NASA Technical Memorandum 100542

AVSCOM
Technical Memorandum 88-B-005

INFLOW MEASUREMENT MADE WITH A LASER VELOCIMETER ON A HELICOPTER MODEL IN FORWARD FLIGHT

Volume II RECTANGULAR PLANFORM BLADES AT AN ADVANCE RATIO OF 0.23

Joe W. Elliott and Susan L. Althoff
Aerostructures Directorate
USAARTA-AVSCOM
Langley Research Center
Hampton, Virginia

Richard H. Sailey
PRC Kentron Inc.
Aerospace Technologies Division
Hampton, Virginia

April 1988

National Aeronautics and
Space Administration

Langley Research Center
Hampton, Virginia 23665-5225

SUMMARY

An experimental investigation was conducted in the 14- by 22-Foot Subsonic Tunnel at NASA Langley Research Center to measure the inflow into a scale model helicopter rotor in forward flight ($\mu_\infty = 0.23$). The measurements were made with a two component Laser Velocimeter (LV) one chord above the plane formed by the path of the rotor tips (tip path plane). A conditional sampling technique was employed to determine the azimuthal position of the rotor at the time that each velocity measurement was made so that the azimuthal fluctuations in velocity could be determined. Measurements were made at a total of 180 separate locations in order to clearly define the inflow character. This data is presented herein without analysis.

INTRODUCTION

One of the many problems confronting the helicopter aerodynamic community is the lack of a comprehensive database which includes the measurements of the velocities into and through the rotor systems. These measurements are necessary for a more complete understanding of the fluid dynamics associated with the rotor and its thrust/lift producing process, and to provide data for the validation of the rapidly emerging computer codes intended to predict the behavior of this process. One explanation for the lack of available data is the absence, until recent years, of a suitable device for making such measurements. Making measurements in and around a system of rotating blades requires a nonintrusive measurement capability that presents a minimum risk to the systems involved and provides an accurate means of making such measurements. The Laser Velocimeter (LV), which uses high energy light beams to measure velocities, is ideally suited to this task.

The Laser Velocimeter has been successfully used to measure specific areas and localized phenomena within the rotor disk (refs. 1 through 3). In addition, the hotwire anemometer and pressure probes, both having directional measuring limitations, have been employed in similar programs (refs. 4 and 5). This is, however, the first time that a comprehensive program has been undertaken to map the flow into the complete rotor disk. An investigation has been conducted to measure the flow into a representative rotor system as a function of azimuth using a two-component (stream wise and vertical direction) LV system.

NOTATION

A_0 constant term in Fourier series of blade feathering (collective) at $r/R = 0.75$, deg

A_1 coefficient of cosine term in Fourier series of blade feathering, deg

B_1 coefficient of sin term in Fourier series of blade feathering, deg

b number of blades

C_D rotor drag coefficient, $D/\rho A (V_{tip})^2$, nondimensional

C_Q rotor torque coefficient, $Q/\rho A R (V_{tip})^2$, nondimensional

C_T rotor thrust coefficient, $T/\rho A (V_{tip})^2$, nondimensional

c rotor blade chord, inches

D rotor Drag, positive to the rear

Q rotor Torque, ft-lb

q dynamic pressure, lb/ft^2

r local radius of the rotor system, ft

R rotor radius, ft

T thrust produced by the rotor, lbf

U free-stream component of velocity, positive downstream, ft/sec

U_∞ free-stream velocity, positive downstream, ft/sec

u_i induced component of velocity parallel to the tip path plane (positive flow down stream), ft/sec

V vertical component of velocity, positive up, ft/sec

v_i induced component of velocity normal to the tip path plane (positive flow up), ft/sec

V_{tip} rotor blade tip velocity, ft/sec

Greek

α angle between rotor disk and free-stream velocity (positive nose up), deg

λ inflow ratio normal to Tip Path Plane (positive up), $(U_\infty \sin \alpha + v_i)/V_{tip}$

λ_i induced inflow ratio normal to Tip Path Plane, (positive up), v_i/V_{tip}

μ_∞ rotor advance ratio, $U_\infty \cos \alpha/V_{tip}$

μ inflow ratio parallel to Tip Path Plane (positive down stream), $(U \cos \alpha + u_i)/V_{tip}$

μ_i induced inflow ratio parallel to Tip Path Plane (positive down stream), u_i/V_{tip}

Ω rotor rotational speed, radians/sec

ψ rotor azimuth measured from downstream position positive counterclockwise as viewed from above, deg

ρ air density, $slugs/ft^3$

θ blade pitch angle at a specific azimuth, $\theta = A_0 - A_1 \cos \psi - B_1 \sin \psi$, deg

$\overline{xx}$ mean values

EXPERIMENTAL APPARATUS

The experimental apparatus used in this investigation included the NASA Langley Research Center 14- by 22-Foot Subsonic Tunnel, the 2-Meter Rotor Test System (2MRTS), and a two-component laser velocimeter system.

The 14- by 22-Foot Subsonic Tunnel is an atmospheric, closed-circuit wind tunnel of conventional design with enhancements for the testing of powered and high-lift configurations (ref. 6). The tunnel is shown in figure 1 and schematically in figure 2. When the test section is configured open, with the walls and ceiling lifted out of the flow leaving only a solid floor and a flow collector at the rear, it can be driven to about 170 knots. This investigation was conducted with the tunnel in this configuration to allow complete optical access to the rotor flowfield produced by the 2MRTS that was mounted on a strut in the forward part of the test section as is shown in figure 3.

The 2MRTS is a general purpose rotorcraft model testing system. The system consists of a 29-horsepower electric drive motor and 90° speed-reducing transmission, a blade pitch control system, and two six-component strain gage balances used for measuring forces and moments on the rotor system and fuselage shell. The four-bladed rotor hub is fully articulated with viscous dampers for lead-lag motion and coincident flap and lag hinges. A more detailed description of the 2MRTS including the ROBIN fuselage can be found in reference 7. The characteristics of rotor blades used in this investigation can be found in table 1. No attempt was made to dynamically scale the rotor blades, rather they were made as stiff as possible to minimize deflection while being tested.

The LV system used in this investigation was designed to measure the instantaneous components of velocity in the longitudinal (free stream) and vertical directions. The LV system is described in reference 8. The system is comprised of four subsystems: optics, traverse, data acquisition, and seeding. The optics subsystem, which is shown in figure 4, operates in backscatter mode and at high power (4 watts in all lines) in order to accommodate the long focal lengths needed to scan the wide test section. The transmitting and receiving optics packages are augmented by a zoom lens system consisting of a 3-in. clear aperture negative lens and a 12-in. clear aperture positive lens. Bragg cells in each of the optical paths provide a directional measurement capability. The velocity measurements are made at a point in space where the four beams cross, called the sample volume. The length of the sample volume (transverse to the flow direction) increases as the sample volume is moved away from the optics assembly. This length, over the 10- to 20 ft focal length of the system, is less than 1 cm and has a constant diameter of 0.2 mm.

The traverse subsystem provides five degrees of freedom in positioning the sample volume and is controlled by the same computer that is used for data acquisition. Translation of the sample volume in the horizontal and vertical direction is accomplished by displacing the entire optics platform. Translation along the lateral axes is accomplished by displacing the negative lens located in the zoom lens assembly, thus refocusing the sample volume along the axis of optical transmission. The other two degrees of freedom, pan and tilt, are implemented by rotating the final mirror about its vertical and horizontal axis in order to change the direction of optical

6 ft streamwise, 16.5 ft laterally, and 10° in both pan and tilt. Measurements can be made outside of this envelope by repositioning the optics platform, which is mounted on wheels to facilitate such relocations. For this study the traversing system was positioned to the right of the test section when looking upstream as shown in figure 5.

The data acquisition subsystem is shown schematically in figure 6 and interfaces with the optical signal processing equipment to receive two channels of raw LV data and up to five channels of auxiliary data. In this investigation four of the auxiliary channels were used for the acquisition of data relative to blade position. Two of the channels (one each for the U and V components) measured the azimuthal position of the rotor shaft and the other two the lead/lag and flapping motion. The system converts the raw LV data to engineering units and determines the statistical characteristics of the acquired data so that the test results can be evaluated during the acquisition process. The raw data which is acquired from the buffer interface device, the data which has been converted to engineering units, and up to 64 parameters which are acquired from the tunnel static data acquisition system are written to magnetic tape for later analysis. The final function performed by the data system is to interface with and control the five degree-of-freedom scan system.

The seeding subsystem, shown schematically in figure 7, is a solid particle, liquid dispensing system (ref. 9). Polystyrene latex microspheres are suspended in a mixture containing, by volume, 50 percent water and 50 percent ethyl alcohol. The advantage of the polystyrene particles is their low density, high reflectivity, and precise particle size. The size of the particles used in this investigation was 1.7 microns in diameter with a standard deviation of 0.0239 microns. This mixture is pumped to an array of 32 nozzles where compressed air is used to atomize the mixture. These nozzles are mounted on a frame 8 ft wide by 6 ft high which is suspended on cables in the settling chamber of the tunnel. The low vapor pressure of water/alcohol mixture allows it to evaporate as it travels the 85 ft from the settling chamber to the test section. This process provides isolated single particles in the flow field whose velocities are measured as they pass through the sample volume, from which the local fluid velocity is inferred.

ERROR ANALYSIS

The overall LV system error is obtained by summing the error of all of the components that contribute to an error in the velocity measurement. The error sources are summarized in the table below, and are defined in refs. 10 and 11. They result in a bias error of -0.81 percent to 1.82 percent and a random error of 1.12 percent. Taking the square root of the sum of the squares of these gives a total system error of 1.38 percent to 2.14 percent (1.76 percent ± 0.38 percent).

Error source	Bias percent	Random percent
Cross beam angle measurement	0.81	None
Diverging fringes	A	A
Time jitter	N/A	N/A
Clock synchronization	0.51	± 0.51
Quantization	A	± 0.99
Velocity bias	B	B
Brag bias	B	B
Velocity gradient	B	B
Particle lag	± 0.50	B
Total error	-0.81 to 1.82	1.12
A NOT MEASURED B NEGLIGIBLE		

TEST PROCEDURES

In all cases, measurements were made at azimuthal increments of 30° from $\psi = 0$, at 3.0 in. (approximately one chord) above the plane formed by the tips of the blades. Measurements were made from radial location of $r/R = 0.2$ to $r/R = 1.1$, with the majority of the measurement locations concentrated toward the outboard portion of the disk. Figure 8 shows the measurement locations super-imposed on the rotor disk. During the test the rotor tip path plane was maintained at -3° relative to the free stream by zeroing the blade flapping relative to the shaft and setting the shaft angle to -3°. The operating rotor speed for the test was held at 2113 rpm, the nominal tunnel speed was 143 ft/sec ($\mu_\infty = 0.23$), and the nominal rotor thrust coefficient was 0.0064. Table 2 lists the target flight conditions, and selected parameters acquired during the test. The acquisition process consisted of placing the sample volume at the location to be measured and acquiring data for a period of two minutes or until 4096 velocity measurements were made in either the U or the V components. During this time conditional sampling techniques were employed to determine the location of the four blades and to permanently associate each measured velocity with the location of the blade when the measurement was made. At the conclusion of that process the measurement location was changed and the acquisition process was repeated.

DATA REDUCTION

Independent velocity measurements in the free stream and vertical direction were made at each measurement location. At the same instant in time that a velocity measurement was made, the location of the blades was recorded for that velocity

component. The maximum time required to acquire this data was two minutes (4200 rotor revolutions for this test) and the minimum approximately 20 sec. These data were collected over many spaced azimuth segments that are representative of blade position and include the corrections for blade lead/lag motion. The velocity value assigned to each azimuthal interval is the arithmetic mean of all of the measurements that were taken in the respective 2.81° wide azimuth range. The results of this sorting process provide the azimuth dependent velocity data. The "mean" velocity value refers to the arithmetic mean, calculated from all of the measurements made at a single measurement location.

EXPERIMENTAL RESULTS

Table 3 lists the measurement locations, the mean and standard deviation of the 2 components of induced inflow velocity, and the number of measurements made on the U and V components. In figure 9 the mean induced component of velocity (longitudinal) μ_i with a band of ± one standard deviation is plotted vs. radius for each radial scan. Figure 10 presents in the same format the mean induced component of velocity (normal) λ_i. The ± one standard deviation is not indicative of the error but rather of the unsteady nature of the flow. The error of 1.76 percent ±0.38 percent is approximately equal to the size of the symbols in figures 9 and 10. The same data, without the one standard deviation, is presented in a contour plot format in figures 11 and 12 in order to more clearly show the mean induced flow over the whole disk (viewed from above). The format of each of figures 13 through 192 is the induced velocity vs. azimuth at the top of the figure, the number of measurements that went into determining the mean for each bin in the center, and an order ratio analysis of the time dependent data at the bottom of the figure. The figure numbers for the azimuthal and radial locations are indicated below.

Azimuth / r/R	0	30	60	90	120	150	180	210	240	270	300	330
0.20	13	28	43	58	73	88	103	118	133	148	163	178
0.40	14	29	44	59	74	89	104	119	134	149	164	179
0.50	15	30	45	60	75	90	105	120	135	150	165	180
0.60	16	31	46	61	76	91	106	121	136	151	166	181
0.70	17	32	47	62	77	92	107	122	137	152	167	182
0.74	18	33	48	63	78	93	108	123	138	153	168	183
0.78	19	34	49	64	79	94	109	124	139	154	169	184
0.82	20	35	50	65	80	95	110	125	140	155	170	185
0.86	21	36	51	66	81	96	111	126	141	156	171	186
0.90	22	37	52	67	82	97	112	127	142	157	172	187
0.94	23	38	53	68	83	98	113	128	143	158	173	188
0.98	24	39	54	69	84	99	114	129	144	159	174	189
1.02	25	40	55	70	85	100	115	130	145	160	175	190
1.04	26	41	56	71	86	101	116	131	146	161	176	191
1.10	27	42	57	72	87	102	117	132	147	162	177	192

The results shown in table 3, the mean and standard deviation of the induced inflow velocities, and the results shown in figures 13 through 192, the azimuth dependent induced inflow velocities, are included on a 5.25 in. floppy disk in Microsoft Corporation MS-DOS format (see pocket inside rear cover). The details of the data format, and file structure is located in the file "readme.com". The disk format is 360 kbyte double sided written using DOS 3.2.

CONCLUDING REMARKS

The Laser Velocimeter provides a effective system for making measurements in the dynamic environment associated with rotorcraft. It has in fact been used on numerous occasions to measure the localized phenomena encountered in such flows. This investigation demonstrates the use of a mature system in mapping the flow into a representative rotor in forward flight. These measurements provide not only the mean values but azimuth dependent values as well, and they provide a detailed look at the nature of this flow.

REFERENCES

1. Landgrebe, A. J.; and Johnson, B. V.: Measurement of Model Helicopter Rotor Flow Velocities With a Laser Doppler Velocimeter. American Helicopter Society, Journal, Vol. 19, July 1974, pp. 39-43.

2. Biggers, J. C.; and Orloff, K. L.: Laser Velocimeter Measurements of the Helicopter Rotor-Induced Flowfield. American Helicopter Society, Annual National V/STOL Forum, 30th, Washington, D.C., May 7-9, 1974.

3. Owen, F. K.; and Taubert, M. E.: Measurement and Prediction of Model-Rotor Flowfields. AIAA, 18th Fluid Dynamics, Plasmadynamics and Laser Conference, Cincinnati, Ohio, July 16-18, 1985.

4. Tangler, J. L.; Wohlfeld, R. M.; and Miley, S. J.: Analysis of Wakes Generated by Hovering Model Propellers and Rotors Using Schlieren Photography and Hot-Wire Anemometry. Bell Helicopter Company, Forth Worth, Texas, NASA CR-2305, September 1973.

5. Junker, B.: Investigations of Blade-Vortices in the Rotor Downwash. Twelfth European Rotorcraft Forum, Garmish-Partenkirchen, Federal Republic of Germany, September 22-25, 1986.

6. Applin, Z. T.: Flow Improvements in the Circuit of the Langley 4- by 7-Meter Tunnel. NASA TM-85662, December 1983.

7. Phelps, A. E. III; and Berry, J. D.: Description of the U.S. Army 2-Meter Rotor Test System. NASA TM-87762, AVSCOM TM-86-B-4, January 1987.

8. Sellers, W. L.; and Elliott, J. W.: Applications of a Laser Velocimeter in the Langley 4- by 7-Meter Tunnel. Proceedings of the Workshop on Flow Visualization and Laser Velocimetry for Wind Tunnels. NASA CP-2243, March 1982, pp. 283-293.

9. Elliott, J. E.; and Nichols, C. E.: Seeding Systems for use With a Laser Velocimeter in Large Scale Wind Tunnels. Proceedings of the Workshop on Wind Tunnel Seeding Systems for Laser Velocimeters, NASA CP-2393, March 1985, pp. 93-103.

10. Young, W. H.; Meyers, J. F.; and Hepner, T. E.: Laser Velocimeter Systems Analysis to a Flow Survey Above a Stalled Wing. NASA TN D-8408, August 1977.

11. Dring, R. P.: Sizing Criteria for Laser Anemometry Particles. Journal of Fluid Engineering, Vol. 104, March 1982, pp. 15-17.

TABLE 1.- 2MRTS ROTOR AND BLADE CHARACTERISTICS

Hub type	Fully Articulated
Number of blades	4
Airfoil section	NACA 0012
Hinge offset, in., r/R	2.00,.06
Root cutout, in., r/R	8.25,.24
Pitch-flap coupling angle, deg	0.0
Twist linear, deg	-8.0
Radius, R, in.	33.88
Airfoil chord, C, in.	2.6
Rotor solidity, bc/πR	0.0977
Blade stiffness	
Flapwise lb-in^2	11500
Torsional lb-in^2	25500
Blade weight, grams	259.3
Lead/lag damping in-lb/deg/sec	182.4

TABLE 2.- NOMINAL ROTOR CONTROLS AND PERFORMANCE PARAMETERS

Propulsive Force, (Drag/q) ft^2	0.00
α, deg	-3,04
A_0, deg	8.16
A_1, deg	-1,52
B_1, deg	4.13
μ_∞	0.230
V_∞, knots	85.258
V_{tip}, ft/sec	624.50
M_{tip}, nondimensional	0.5479
Lag angle, (mean), deg	0.90

TABLE 3.- INFLOW VELOCITY SUMMARY

		μ_1			λ_1		
ψ	r/R	Mean	Standard deviation	# measurements	Mean	Standard deviation	# measurements
0	.20	.0227	.0080	2762	-.0019	.0117	2100
0	.40	.0218	.0078	2237	-.0134	.0111	2115
0	.50	.0213	.0075	1862	-.0155	.0106	1990
0	.60	.0213	.0077	1865	-.0209	.0099	2012
0	.70	.0200	.0077	1904	-.0248	.0085	1819
0	.74	.0195	.0067	1805	-.0254	.0108	2025
0	.78	.0181	.0067	1995	-.0265	.0106	2092
0	.82	.0182	.0067	1920	-.0281	.0094	1918
0	.86	.0151	.0064	2016	-.0298	.0095	1990
0	.90	.0147	.0079	2639	-.0309	.0091	2126
0	.94	.0132	.0078	2470	-.0320	.0093	2094
0	.98	.0113	.0075	2331	-.0325	.0079	2064
01	.02	.0102	.0087	2431	-.0324	.0067	2003
01	.04	.0077	.0092	2659	-.0326	.0067	2047
01	.10	.0063	.0091	2612	-.0317	.0064	2079
30	.20	.0204	.0092	1069	-.0011	.0129	2155
30	.40	.0213	.0068	1322	-.0166	.0092	2338
30	.50	.0192	.0062	1212	-.0260	.0122	2080
30	.60	.0171	.0057	1749	-.0299	.0096	2425
30	.70	.0132	.0063	2385	-.0338	.0100	2711
30	.74	.0121	.0063	2343	-.0345	.0100	2338
30	.82	.0101	.0059	1858	-.0358	.0100	3052
30	.86	.0086	.0053	1053	-.0355	.0093	1442
30	.90	.0079	.0050	936	-.0334	.0081	660
30	.94	.0055	.0052	1163	-.0323	.0085	883
30	.98	.0044	.0054	1787	-.0314	.0075	1176
30	1.02	.0036	.0051	2184	-.0311	.0066	1322
30	1.04	.0029	.0048	2971	-.0307	.0073	1788
30	1.10	.0010	.0042	3086	-.0287	.0067	1929
60	.20	.0181	.0076	1095	-.0016	.0065	1988
60	.40	.0187	.0068	905	-.0209	.0079	1859
60	.50	.0168	.0069	913	-.0225	.0082	1630
60	.60	.0148	.0066	1236	-.0220	.0104	2619
60	.70	.0144	.0062	3427	-.0210	.0074	2388
60	.74	.0142	.0059	3698	-.0212	.0076	2065
60	.78	.0126	.0059	3797	-.0208	.0079	1865
60	.82	.0114	.0056	3794	-.0204	.0074	1955
60	.86	.0112	0069	3821	-.0181	.0067	1786
60	.90	.0091	.0048	2086	-.0172	.0069	2242
60	.94	.0083	.0051	2820	-.0153	.0071	2233
60	.98	.0074	.0047	2570	-.0124	.0065	2211
60	1.04	.0037	.0043	2502	-.0037	.0058	2036
60	1.10	.0016	.0041	3257	.0169	.0045	1894
90	.20	.0160	.0068	2675	-.0027	.0051	1935
90	.40	.0173	.0073	3263	-.0140	.0068	2189

TABLE 3.- Continued

		μ_1			λ_1		
ψ	r/R	Mean	Standard deviation	# measurements	Mean	Standard deviation	# measurements
90	.50	.0183	.0078	2853	-.0131	.0071	2341
90	.60	.0171	.0074	2305	-.0095	.0082	2187
90	.70	.0157	.0066	3143	-.0073	.0078	2150
90	.74	.0149	.0065	2971	-.0037	.0063	1749
90	.78	.0142	.0059	2783	-.0017	.0065	1440
90	.82	.0127	.0059	2674	.0014	.0069	1476
90	.86	.0112	.0057	3081	.0047	.0060	2123
90	.90	.0098	.0053	2895	.0076	.0051	2063
90	.94	.0078	.0051	3067	.0114	.0040	2123
90	.98	.0059	.0047	3205	.0135	.0041	2000
90	1.02	.0049	.0042	3334	.0145	.0042	1858
90	1.04	.0031	.0040	3389	.0143	.0041	1732
90	1.10	.0027	.0035	3240	.0128	.0038	1553
120	.20	.0105	.0049	3572	.0006	.0056	1925
120	.40	.0165	.0054	3576	-.0063	.0075	2732
120	.50	.0169	.0062	3557	-.0048	.0077	3091
120	.70	.0142	.0063	2663	.0040	.0069	2915
120	.74	.0129	.0058	2483	.0072	.0072	3153
120	.78	.0123	.0059	2286	.0078	.0071	3162
120	.82	.0109	.0056	2250	.0092	.0072	3254
120	.86	.0091	.0049	2178	.0105	.0067	3367
120	.90	.0082	.0056	3740	.0113	.0069	3319
120	.94	.0069	.0052	3736	.0120	.0061	3369
120	.98	.0059	.0049	3250	.0120	.0057	3268
120	1.02	.0037	.0045	3413	.0112	.0059	3220
120	1.04	.0030	.0041	3207	.0109	.0059	3169
120	1.10	.0016	.0036	3154	.0099	.0063	3082
150	.20	.0071	.0054	3276	.0038	.0066	2691
150	.40	.0150	.0053	3465	-.0004	.0071	2152
150	.50	.0156	.0051	3399	.0029	.0085	2795
150	.60	.0157	.0055	3412	.0055	.0088	2953
150	.70	.0137	.0056	3452	.0082	.0079	2606
150	.74	.0112	.0057	3492	.0098	.0089	2848
150	.78	.0113	.0050	3502	.0108	.0089	3069
150	.82	.0104	.0052	3537	.0107	.0079	3058
150	.86	.0085	.0055	3492	.0112	.0075	3067
150	.94	.0047	.0055	3267	.0111	.0063	3134
150	.98	.0028	.0052	3390	.0112	.0063	3084
150	1.02	.0019	.0046	3366	.0105	.0051	3017
150	1.04	.0023	.0043	3111	.0102	.0050	3119
150	1.10	.0001	.0039	3261	.0093	.0063	3185
180	.20	.0072	.0066	2548	.0025	.0054	773
180	.40	.0111	.0060	1879	-.0004	.0093	523
180	.50	.0128	.0061	1906	.0009	.0092	512
180	.60	.0120	.0064	2624	.0053	.0067	591

TABLE 3.- Continued

		μ_l			λ_l		
ψ	r/R	Mean	Standard deviation	# measurements	Mean	Standard deviation	# measurements
180	.70	.0107	.0067	2590	.0064	.0078	571
180	.74	.0107	.0069	2448	.0084	.0066	472
180	.78	.0085	.0069	2467	.0093	.0069	550
180	.82	.0069	.0071	2130	.0118	.0090	2634
180	.86	.0049	.0073	2144	.0117	.0087	2679
180	.90	.0039	.0071	2400	.0118	.0080	2675
180	.94	.0052	.0072	2483	.0122	.0068	2604
180	.98	.0030	.0067	2855	.0109	.0054	2385
180	1.02	.0011	.0061	2856	.0098	.0062	2281
180	1.04	.0026	.0057	2875	.0094	.0061	2331
180	1.10	.0006	.0055	2788	.0085	.0059	2153
210	.40	.0110	.0076	2953	.0009	.0092	2419
210	.50	.0138	.0074	3143	.0007	.0094	2357
210	.60	.0162	.0073	2930	.0037	.0091	2466
210	.70	.0166	.0091	2709	.0082	.0133	2783
210	.74	.0162	.0097	2653	.0073	.0157	2877
210	.78	.0147	.0097	2550	.0131	.0137	2881
210	.82	.0125	.0099	2427	.0112	.0096	2452
210	.86	.0119	.0097	2330	.0106	.0097	2604
210	.90	.0104	.0089	2516	.0107	.0090	2626
210	.94	.0083	.0081	2544	.0108	.0085	2579
210	.98	.0060	.0074	2647	.0115	.0073	2570
210	1.02	.0049	.0063	2710	.0103	.0077	2591
210	1.04	.0038	.0064	2794	.0097	.0080	2667
210	1.10	.0032	.0061	2719	.0081	.0063	2317
240	.20	.0100	.0060	2745	.0007	.0048	2411
240	.40	.0131	.0073	3004	-.0049	.0065	2298
240	.50	.0142	.0067	1515	-.0051	.0076	1097
240	.60	.0132	.0069	1617	-.0051	.0071	1626
240	.70	.0152	.0083	2411	.0004	.0105	2468
240	.74	.0150	.0091	2429	.0028	.0121	2567
240	.82	.0135	.0101	2208	.0058	.0134	2369
240	.86	.0127	.0099	2496	.0071	.0127	2643
240	.90	.0130	.0094	2651	.0092	.0105	2653
240	.94	.0101	.0086	2461	.0107	.0092	2554
240	.98	.0075	.0075	2460	.0116	.0082	2605
240	1.02	.0055	.0072	2546	.0121	.0081	2503
240	1.04	.0056	.0071	2461	.0106	.0064	2197
240	1.10	.0042	.0068	2312	.0097	.0064	1893
270	.20	.0156	.0044	2773	.0008	.0058	3098
270	.40	.0124	.0063	2433	-.0045	.0074	1660
270	.50	.0121	.0075	1659	-.0080	.0073	1073
270	.60	.0136	.0081	2309	-.0087	.0100	1496
270	.70	.0147	.0087	3348	-.0124	.0096	1571
270	.74	.0145	.0086	3206	-.0122	.0089	1484

TABLE 3.- Continued

		μ_1			λ_1		
ψ	r/R	Mean	Standard deviation	# measurements	Mean	Standard deviation	# measurements
270	.78	.0142	.0087	3176	-.0109	.0085	1608
270	.82	.0143	.0088	3118	-.0088	.0103	1762
270	.86	.0140	.0090	3094	-.0063	.0109	1791
270	.90	.0143	.0090	3123	-.0002	.0136	2287
270	.94	.0133	.0082	2984	.0046	.0126	2521
270	.98	.0105	.0084	2824	.0122	.0095	2621
270	1.02	.0089	.0068	2615	.0159	.0080	2575
270	1.04	.0075	.0065	2455	.0155	.0067	2478
270	1.10	.0065	.0064	2583	.0142	.0072	2288
300	.20	.0187	.0045	2919	-.0023	.0060	3049
300	.40	.0159	.0052	2970	-.0047	.0056	2504
300	.50	.0167	.0064	3406	-.0082	.0069	2631
300	.60	.0141	.0076	2677	-.0116	.0082	1993
300	.70	.0171	.0083	2763	-.0164	.0098	2079
300	.74	.0153	.0083	2195	-.0192	.0095	1635
300	.78	.0157	.0084	2068	-.0206	.0098	1673
300	.82	.0163	.0084	2387	-.0232	.0113	2183
300	.86	.0162	.0076	2444	-.0248	.0108	2081
300	.90	.0103	.0097	1776	-.0246	.0112	2214
300	.94	.0090	.0093	1803	-.0243	.0107	2213
300	.98	.0081	.0097	1362	-.0207	.0093	1910
300	1.02	.0069	.0099	1422	-.0150	.0074	1730
300	1.04	.0076	.0097	1308	-.0128	.0076	1517
300	1.10	.0091	.0108	1422	-.0094	.0100	2292
330	.20	.0181	.0077	1791	-.0005	.0071	2411
330	.40	.0176	.0087	1733	-.0040	.0071	2247
330	.50	.0165	.0090	1268	-.0066	.0080	1970
330	.60	.0163	.0093	1333	-.0080	.0086	1896
330	.70	.0176	.0081	1206	-.0106	.0085	1642
330	.74	.0183	.0084	1418	-.0132	.0098	1919
330	.78	.0171	.0085	1577	-.0150	.0095	1971
330	.82	.0165	.0078	1735	-.0192	.0097	2025
330	.86	.0153	.0085	1985	-.0220	.0108	2162
330	.90	.0146	.0090	2107	-.0236	.0110	2100
330	.94	.0122	.0087	1703	-.0254	.0102	1552
330	.98	.0098	.0097	1803	-.0271	.0104	2211
330	1.02	.0073	.0099	1860	-.0278	.0082	2068
330	1.04	.0050	.0097	2021	-.0272	.0080	2037
330	1.10	.0041	.0086	1803	-.0260	.0075	2243
360	.20	.0227	.0080	2762	-.0019	.0117	2100
360	.40	.0218	.0078	2237	-.0134	.0111	2115
360	.50	.0213	.0075	1862	-.0155	.0106	1990
360	.60	.0213	.0077	1865	-.0209	.0099	2012
360	.70	.0200	.0077	1904	-.0248	.0085	1819
360	.74	.0195	.0067	1805	-.0254	.0108	2025

TABLE 3.- Concluded

		μ_1			λ_1		
ψ	r/R	Mean	Standard deviation	# measurements	Mean	Standard deviation	# measurements
360	.78	.0181	.0067	1995	-.0265	.0106	2092
360	.82	.0182	.0067	1920	-.0281	.0094	1918
360	.86	.0151	.0064	2016	-.0298	.0095	1990
360	.90	.0147	.0079	2639	-.0309	.0091	2126
360	.94	.0132	.0078	2470	-.0320	.0093	2094
360	.98	.0113	.0075	2331	-.0325	.0079	2064
360	1.02	.0102	.0087	2431	-.0324	.0067	2003
360	1.04	.0077	.0092	2659	-.0326	.0067	2047
360	1.10	.0063	.0091	2612	-.0317	.0064	2079

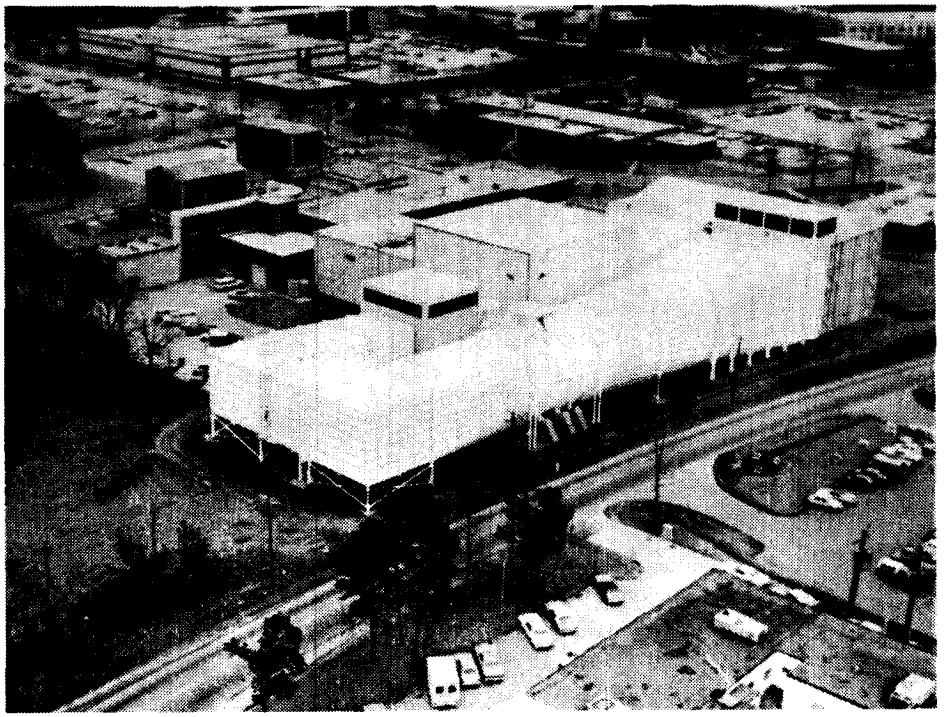

Figure 1.- Aerial view of 14- by 22-foot tunnel.

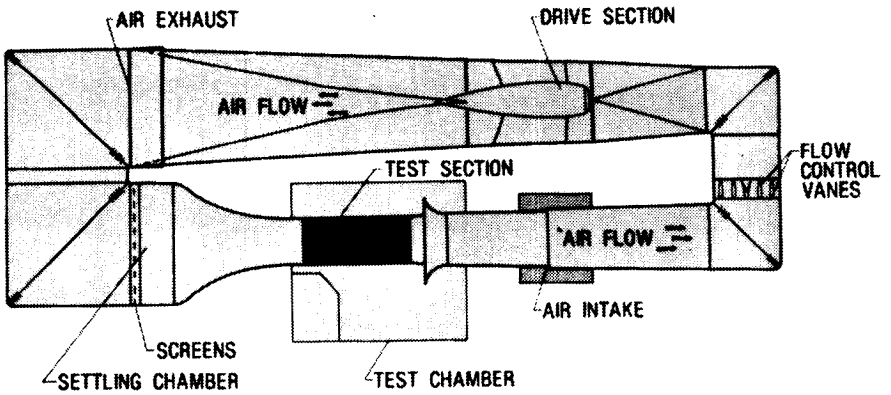

Figure 2.- Schematic view of 14- by 22-foot subsonic wind tunnel.

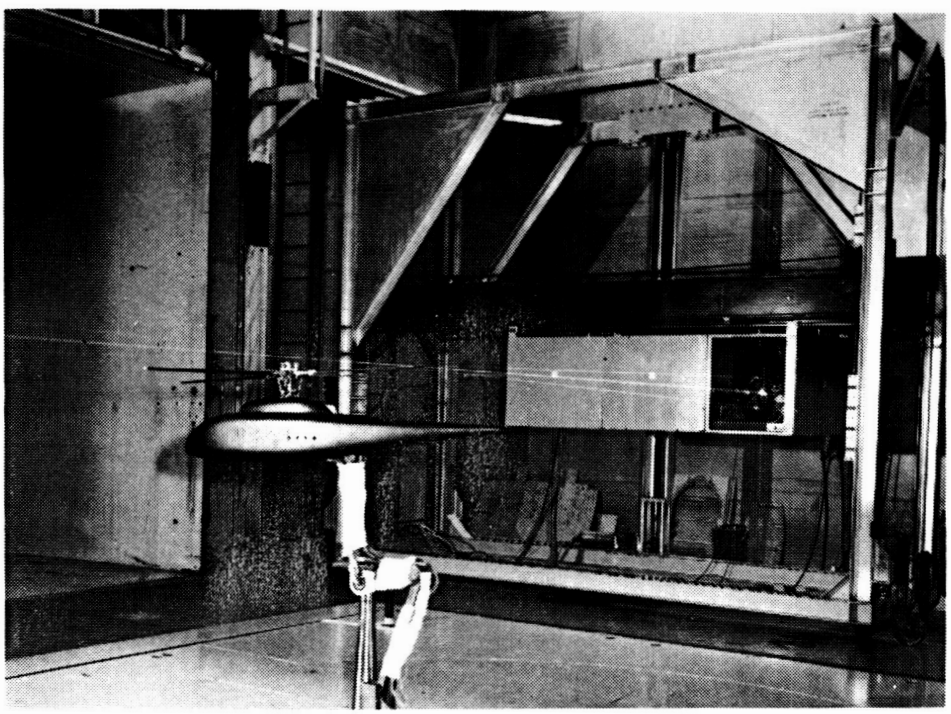

Figure 3.- 2MRTS mounted in forward bay of the test section.

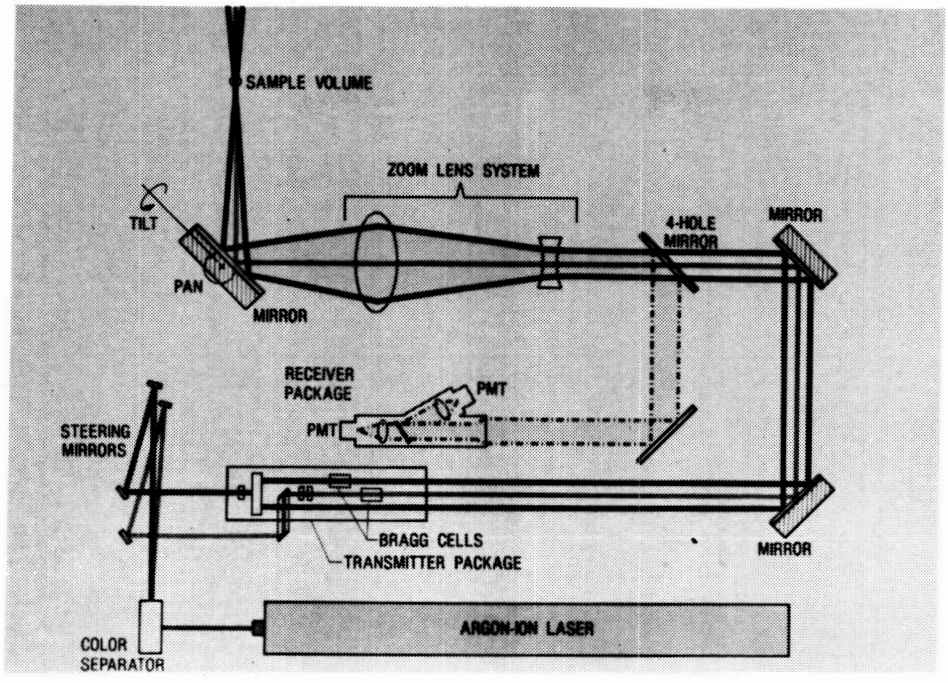

Figure 4.- Schematic diagram of Laser Velocimeter Optics sub-system.

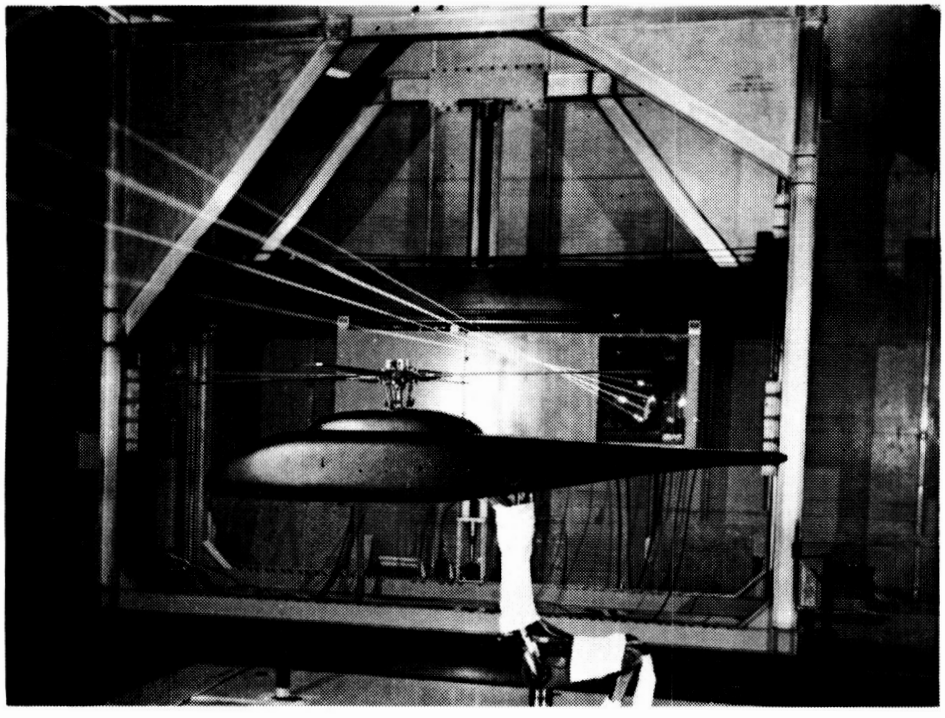

Figure 5.- Laser Velocimeter positioned in test chamber.

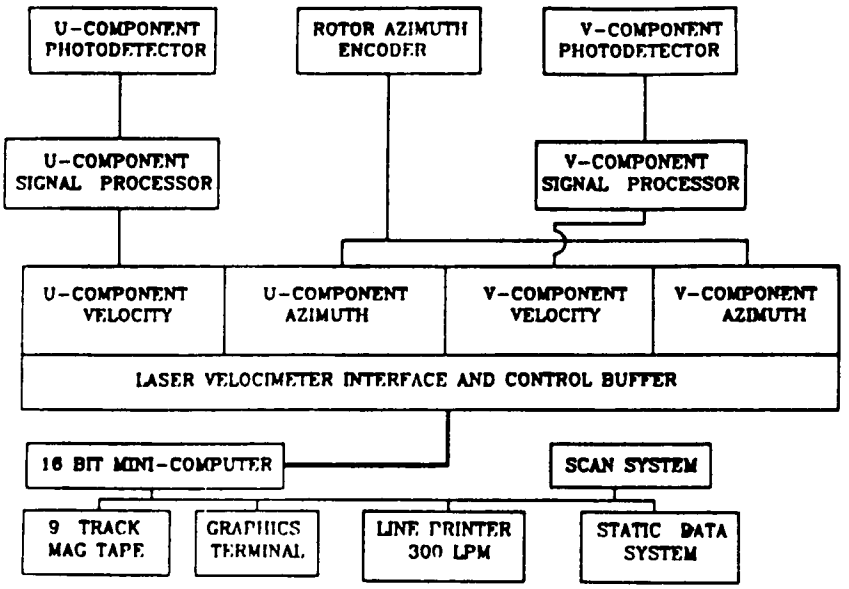

Figure 6.- Schematic view of data acquisition and control sub-system.

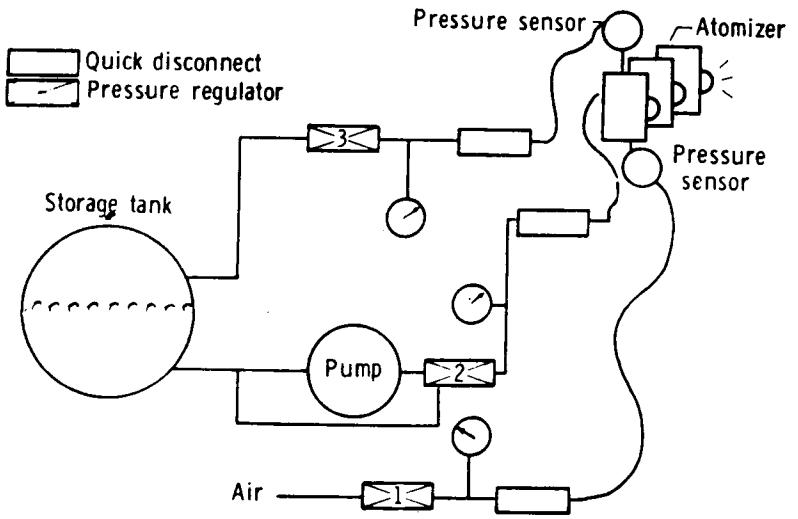

Figure 7.- Schematic of seeding system.

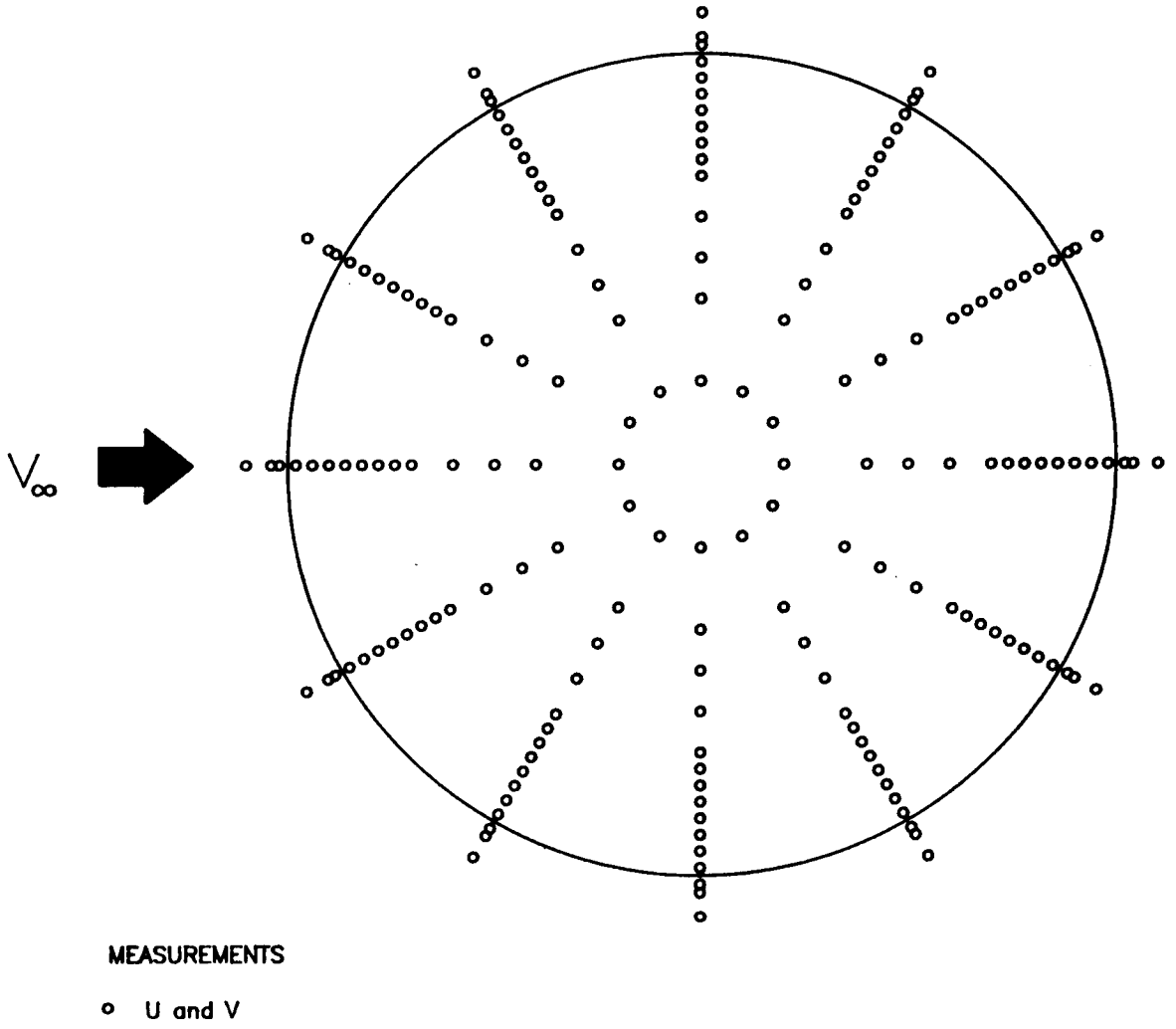

Figure 8.– Locations of velocity measurements, 3.0 inches above rotor tip path plane.

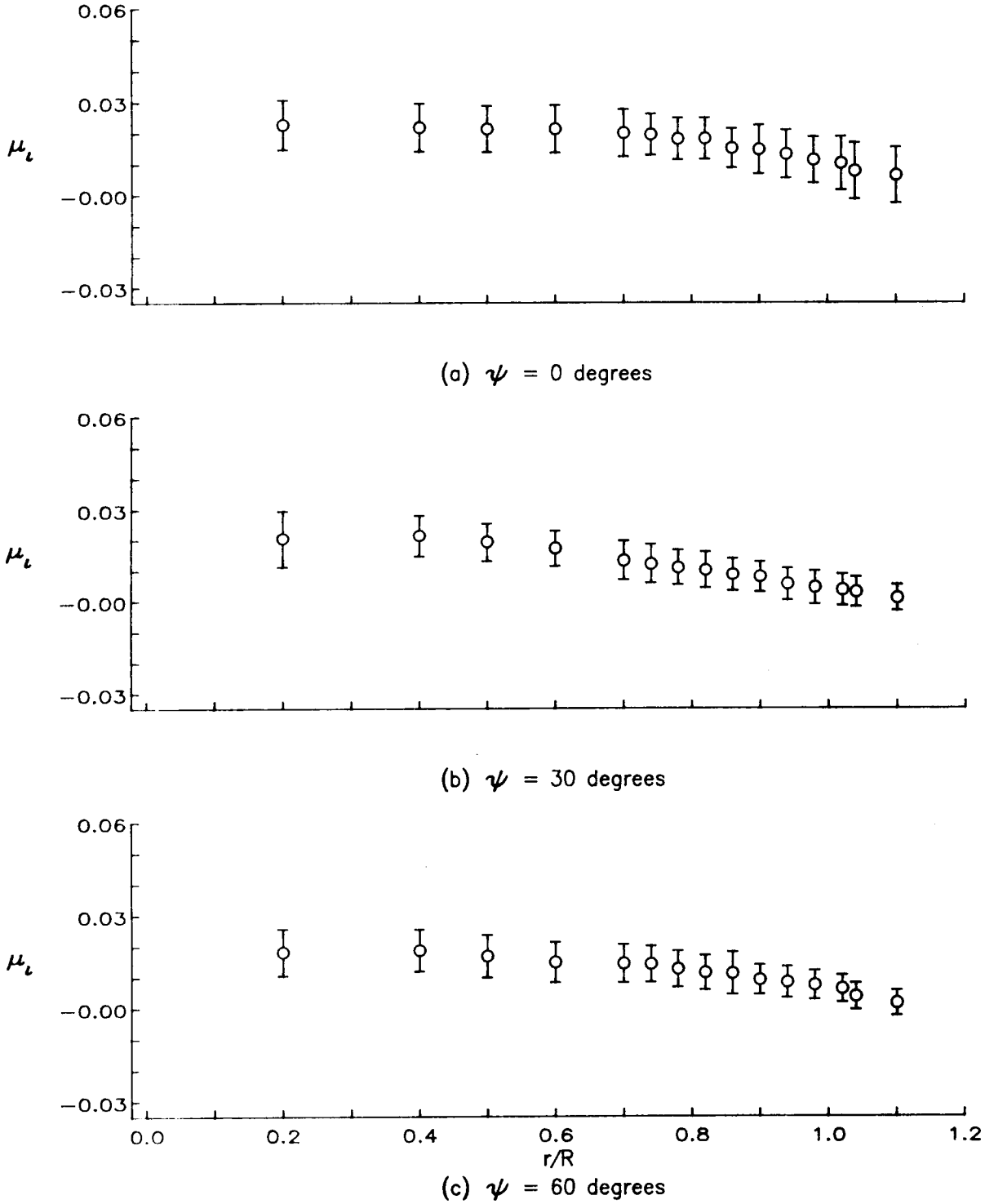

Figure 9.– Radial distribution of mean induced inflow ratio (μ_i).

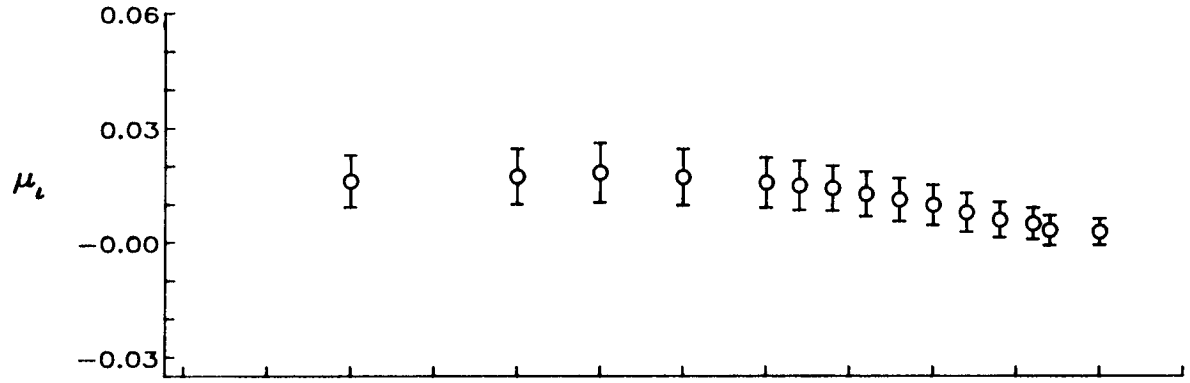

(d) ψ = 90 degrees

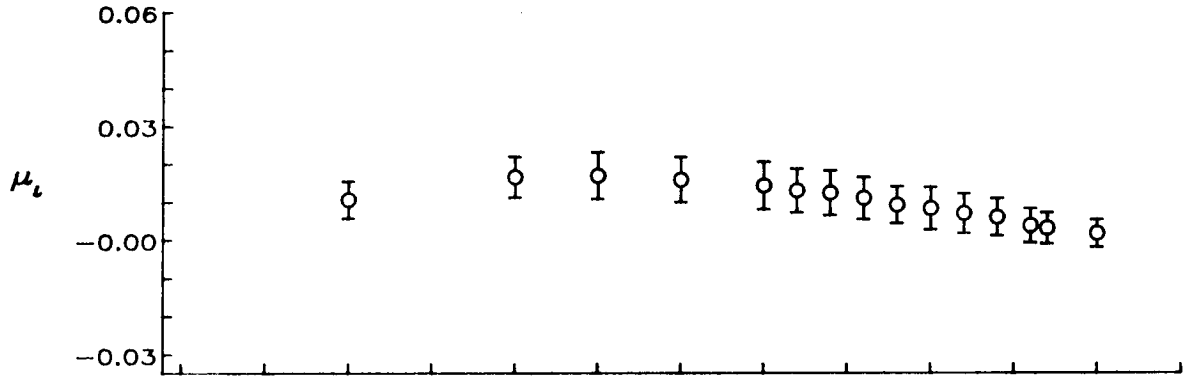

(e) ψ = 120 degrees

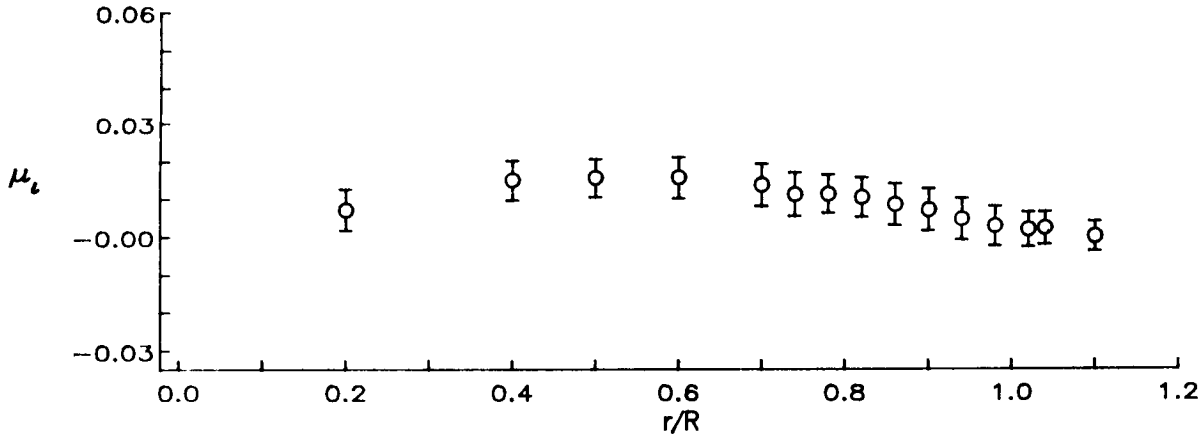

(f) ψ = 150 degrees

Figure 9.– Continued.

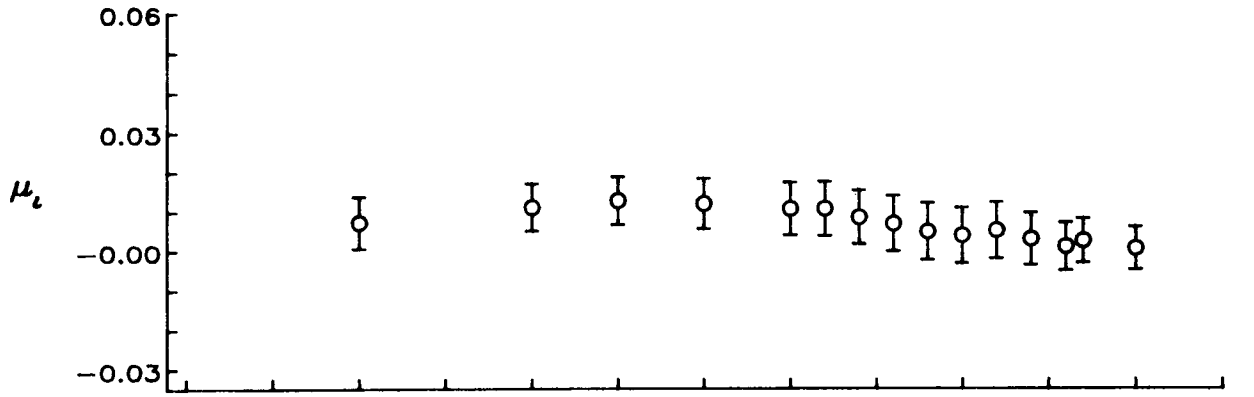

(g) ψ = 180 degrees

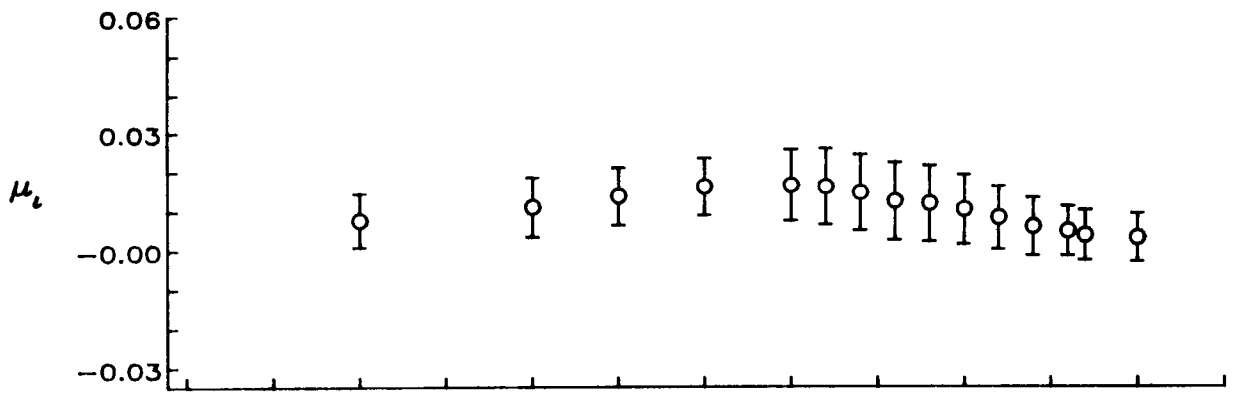

(h) ψ = 210 degrees

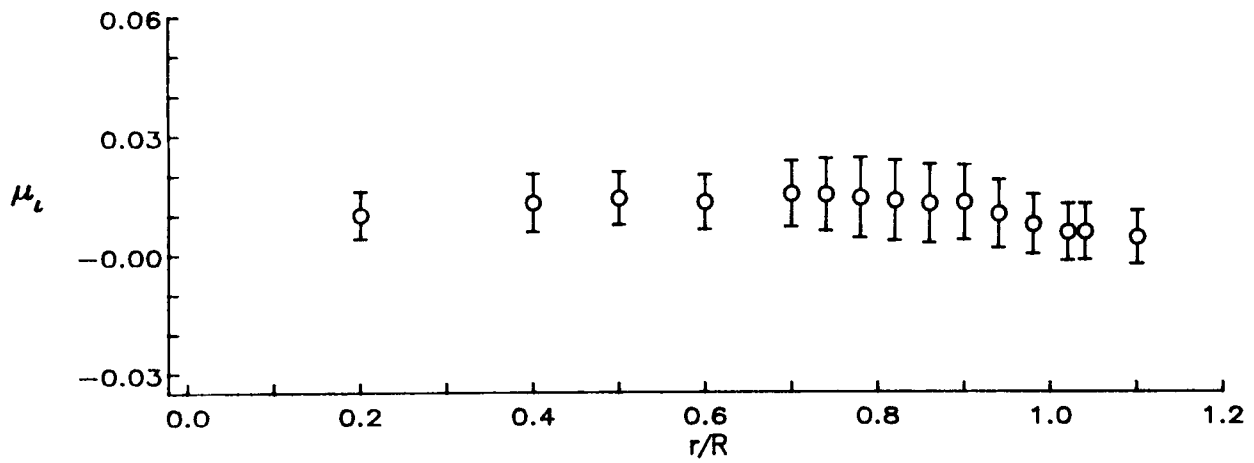

(i) ψ = 240 degrees

Figure 9.– Continued.

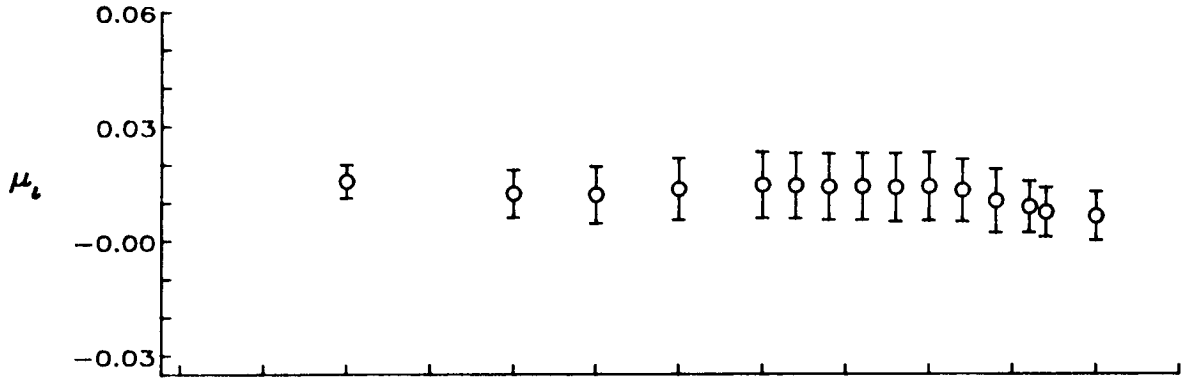

(j) ψ = 270 degrees

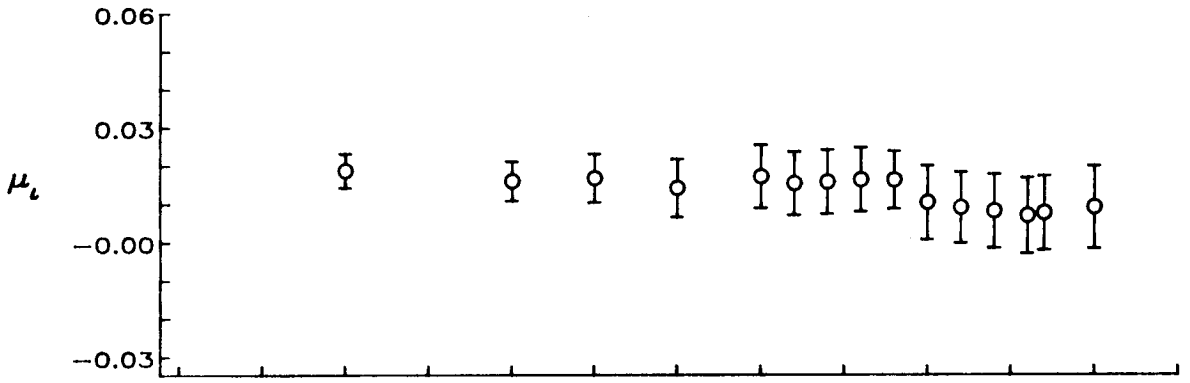

(k) ψ = 300 degrees

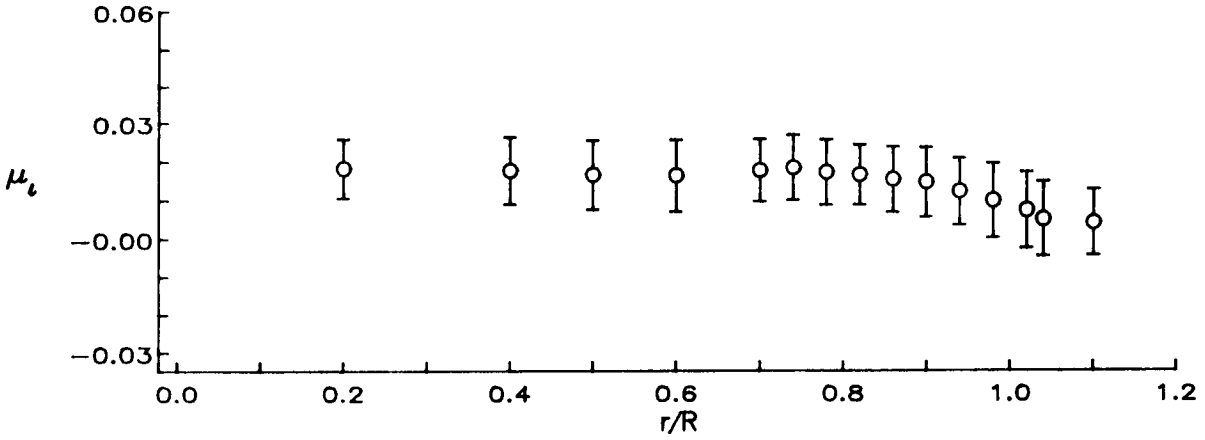

(l) ψ = 330 degrees

Figure 9.– Concluded.

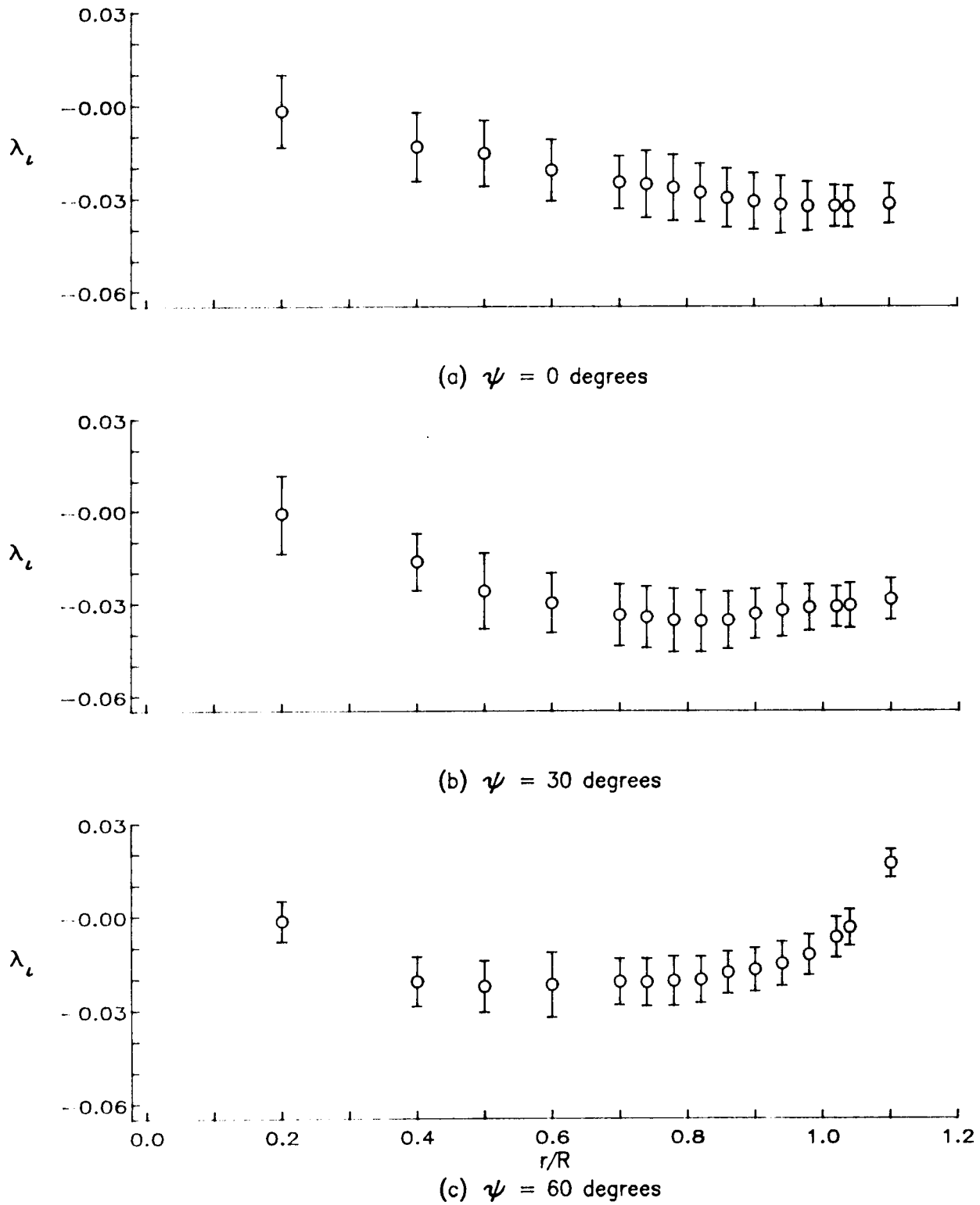

Figure 10.– Radial distribution of mean induced inflow ratio (λ_i).

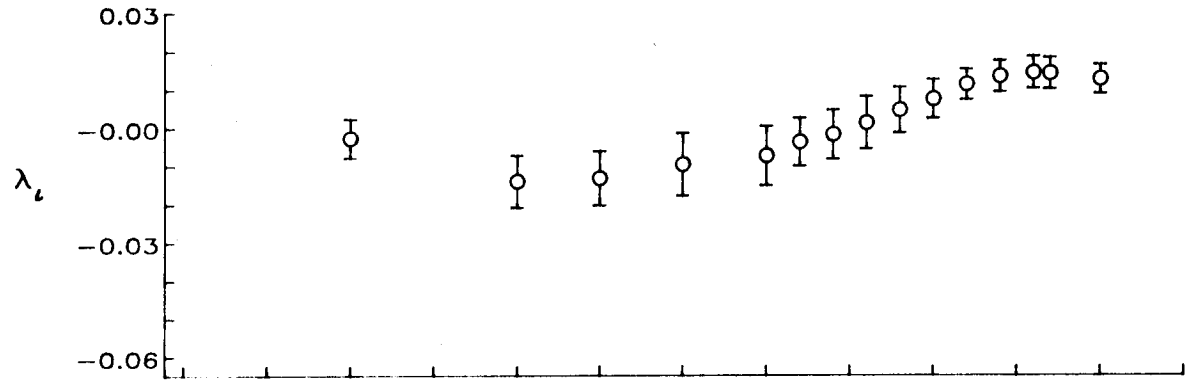

(d) ψ = 90 degrees

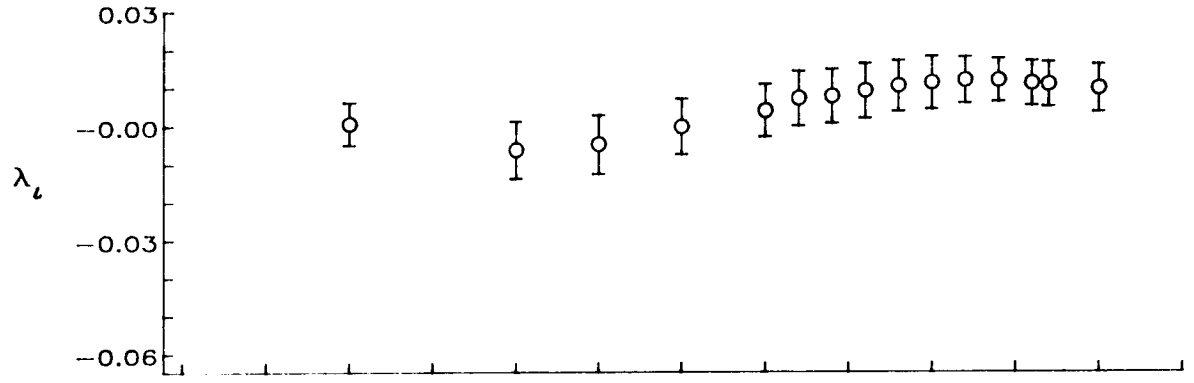

(e) ψ = 120 degrees

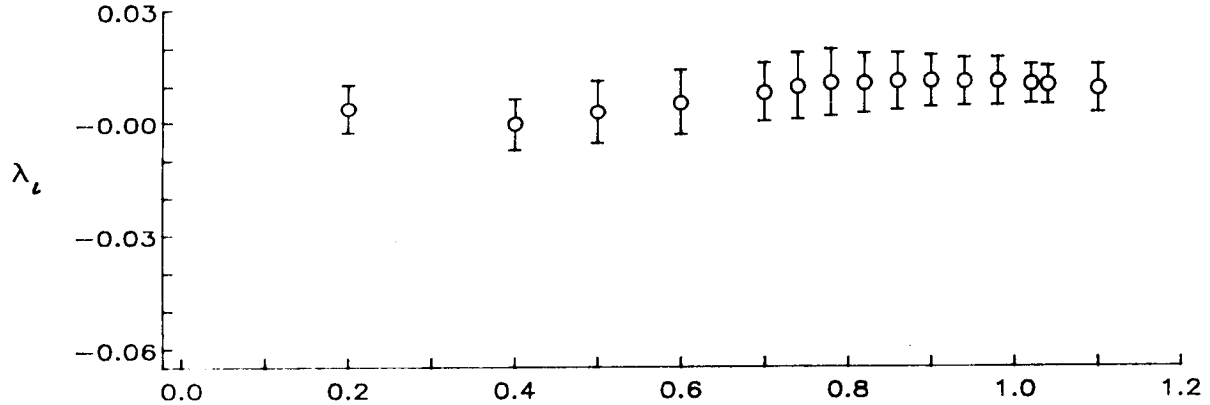

(f) ψ = 150 degrees

Figure 10.– Continued.

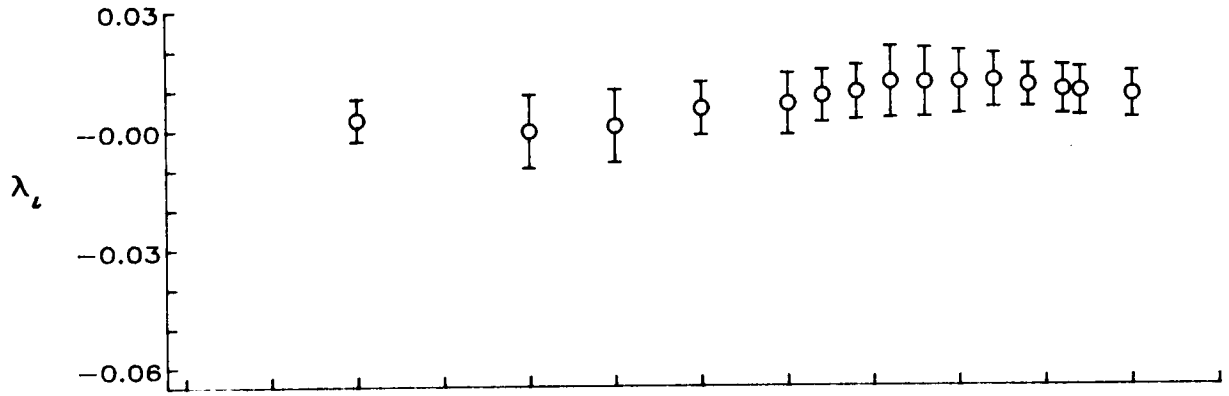

(g) ψ = 180 degrees

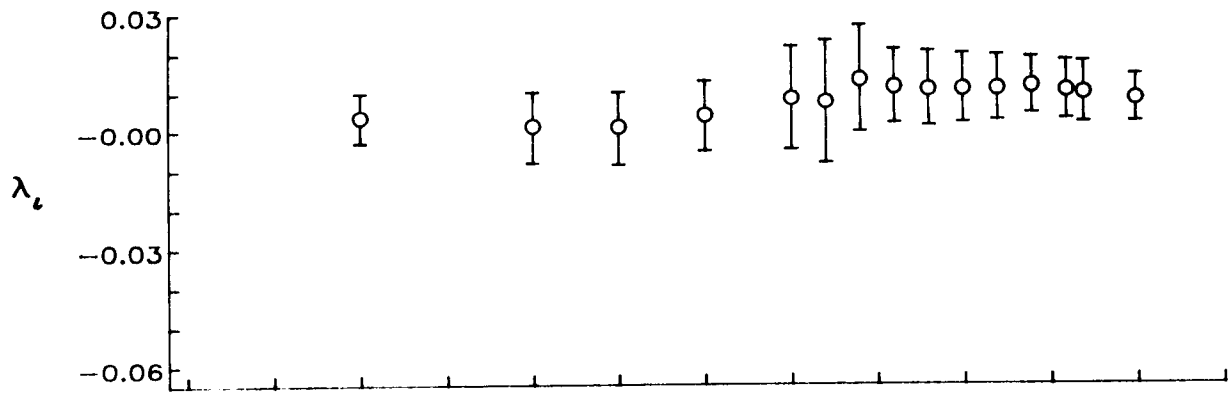

(h) ψ = 210 degrees

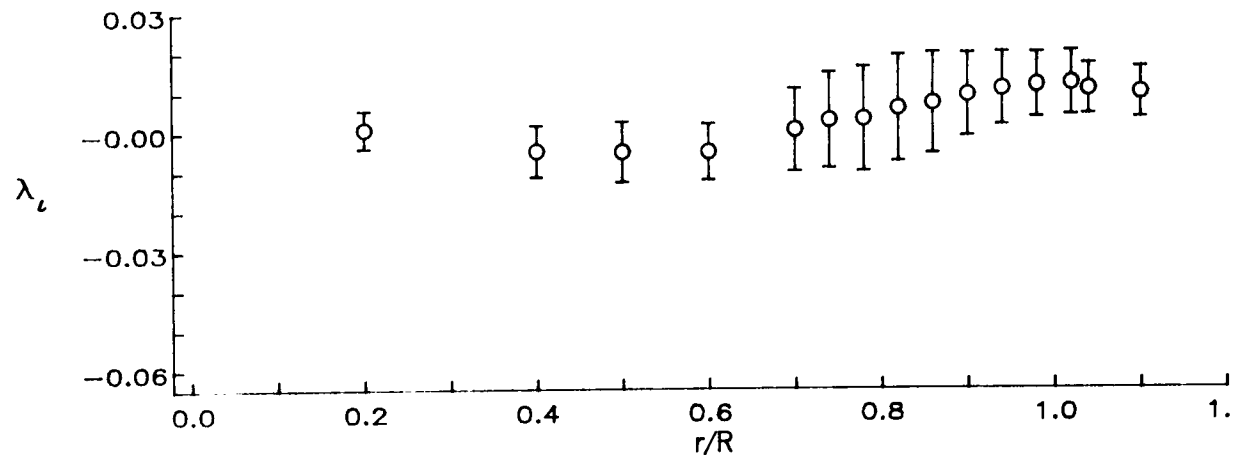

(i) ψ = 240 degrees

Figure 10.– Continued.

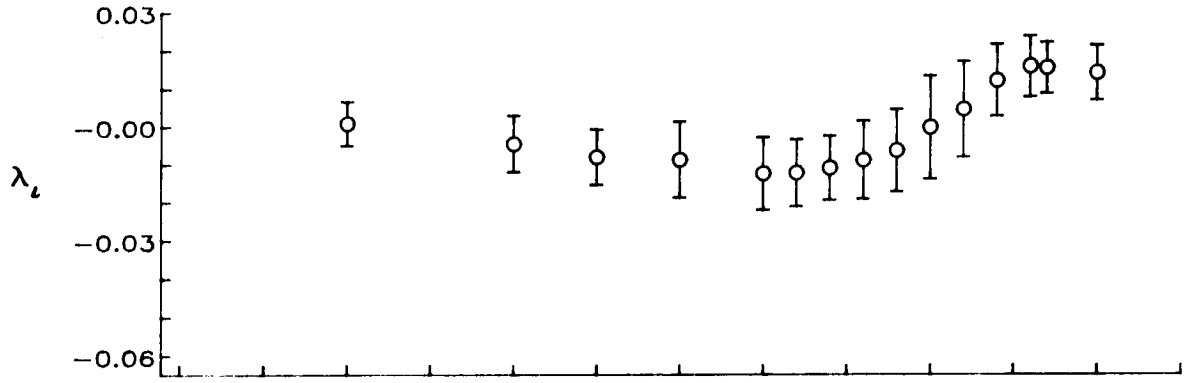

(j) ψ = 270 degrees

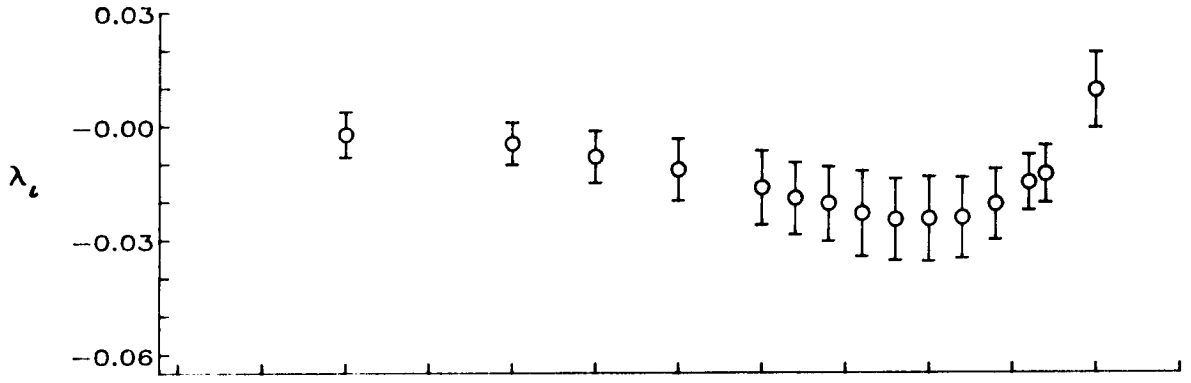

(k) ψ = 300 degrees

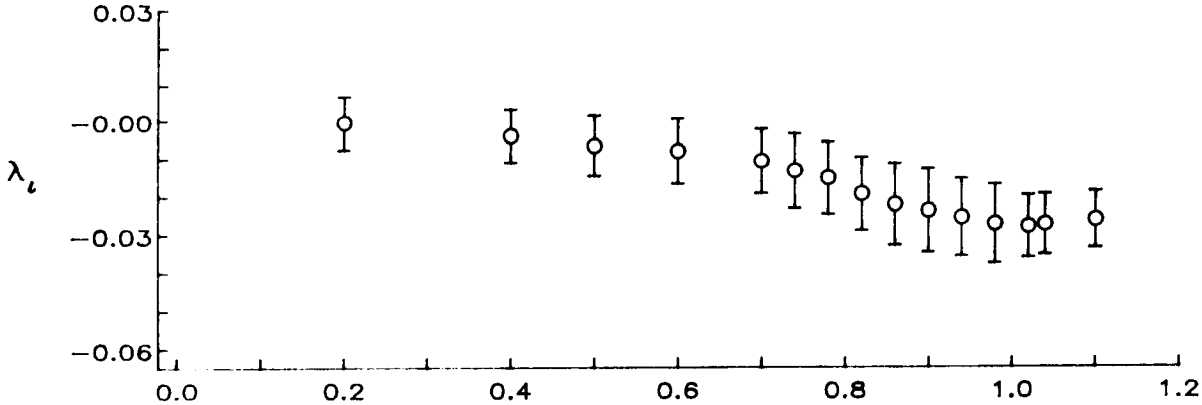

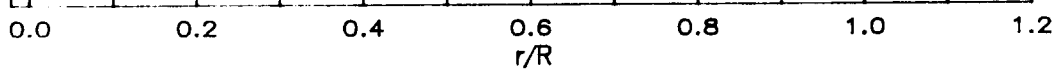

(l) ψ = 330 degrees

Figure 10.– Concluded.

ORIGINAL PAGE
COLOR PHOTOGRAPH

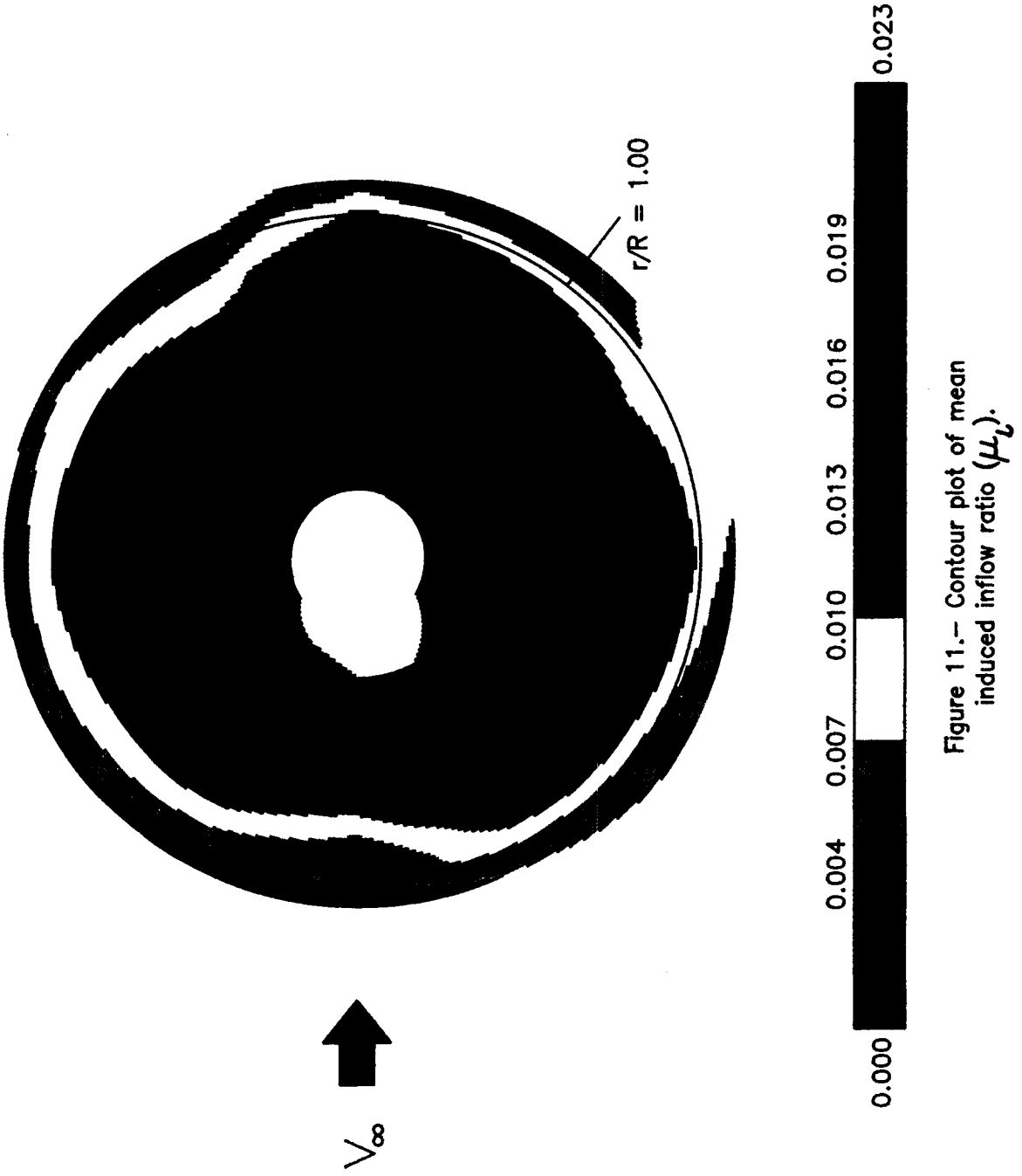

Figure 11.– Contour plot of mean induced inflow ratio (μ_i).

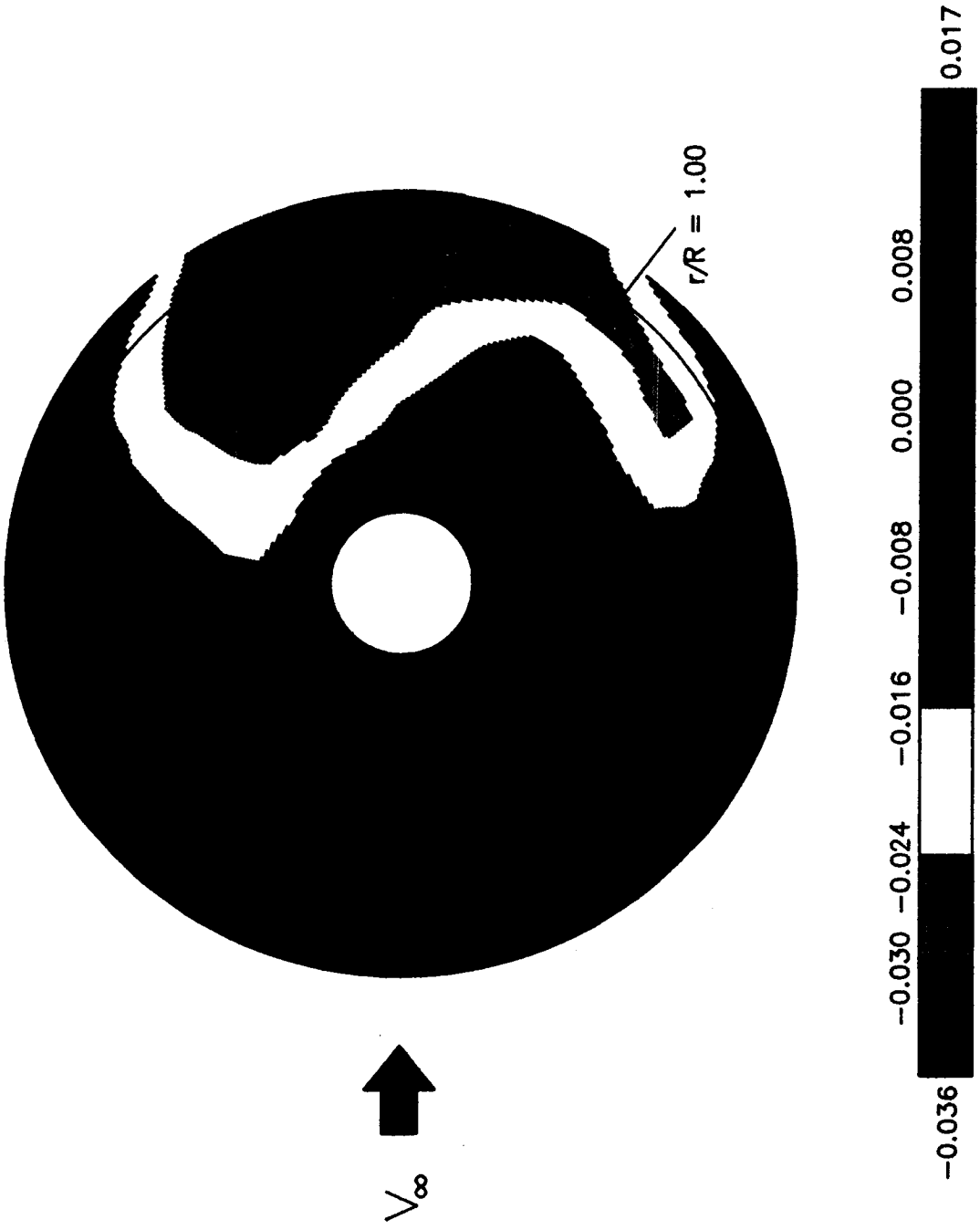

Figure 12.– Contour plot of mean induced inflow ratio (λ_i).

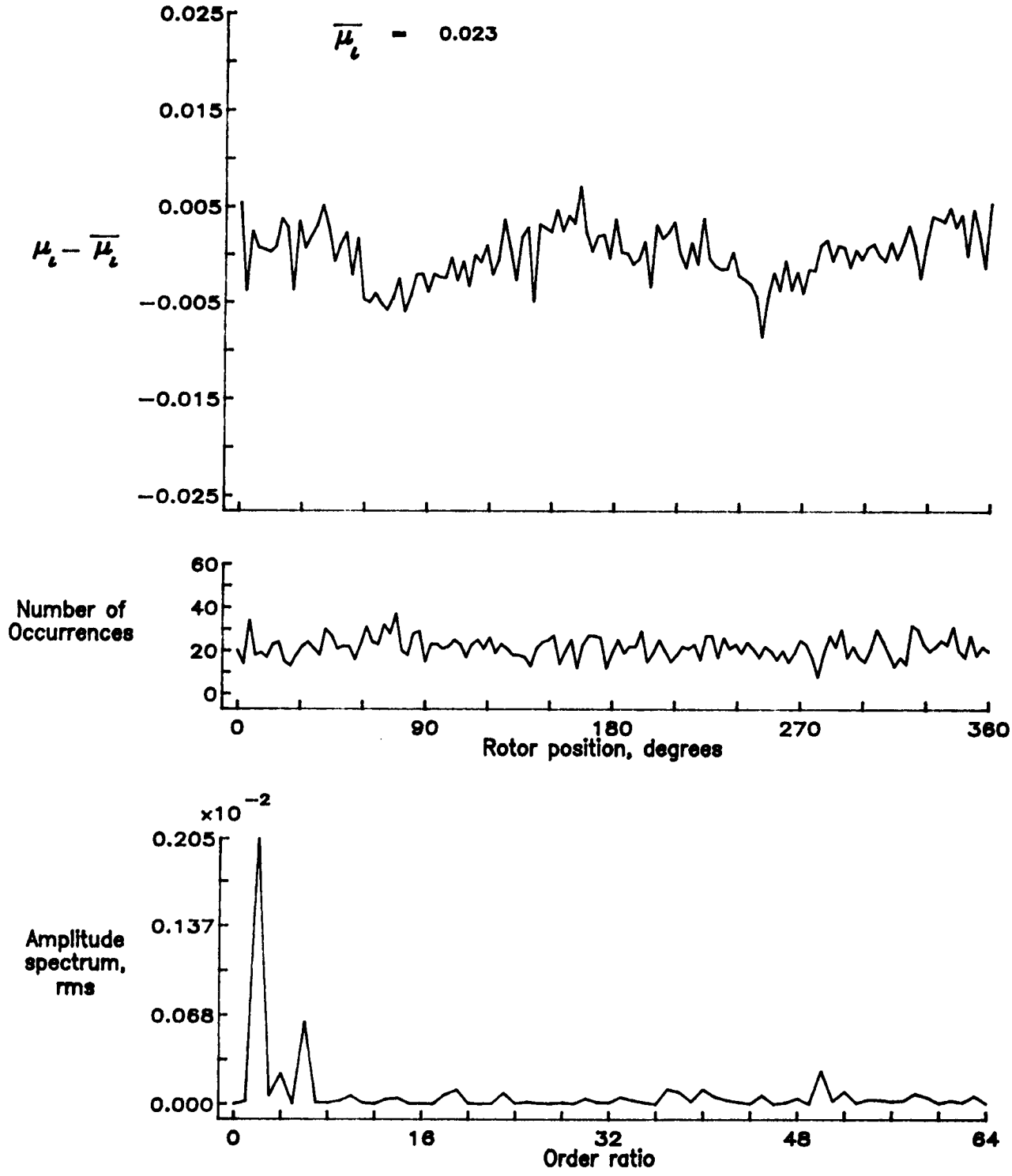

Figure 13.– Induced inflow velocity measured at 0 degrees and r/R of 0.20.

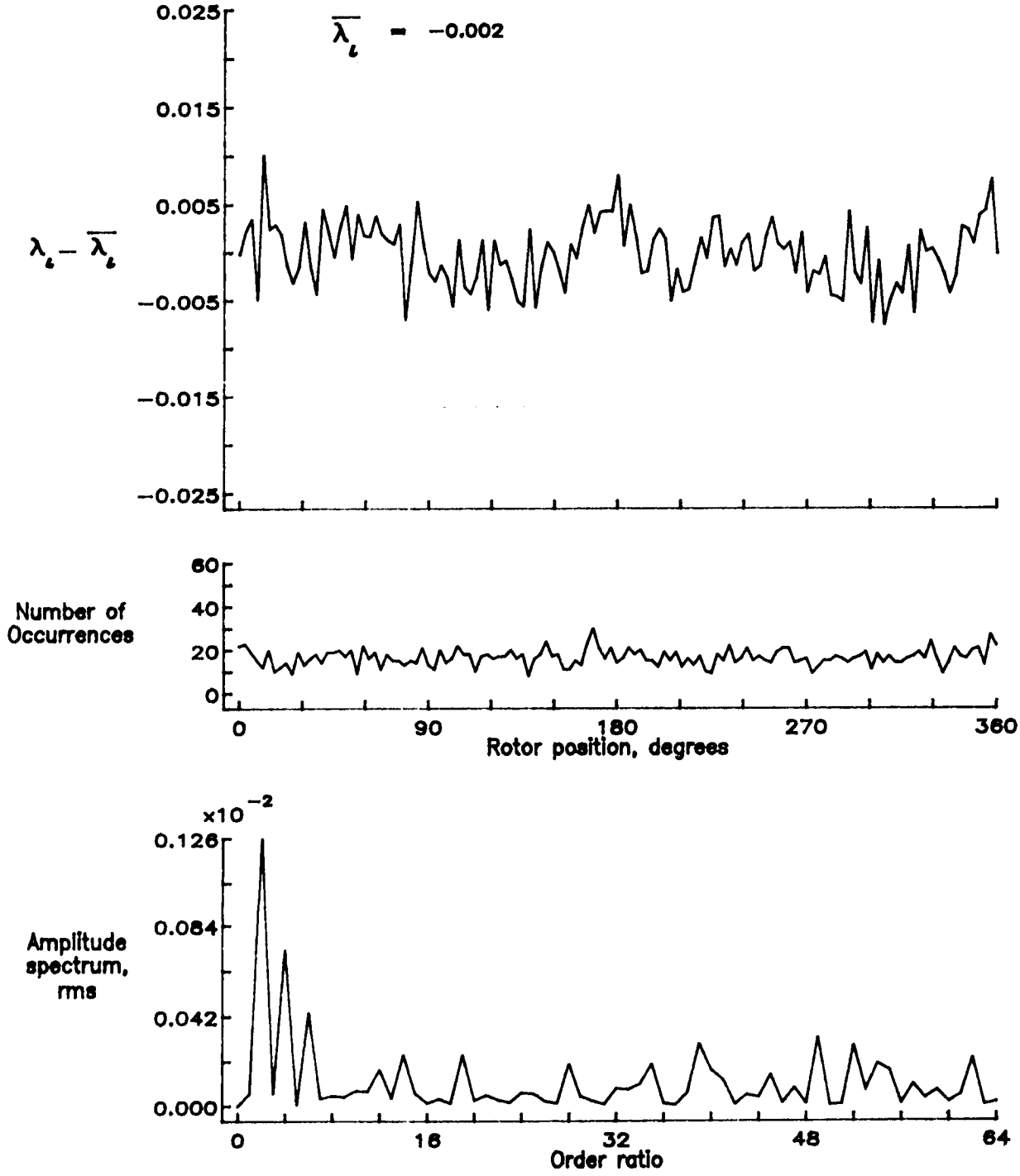

Figure 13.– Concluded.

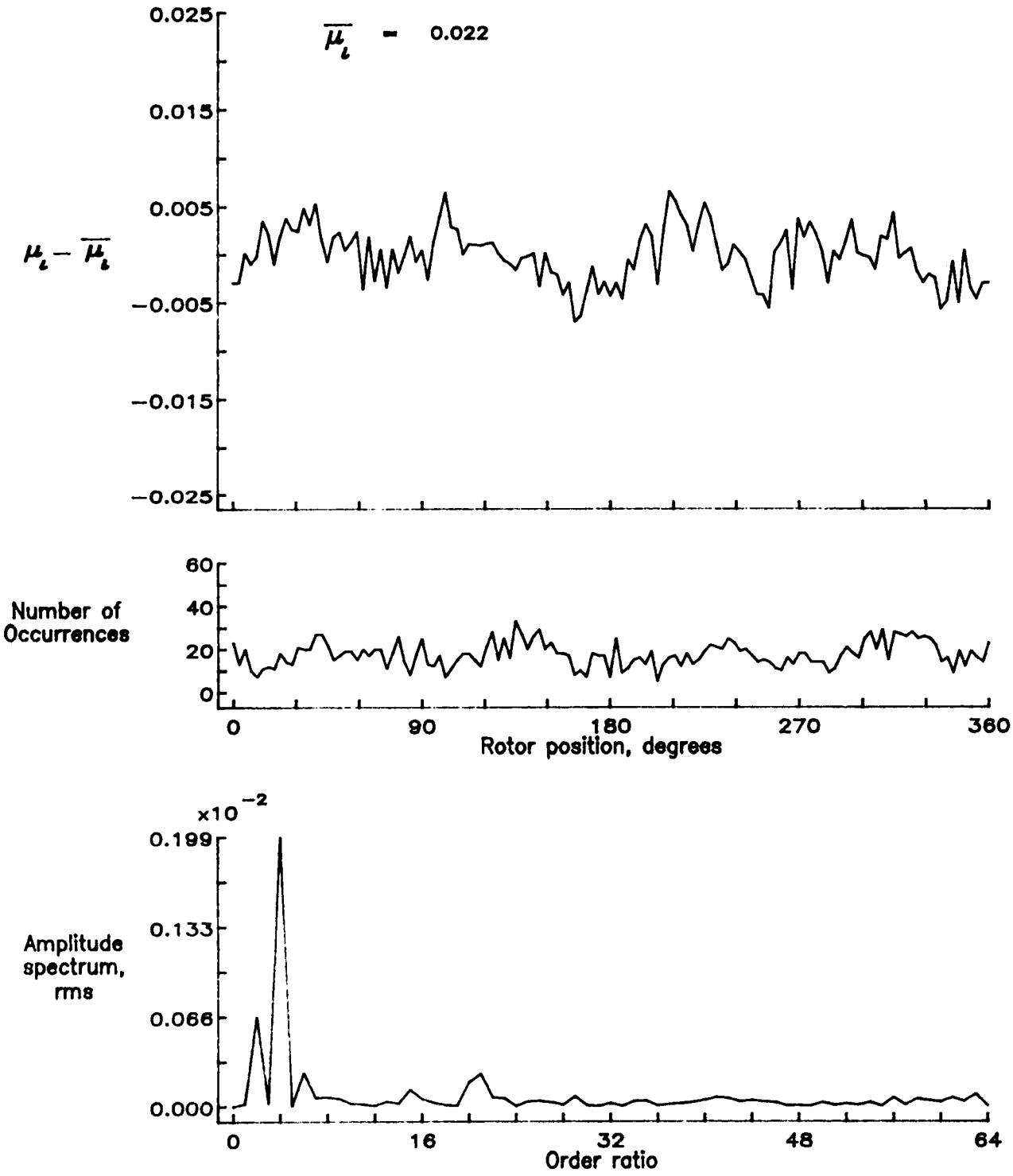

Figure 14.– Induced inflow velocity measured at 0 degrees and r/R of 0.40.

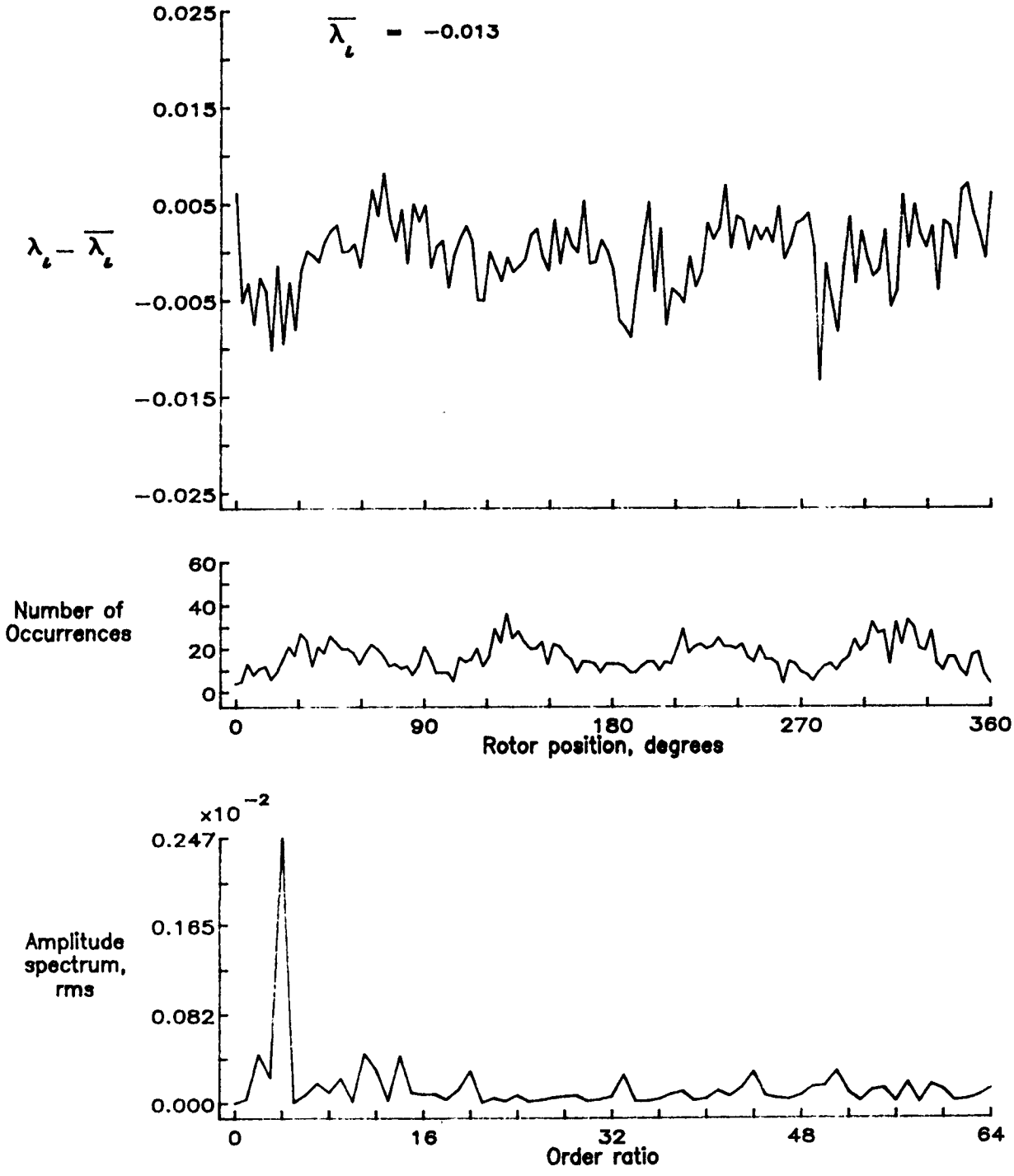

Figure 14.– Concluded.

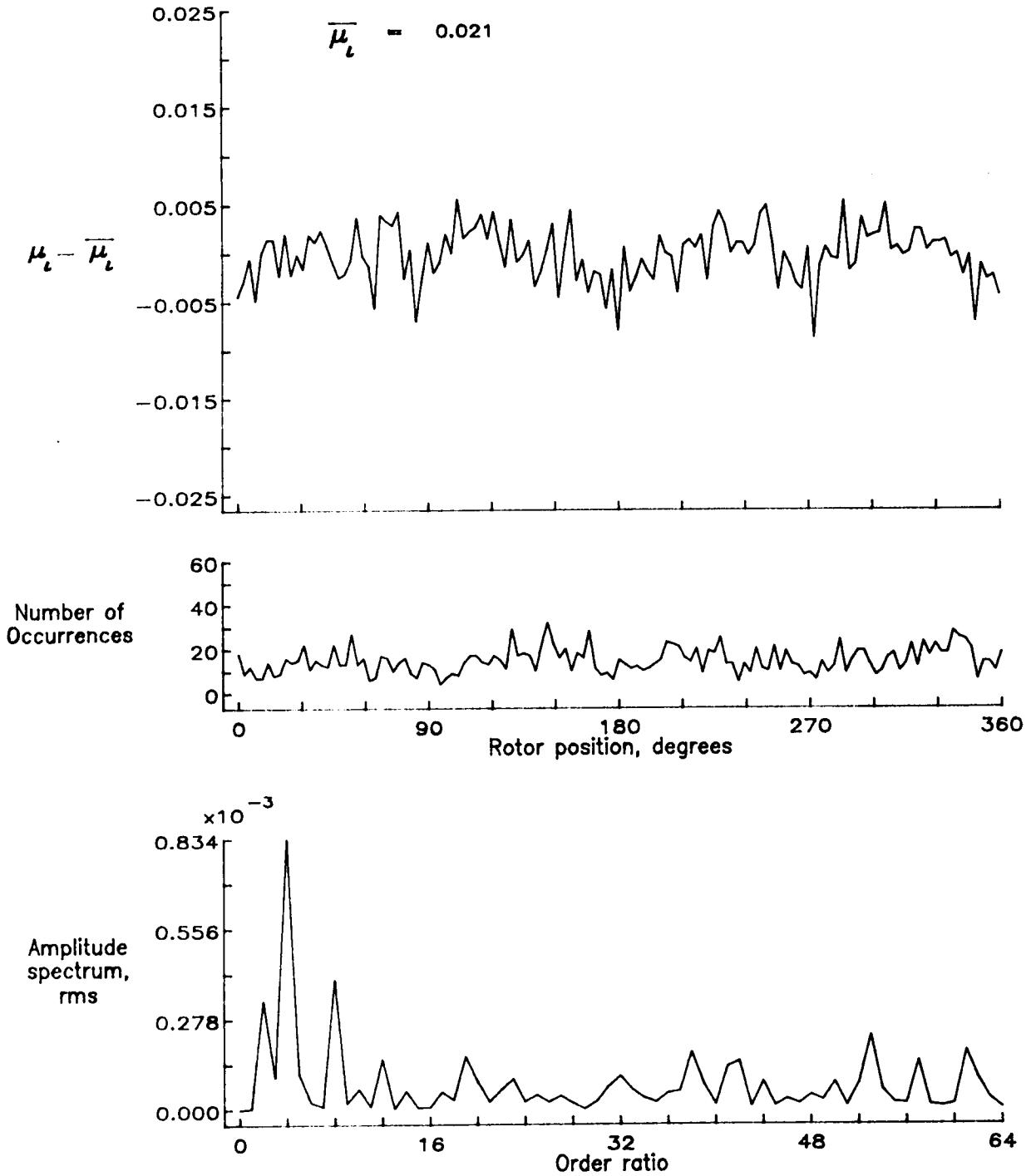

Figure 15.– Induced inflow velocity measured at 0 degrees and r/R of 0.50.

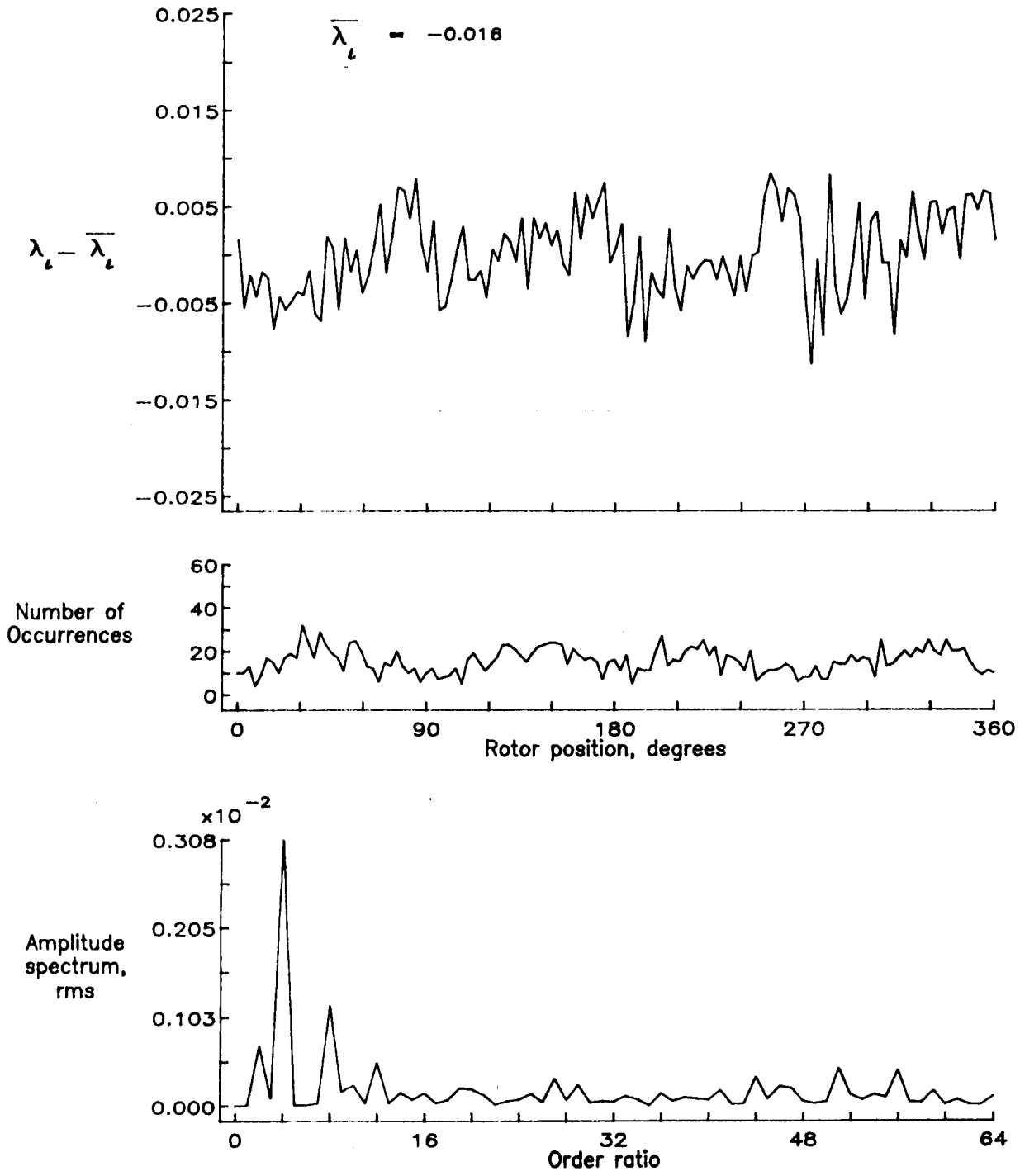

Figure 15.– Concluded.

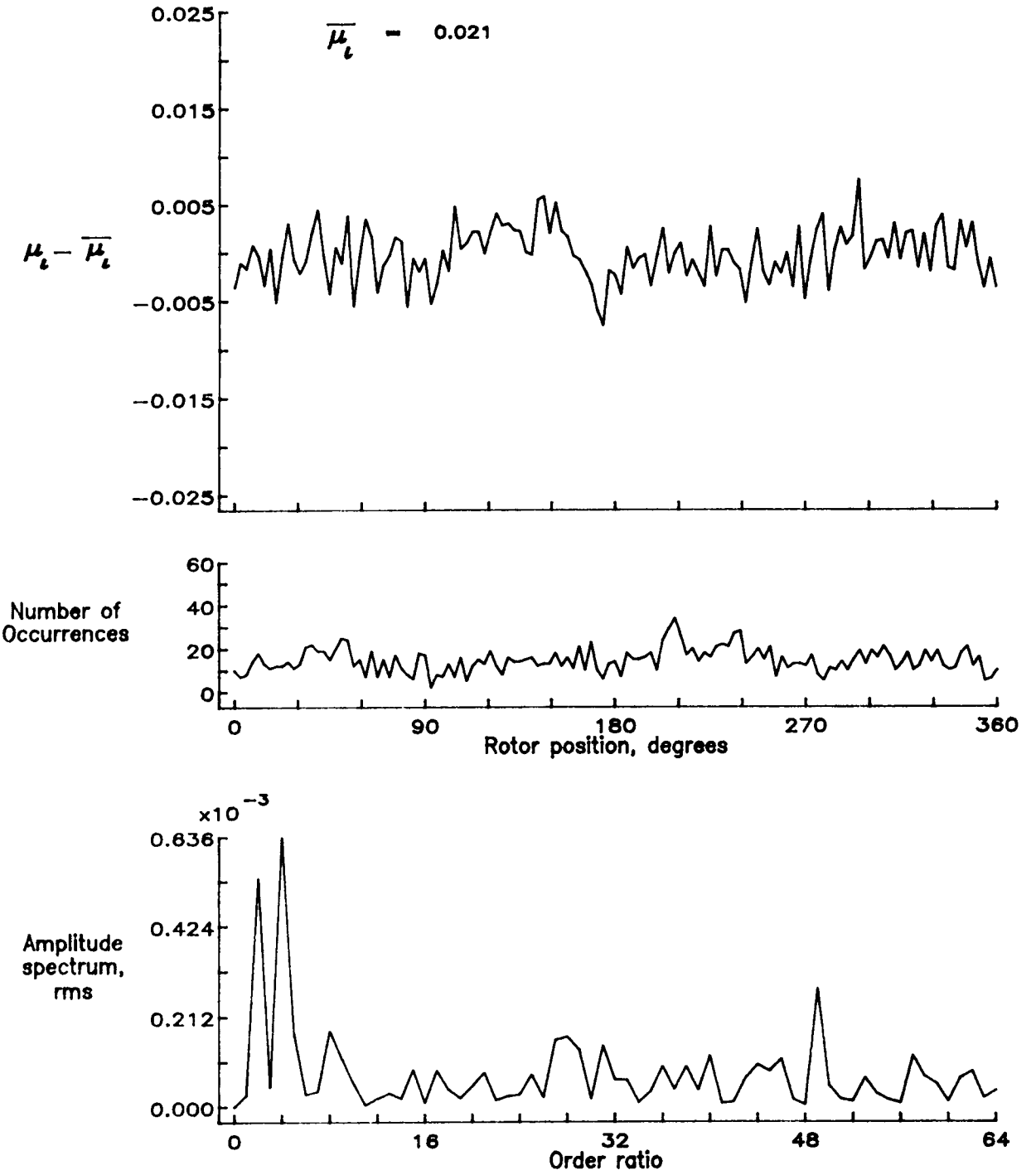

Figure 16.– Induced inflow velocity measured at 0 degrees and r/R of 0.60.

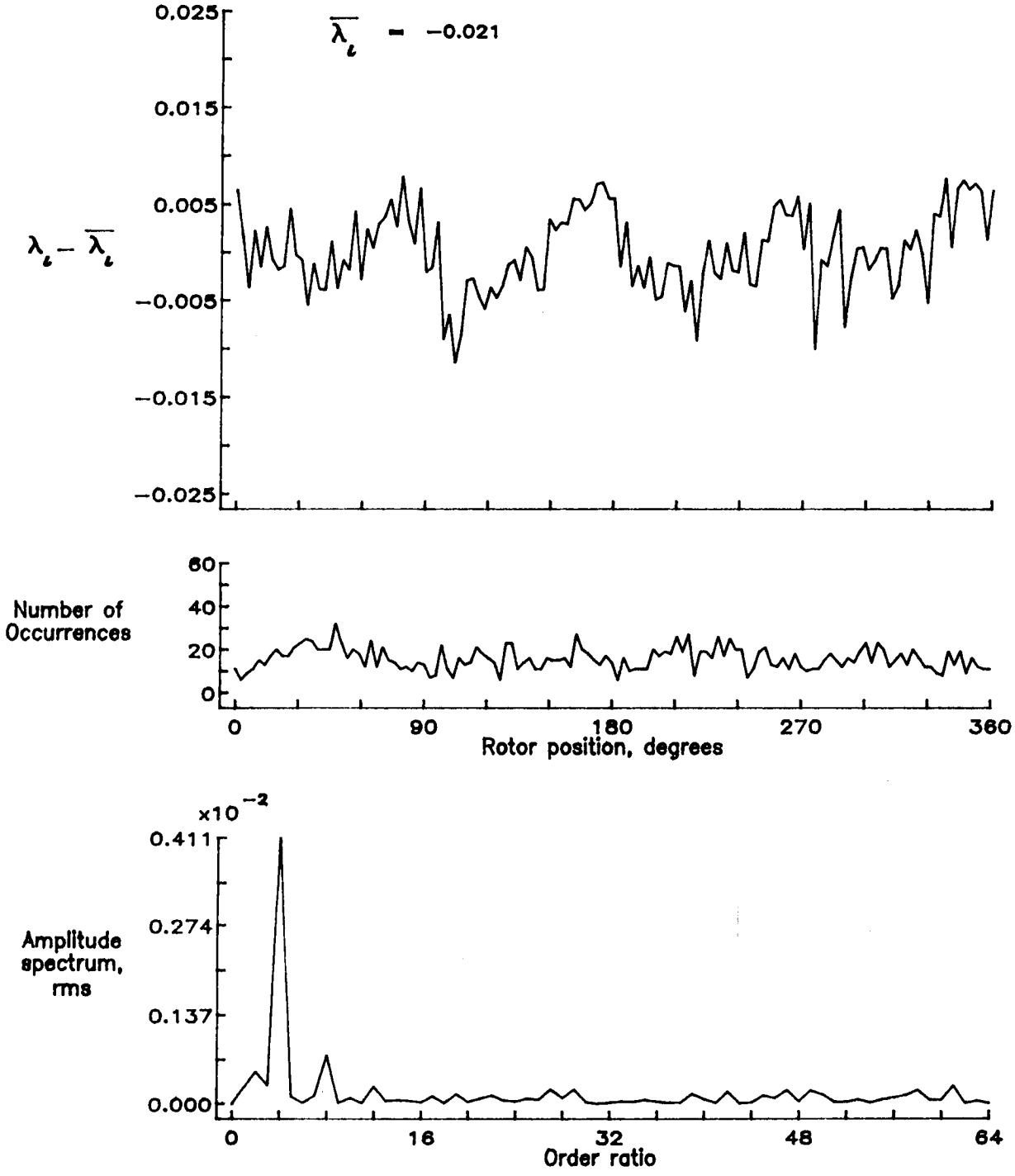

Figure 16.– Concluded.

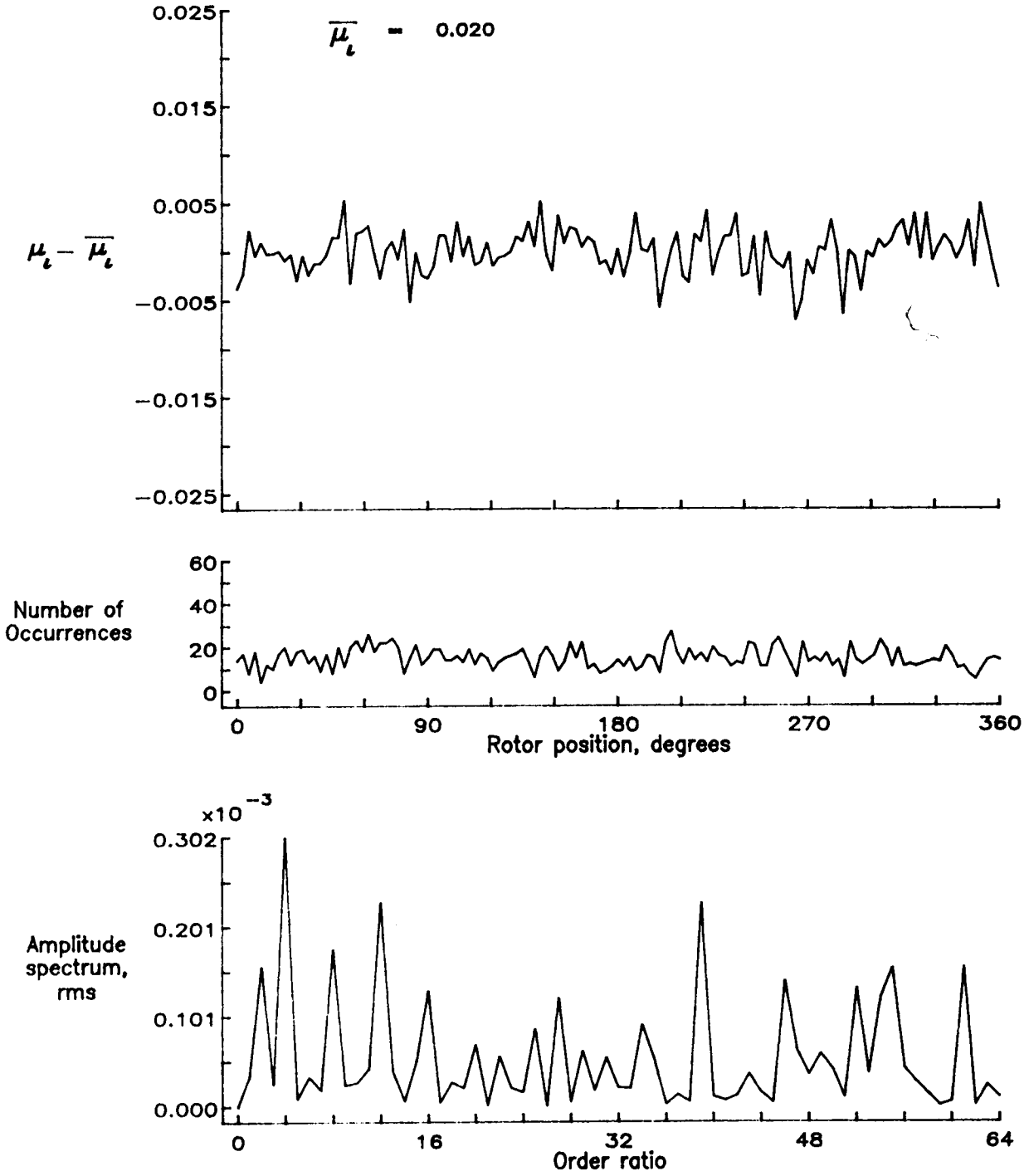

Figure 17.– Induced inflow velocity measured at 0 degrees and r/R of 0.70.

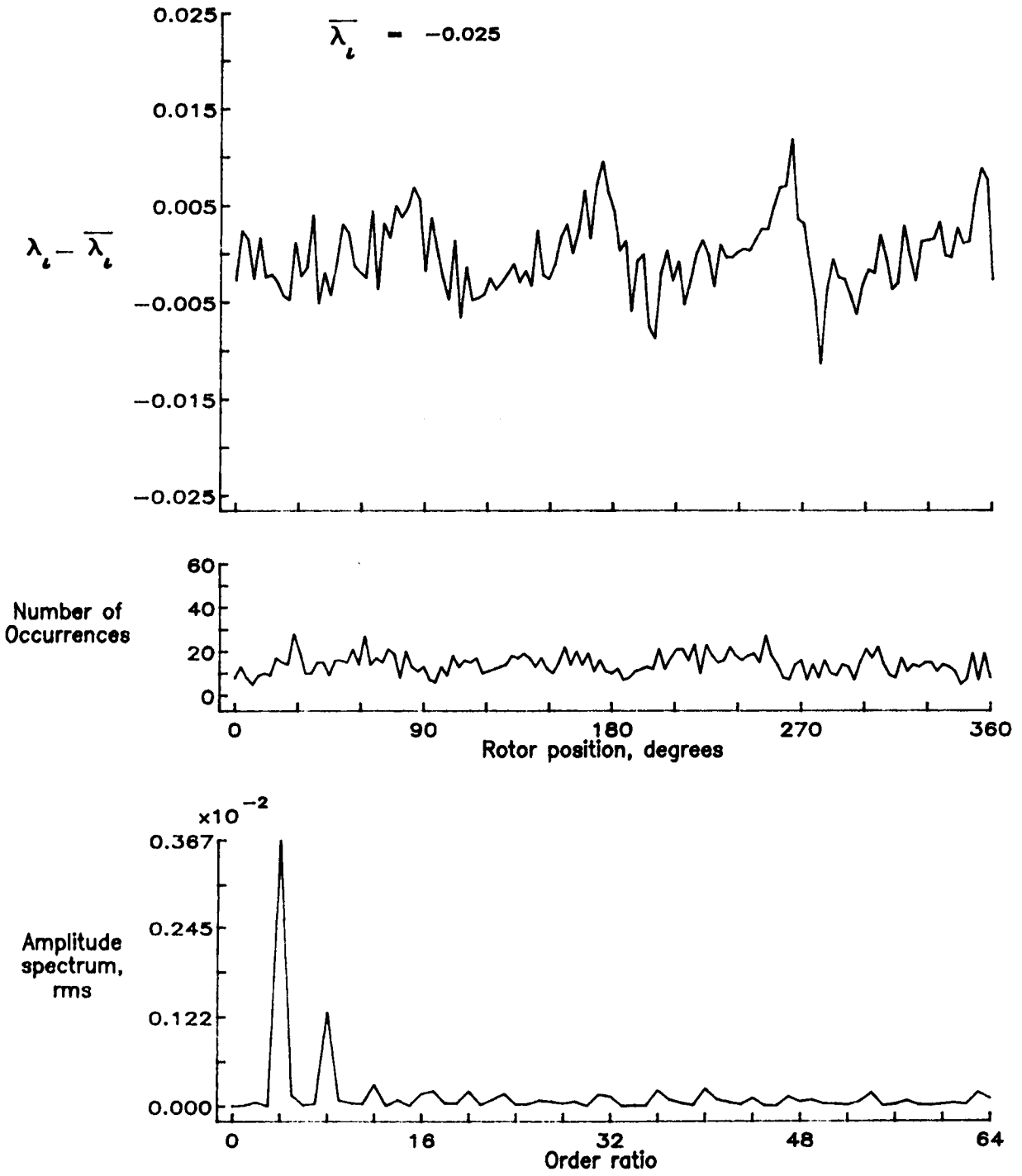

Figure 17.– Concluded.

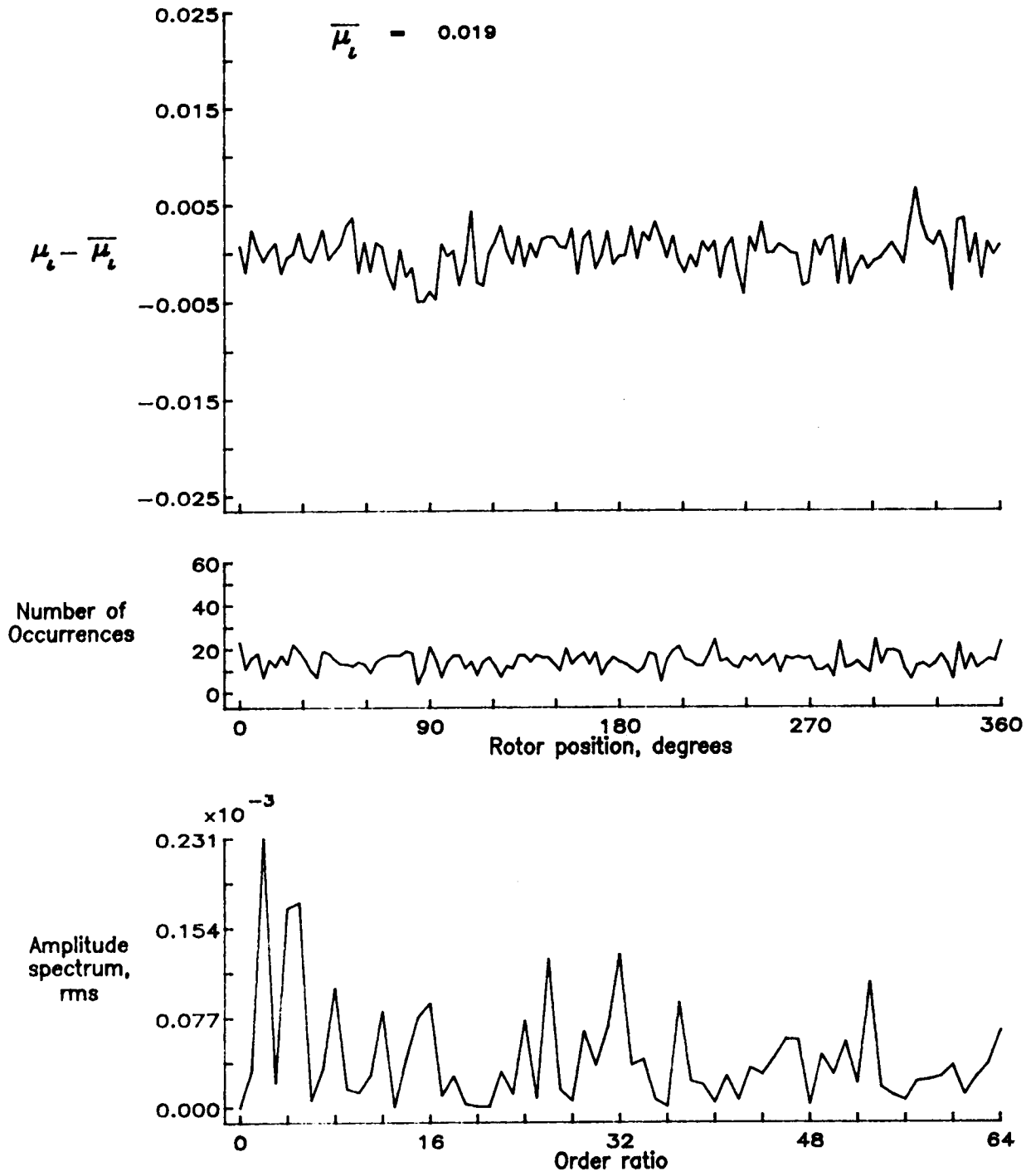

Figure 18.– Induced inflow velocity measured at 0 degrees and r/R of 0.74.

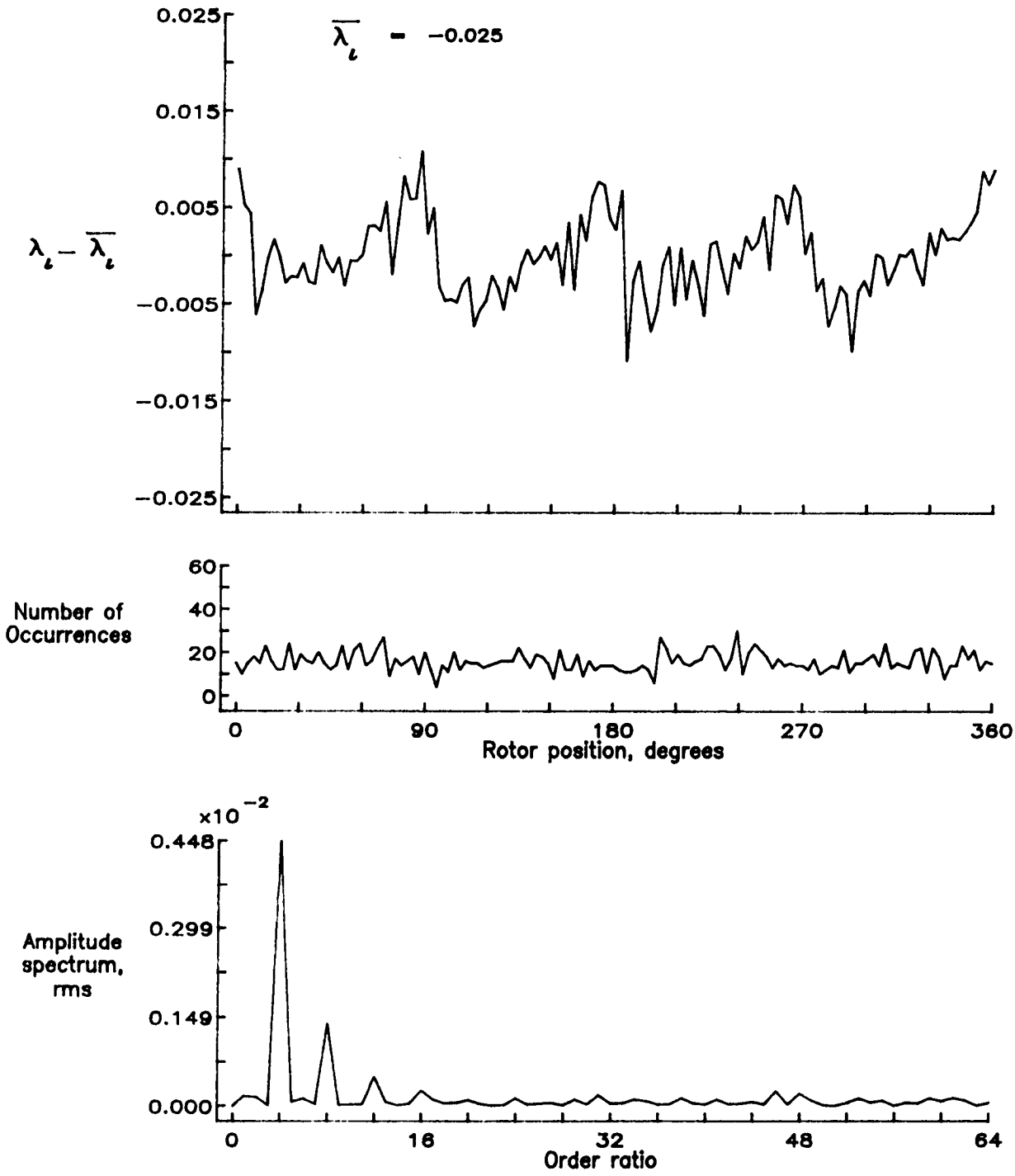

Figure 18.– Concluded.

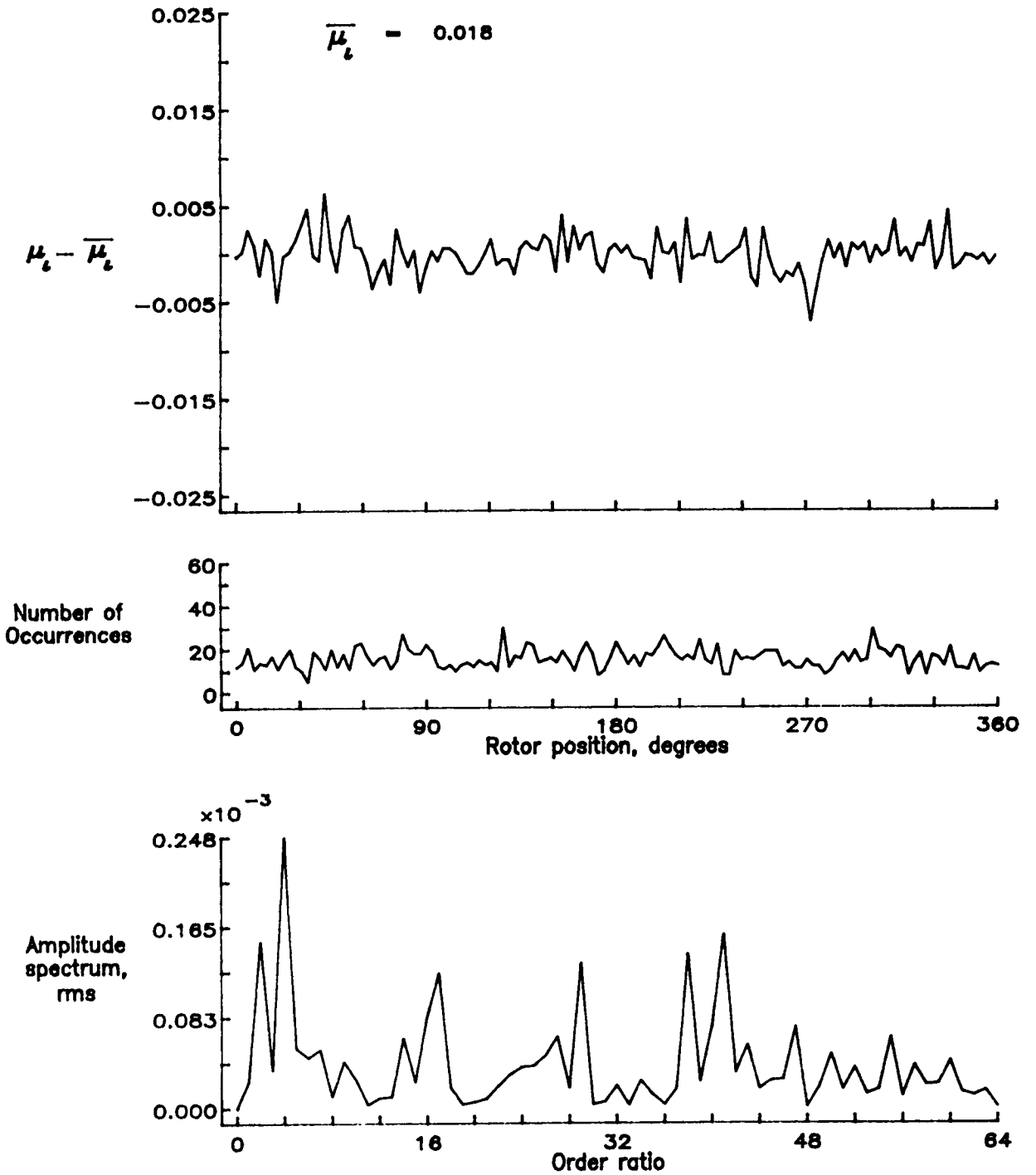

Figure 19.– Induced inflow velocity measured at 0 degrees and r/R of 0.78.

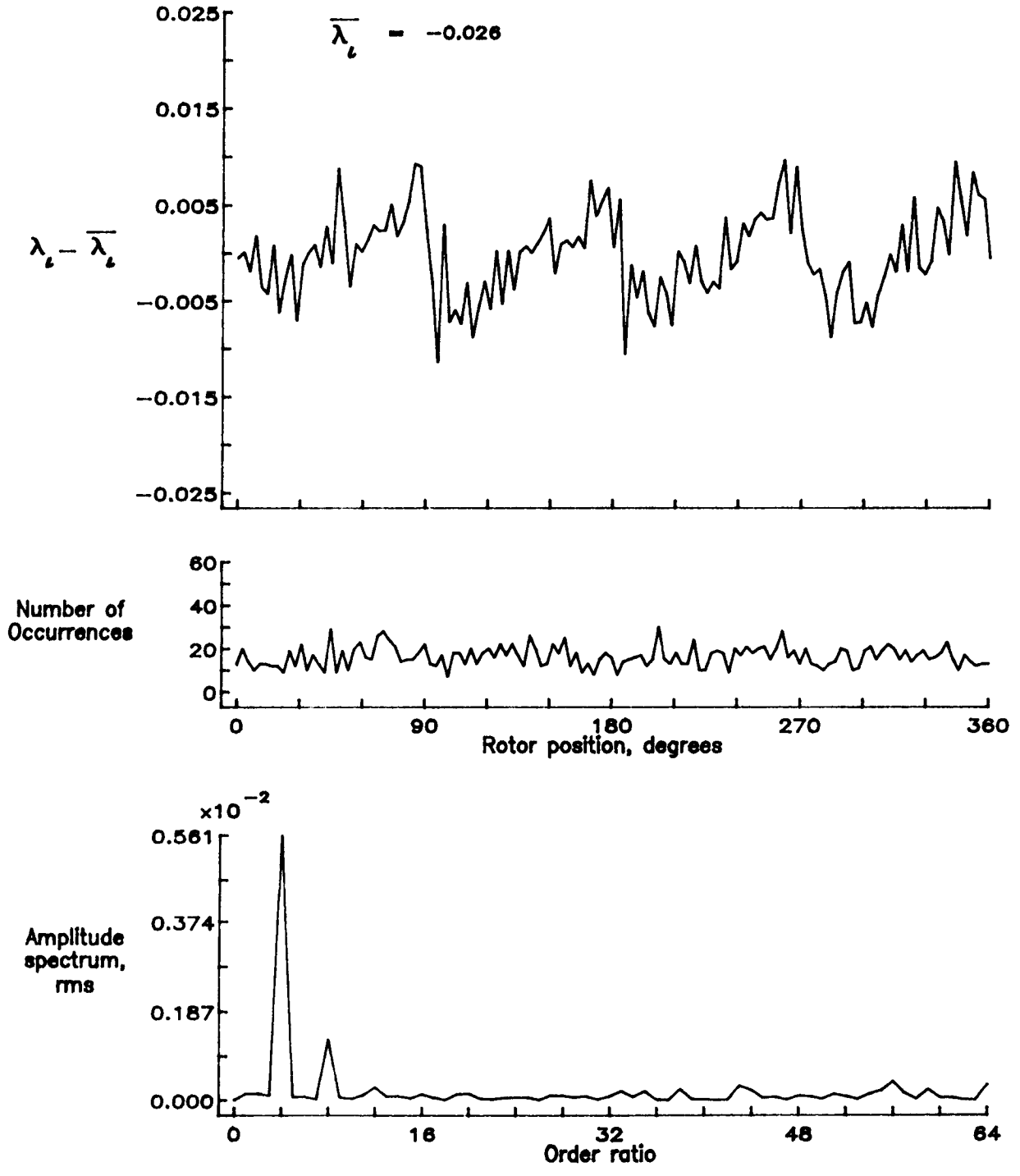

Figure 19.– Concluded.

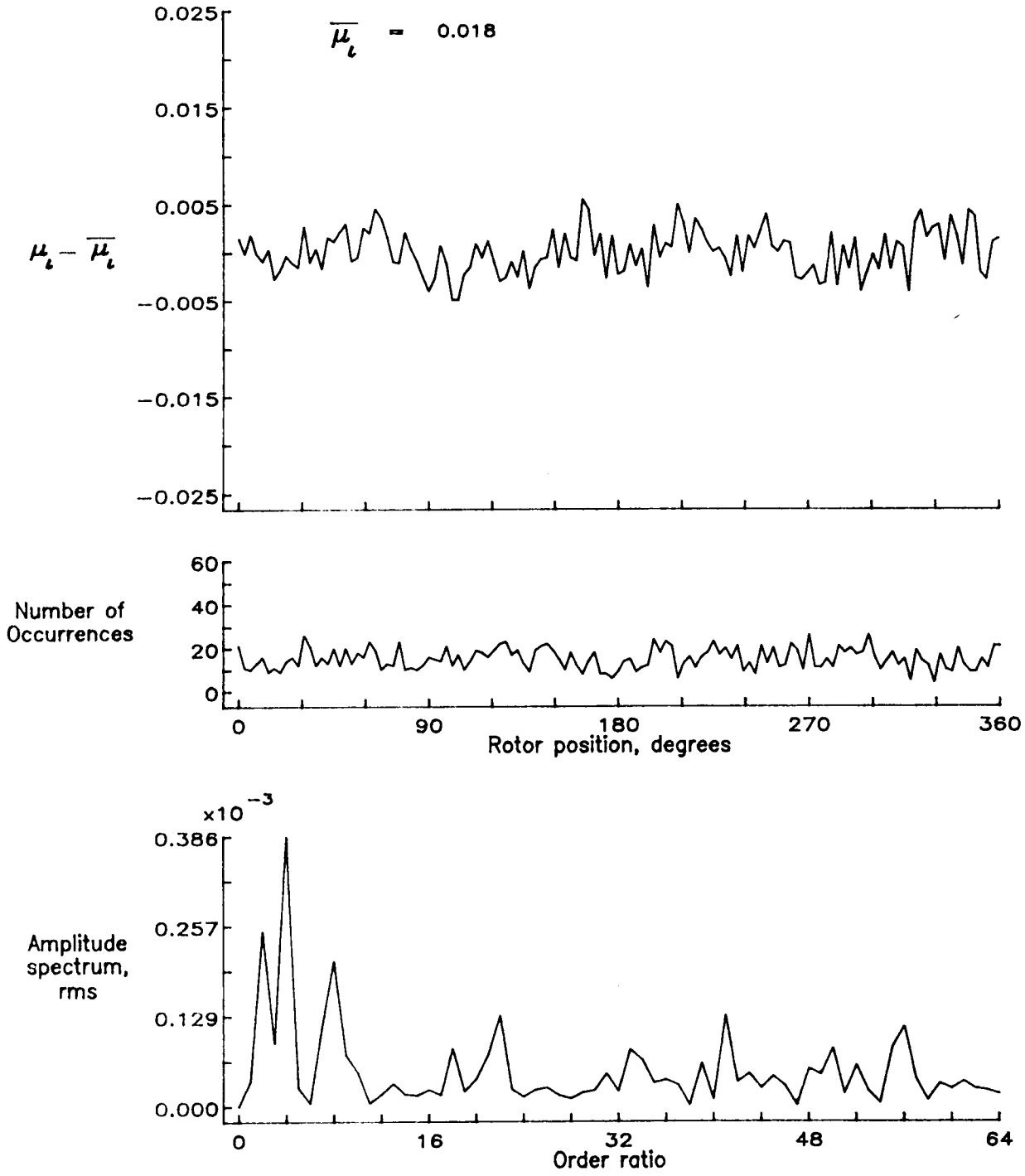

Figure 20.– Induced inflow velocity measured at 0 degrees and r/R of 0.82.

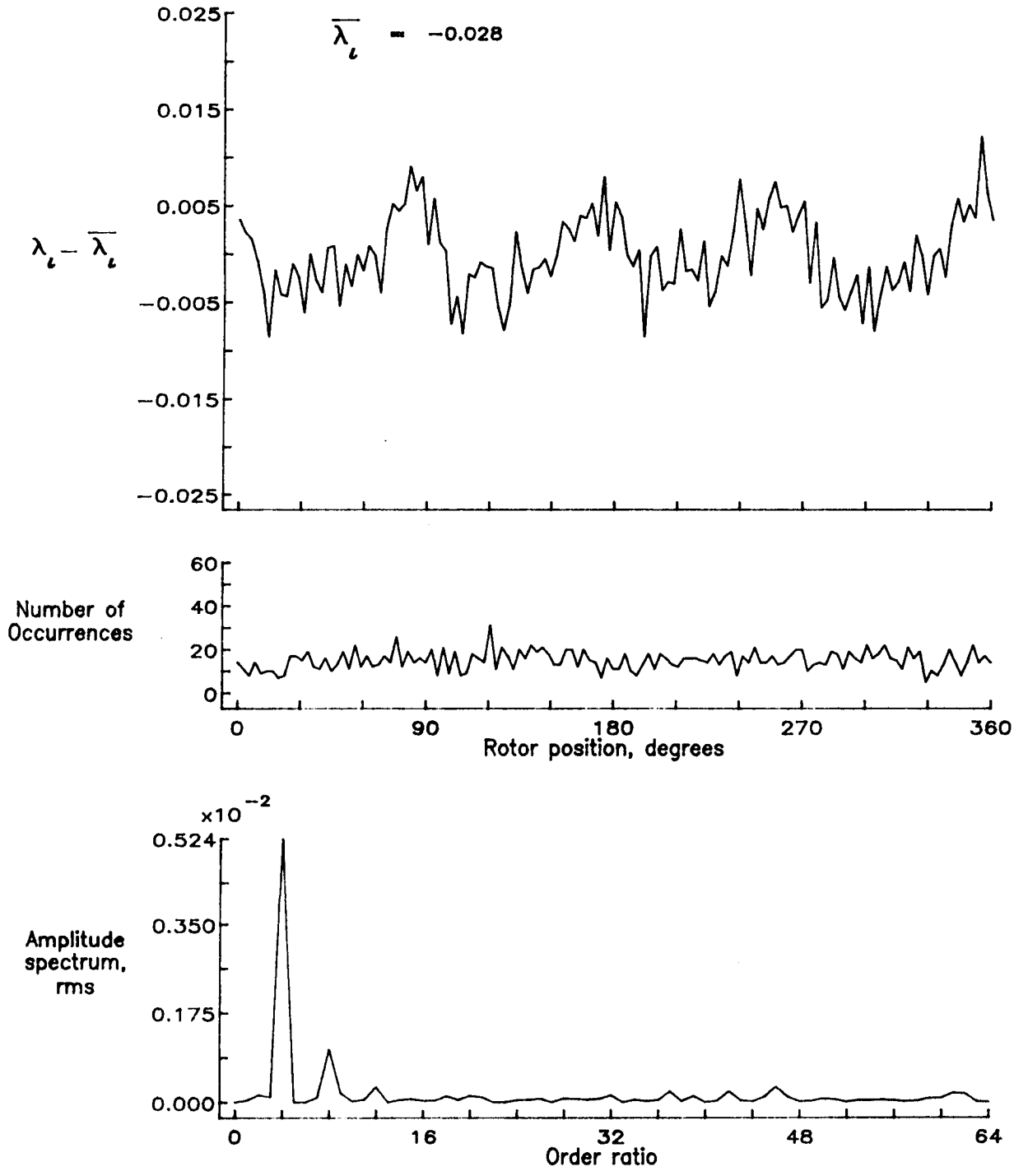

Figure 20.– Concluded.

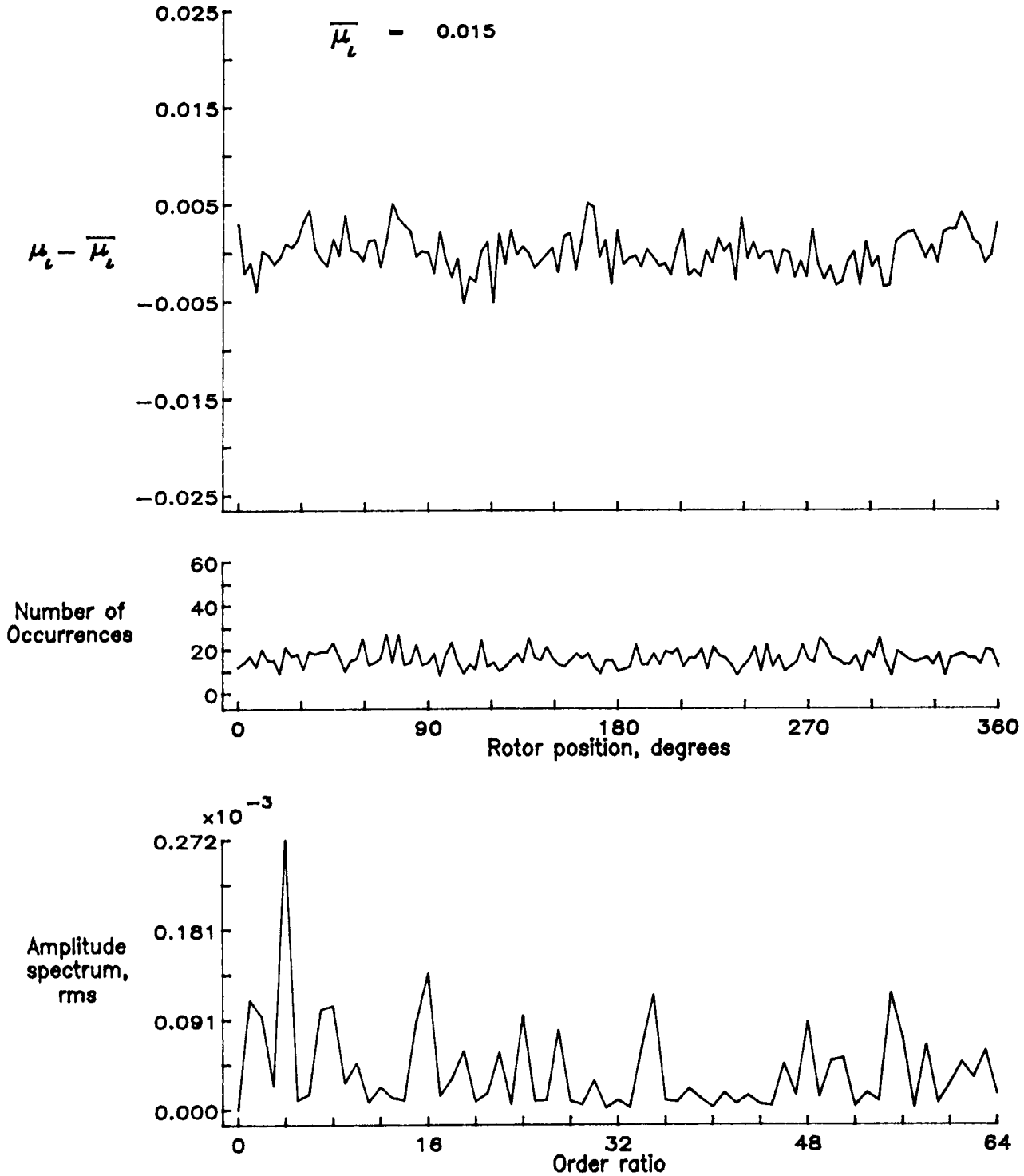

Figure 21.– Induced inflow velocity measured at 0 degrees and r/R of 0.86.

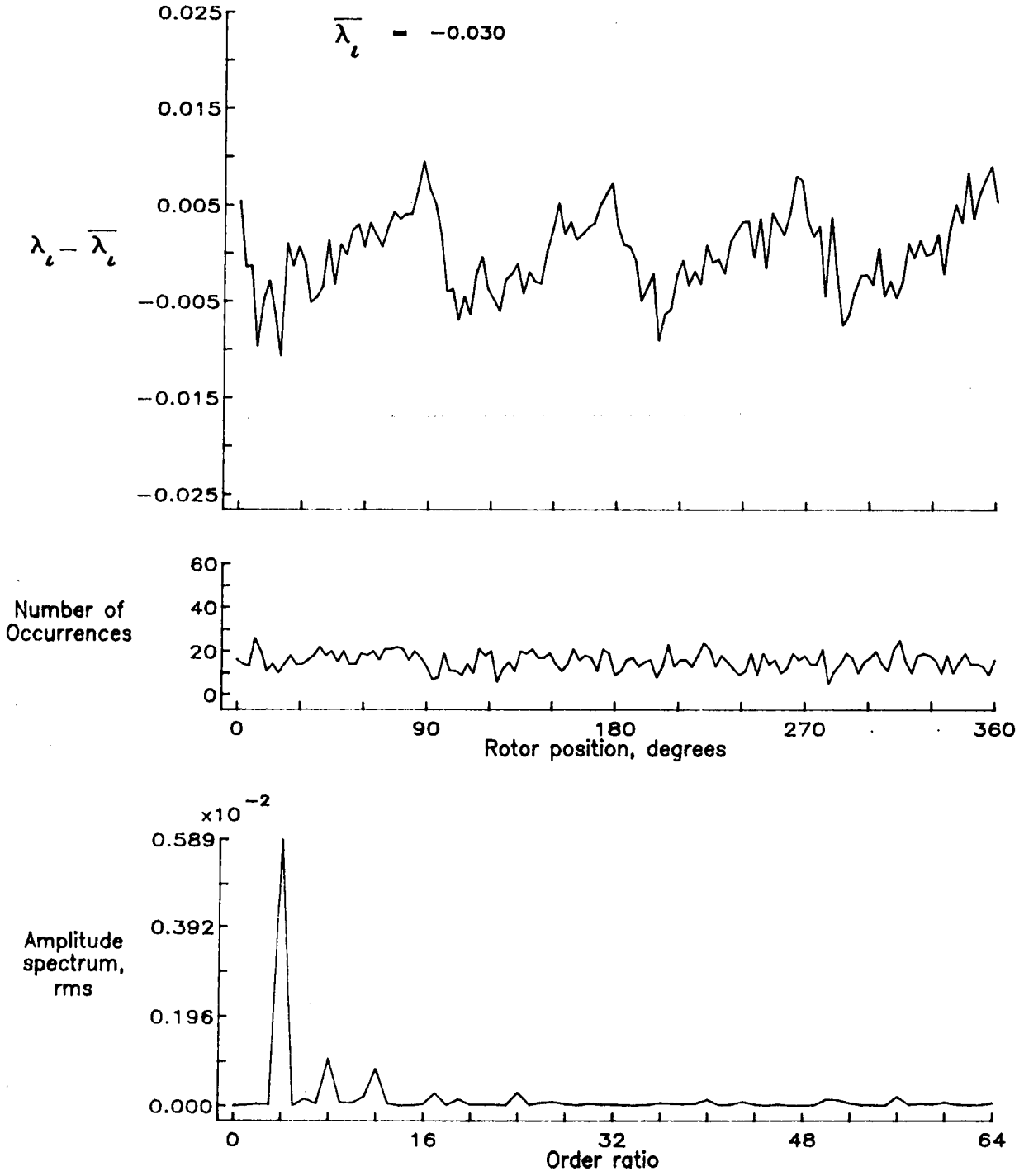

Figure 21.– Concluded.

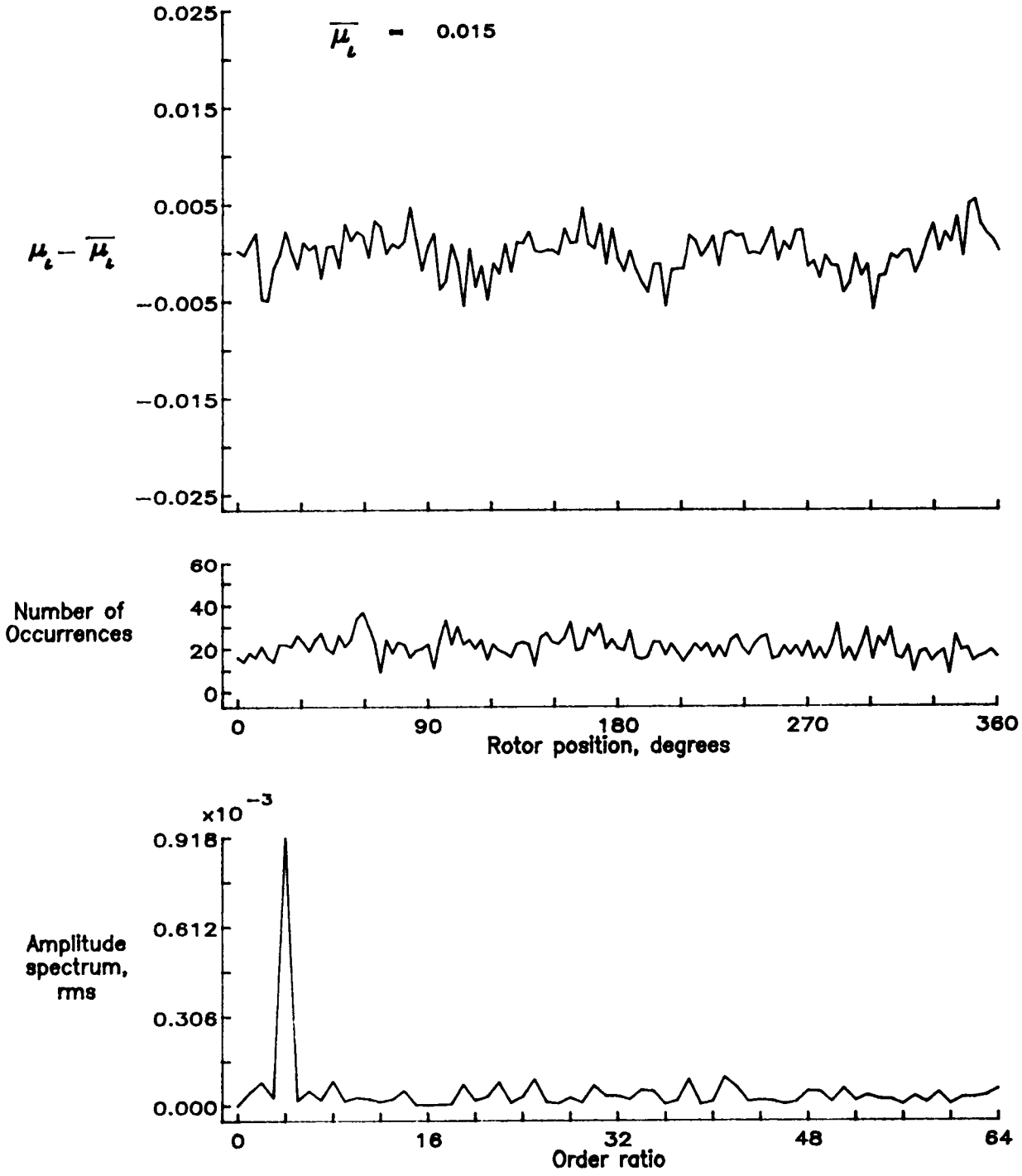

Figure 22.– Induced inflow velocity measured at 0 degrees and r/R of 0.90.

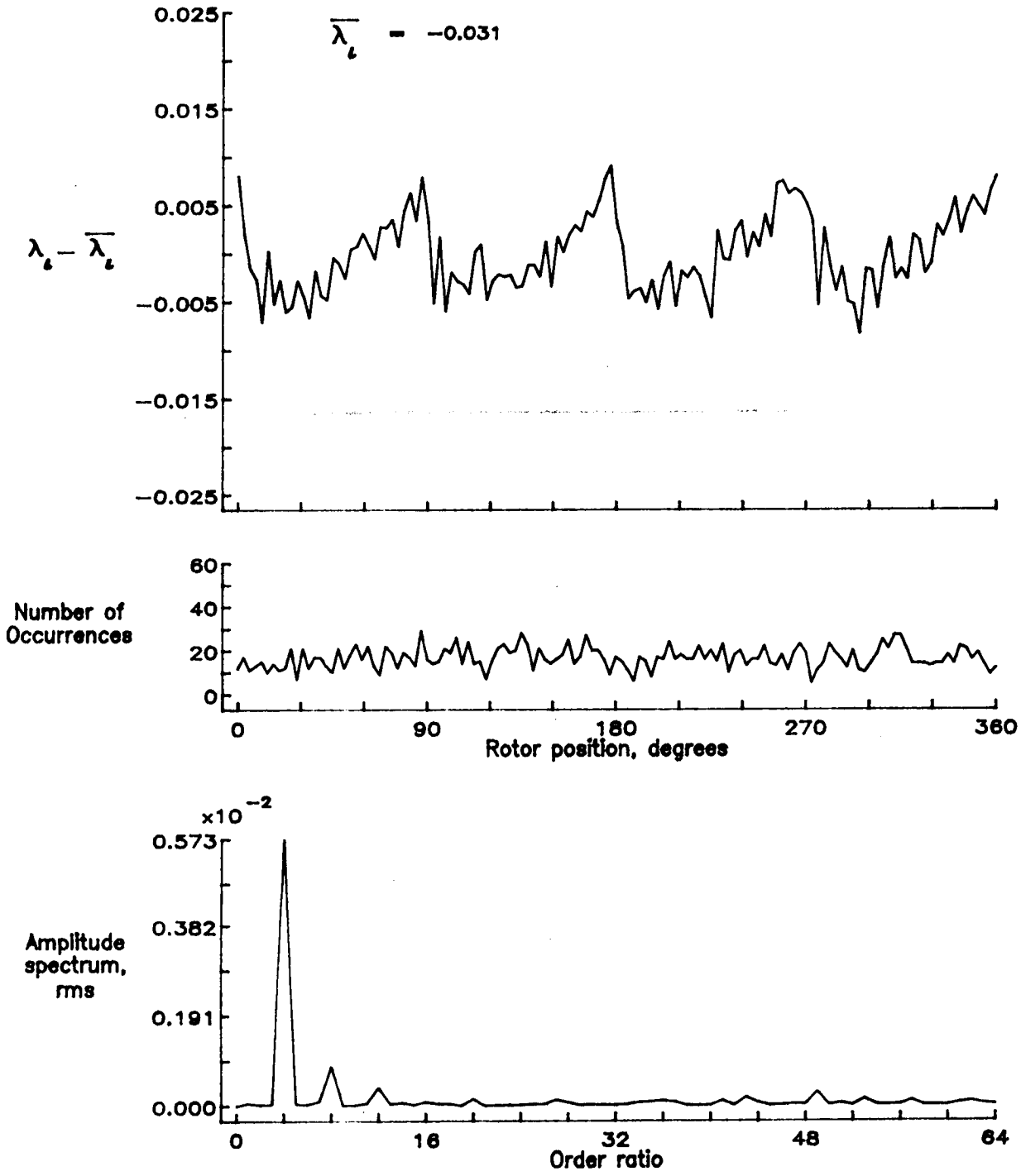

Figure 22.– Concluded.

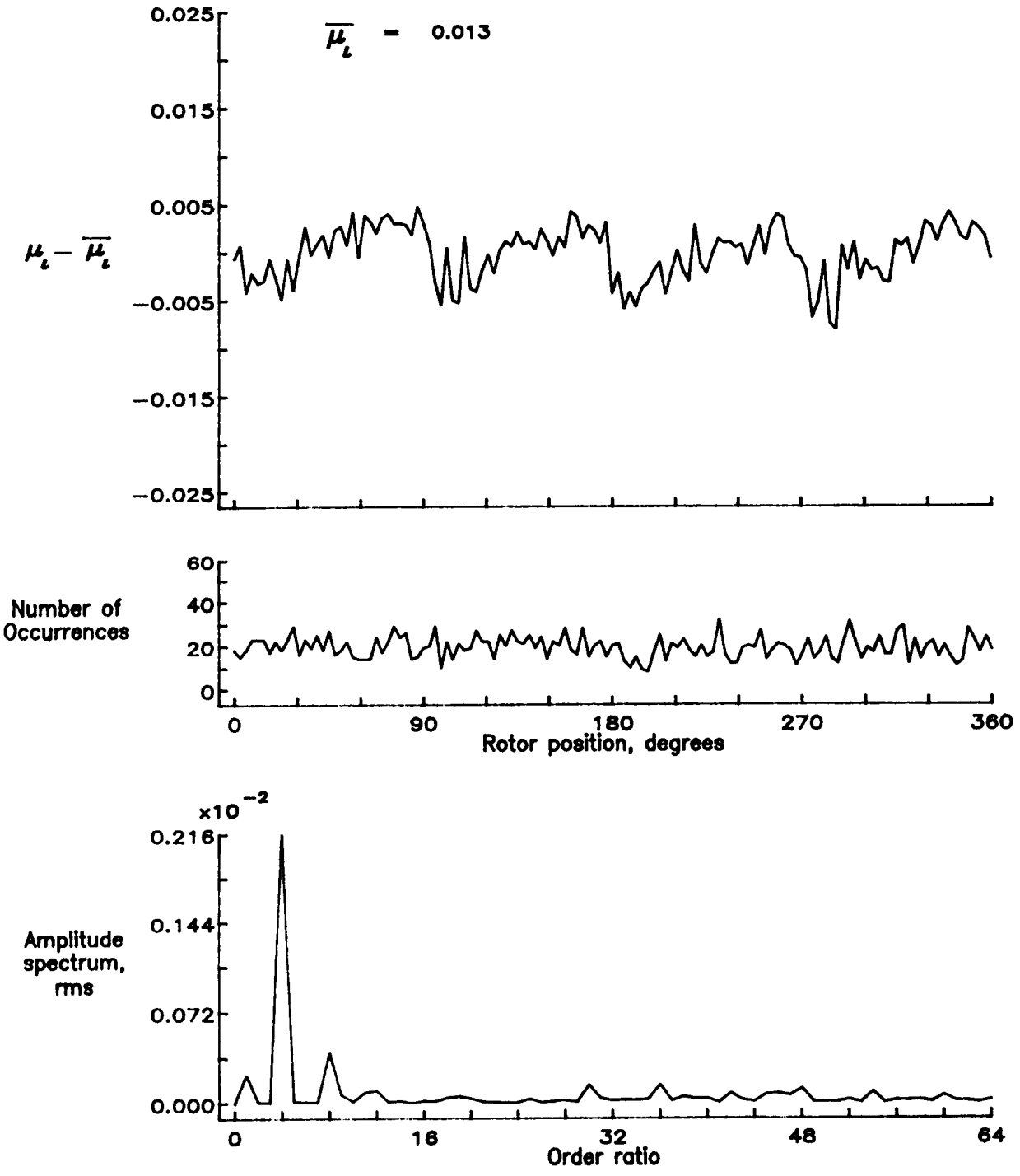

Figure 23.– Induced inflow velocity measured at 0 degrees and r/R of 0.94.

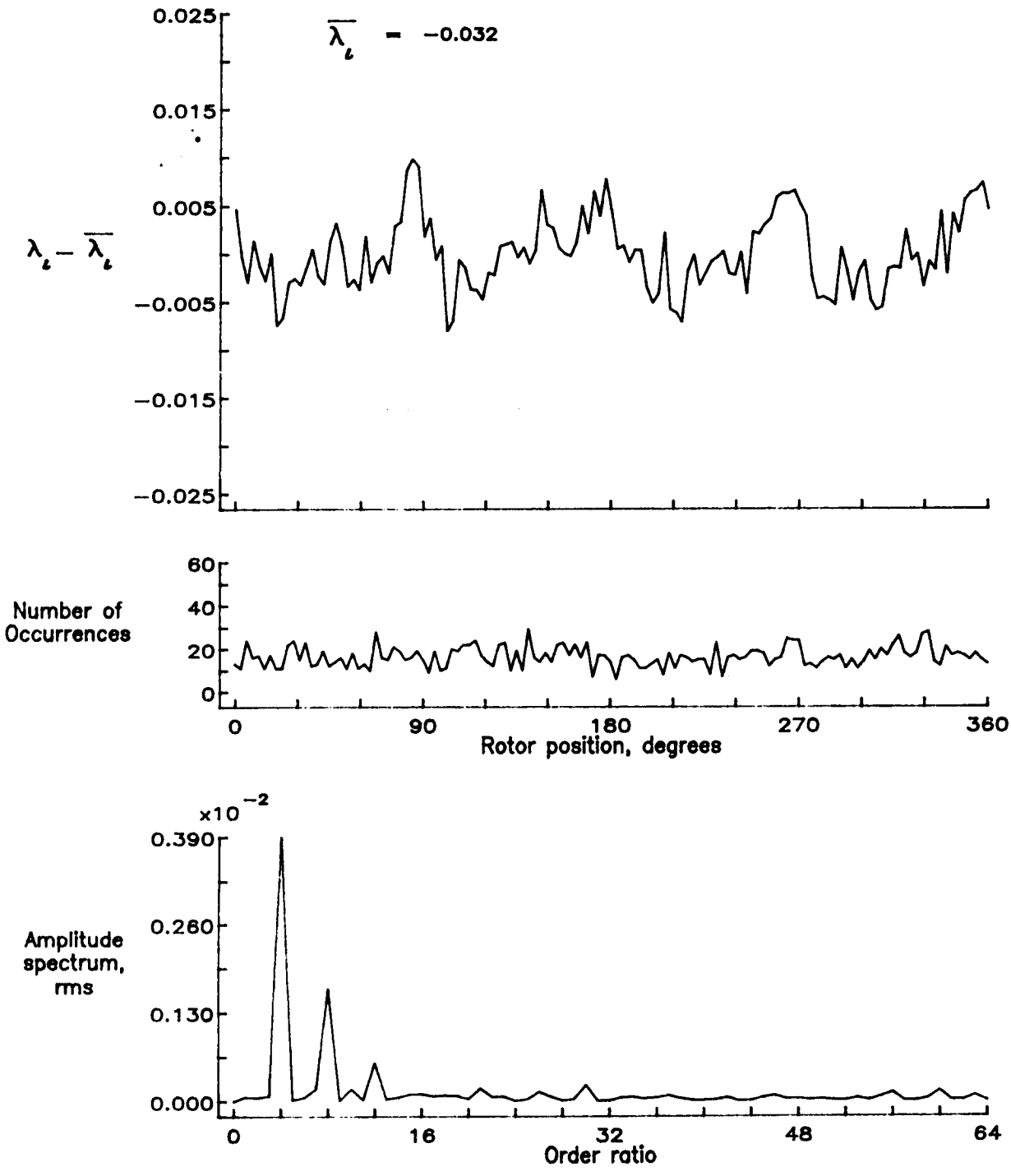

Figure 23.– Concluded.

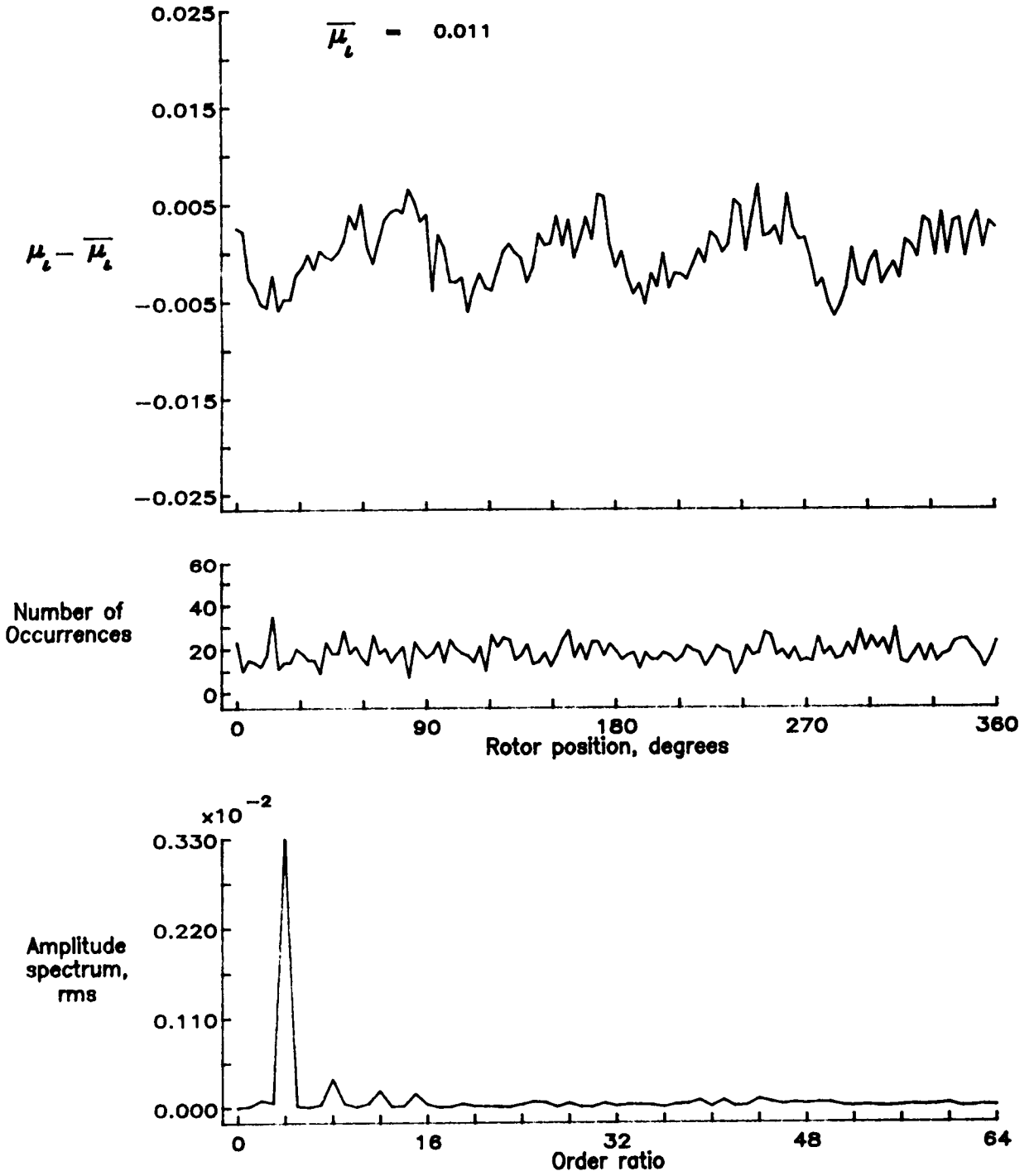

Figure 24.– Induced inflow velocity measured at 0 degrees and r/R of 0.98.

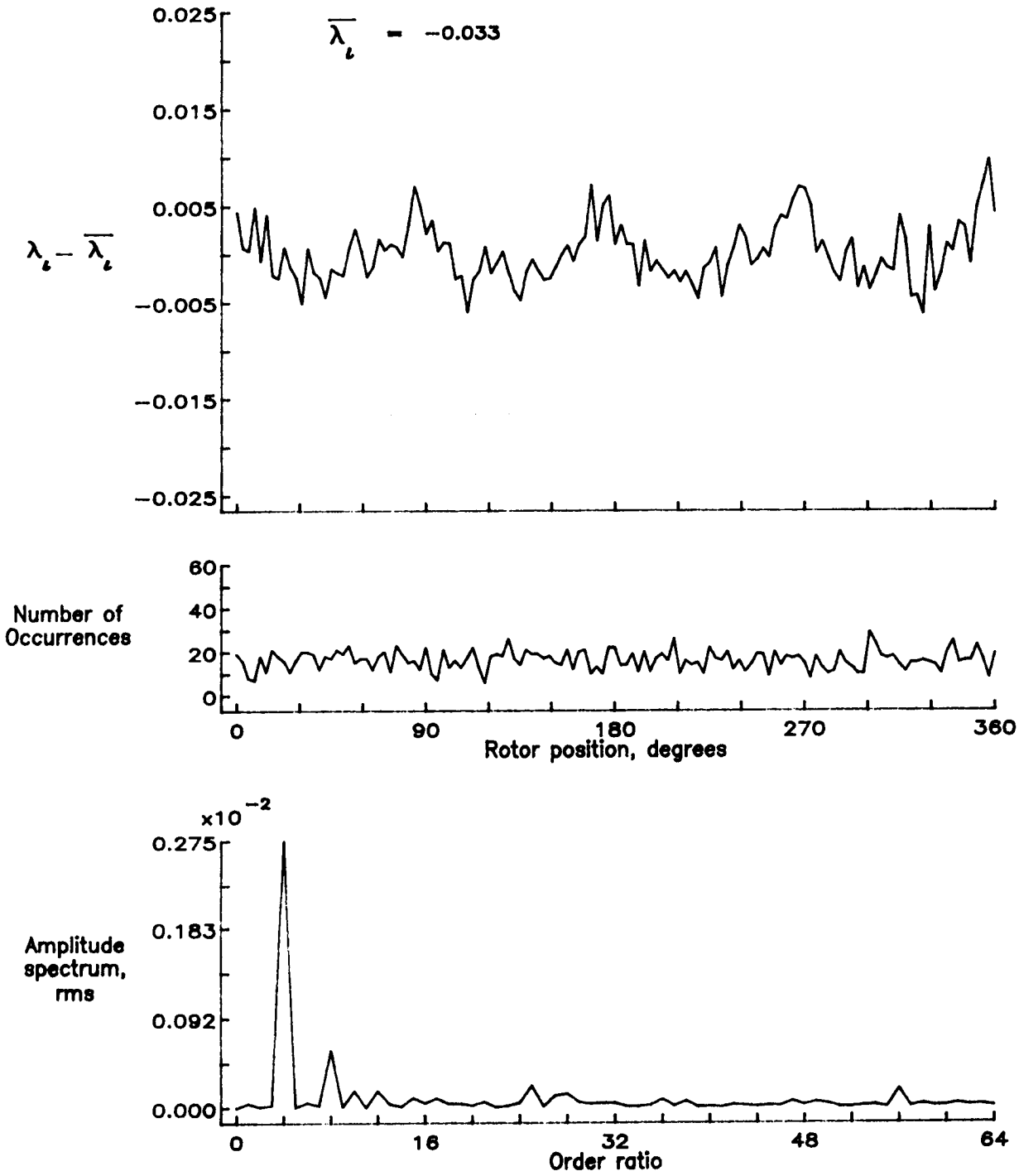

Figure 24.– Concluded.

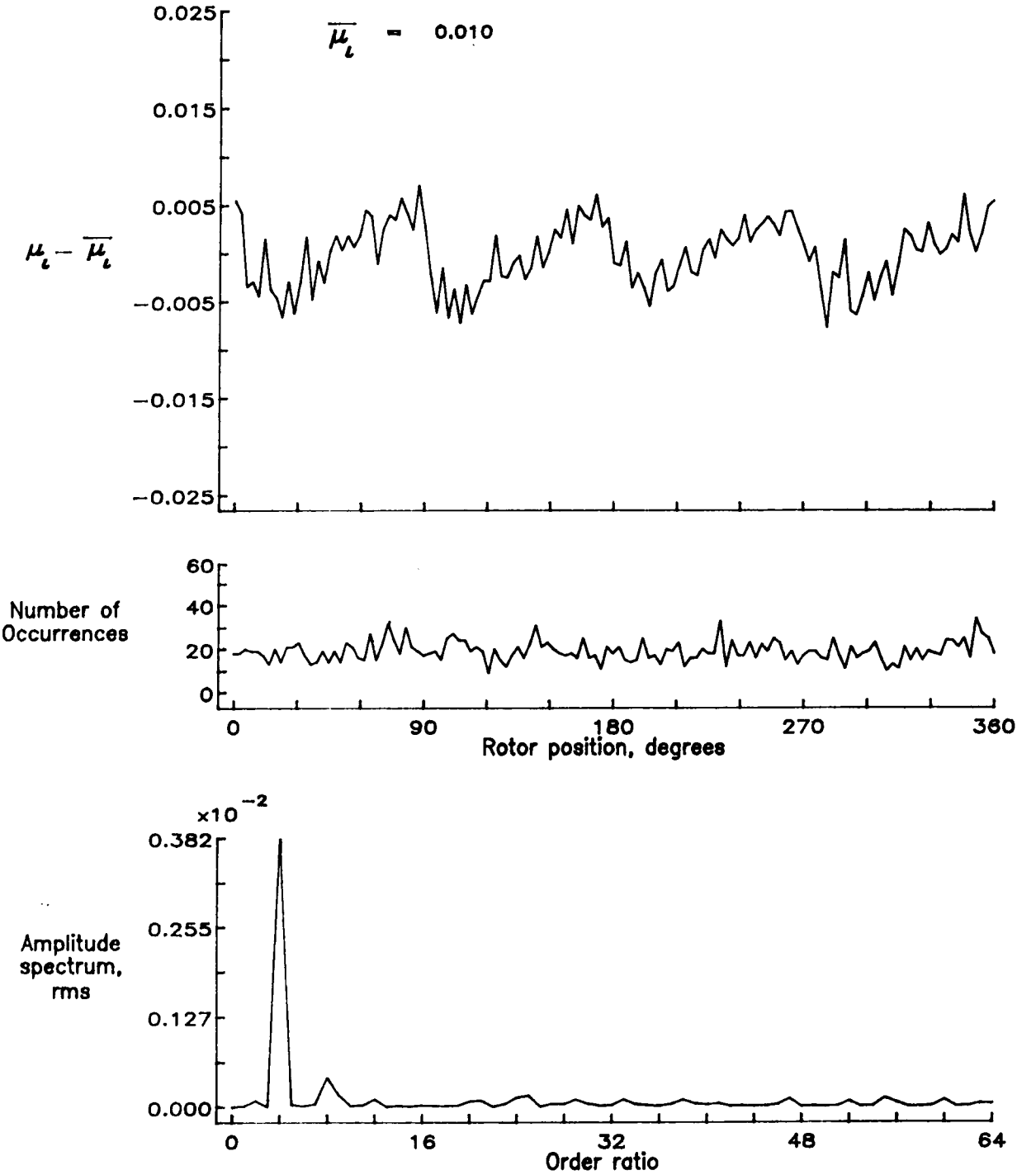

Figure 25.– Induced inflow velocity measured at 0 degrees and r/R of 1.02.

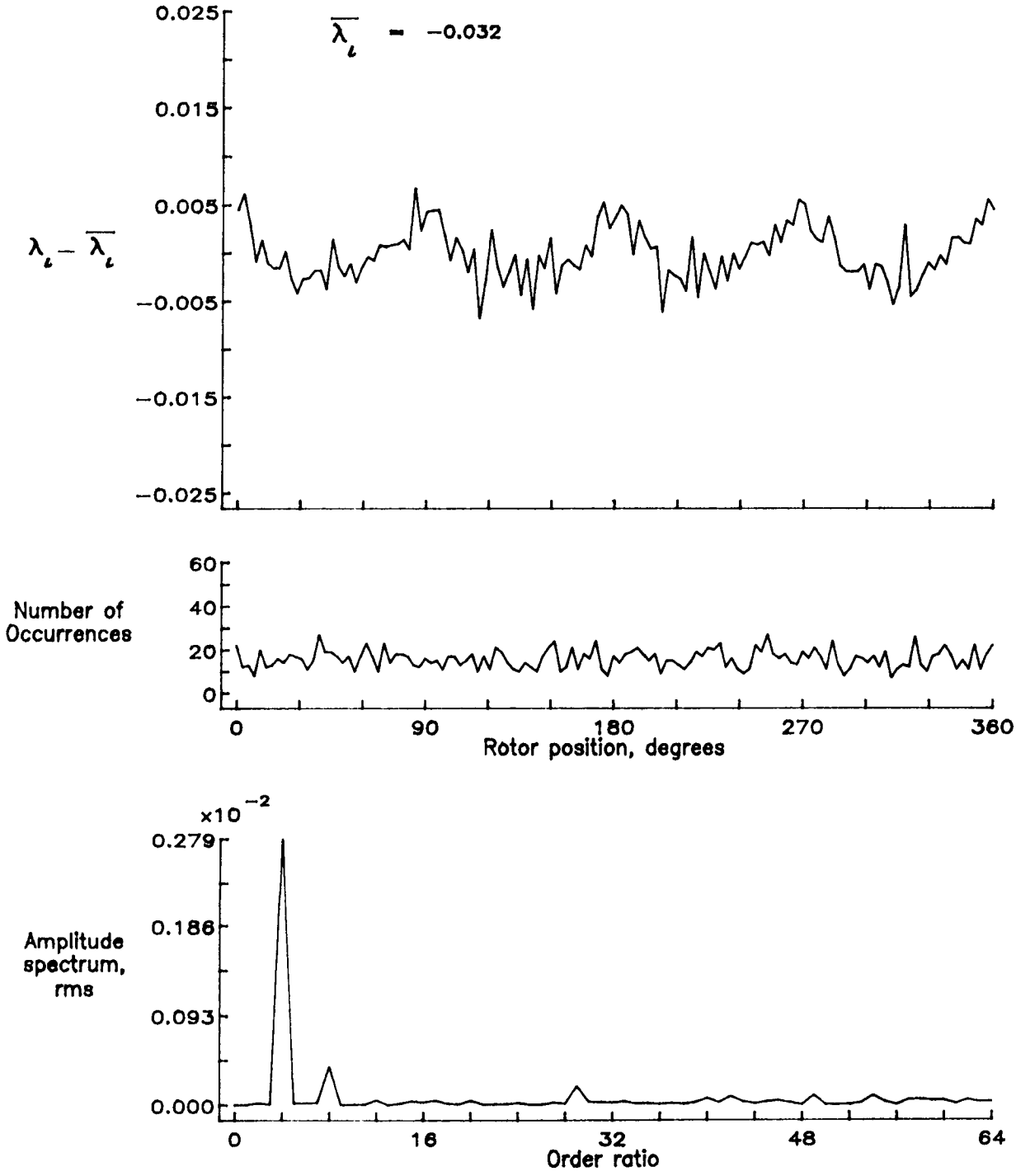

Figure 25.– Concluded.

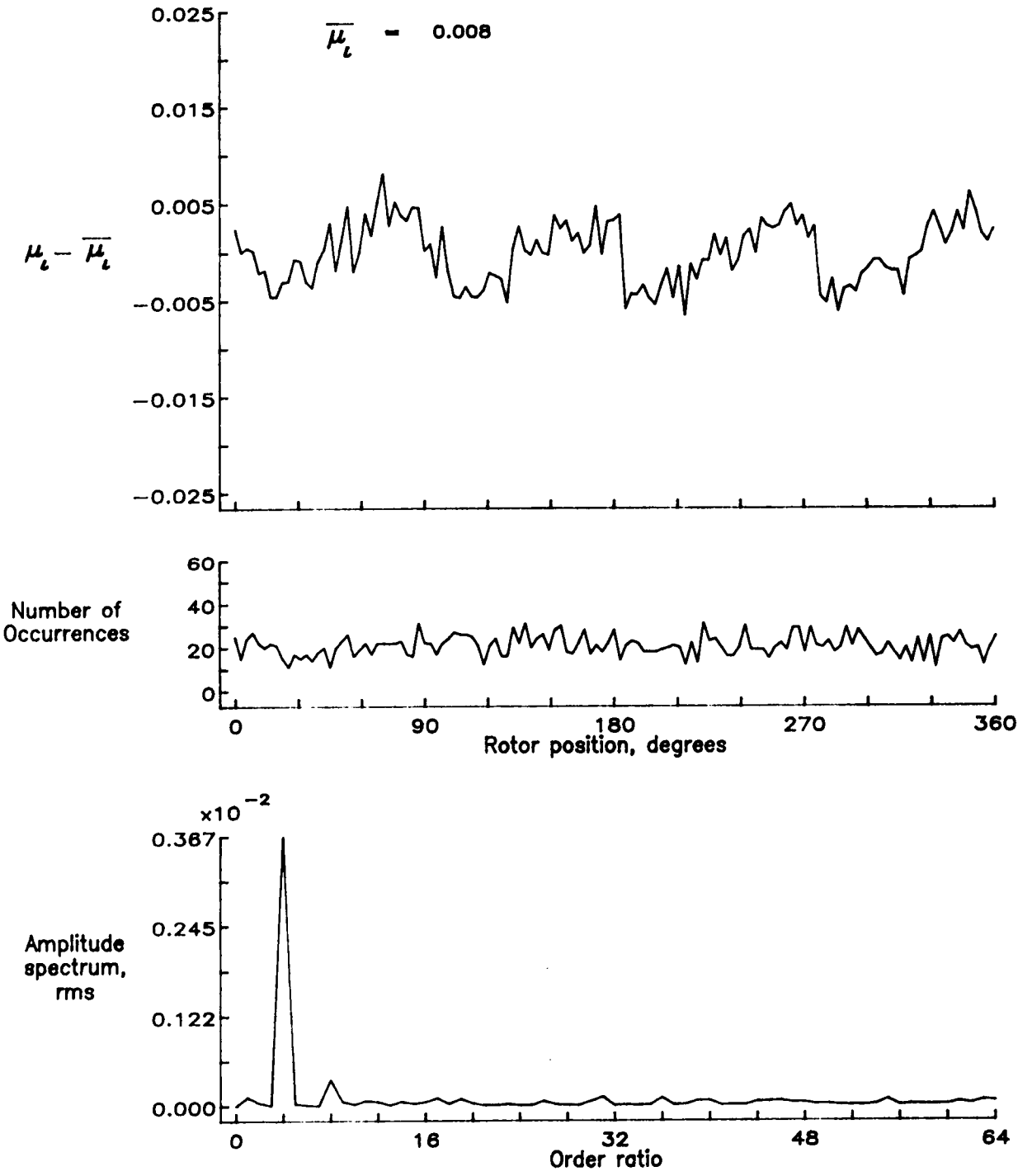

Figure 26.– Induced inflow velocity measured at 0 degrees and r/R of 1.04.

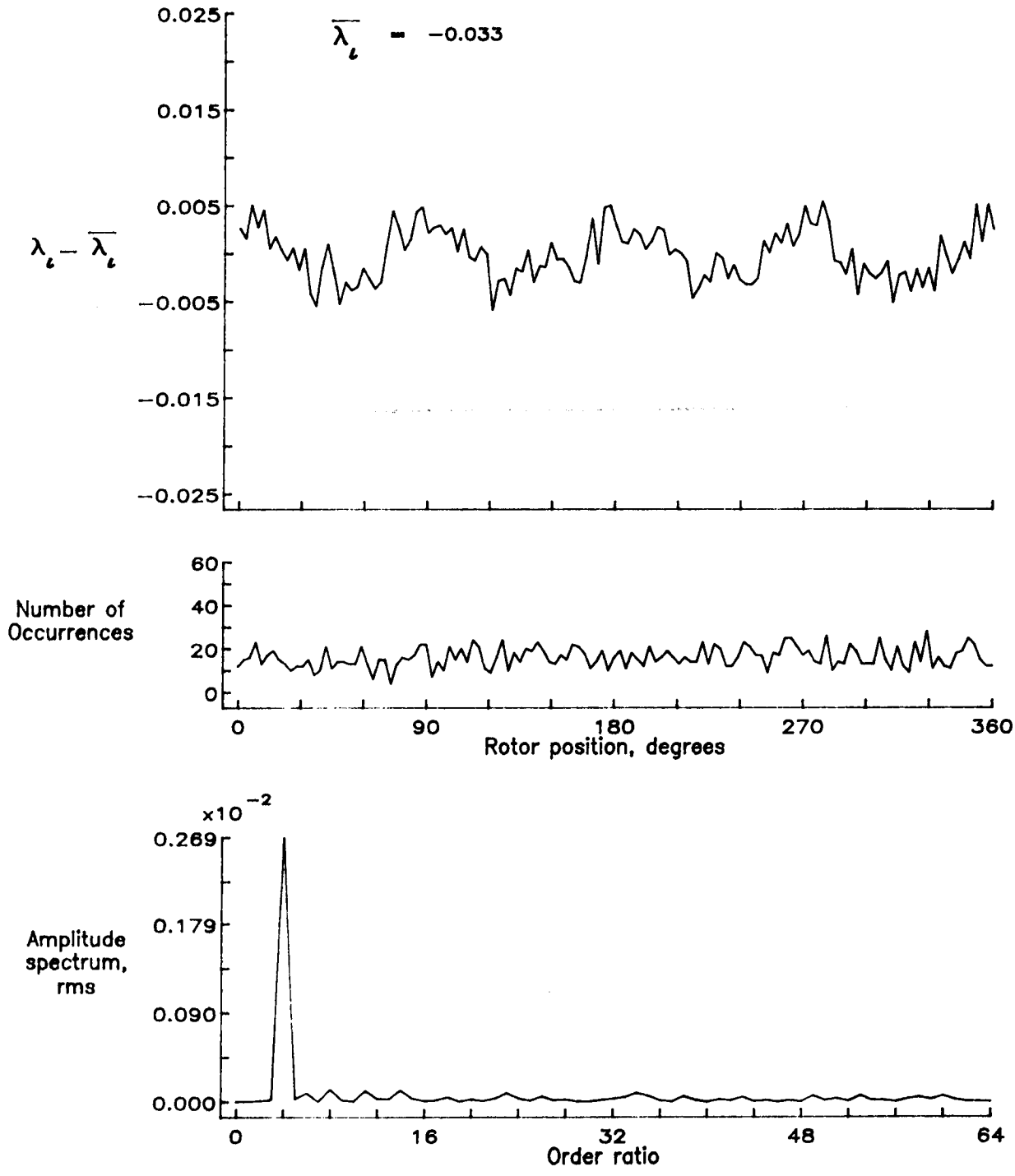

Figure 26.– Concluded.

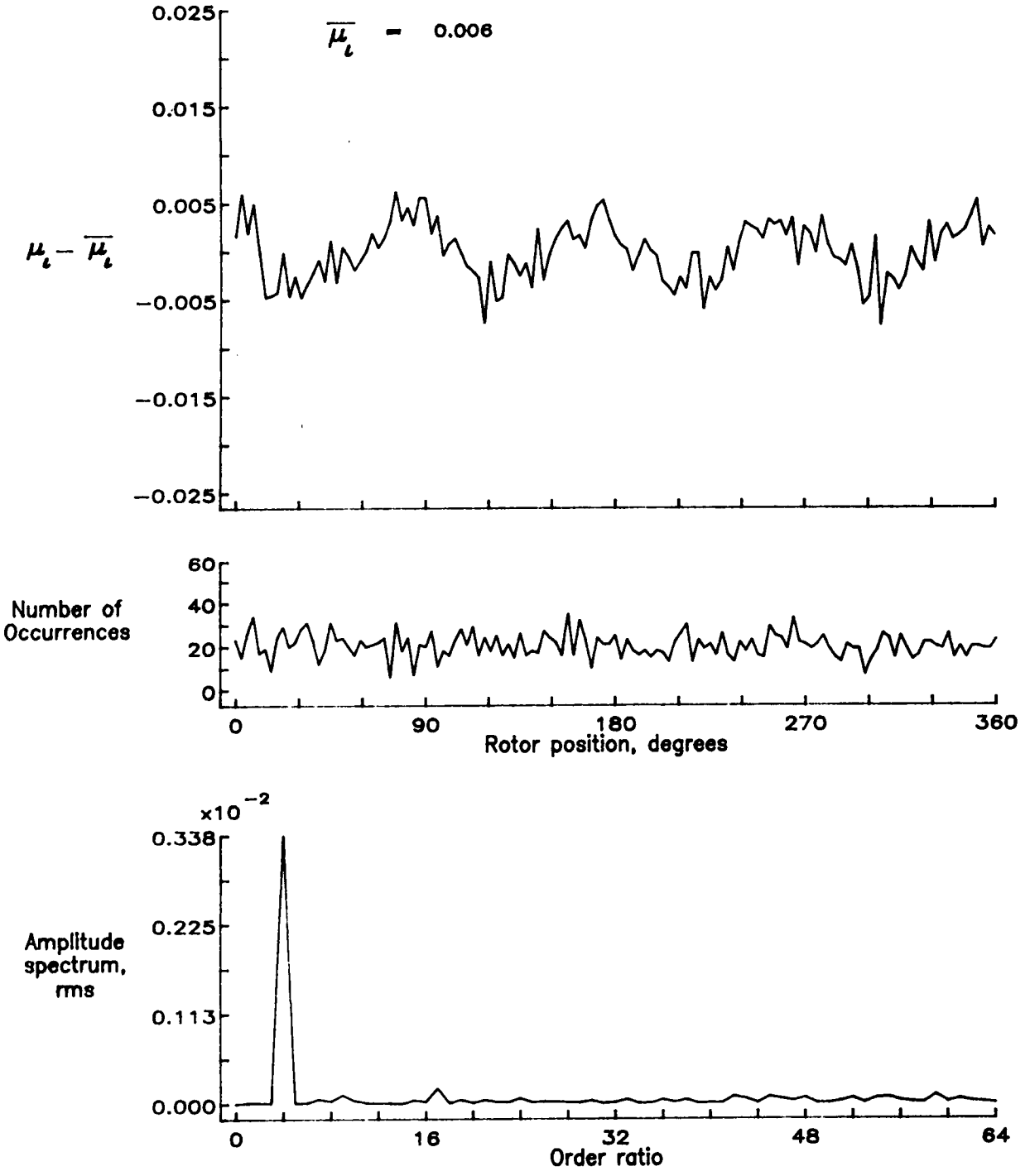

Figure 27.– Induced inflow velocity measured at 0 degrees and r/R of 1.10.

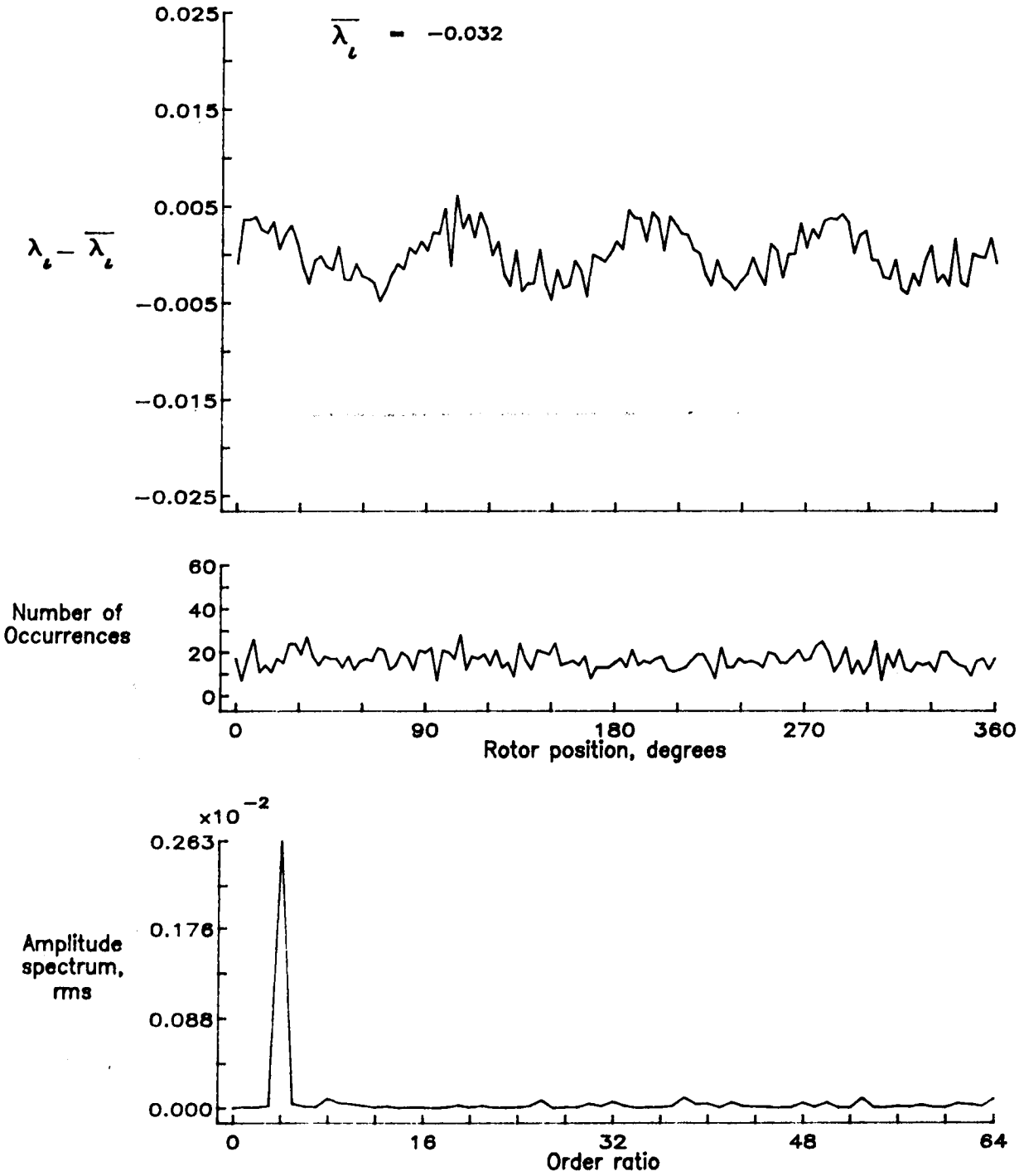

Figure 27.– Concluded.

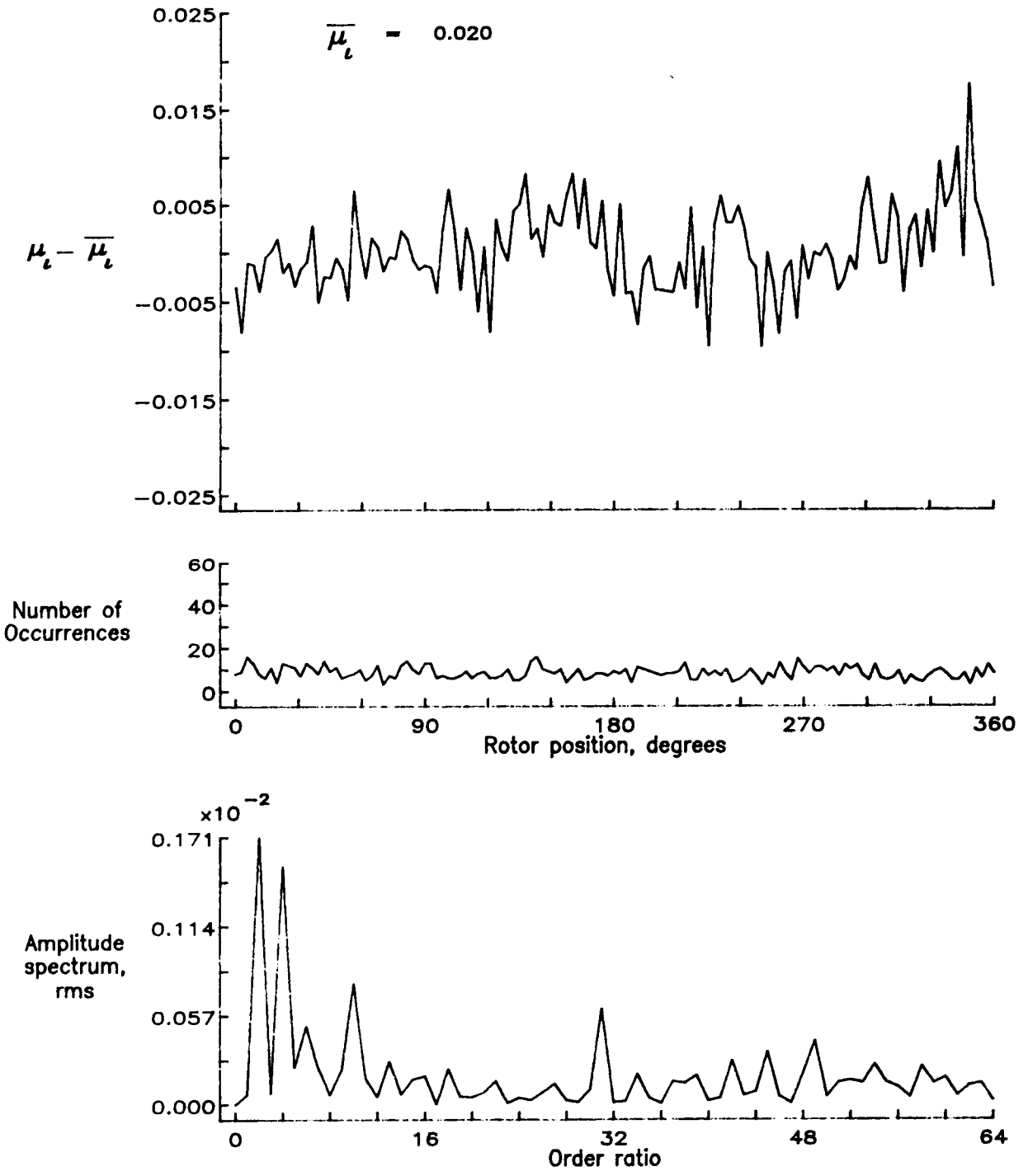

Figure 28.– Induced inflow velocity measured at 30 degrees and r/R of 0.20.

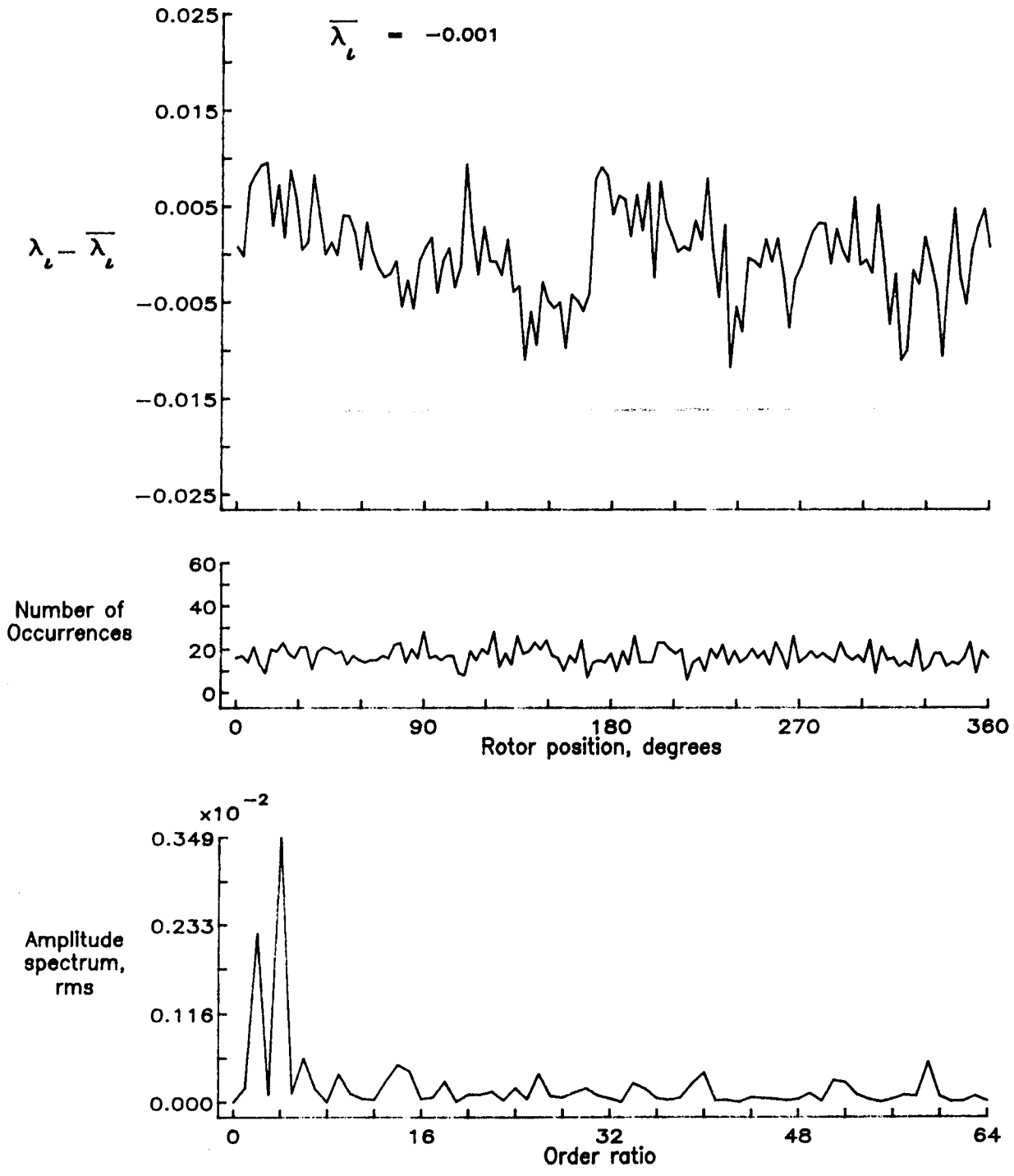

Figure 28.– Concluded.

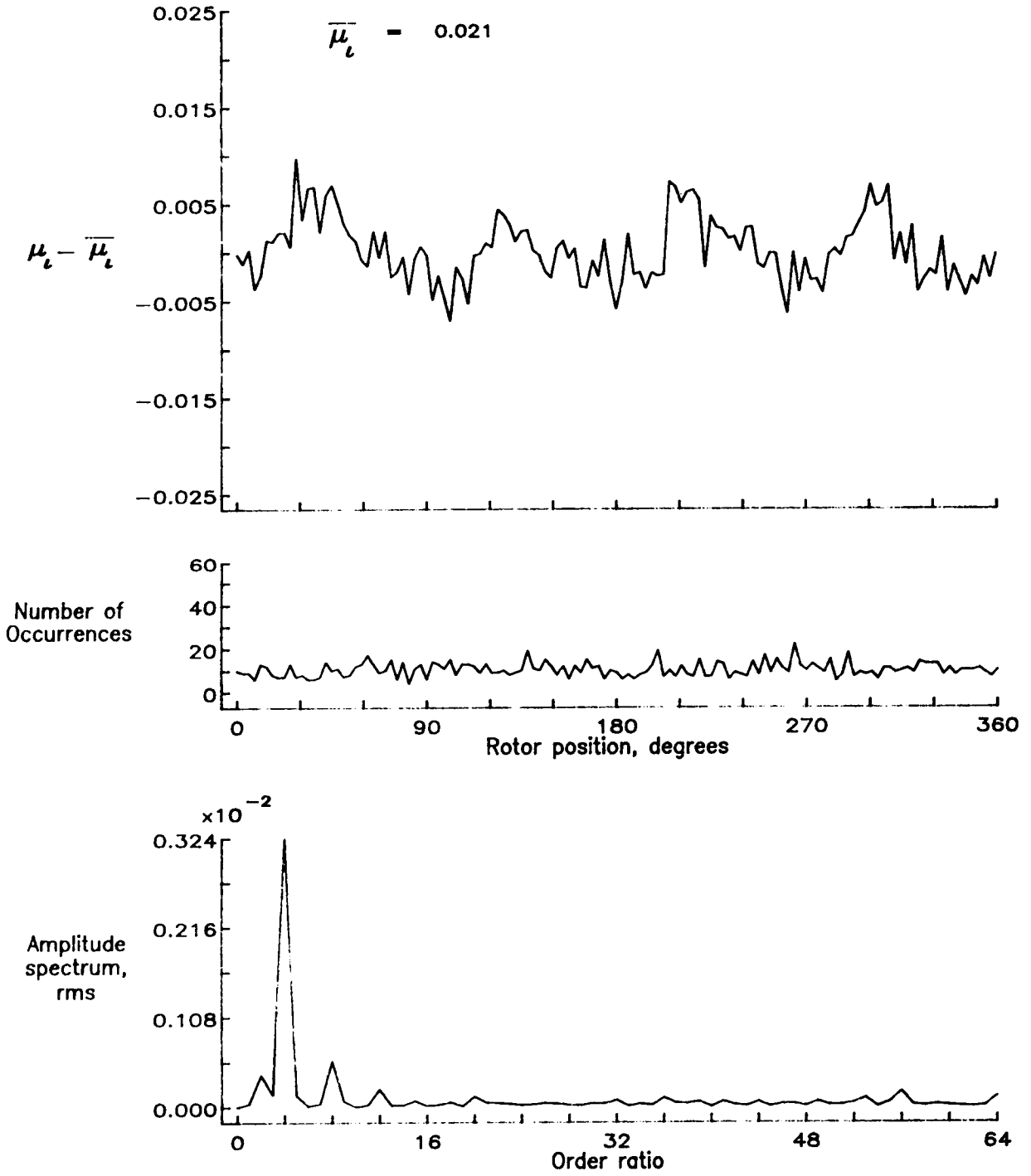

Figure 29.– Induced inflow velocity measured at 30 degrees and r/R of 0.40.

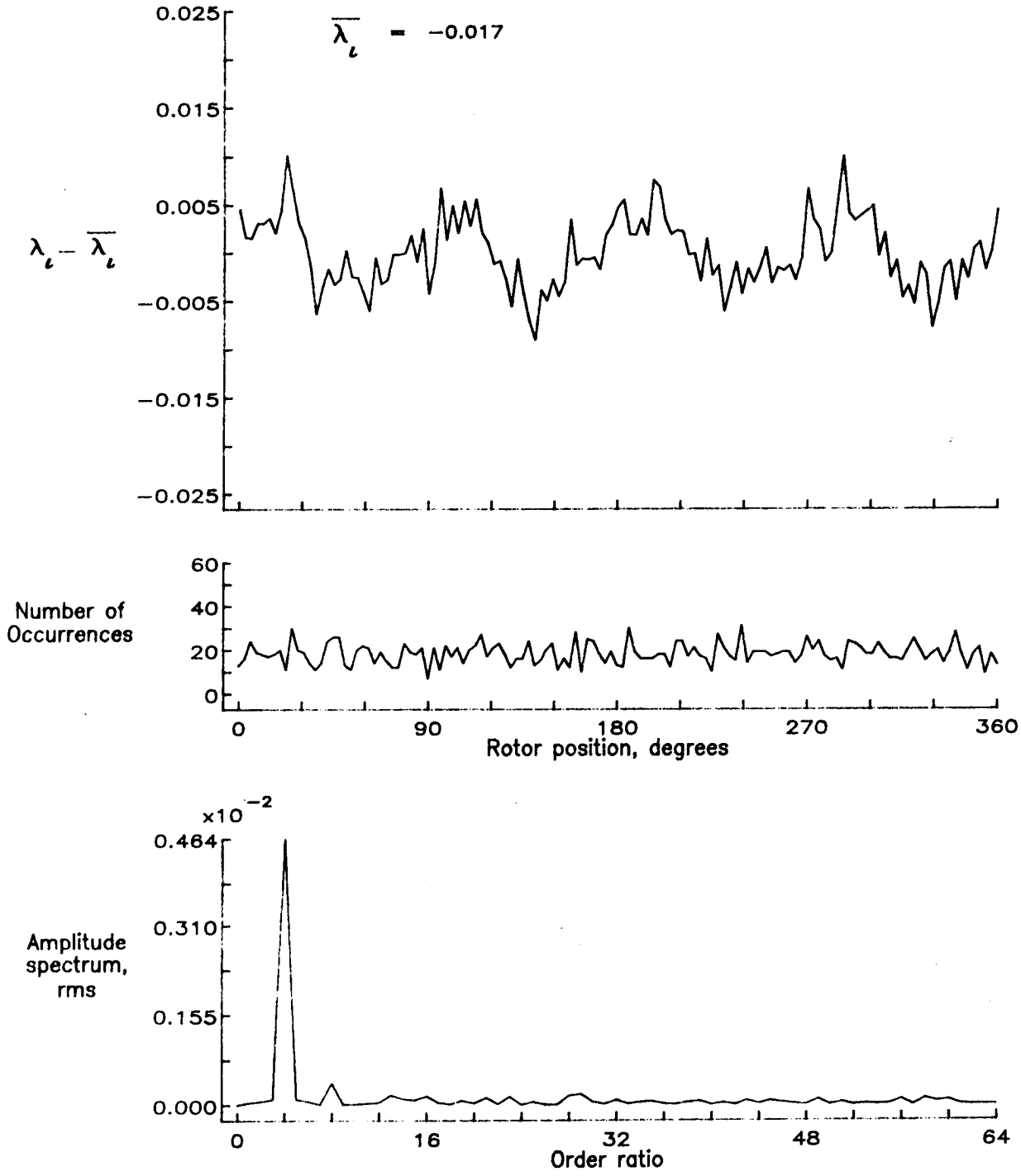

Figure 29.– Concluded.

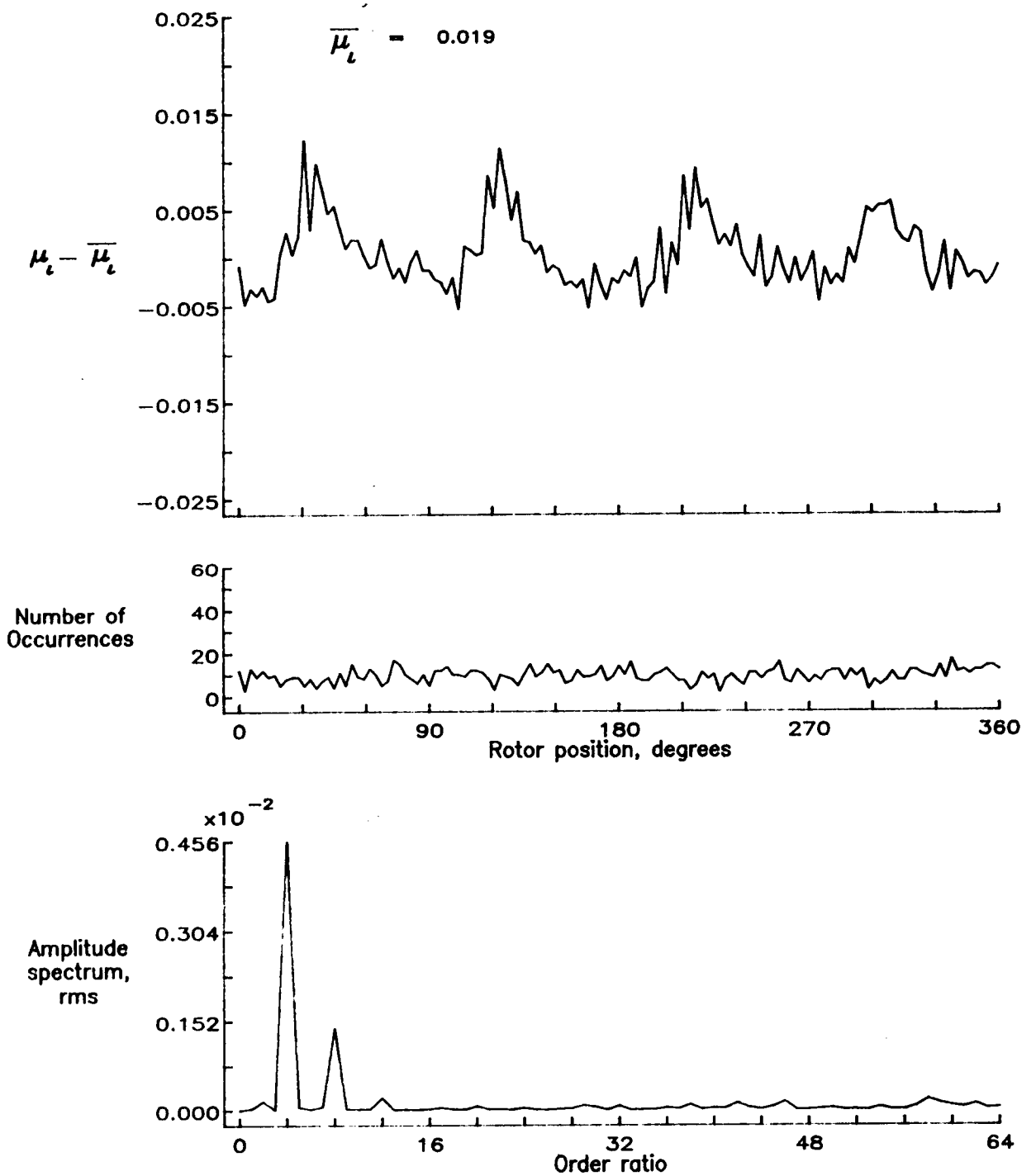

Figure 30.– Induced inflow velocity measured at 30 degrees and r/R of 0.50.

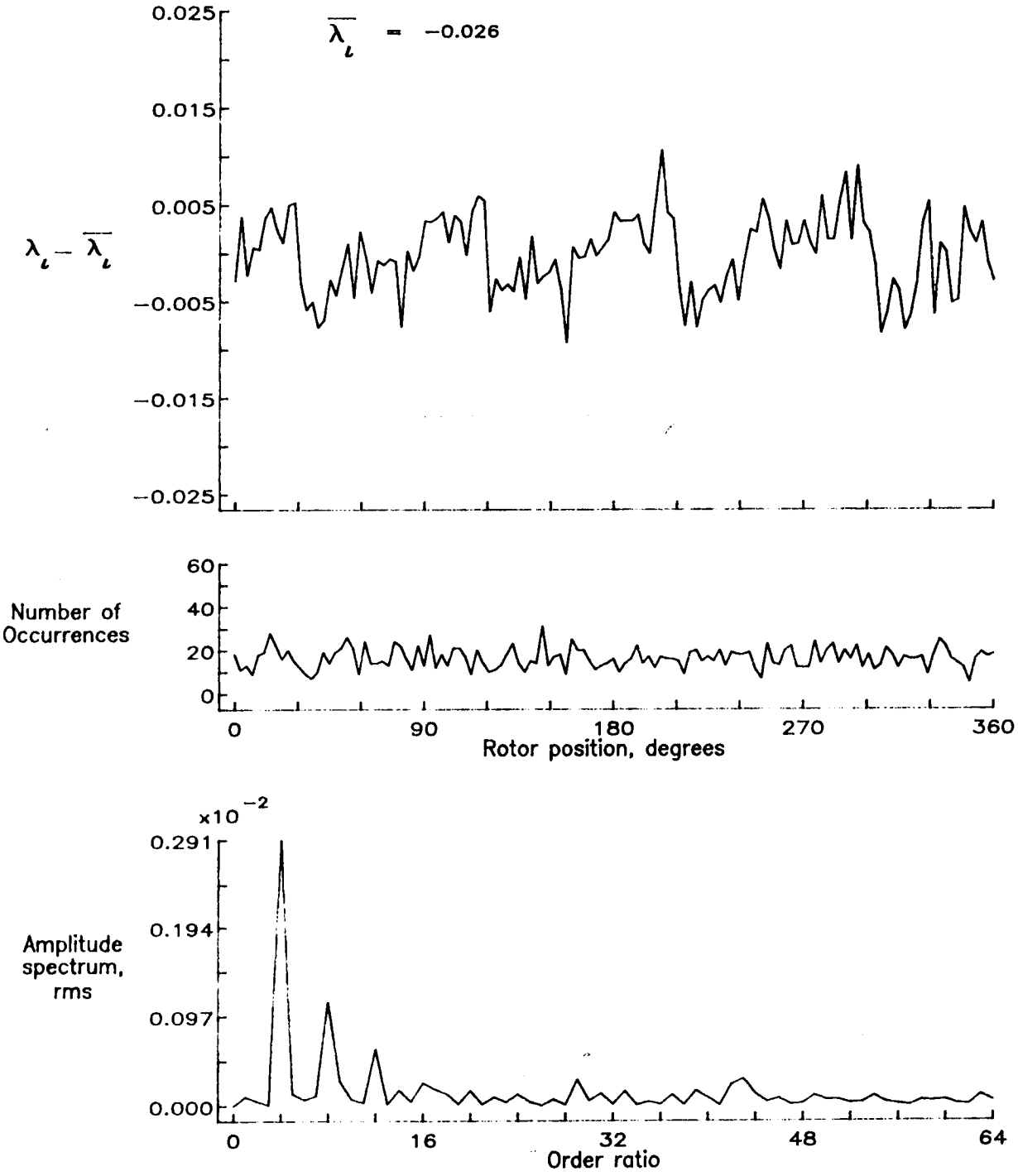

Figure 30.– Concluded.

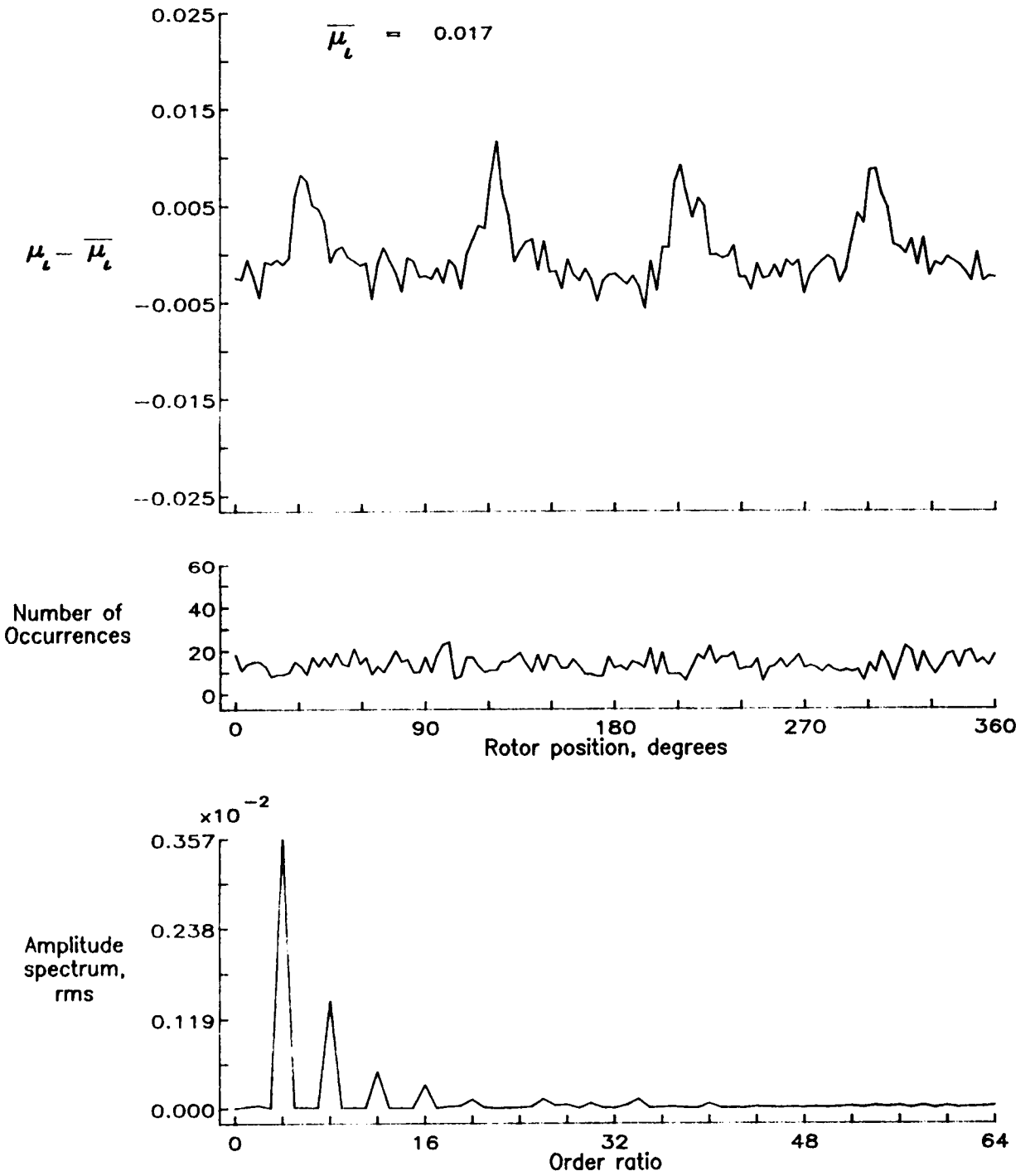

Figure 31.– Induced inflow velocity measured at 30 degrees and r/R of 0.60.

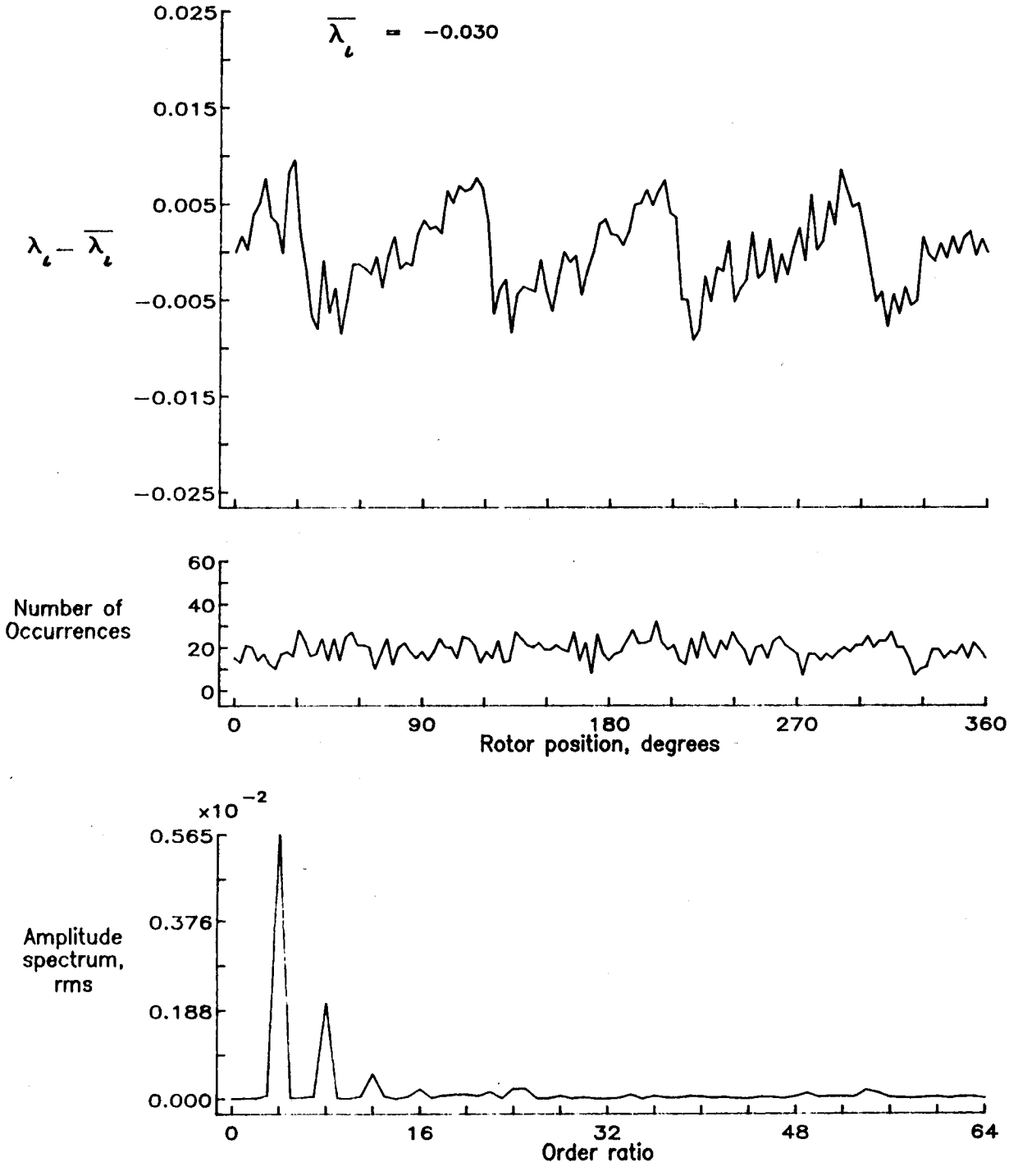

Figure 31.– Concluded.

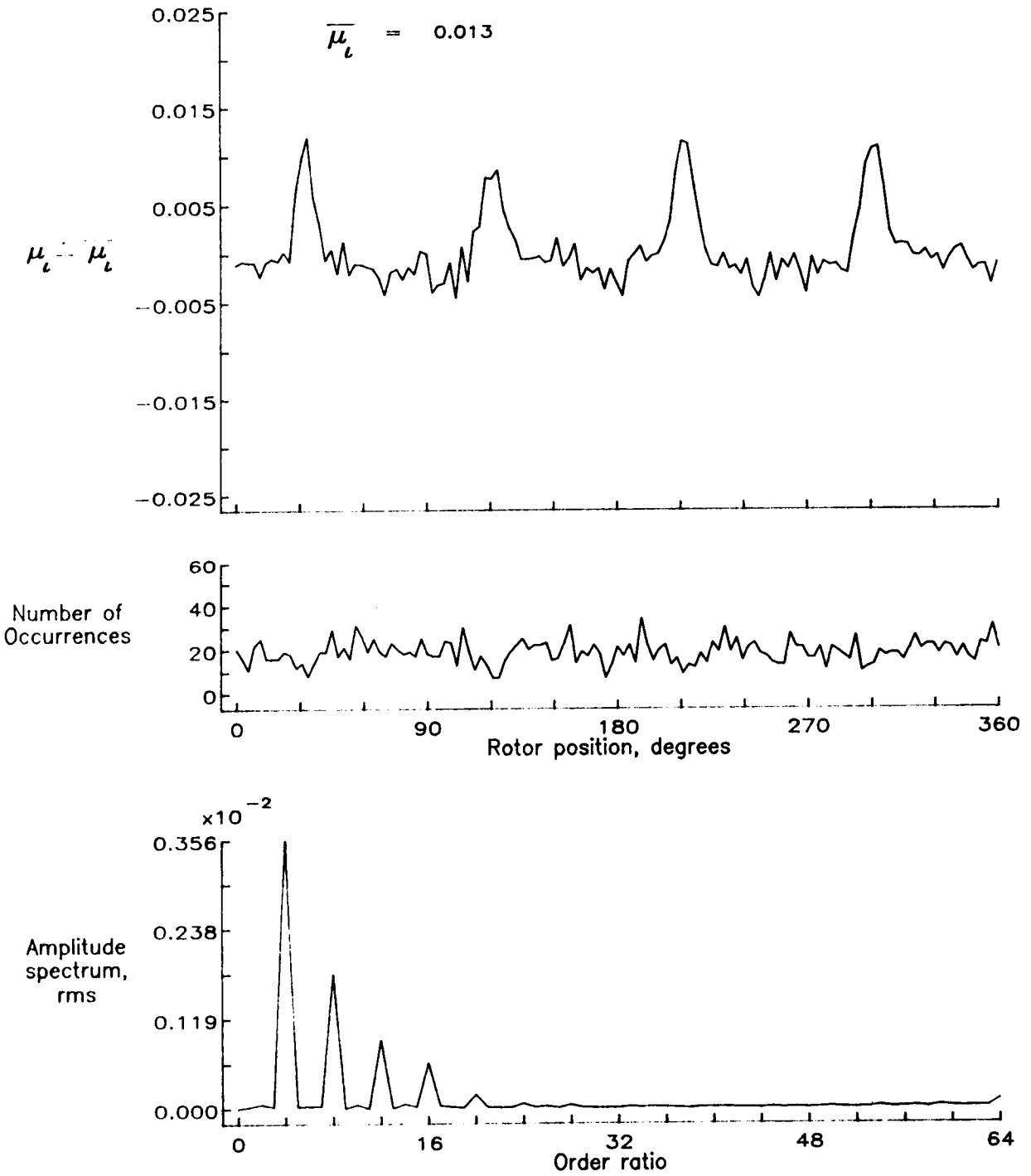

Figure 32.– Induced inflow velocity measured at 30 degrees and r/R of 0.70.

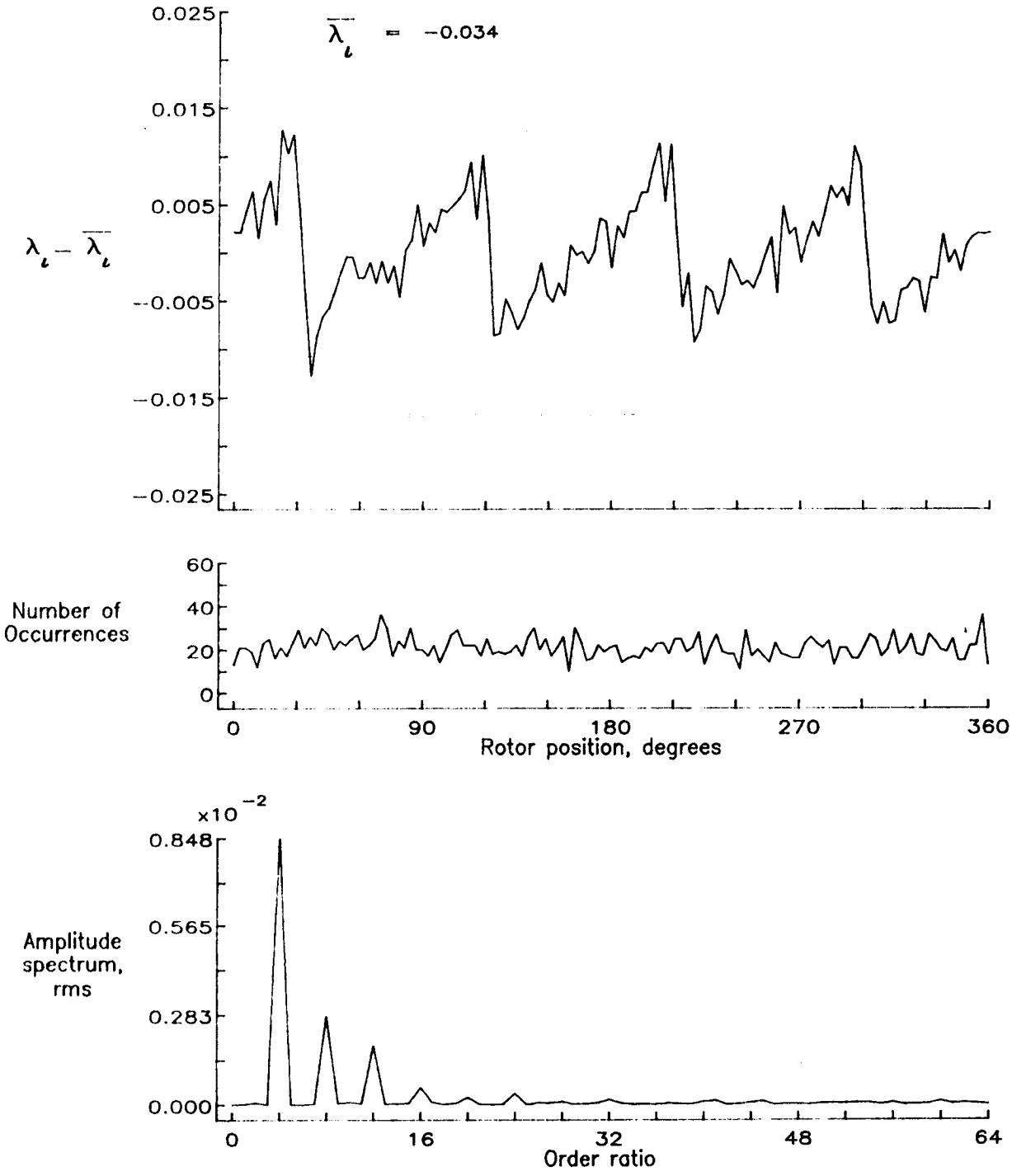

Figure 32.– Concluded.

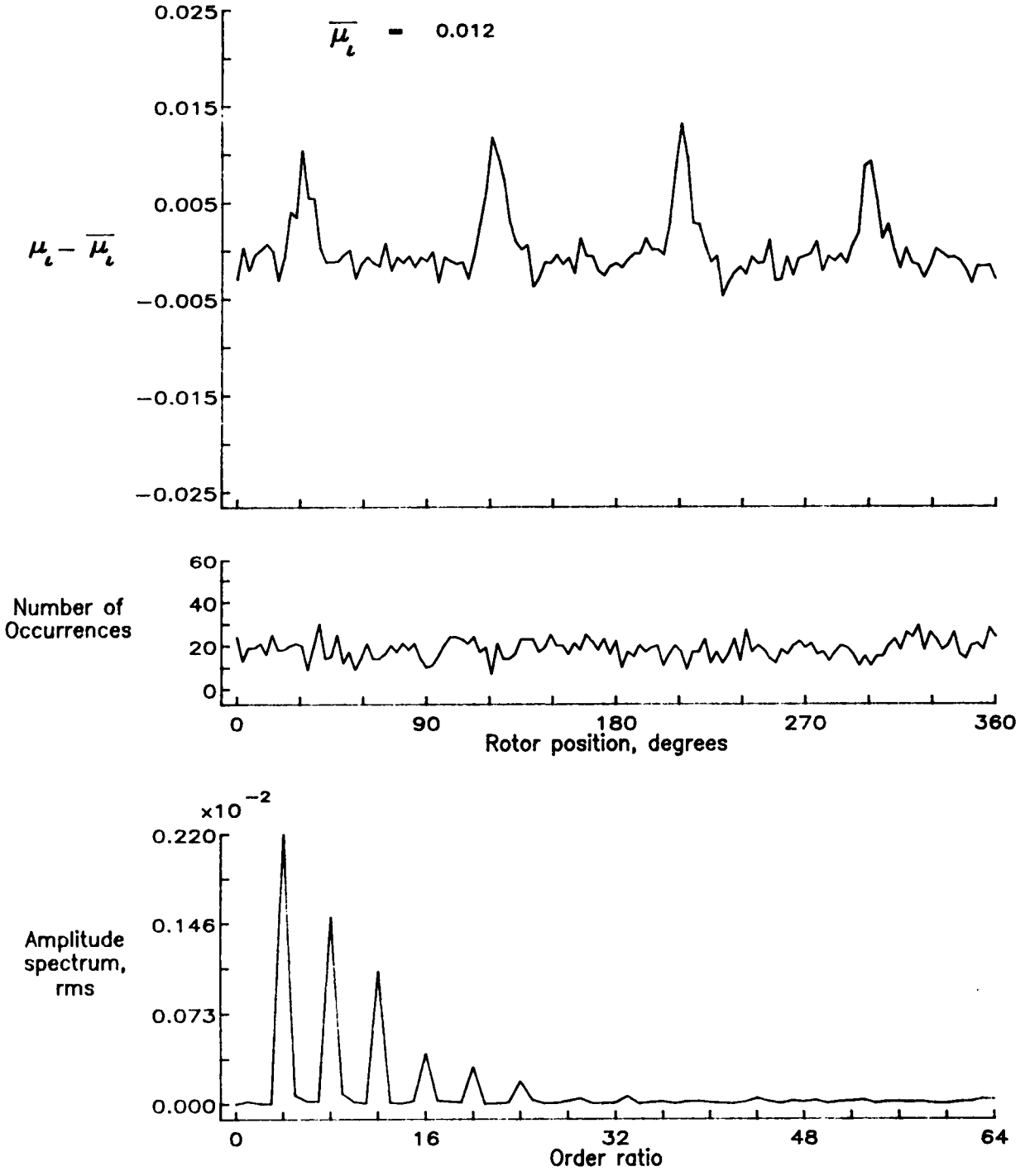

Figure 33.– Induced inflow velocity measured at 30 degrees and r/R of 0.74.

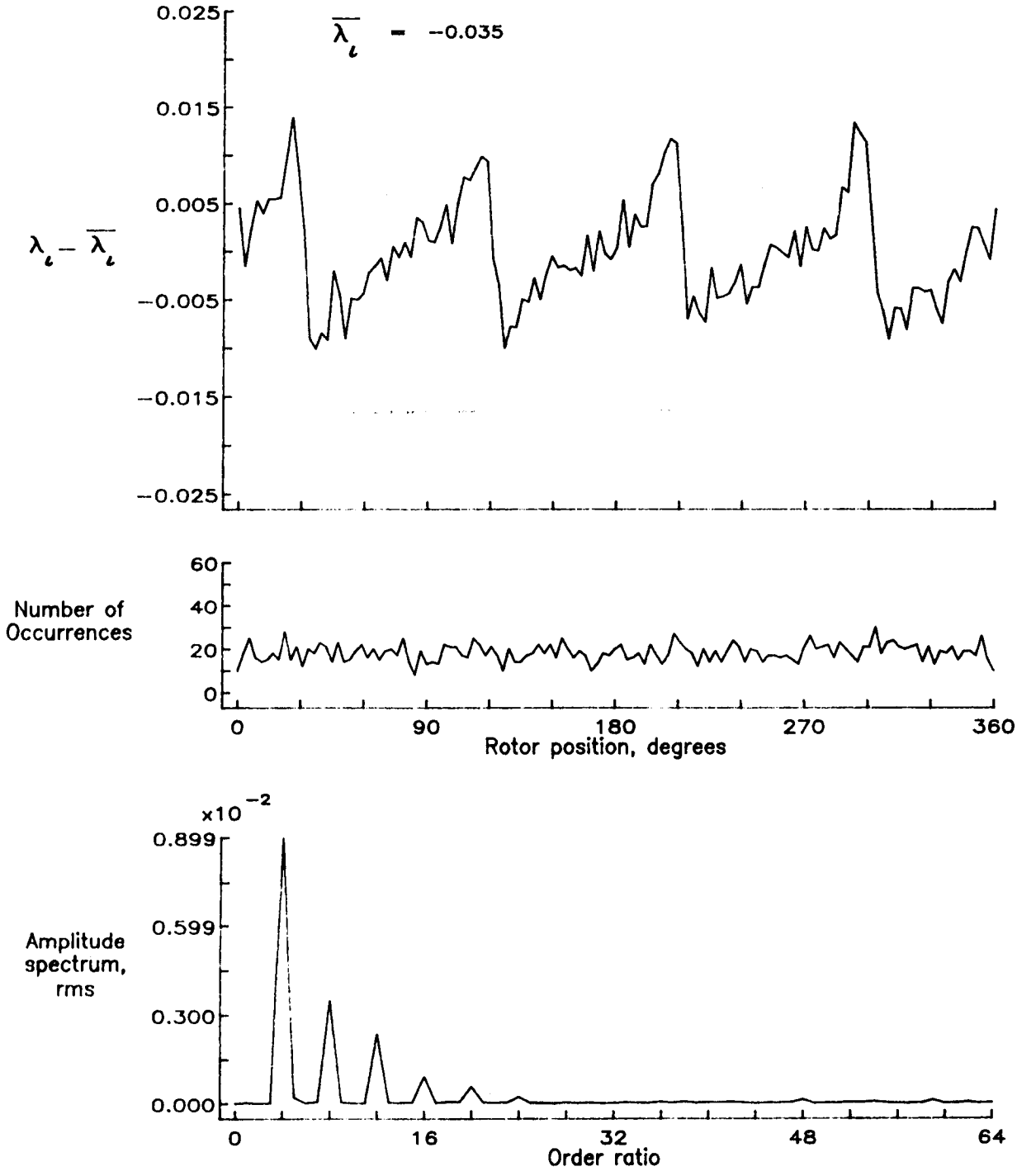

Figure 33.– Concluded.

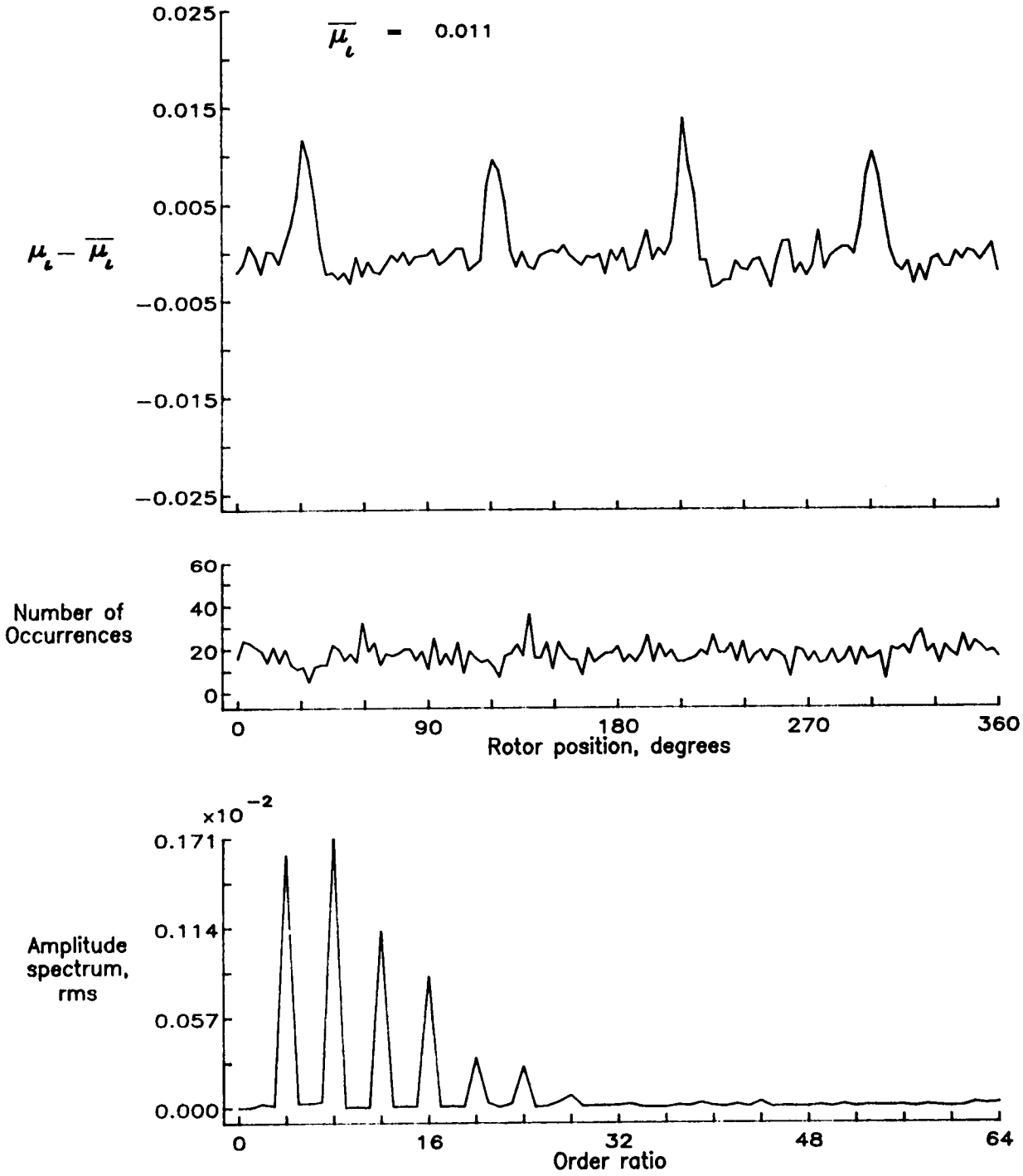

Figure 34.– Induced inflow velocity measured at 30 degrees and r/R of 0.78.

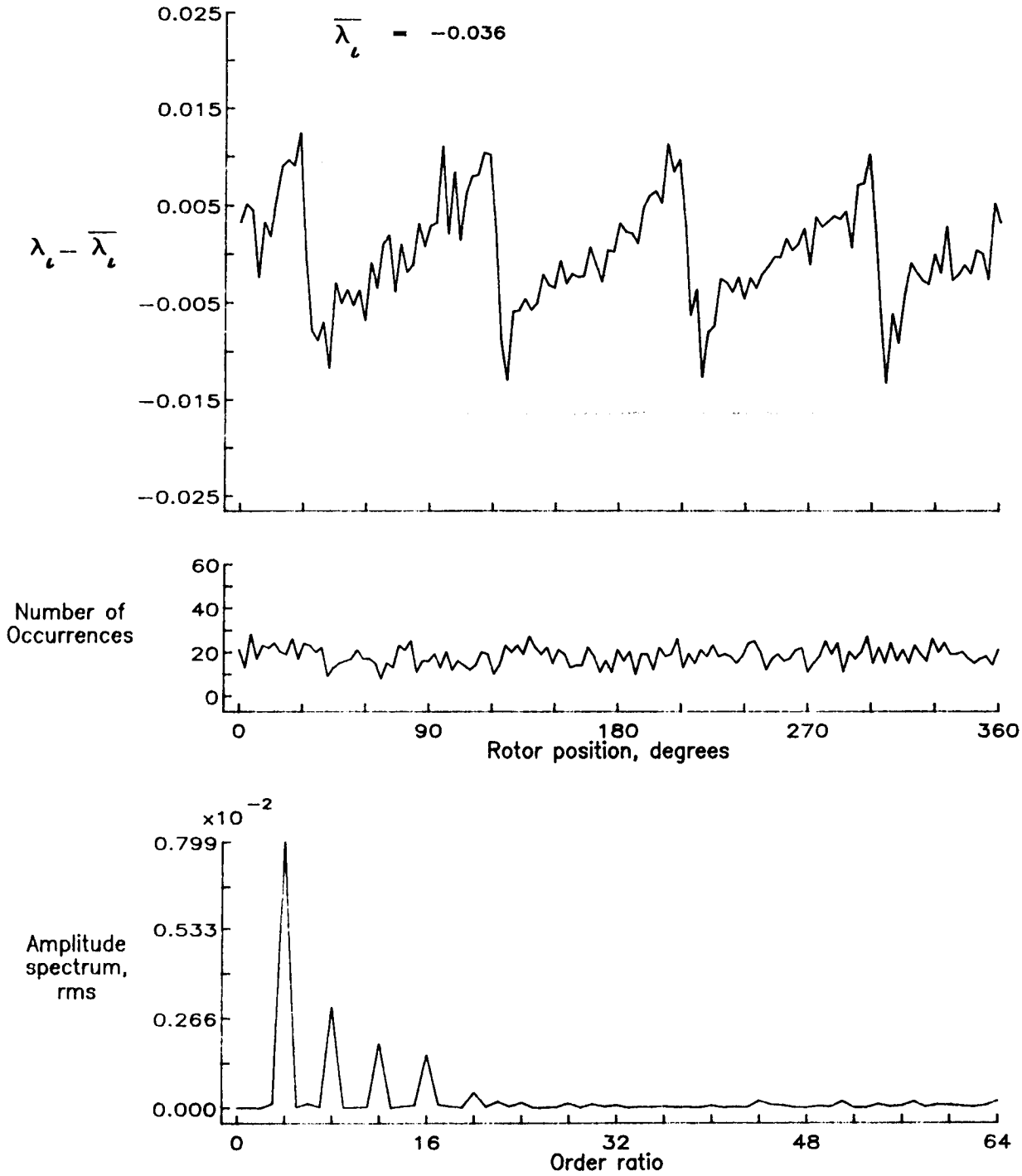

Figure 34.– Concluded.

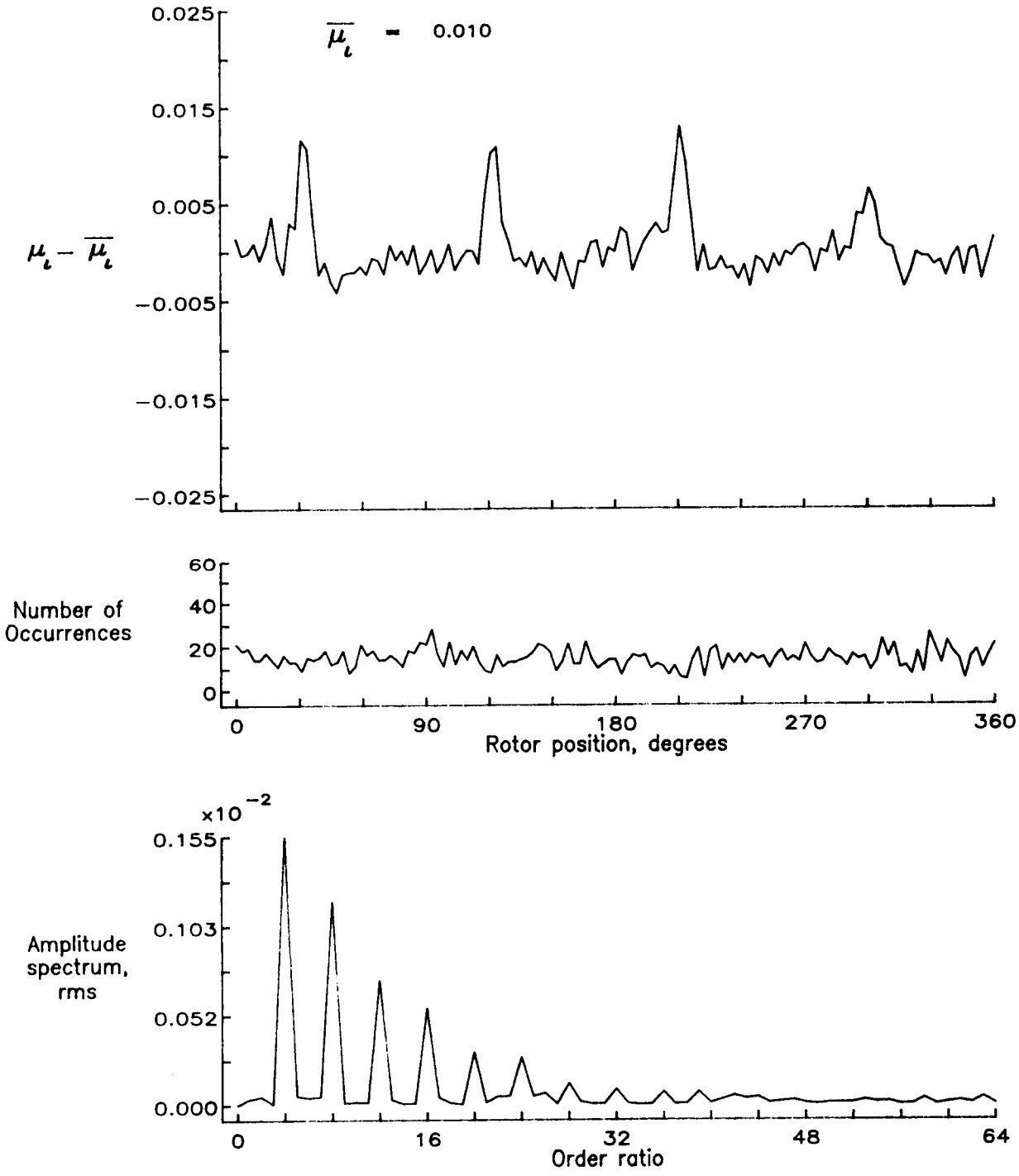

Figure 35.– Induced inflow velocity measured at 30 degrees and r/R of 0.82.

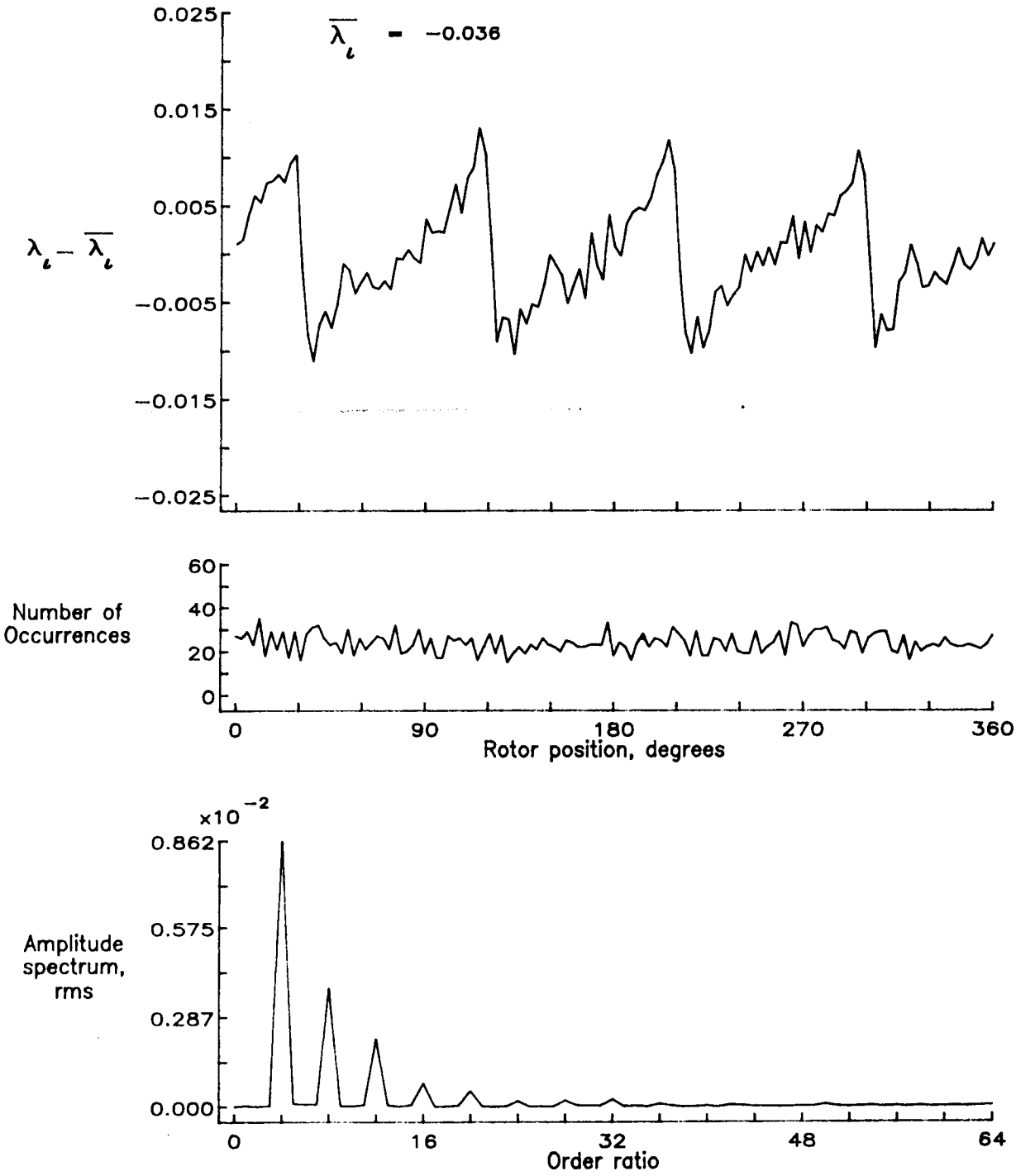

Figure 35.– Concluded.

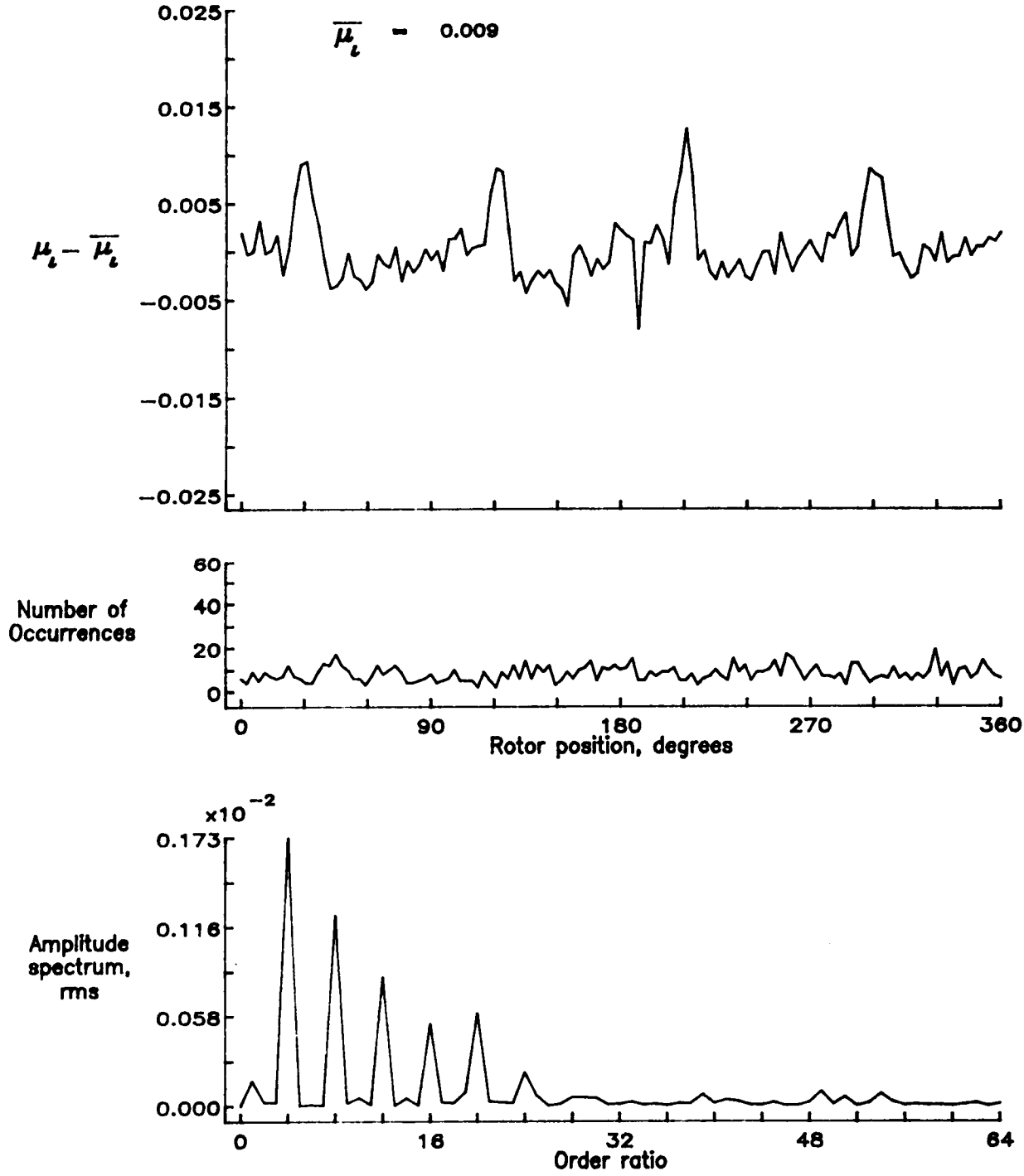

Figure 36.– Induced inflow velocity measured at 30 degrees and r/R of 0.86.

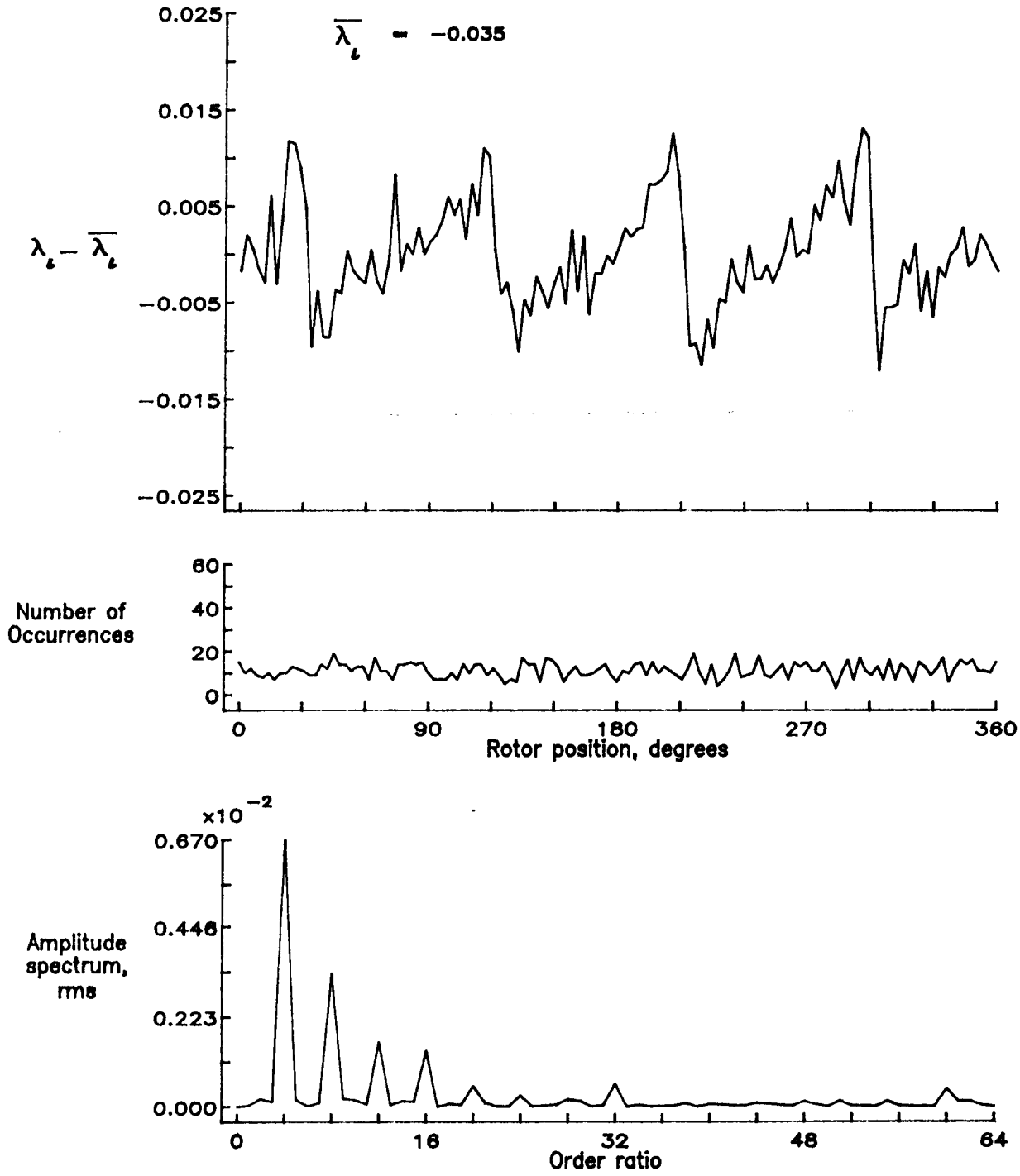

Figure 36.– Concluded.

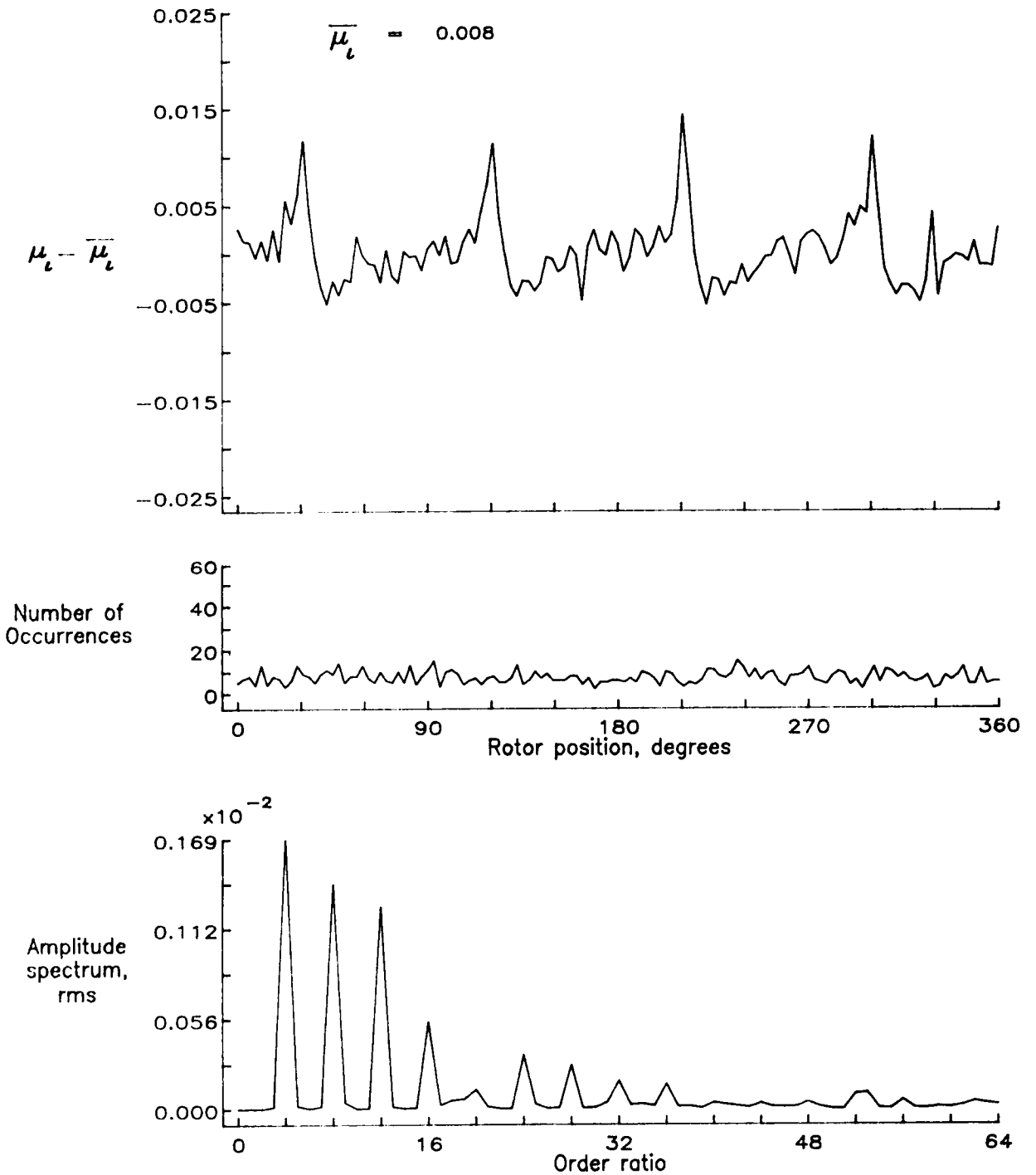

Figure 37.– Induced inflow velocity measured at 30 degrees and r/R of 0.90.

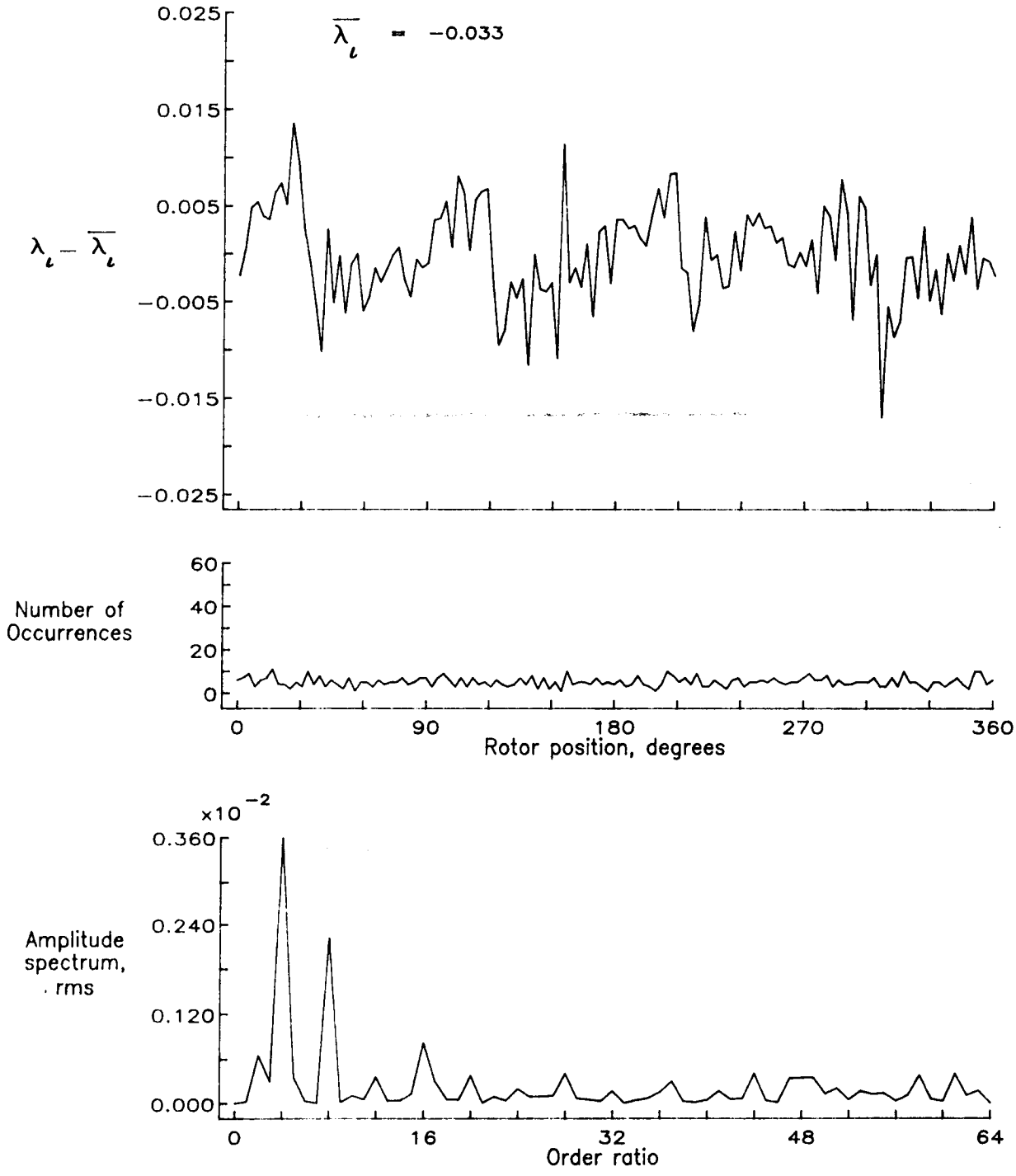

Figure 37.– Concluded.

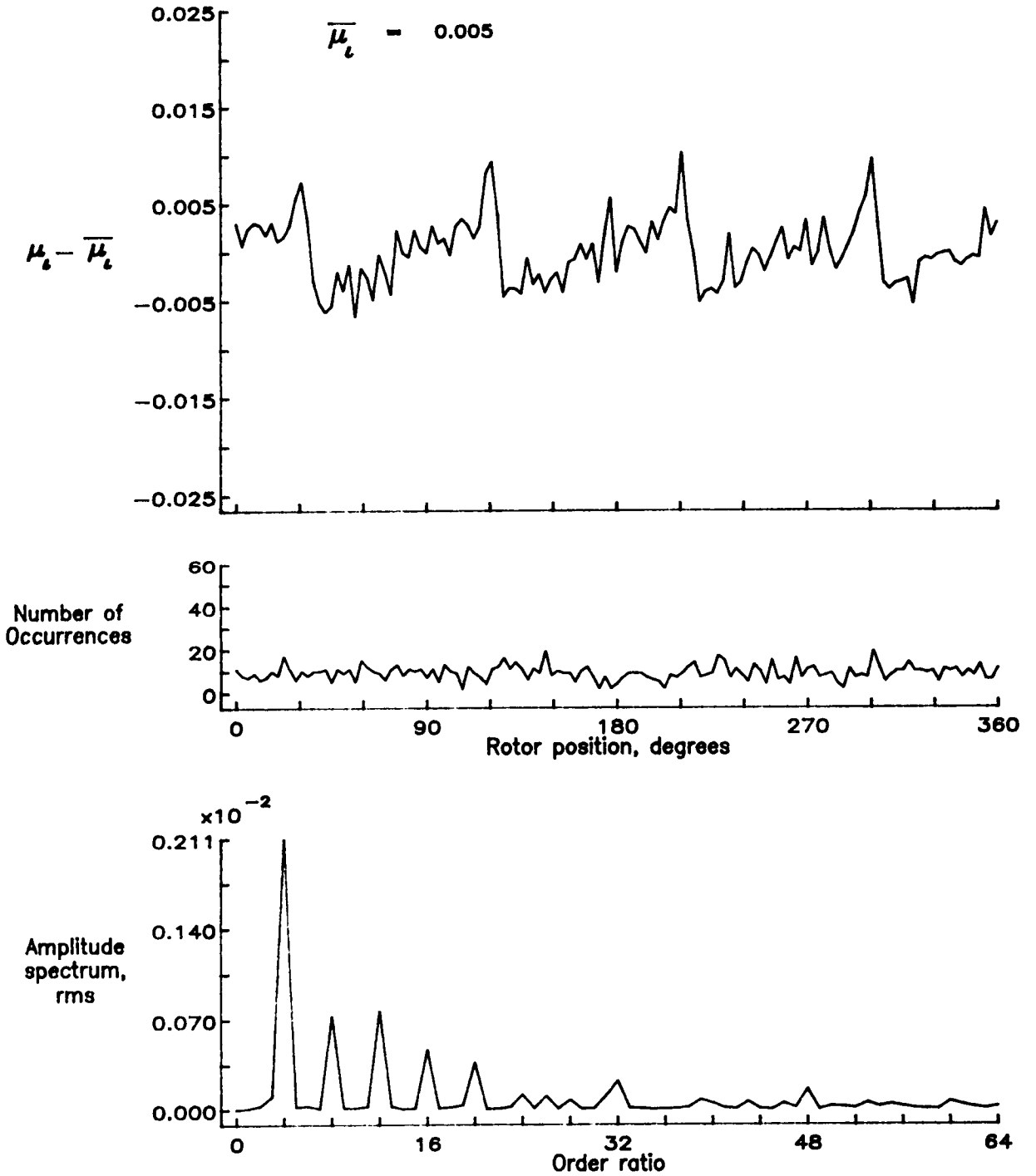

Figure 38.– Induced inflow velocity measured at 30 degrees and r/R of 0.94.

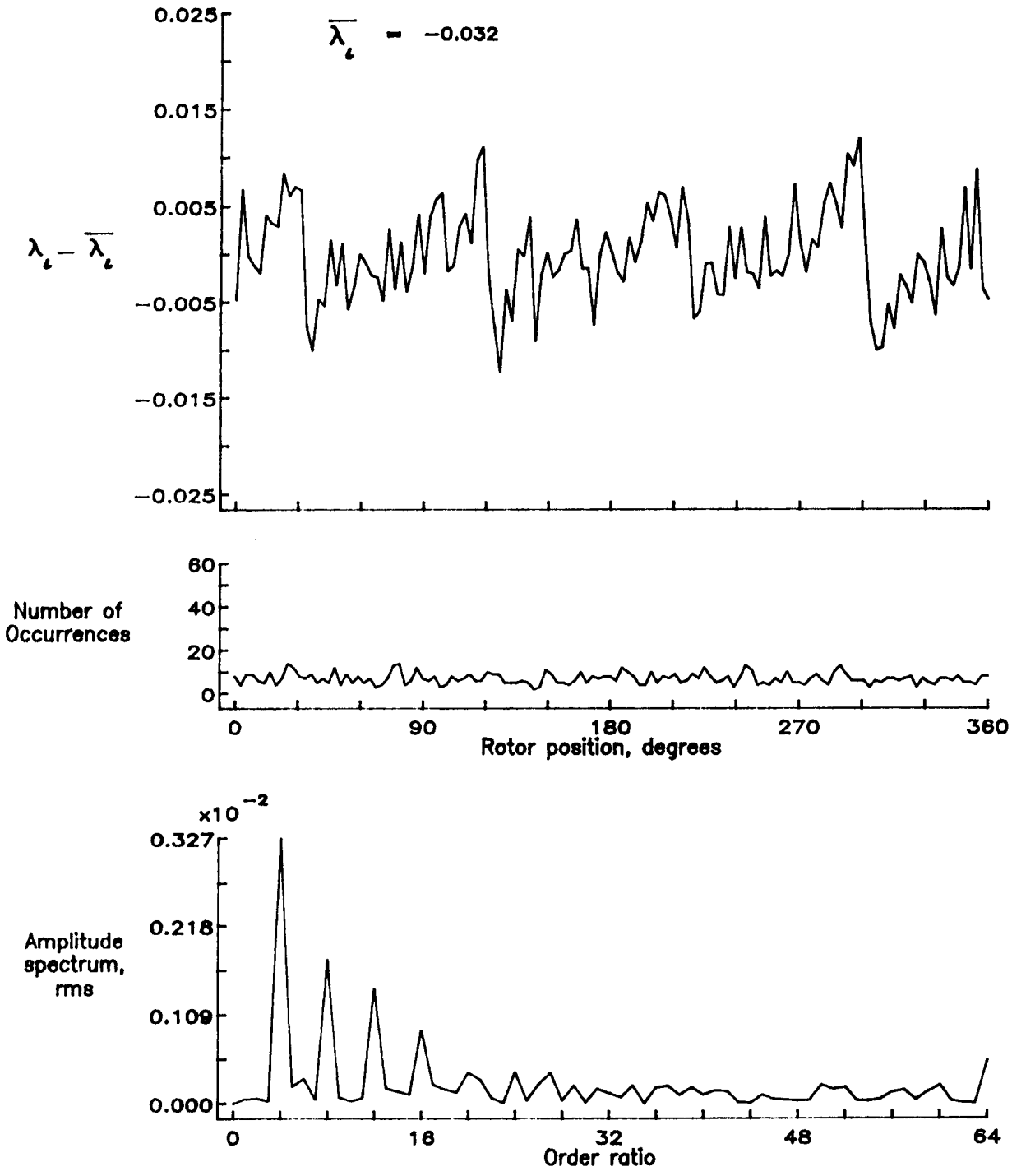

Figure 38.– Concluded.

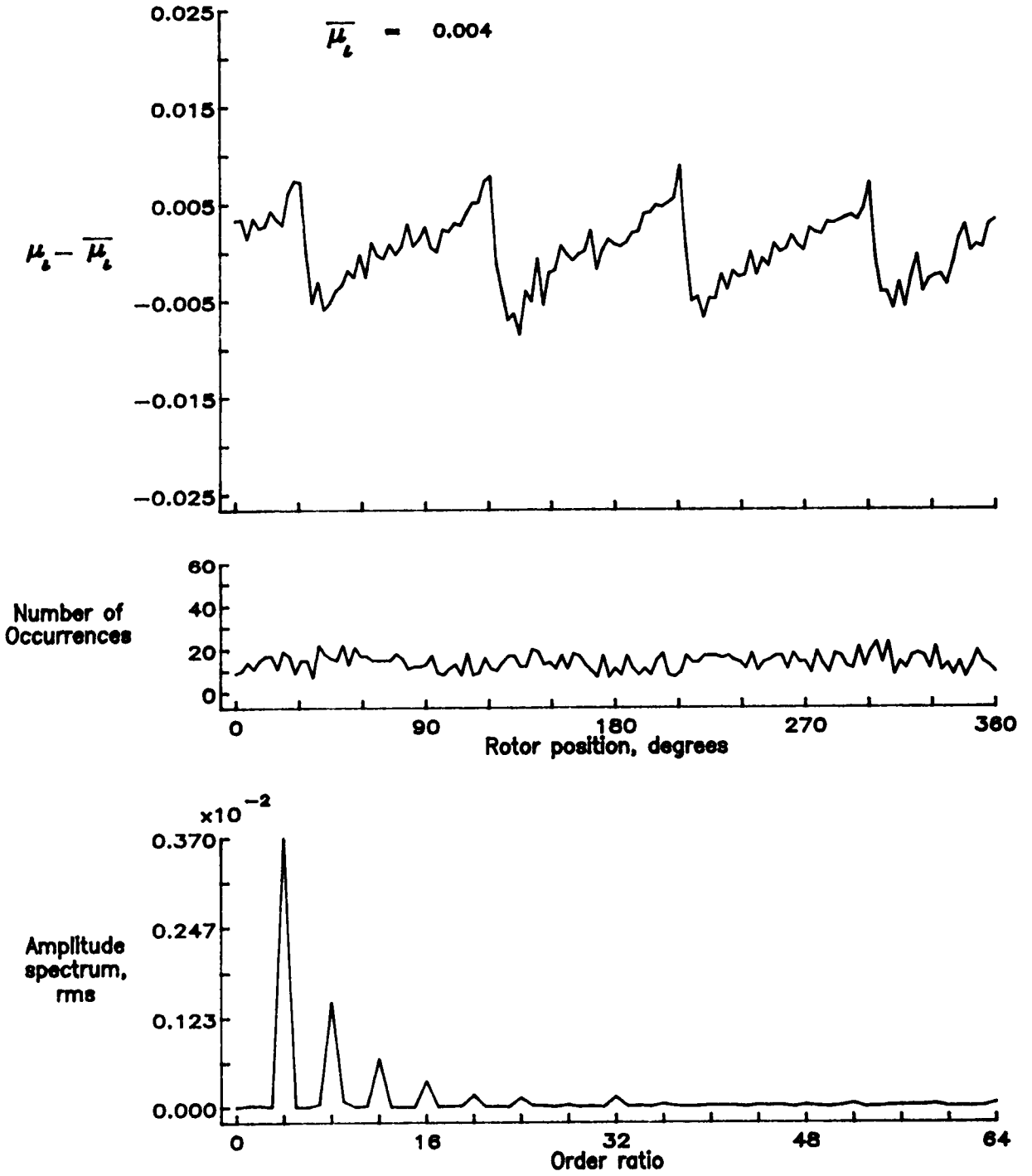

Figure 39.– Induced inflow velocity measured at 30 degrees and r/R of 0.98.

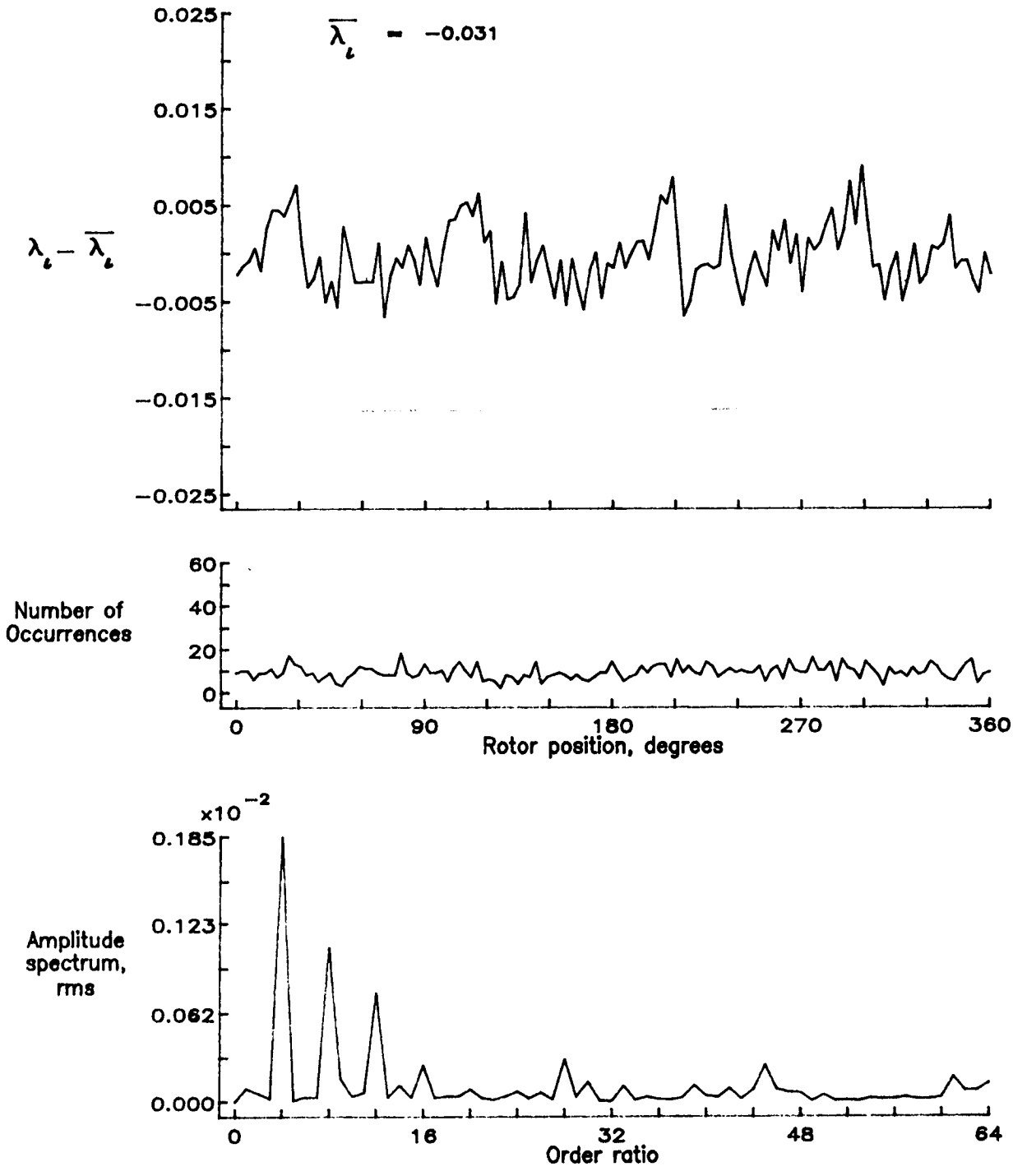

Figure 39.– Concluded.

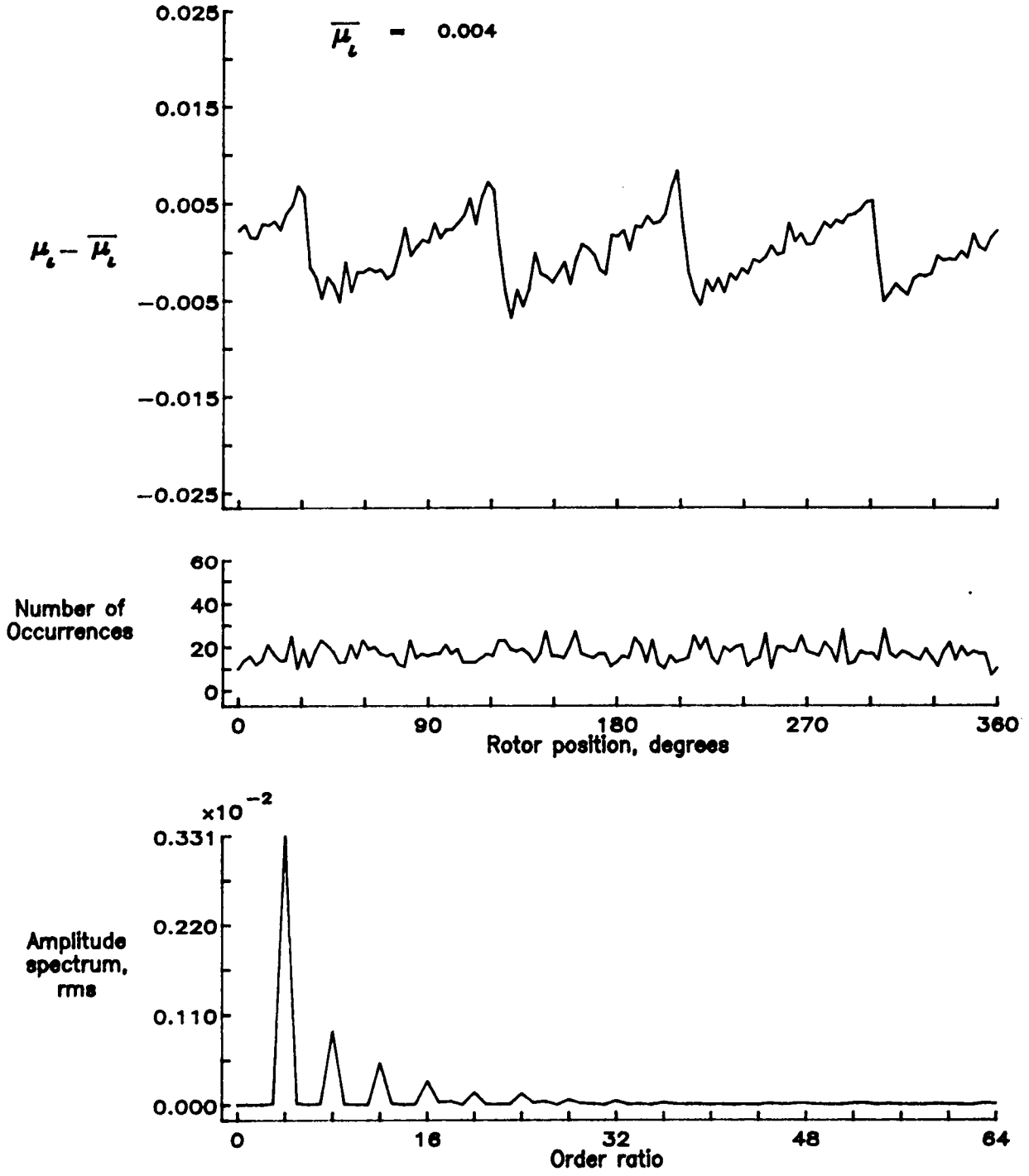

Figure 40.– Induced inflow velocity measured at 30 degrees and r/R of 1.02.

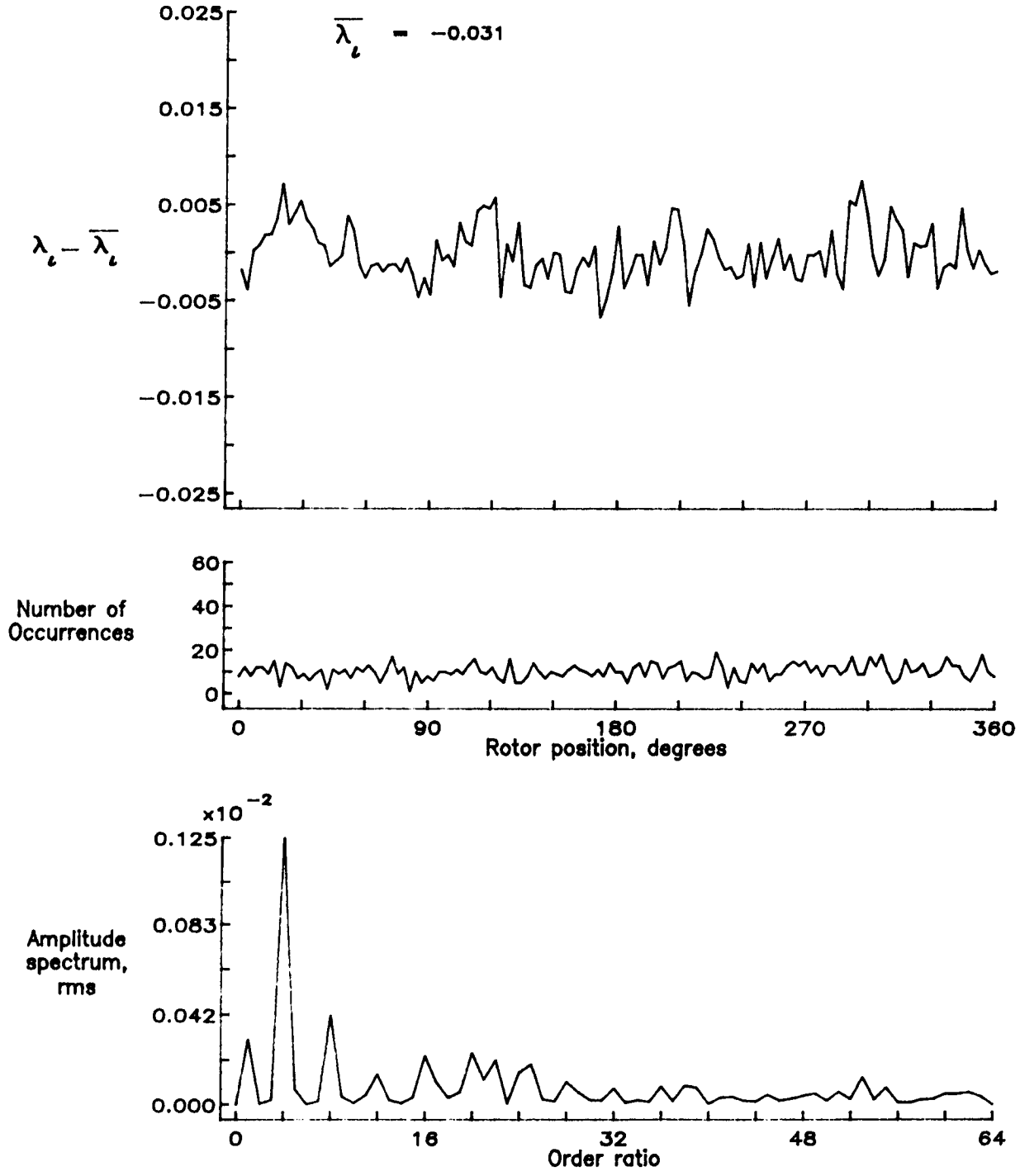

Figure 40.– Concluded.

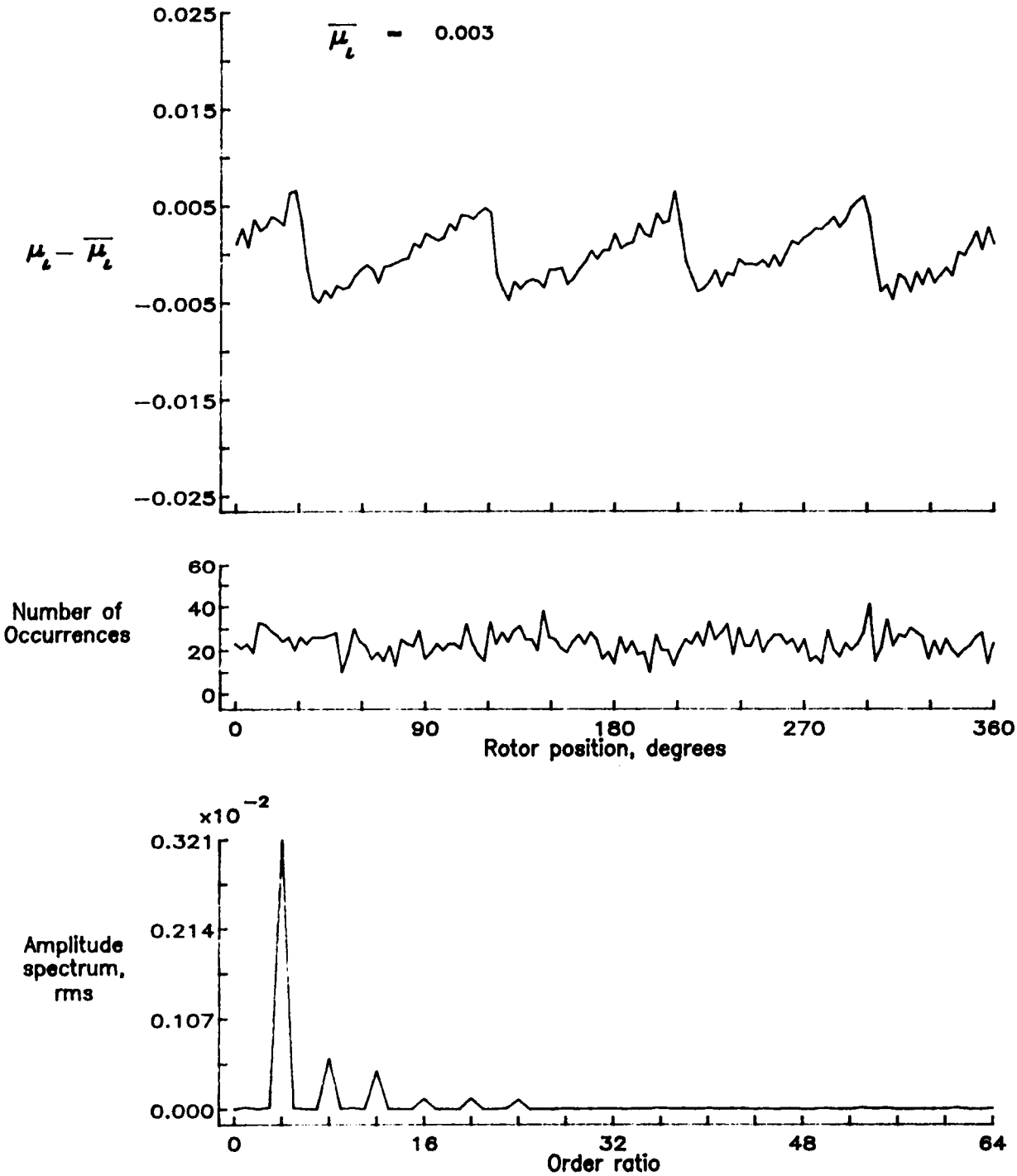

Figure 41.– Induced inflow velocity measured at 30 degrees and r/R of 1.04.

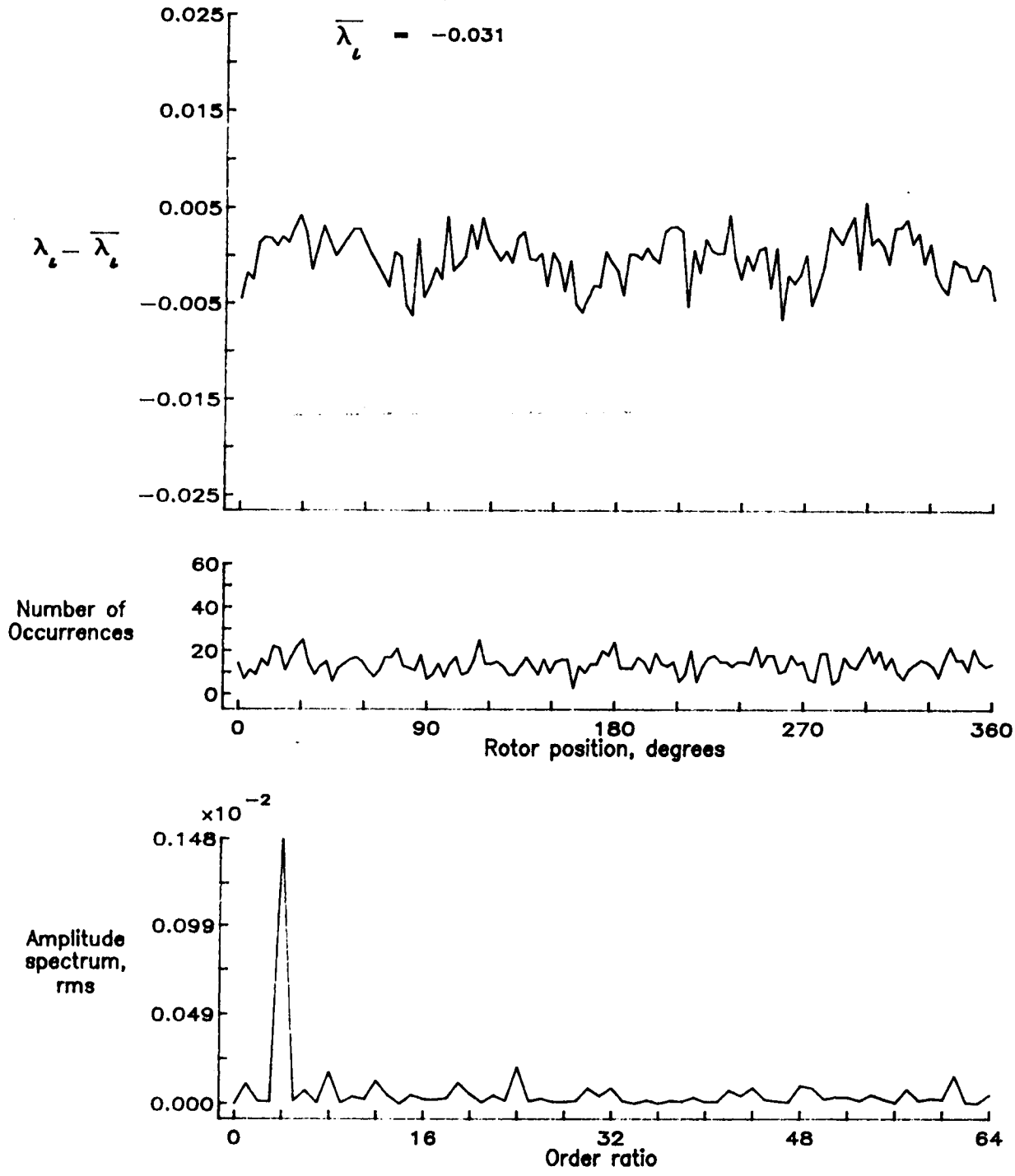

Figure 41.– Concluded.

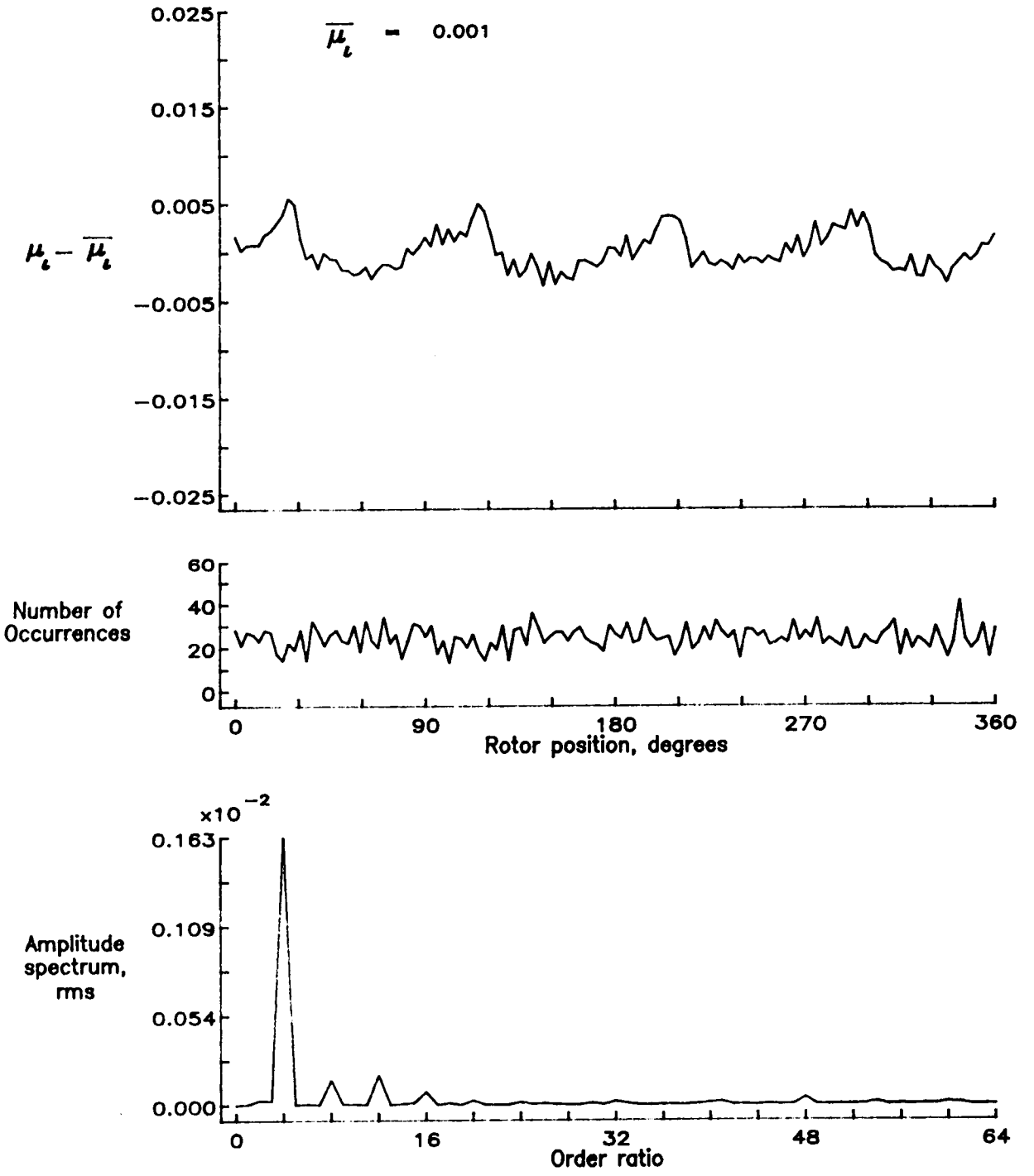

Figure 42.– Induced inflow velocity measured at 30 degrees and r/R of 1.10.

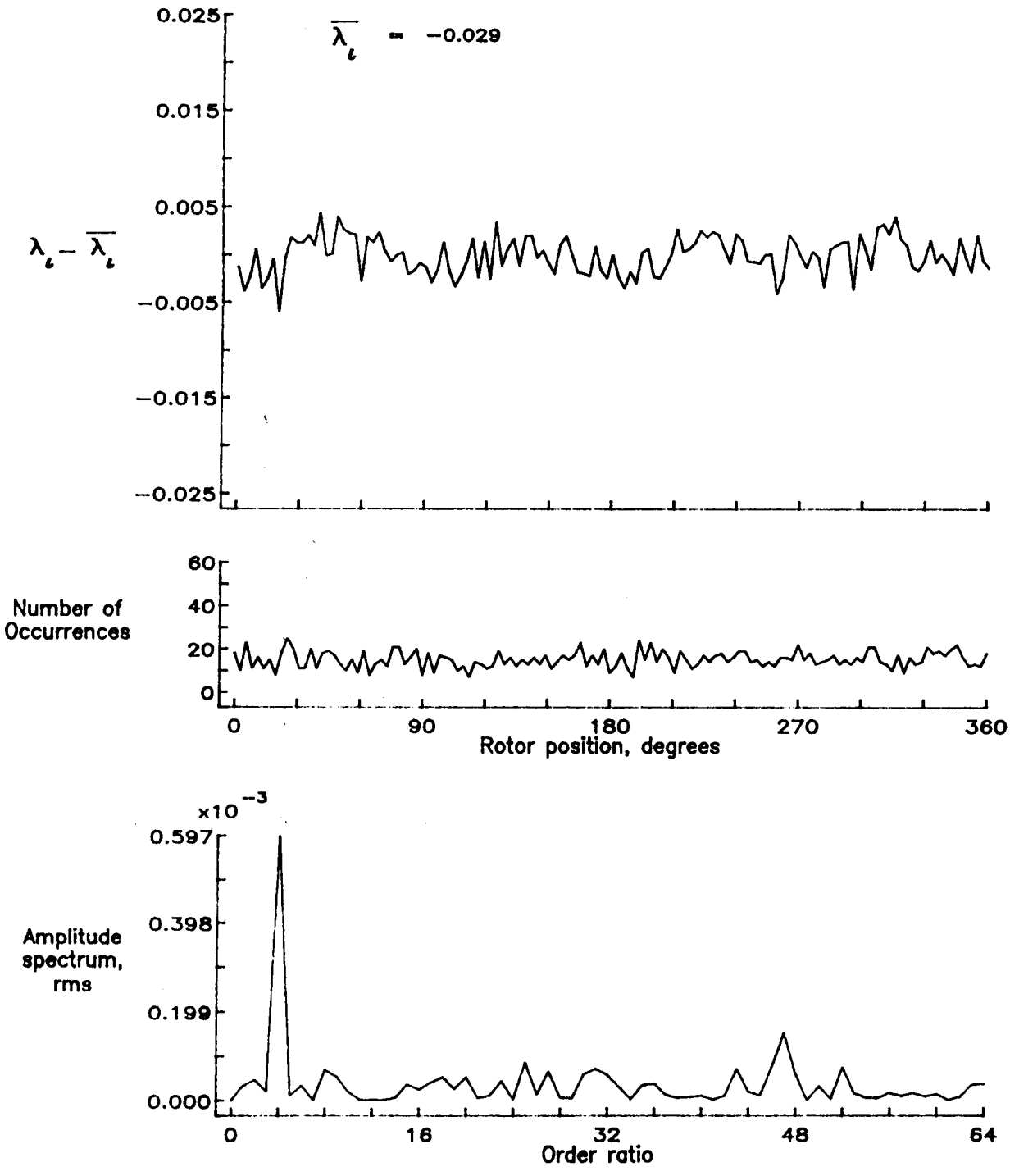

Figure 42.– Concluded.

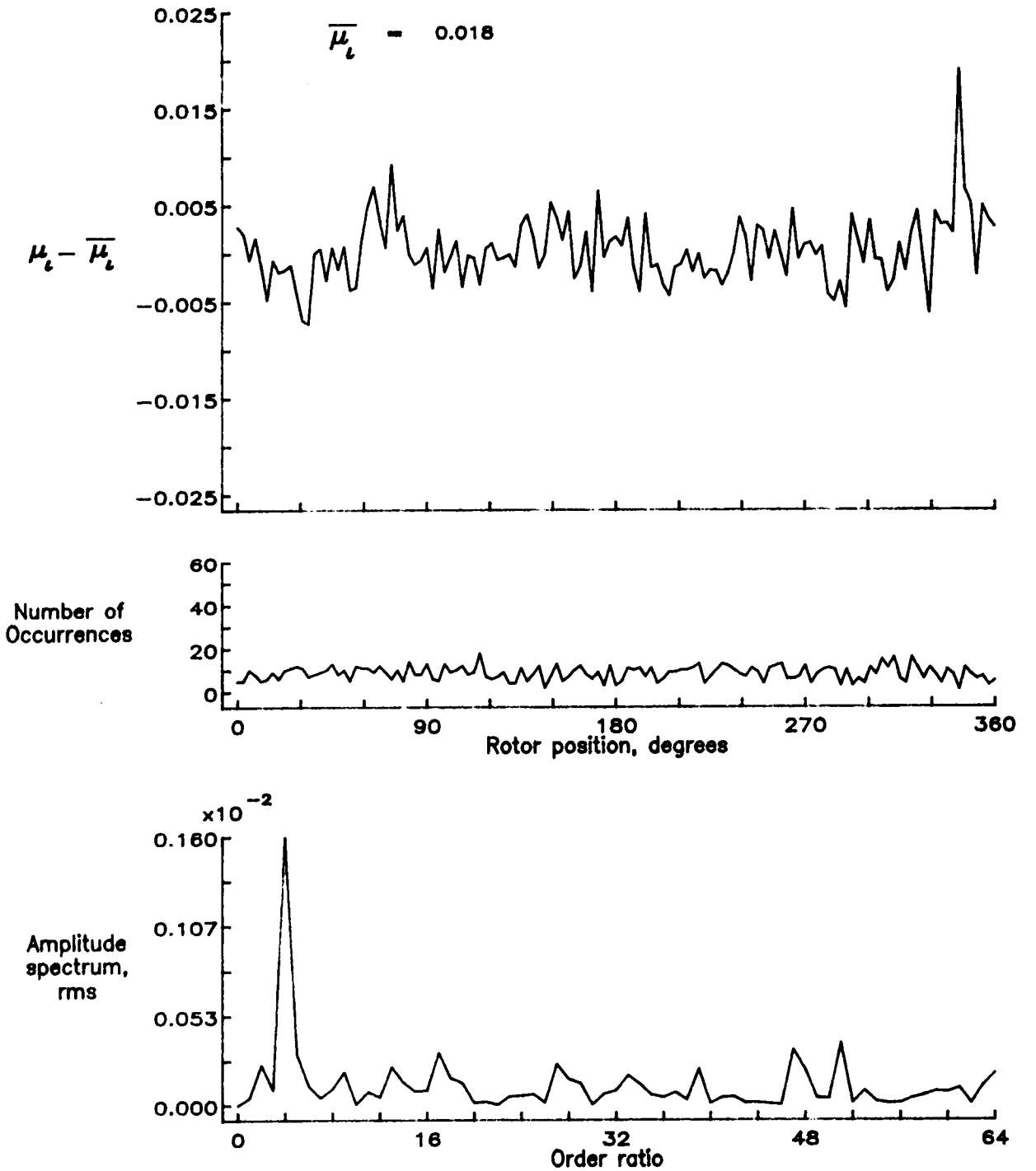

Figure 43.– Induced inflow velocity measured at 60 degrees and r/R of 0.20.

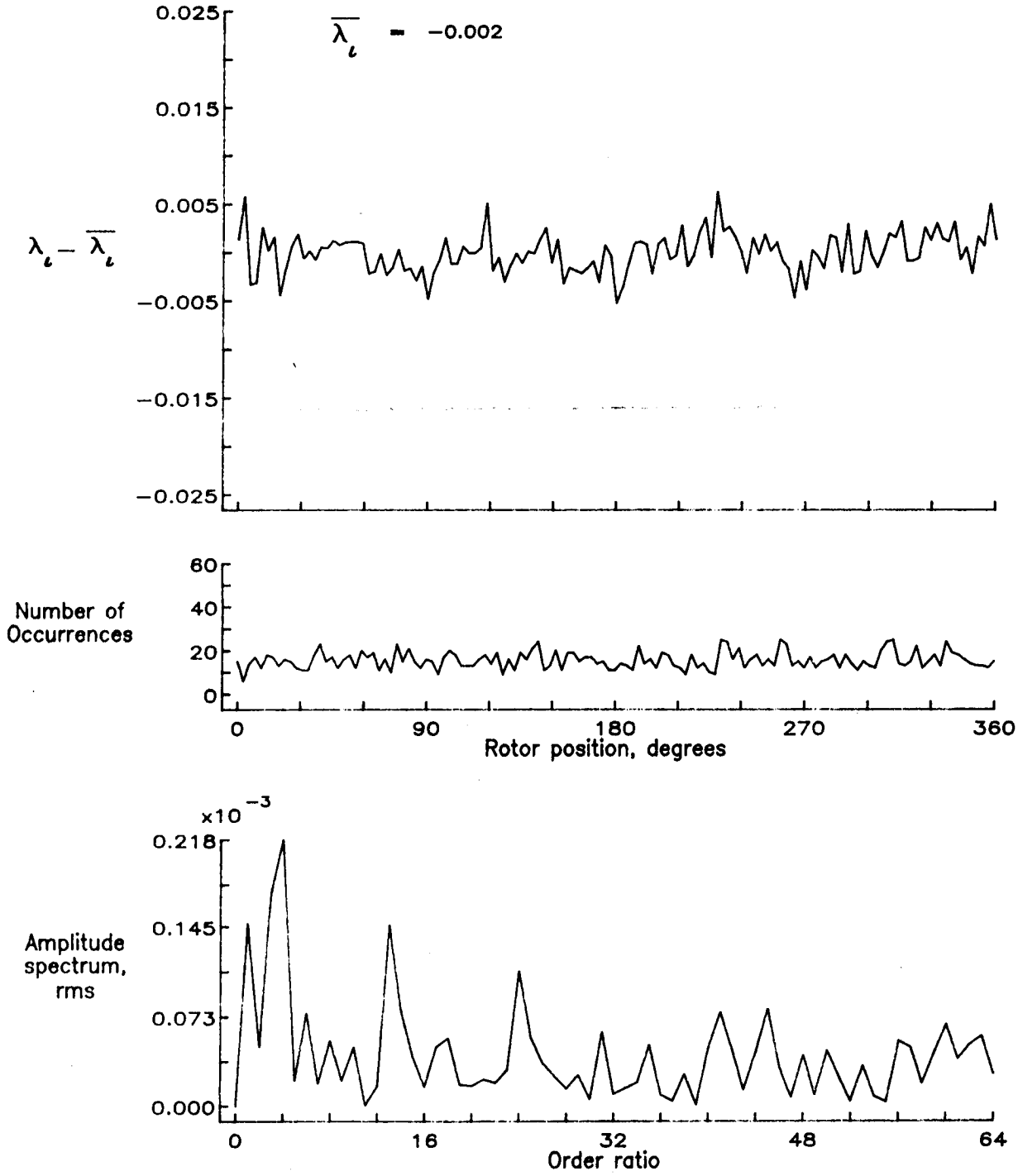

Figure 43.– Concluded.

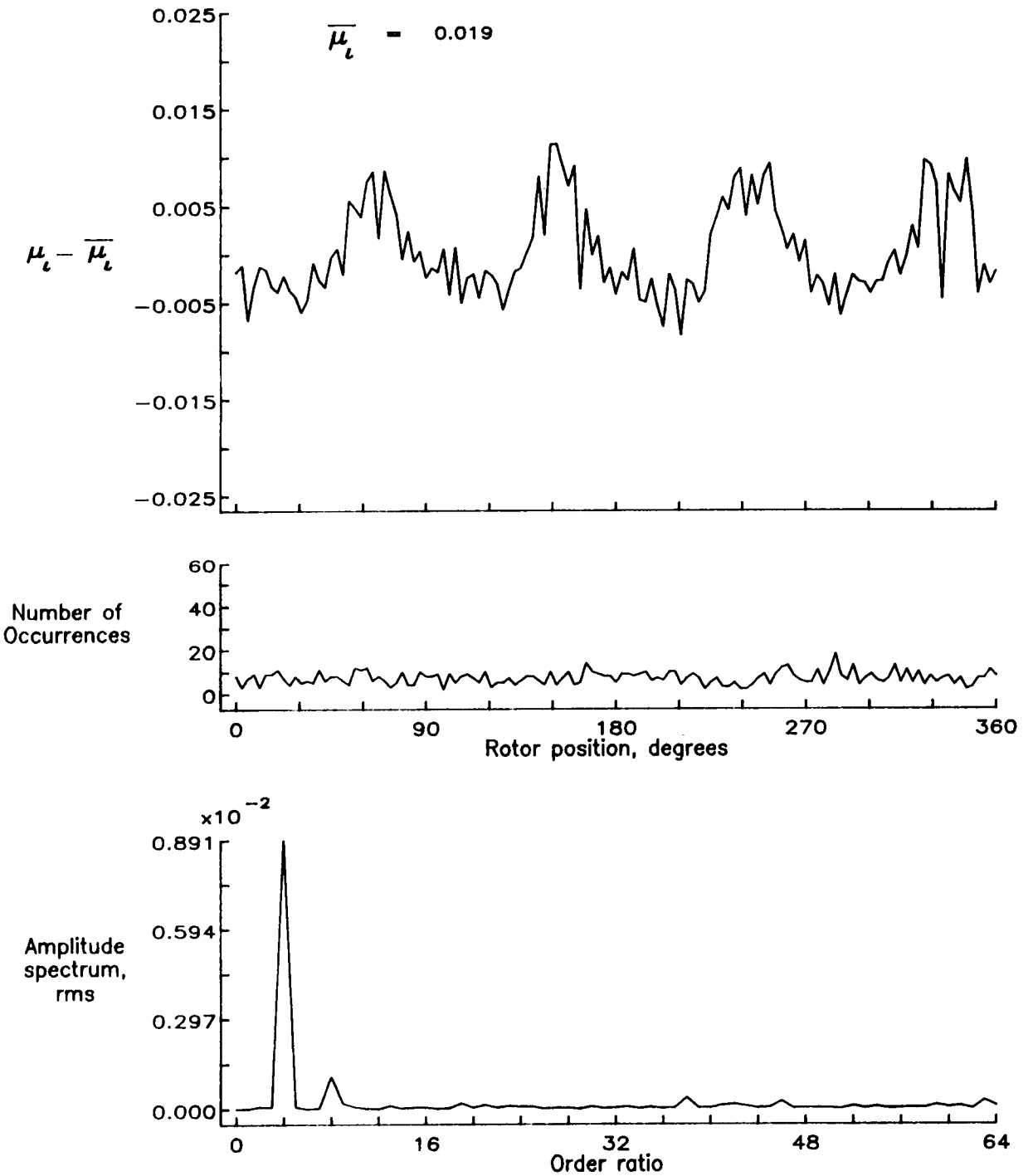

Figure 44.– Induced inflow velocity measured at 60 degrees and r/R of 0.40.

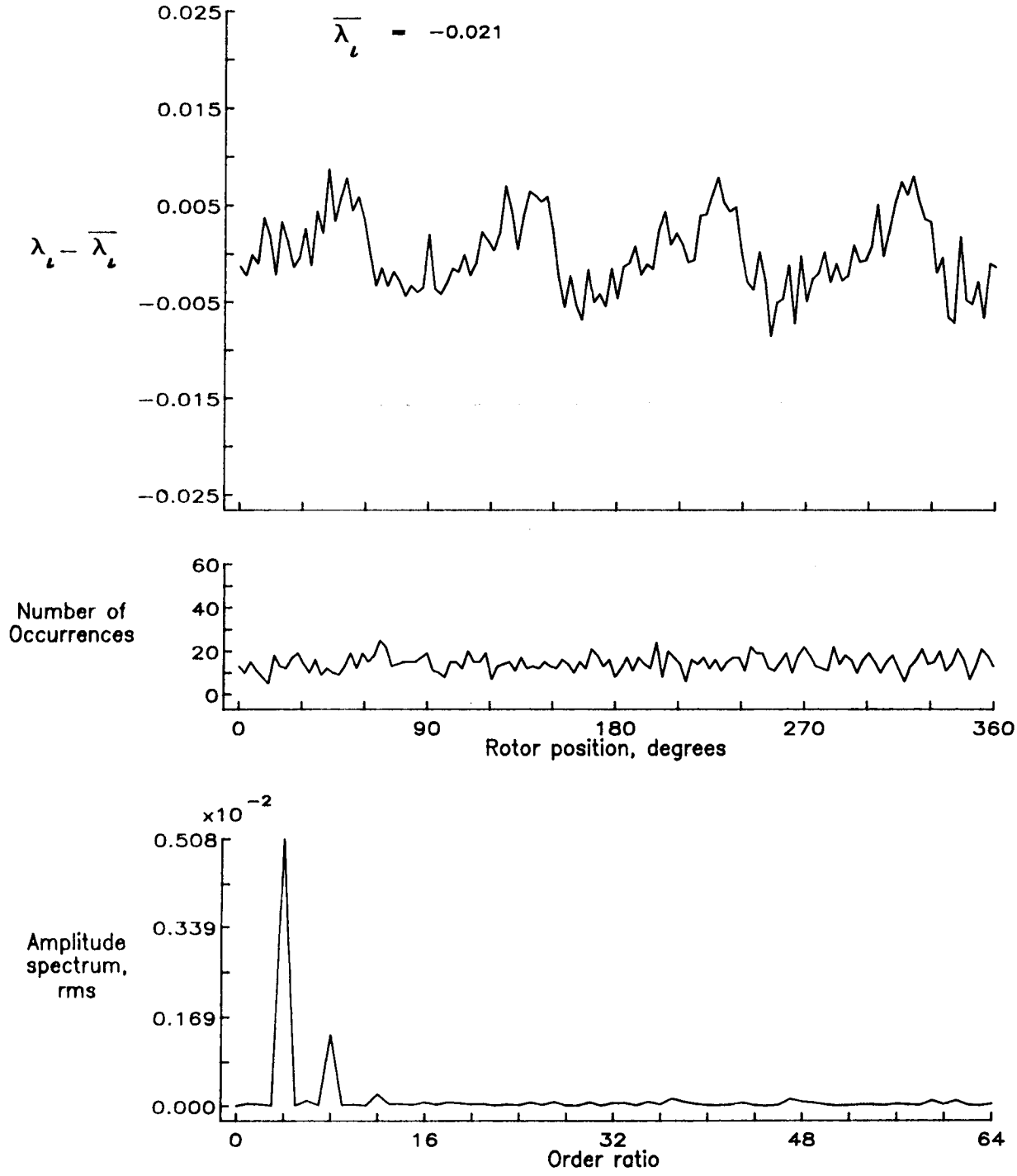

Figure 44.– Concluded.

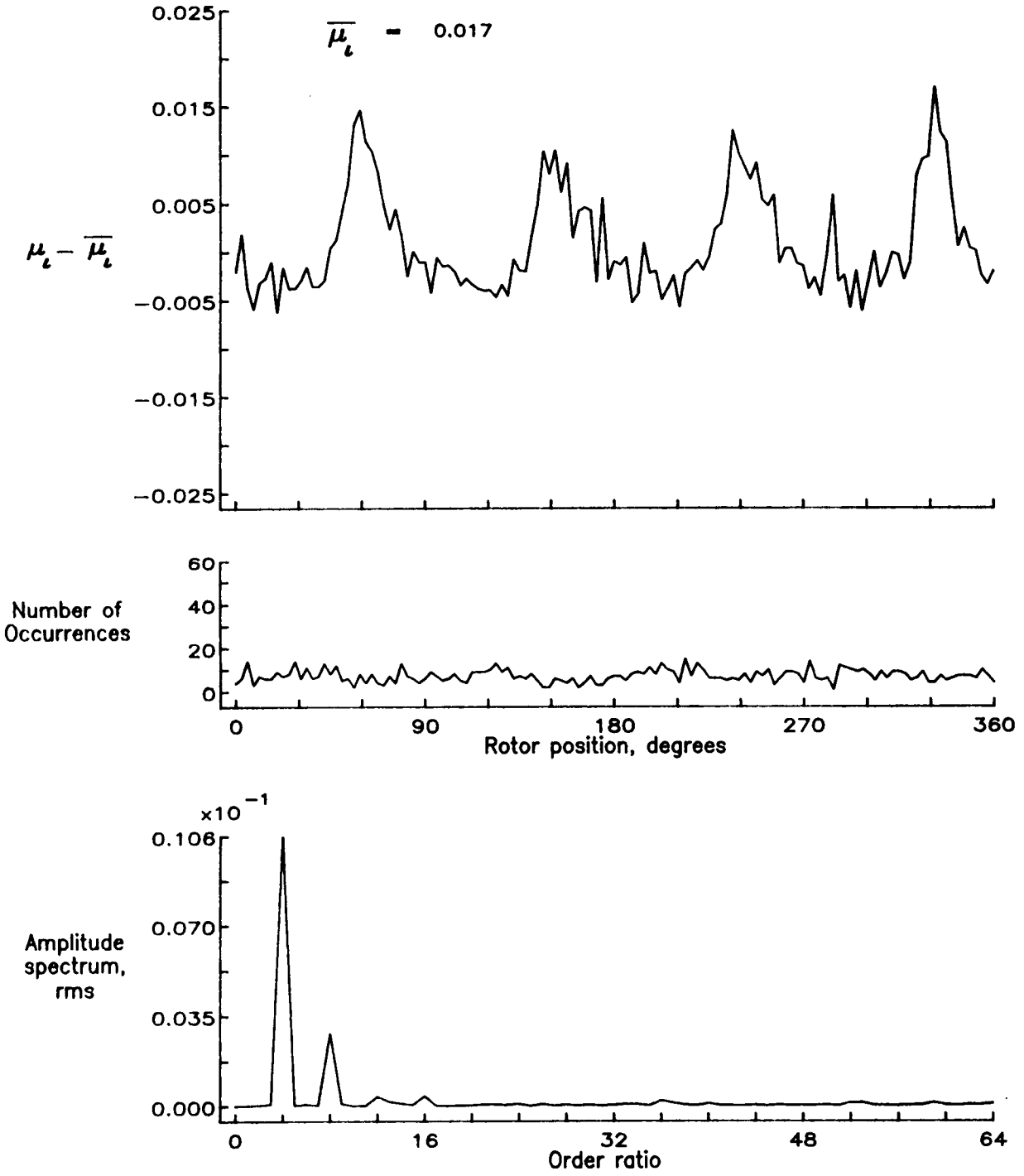

Figure 45.– Induced inflow velocity measured at 60 degrees and r/R of 0.50.

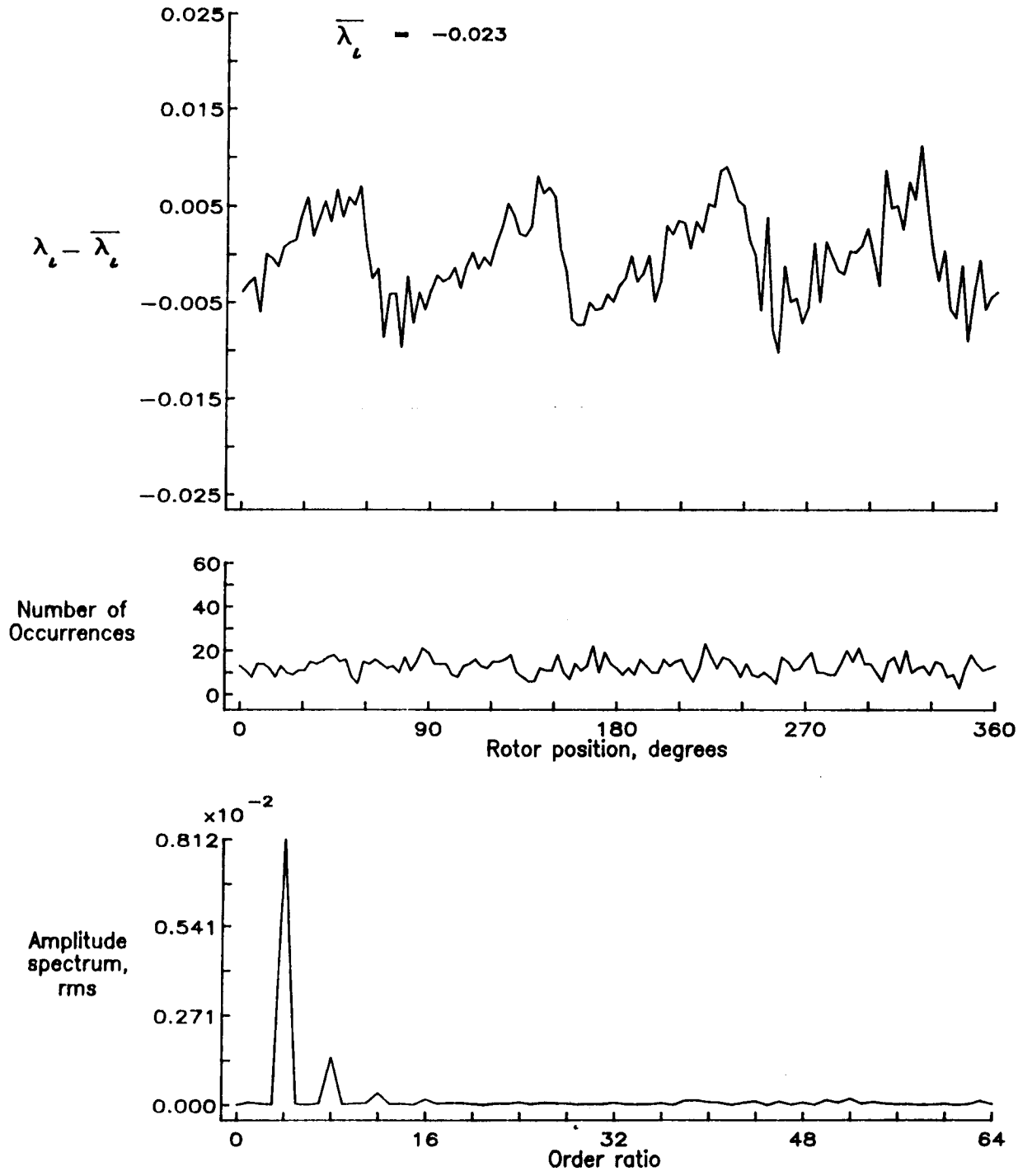

Figure 45.– Concluded.

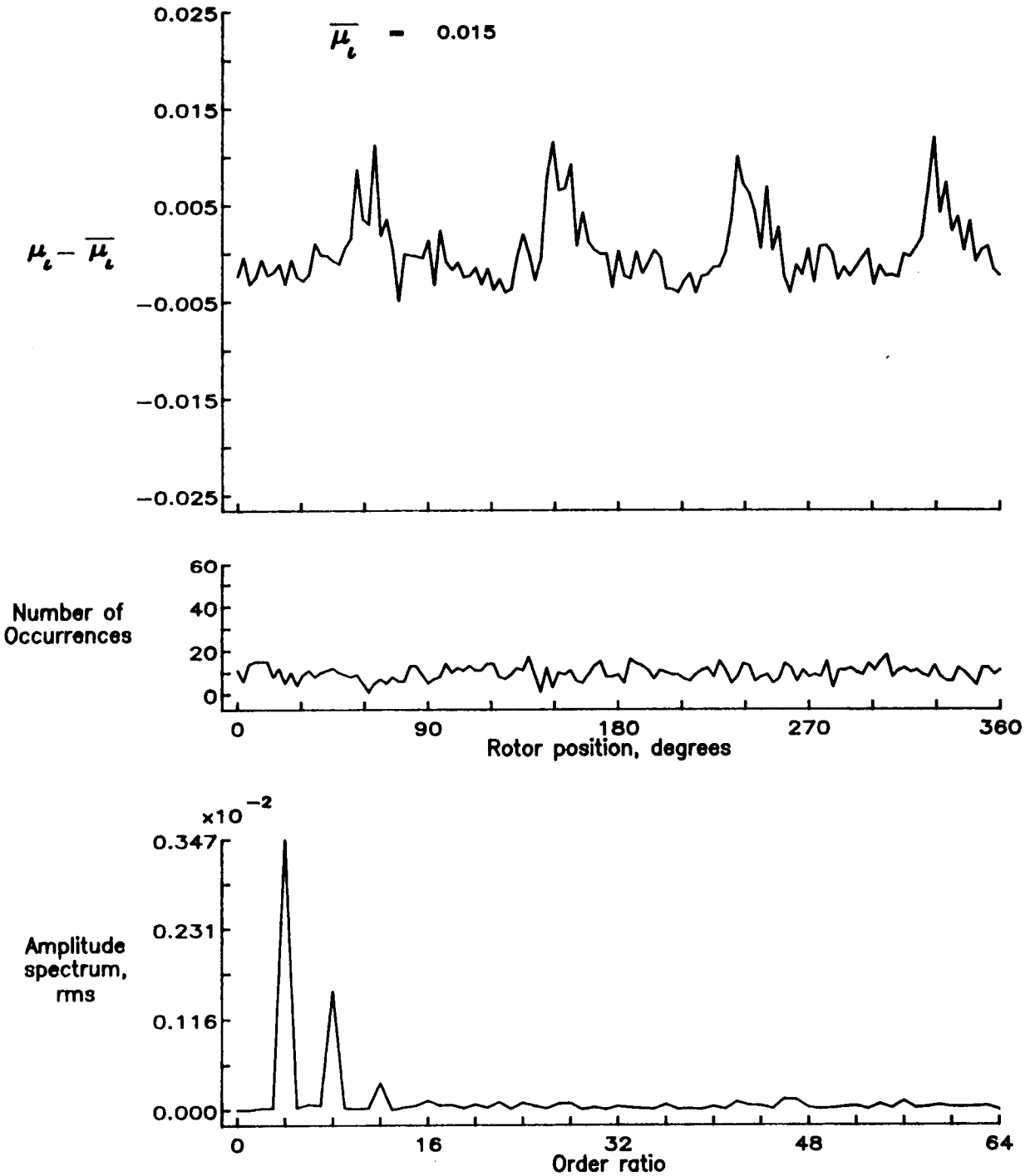

Figure 46.– Induced inflow velocity measured at 60 degrees and r/R of 0.60.

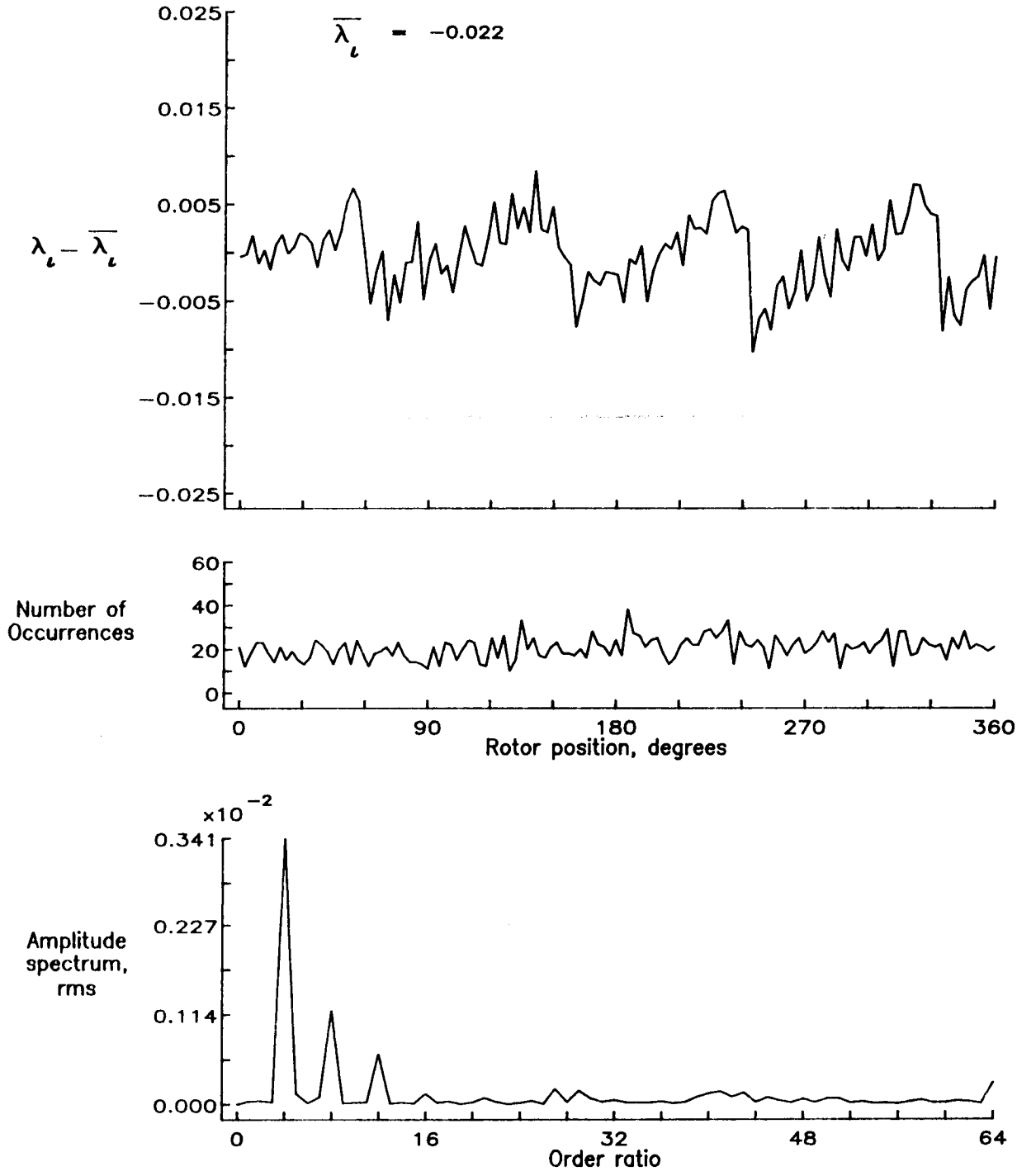

Figure 46.– Concluded.

C-2

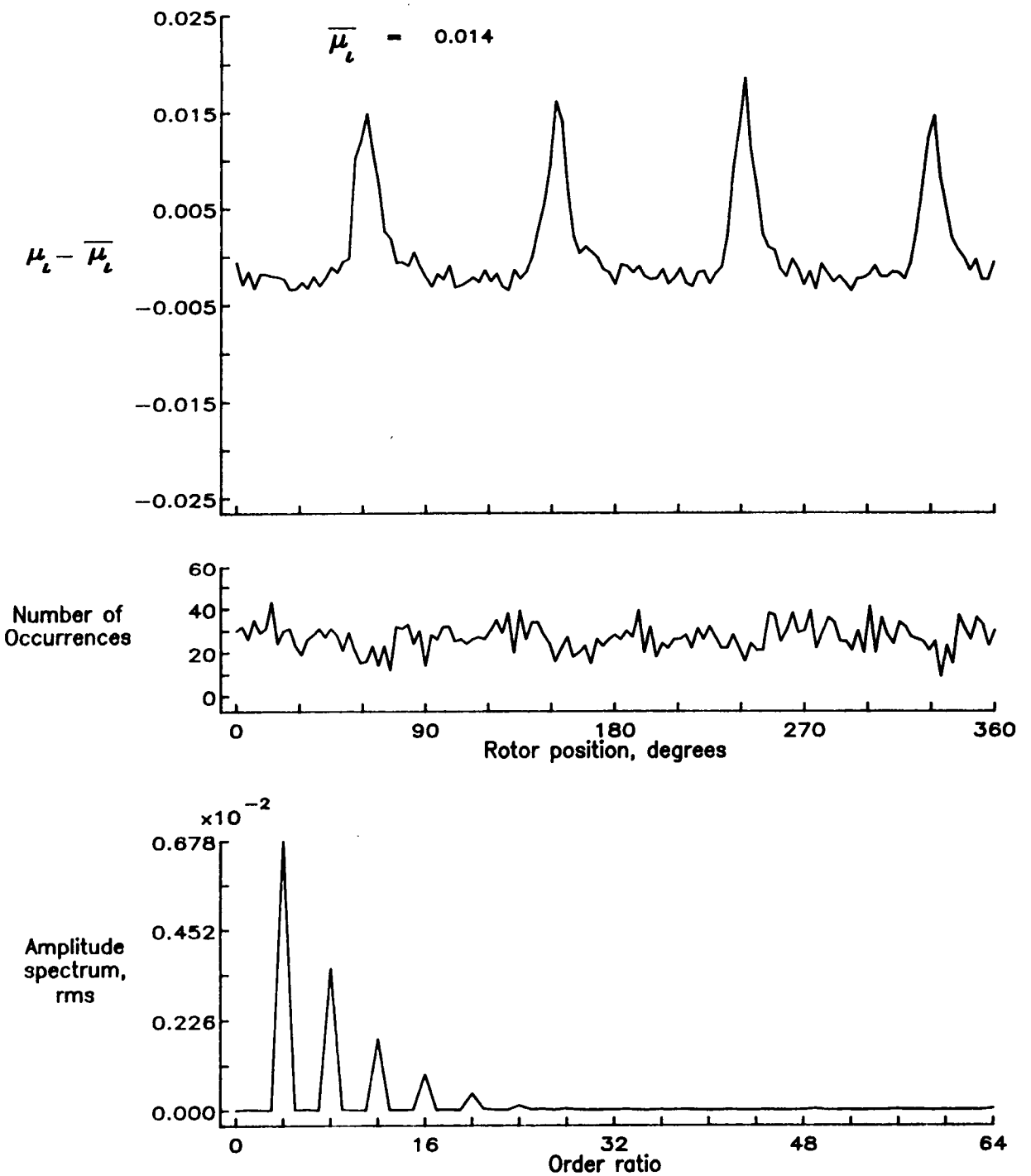

Figure 47.– Induced inflow velocity measured at 60 degrees and r/R of 0.70.

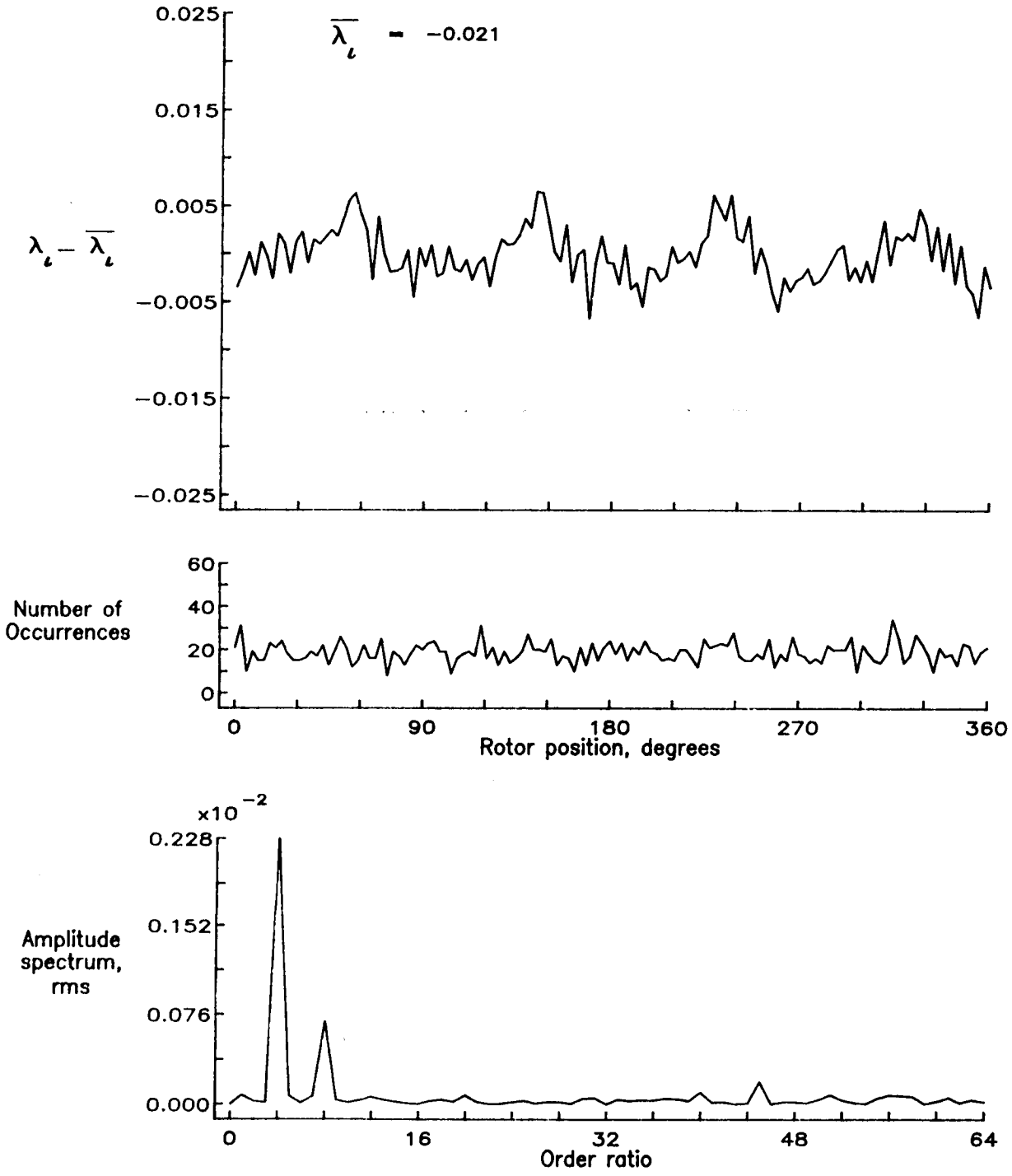

Figure 47.– Concluded.

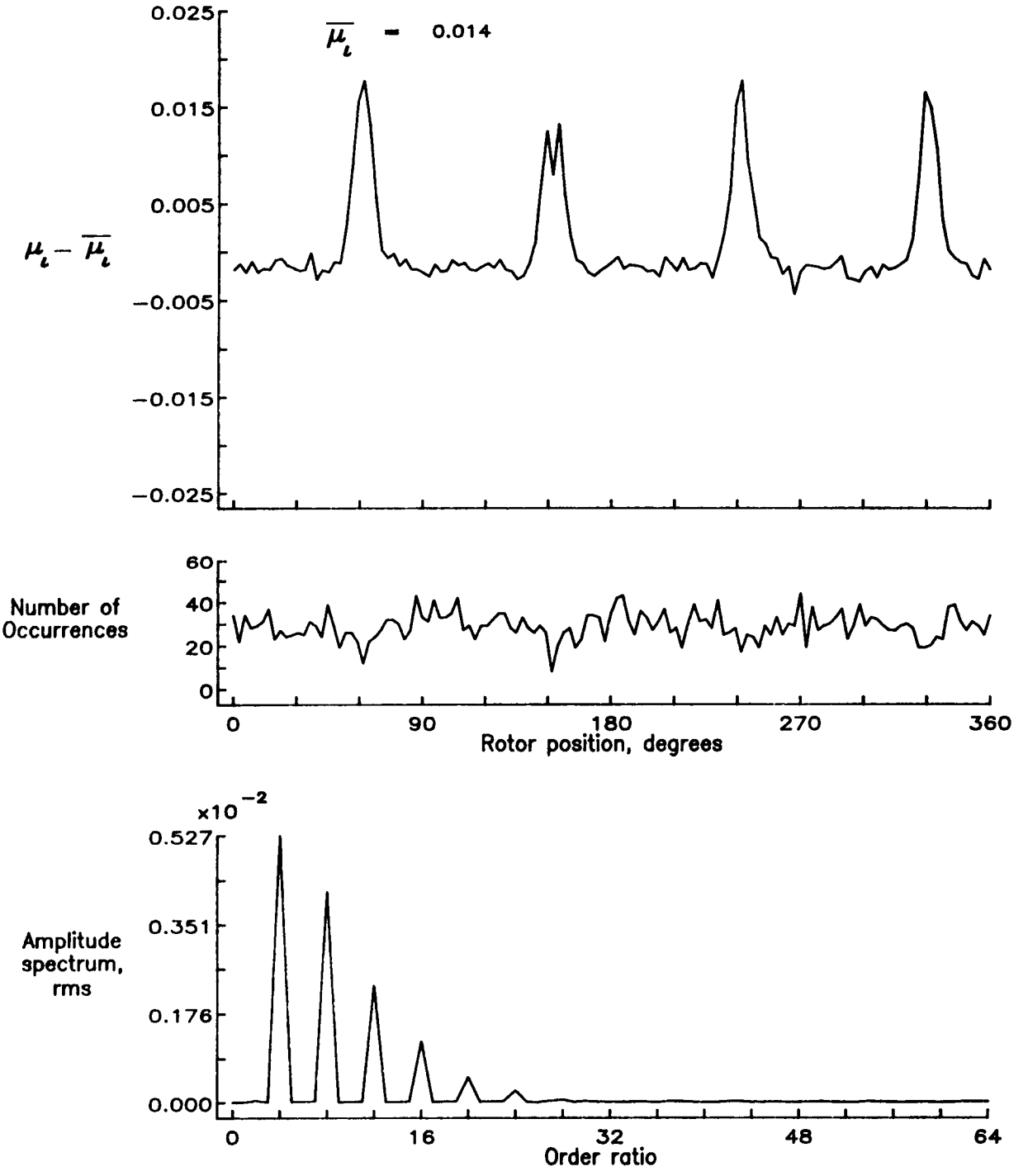

Figure 48.– Induced inflow velocity measured at 60 degrees and r/R of 0.74.

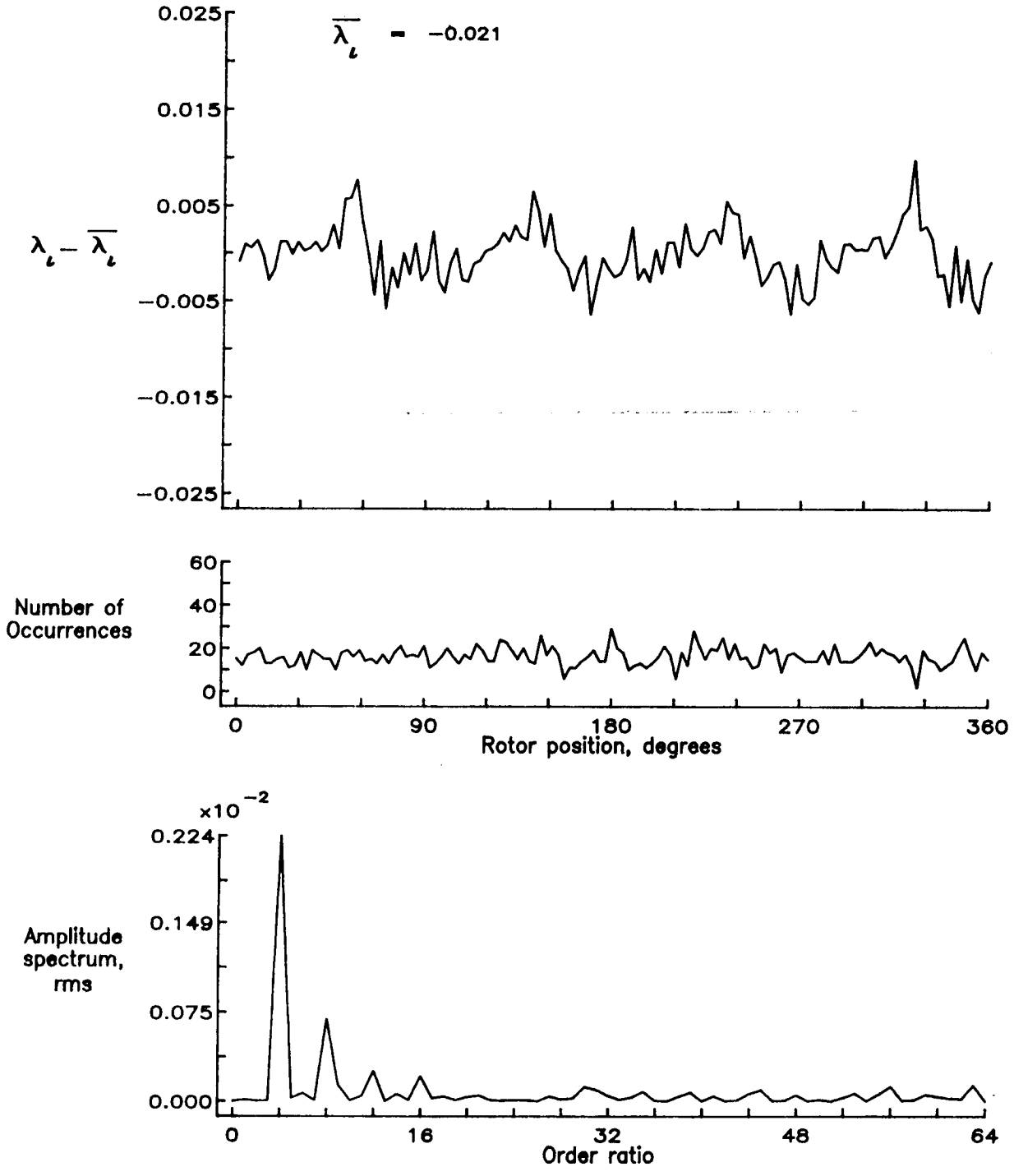

Figure 48.– Concluded.

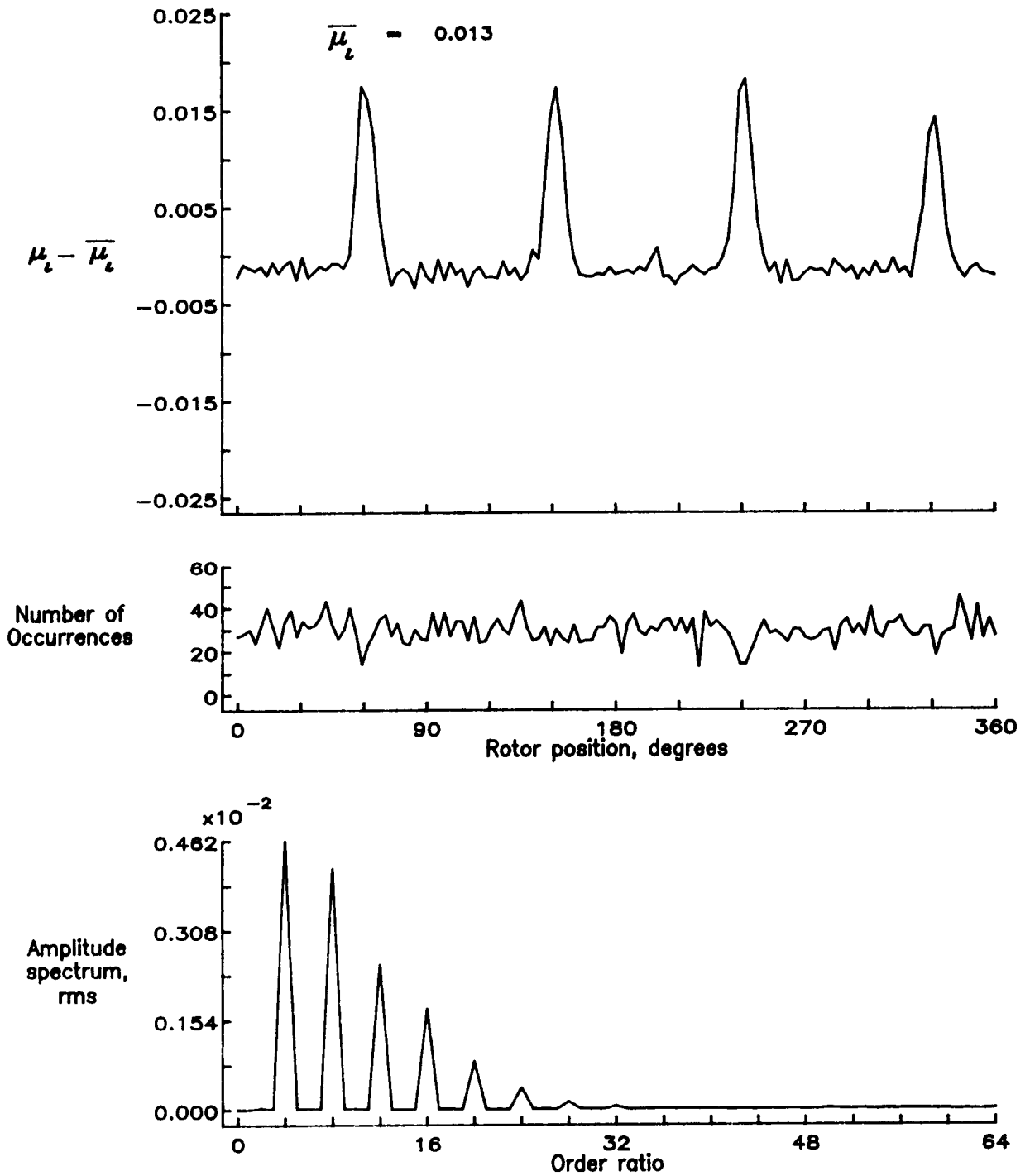

Figure 49.– Induced inflow velocity measured at 60 degrees and r/R of 0.78.

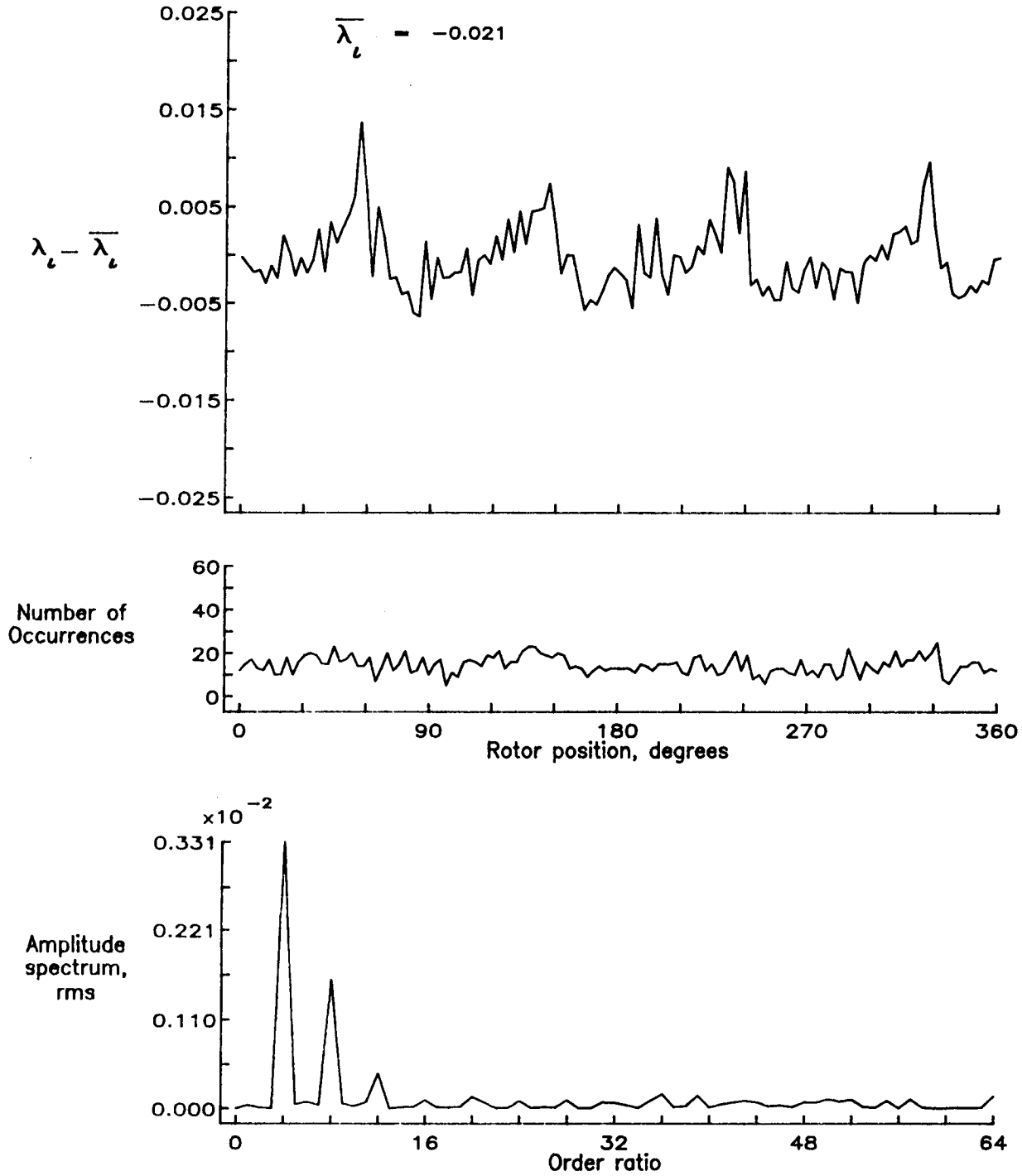

Figure 49.– Concluded.

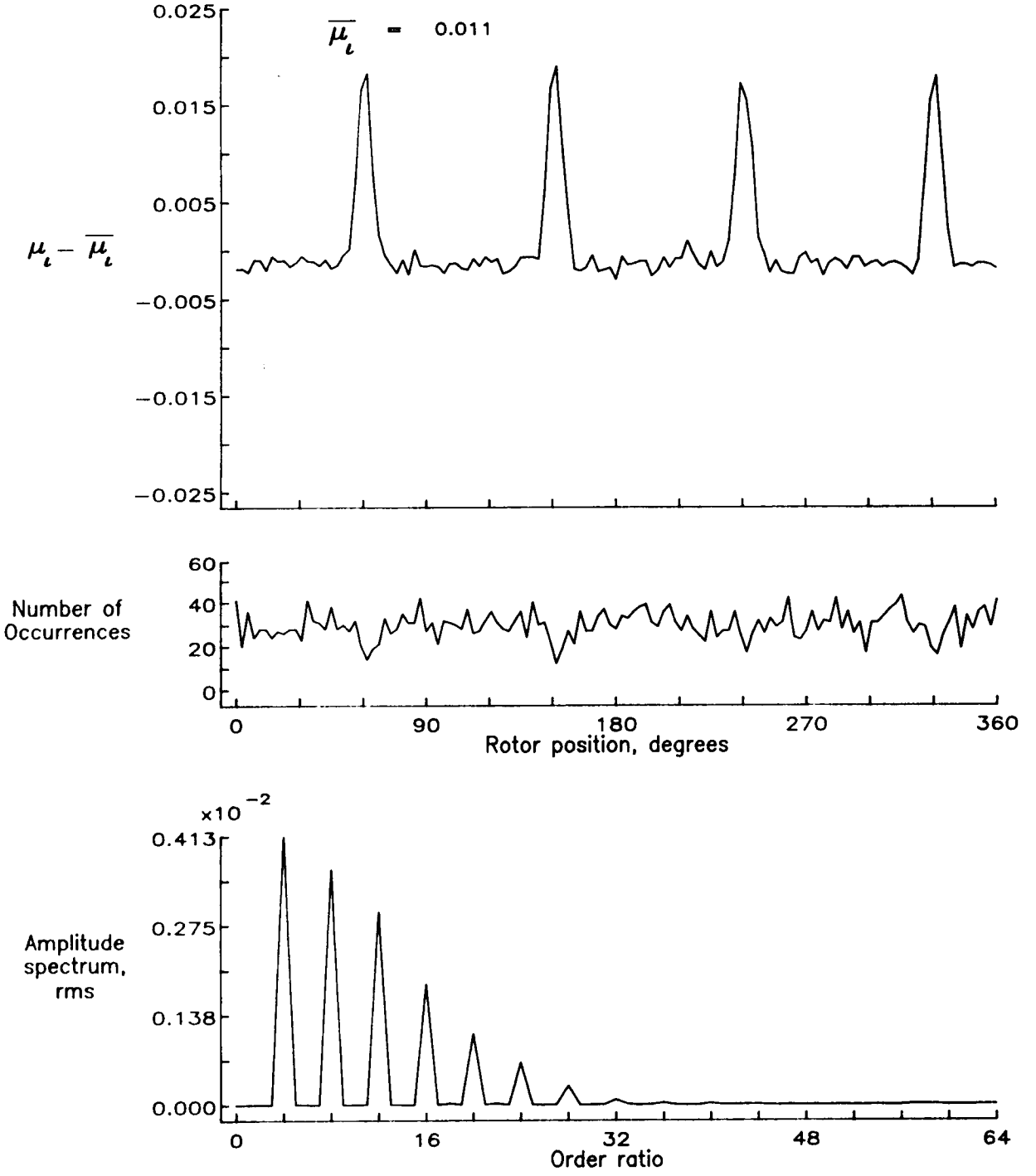

Figure 50.– Induced inflow velocity measured at 60 degrees and r/R of 0.82.

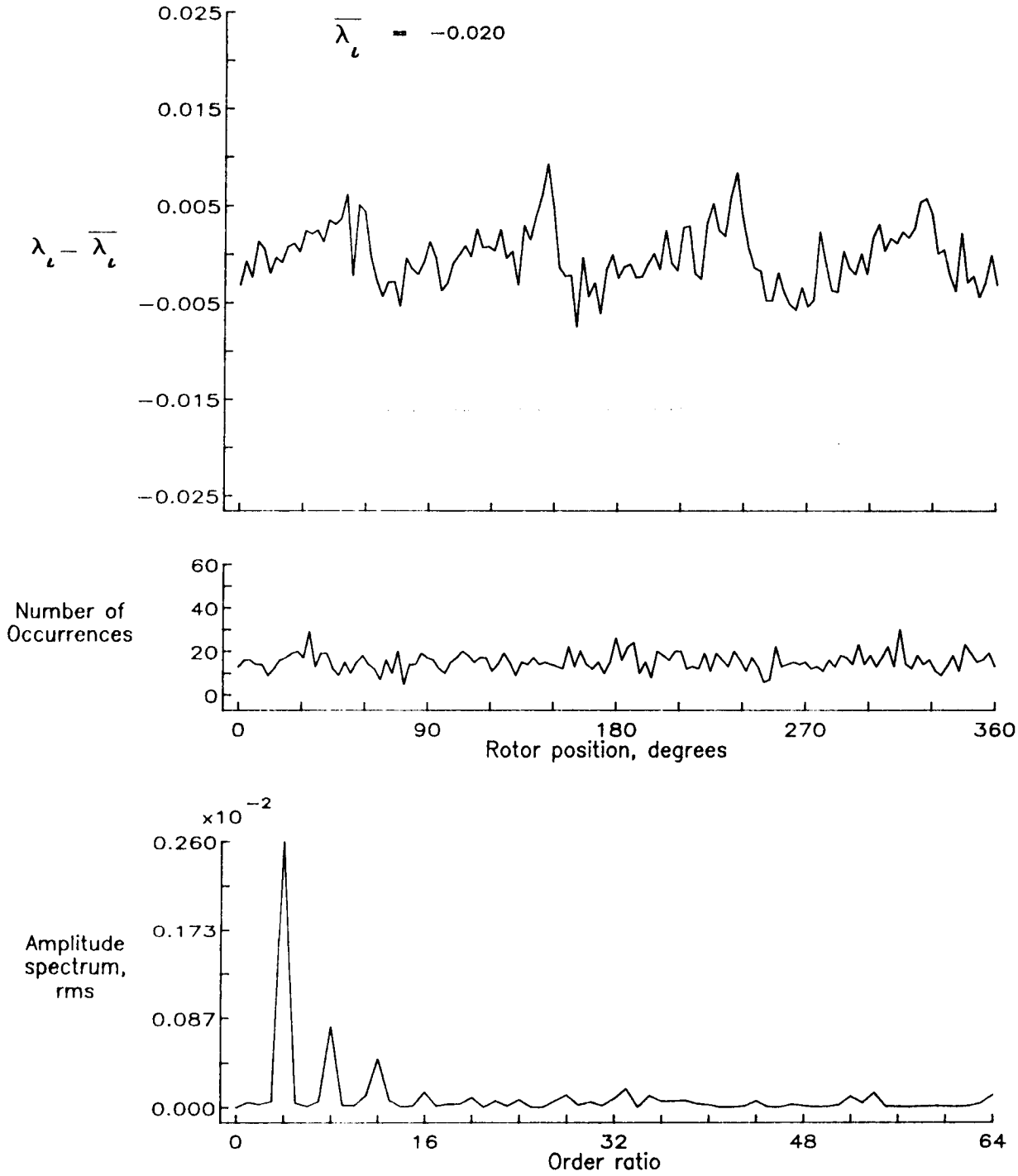

Figure 50.– Concluded.

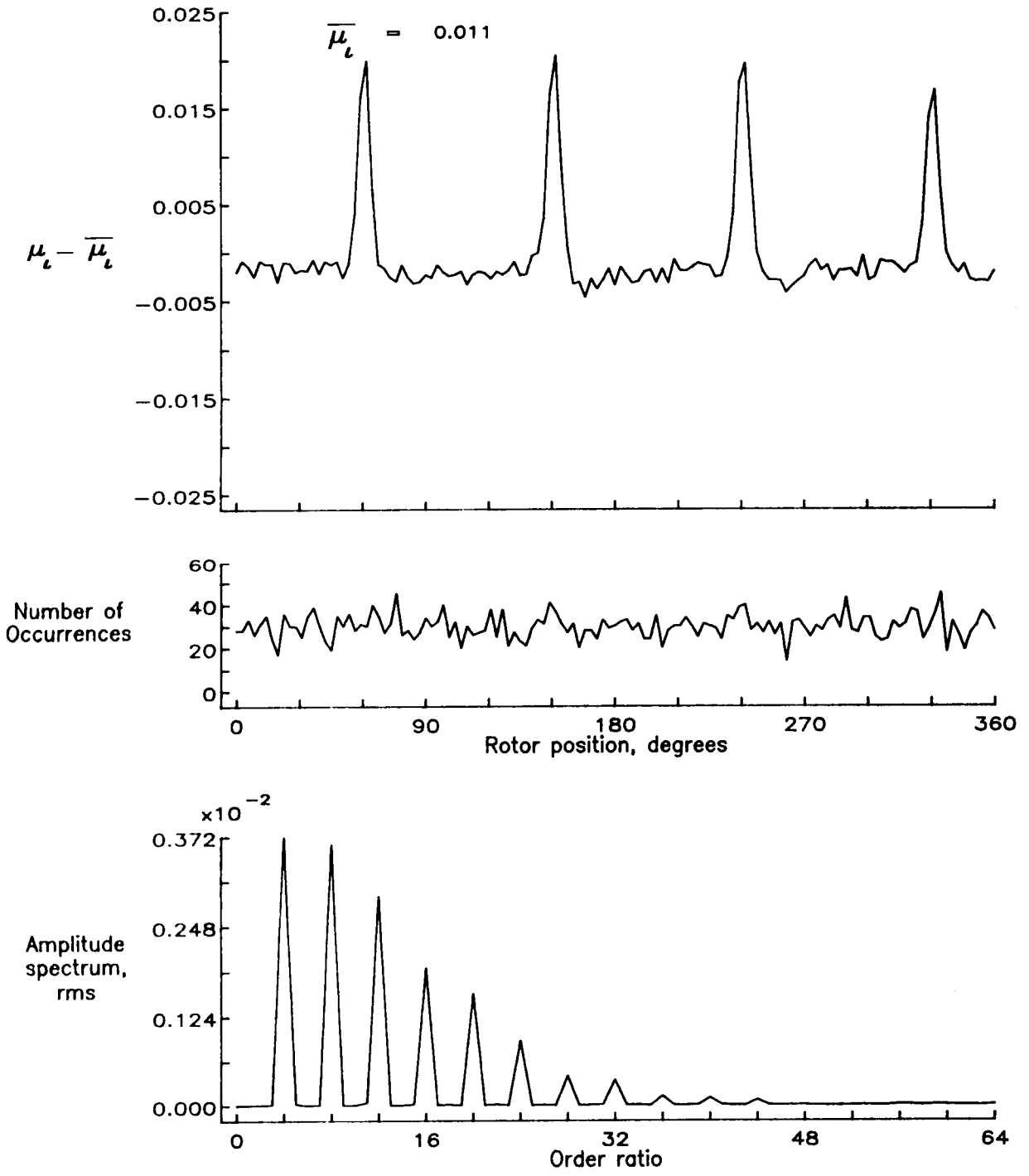

Figure 51.– Induced inflow velocity measured at 60 degrees and r/R of 0.86.

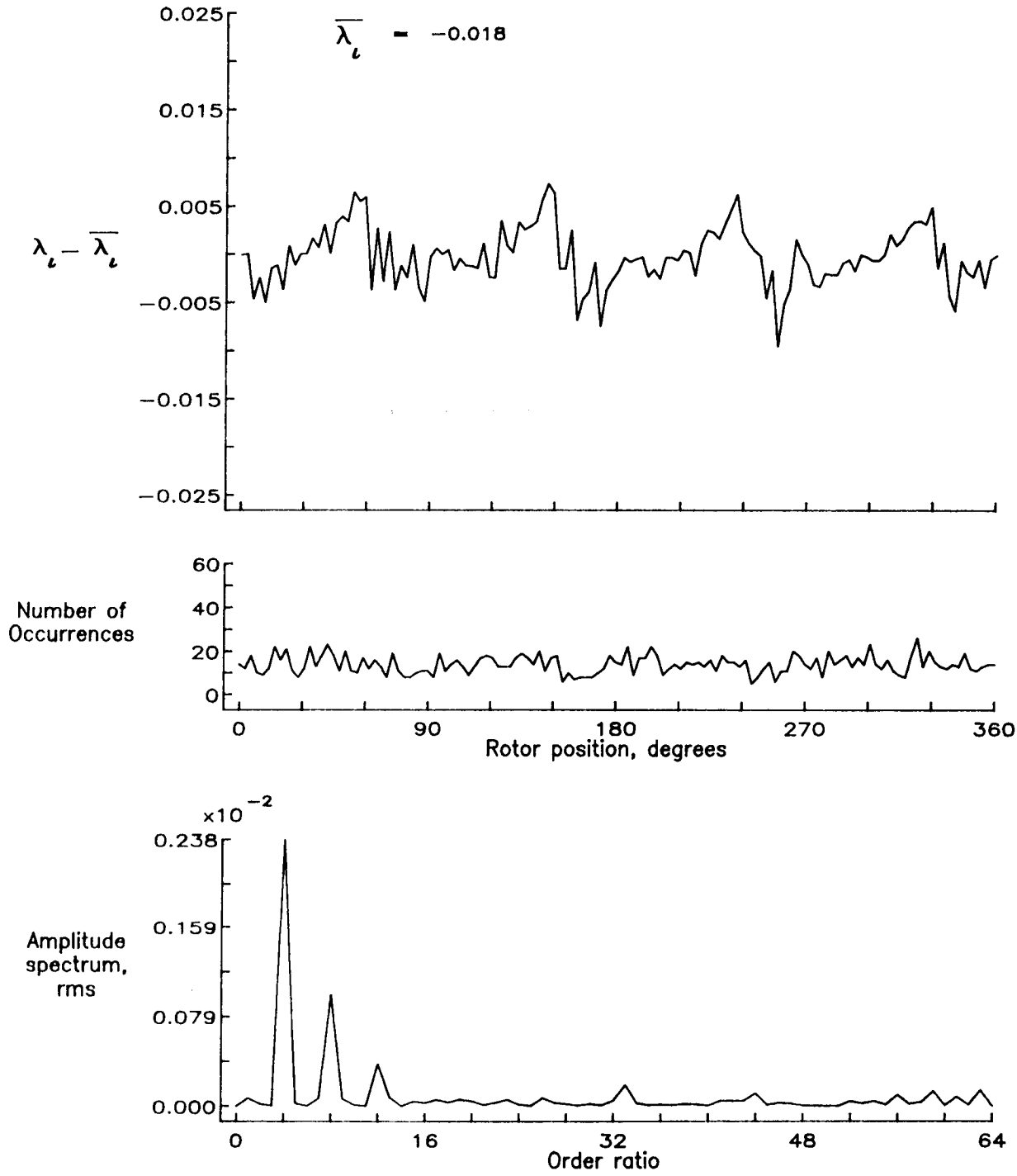

Figure 51.– Concluded.

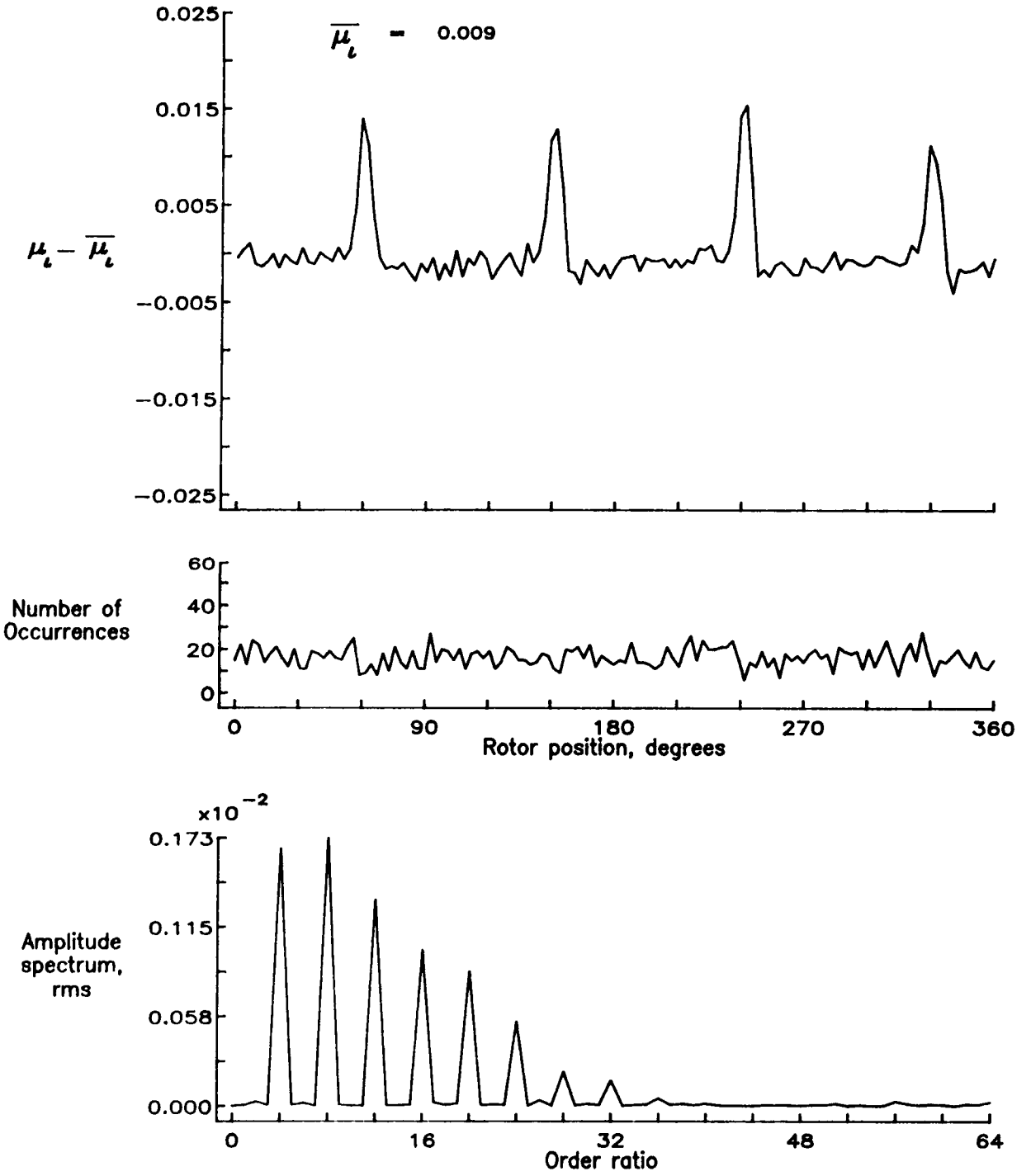

Figure 52.– Induced inflow velocity measured at 60 degrees and r/R of 0.90.

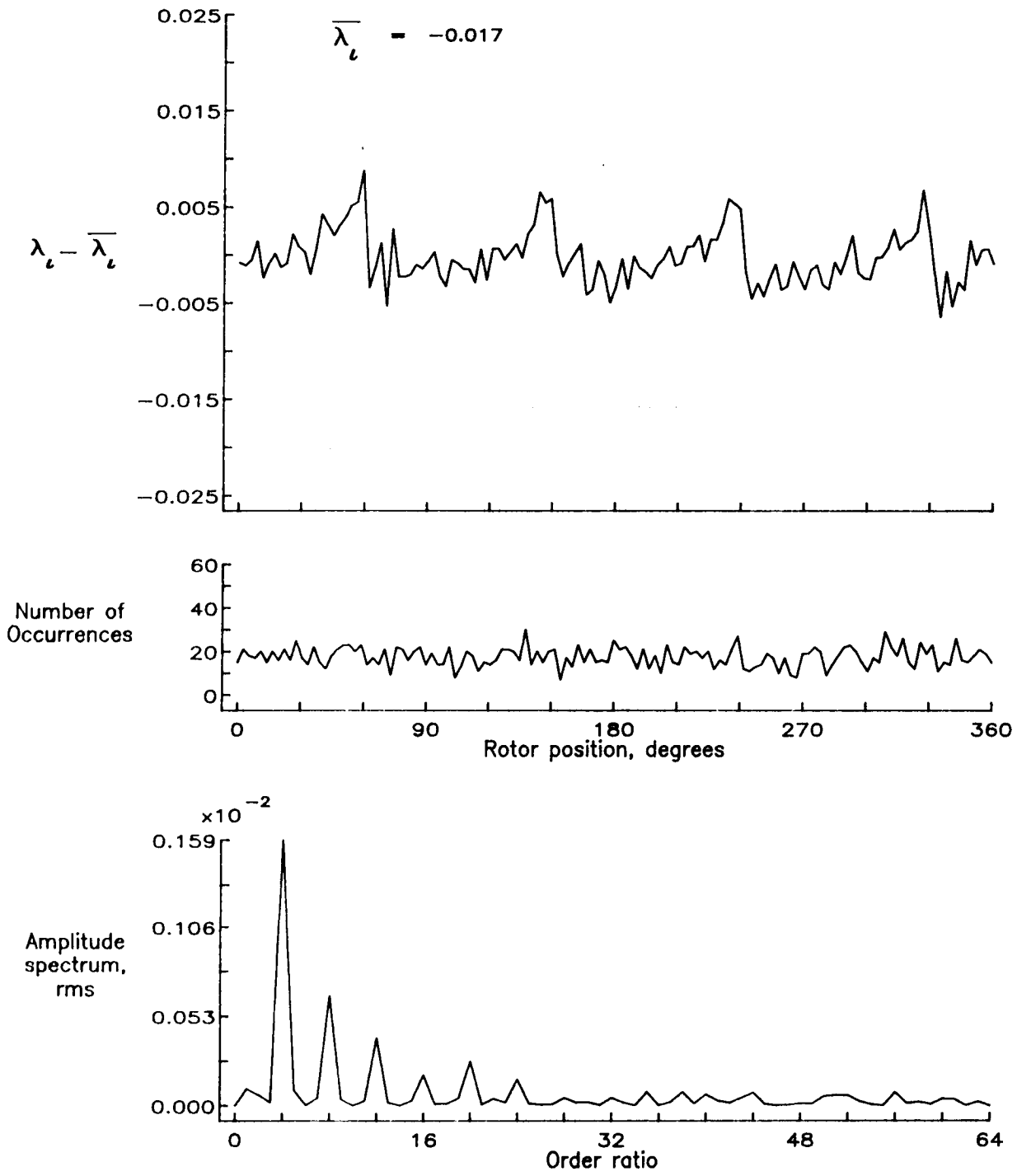

Figure 52.– Concluded.

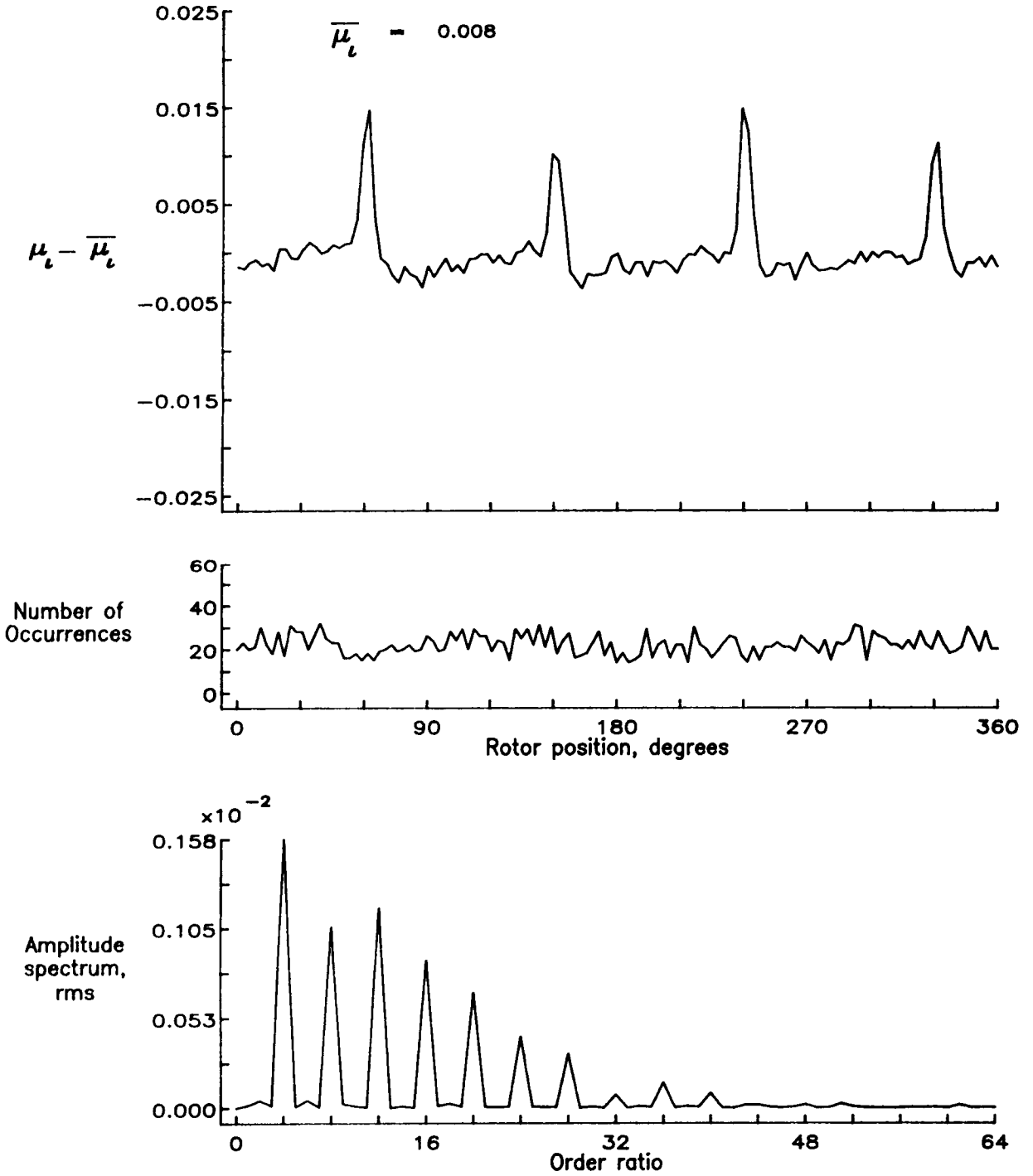

Figure 53.– Induced inflow velocity measured at 60 degrees and r/R of 0.94.

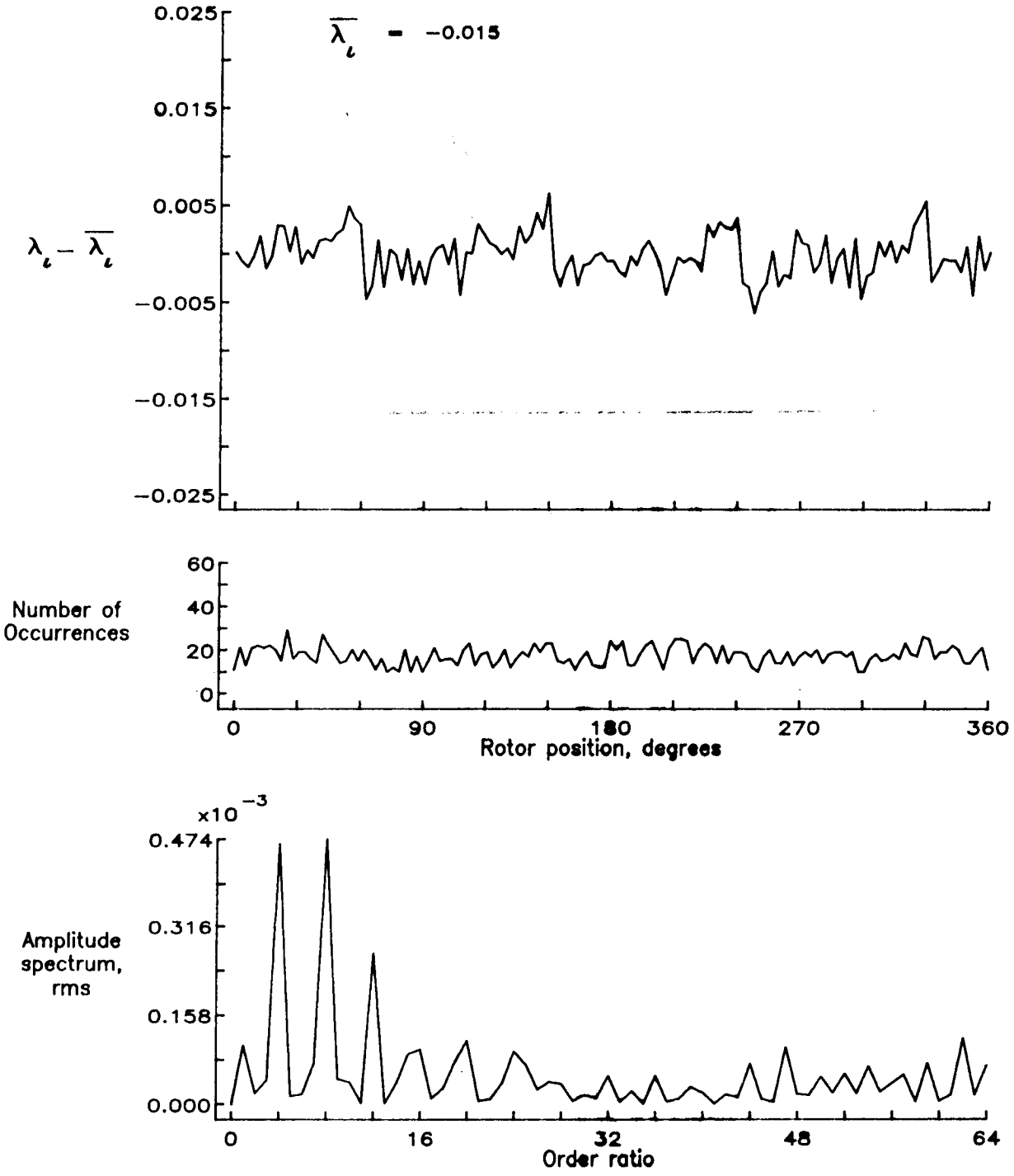

Figure 53.– Concluded.

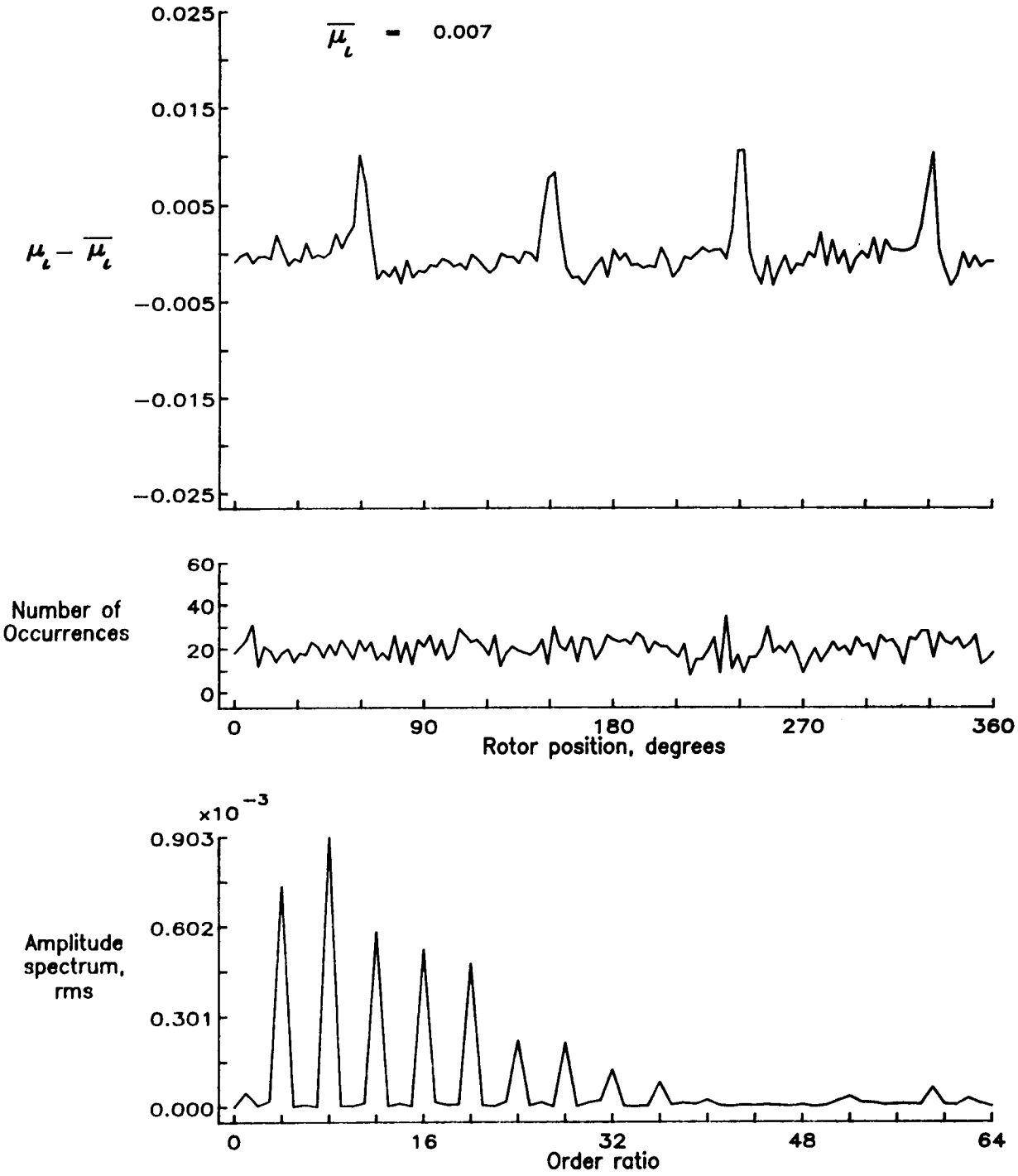

Figure 54.– Induced inflow velocity measured at 60 degrees and r/R of 0.98.

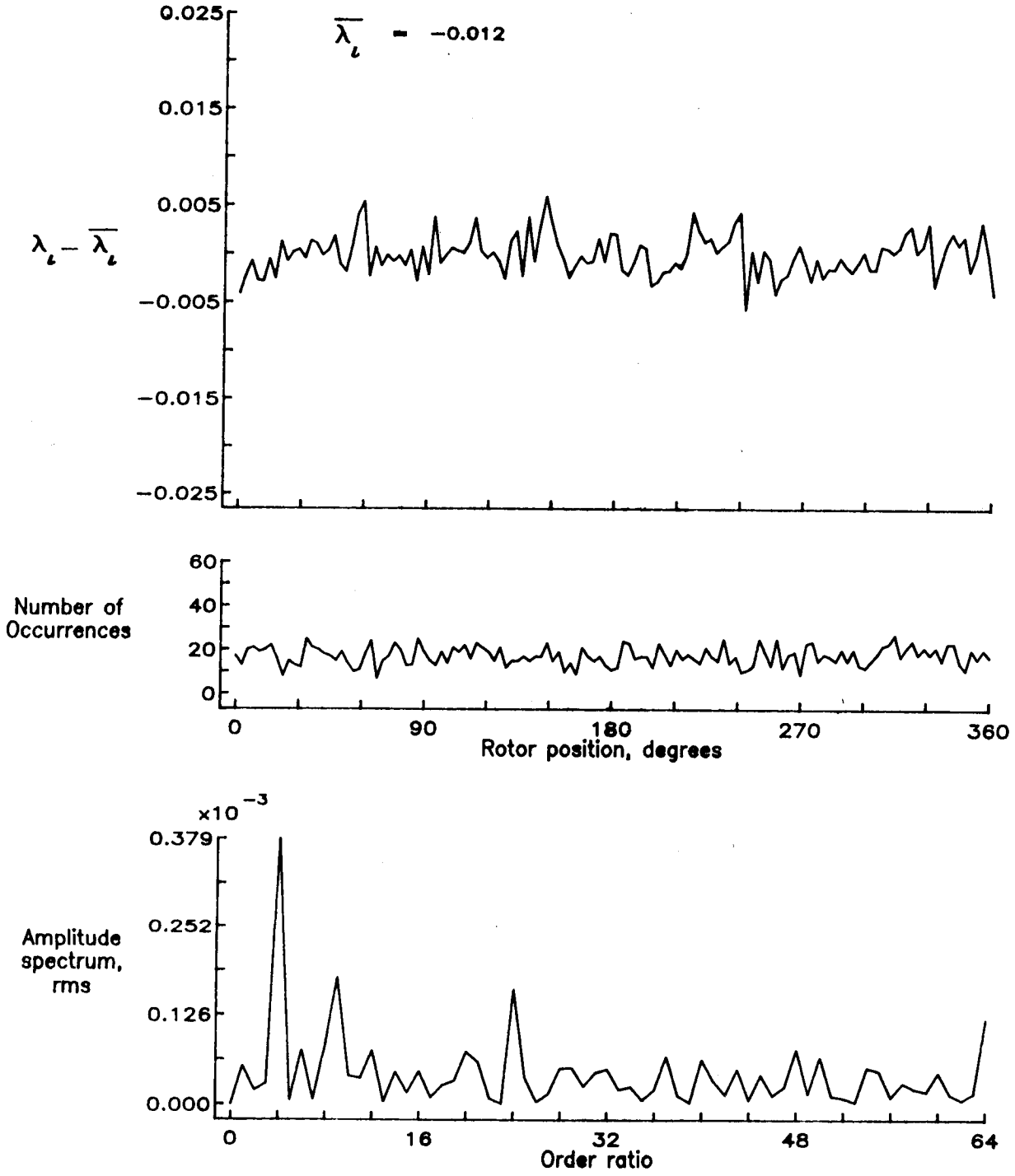

Figure 54.– Concluded.

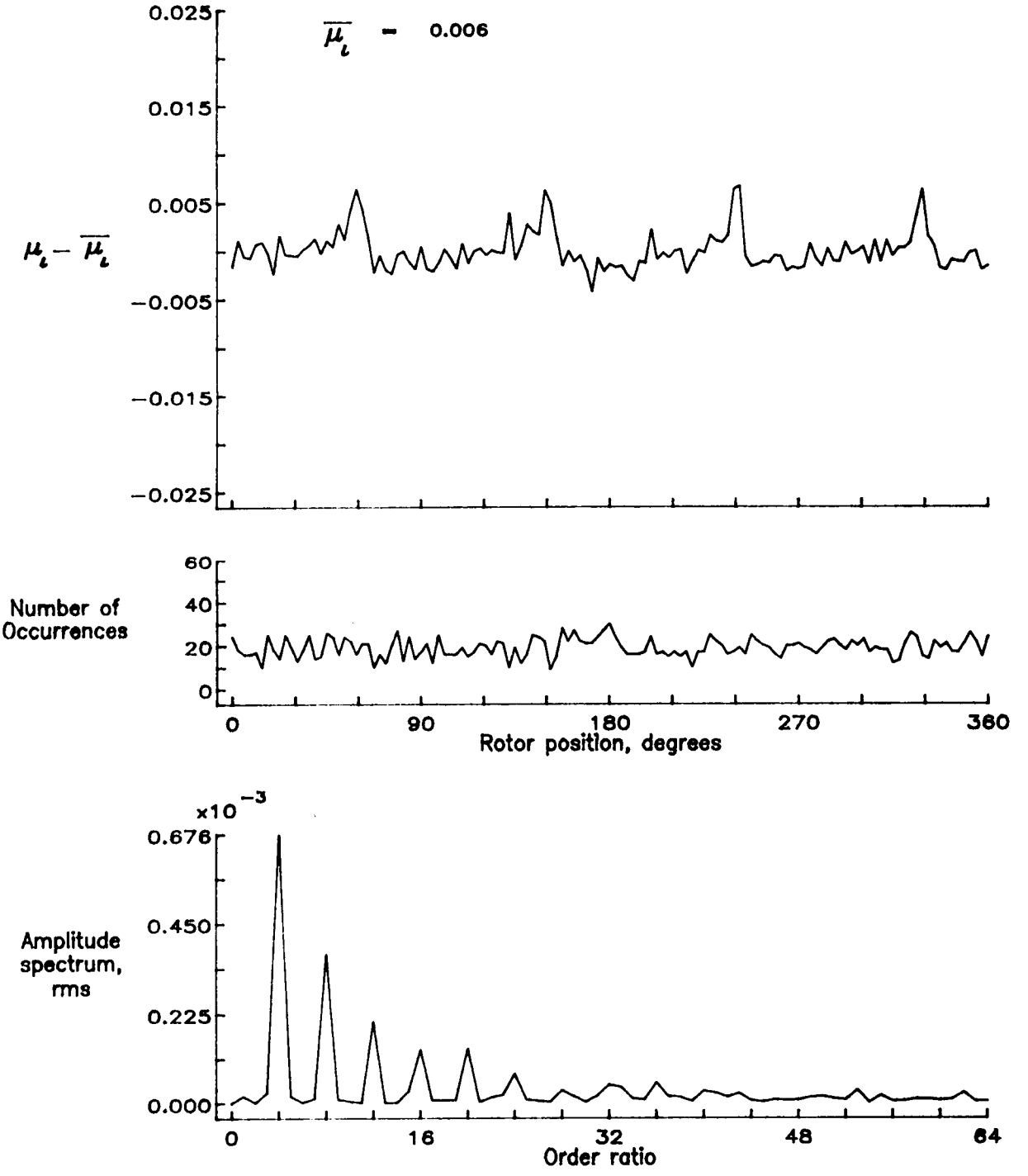

Figure 55.– Induced inflow velocity measured at 60 degrees and r/R of 1.02.

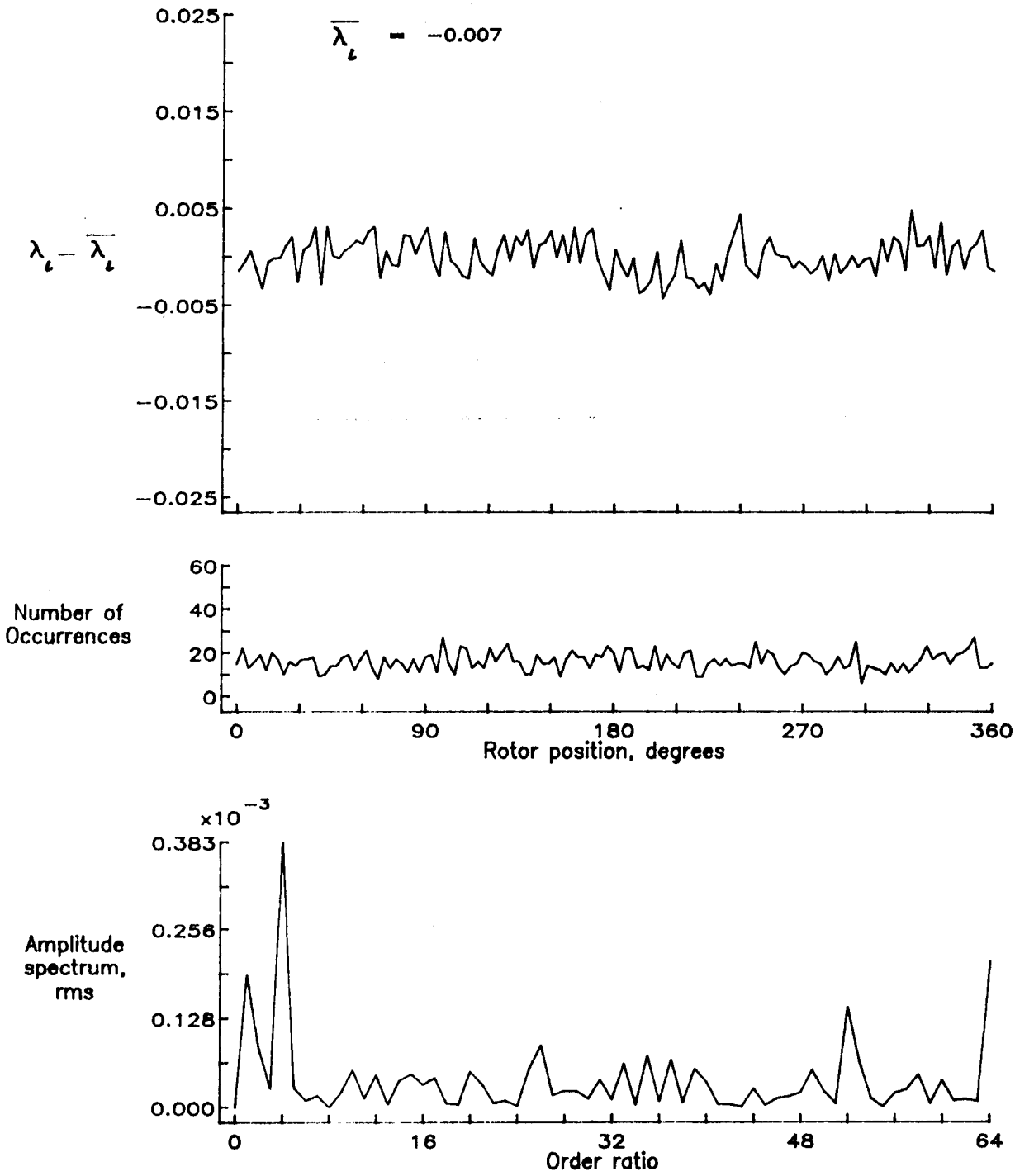

Figure 55.– Concluded.

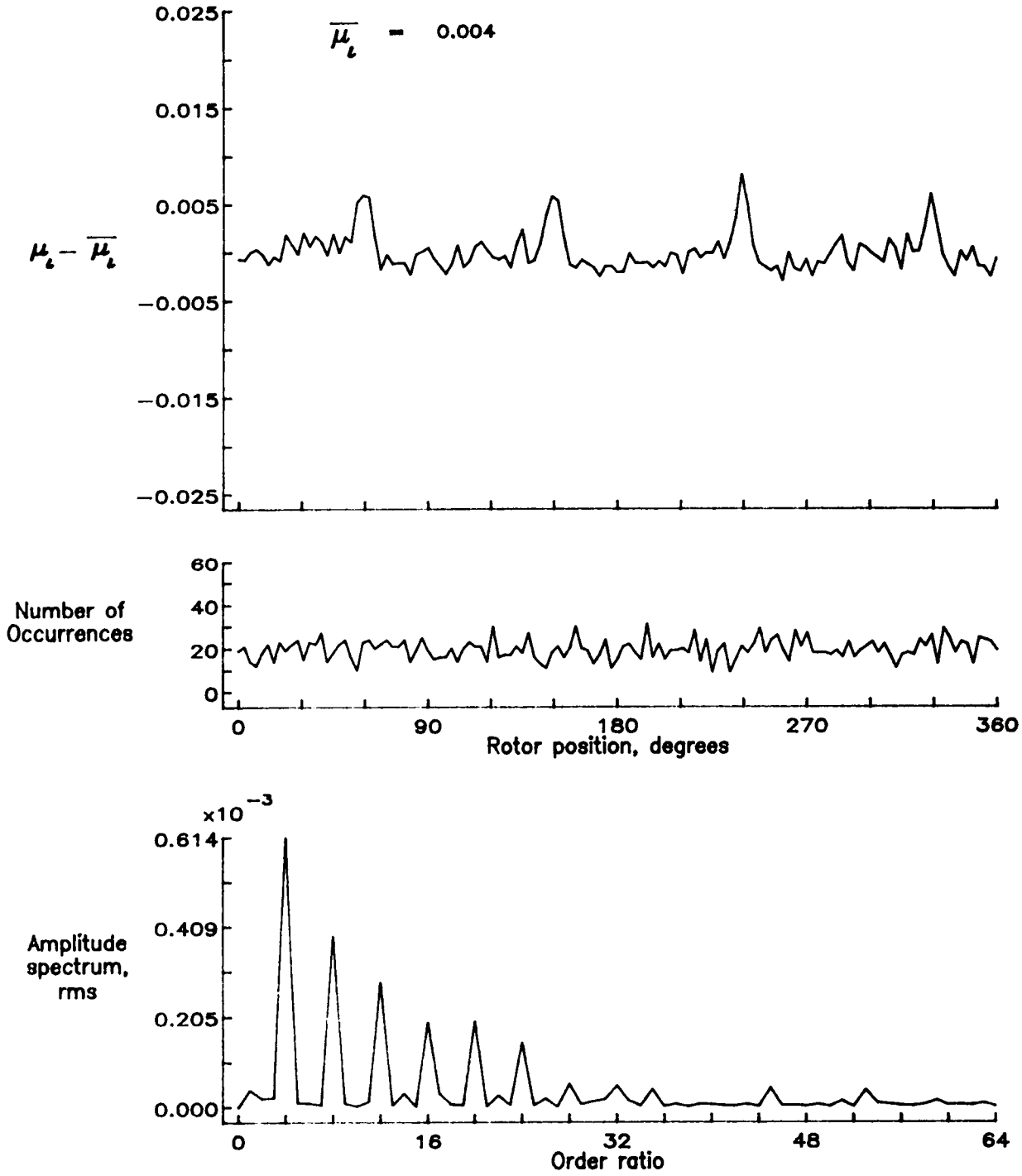

Figure 56.– Induced inflow velocity measured at 60 degrees and r/R of 1.04.

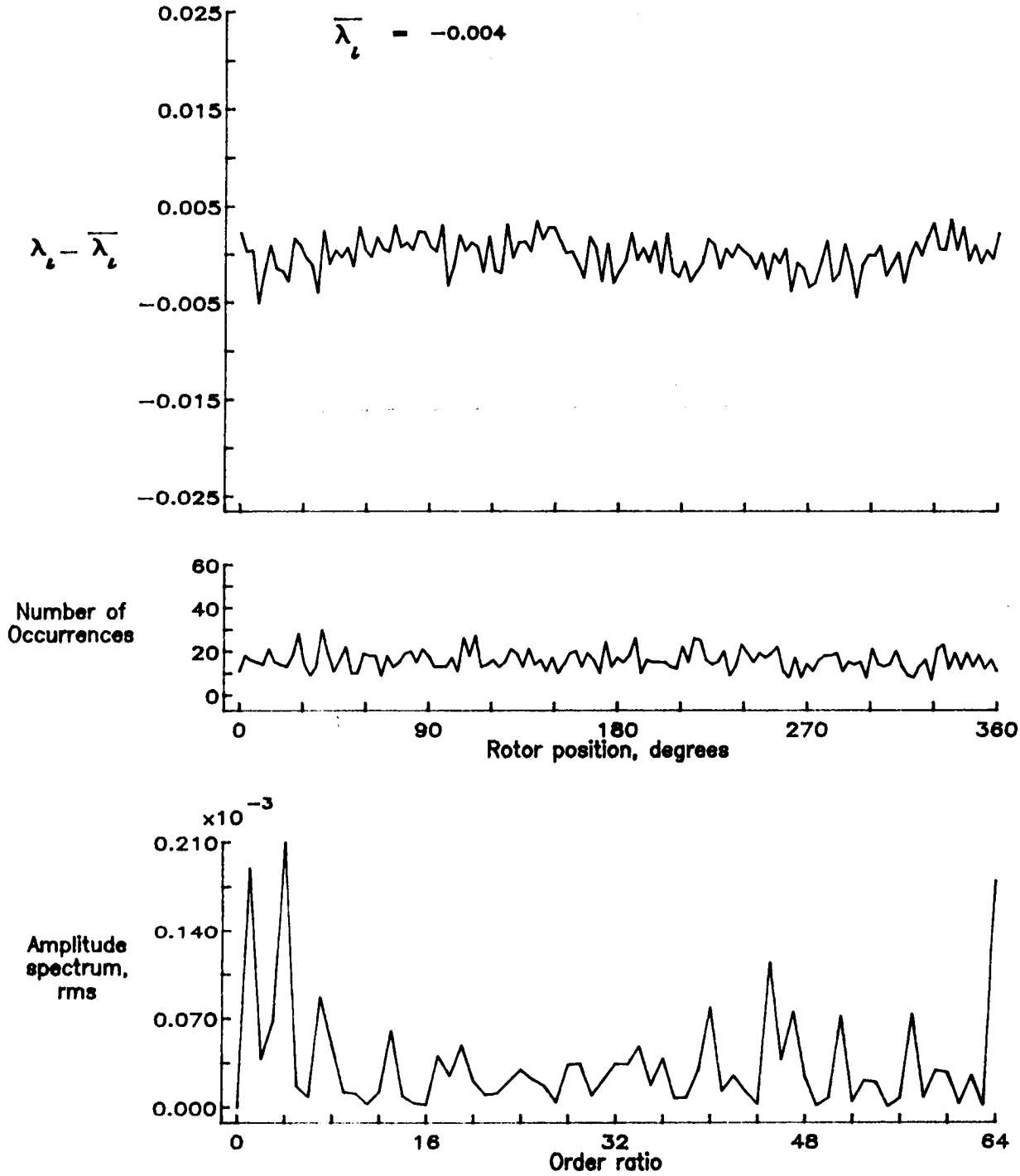

Figure 56.– Concluded.

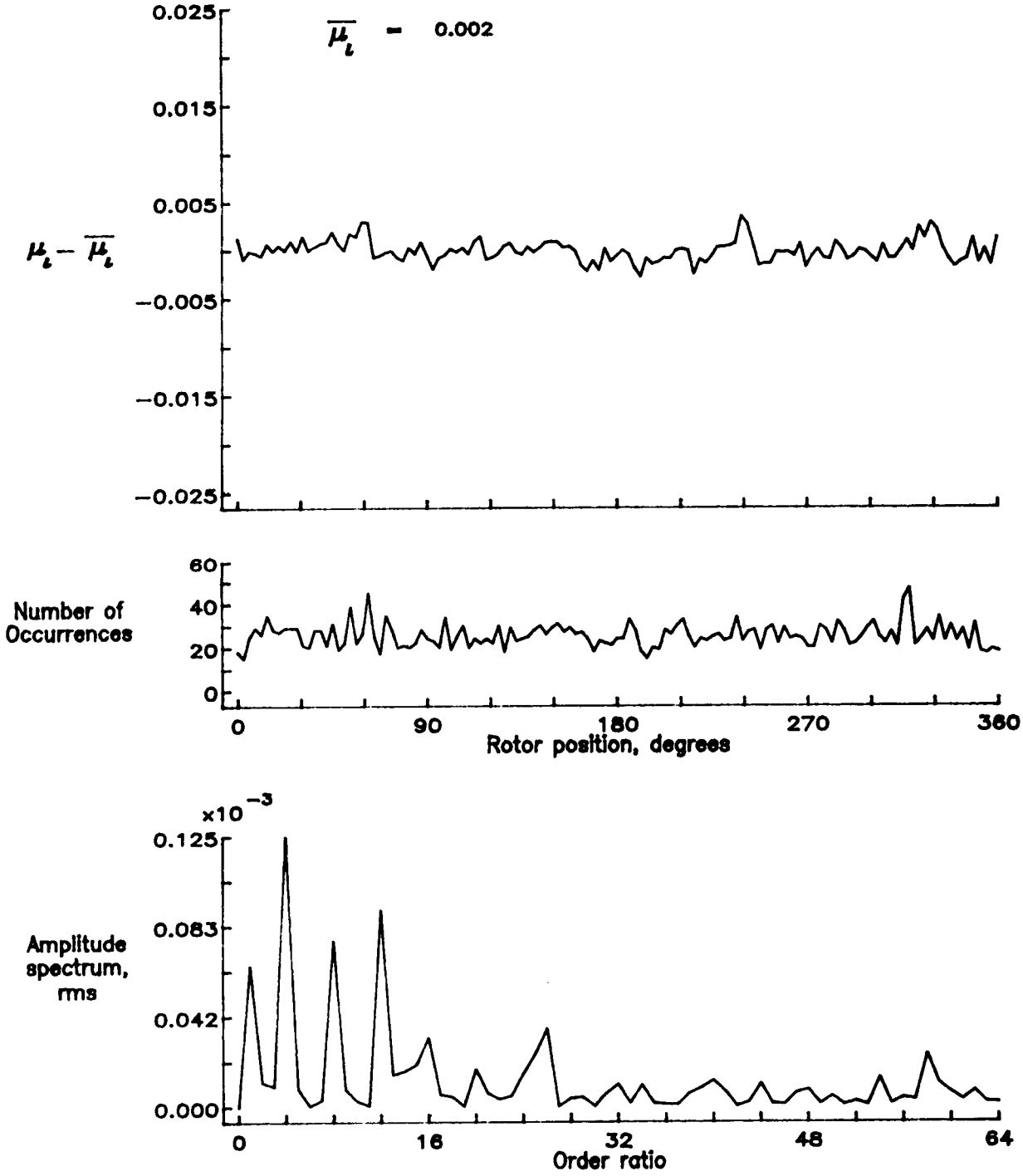

Figure 57.– Induced inflow velocity measured at 60 degrees and r/R of 1.10.

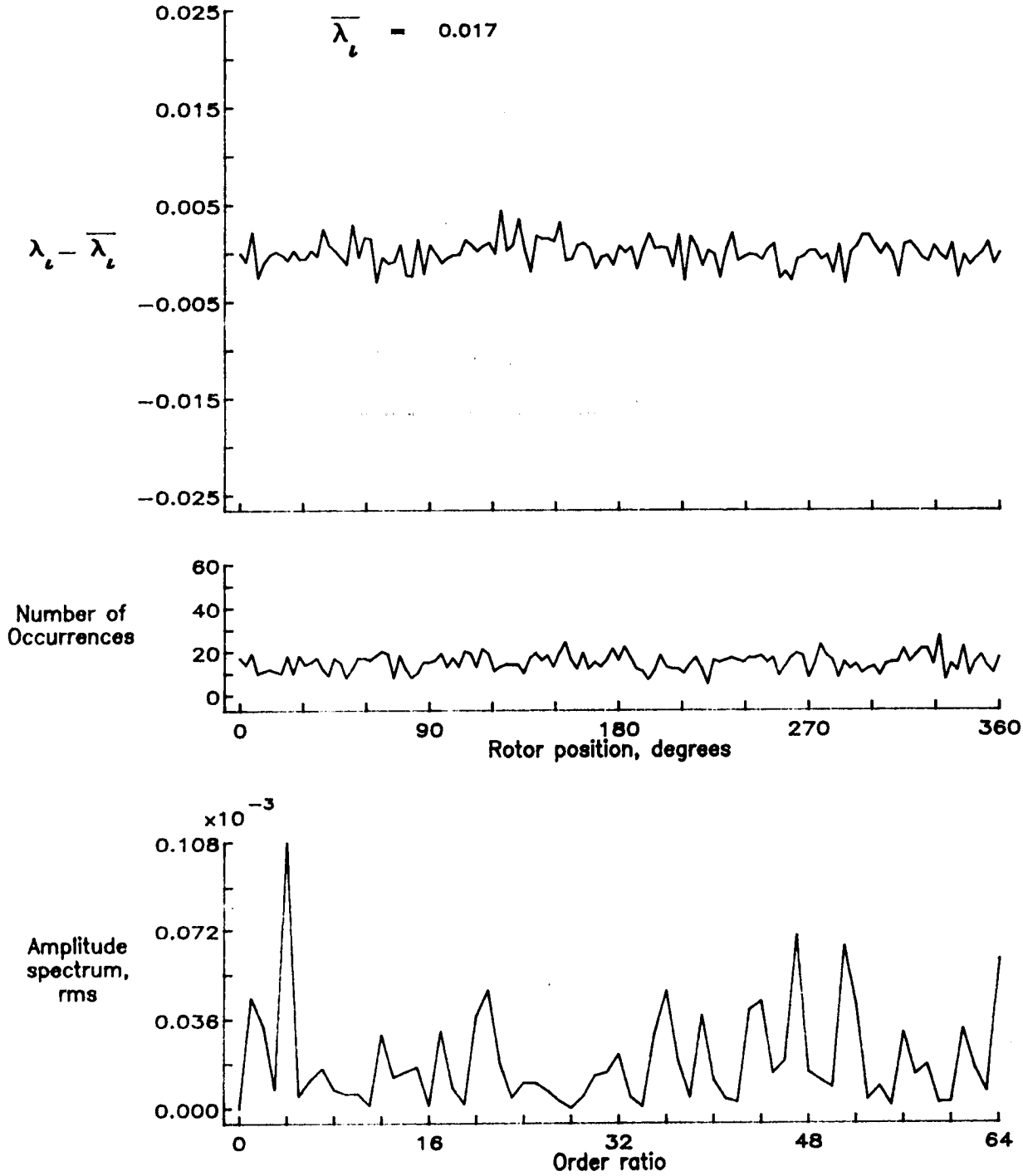

Figure 57.– Concluded.

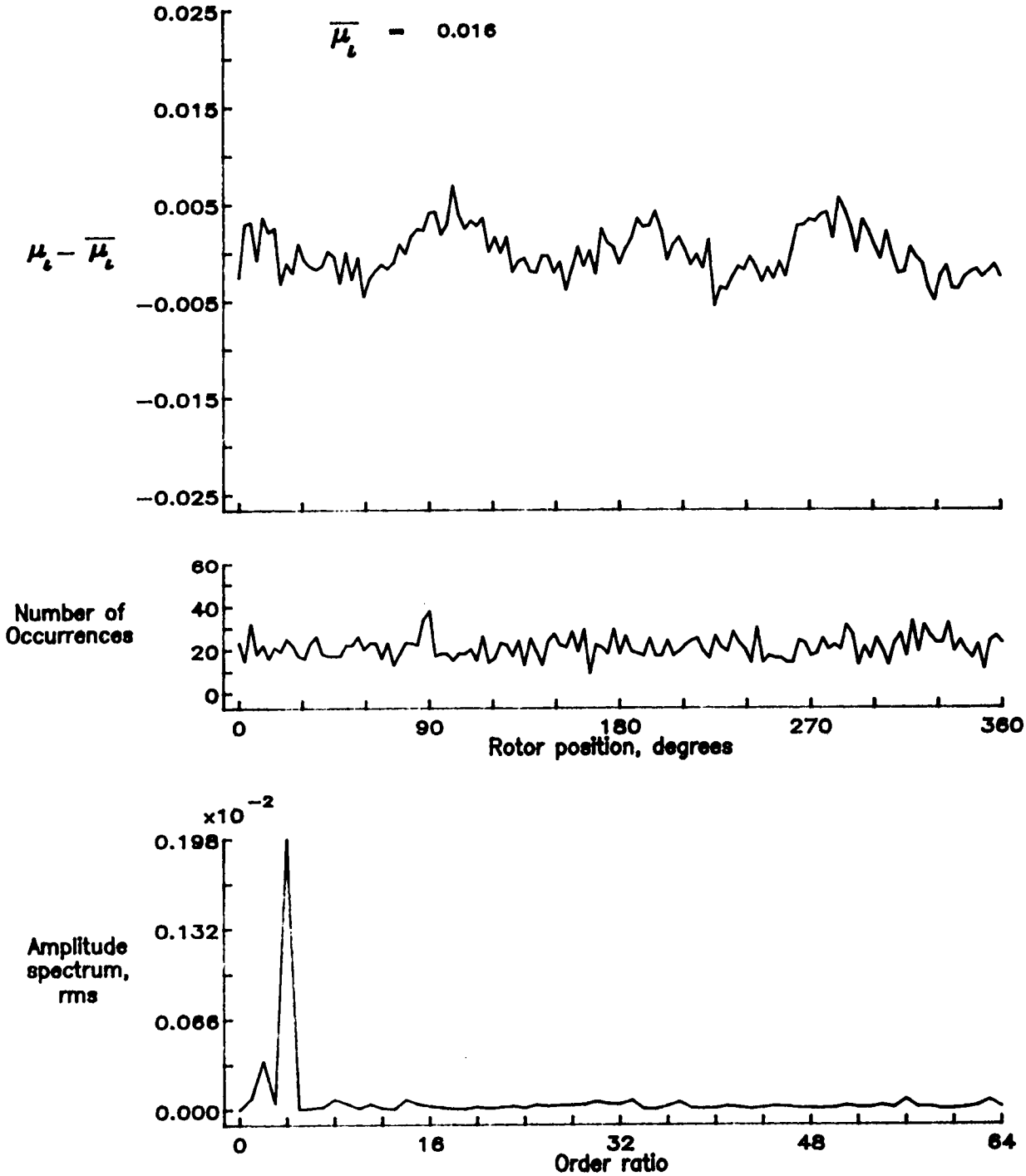

Figure 58.– Induced inflow velocity measured at 90 degrees and r/R of 0.20.

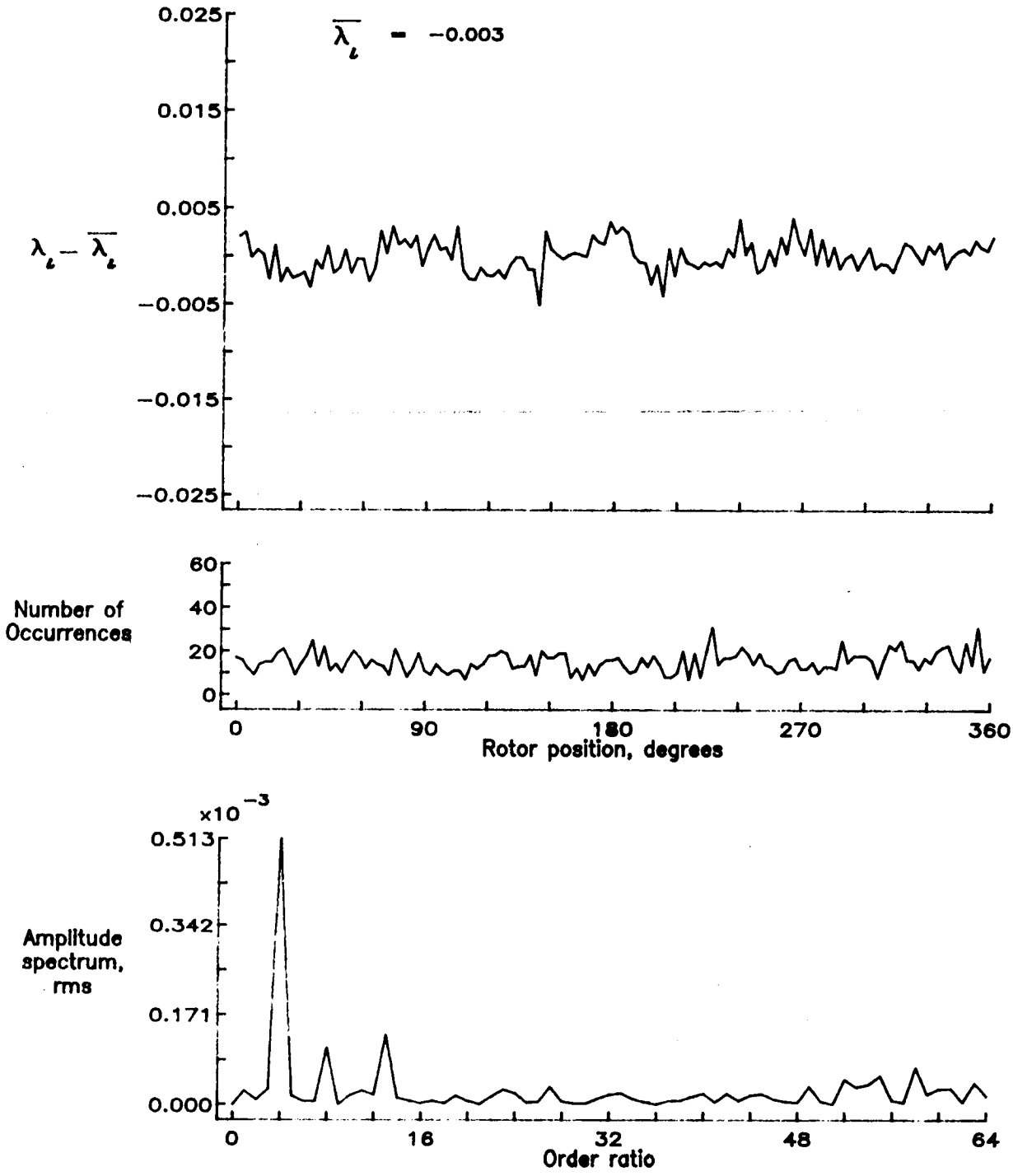

Figure 58.– Concluded.

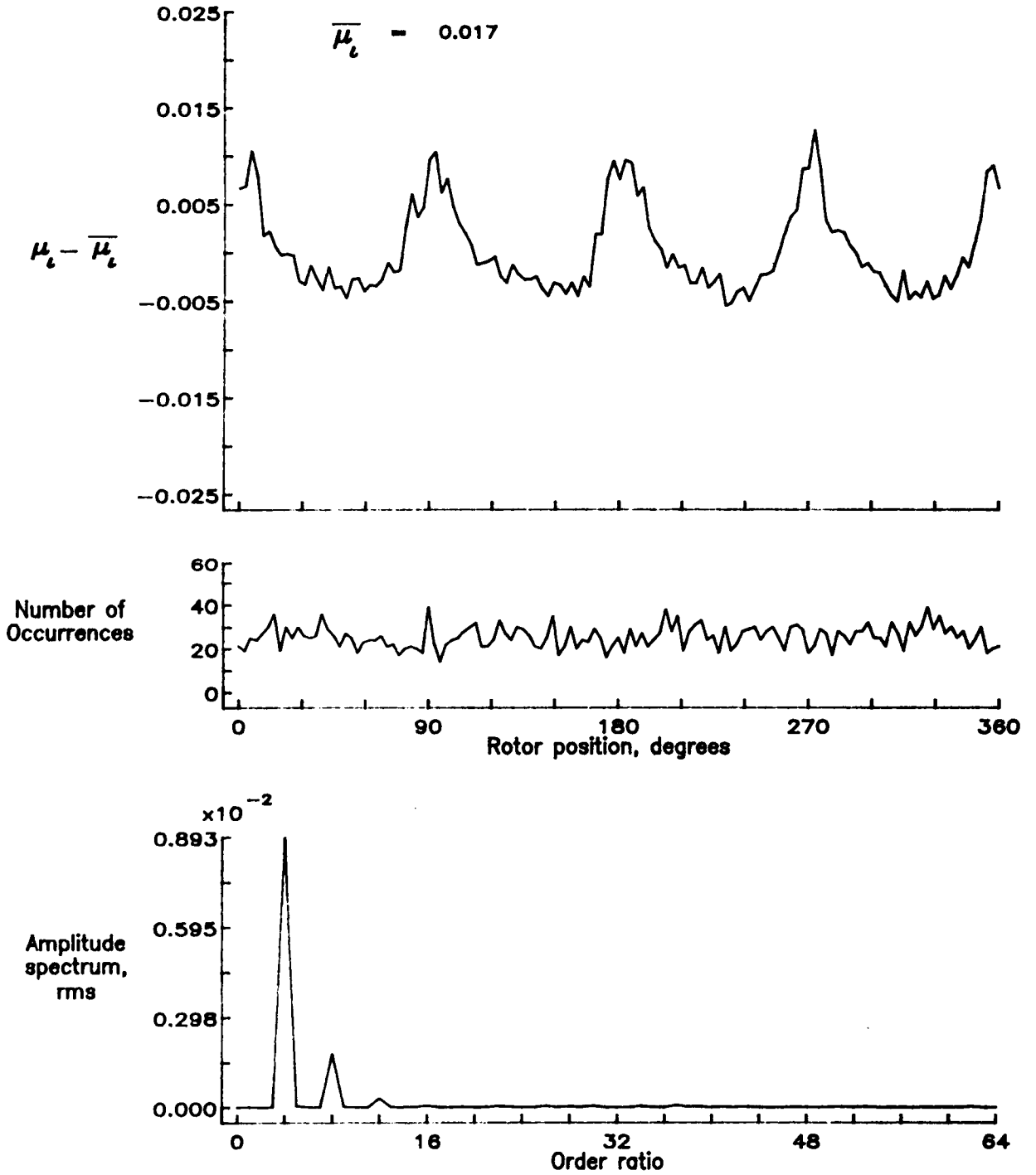

Figure 59.– Induced inflow velocity measured at 90 degrees and r/R of 0.40.

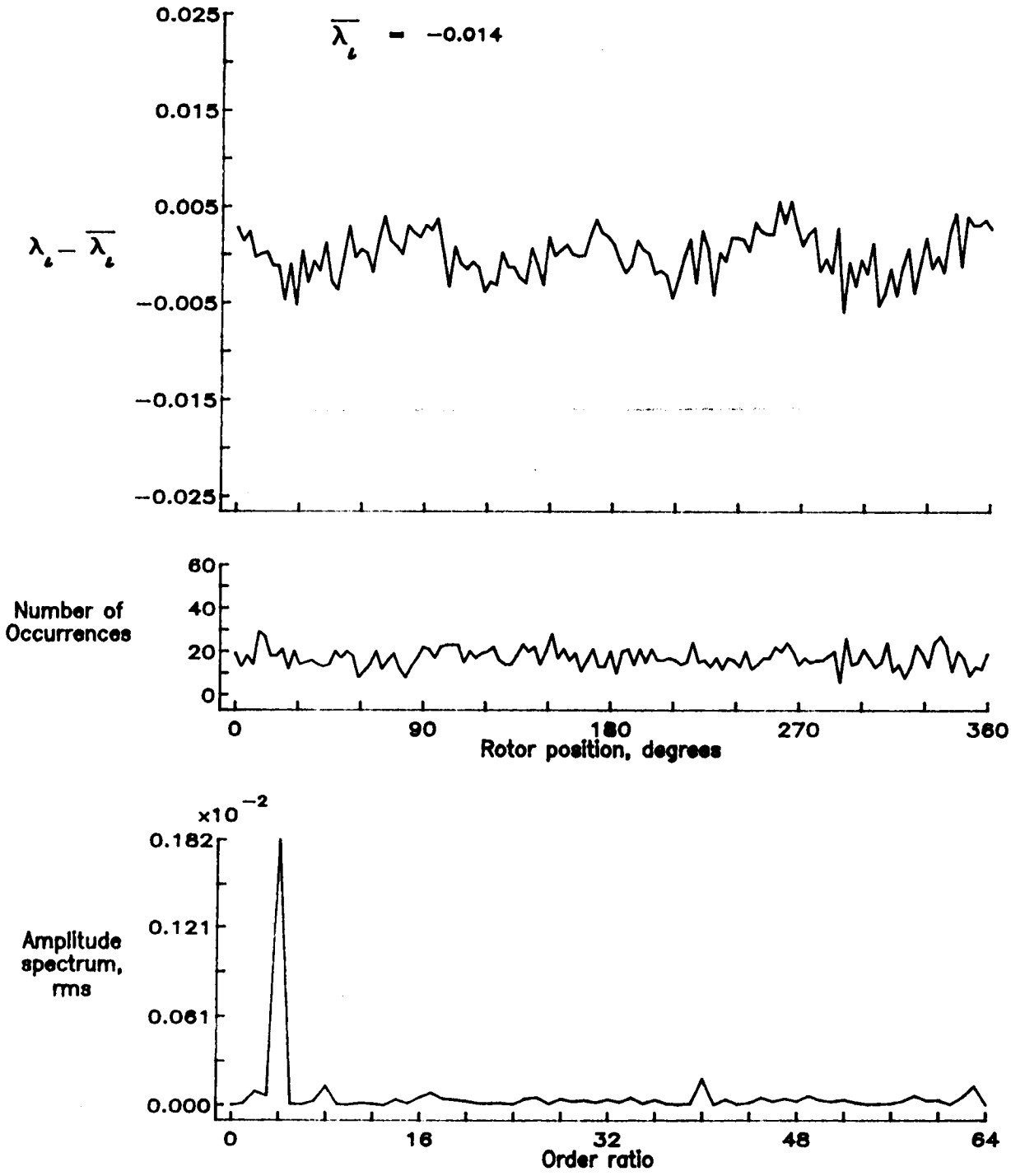

Figure 59.– Concluded.

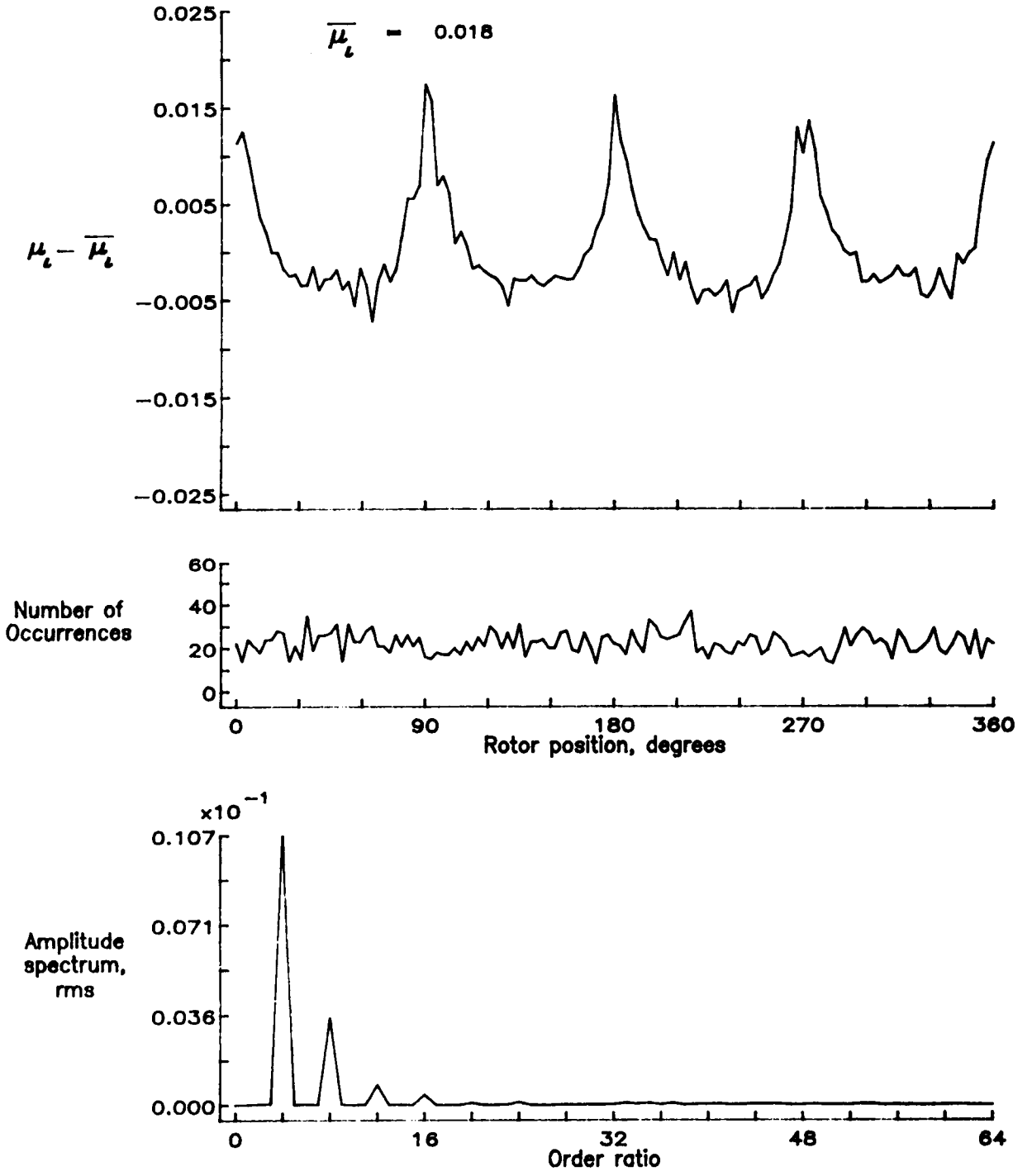

Figure 60.– Induced inflow velocity measured at 90 degrees and r/R of 0.50.

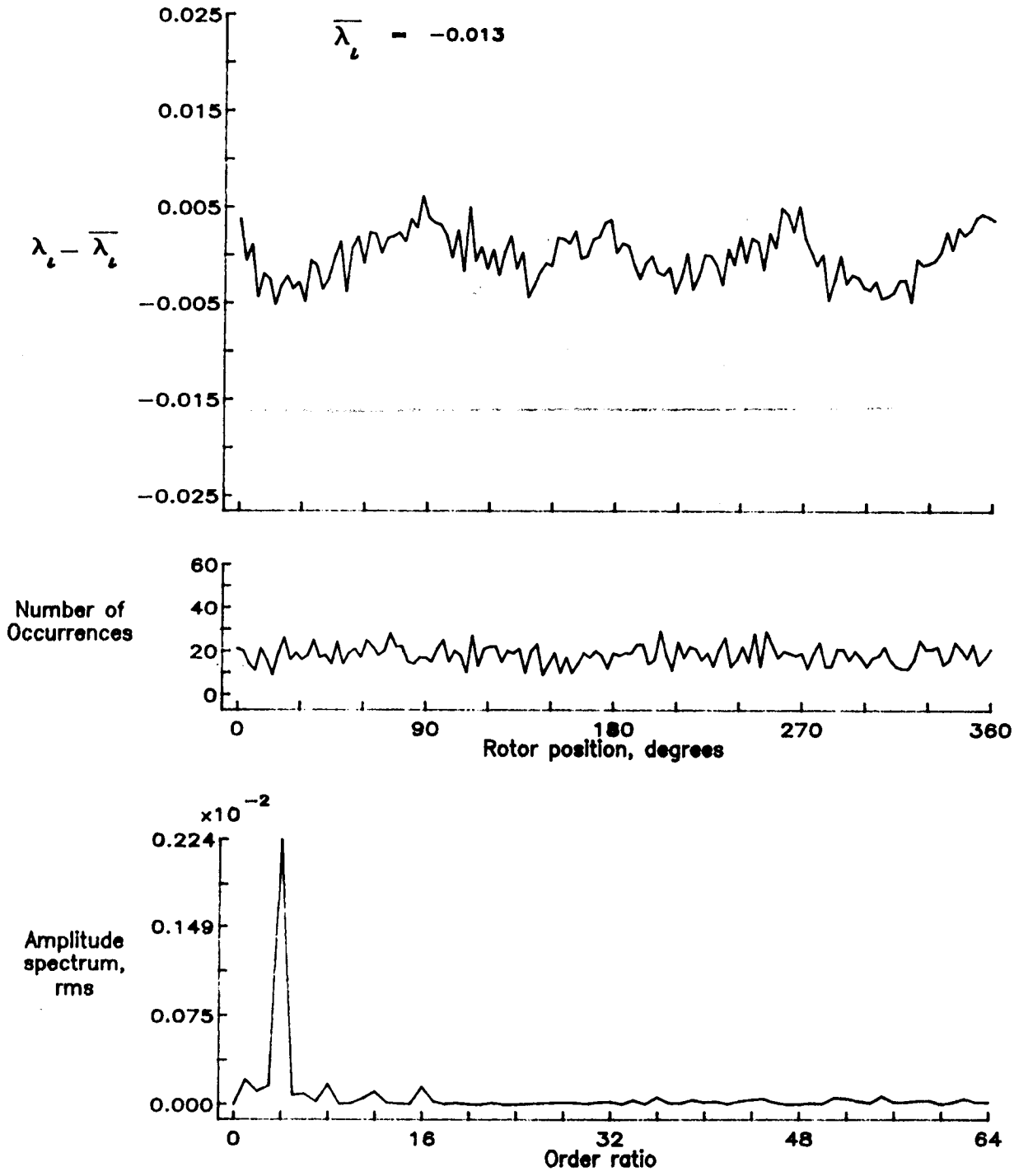

Figure 60.– Concluded.

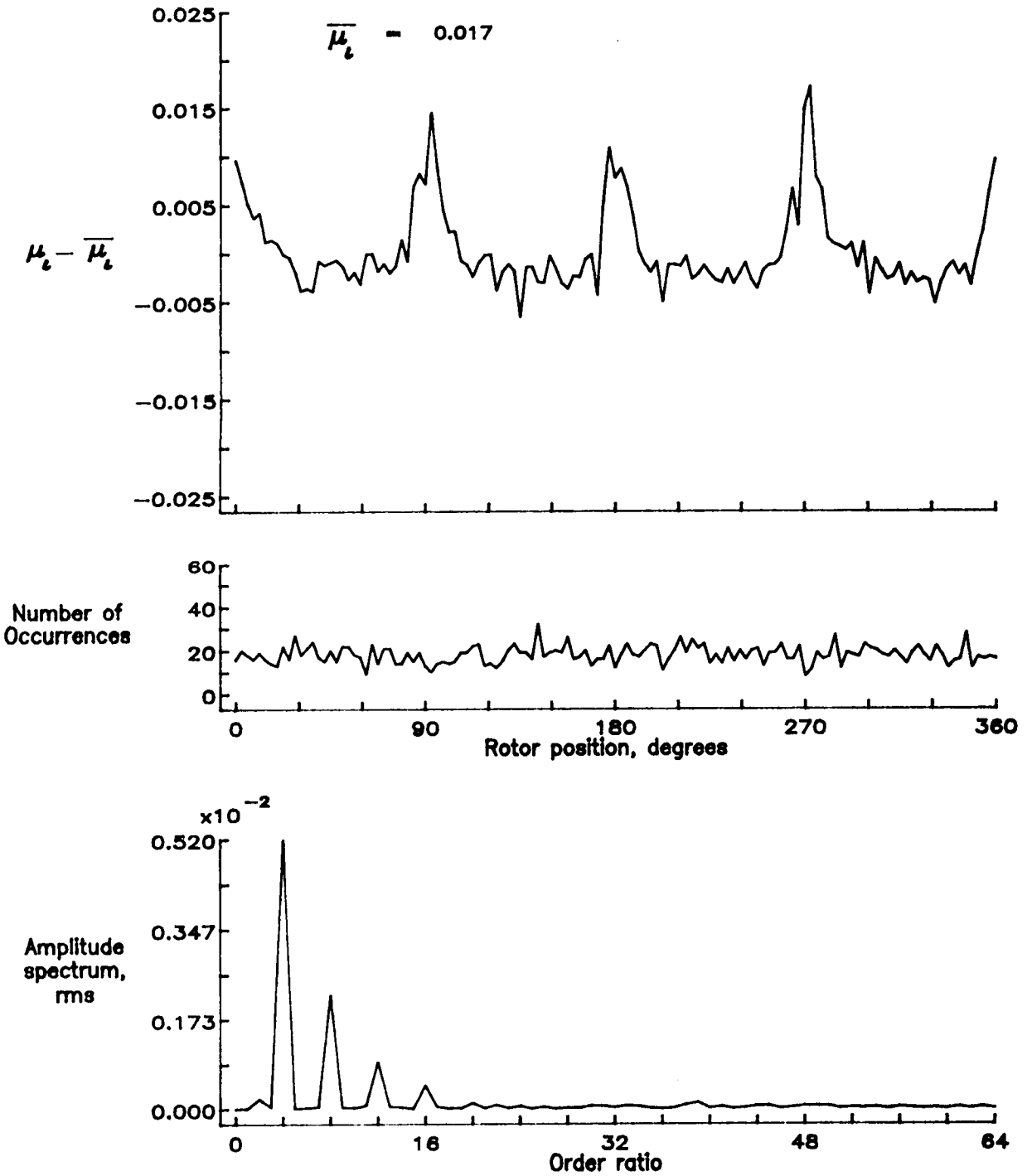

Figure 61.– Induced inflow velocity measured at 90 degrees and r/R of 0.60.

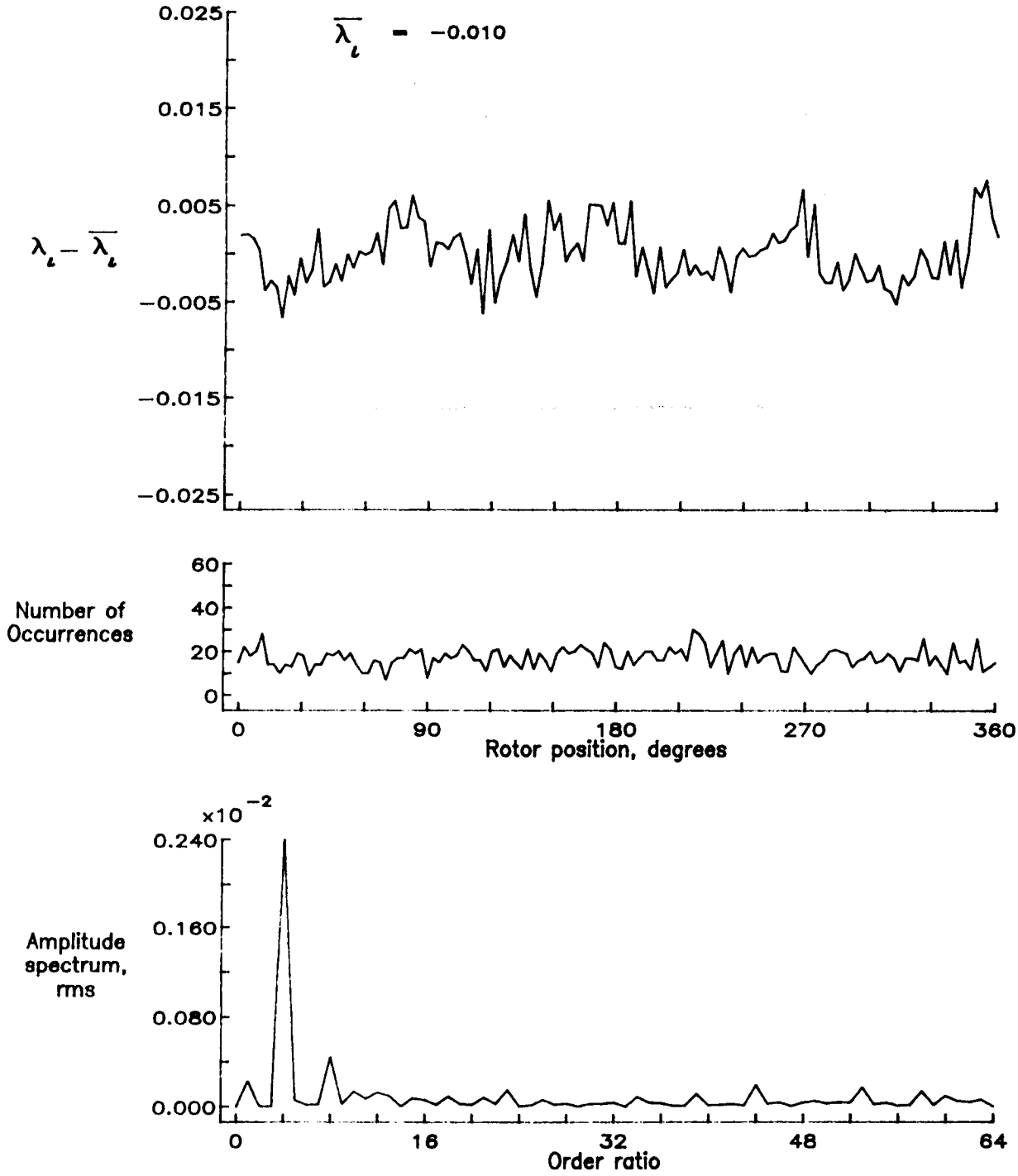

Figure 61.– Concluded.

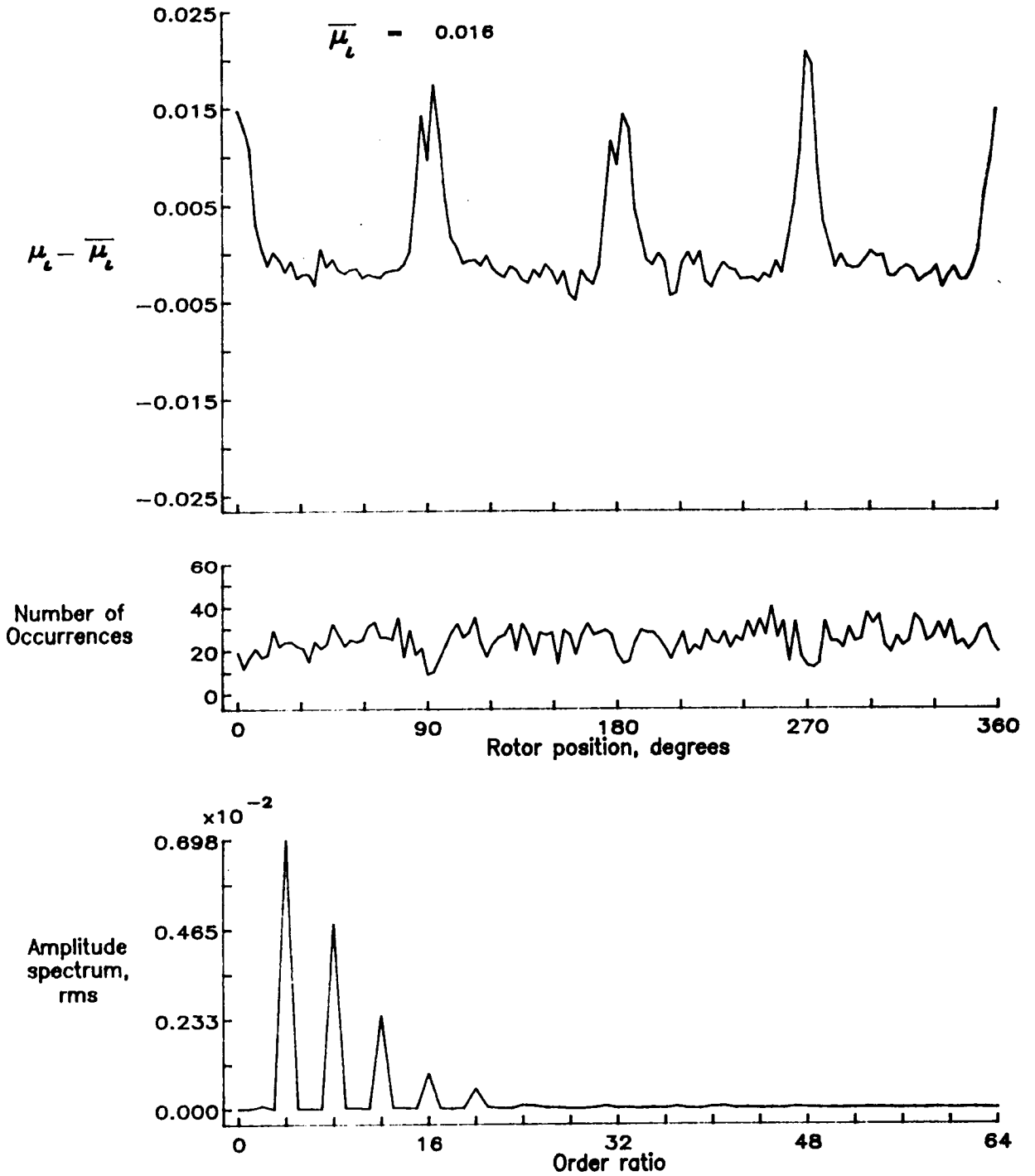

Figure 62.– Induced inflow velocity measured at 90 degrees and r/R of 0.70.

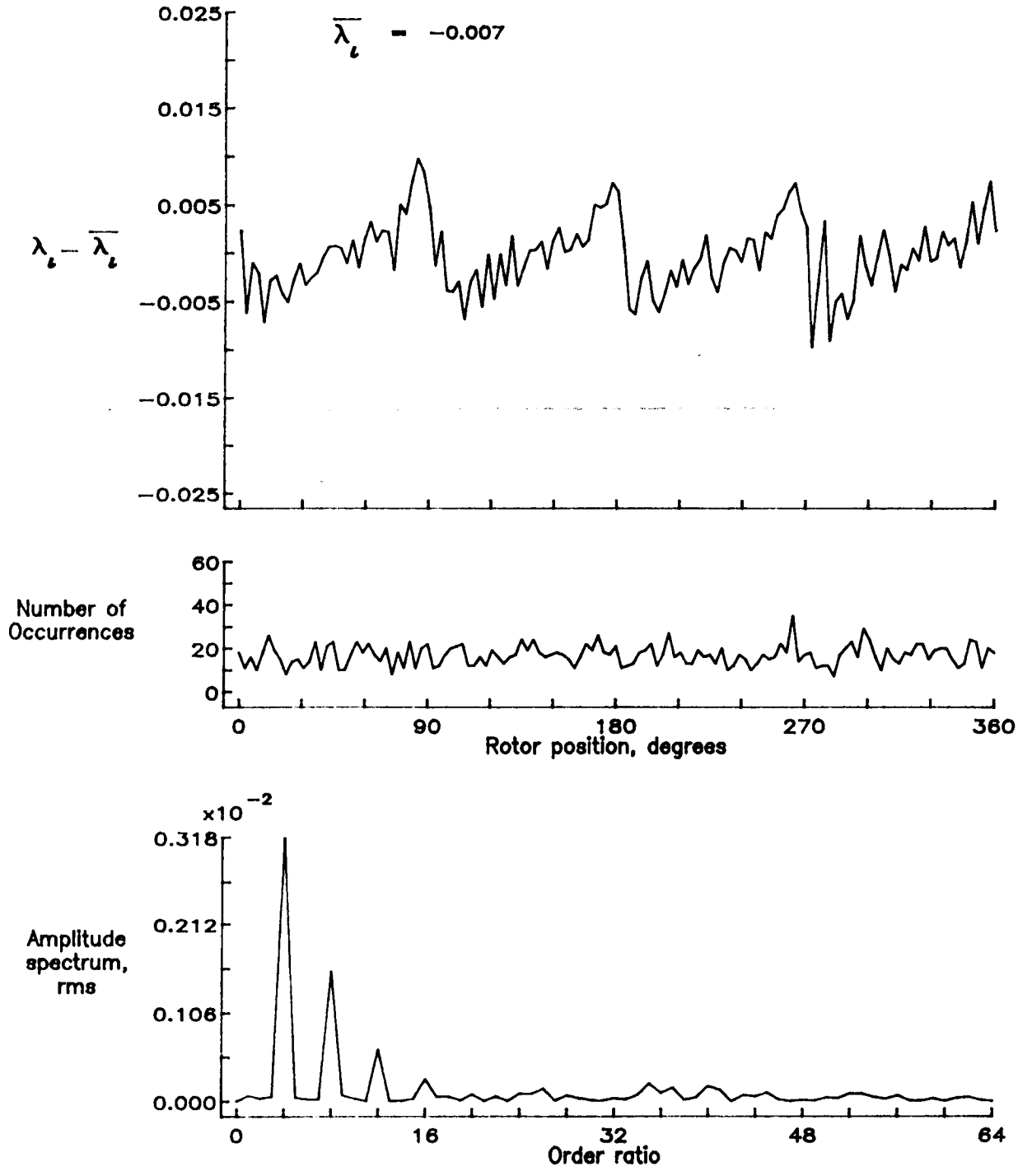

Figure 62.– Concluded.

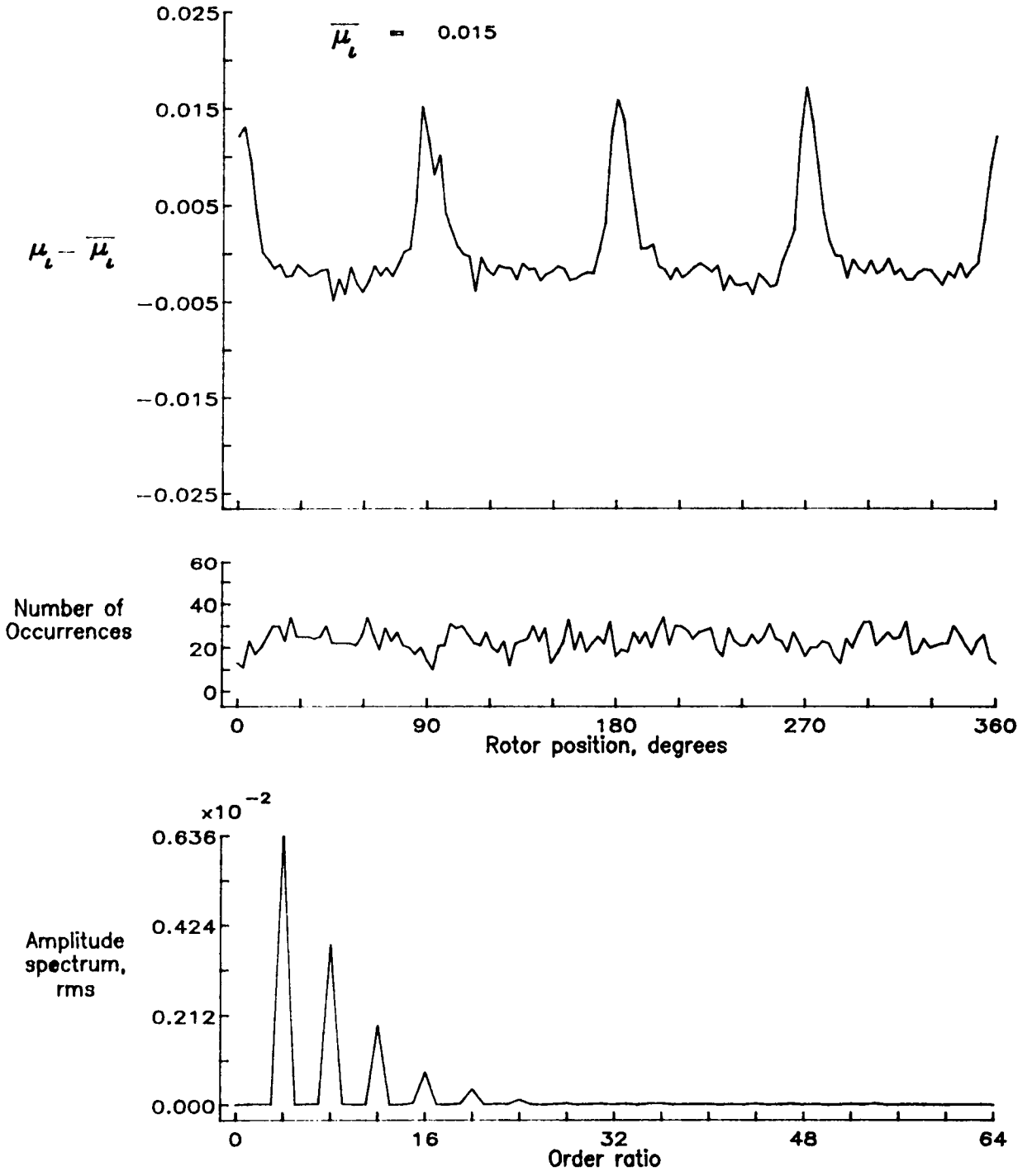

Figure 63.– Induced inflow velocity measured at 90 degrees and r/R of 0.74.

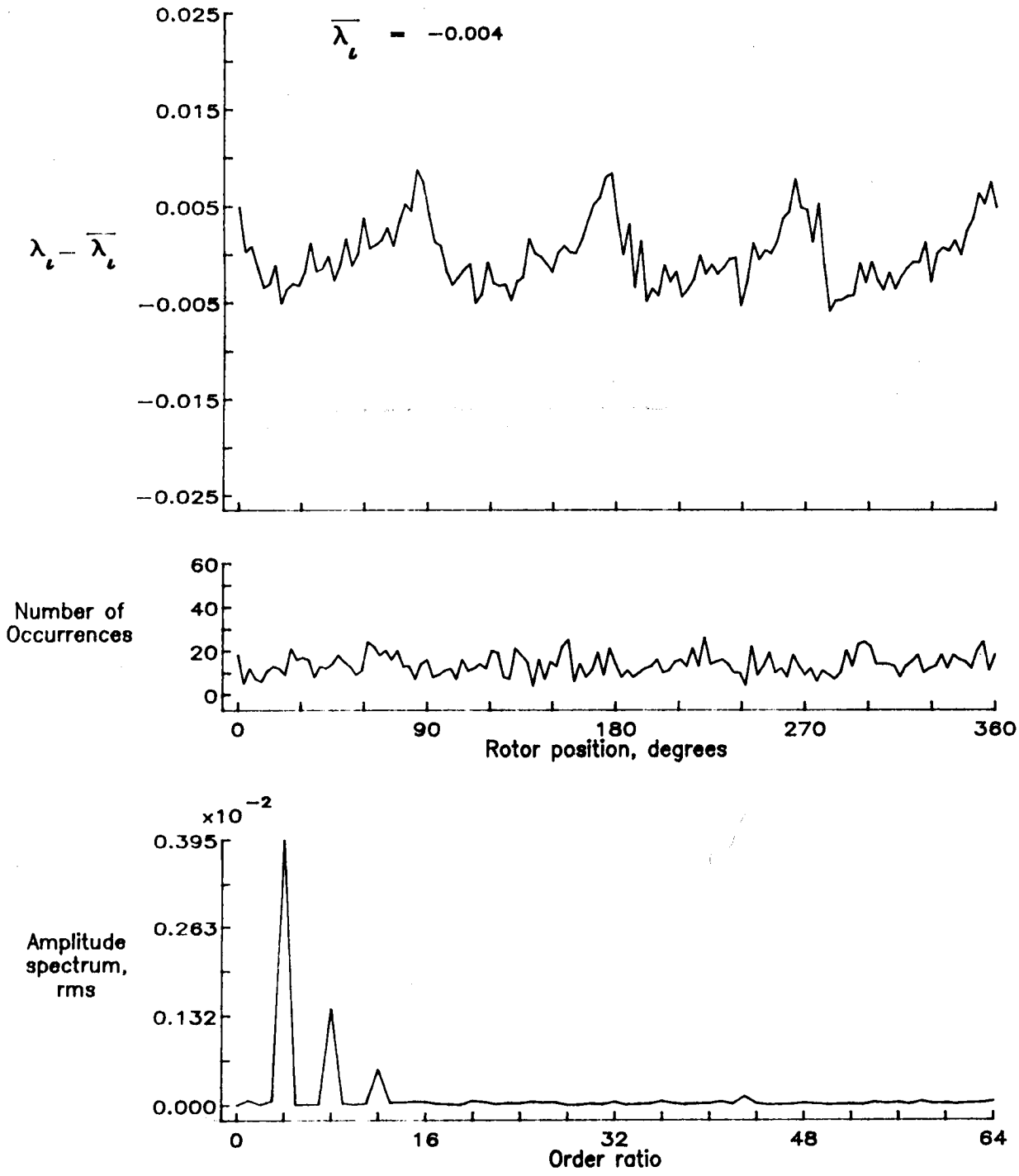

Figure 63.– Concluded.

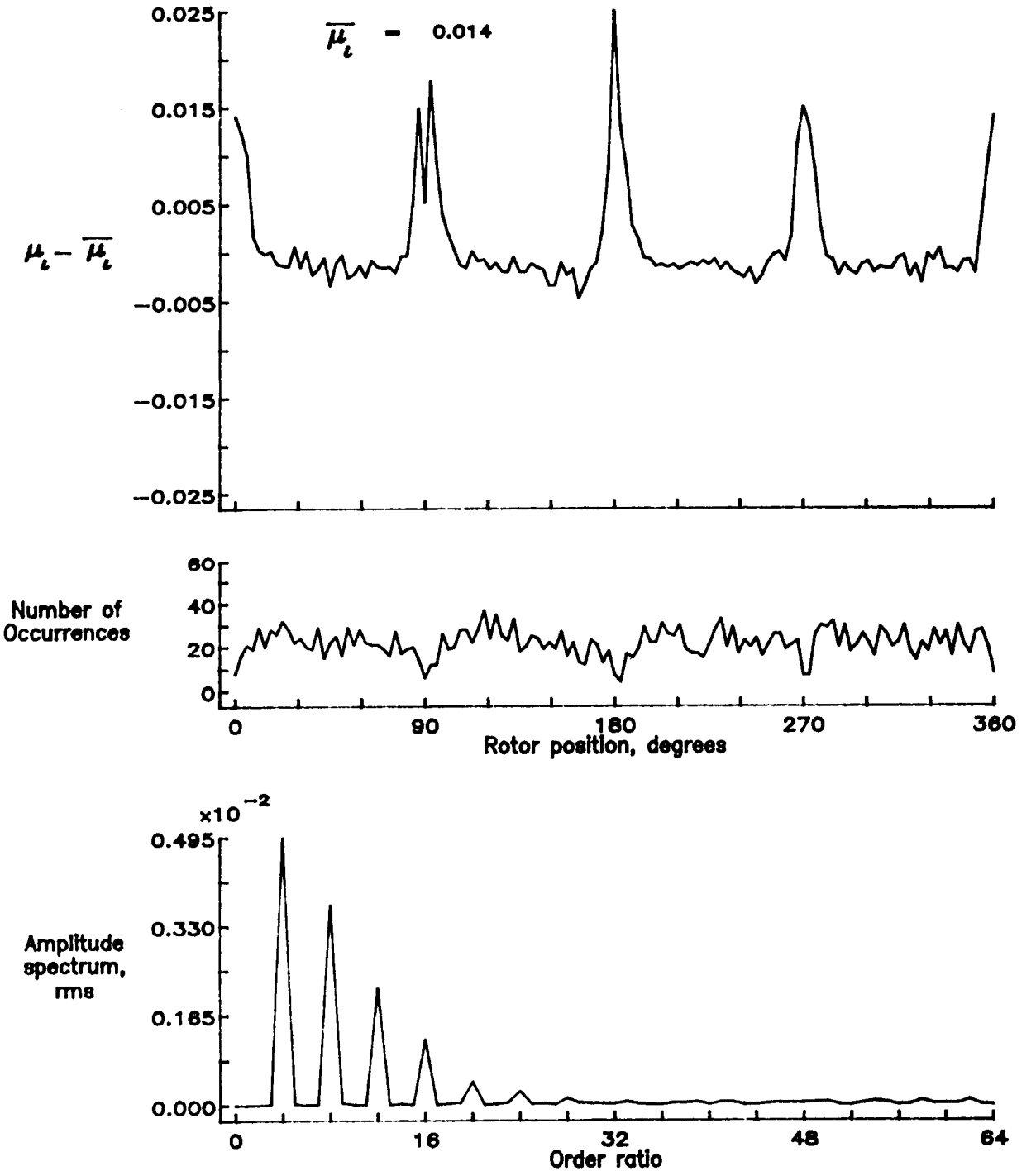

Figure 64.– Induced inflow velocity measured at 90 degrees and r/R of 0.78.

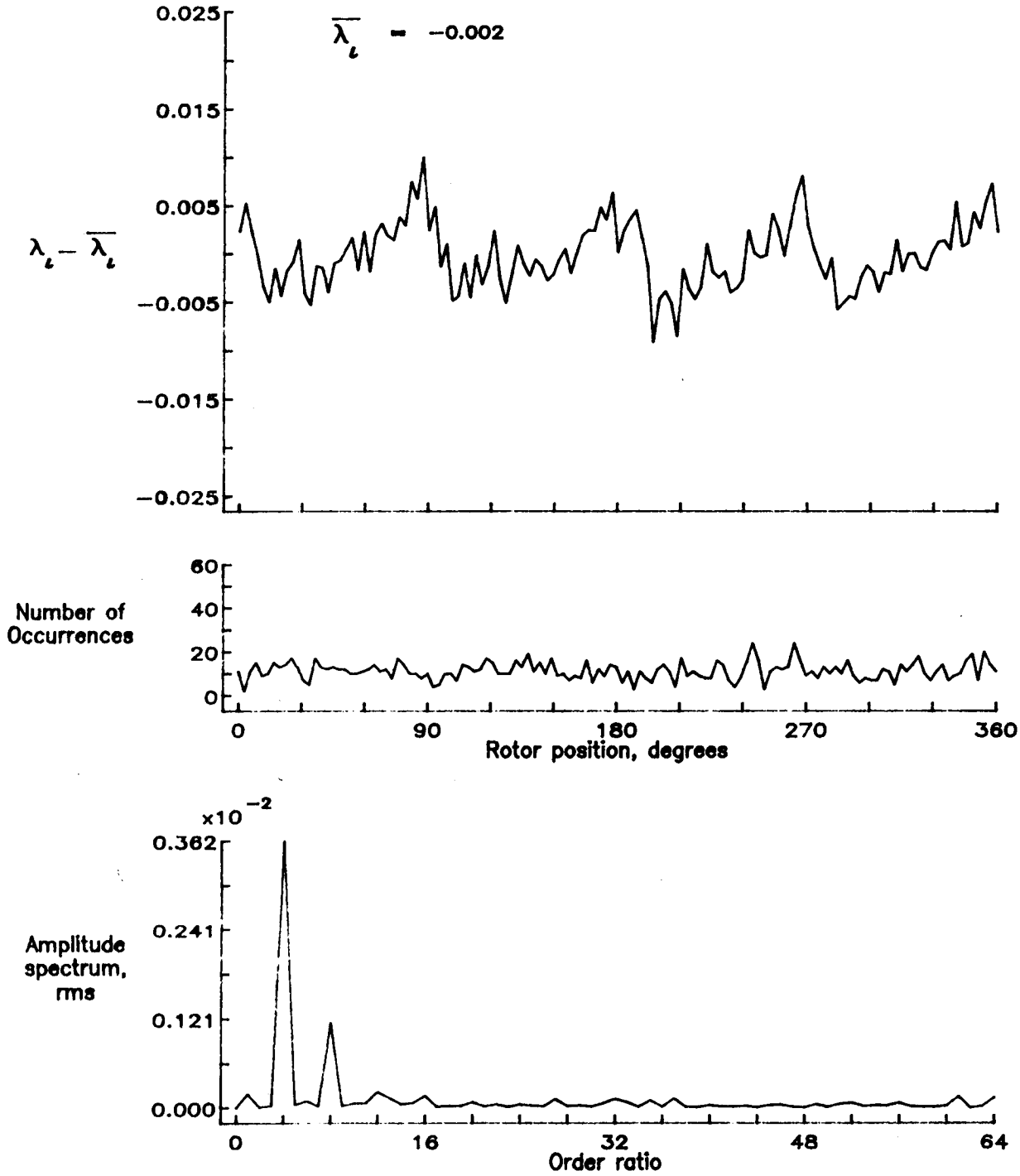

Figure 64.– Concluded.

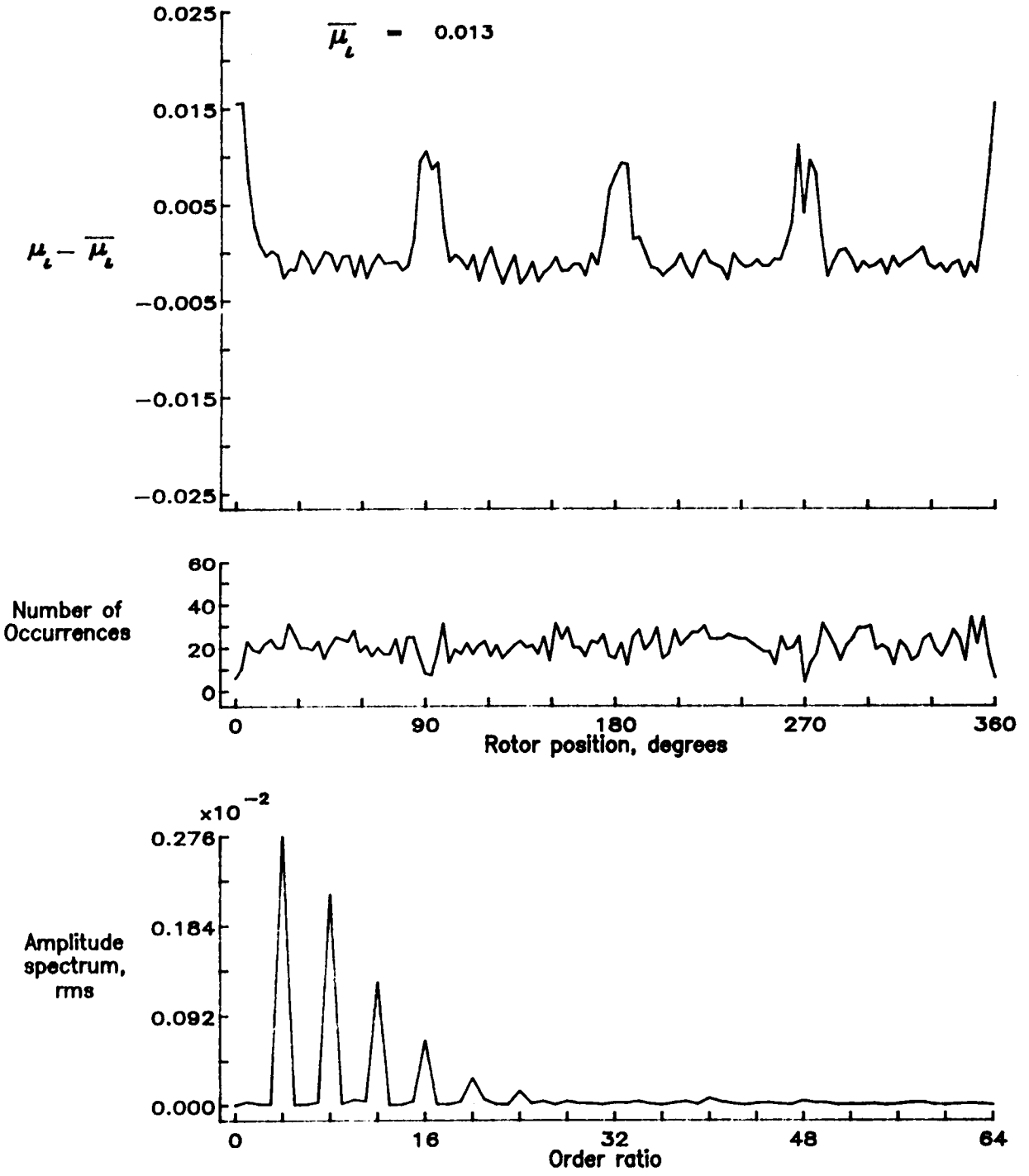

Figure 65.– Induced inflow velocity measured at 90 degrees and r/R of 0.82.

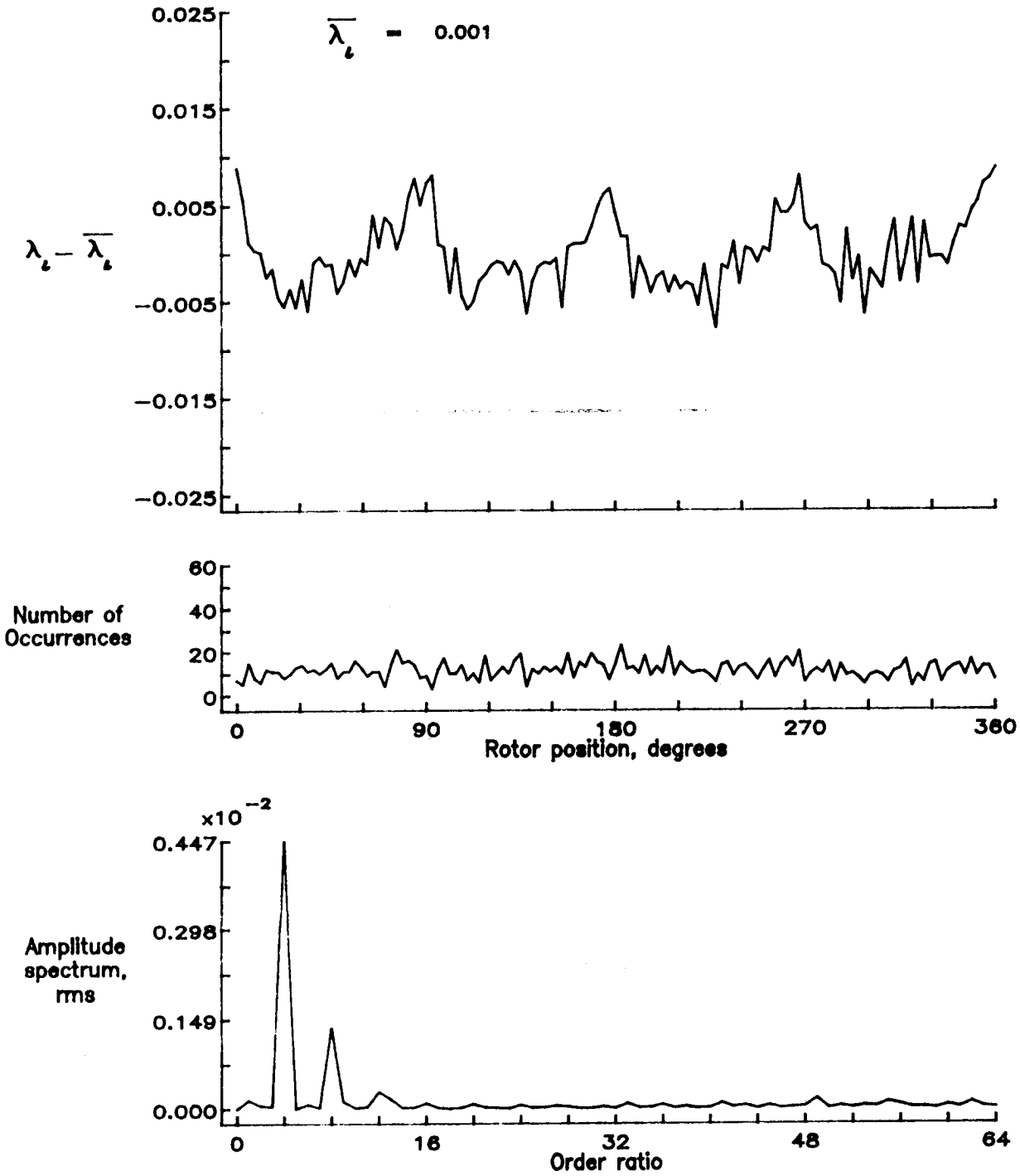

Figure 65.– Concluded.

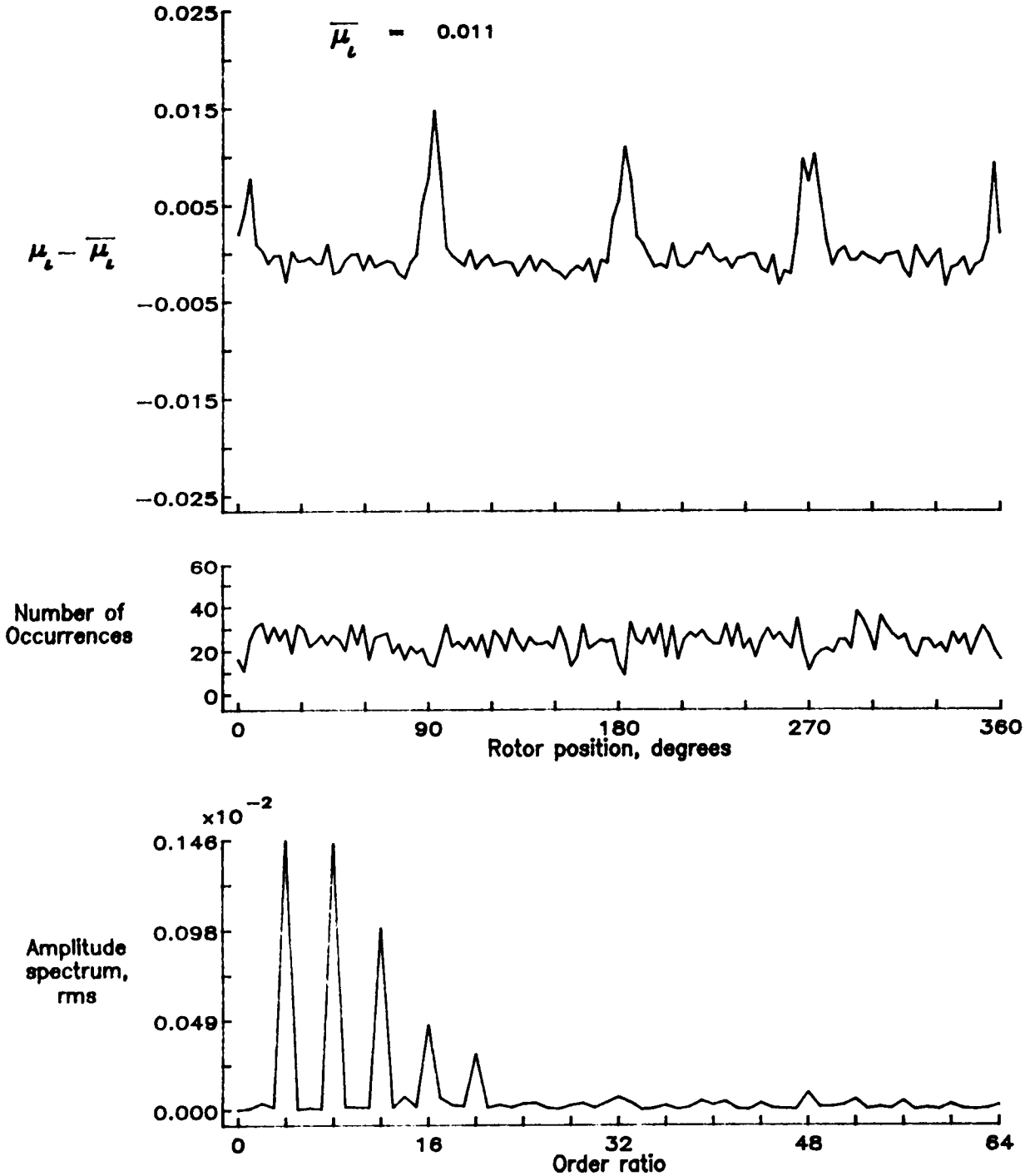

Figure 66.– Induced inflow velocity measured at 90 degrees and r/R of 0.86.

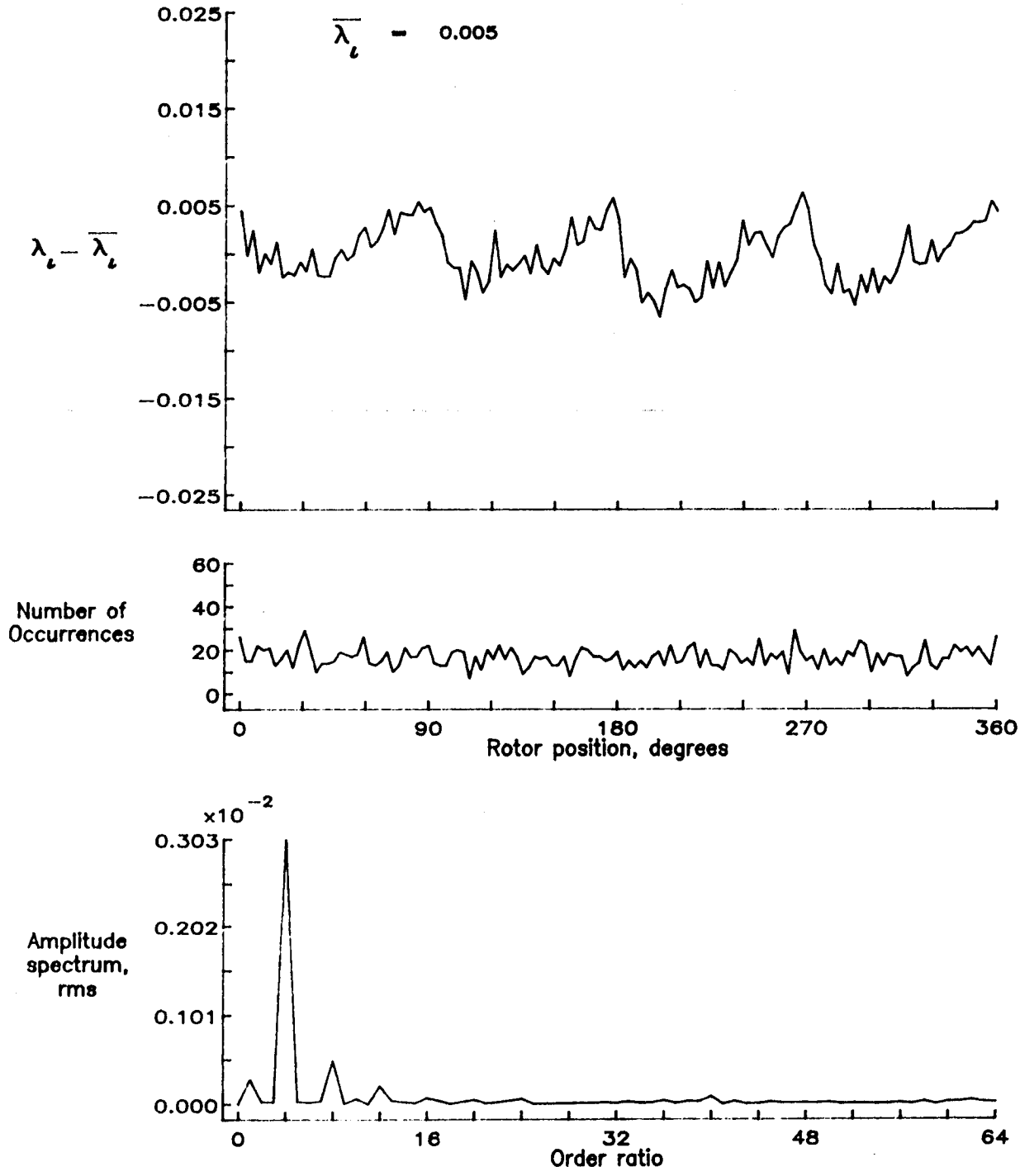

Figure 66.– Concluded.

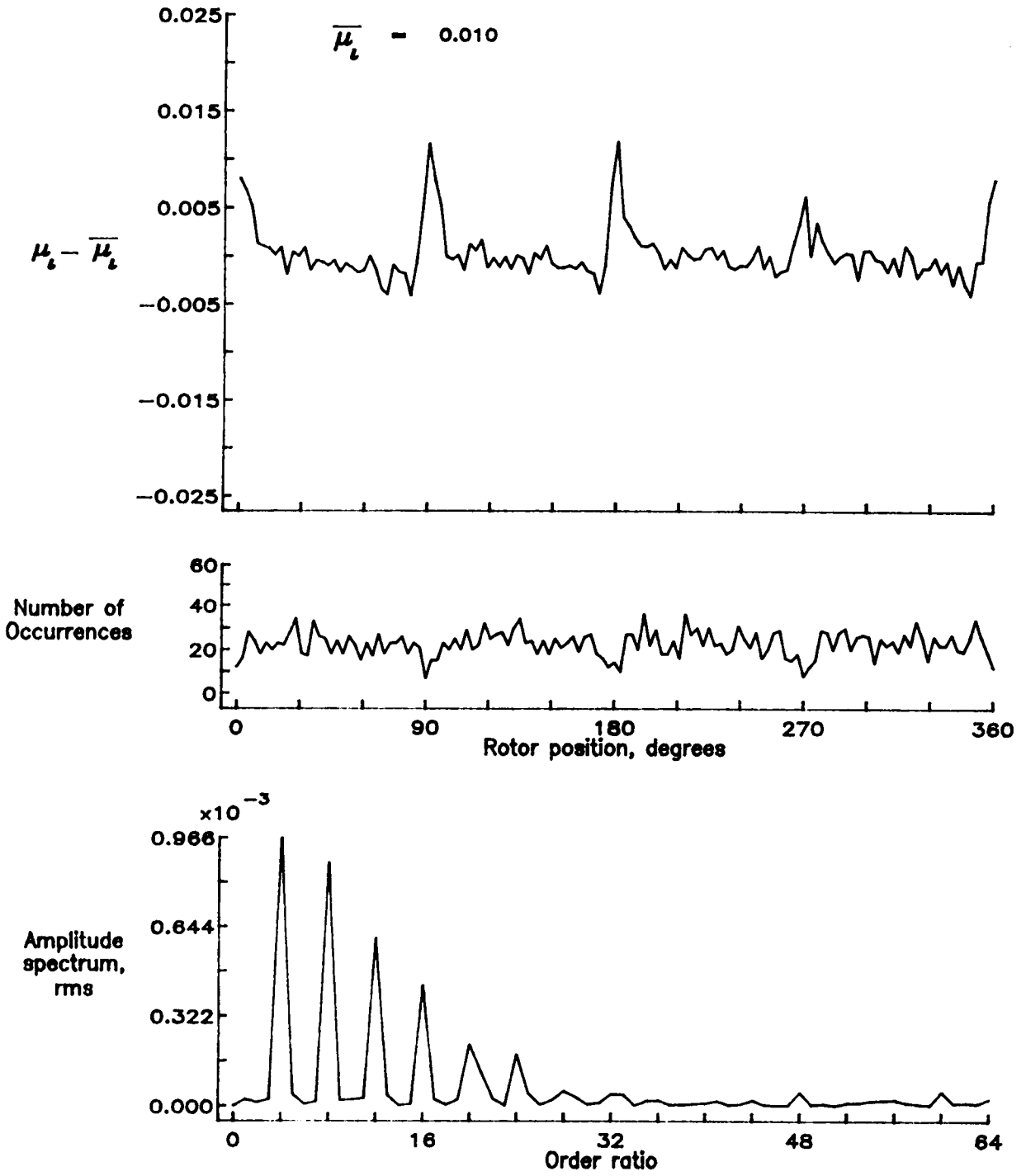

Figure 67.– Induced inflow velocity measured at 90 degrees and r/R of 0.90.

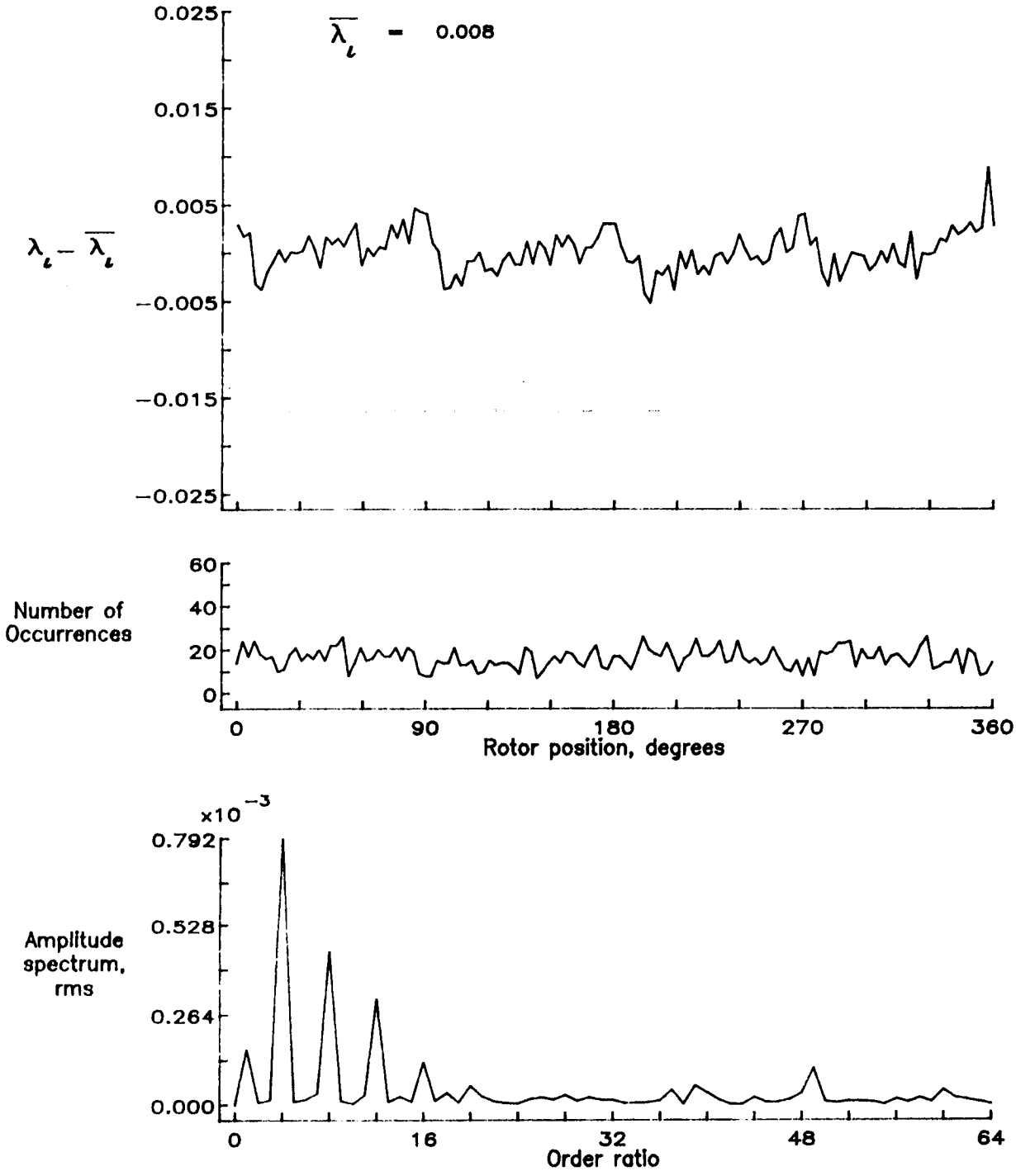

Figure 67.– Concluded.

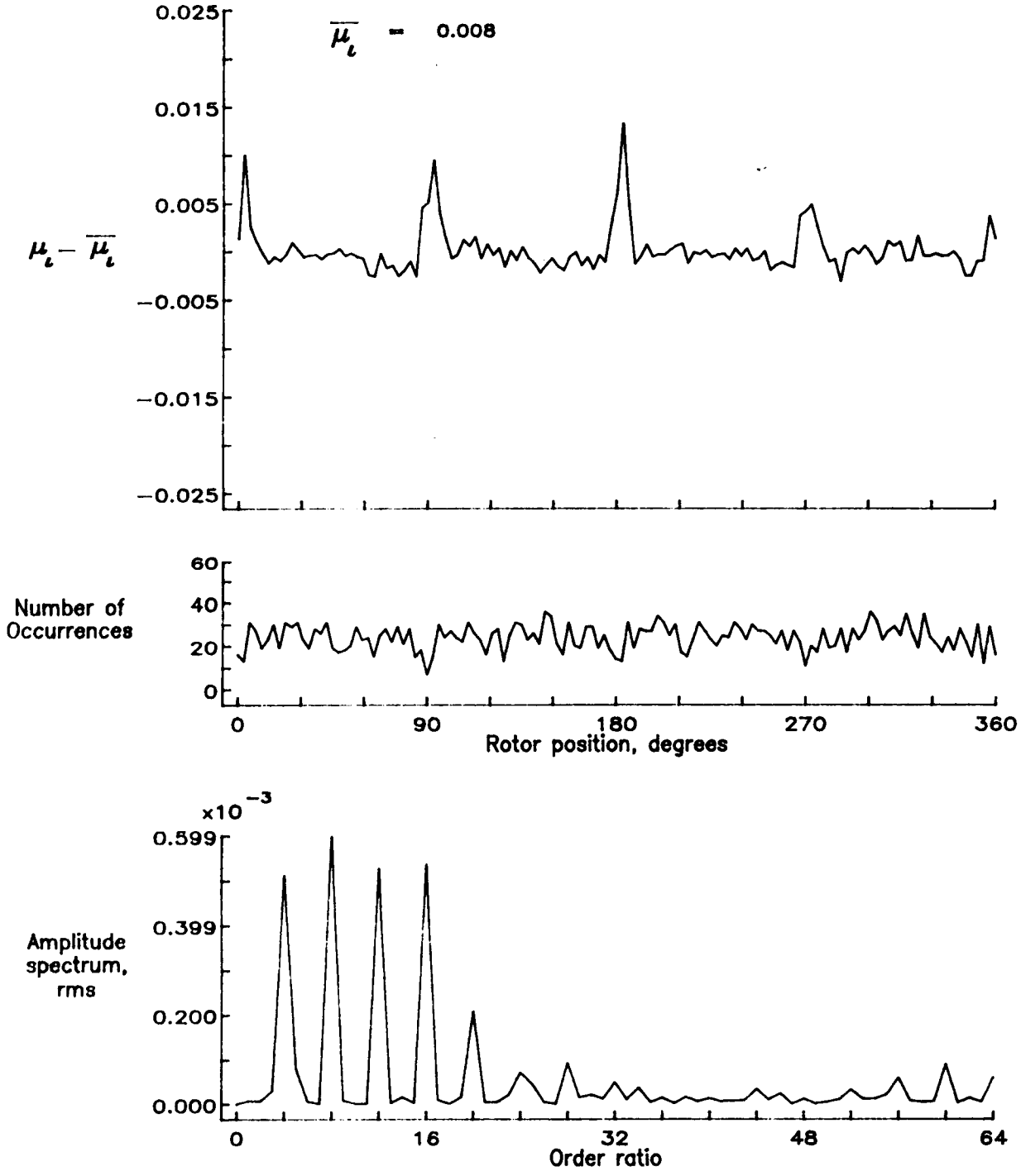

Figure 68.– Induced inflow velocity measured at 90 degrees and r/R of 0.94.

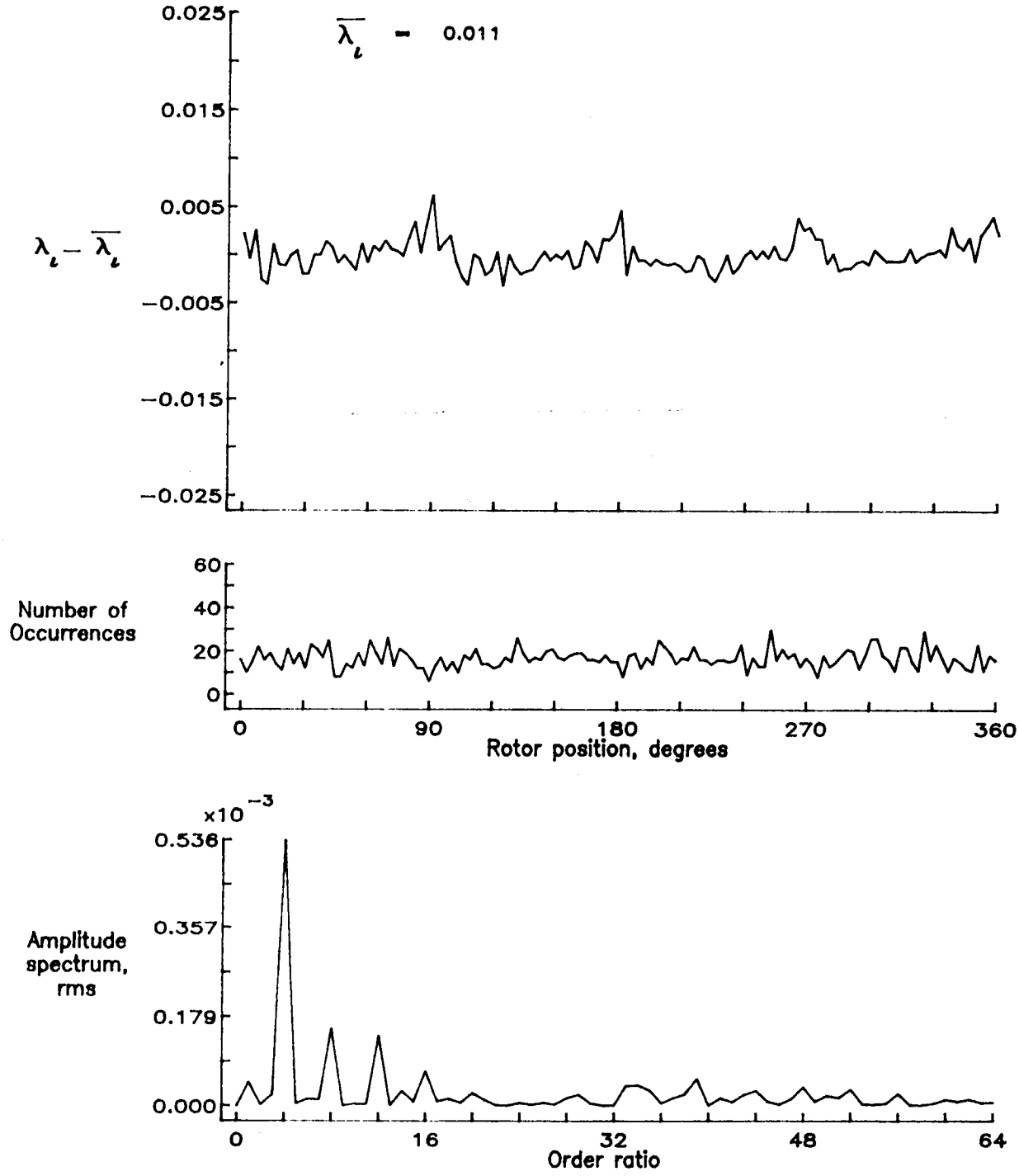

Figure 68.– Concluded.

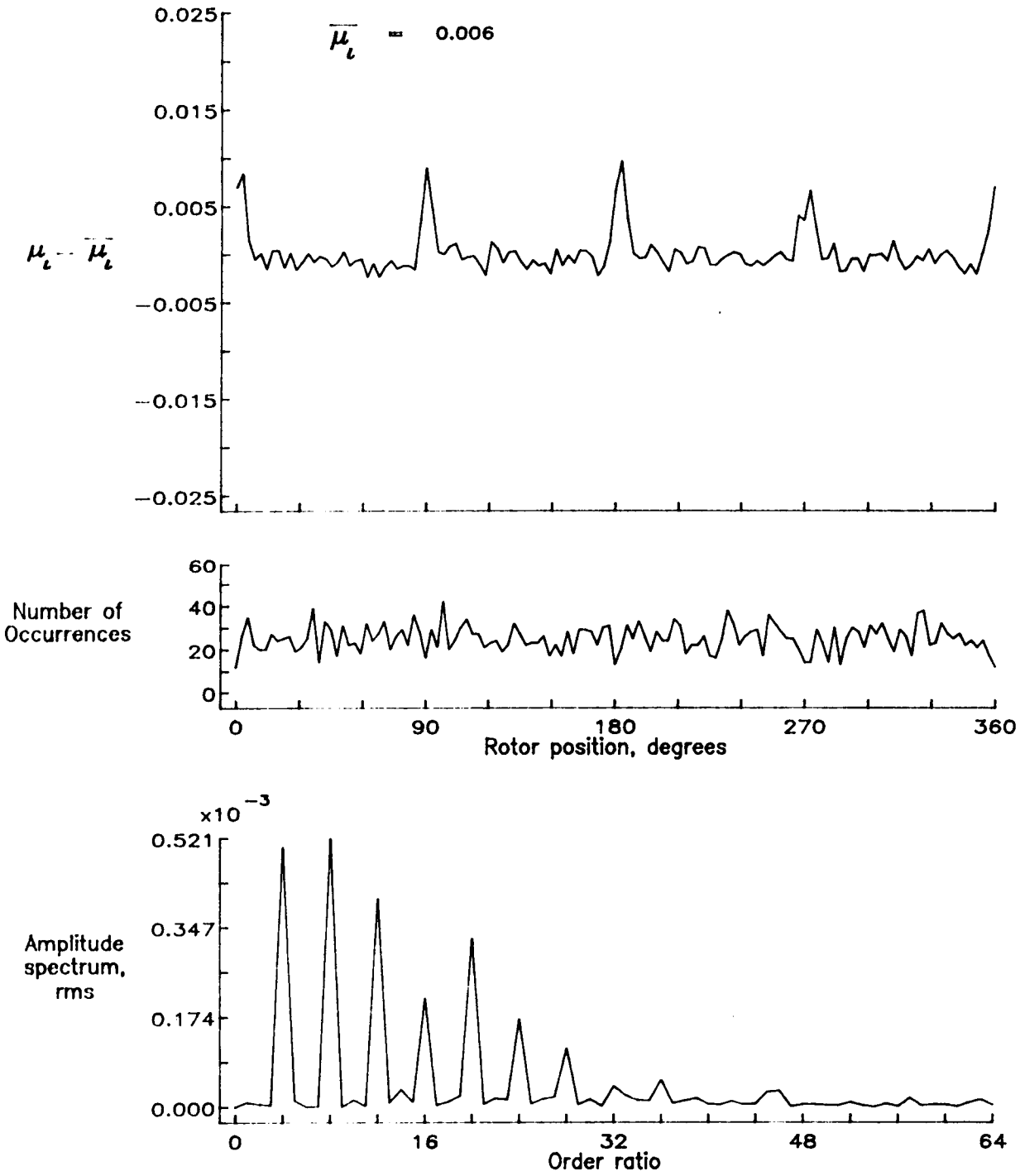

Figure 69.-- Induced inflow velocity measured at 90 degrees and r/R of 0.98.

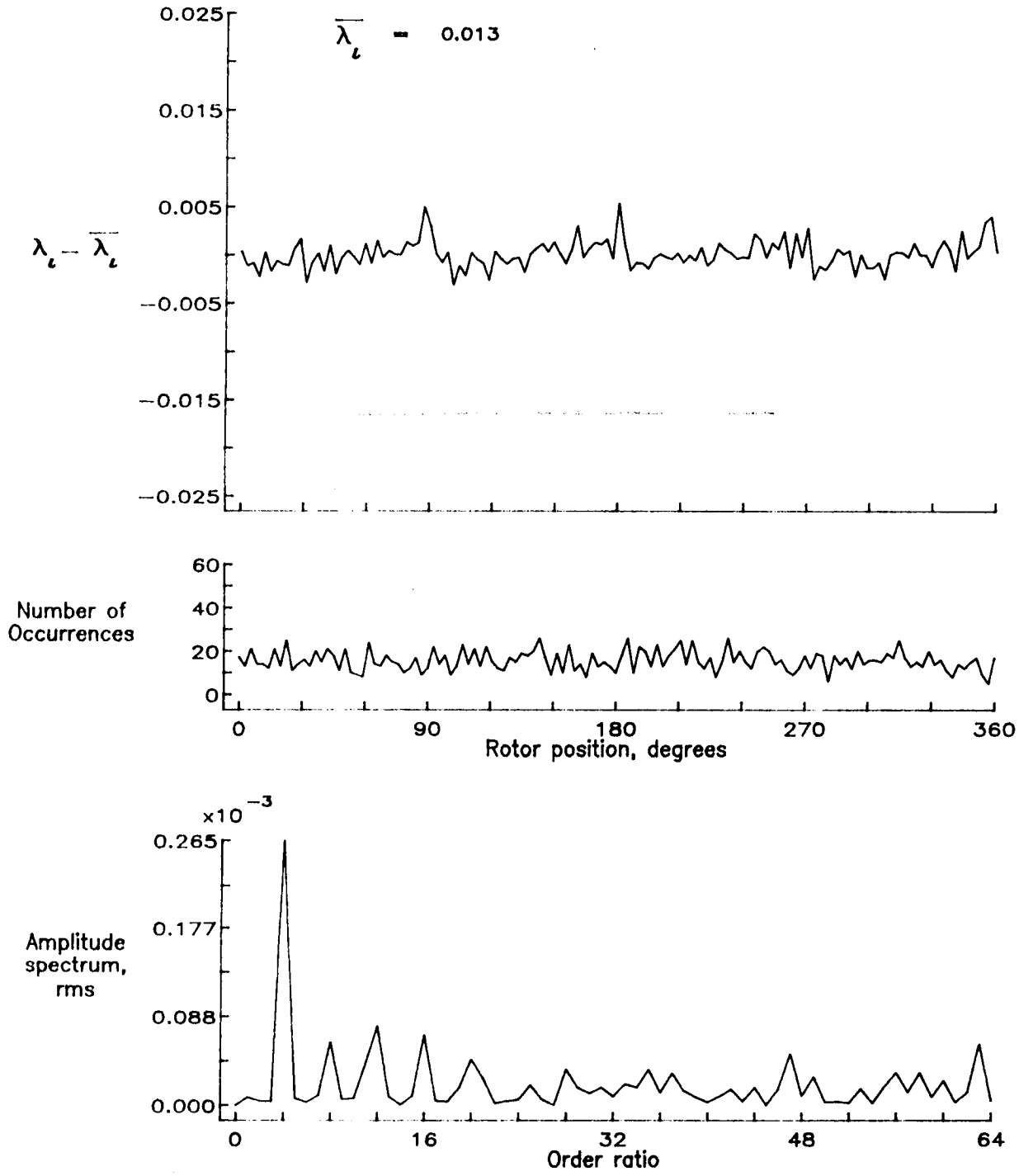

Figure 69.– Concluded.

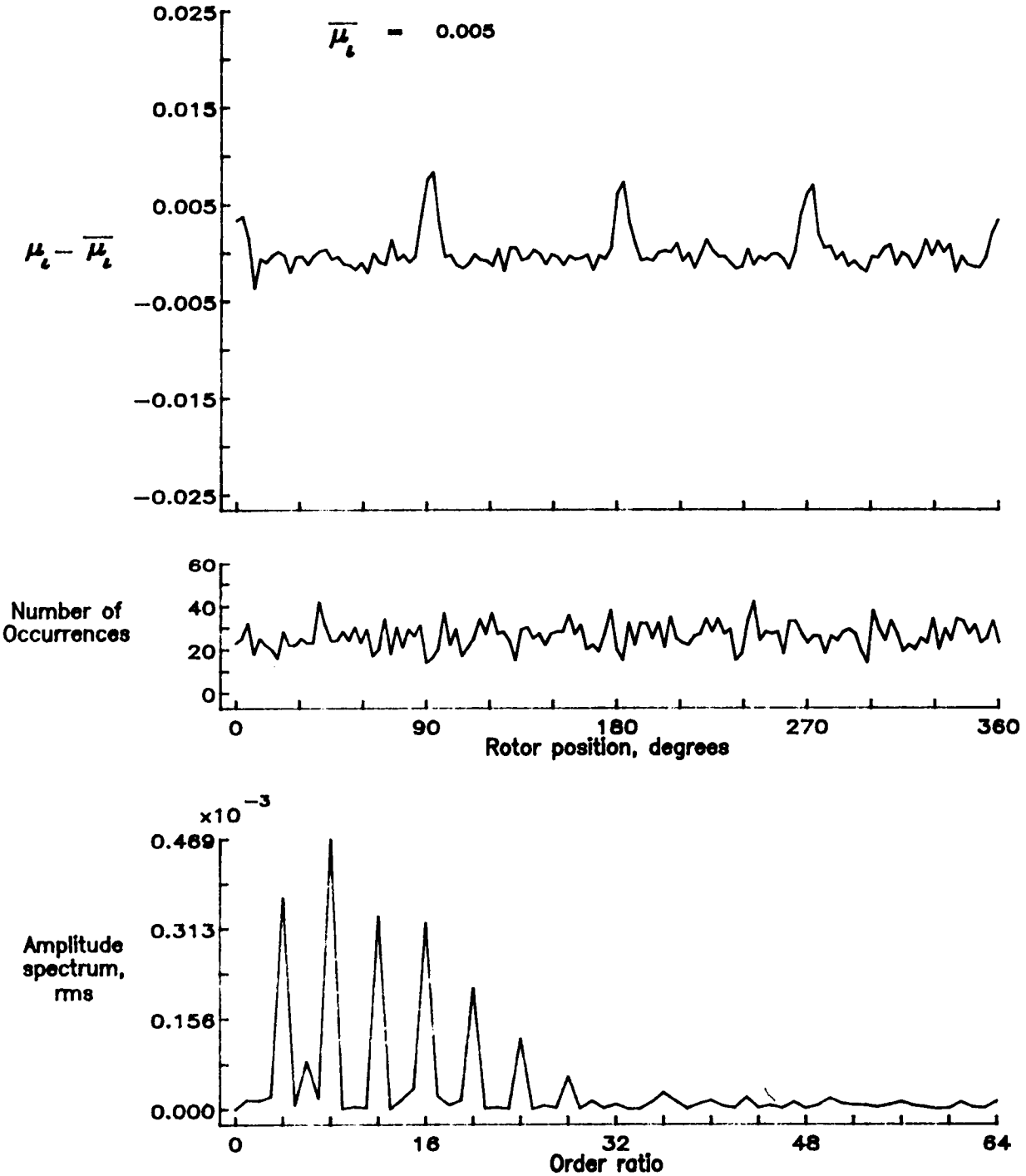

Figure 70.– Induced inflow velocity measured at 90 degrees and r/R of 1.02.

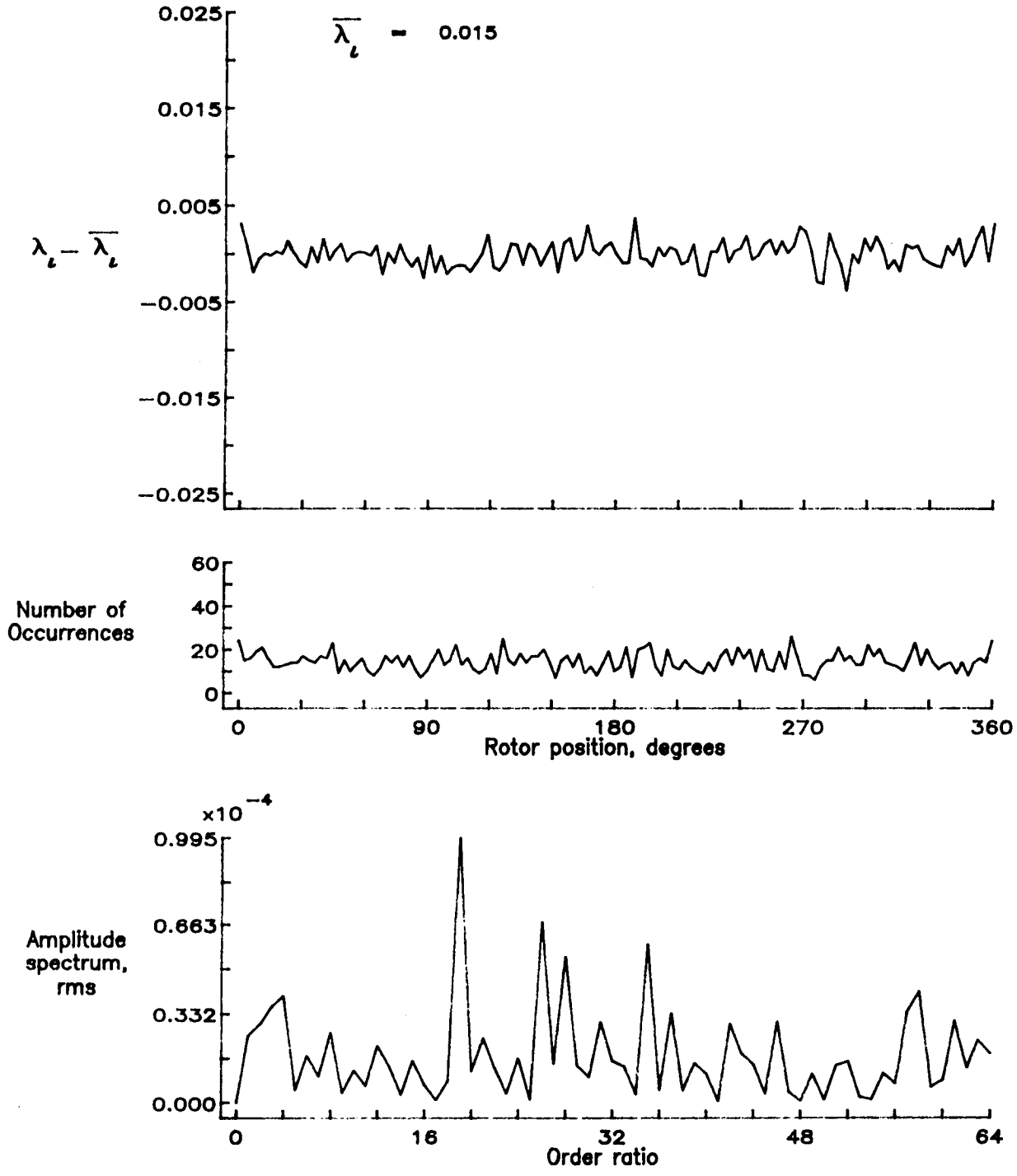

Figure 70.– Concluded.

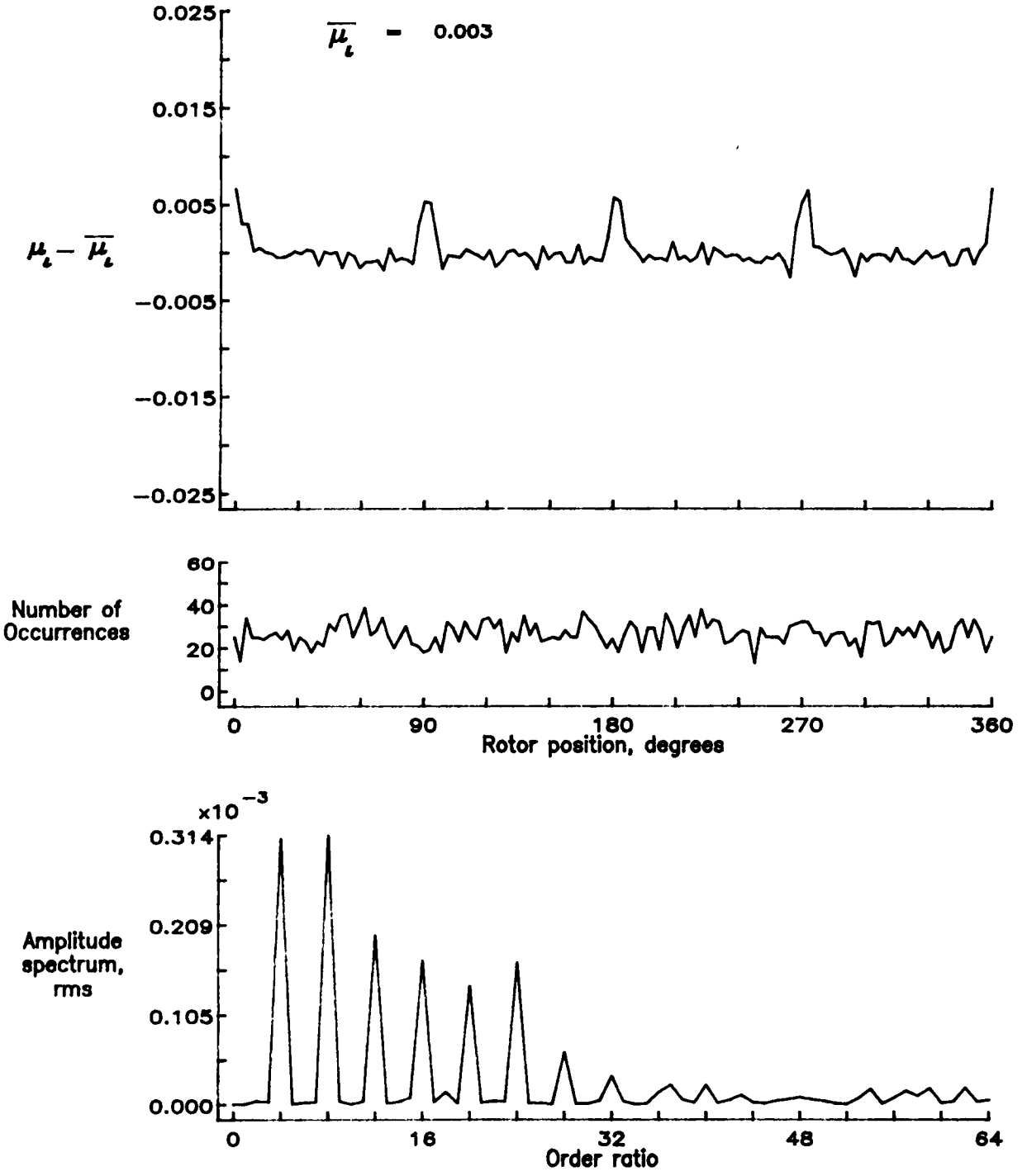

Figure 71.– Induced inflow velocity measured at 90 degrees and r/R of 1.04.

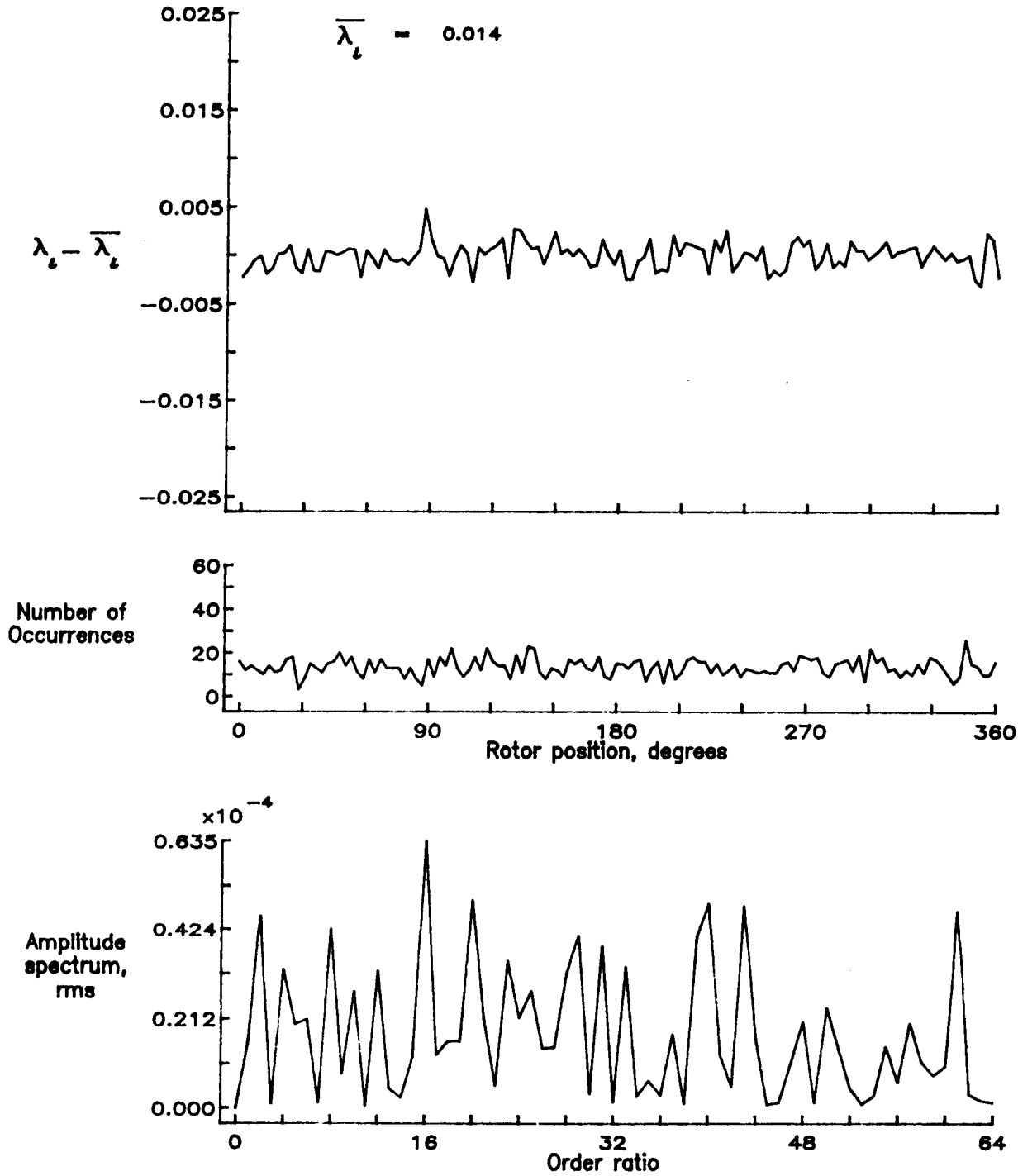

Figure 71.– Concluded.

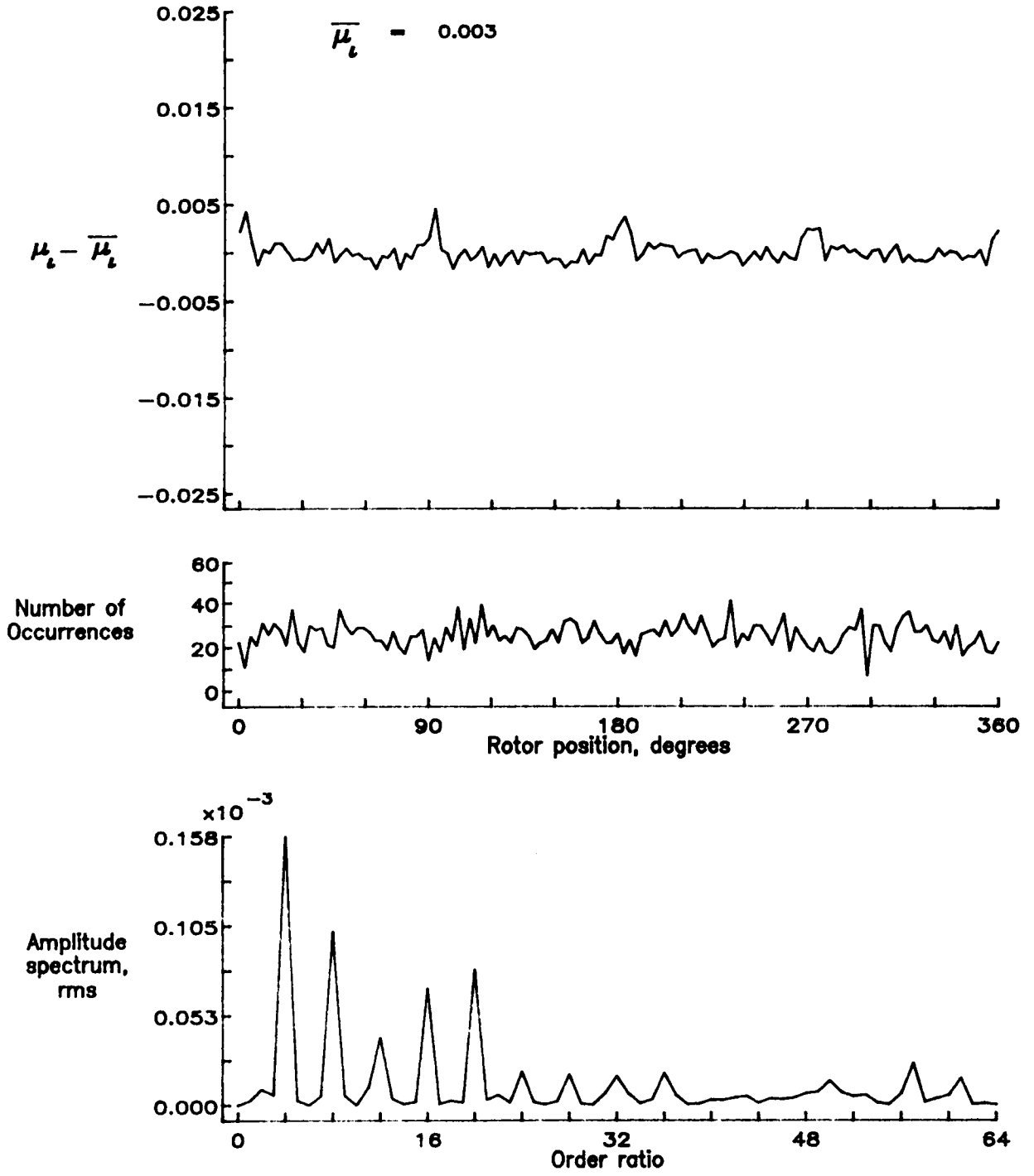

Figure 72.– Induced inflow velocity measured at 90 degrees and r/R of 1.10.

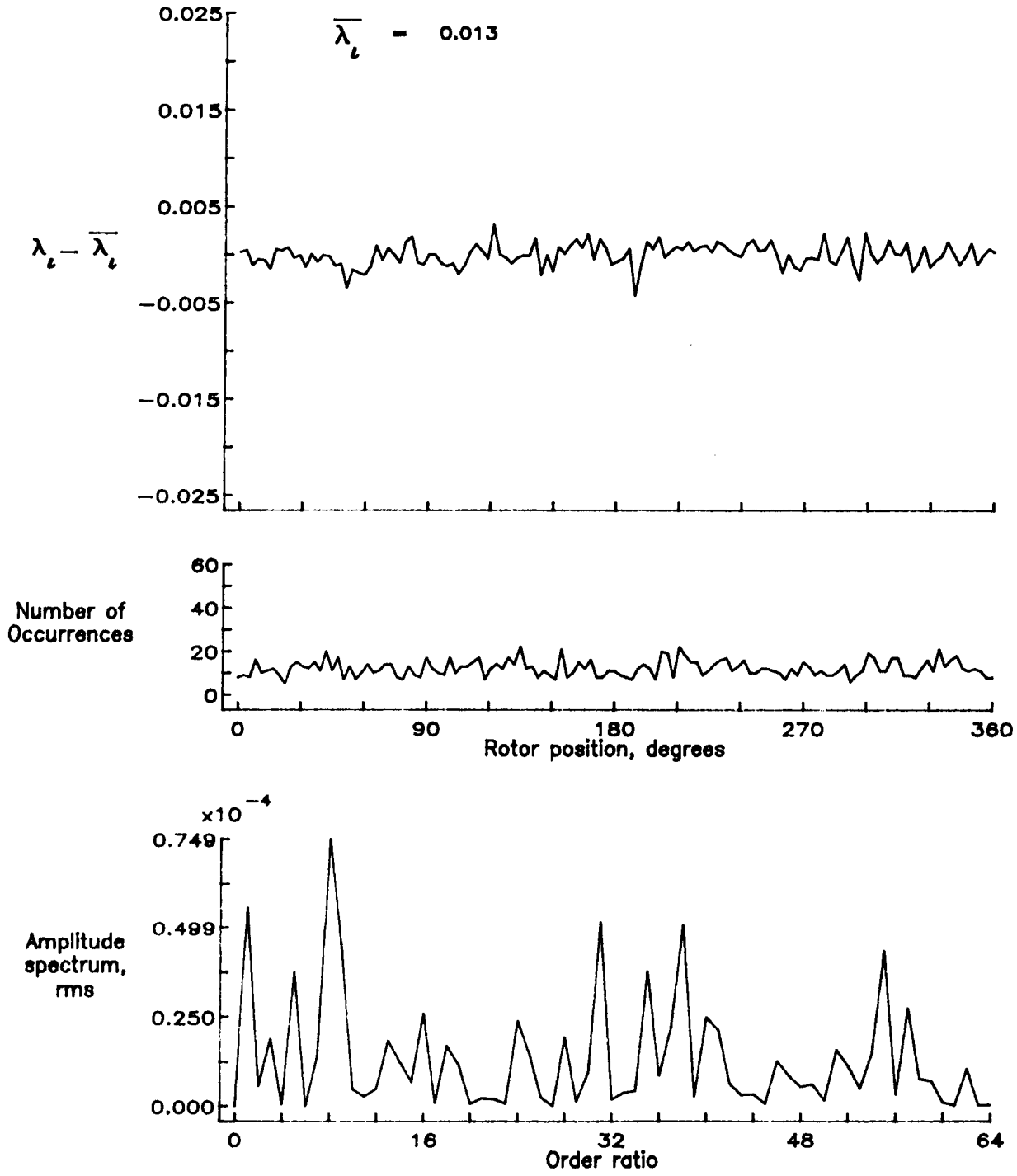

Figure 72.– Concluded.

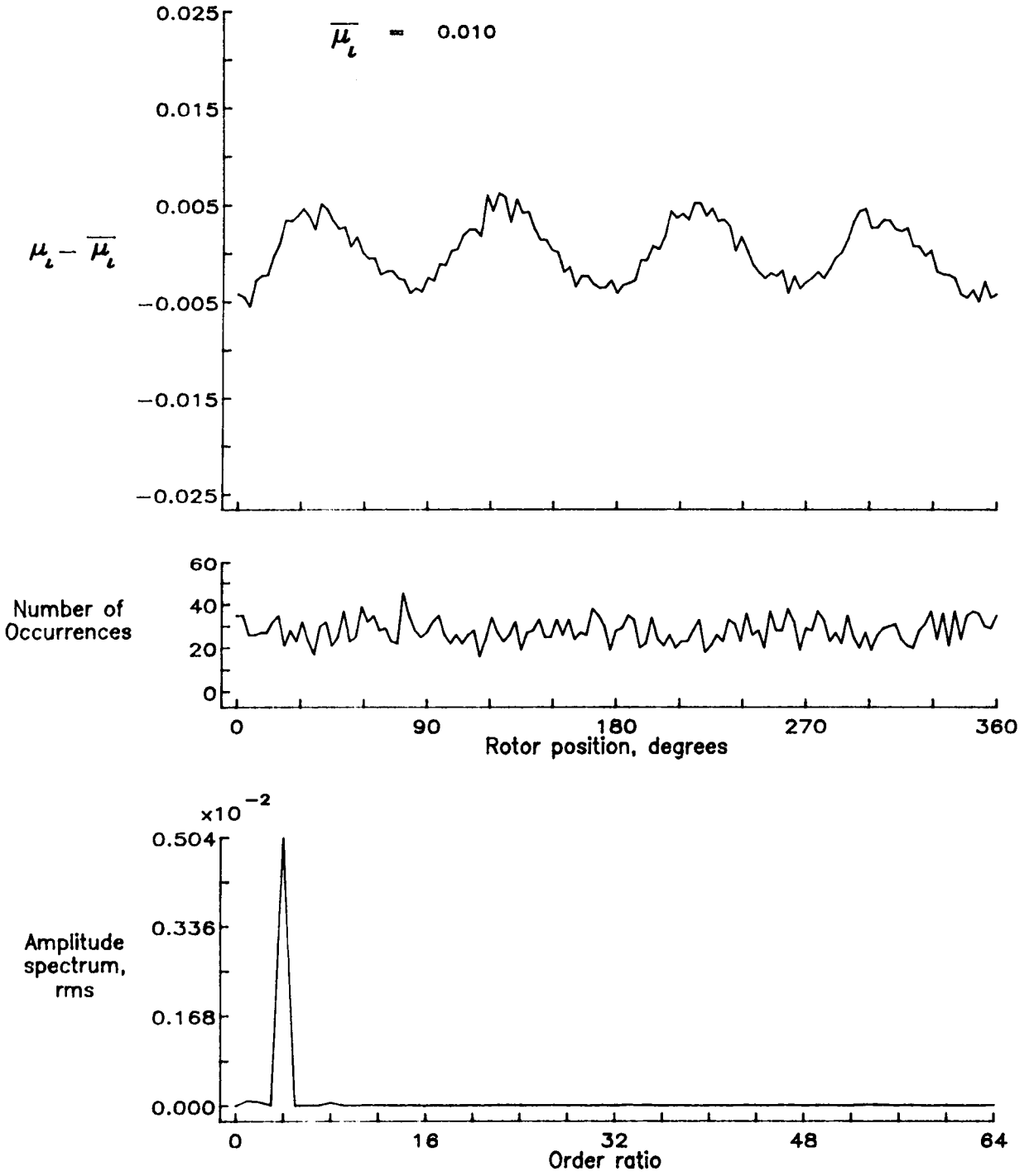

Figure 73.– Induced inflow velocity measured at 120 degrees and r/R of 0.20.

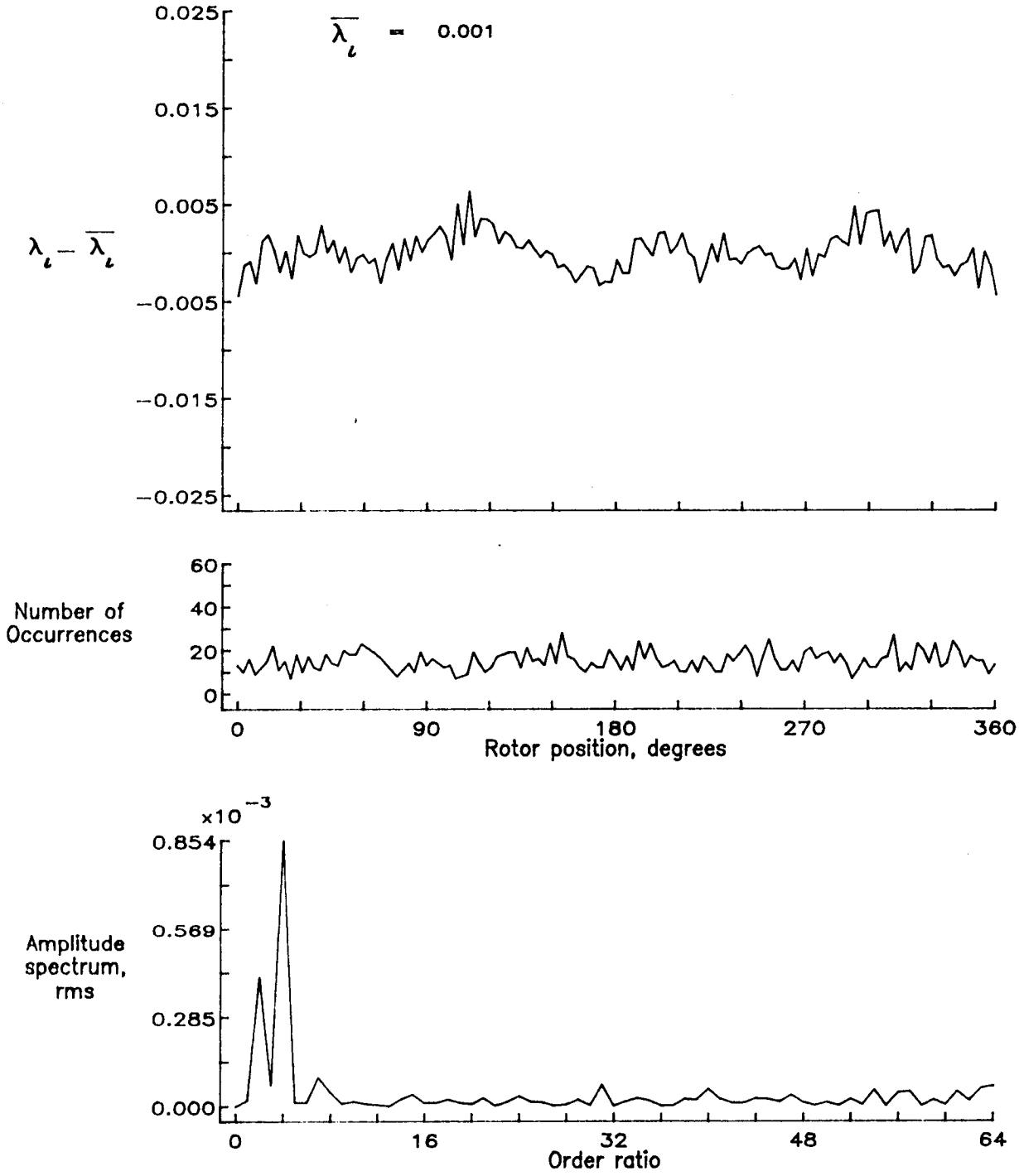

Figure 73.– Concluded.

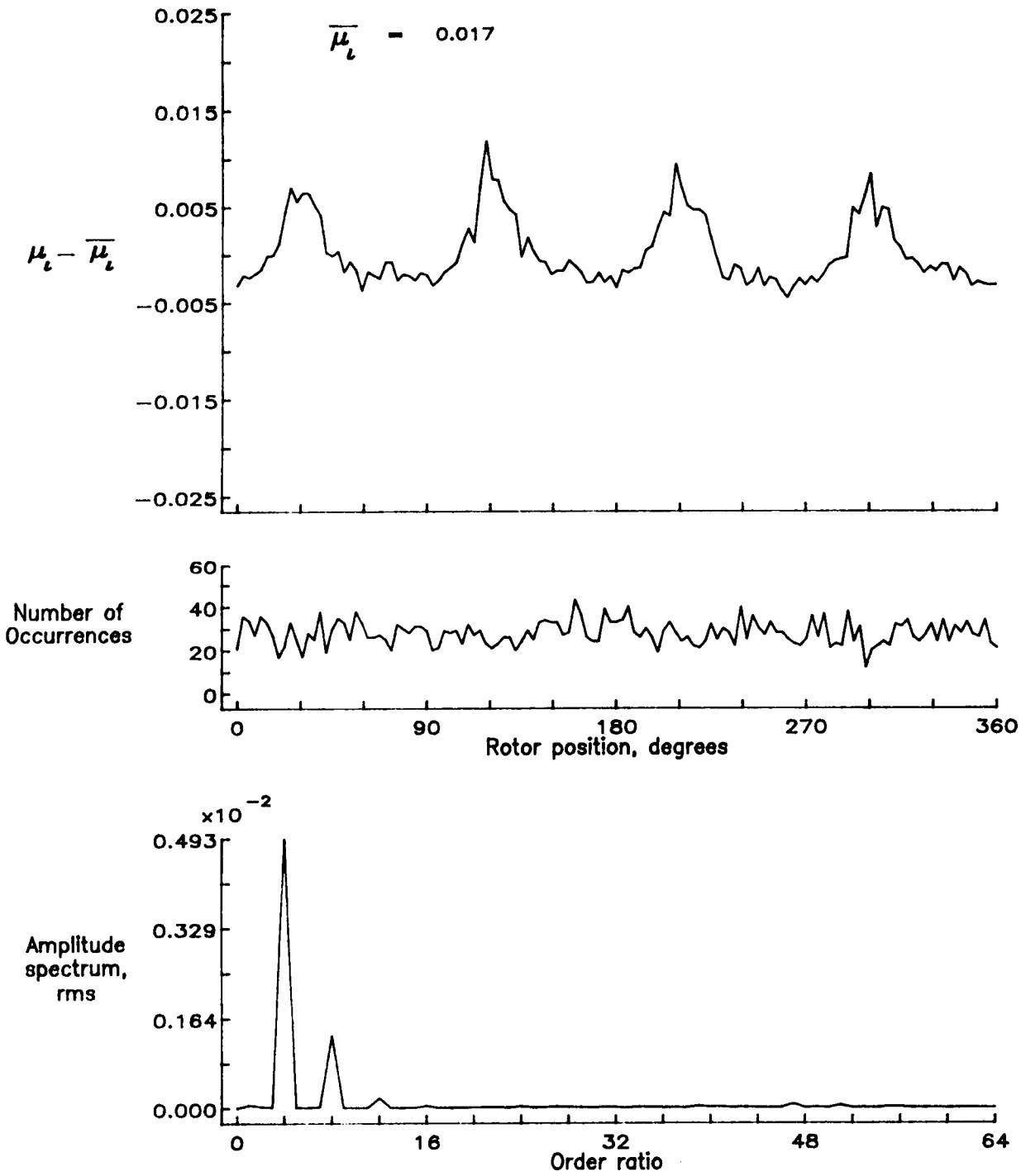

Figure 74.– Induced inflow velocity measured at 120 degrees and r/R of 0.40.

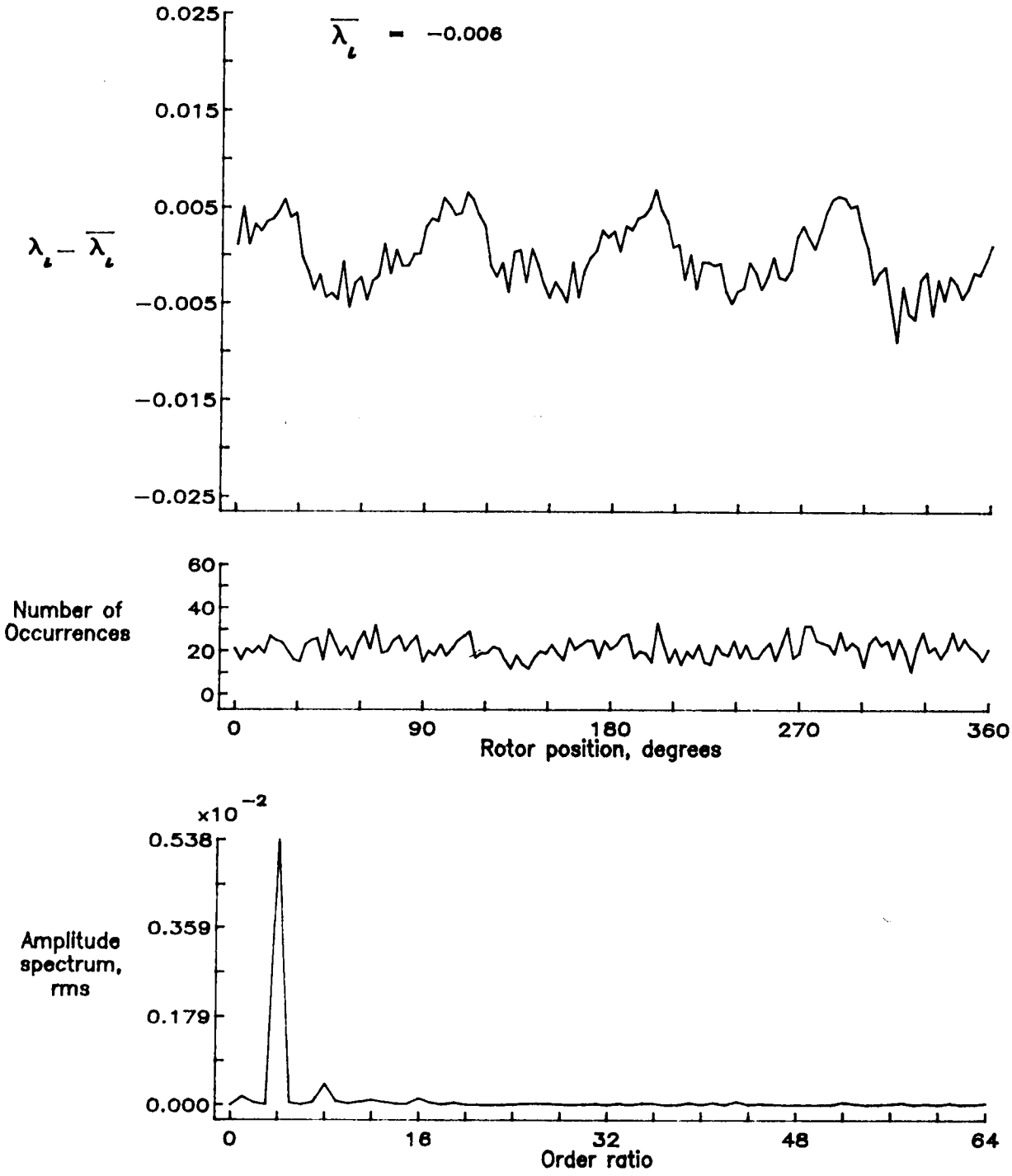

Figure 74.– Concluded.

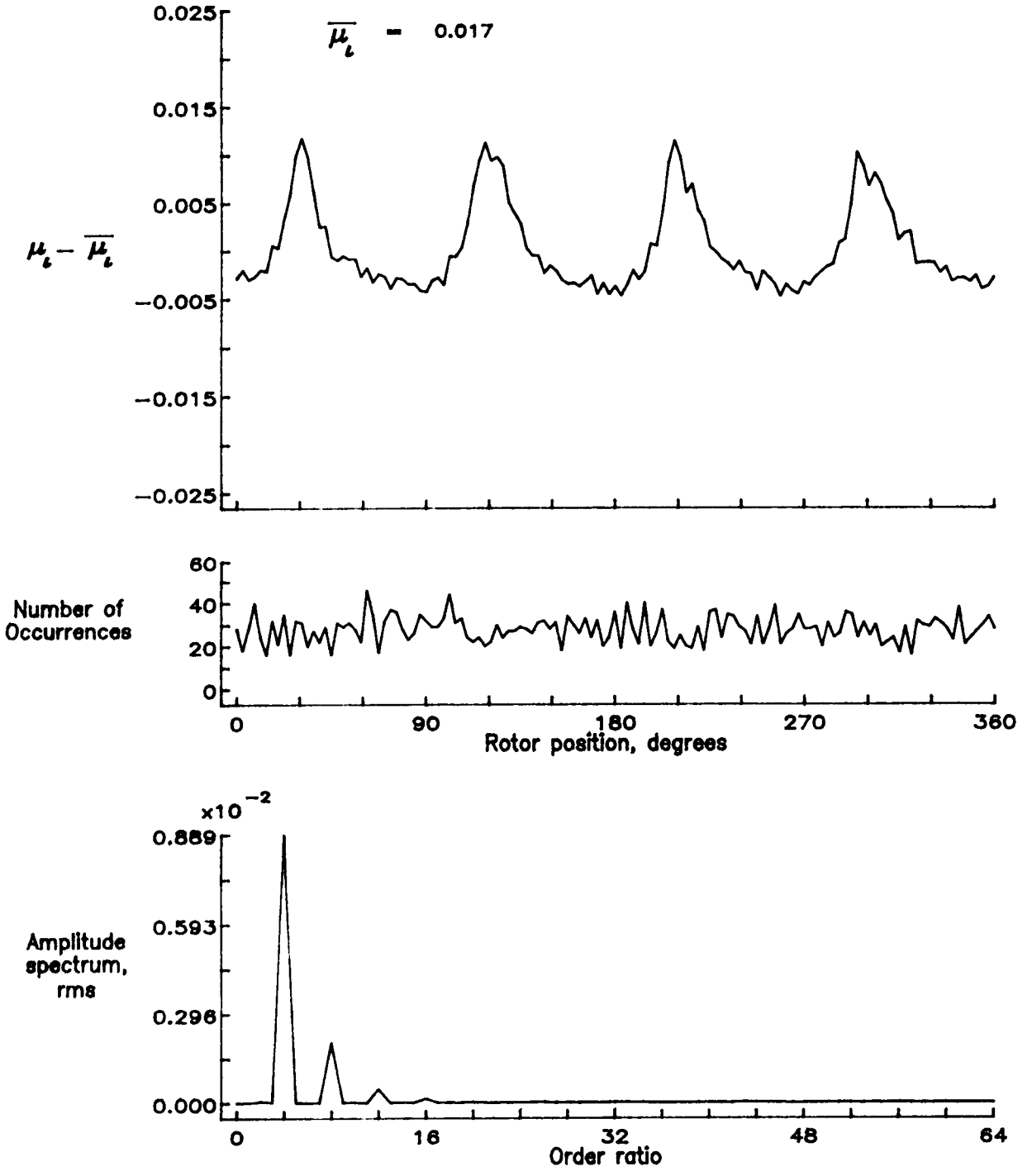

Figure 75.– Induced inflow velocity measured at 120 degrees and r/R of 0.50.

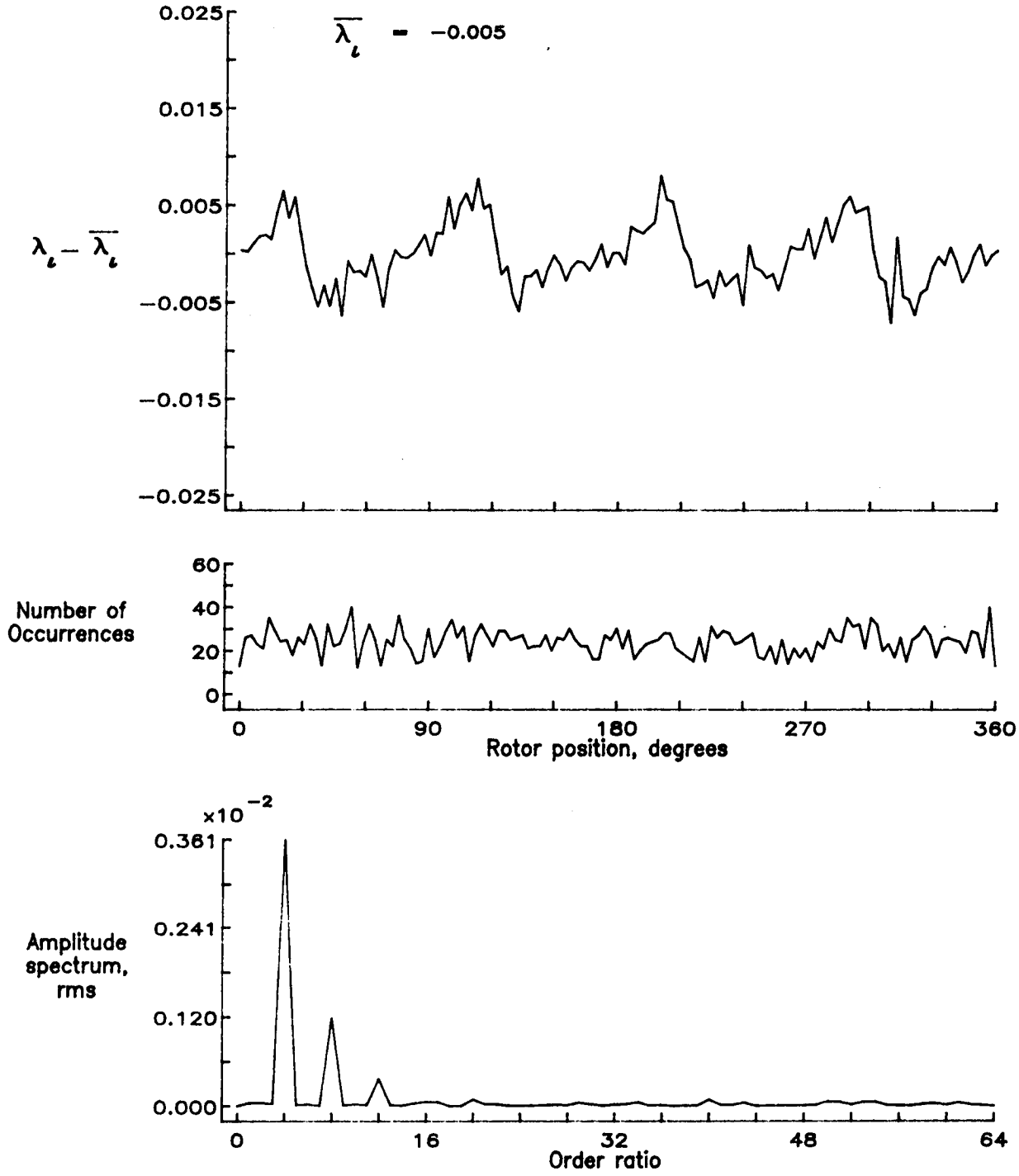

Figure 75.– Concluded.

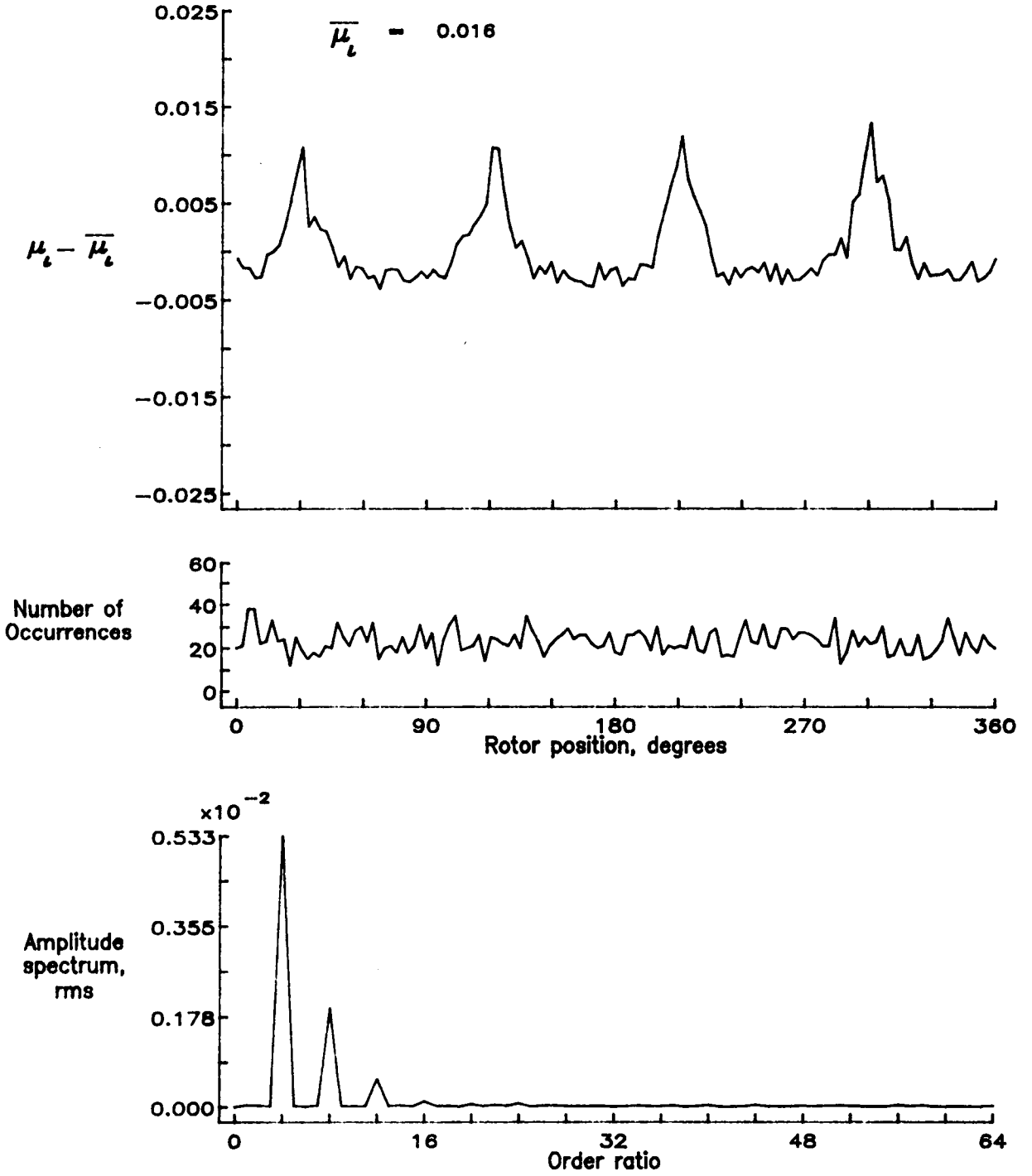

Figure 76.– Induced inflow velocity measured at 120 degrees and r/R of 0.60.

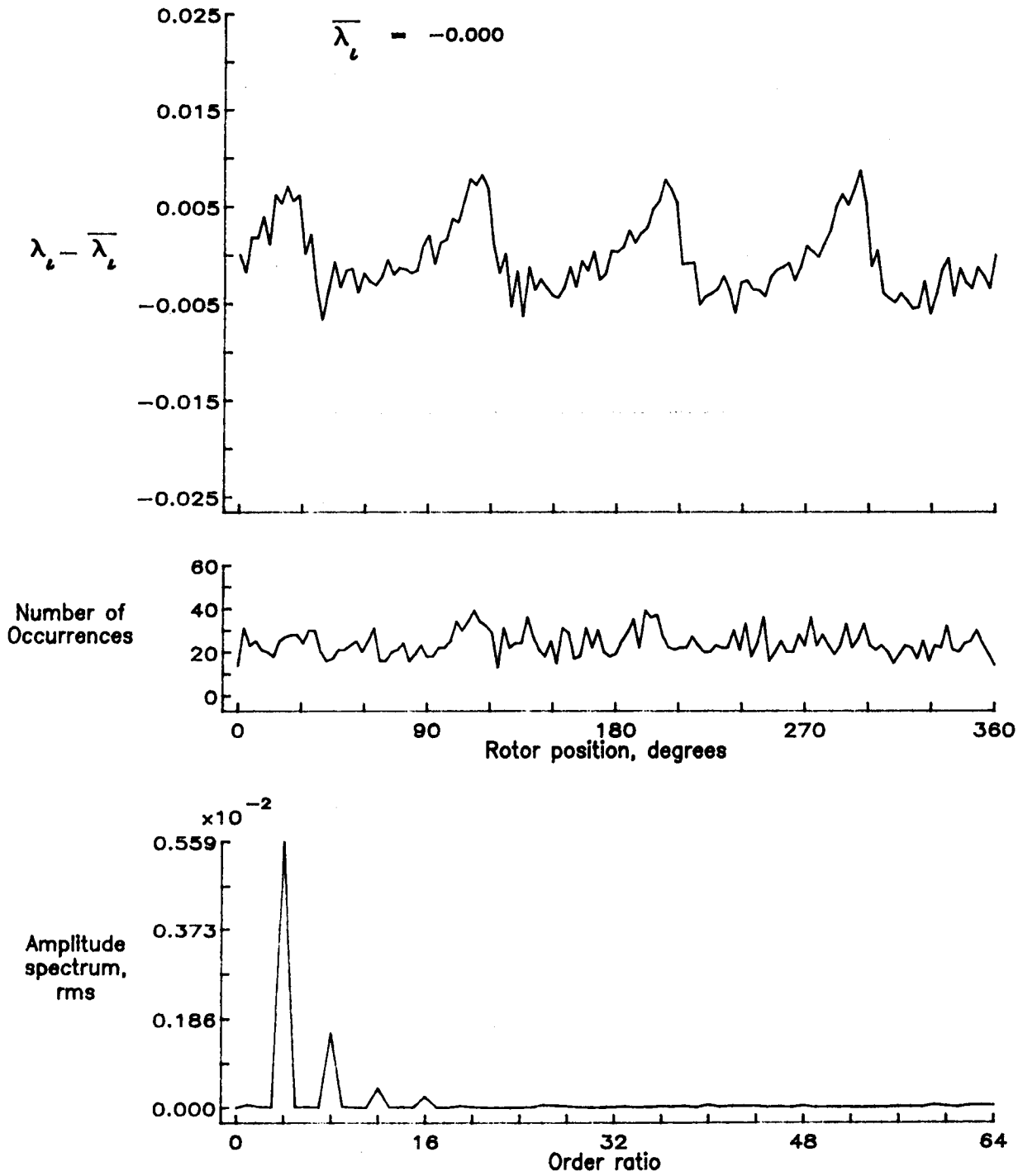

Figure 76.– Concluded.

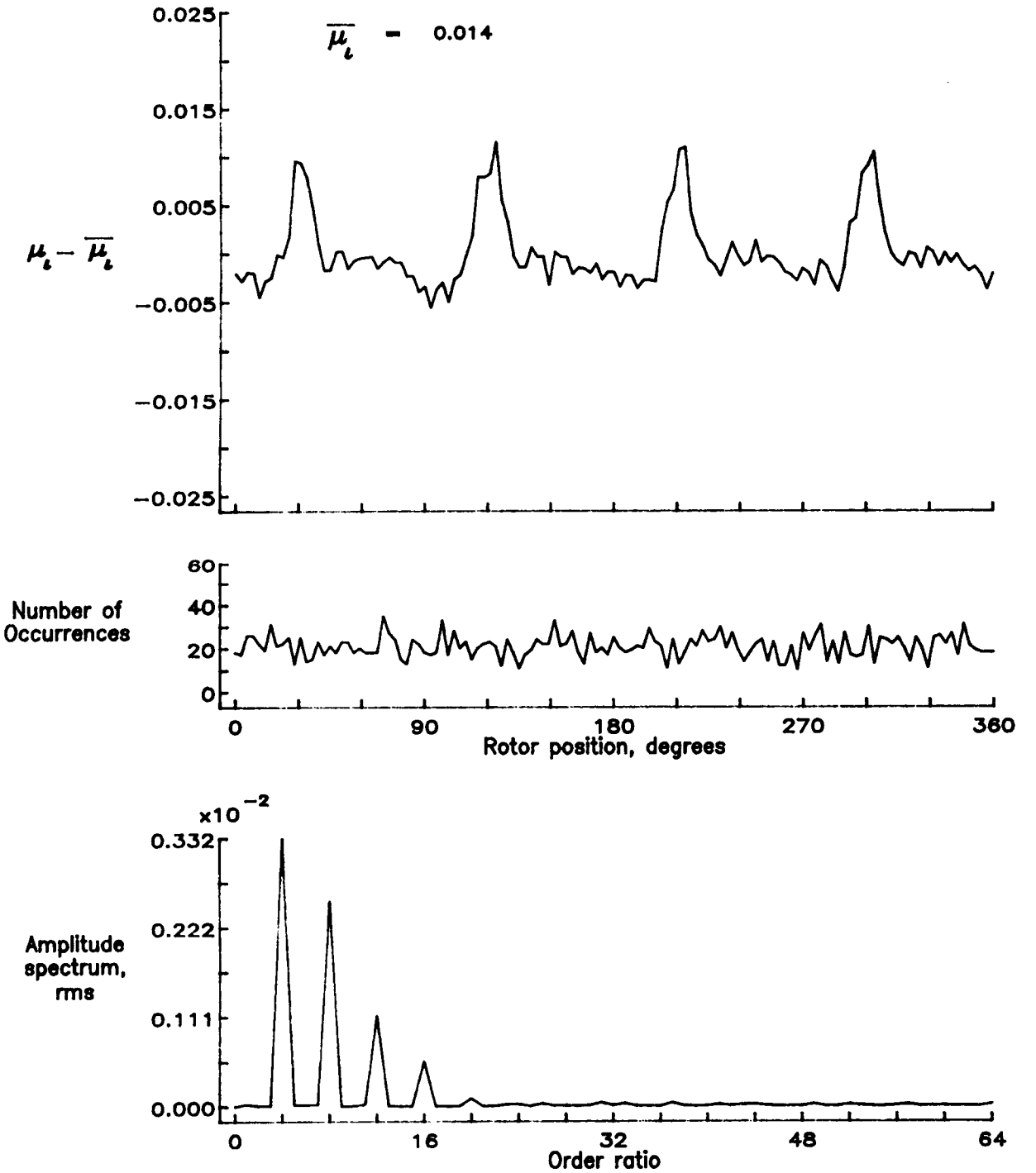

Figure 77.– Induced inflow velocity measured at 120 degrees and r/R of 0.70.

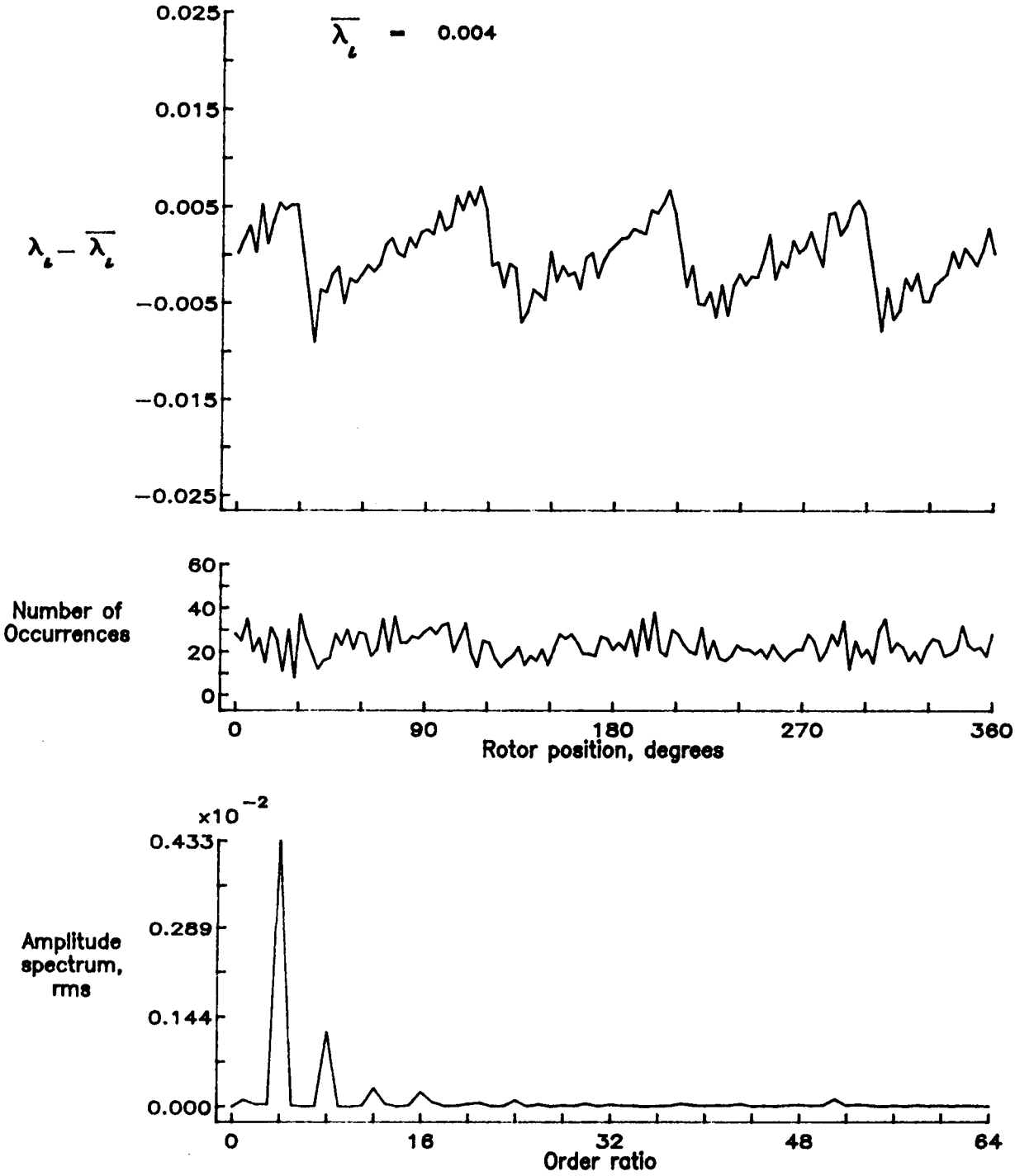

Figure 77.– Concluded.

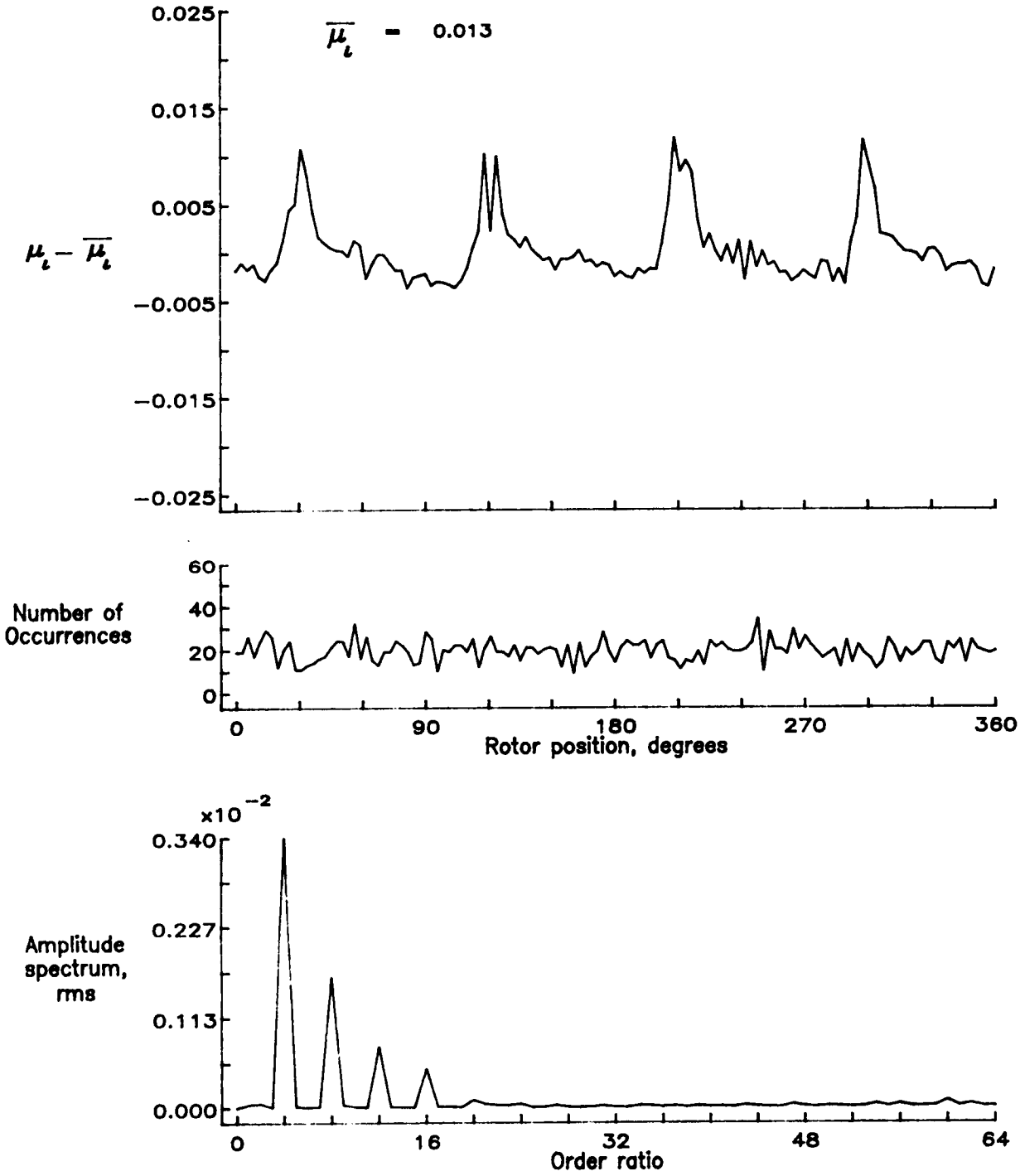

Figure 78.– Induced inflow velocity measured at 120 degrees and r/R of 0.74.

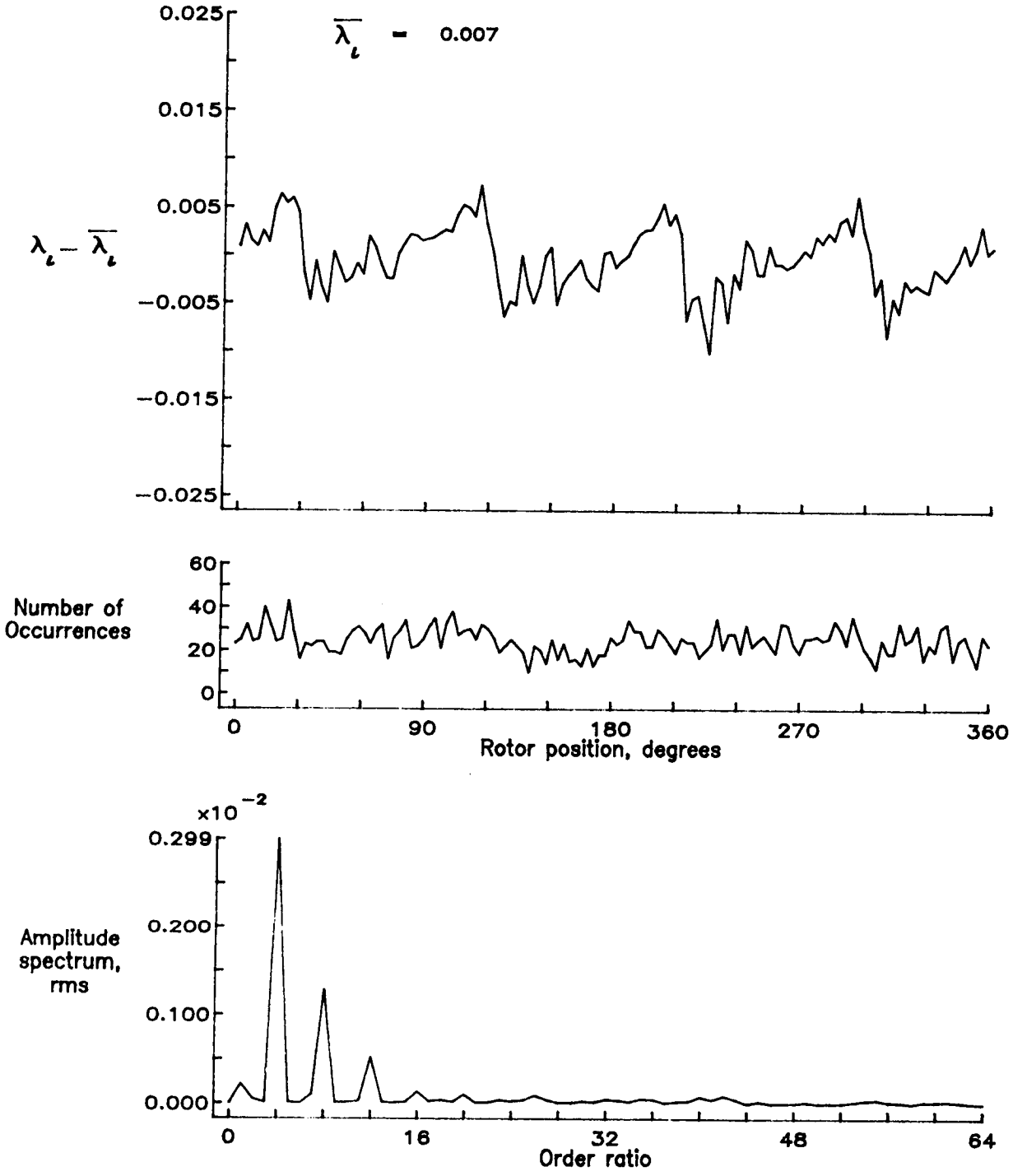

Figure 78.– Concluded.

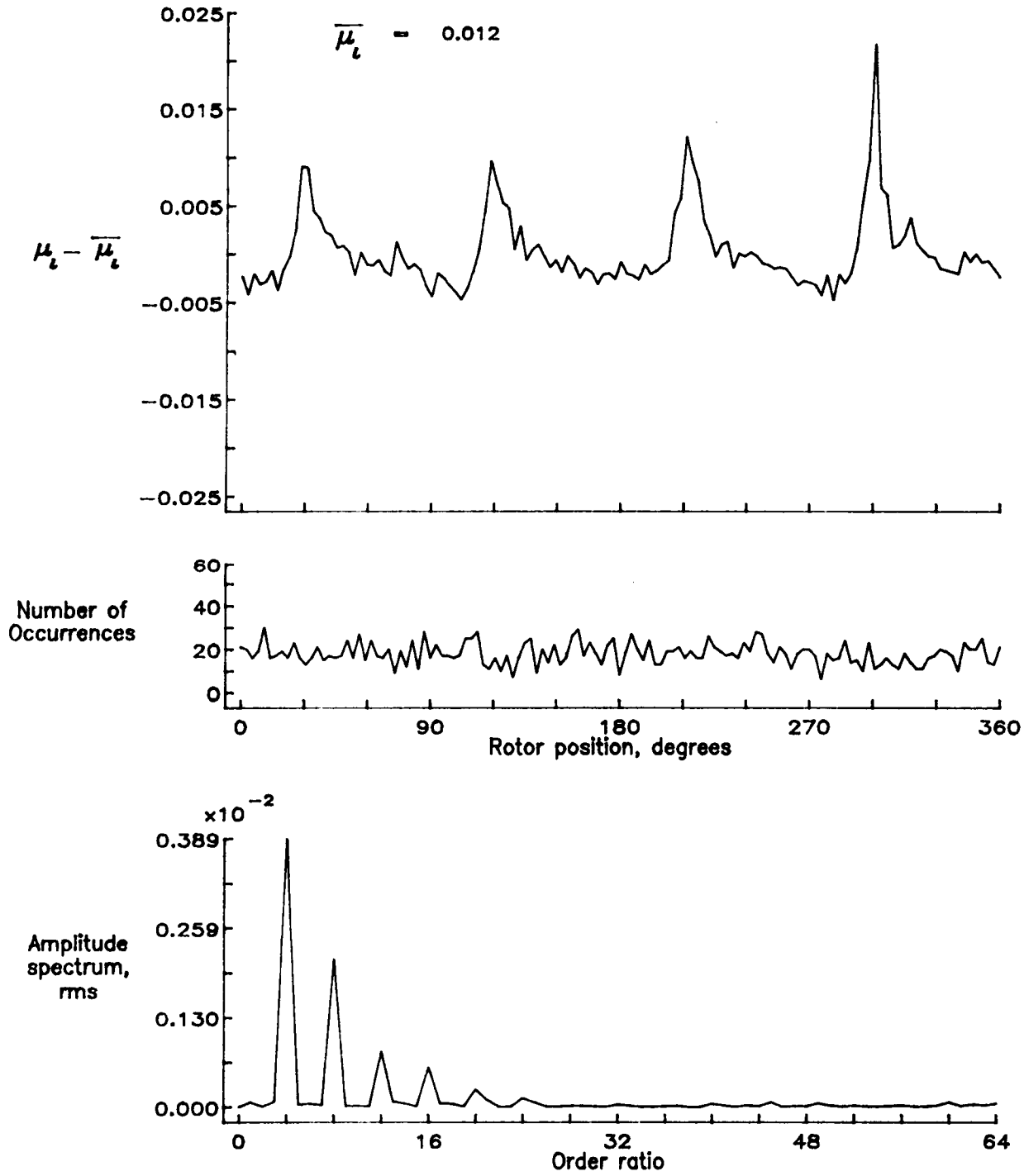

Figure 79.– Induced inflow velocity measured at 120 degrees and r/R of 0.78.

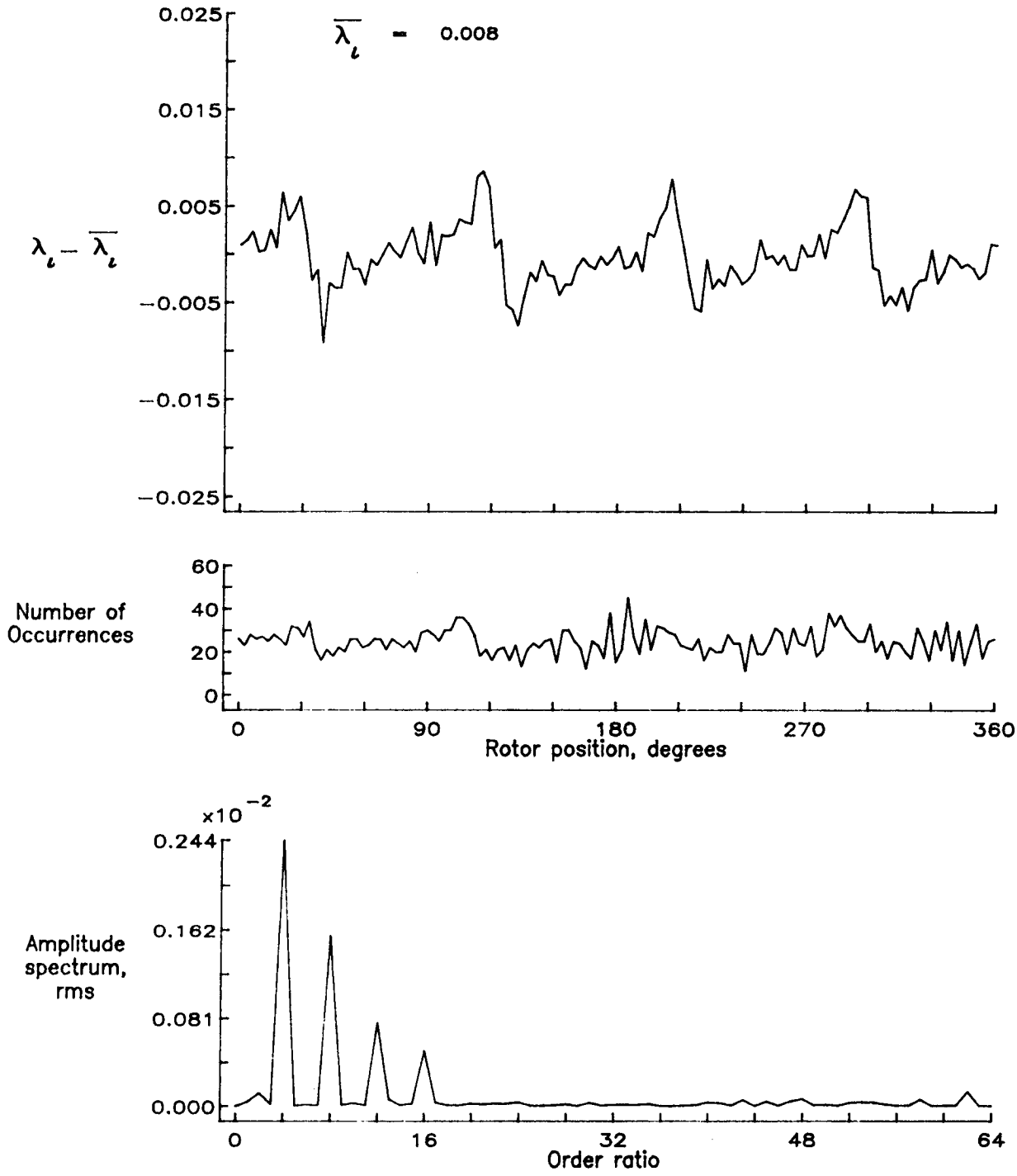

Figure 79.– Concluded.

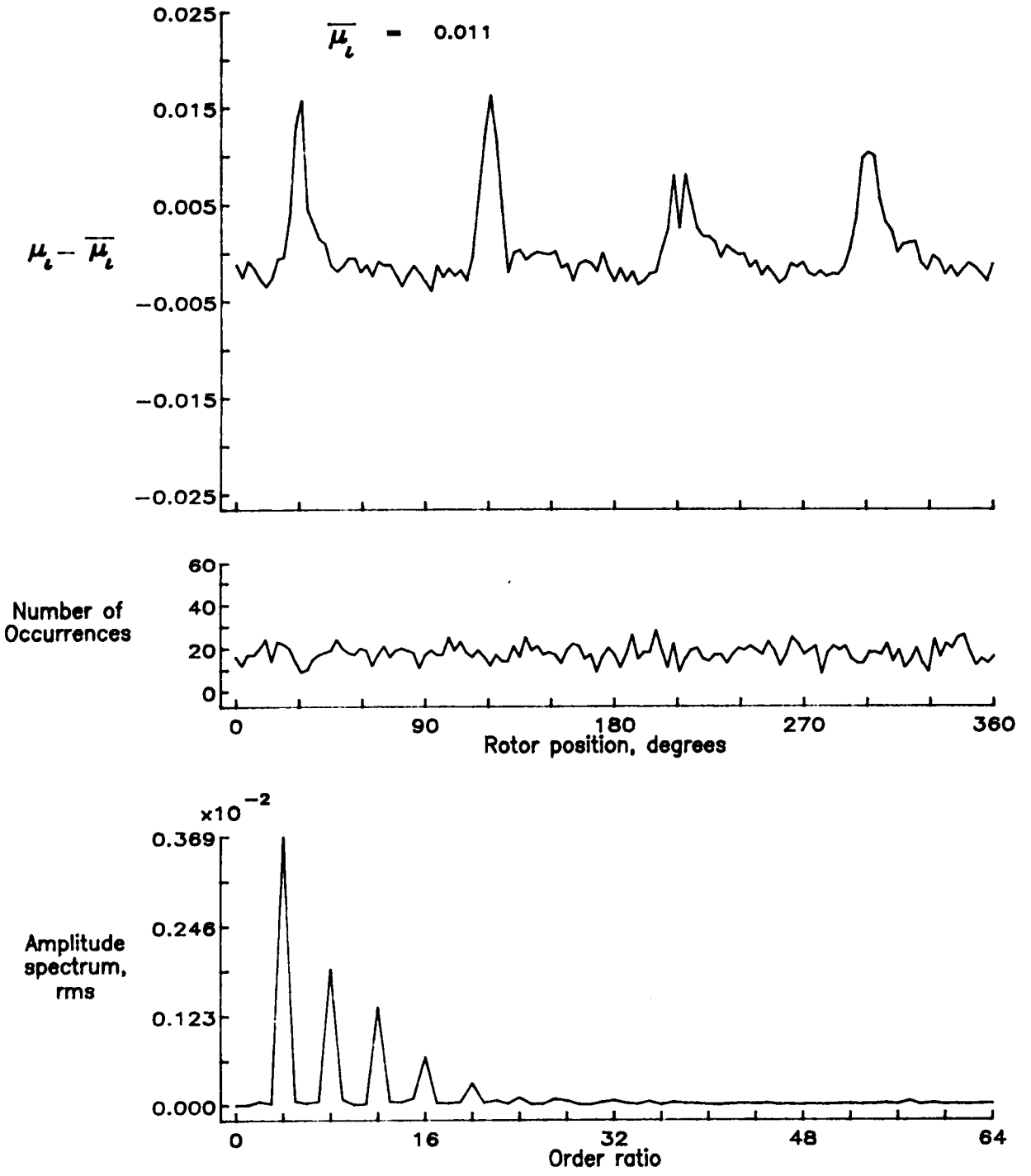

Figure 80.– Induced inflow velocity measured at 120 degrees and r/R of 0.82.

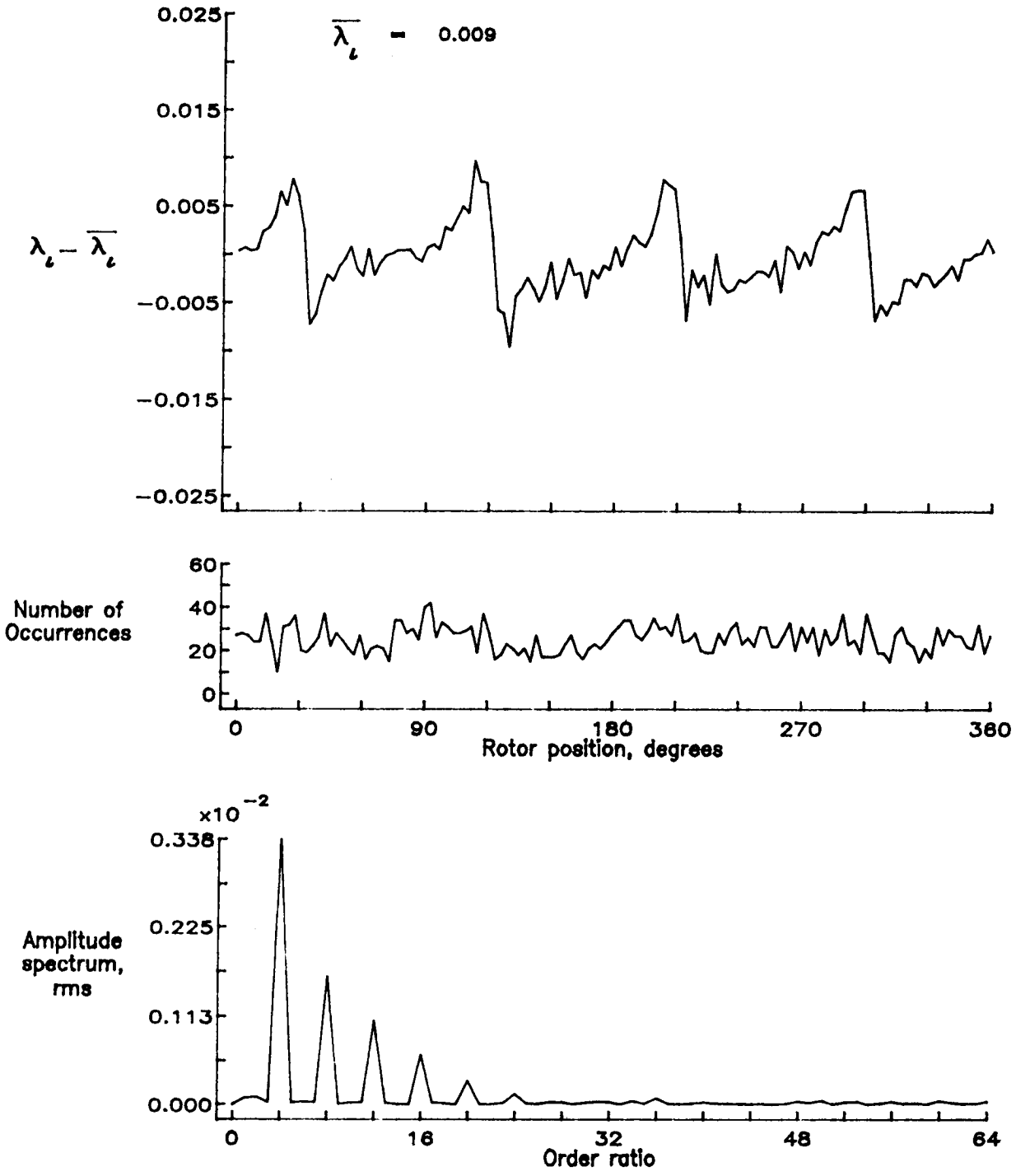

Figure 80.– Concluded.

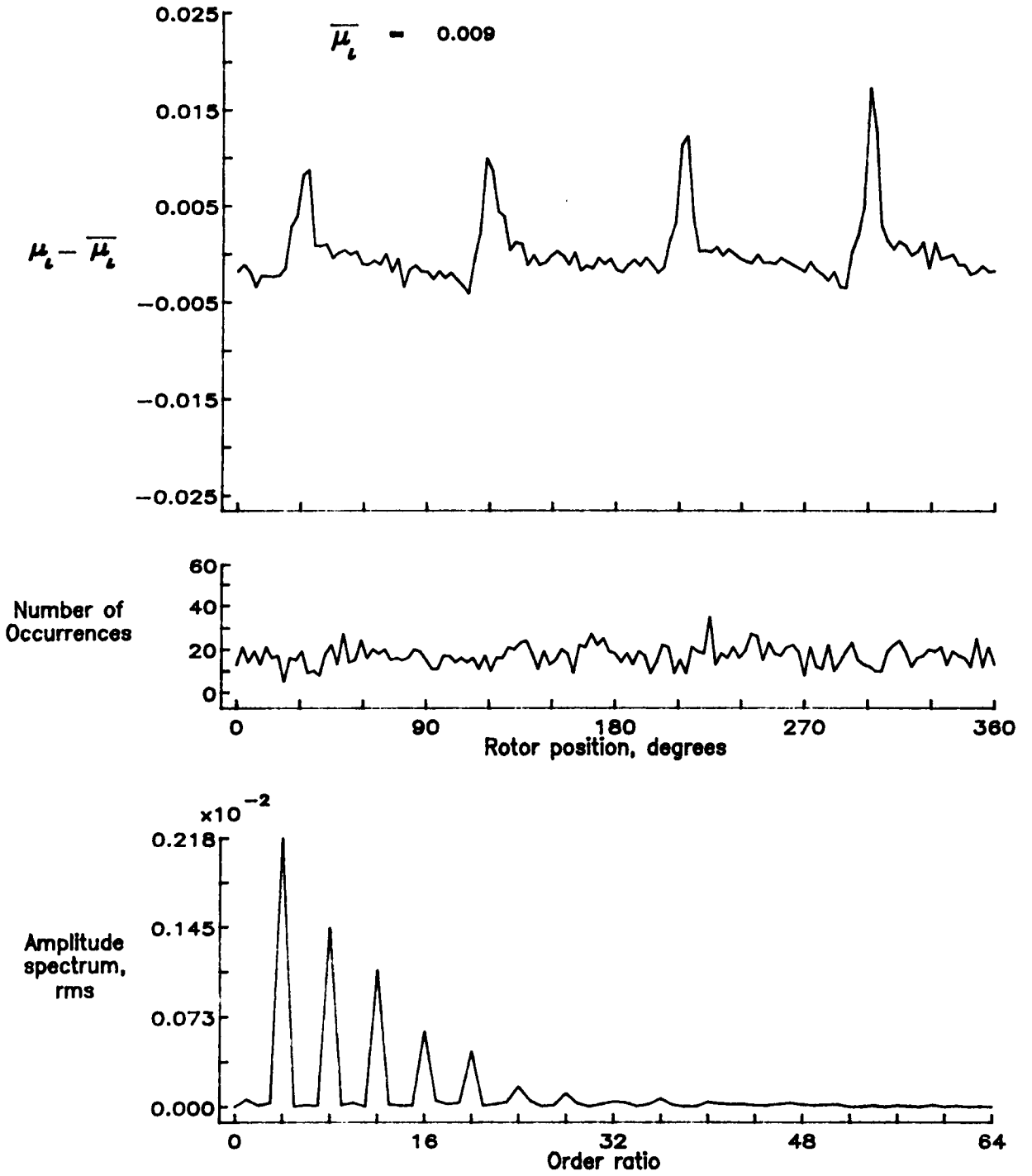

Figure 81.– Induced inflow velocity measured at 120 degrees and r/R of 0.86.

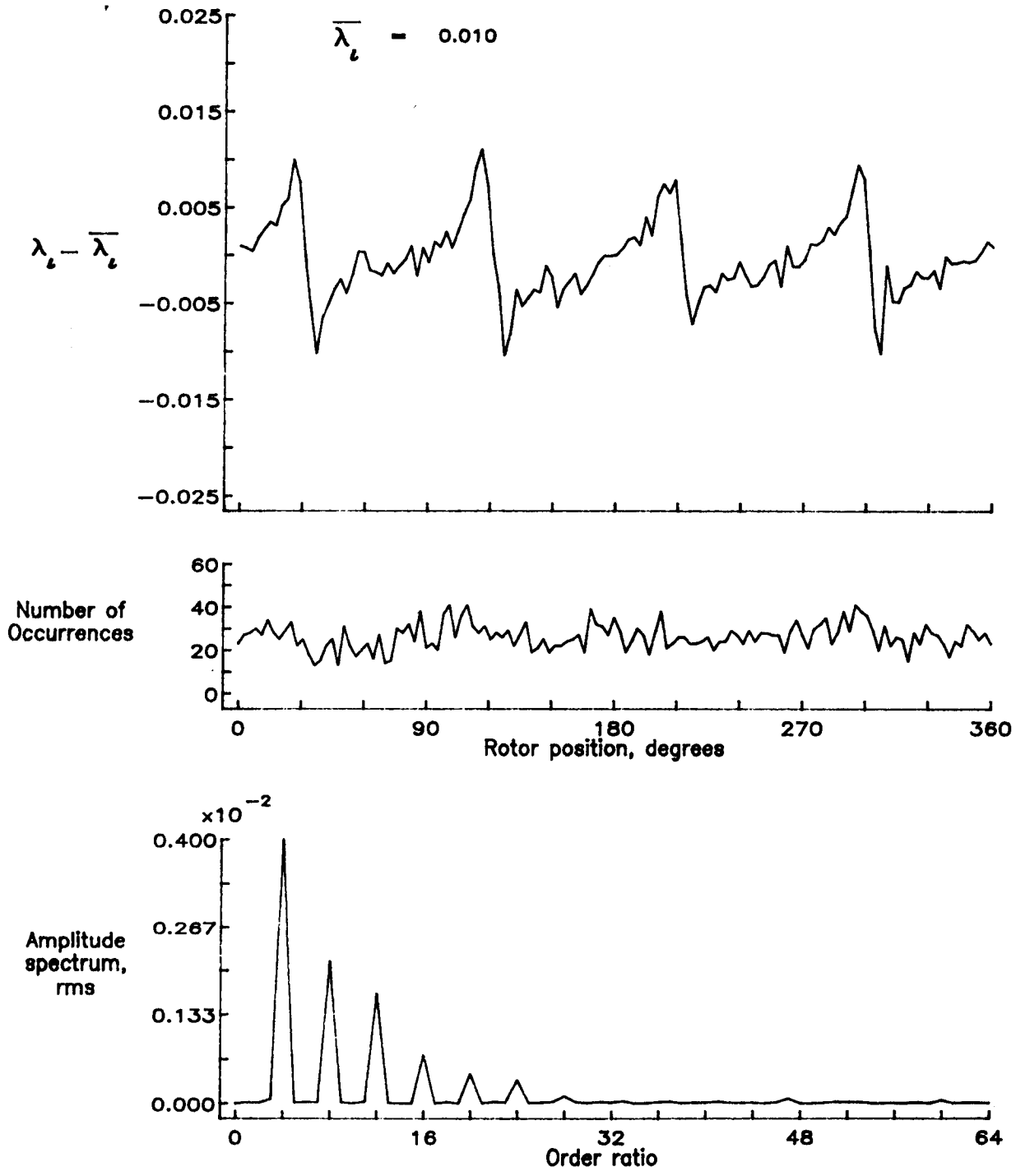

Figure 81.– Concluded.

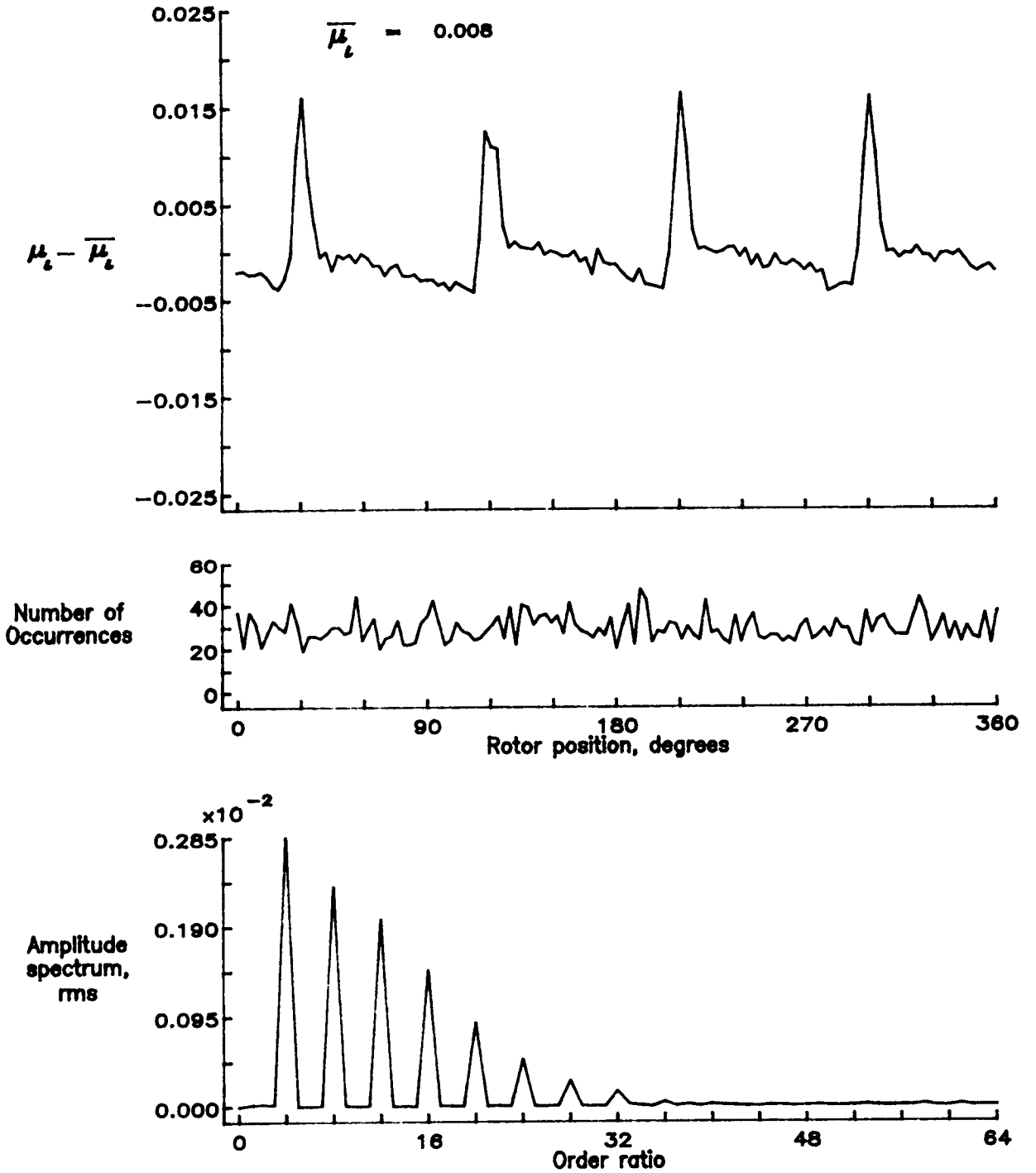

Figure 82.– Induced inflow velocity measured at 120 degrees and r/R of 0.90.

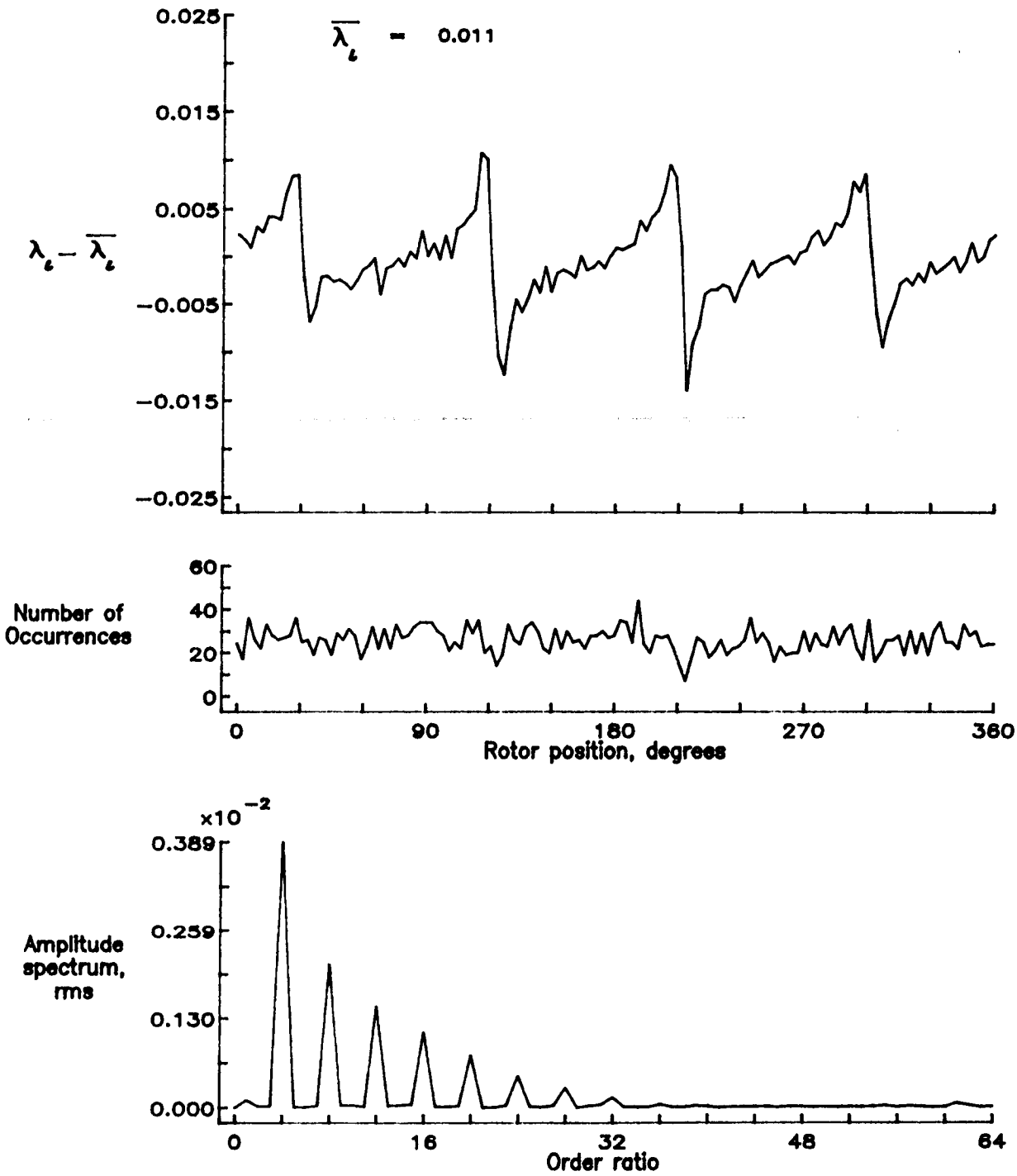

Figure 82.– Concluded.

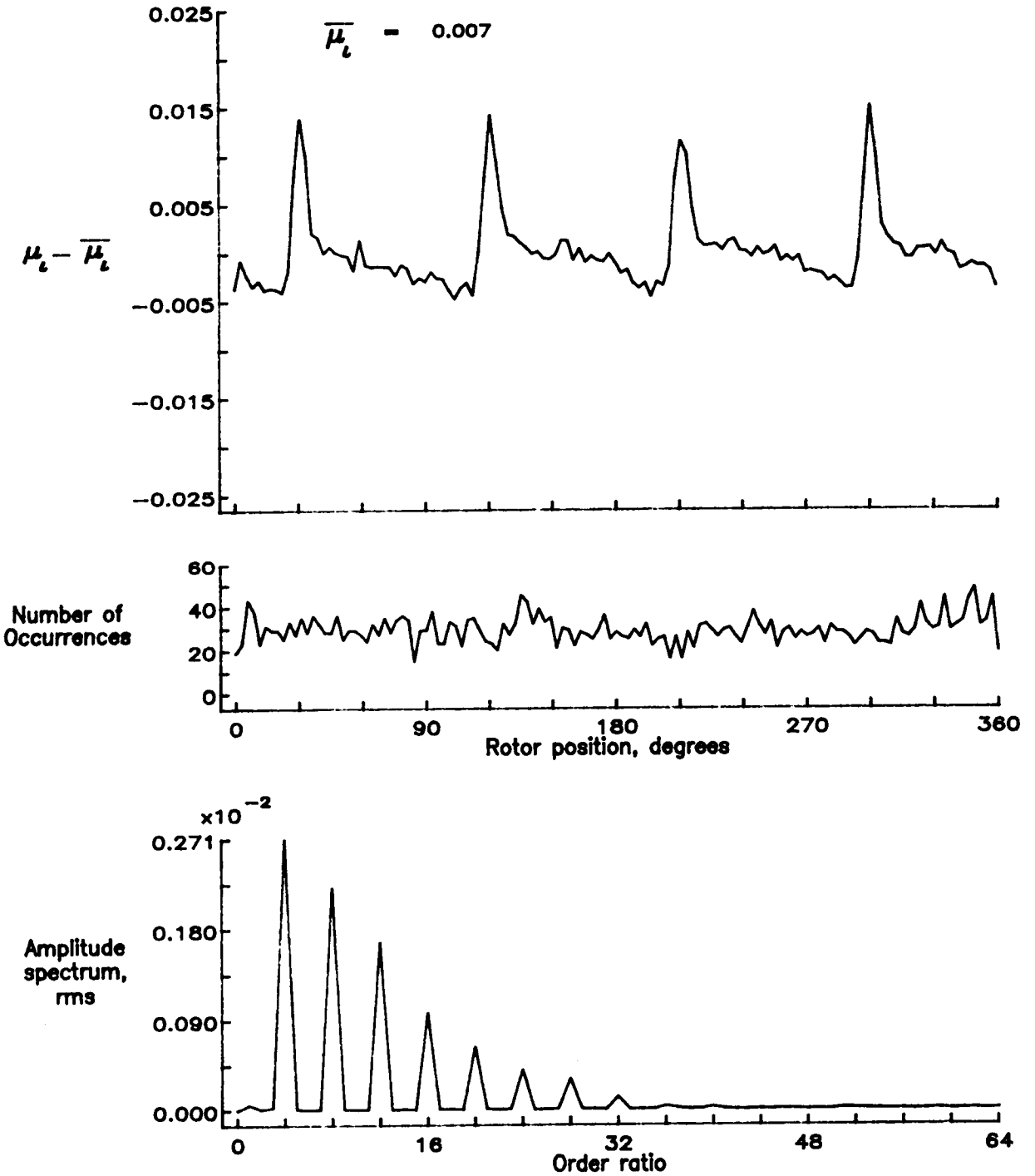

Figure 83.– Induced inflow velocity measured at 120 degrees and r/R of 0.94.

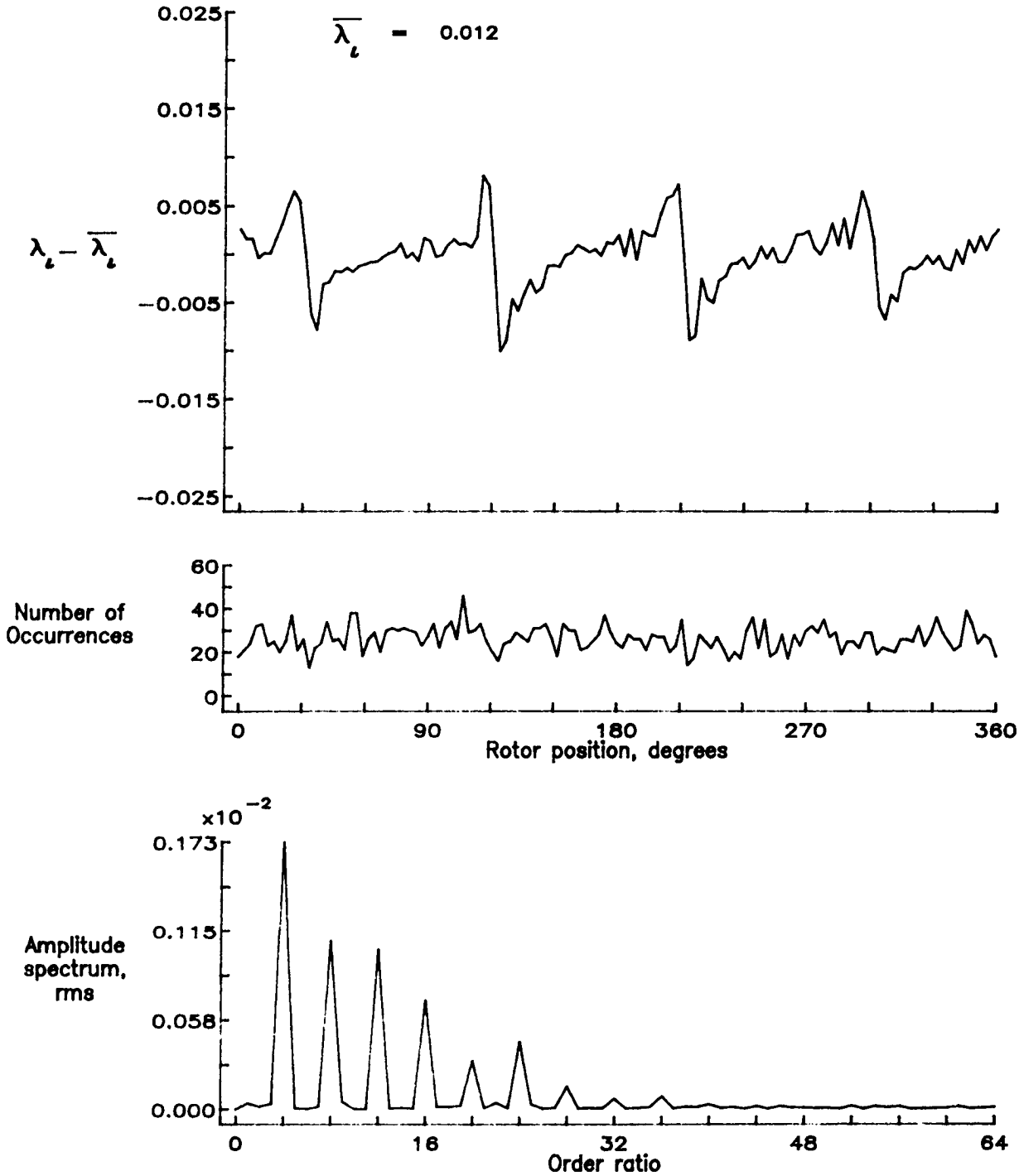

Figure 83.– Concluded.

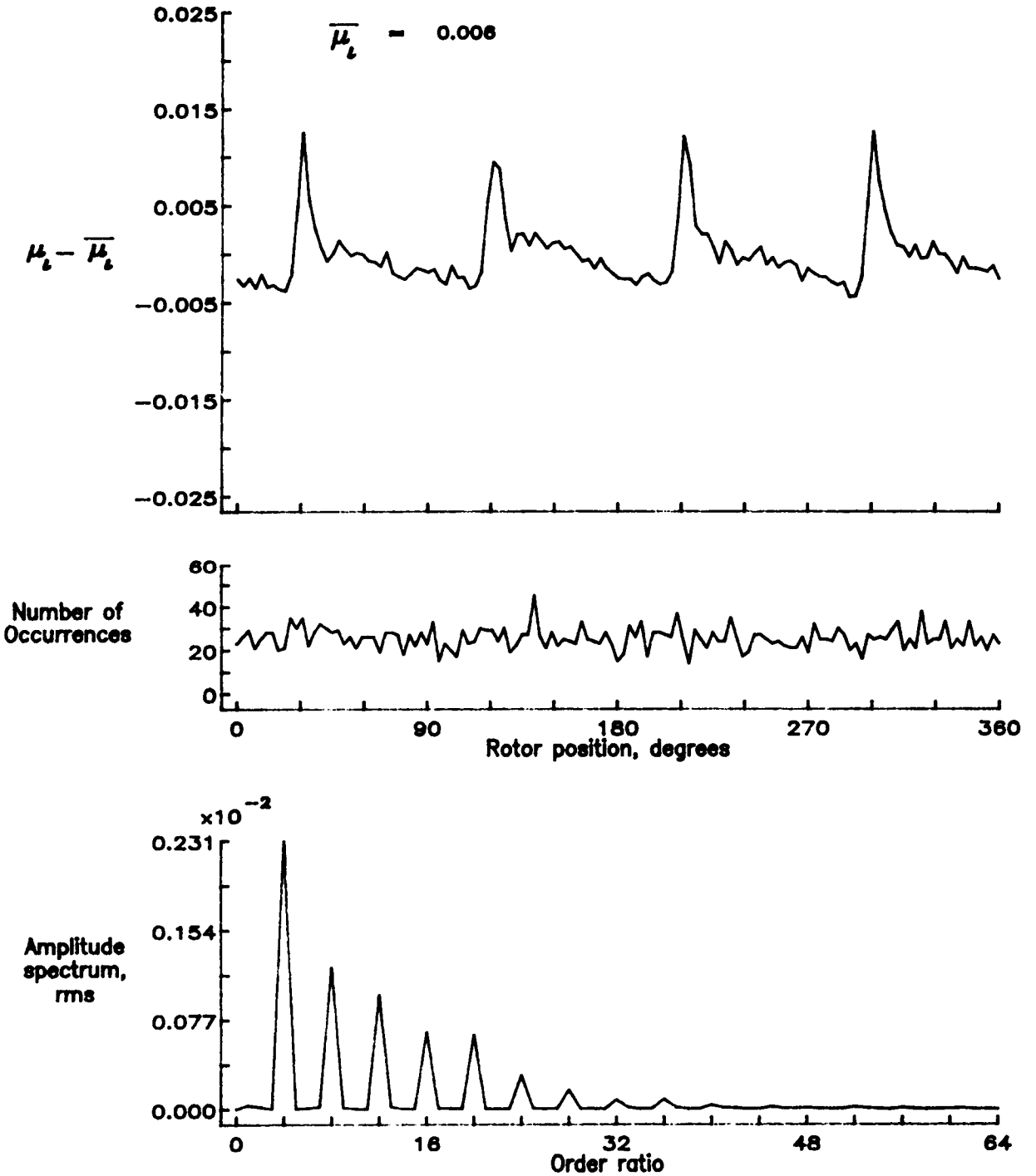

Figure 84.– Induced inflow velocity measured at 120 degrees and r/R of 0.98.

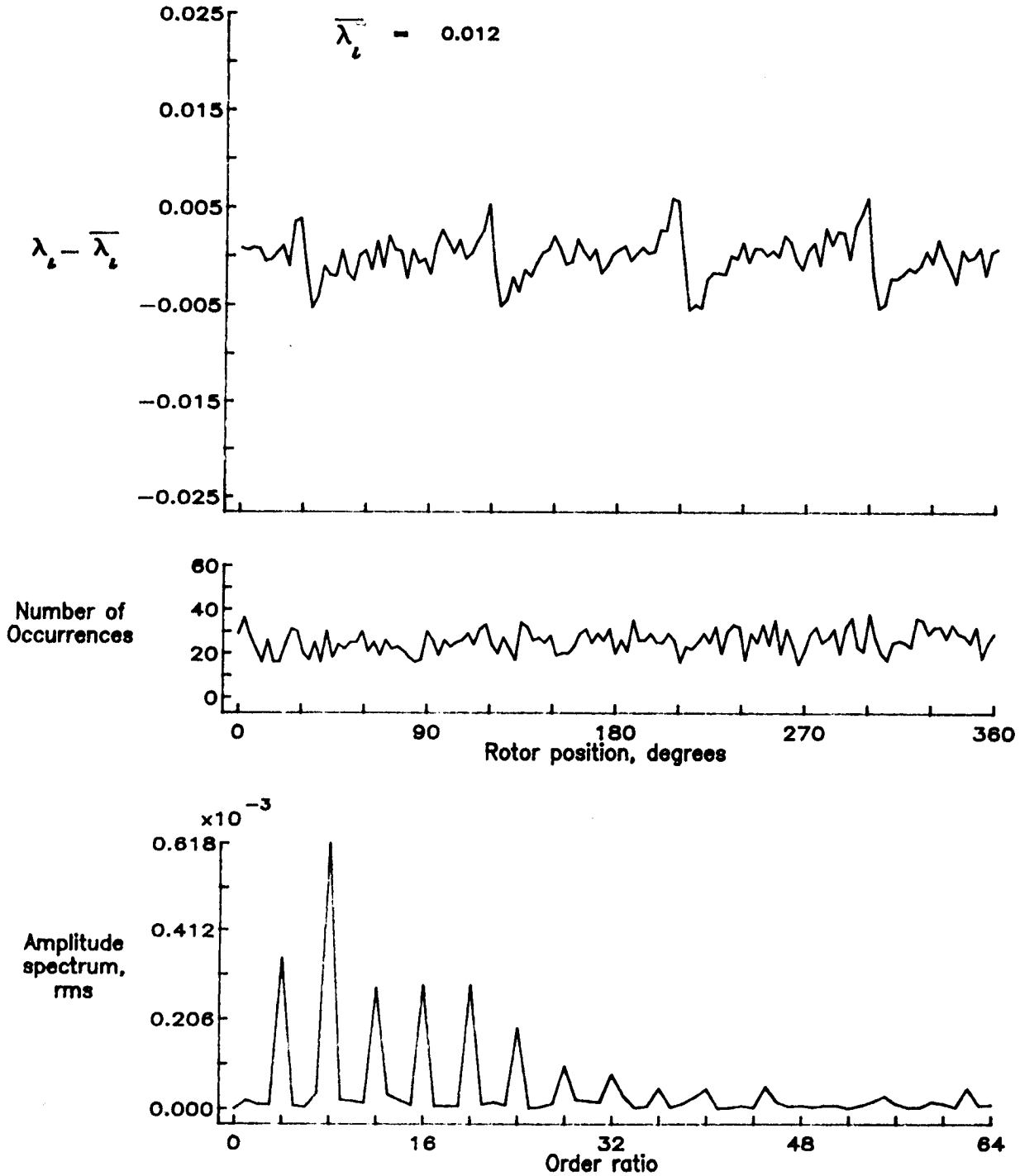

Figure 84.– Concluded.

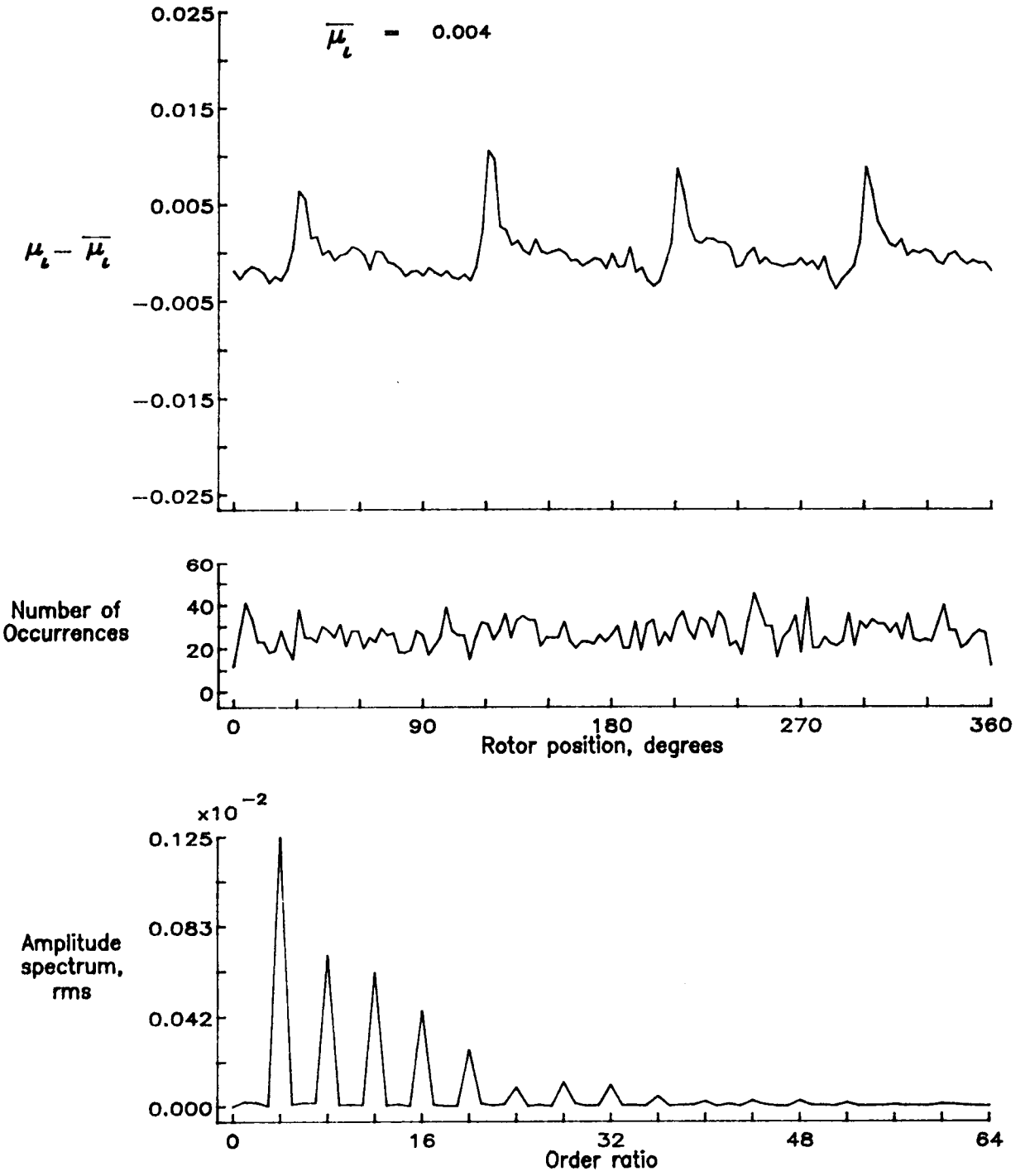

Figure 85.– Induced inflow velocity measured at 120 degrees and r/R of 1.02.

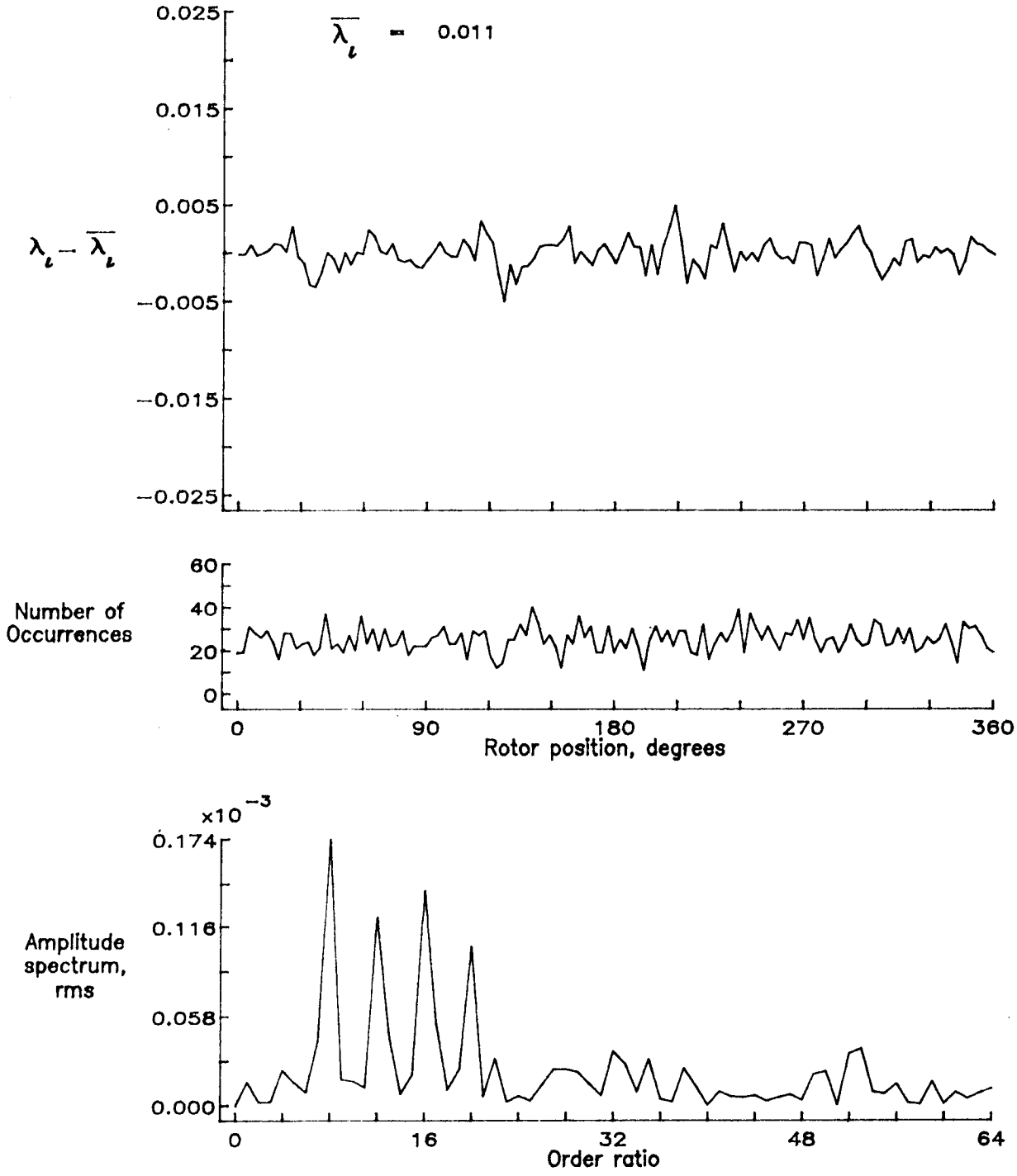

Figure 85.– Concluded.

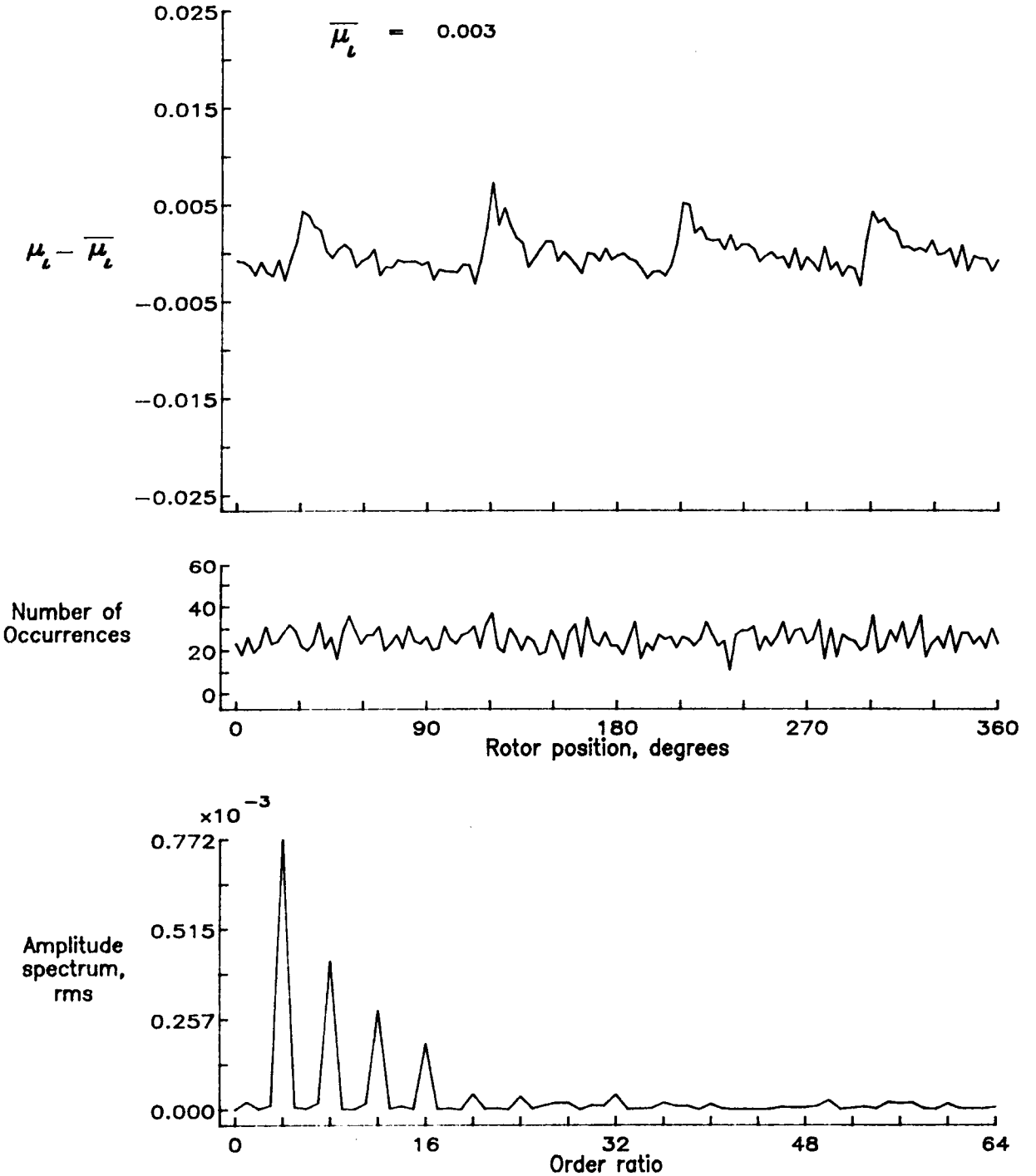

Figure 86.– Induced inflow velocity measured at 120 degrees and r/R of 1.04.

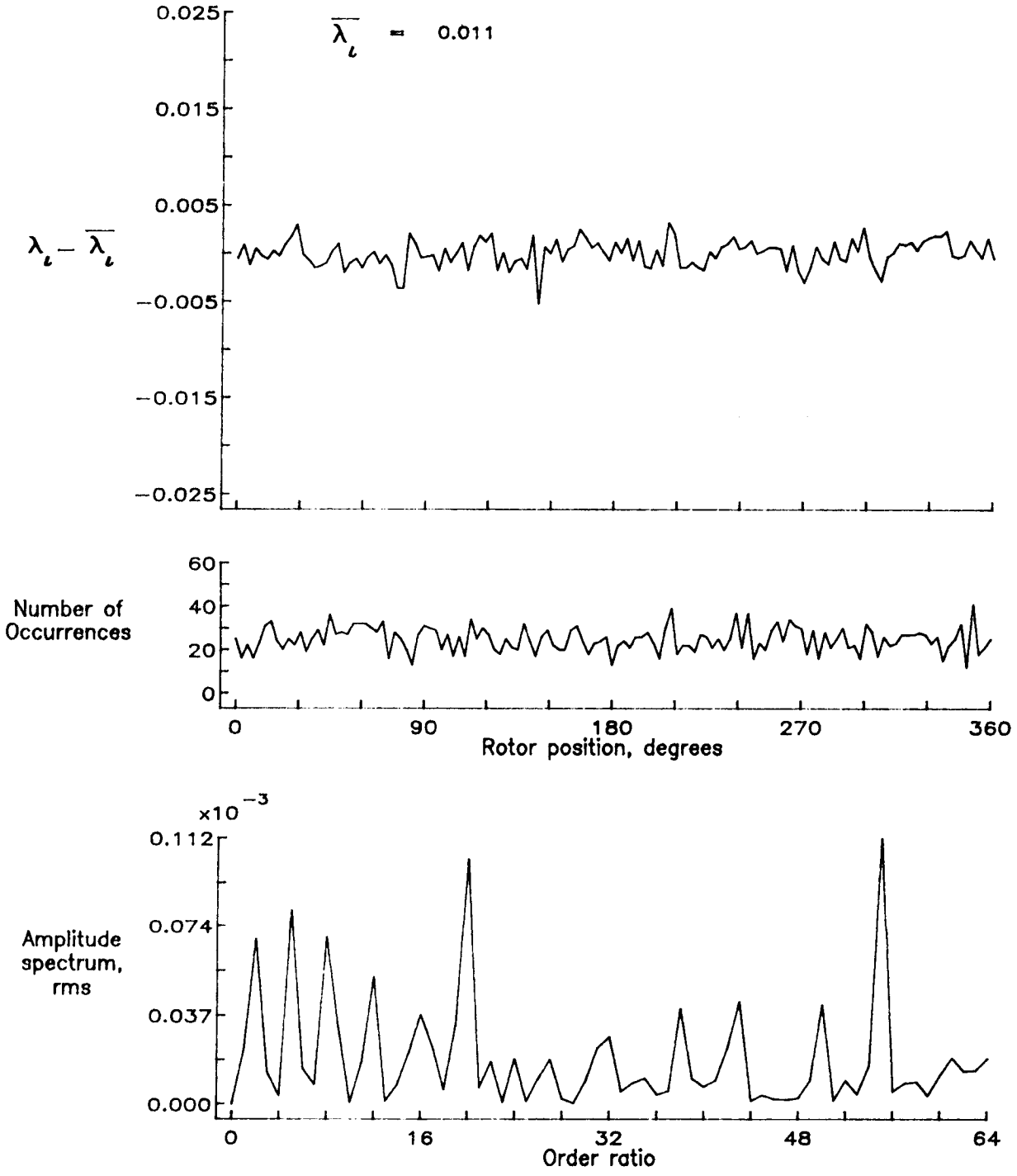

Figure 86.– Concluded.

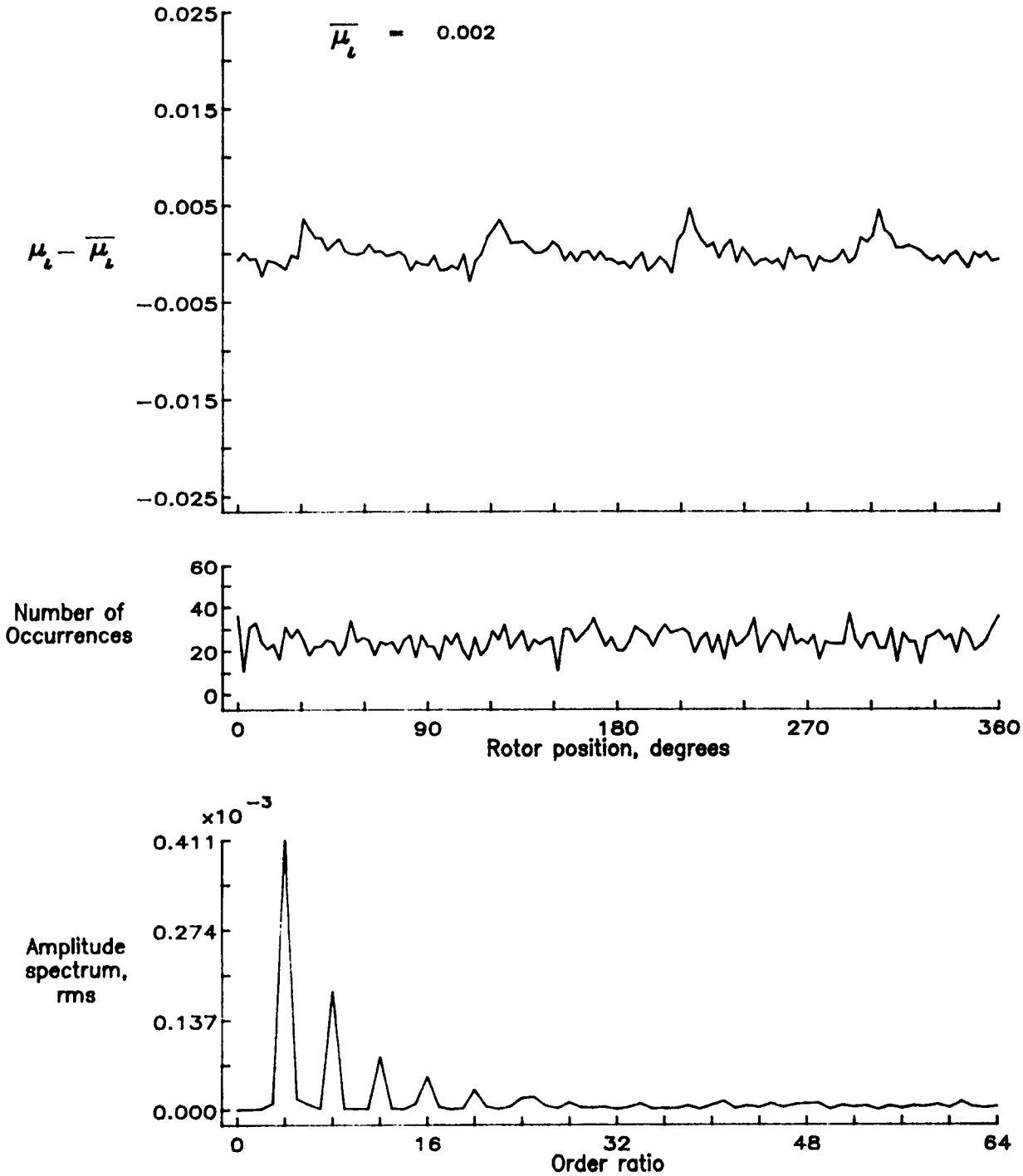

Figure 87.– Induced inflow velocity measured at 120 degrees and r/R of 1.10.

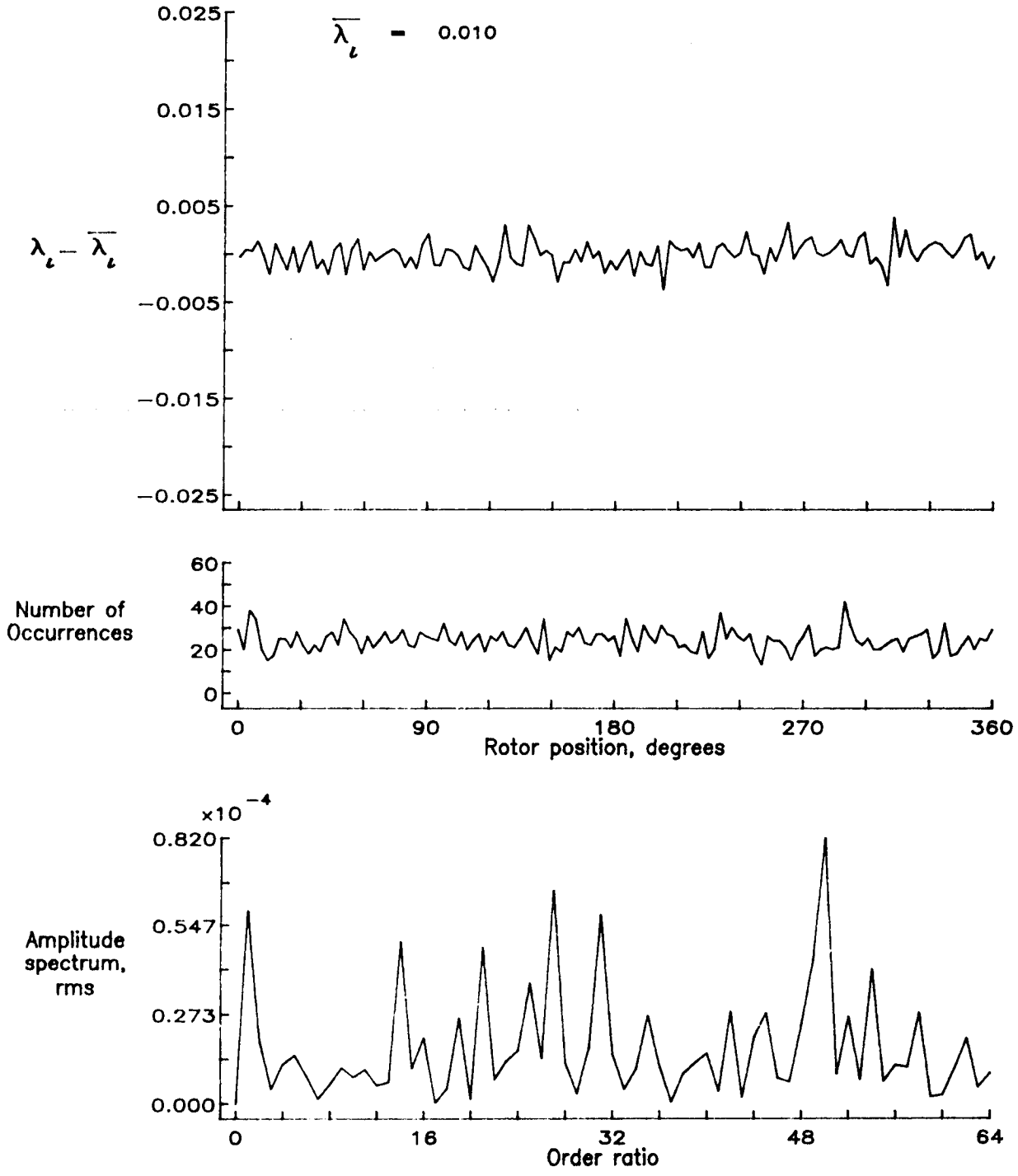

Figure 87.– Concluded.

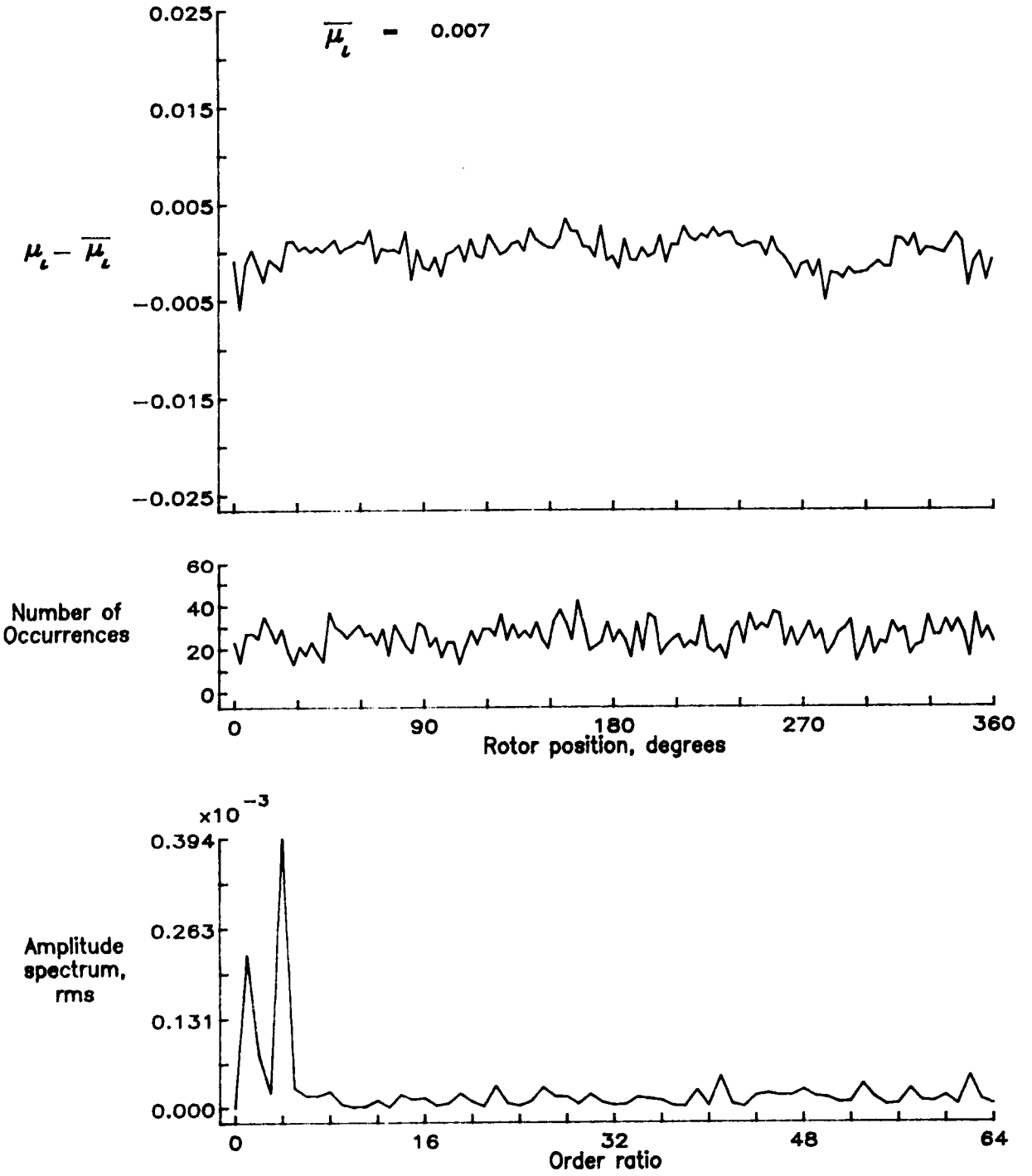

Figure 88.– Induced inflow velocity measured at 150 degrees and r/R of 0.20.

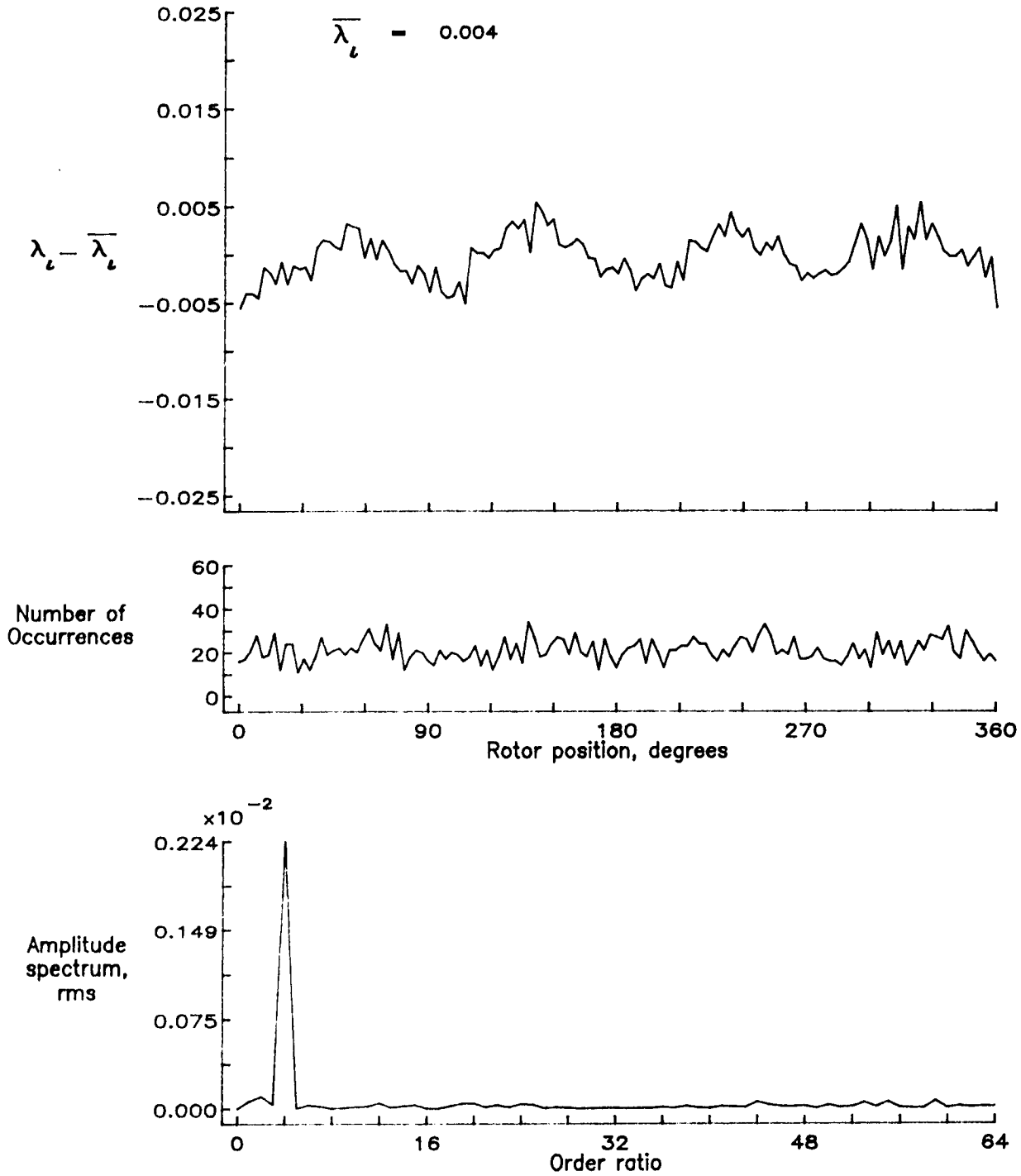

Figure 88.– Concluded.

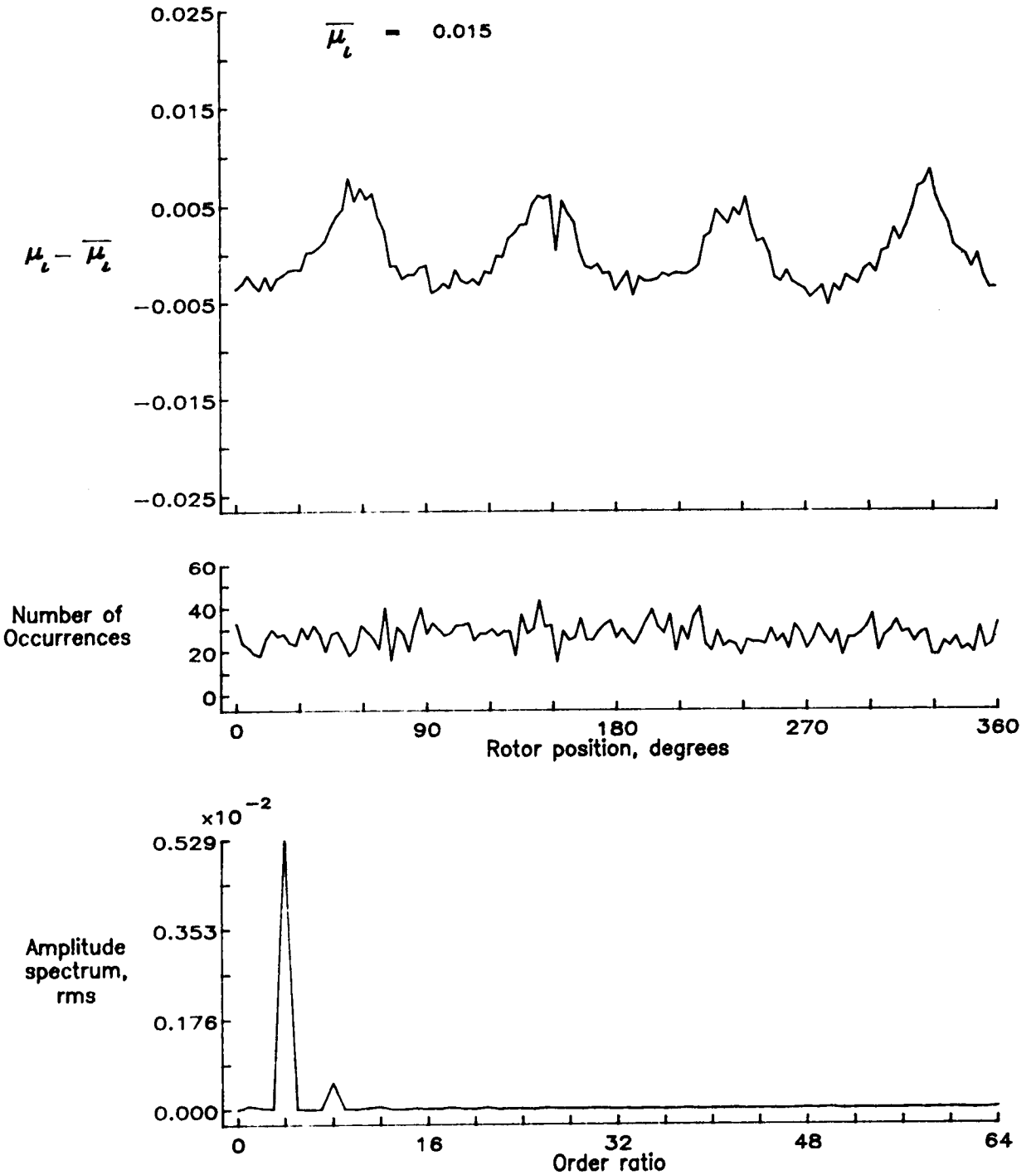

Figure 89.– Induced inflow velocity measured at 150 degrees and r/R of 0.40.

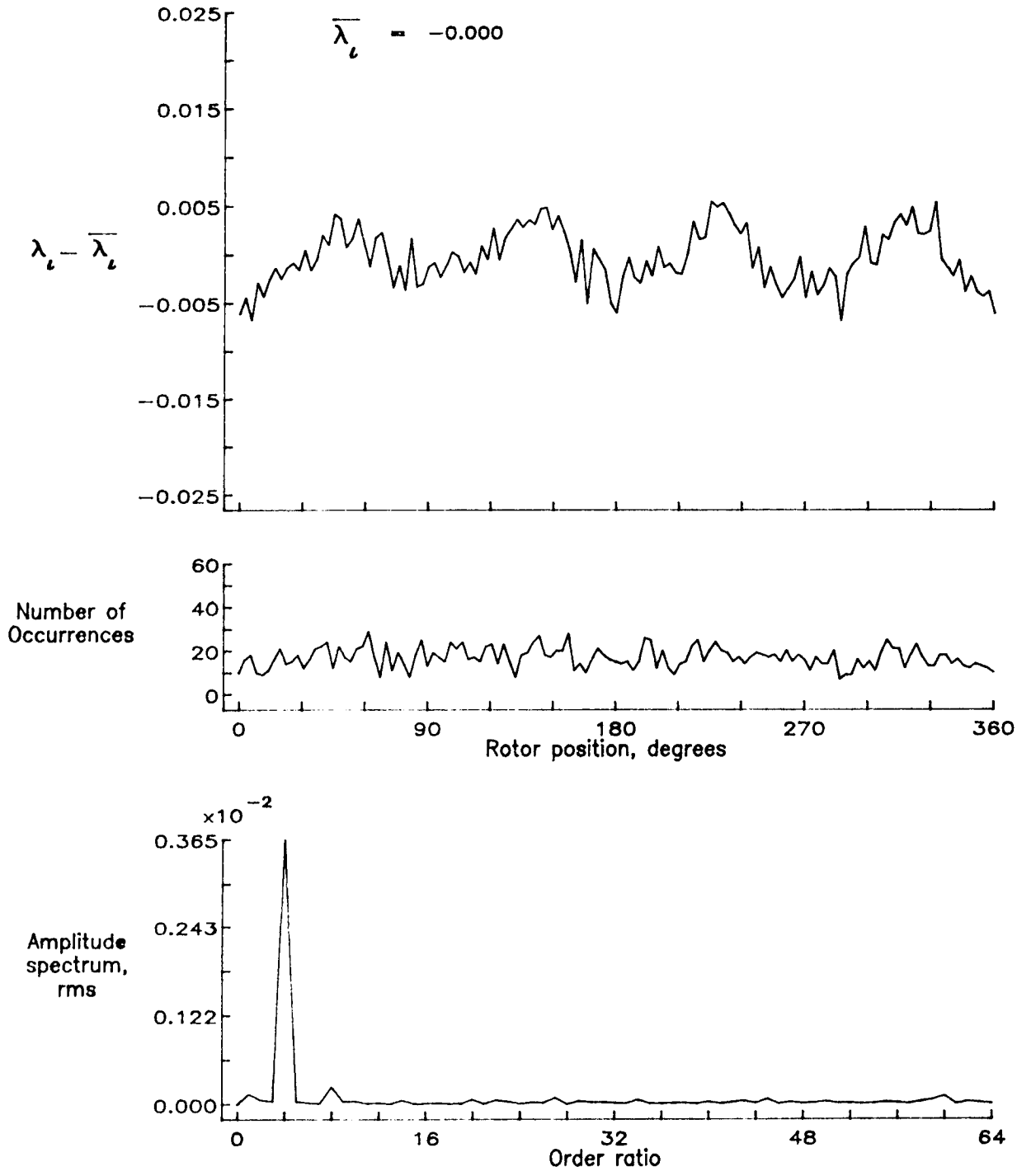

Figure 89.– Concluded.

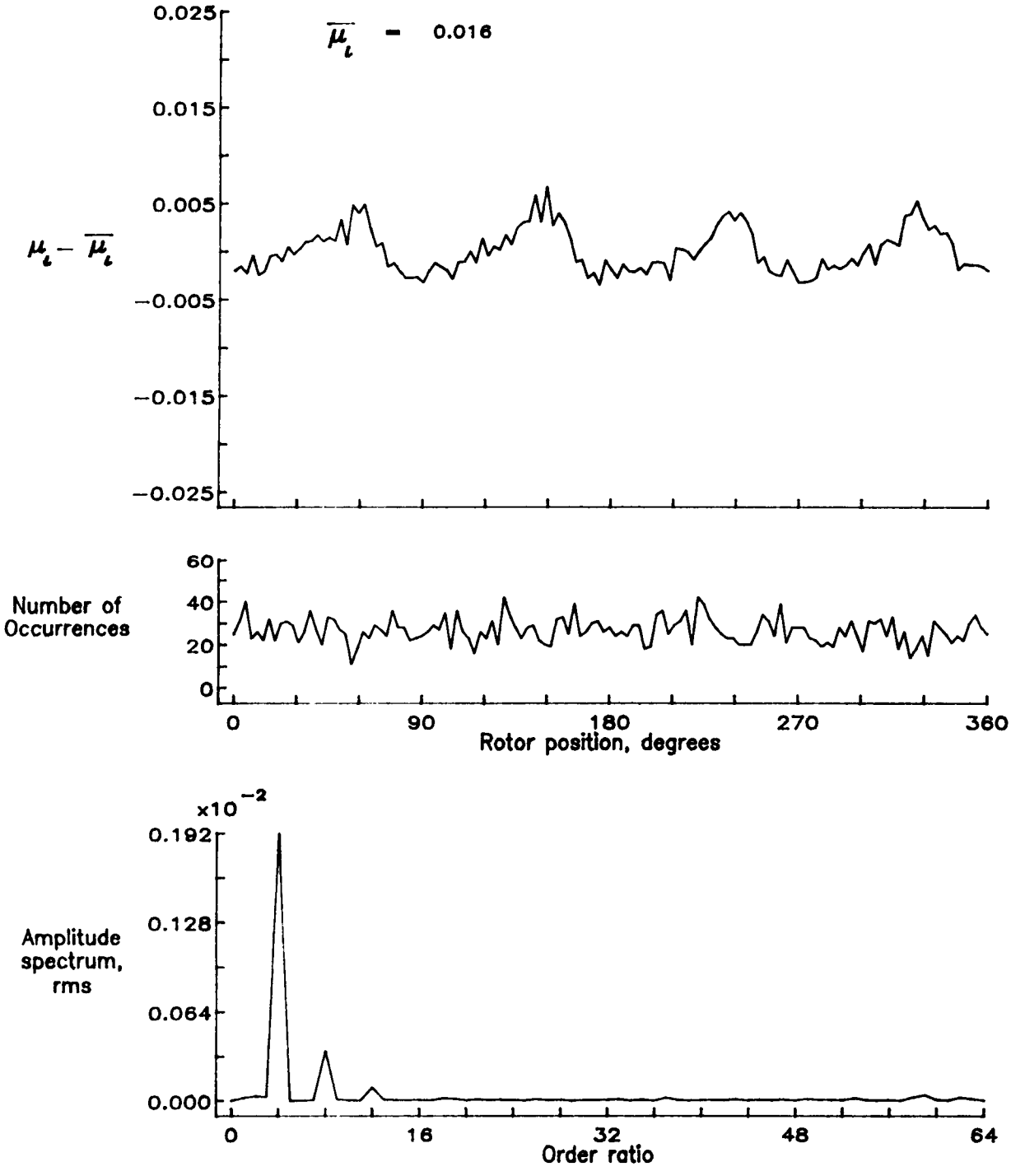

Figure 90.– Induced inflow velocity measured at 150 degrees and r/R of 0.50.

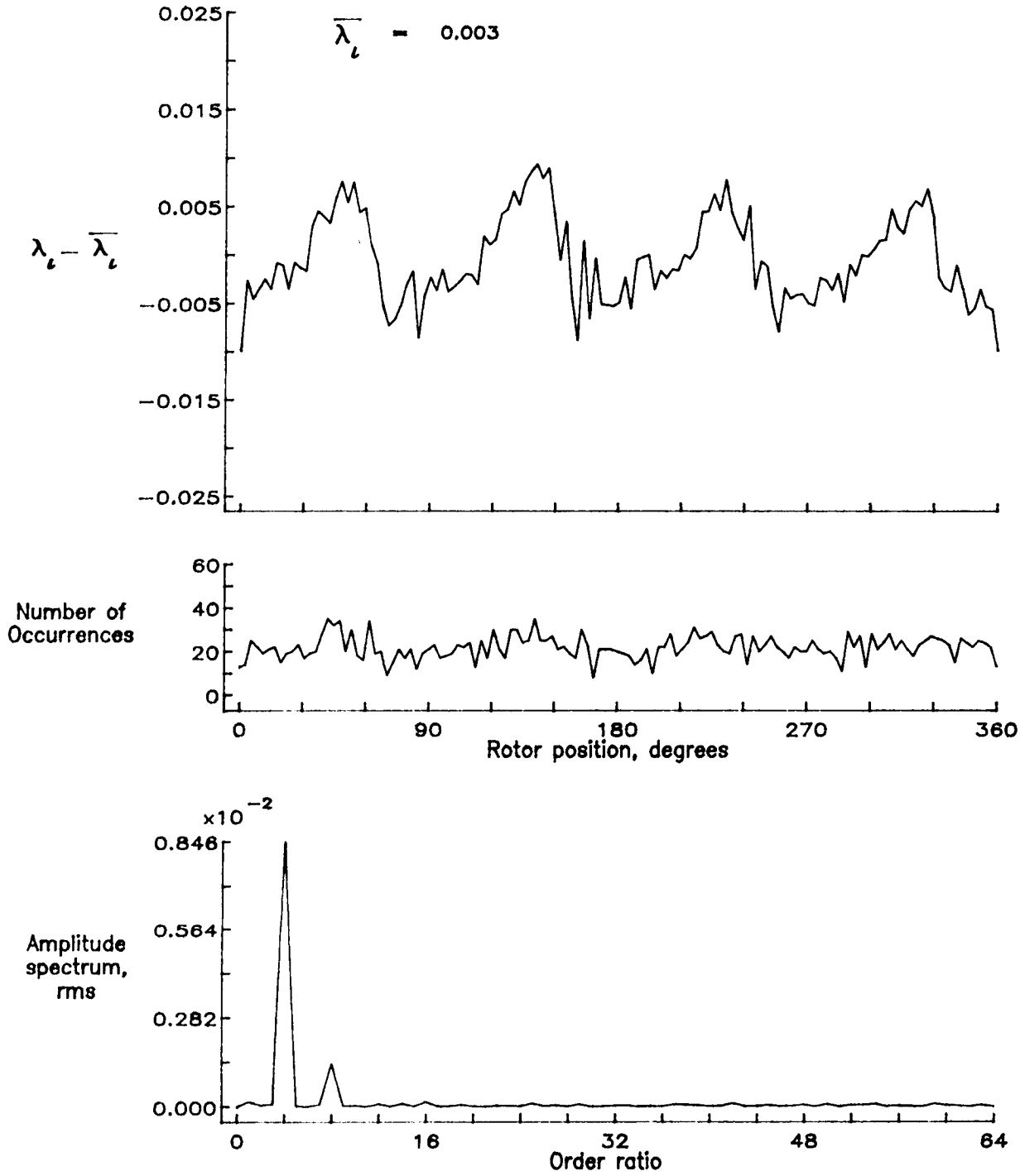

Figure 90.– Concluded.

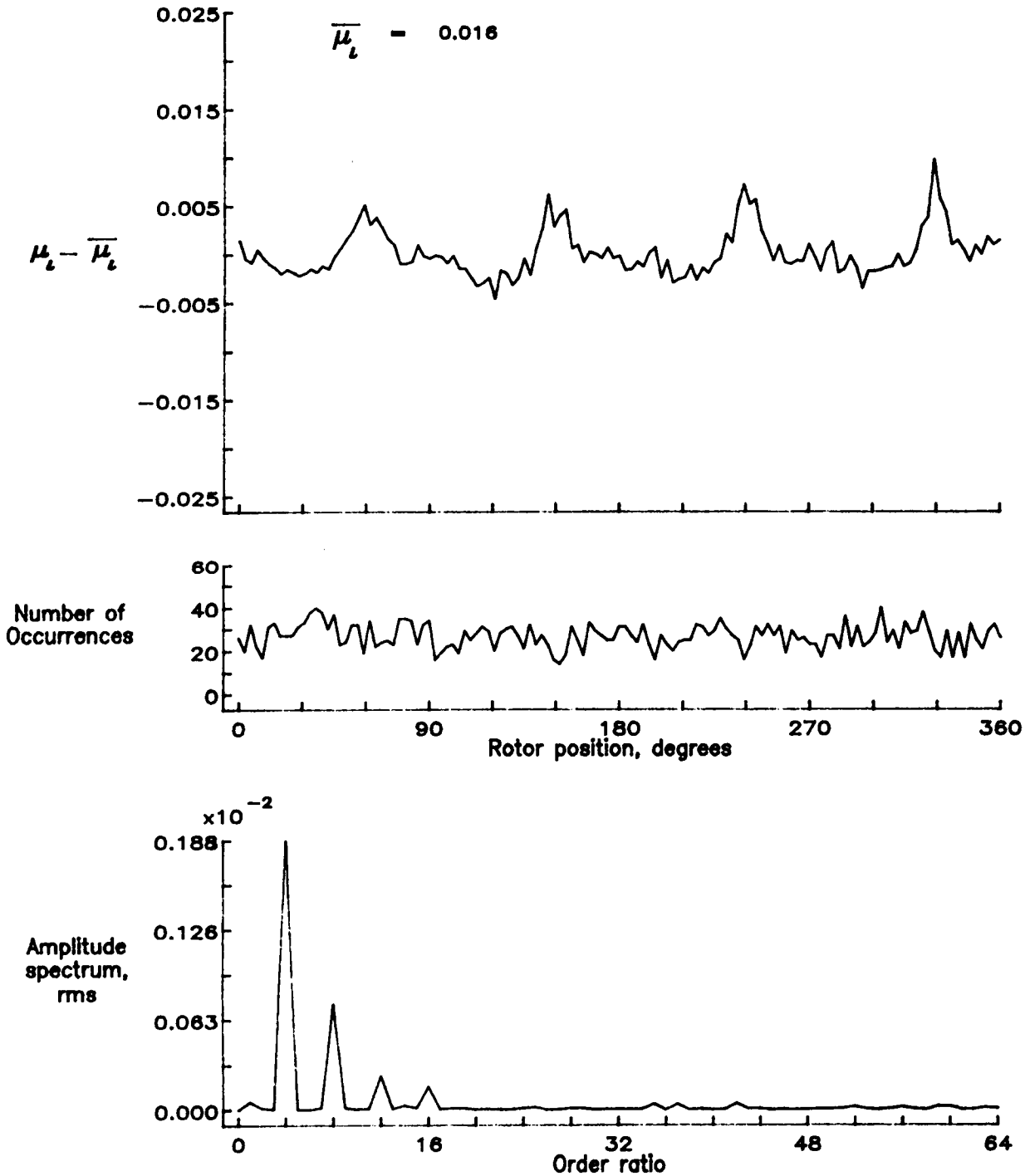

Figure 91.– Induced inflow velocity measured at 150 degrees and r/R of 0.60.

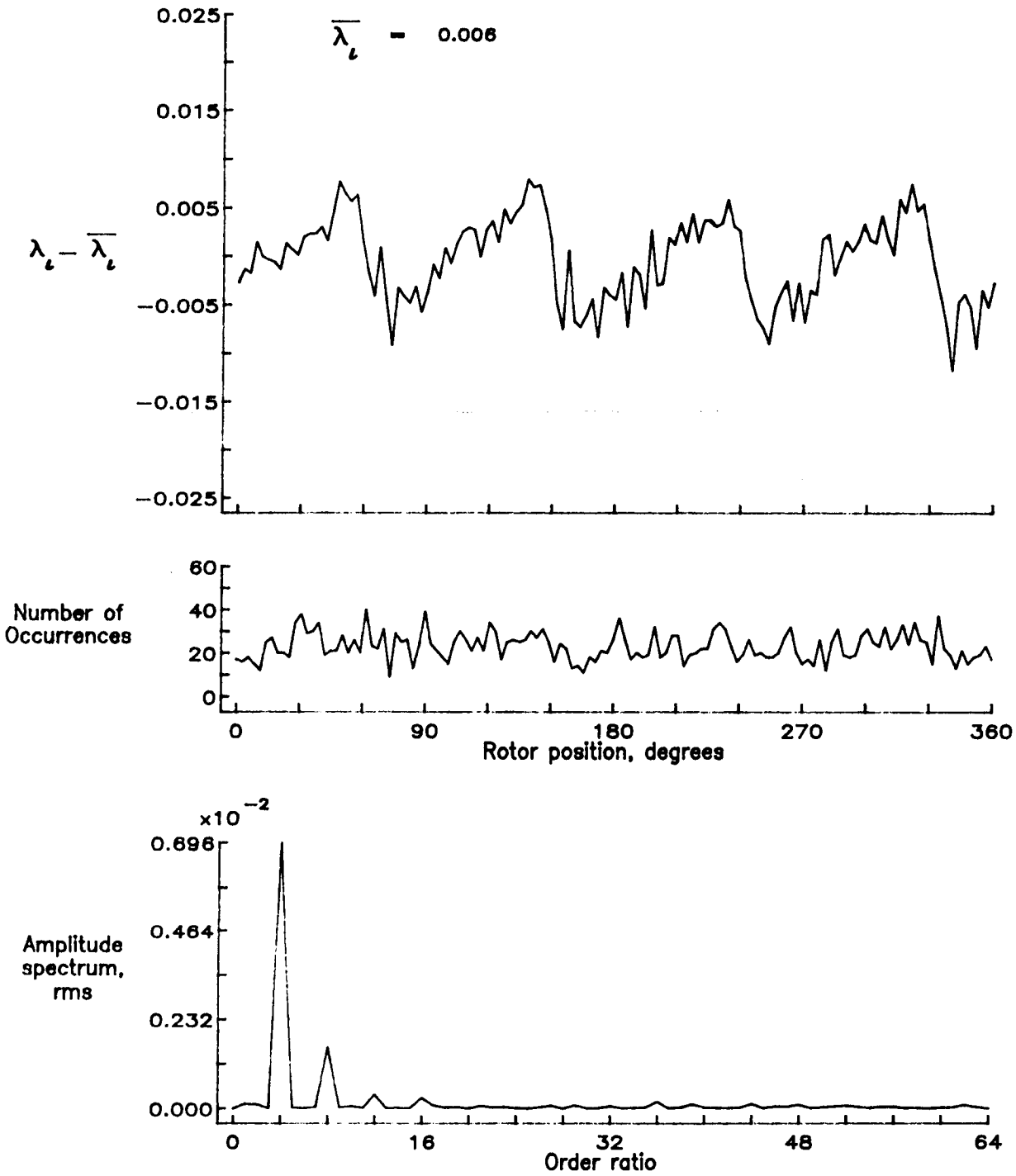

Figure 91.– Concluded.

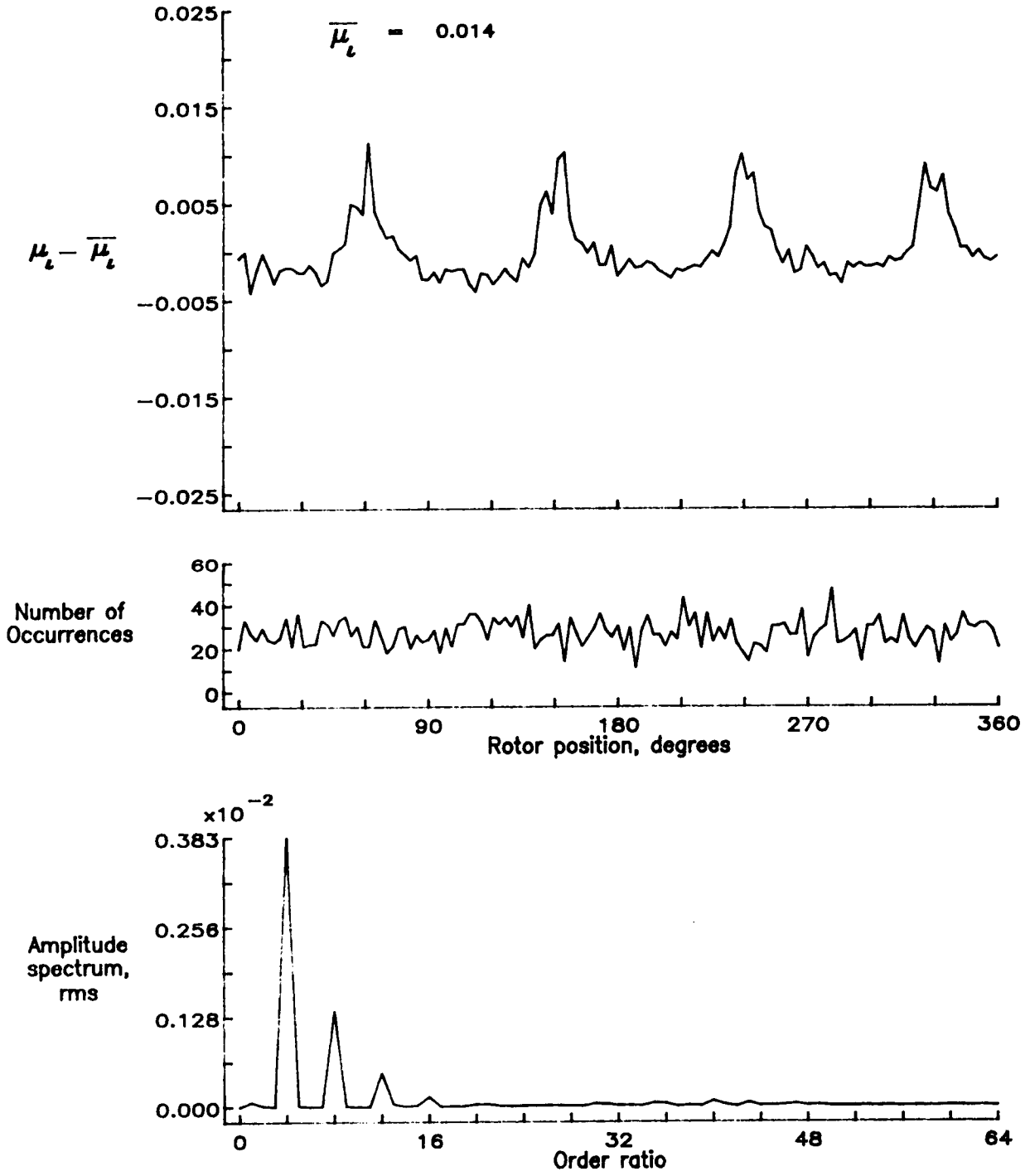

Figure 92.– Induced inflow velocity measured at 150 degrees and r/R of 0.70.

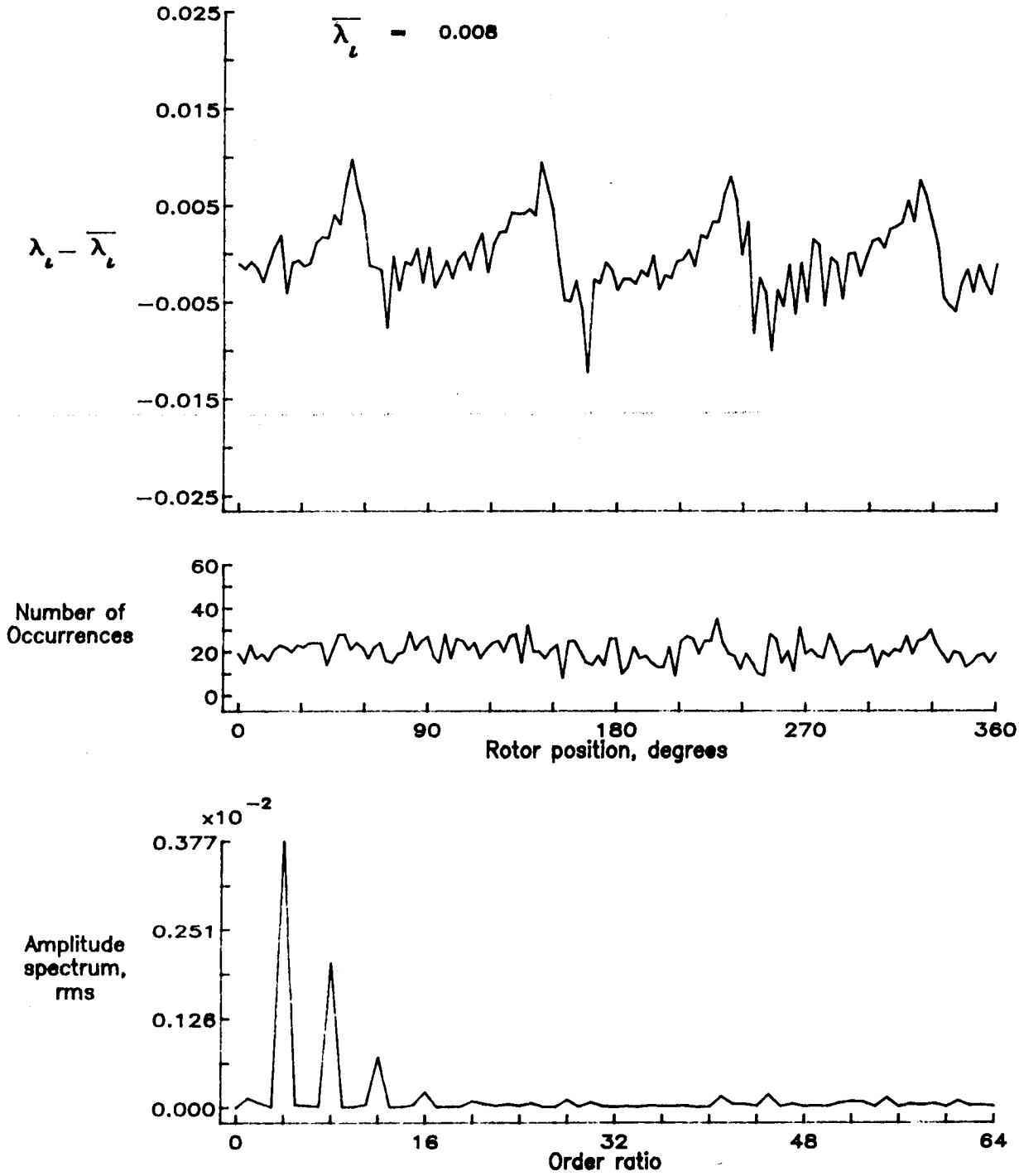

Figure 92.– Concluded.

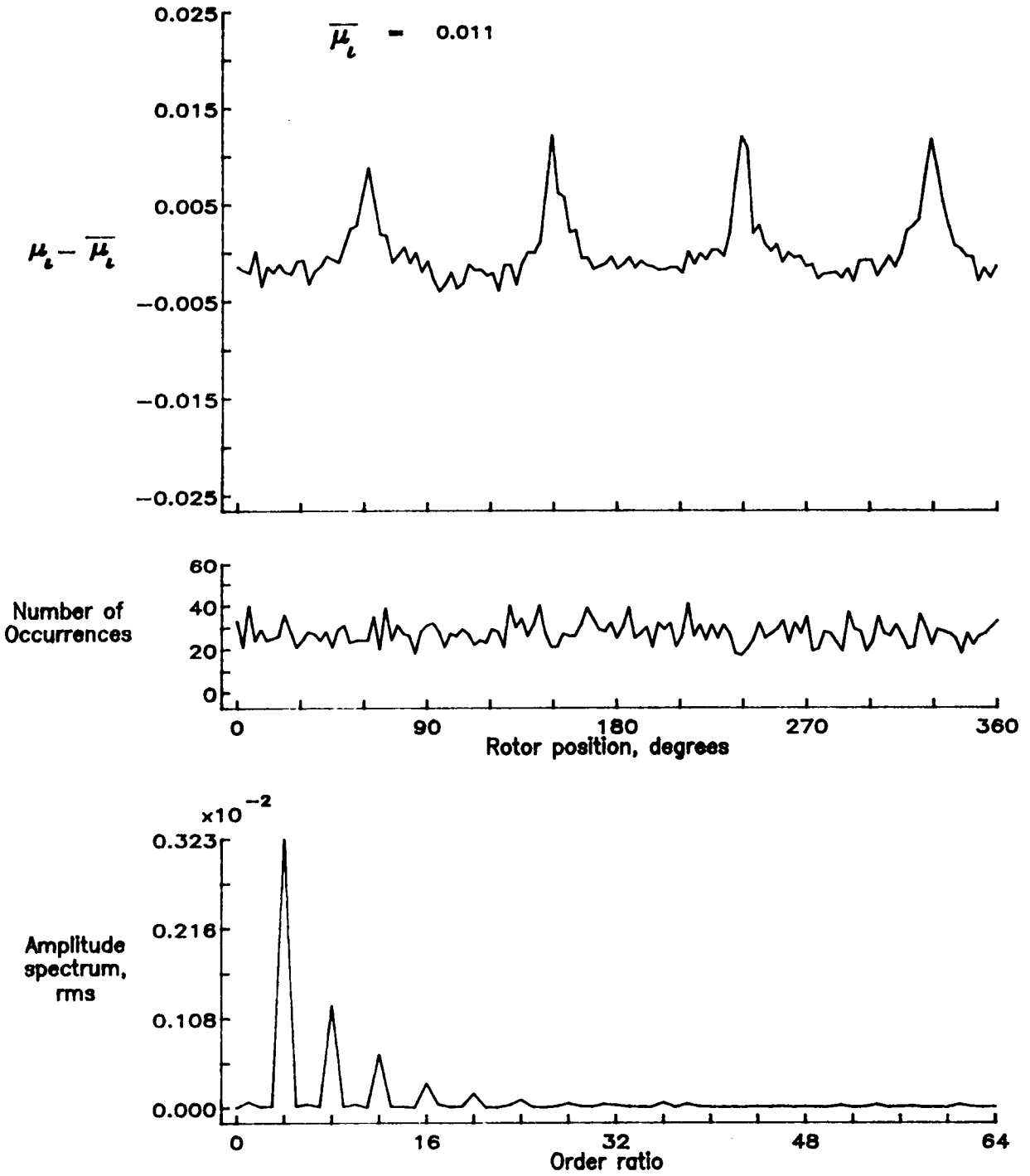

Figure 93.– Induced inflow velocity measured at 150 degrees and r/R of 0.74.

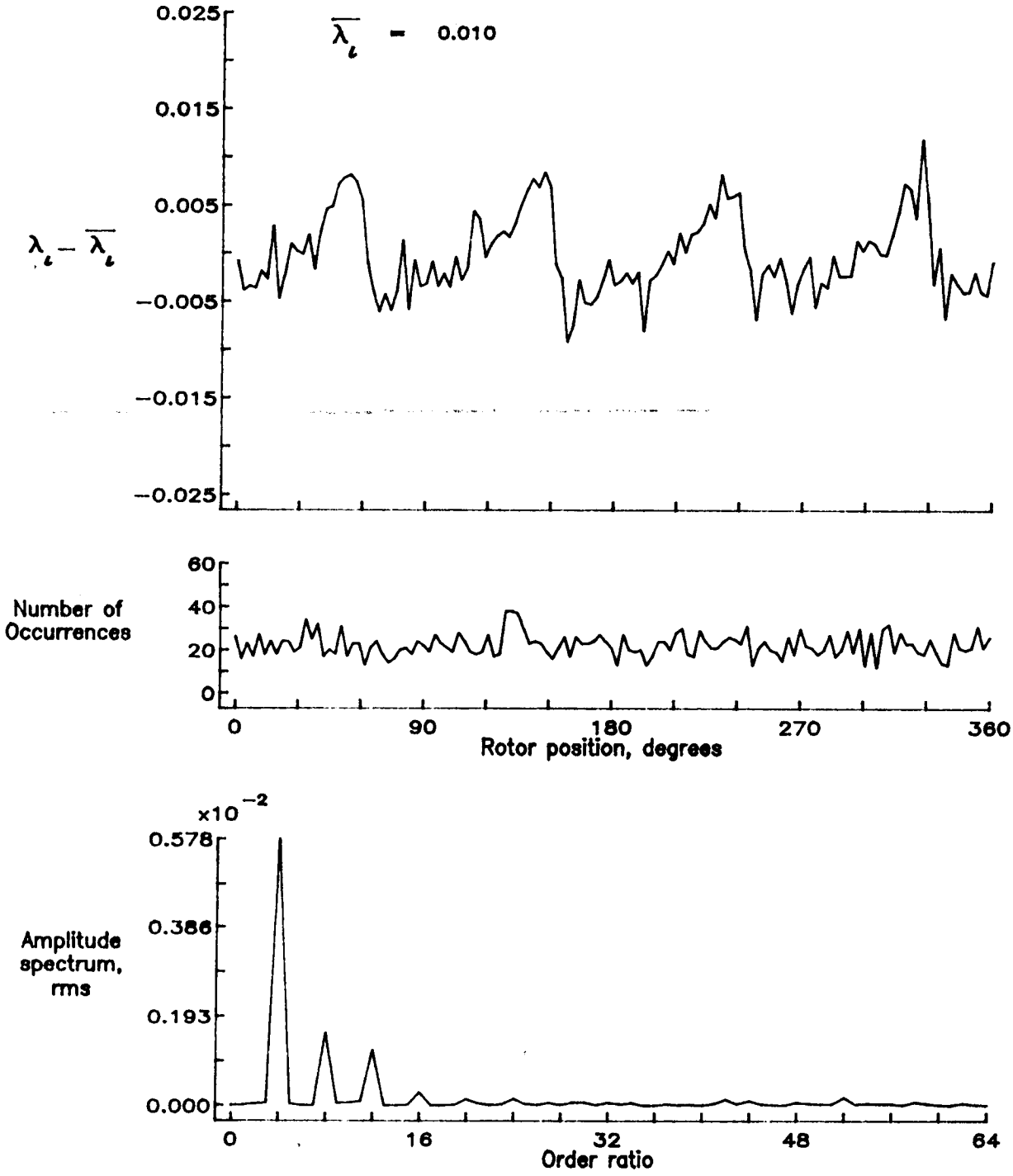

Figure 93.– Concluded.

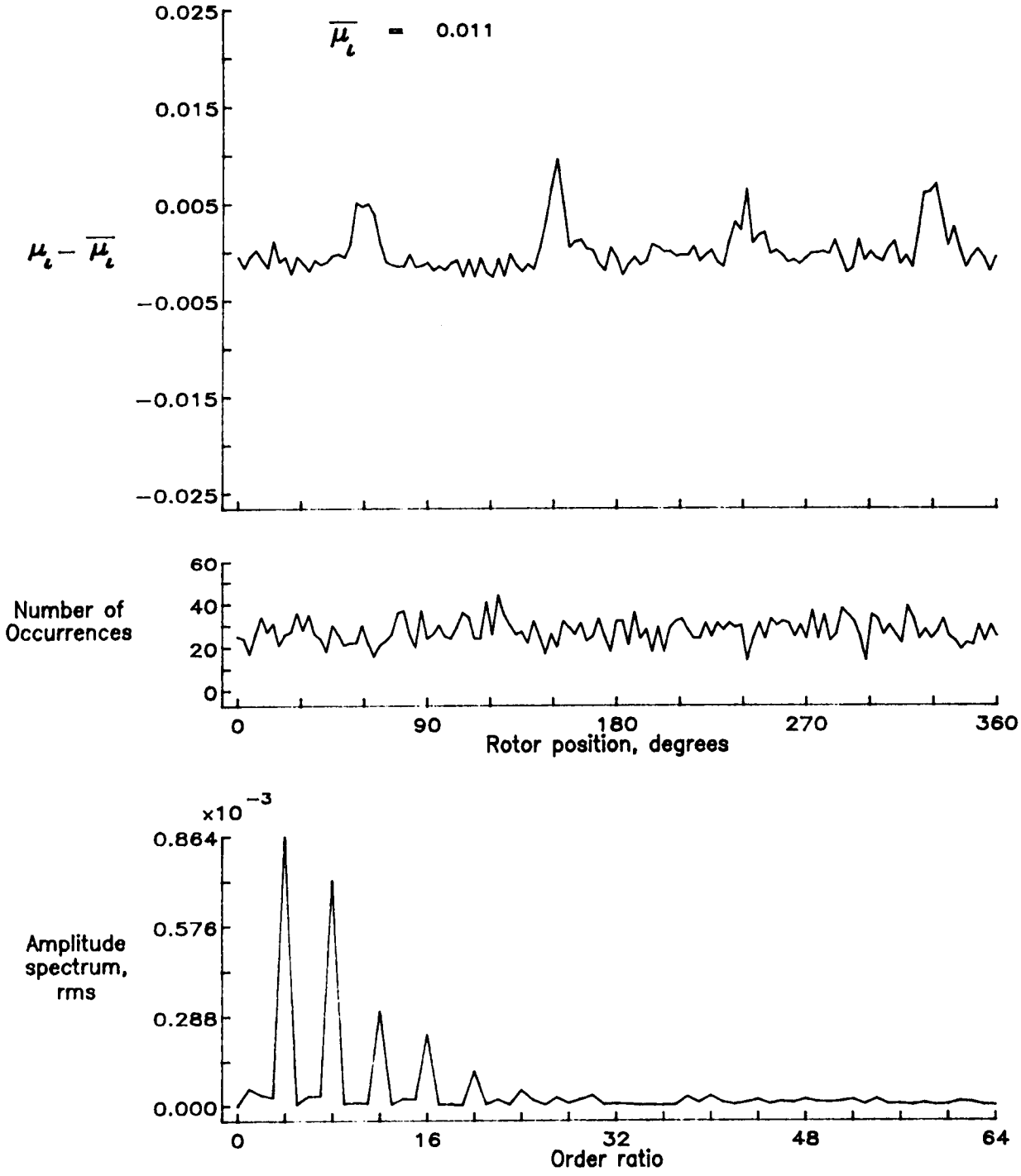

Figure 94.– Induced inflow velocity measured at 150 degrees and r/R of 0.78.

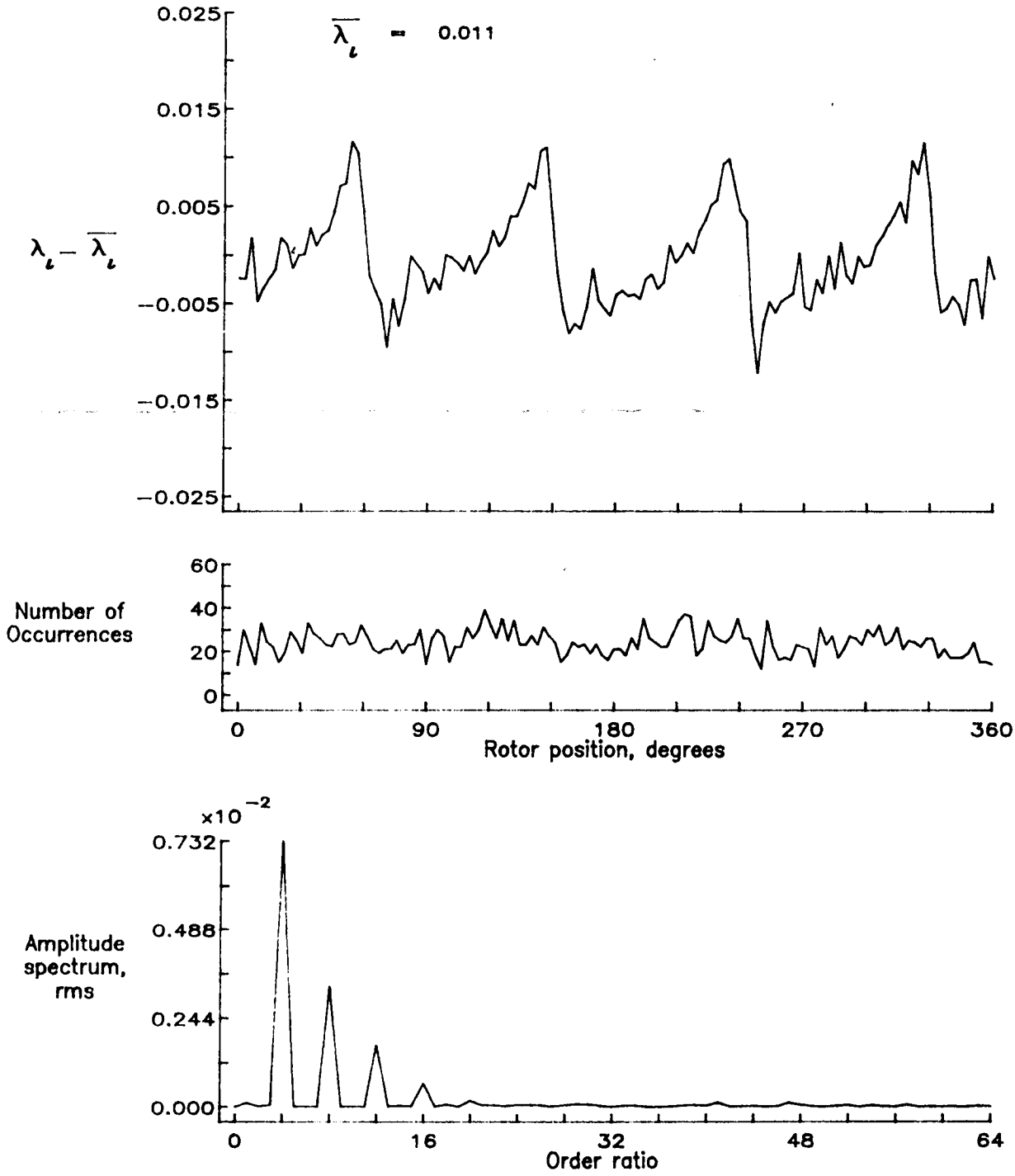

Figure 94.– Concluded.

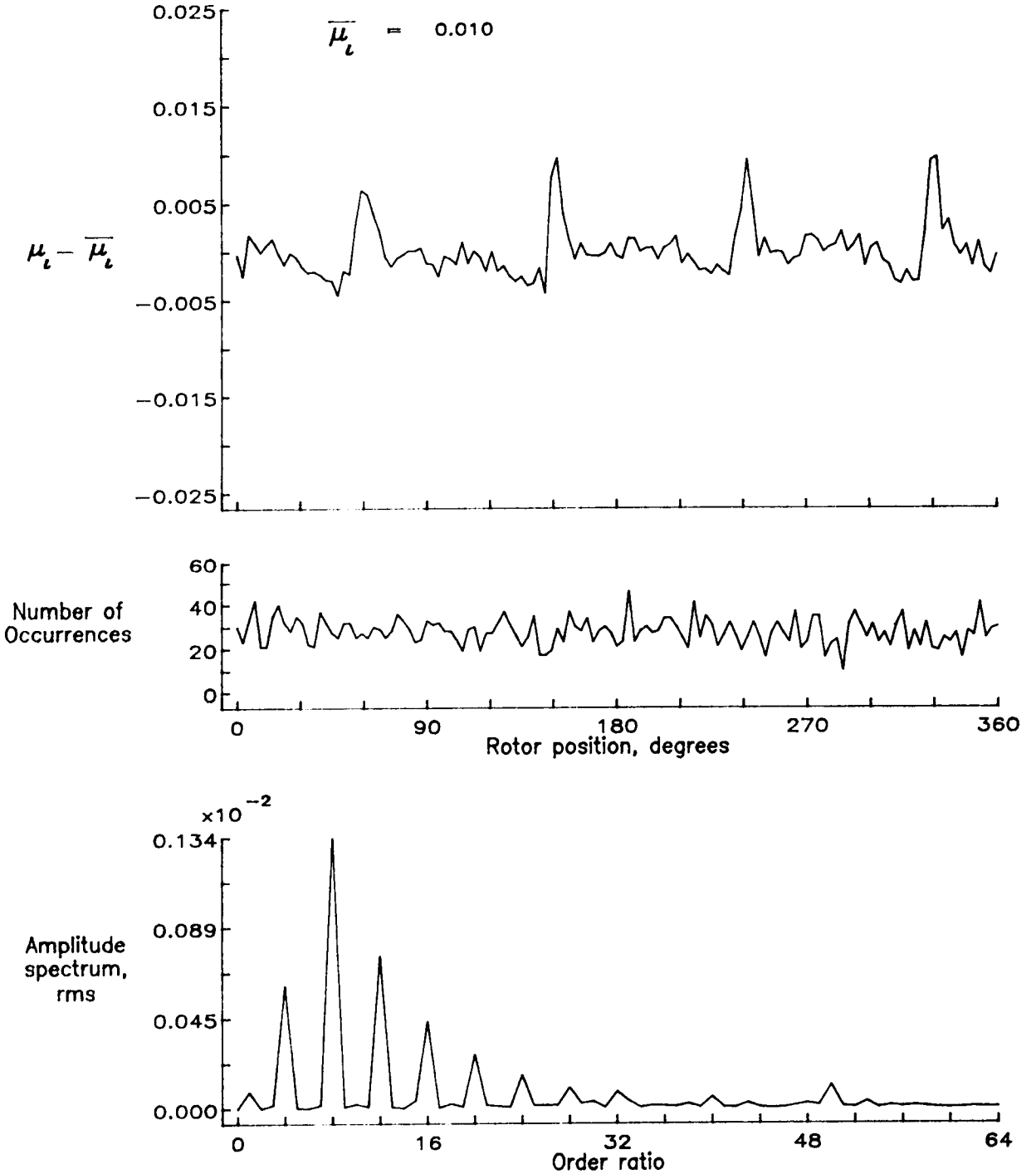

Figure 95.– Induced inflow velocity measured at 150 degrees and r/R of 0.82.

C-3

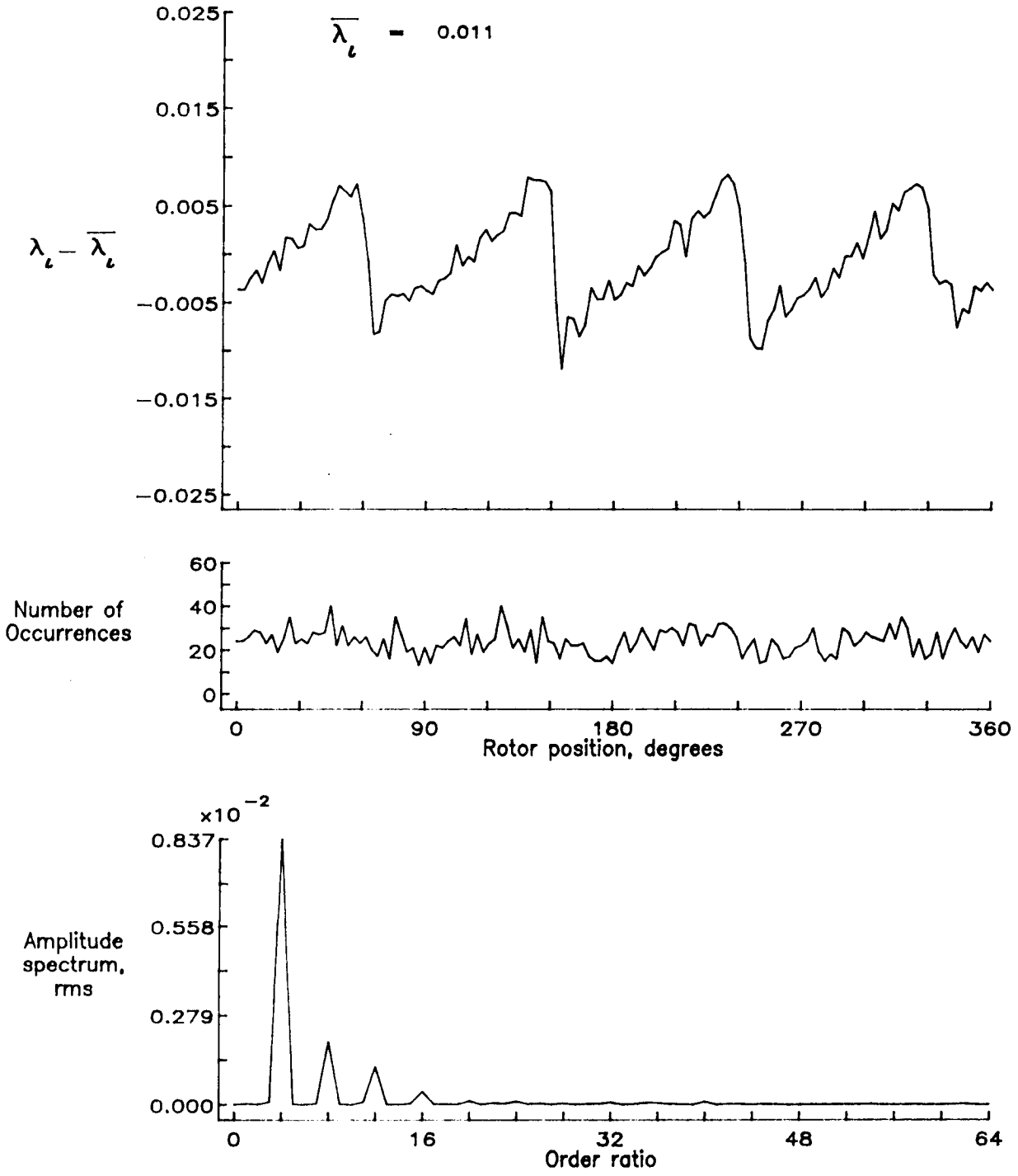

Figure 95.– Concluded.

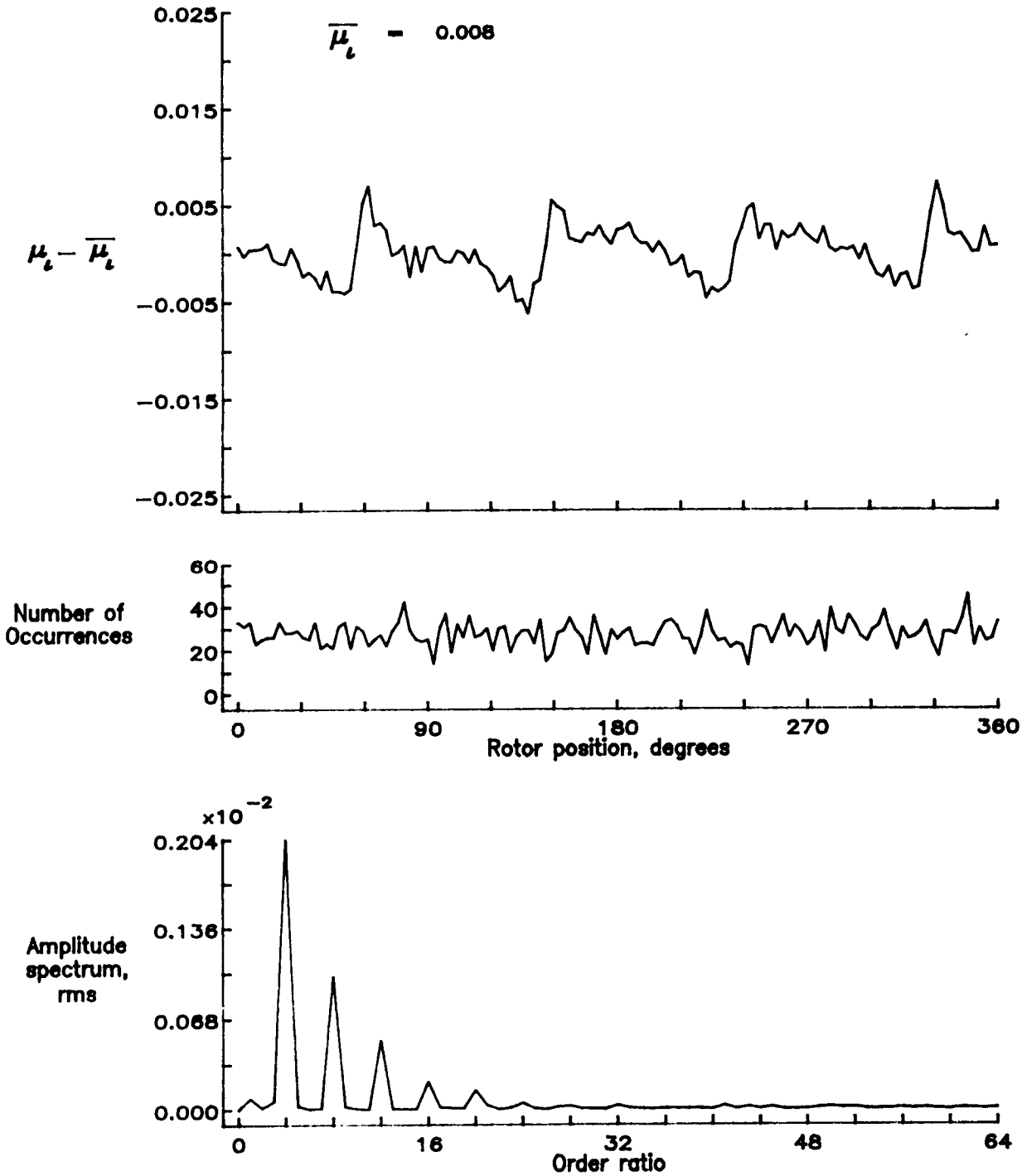

Figure 96.– Induced inflow velocity measured at 150 degrees and r/R of 0.86.

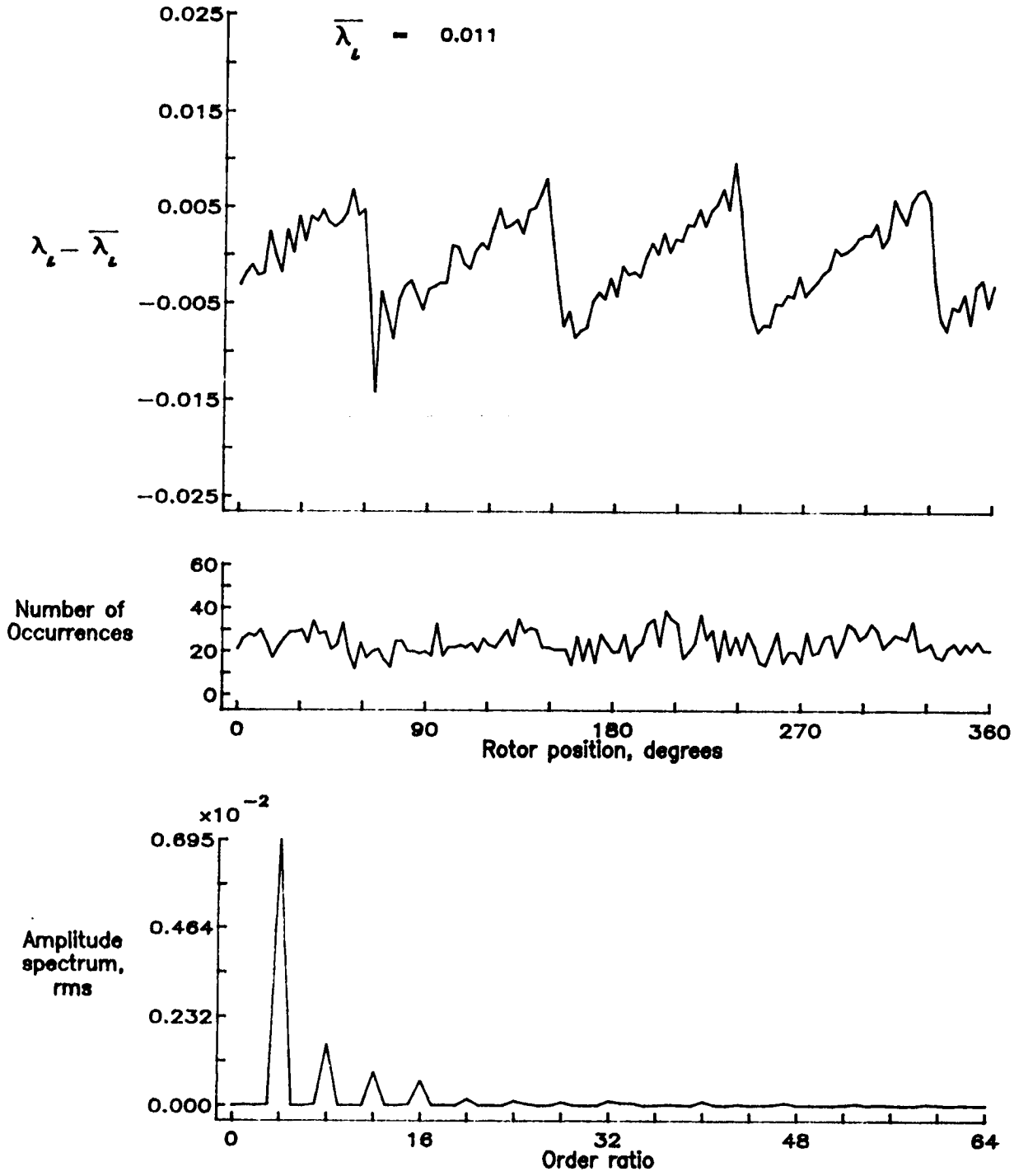

Figure 96.– Concluded.

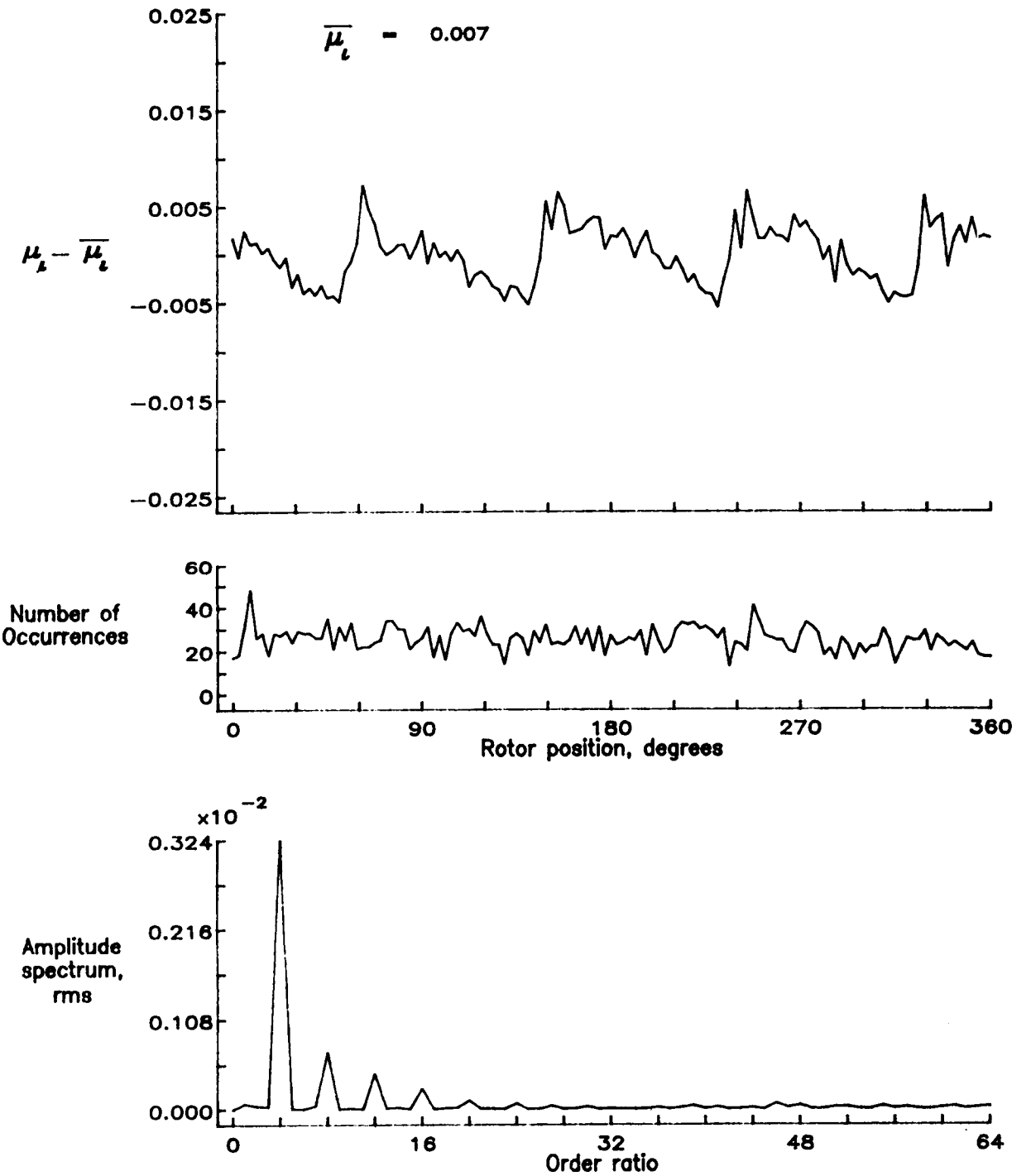

Figure 97.– Induced inflow velocity measured at 150 degrees and r/R of 0.90.

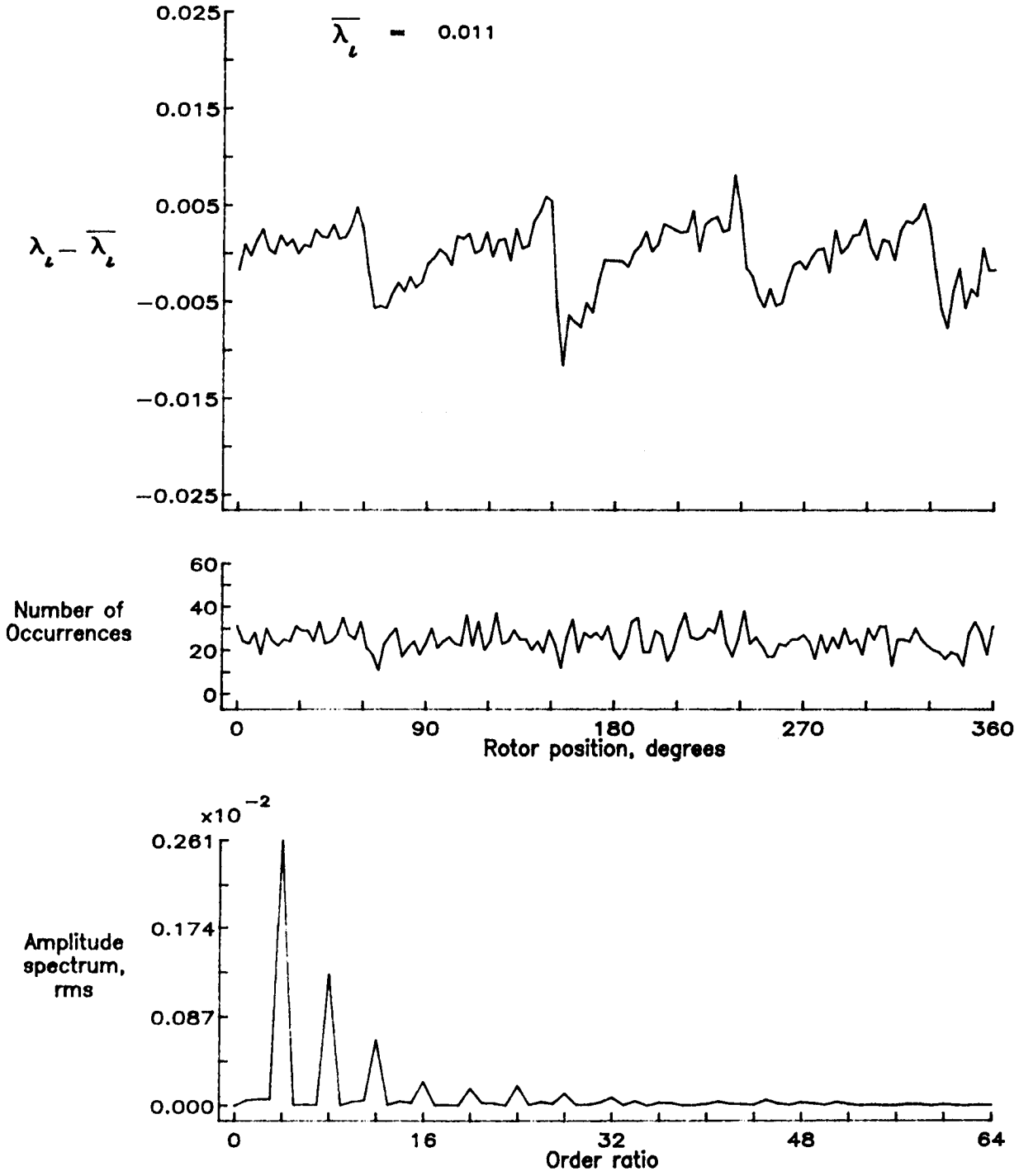

Figure 97.– Concluded.

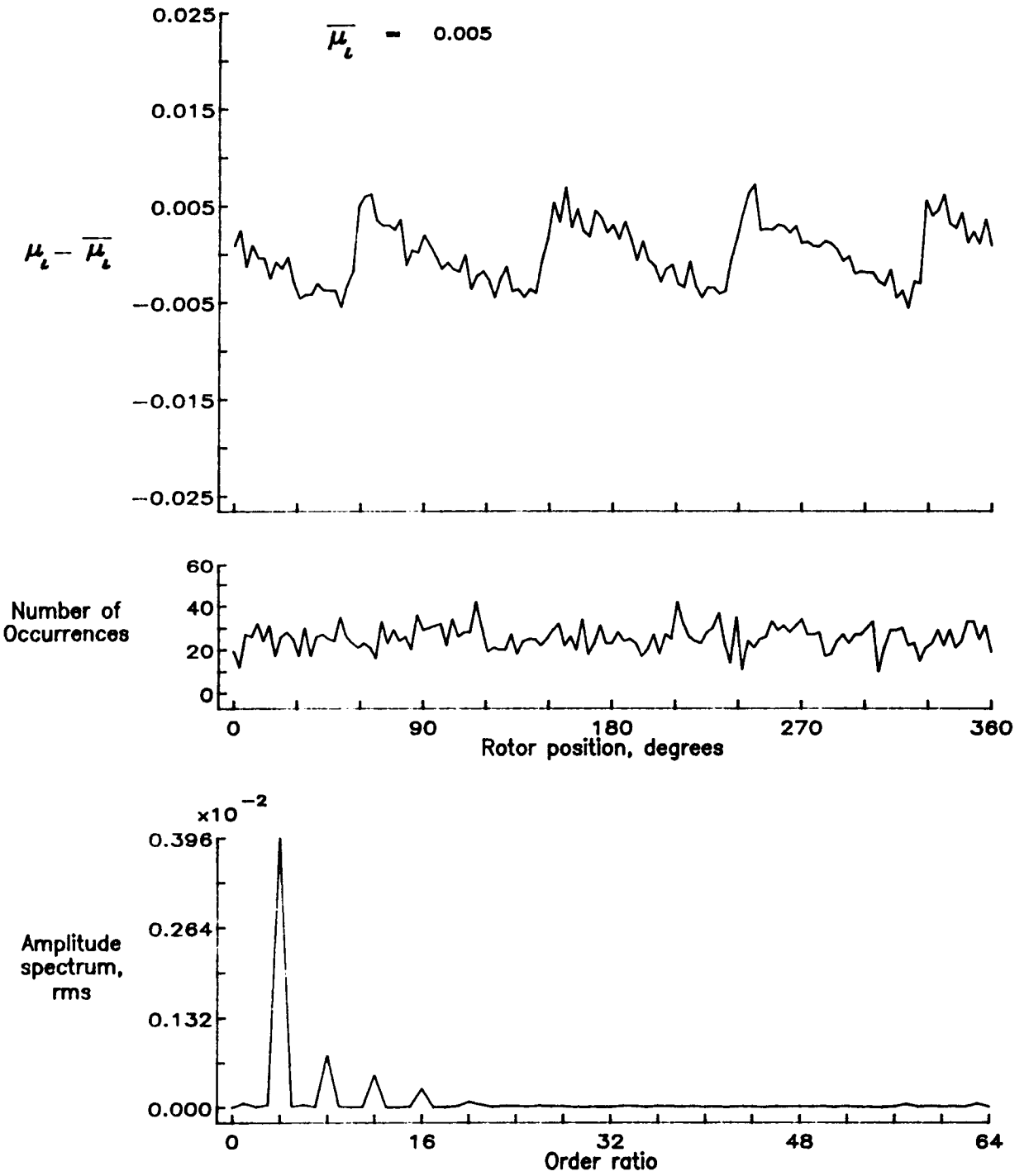

Figure 98.– Induced inflow velocity measured at 150 degrees and r/R of 0.94.

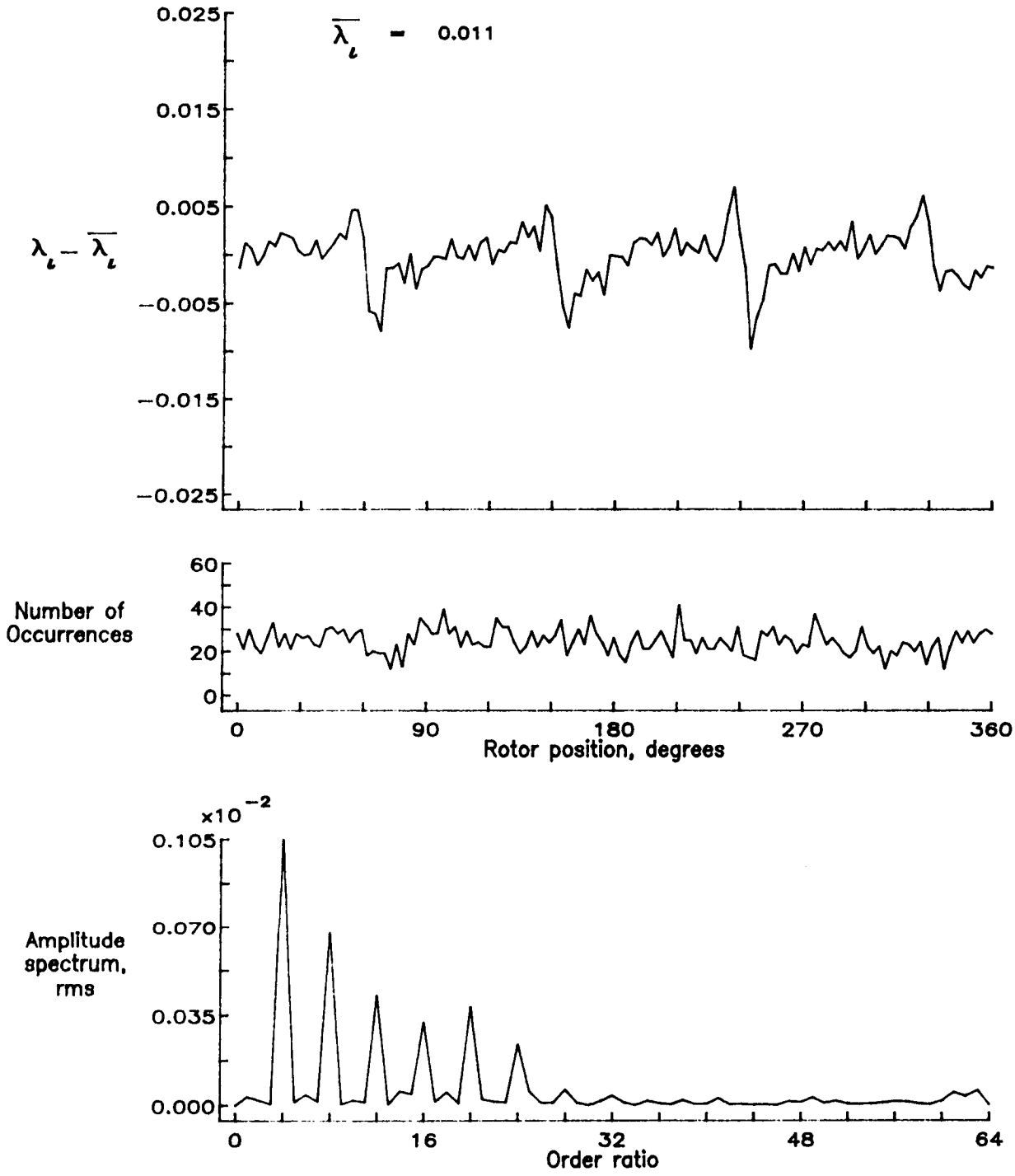

Figure 98.– Concluded.

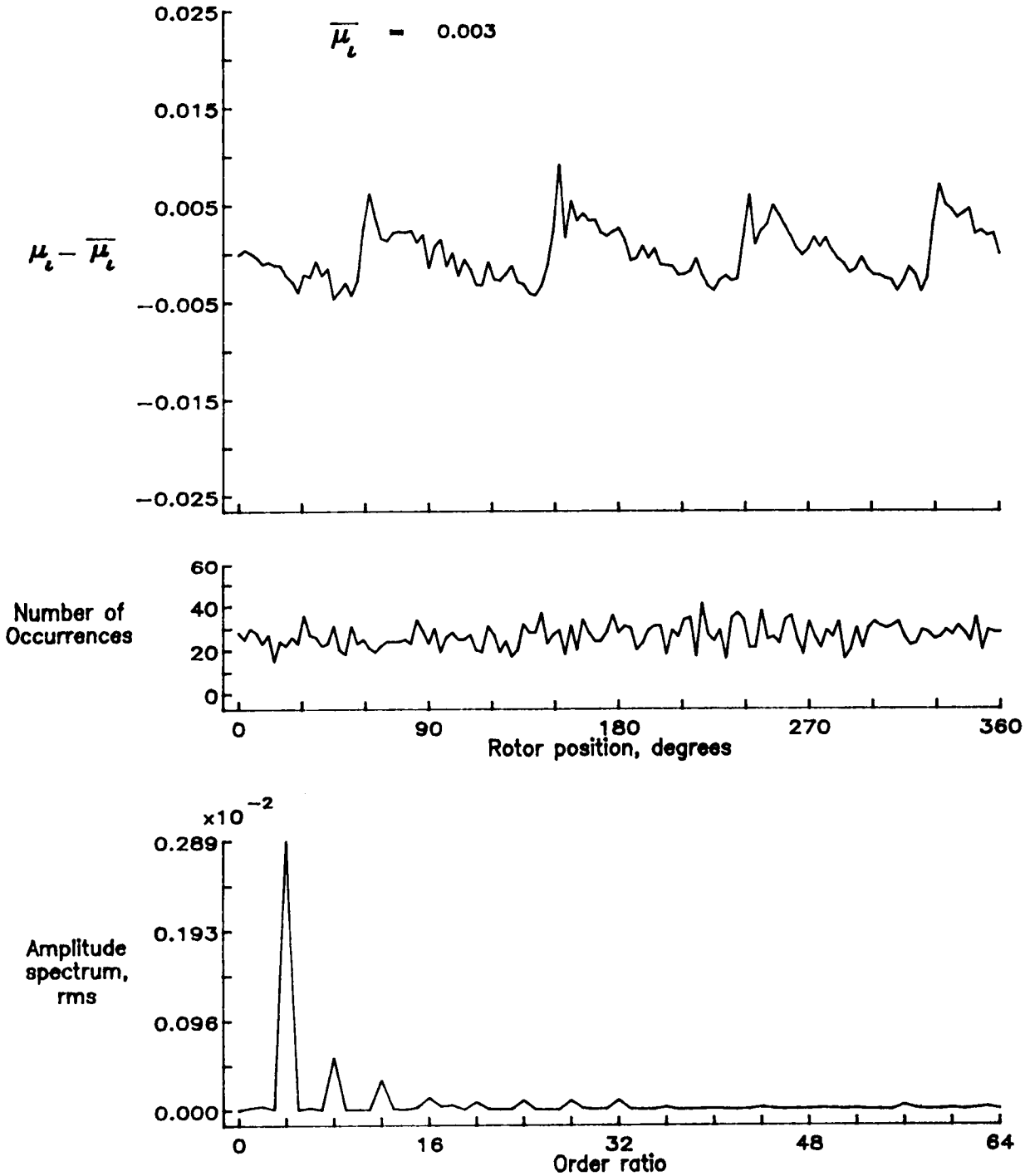

Figure 99.– Induced inflow velocity measured at 150 degrees and r/R of 0.98.

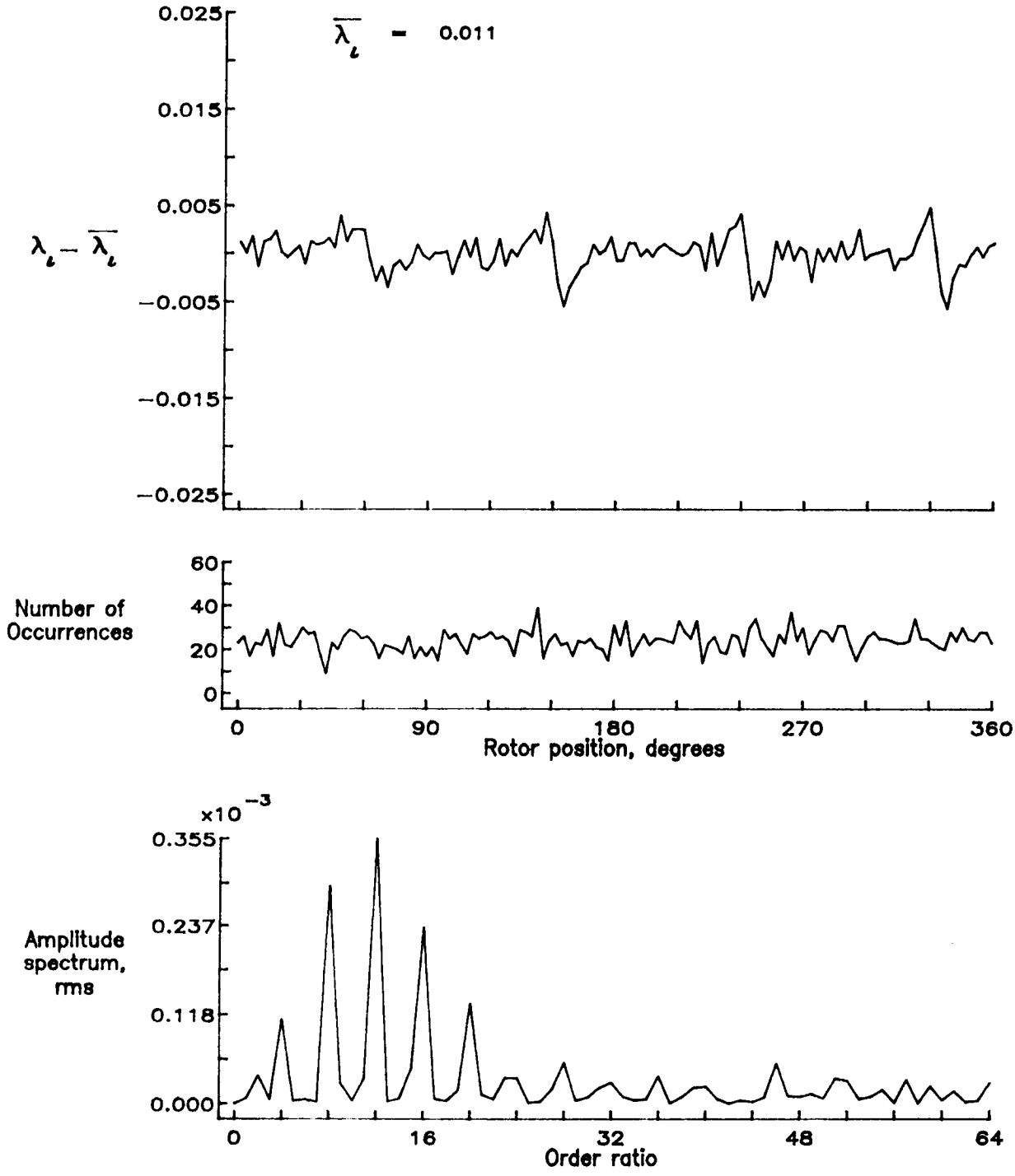

Figure 99.– Concluded.

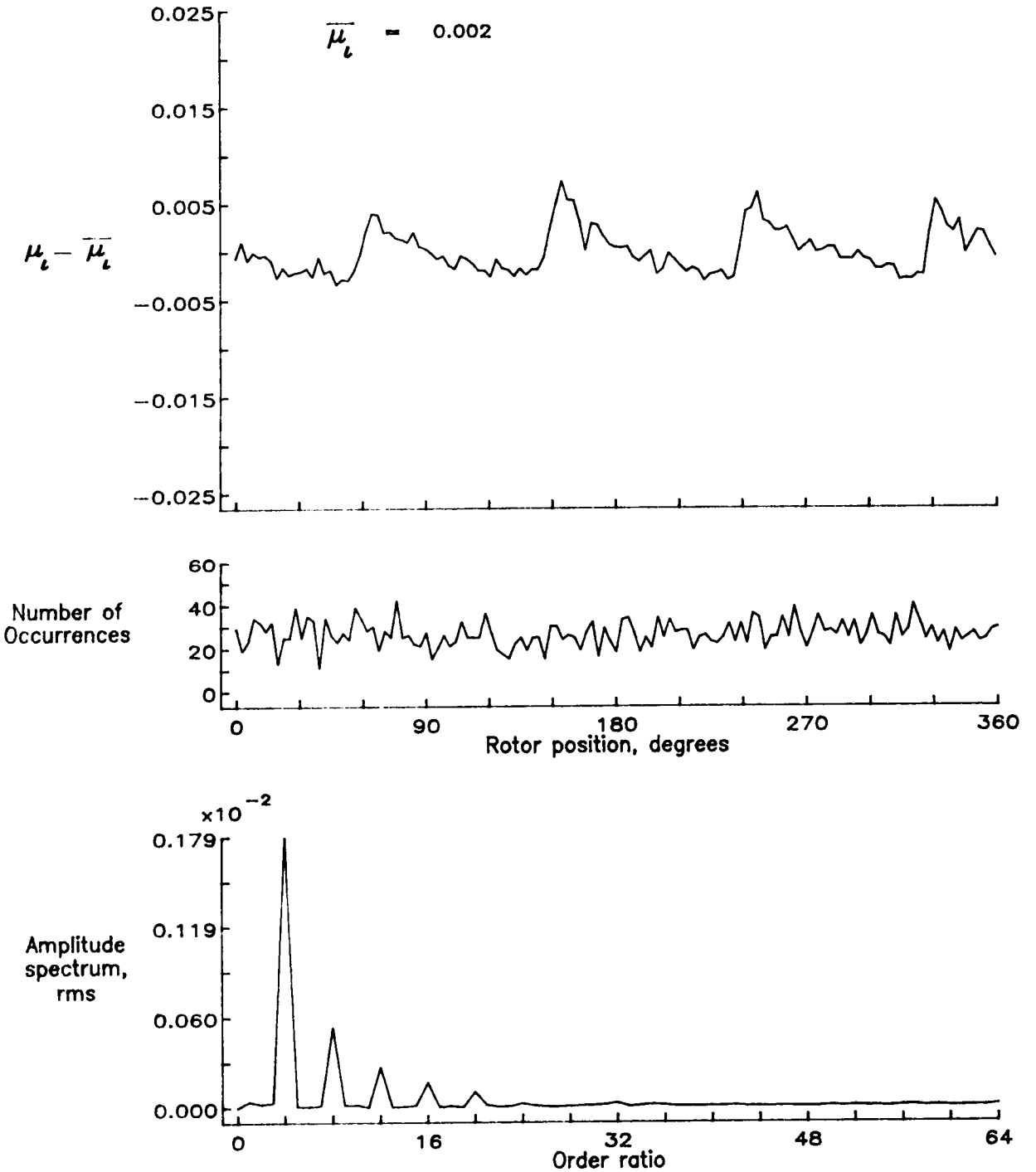

Figure 100.– Induced inflow velocity measured at 150 degrees and r/R of 1.02.

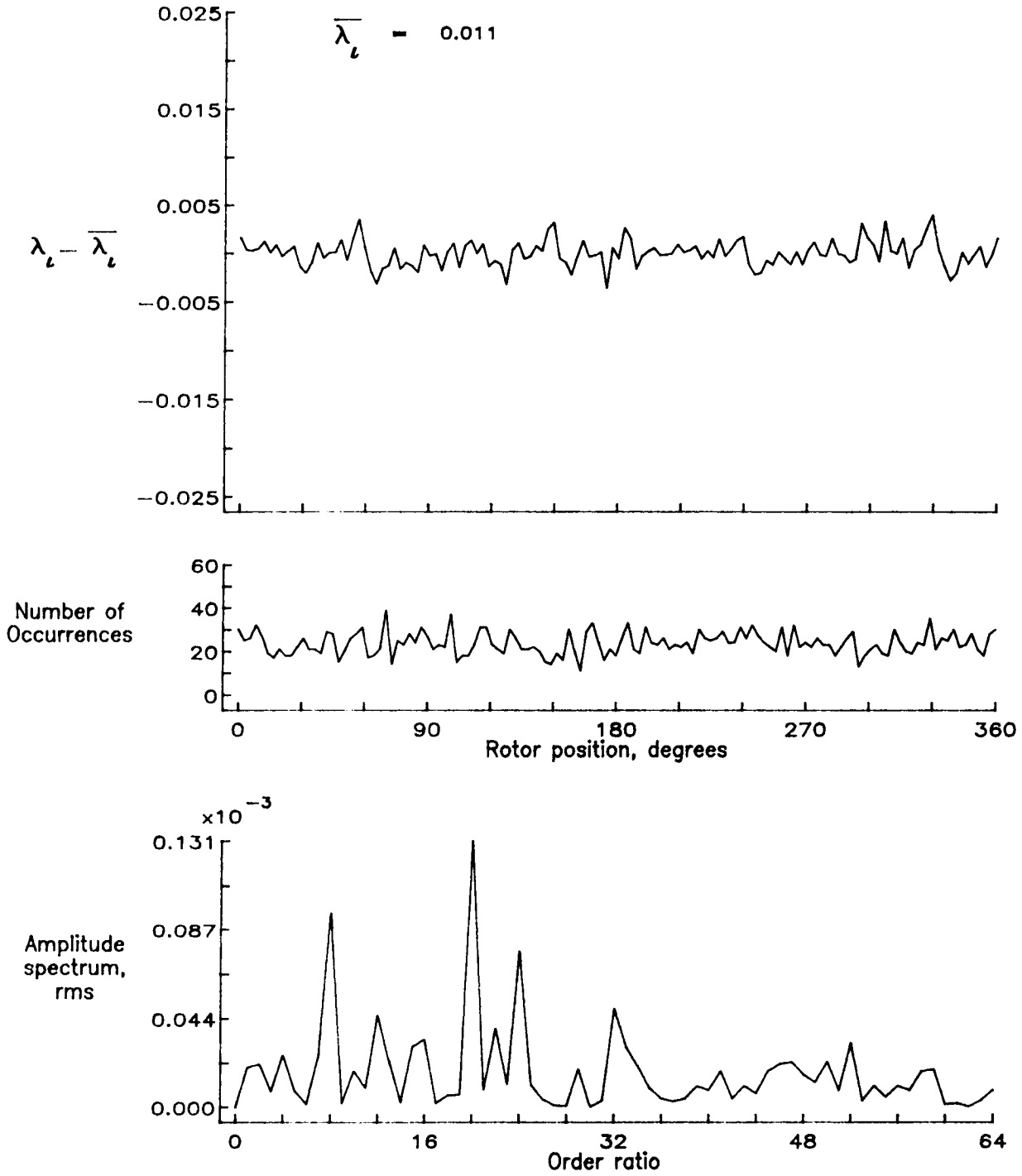

Figure 100.– Concluded.

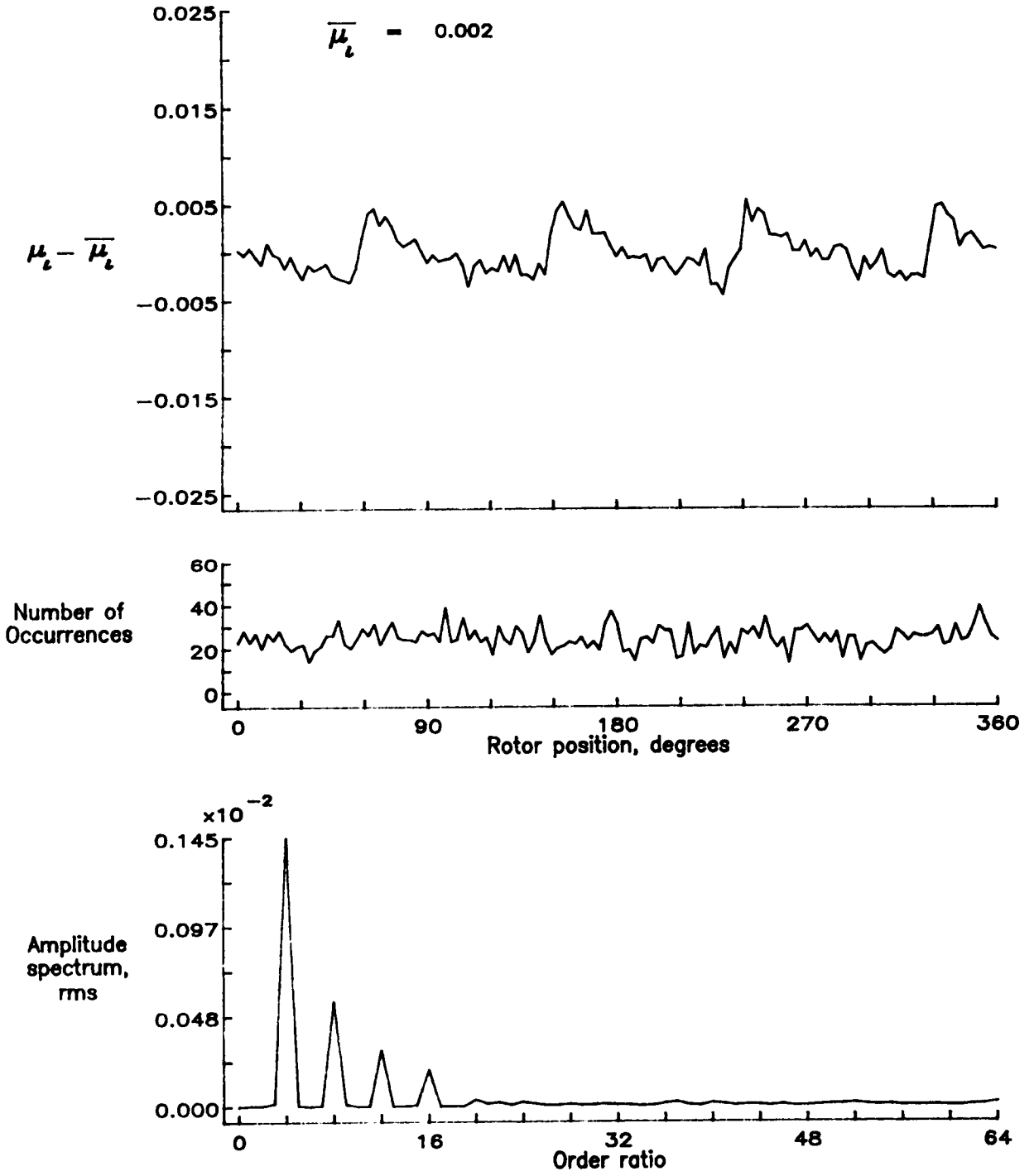

Figure 101.– Induced inflow velocity measured at 150 degrees and r/R of 1.04.

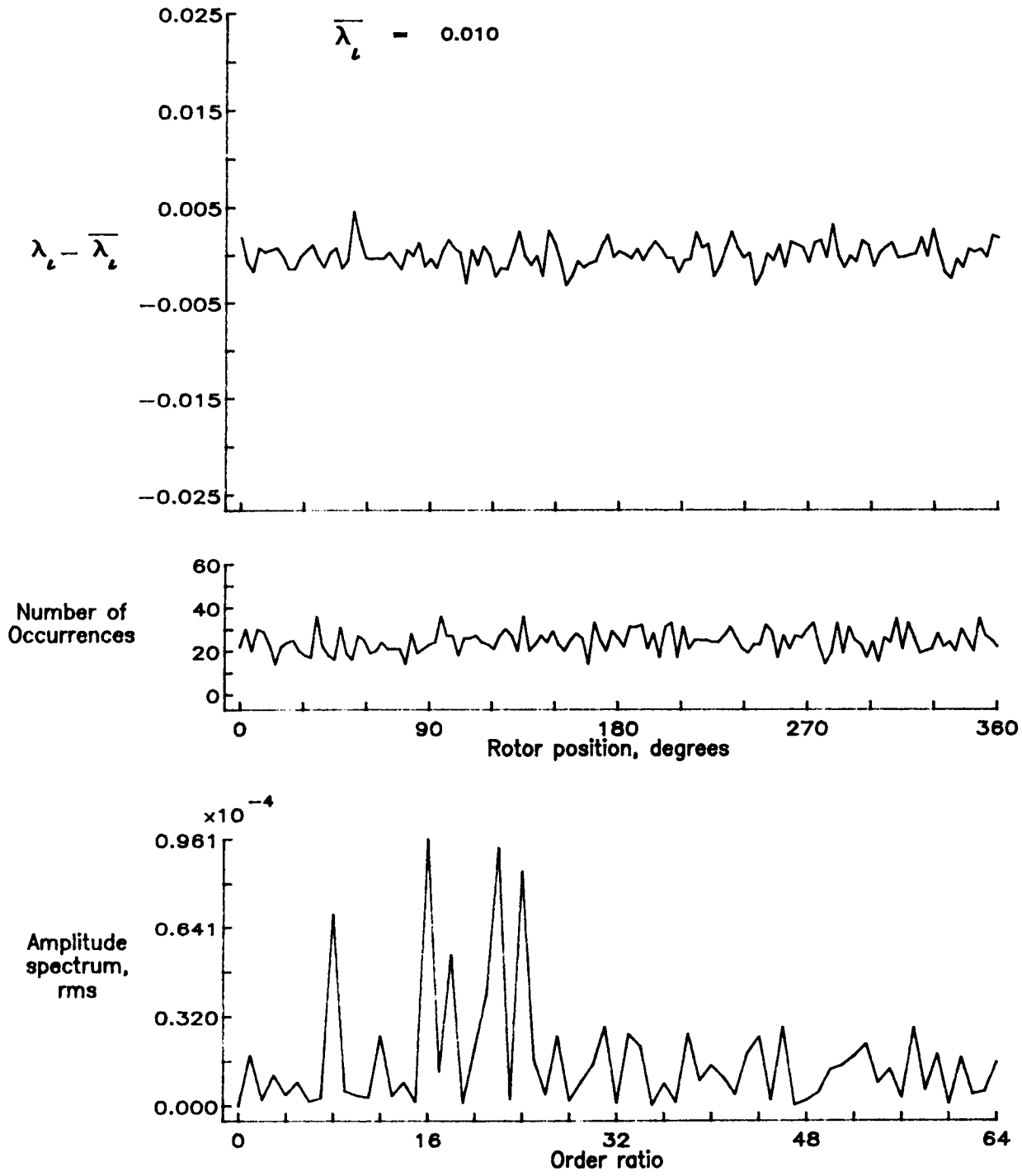

Figure 101.– Concluded.

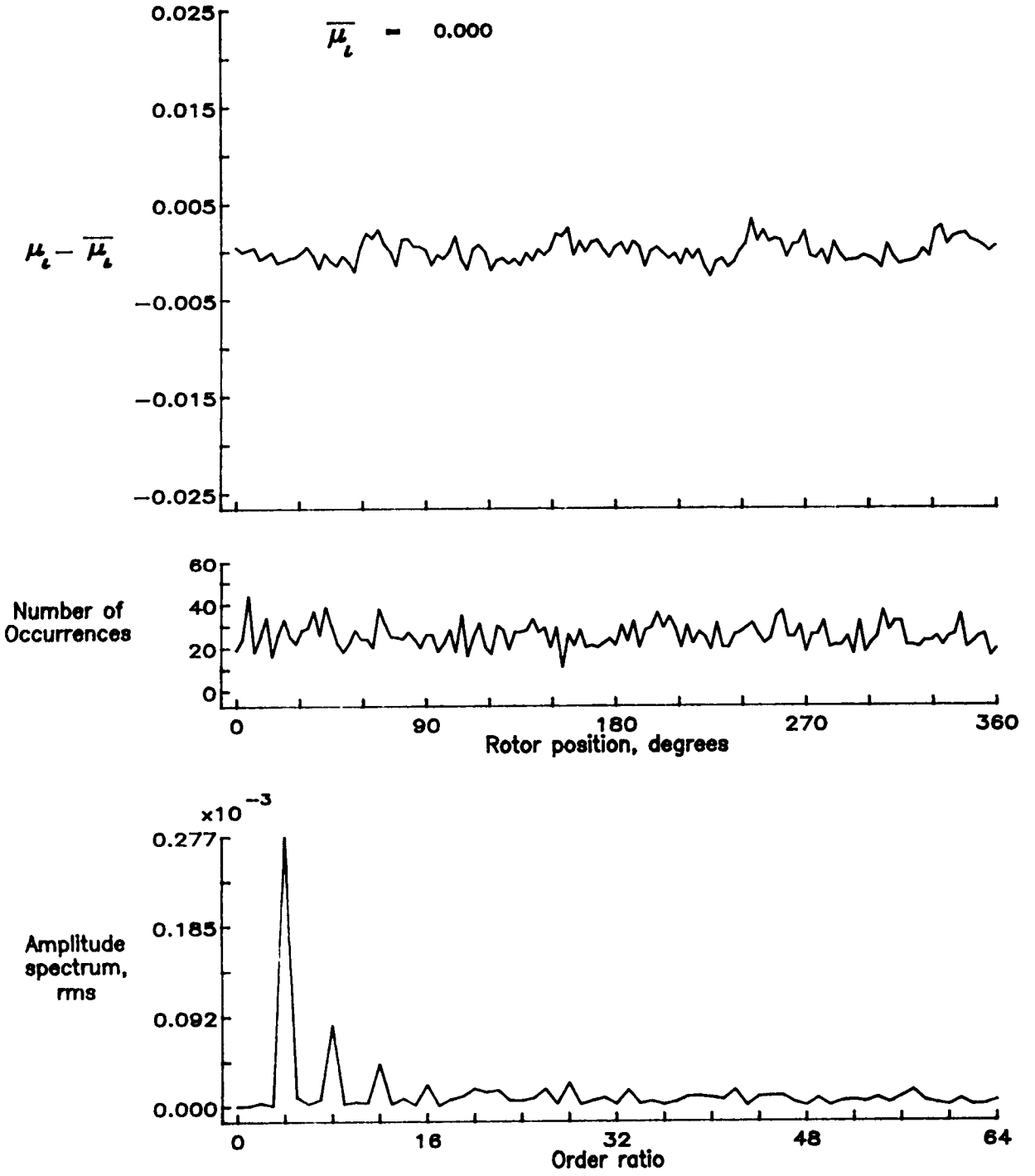

Figure 102.– Induced inflow velocity measured at 150 degrees and r/R of 1.10.

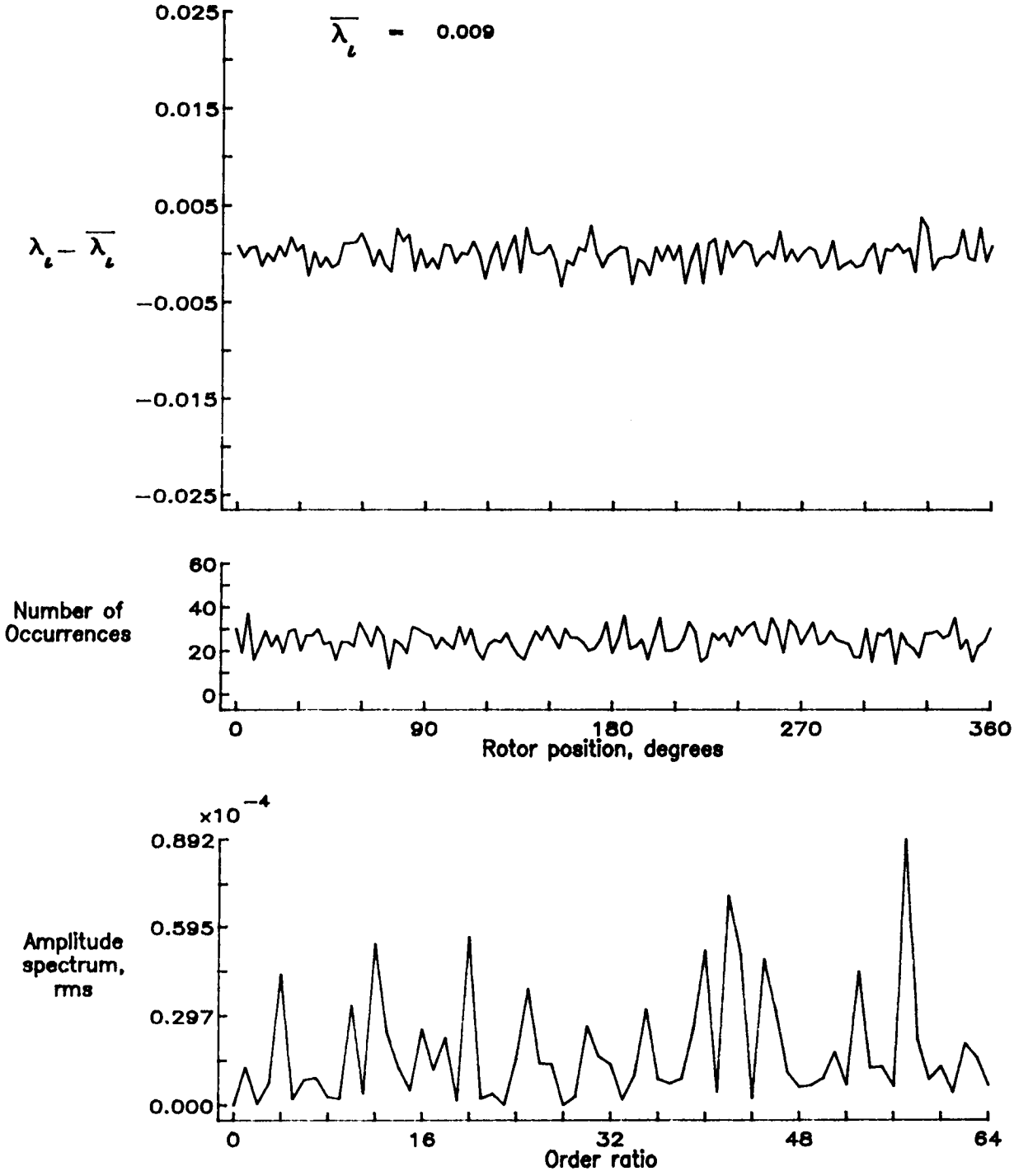

Figure 102.– Concluded.

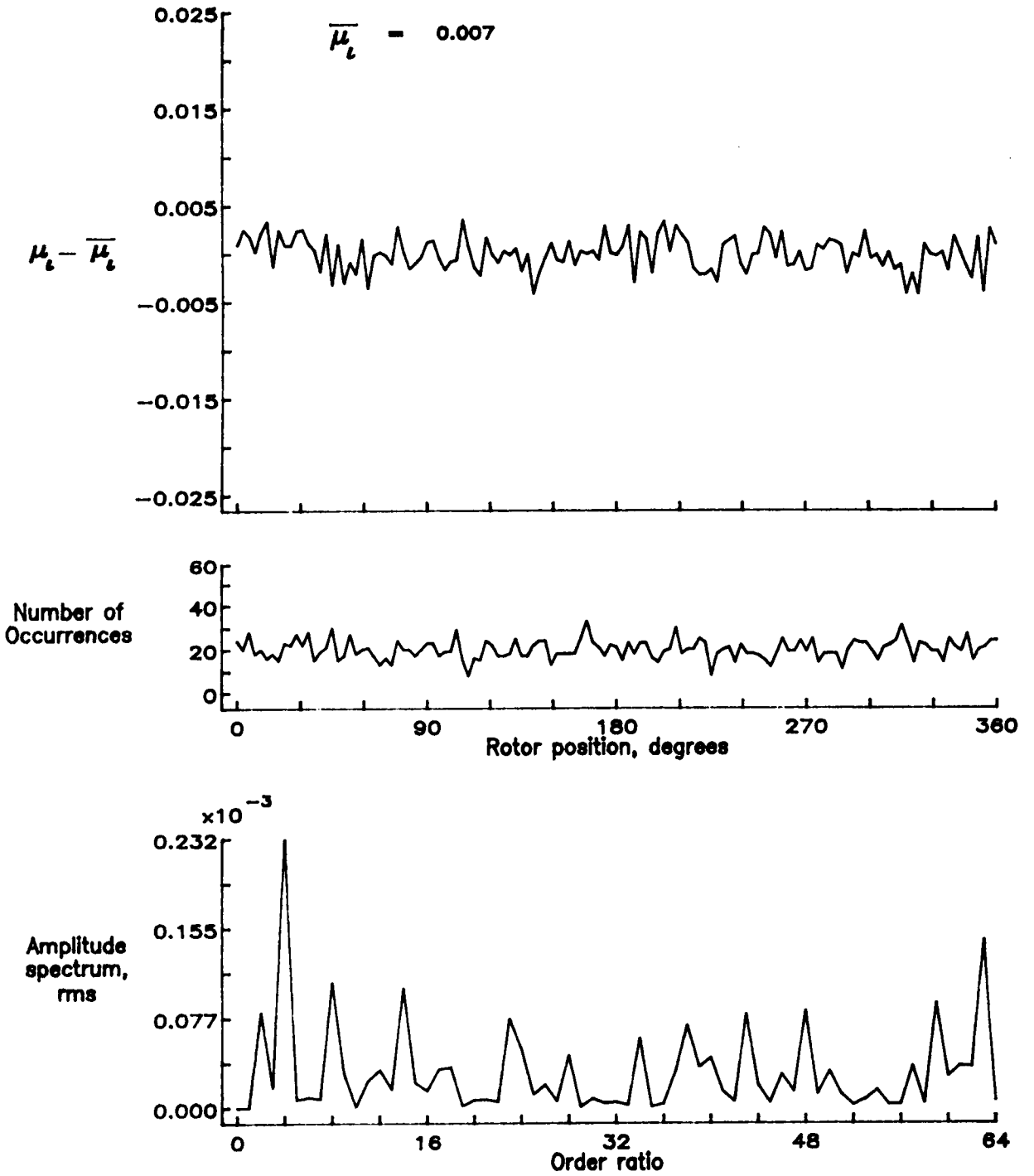

Figure 103.– Induced inflow velocity measured at 180 degrees and r/R of 0.20.

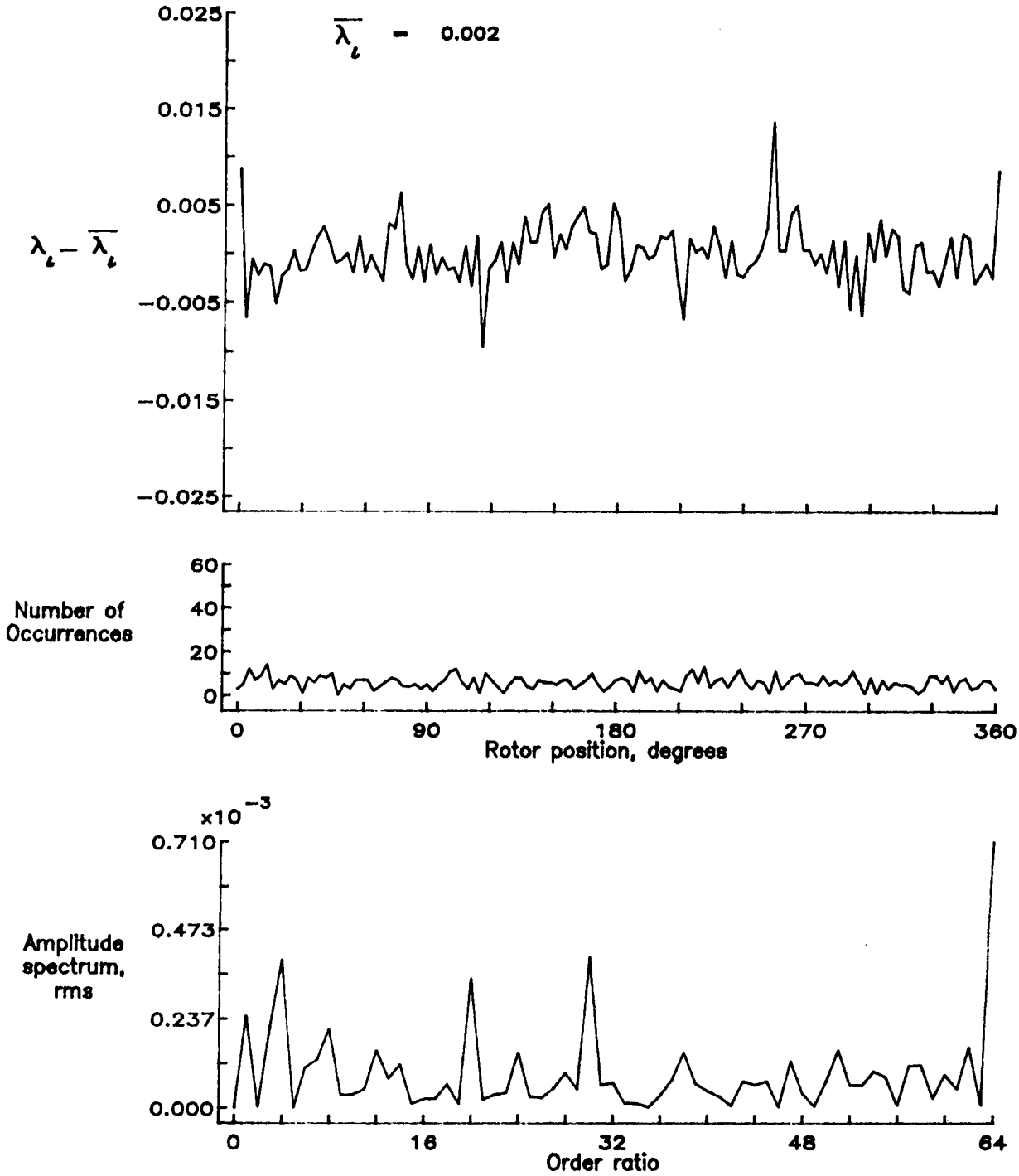

Figure 103.– Concluded.

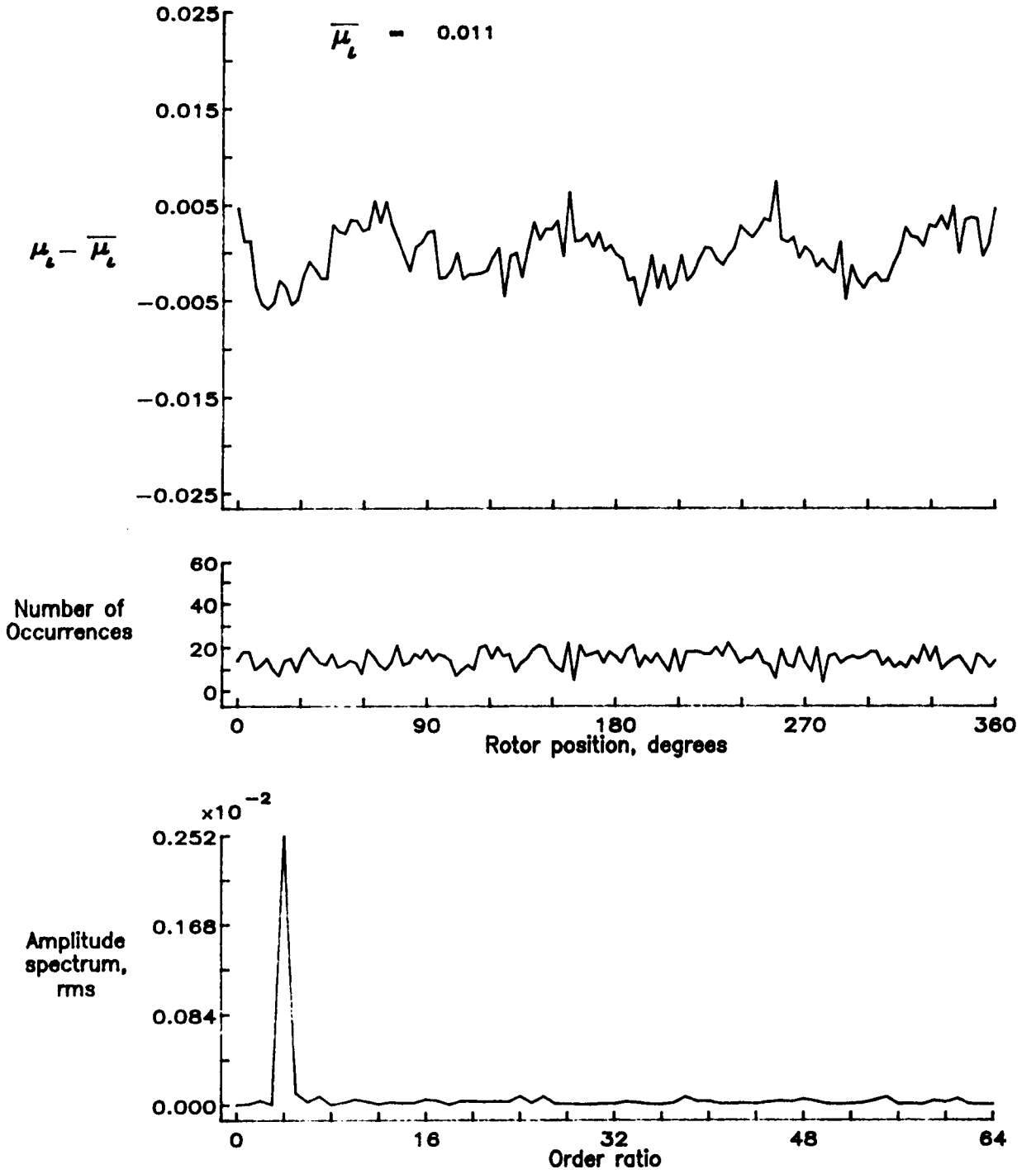

Figure 104.– Induced inflow velocity measured at 180 degrees and r/R of 0.40.

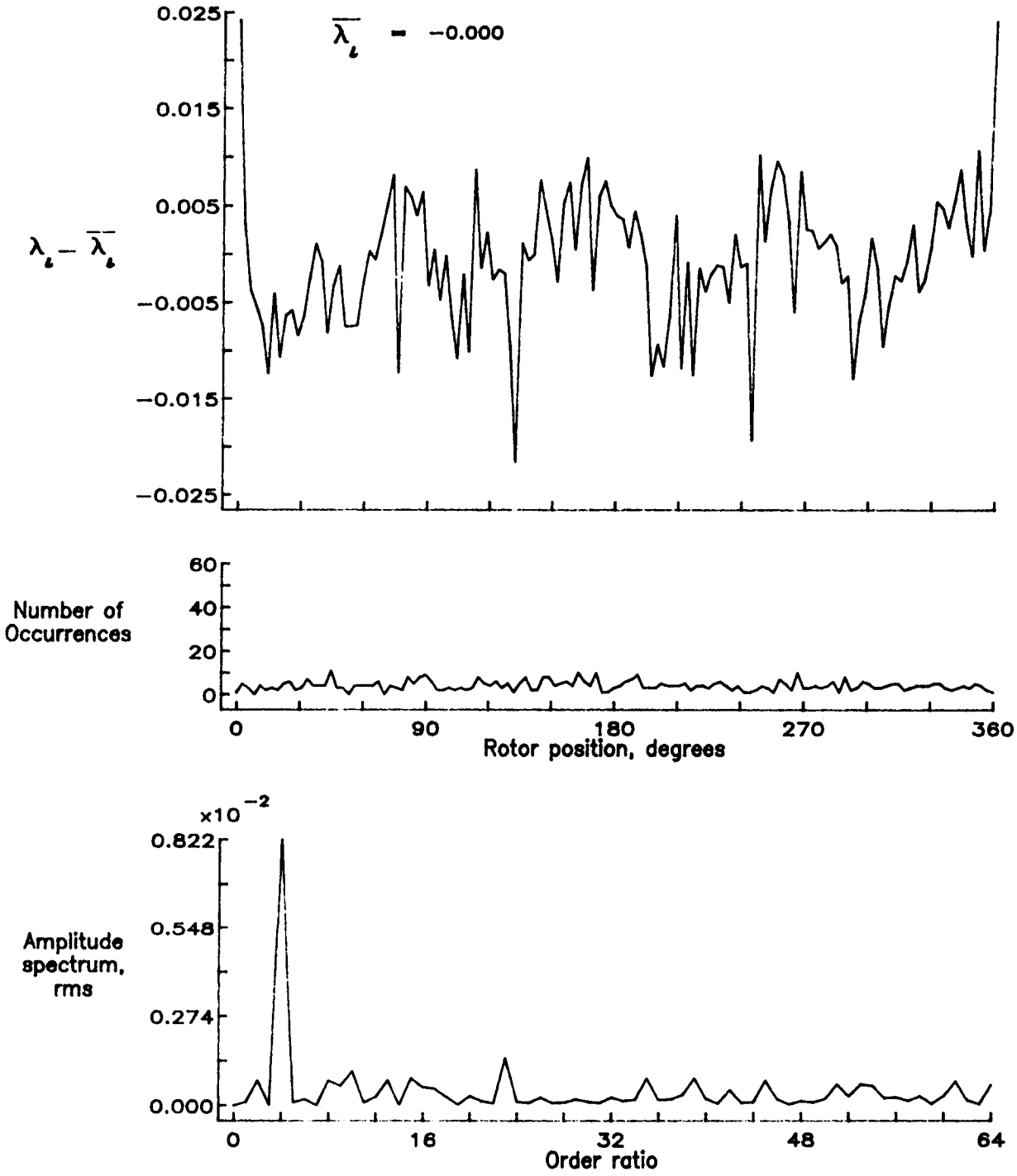

Figure 104.– Concluded.

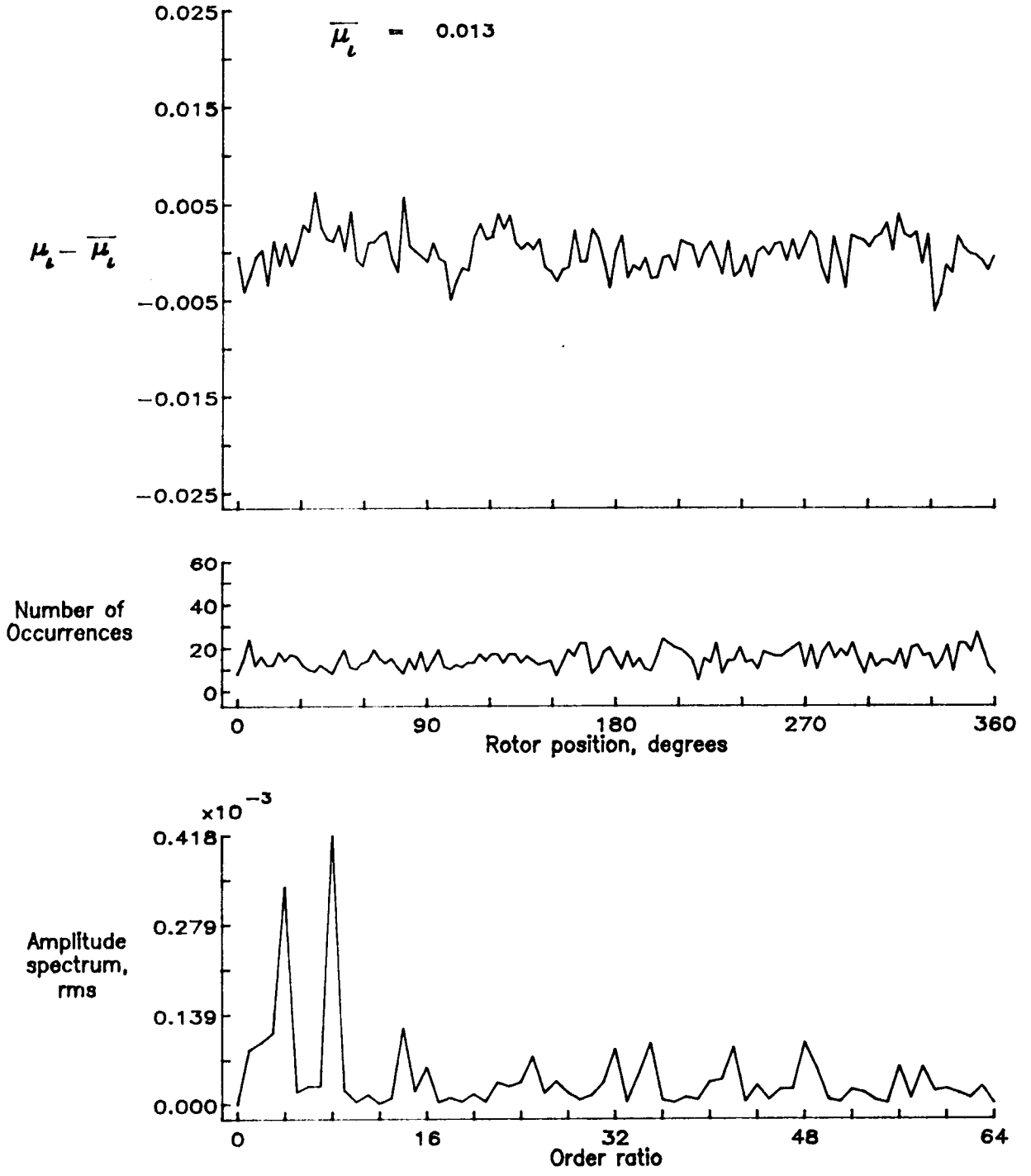

Figure 105.– Induced inflow velocity measured at 180 degrees and r/R of 0.50.

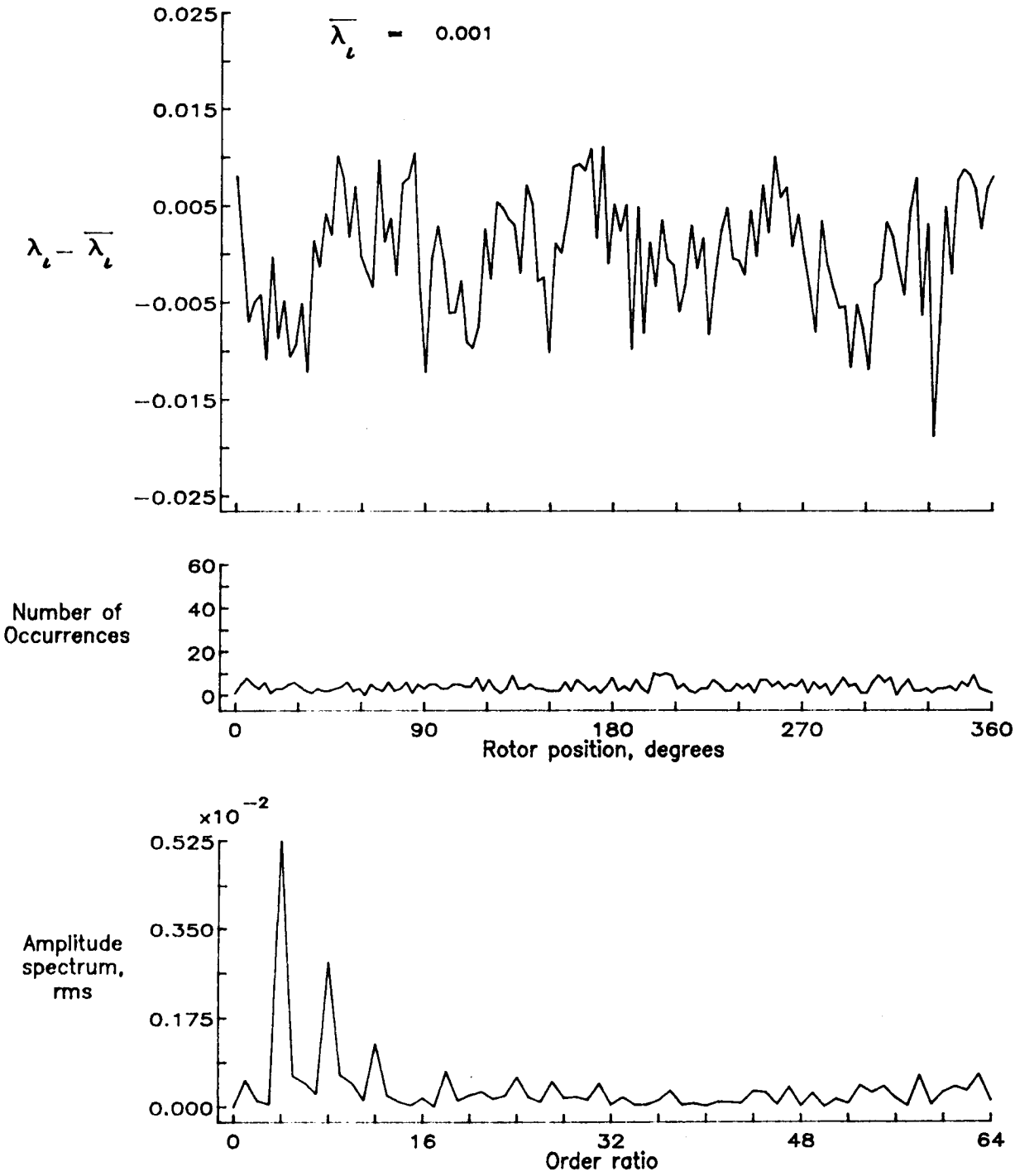

Figure 105.– Concluded.

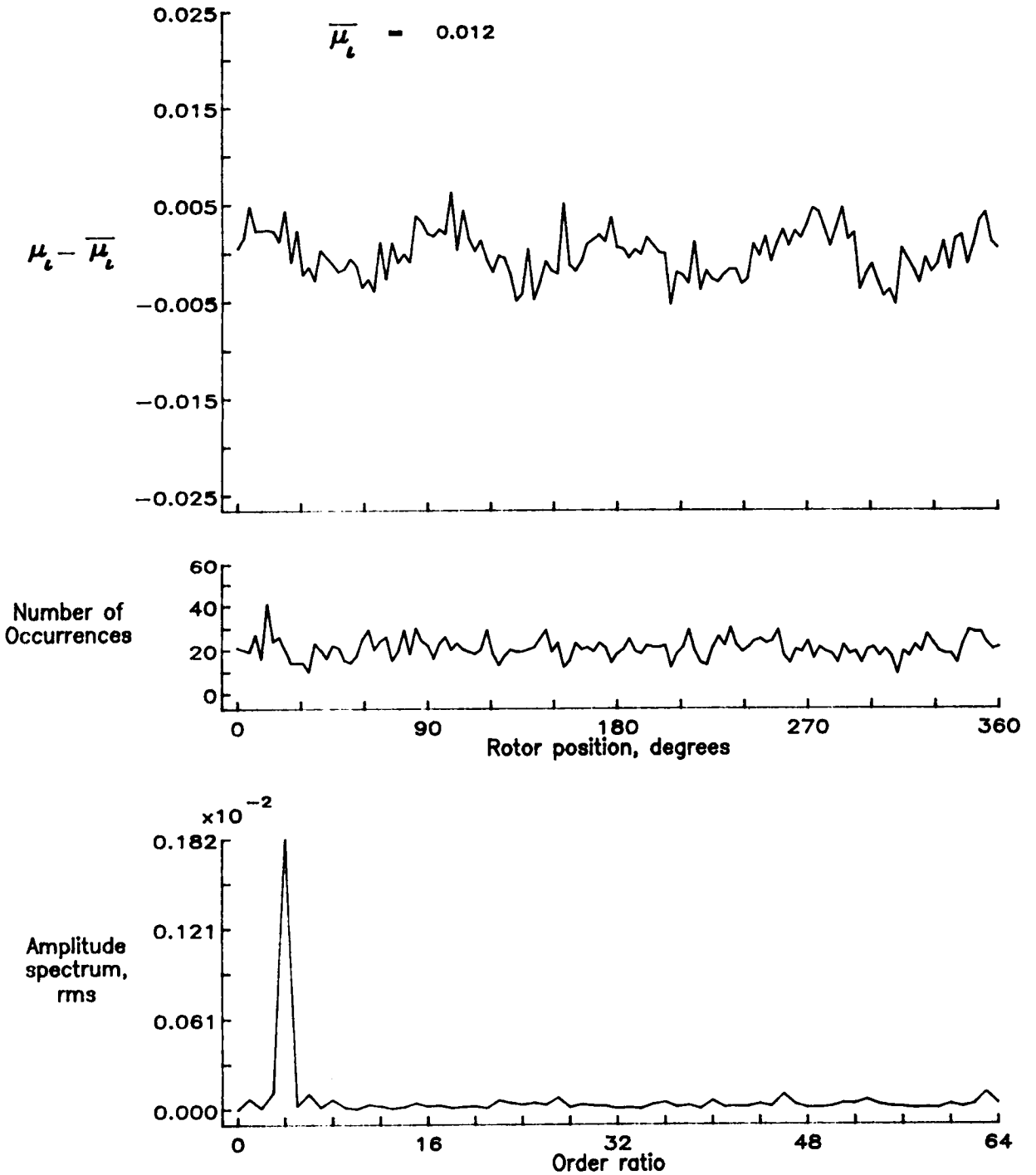

Figure 106.– Induced inflow velocity measured at 180 degrees and r/R of 0.60.

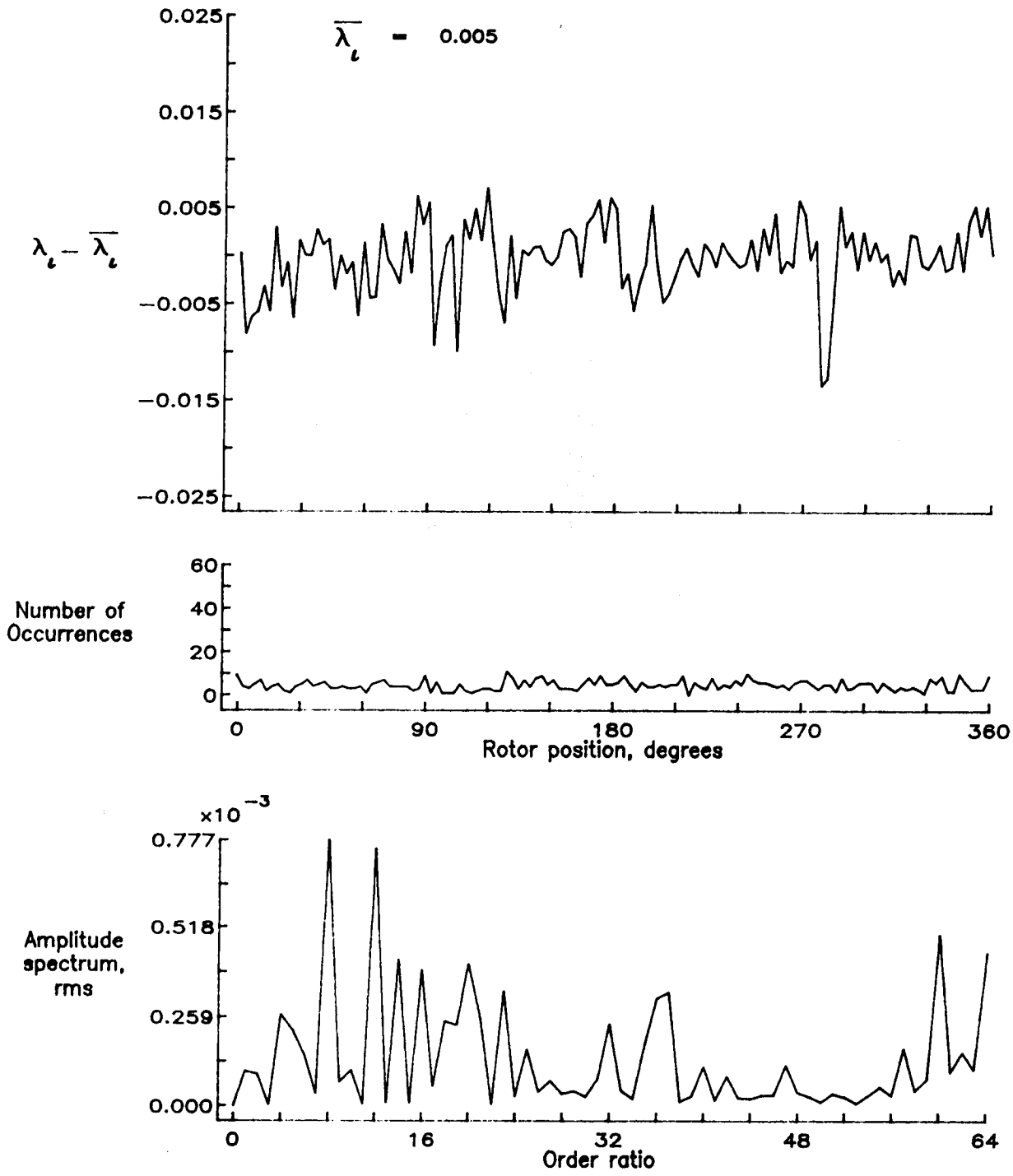

Figure 106.– Concluded.

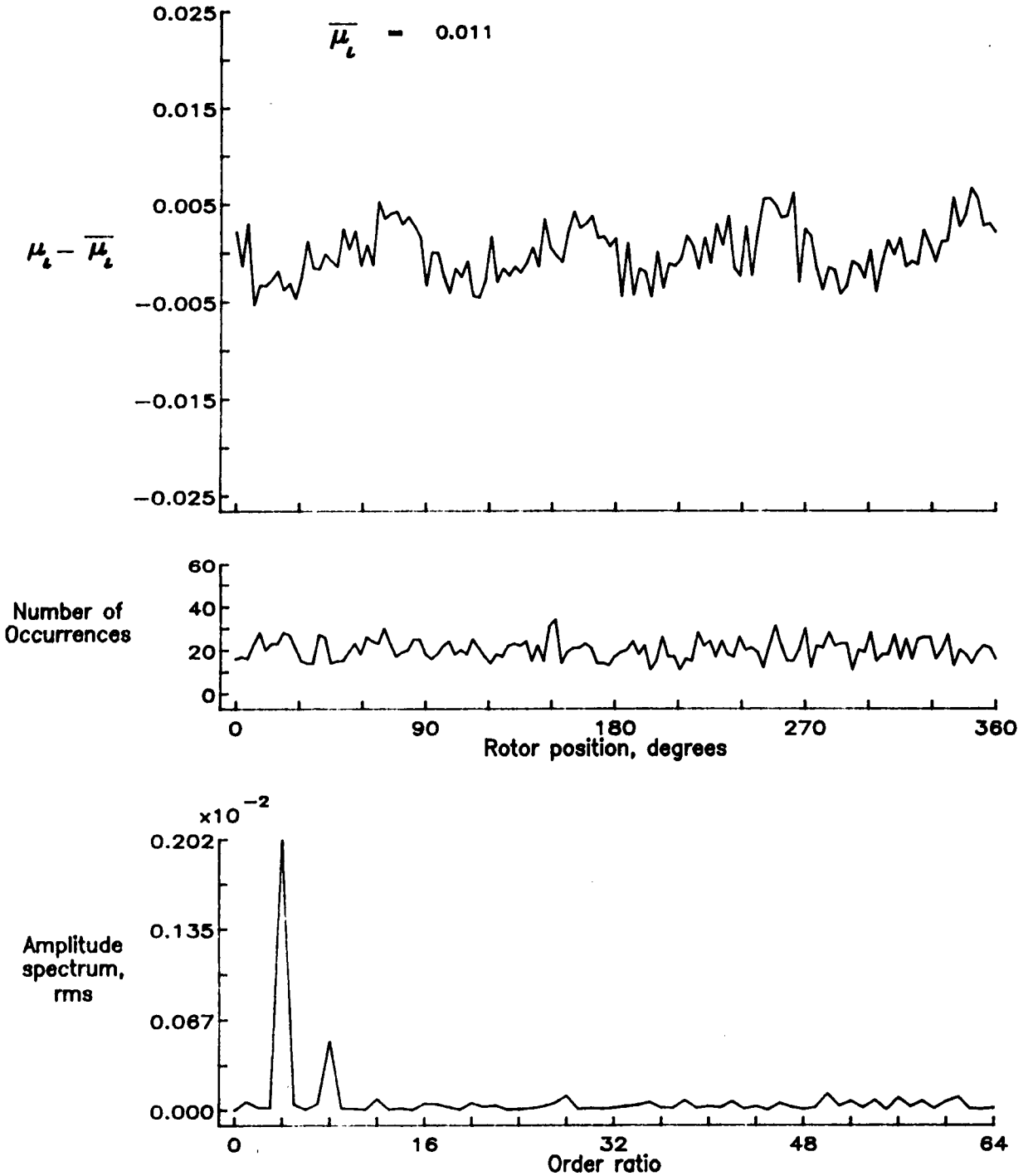

Figure 107.– Induced inflow velocity measured at 180 degrees and r/R of 0.70.

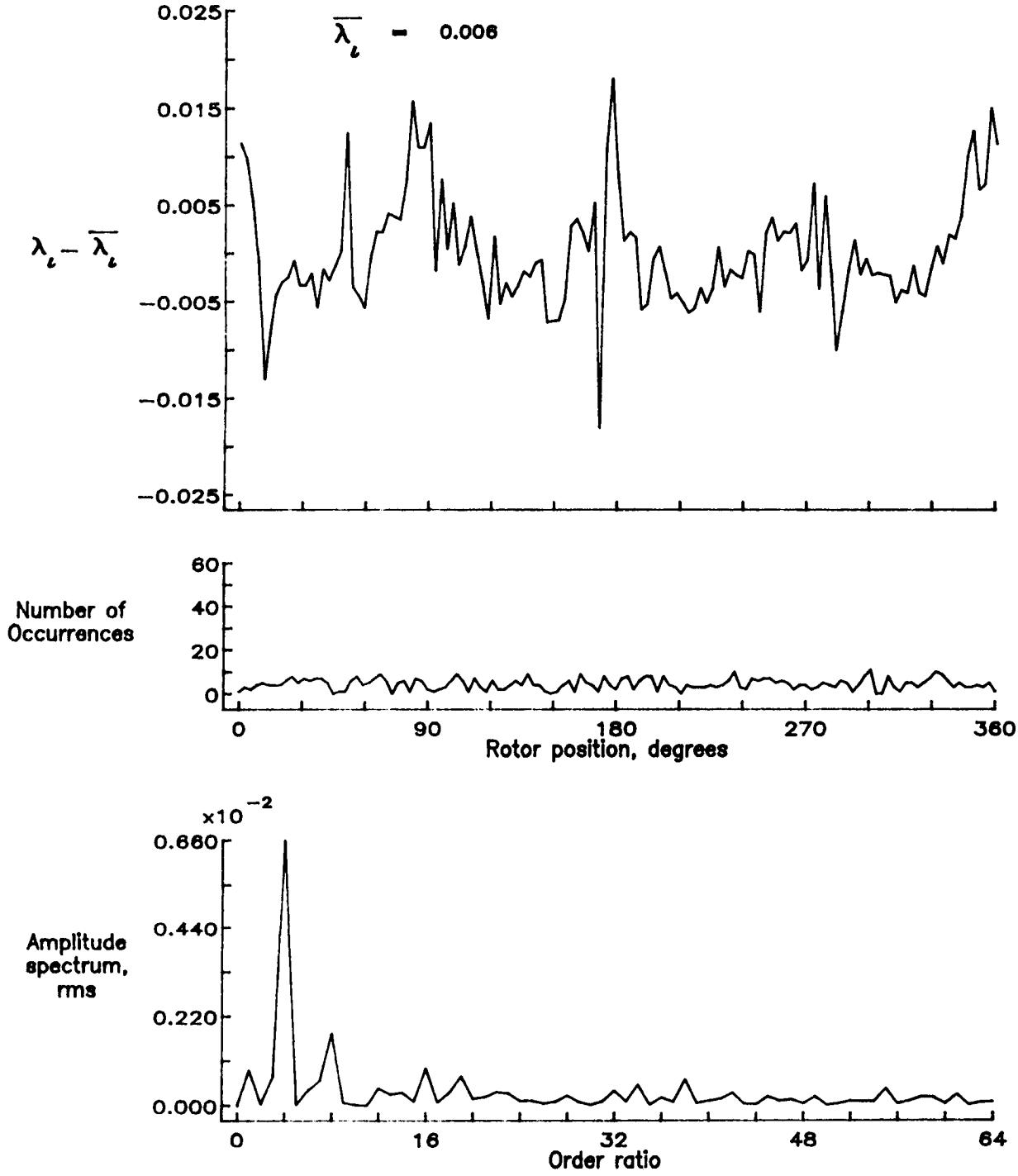

Figure 107.– Concluded.

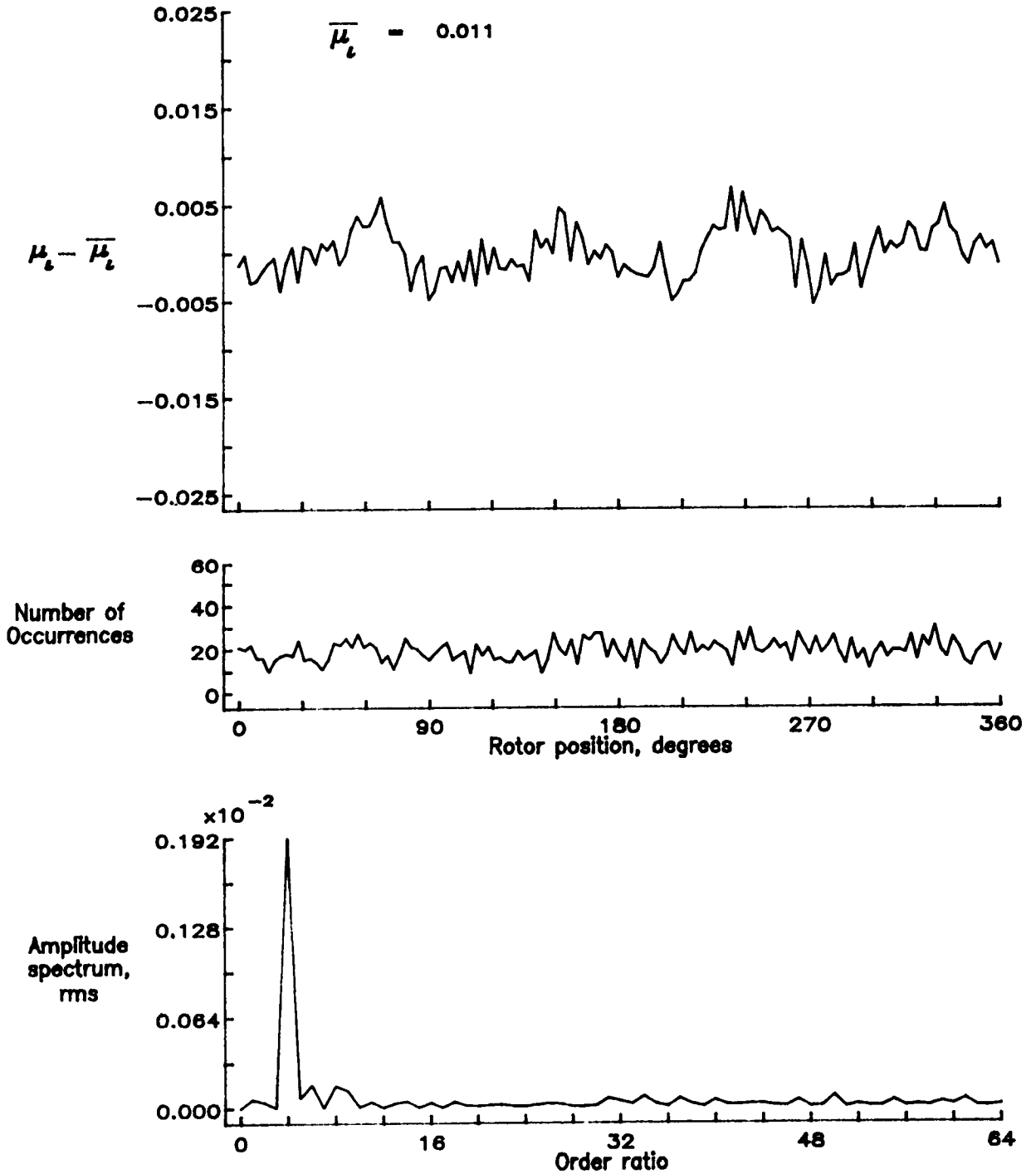

Figure 108.– Induced inflow velocity measured at 180 degrees and r/R of 0.74.

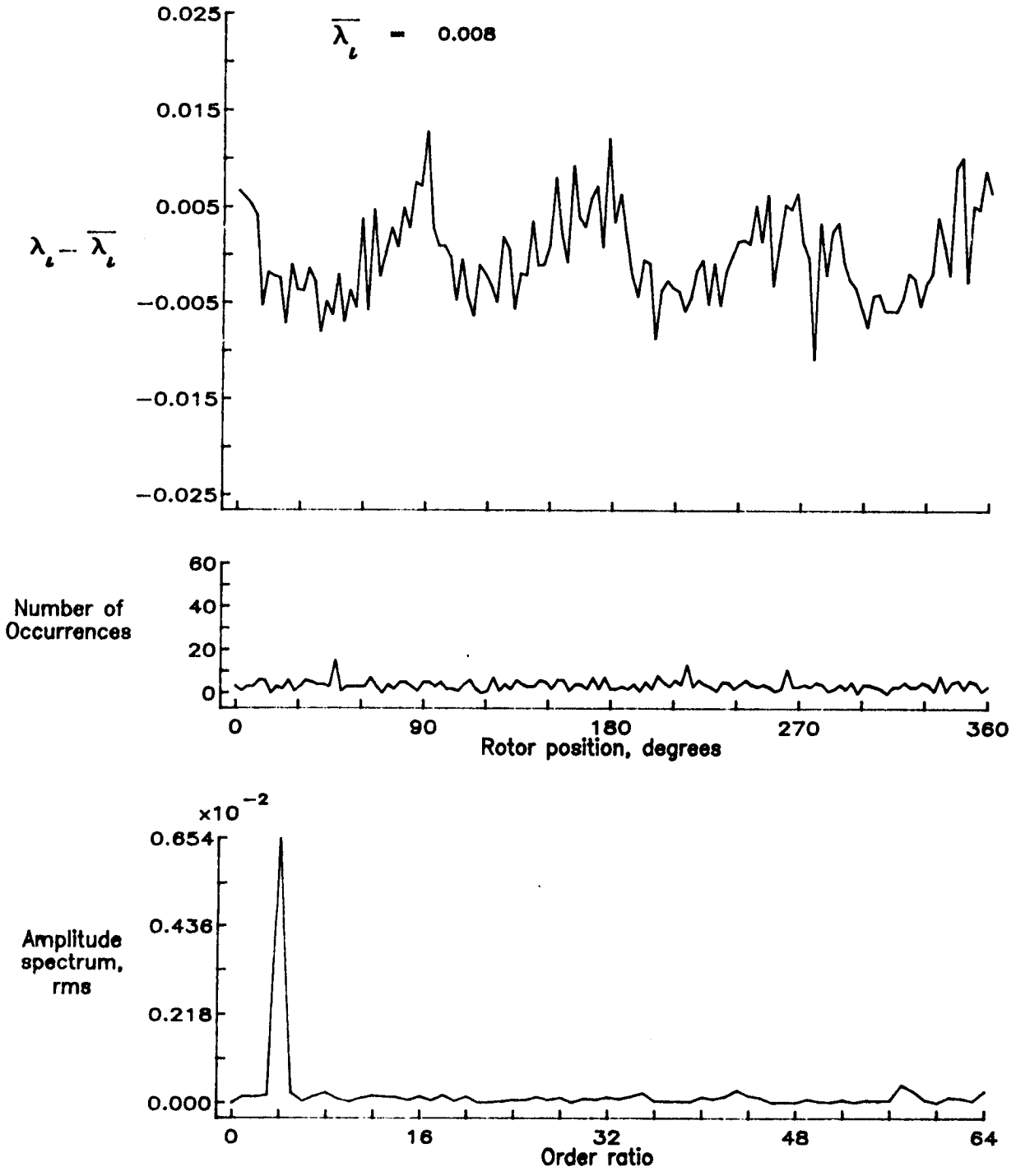

Figure 108.– Concluded.

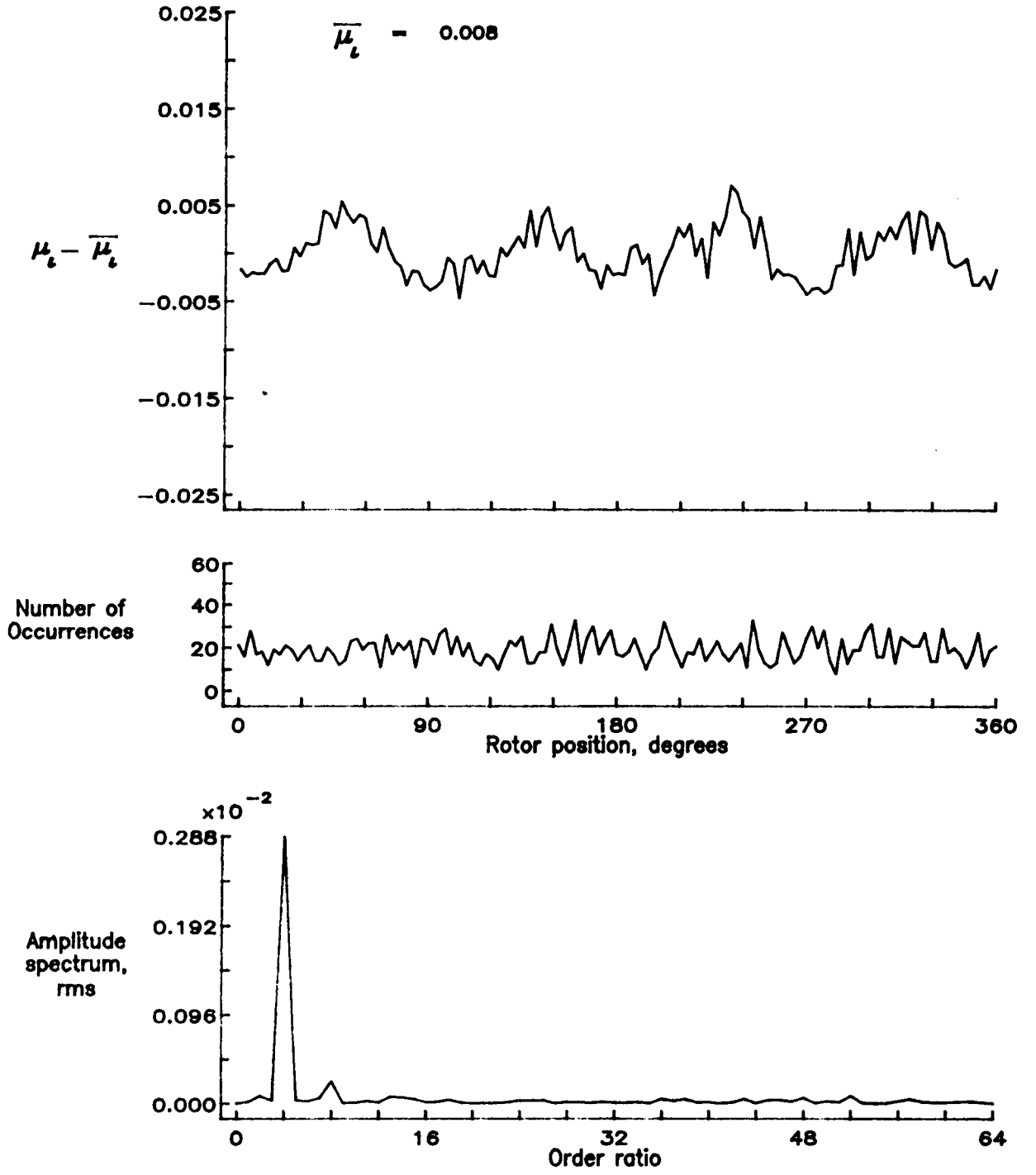

Figure 109.– Induced inflow velocity measured at 180 degrees and r/R of 0.78.

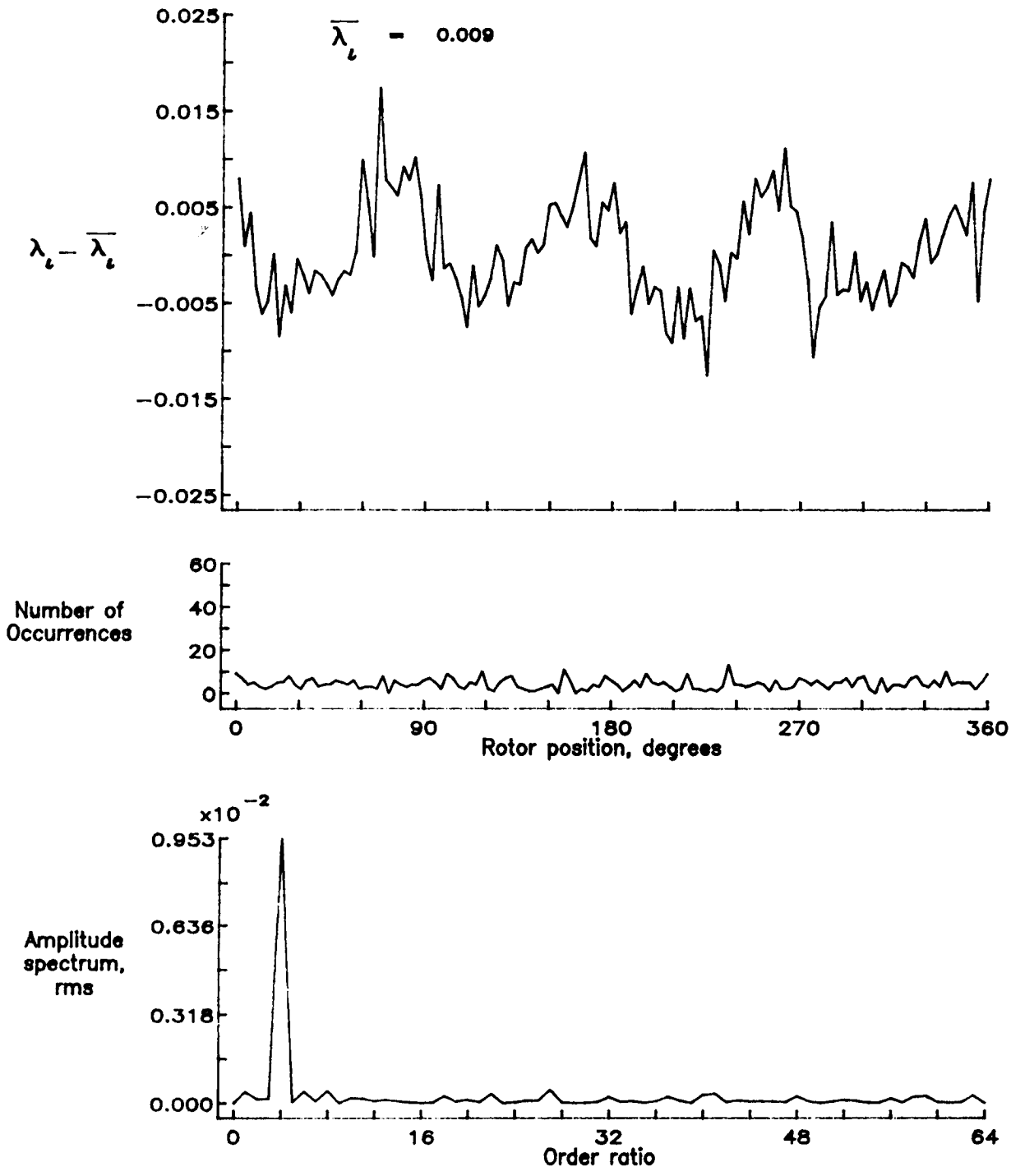

Figure 109.– Concluded.

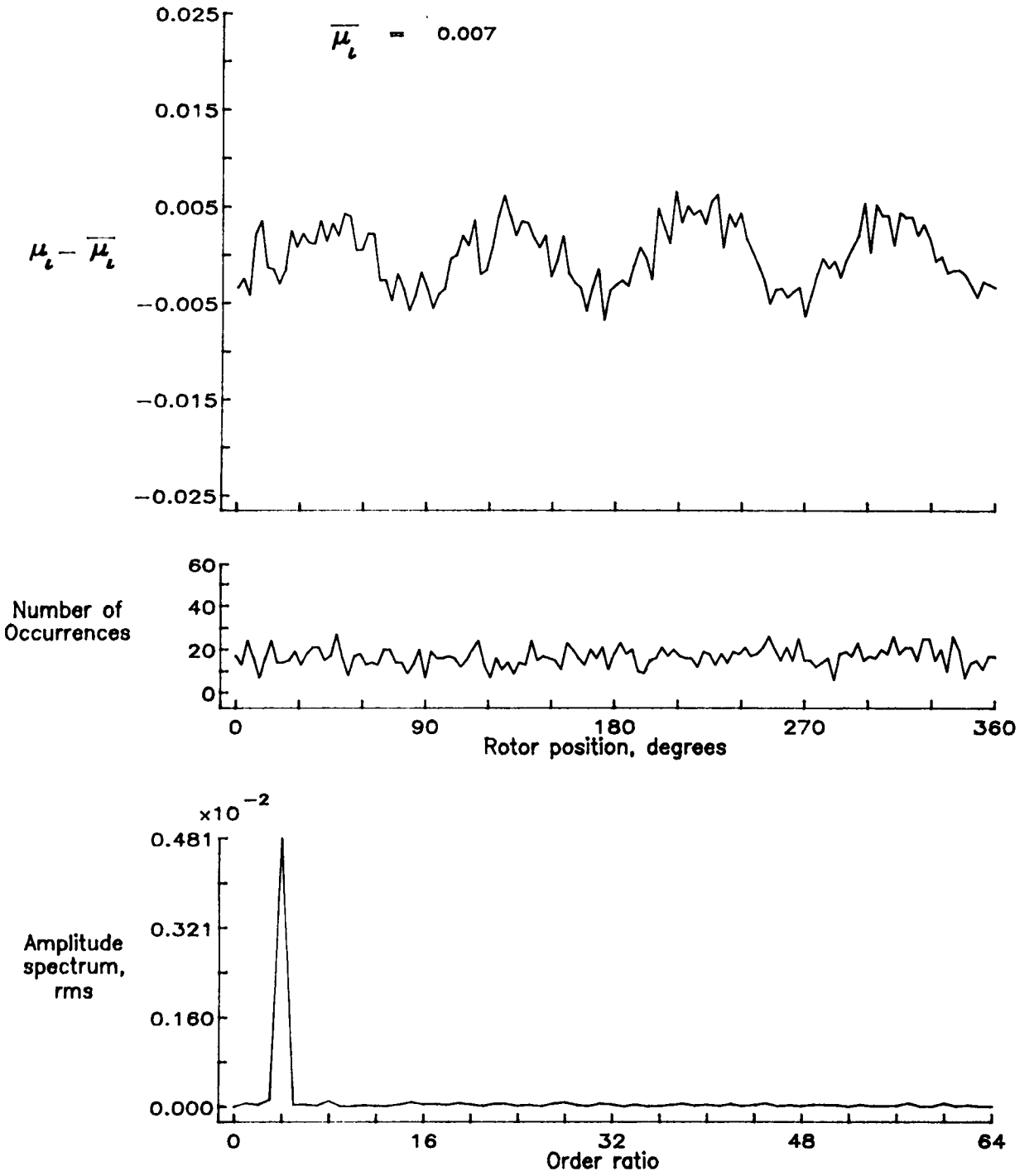

Figure 110.– Induced inflow velocity measured at 180 degrees and r/R of 0.82.

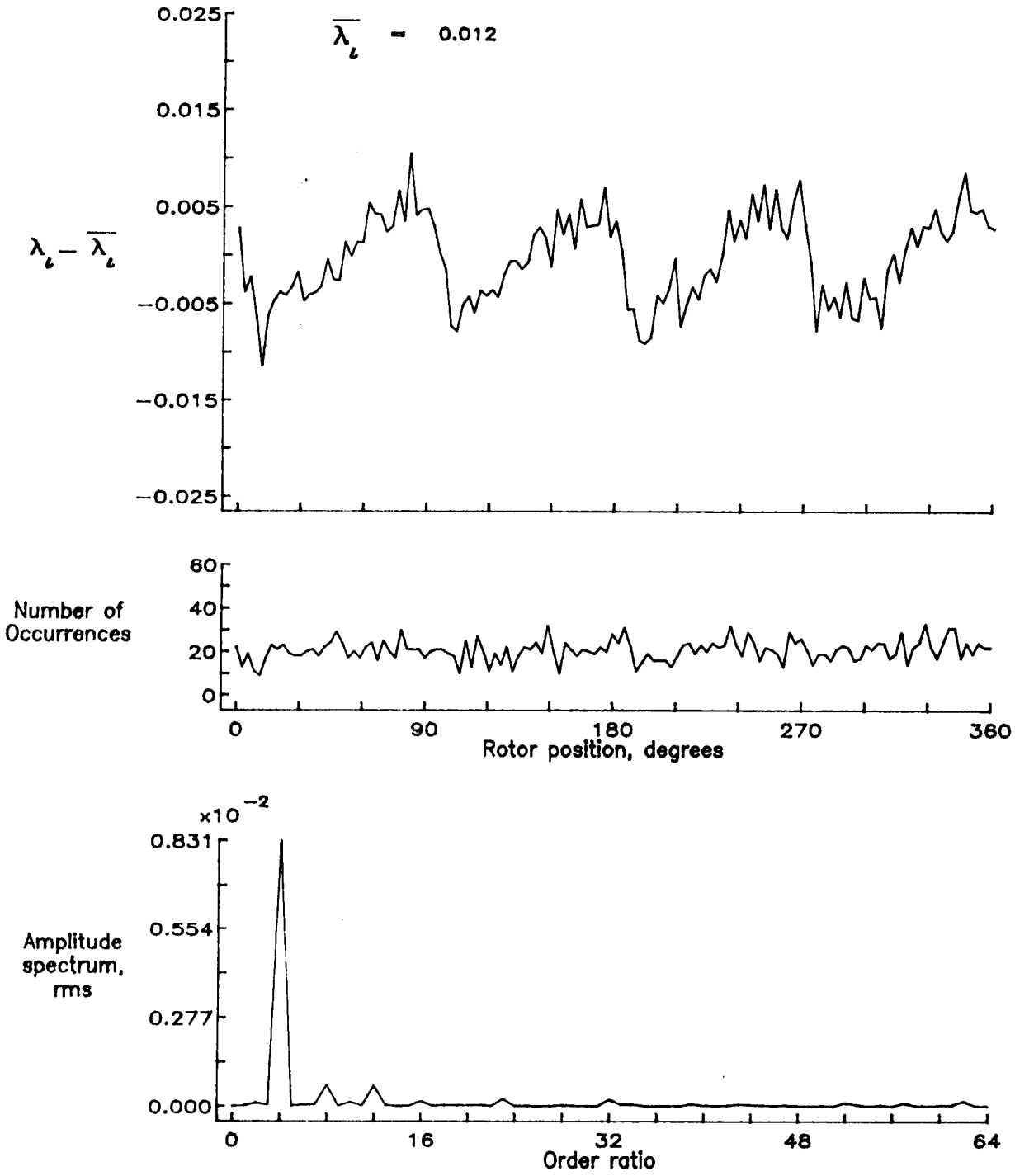

Figure 110.– Concluded.

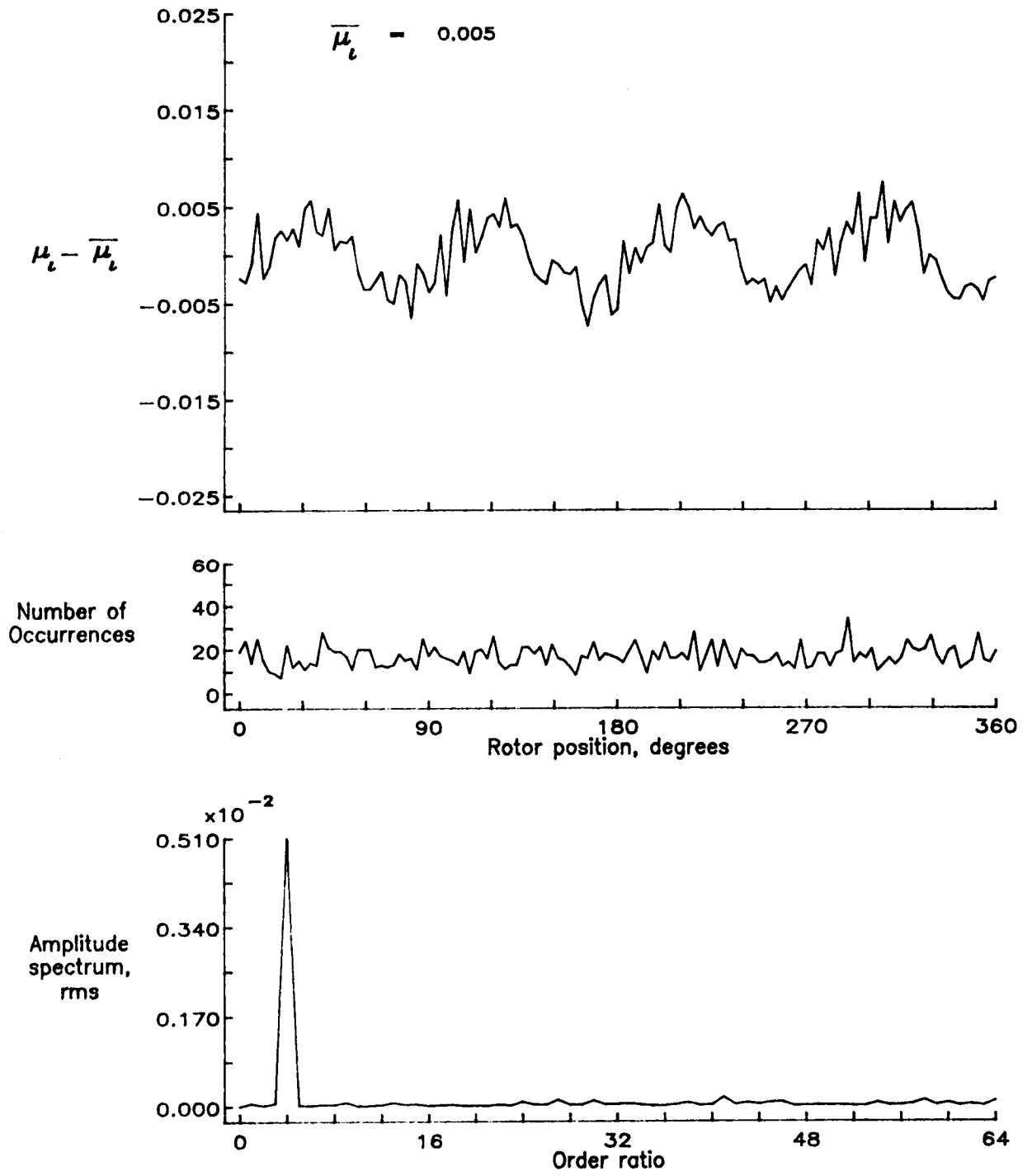

Figure 111.– Induced inflow velocity measured at 180 degrees and r/R of 0.86.

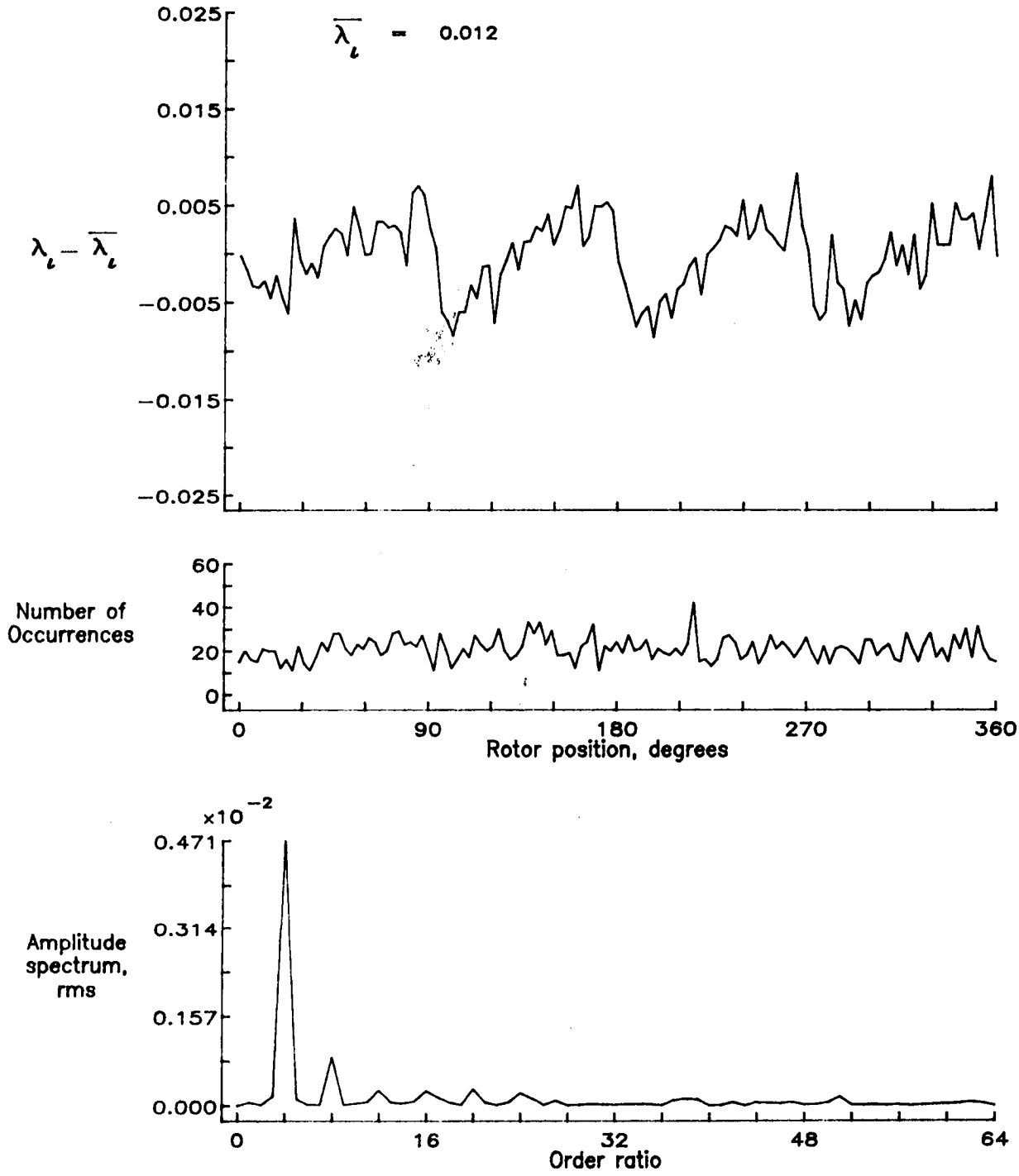

Figure 111.– Concluded.

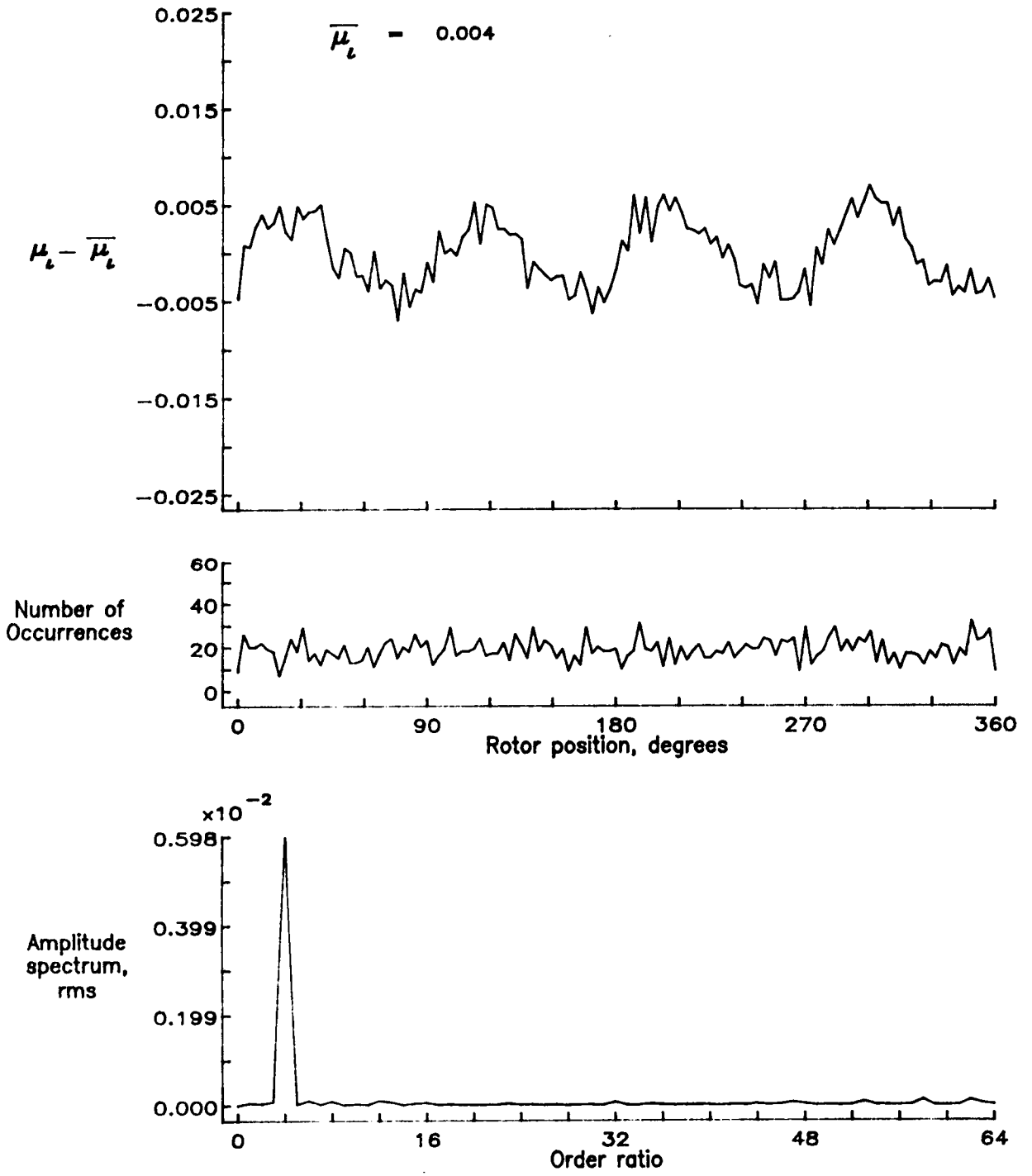

Figure 112.– Induced inflow velocity measured at 180 degrees and r/R of 0.90.

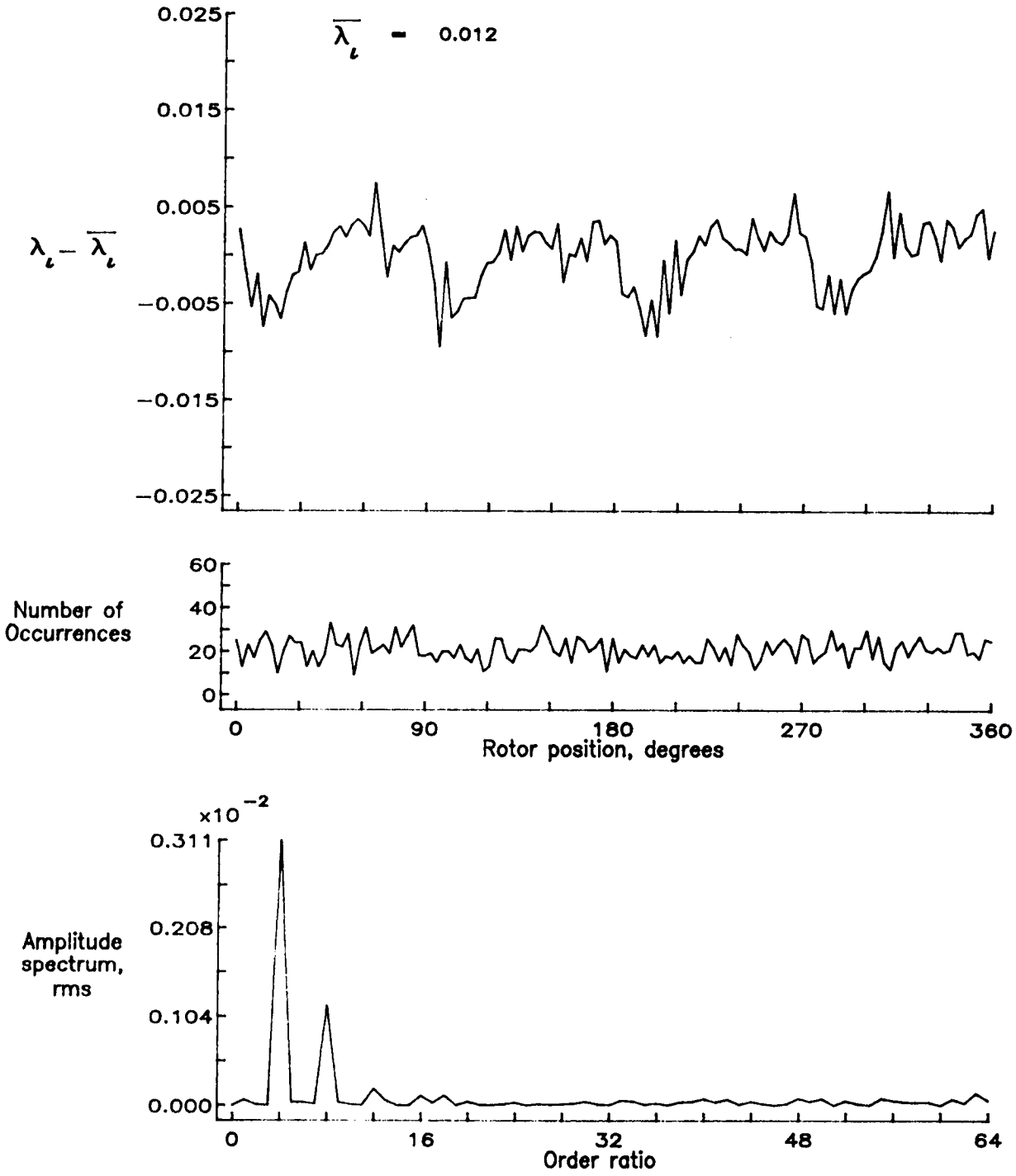

Figure 112.– Concluded.

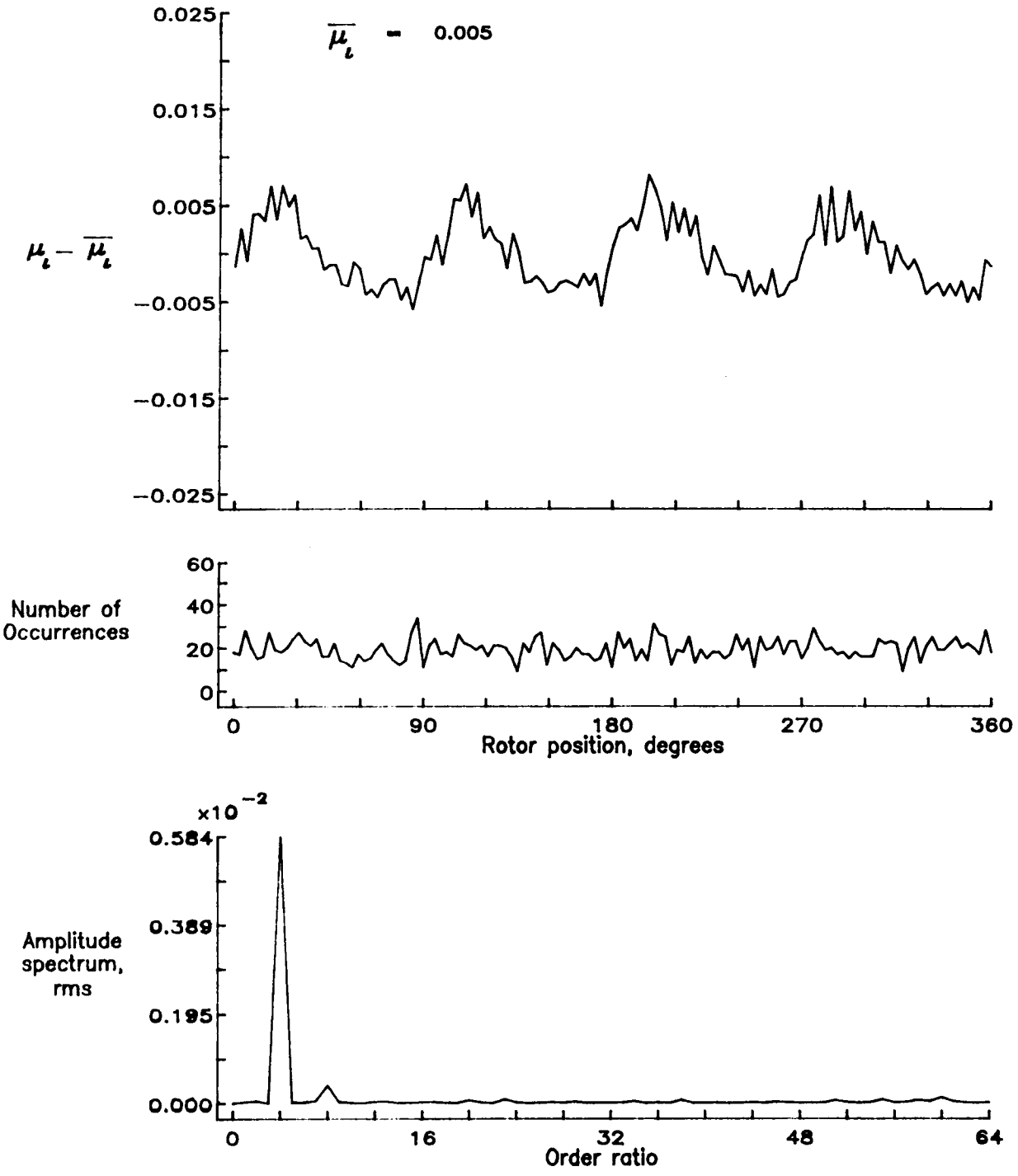

Figure 113.– Induced inflow velocity measured at 180 degrees and r/R of 0.94.

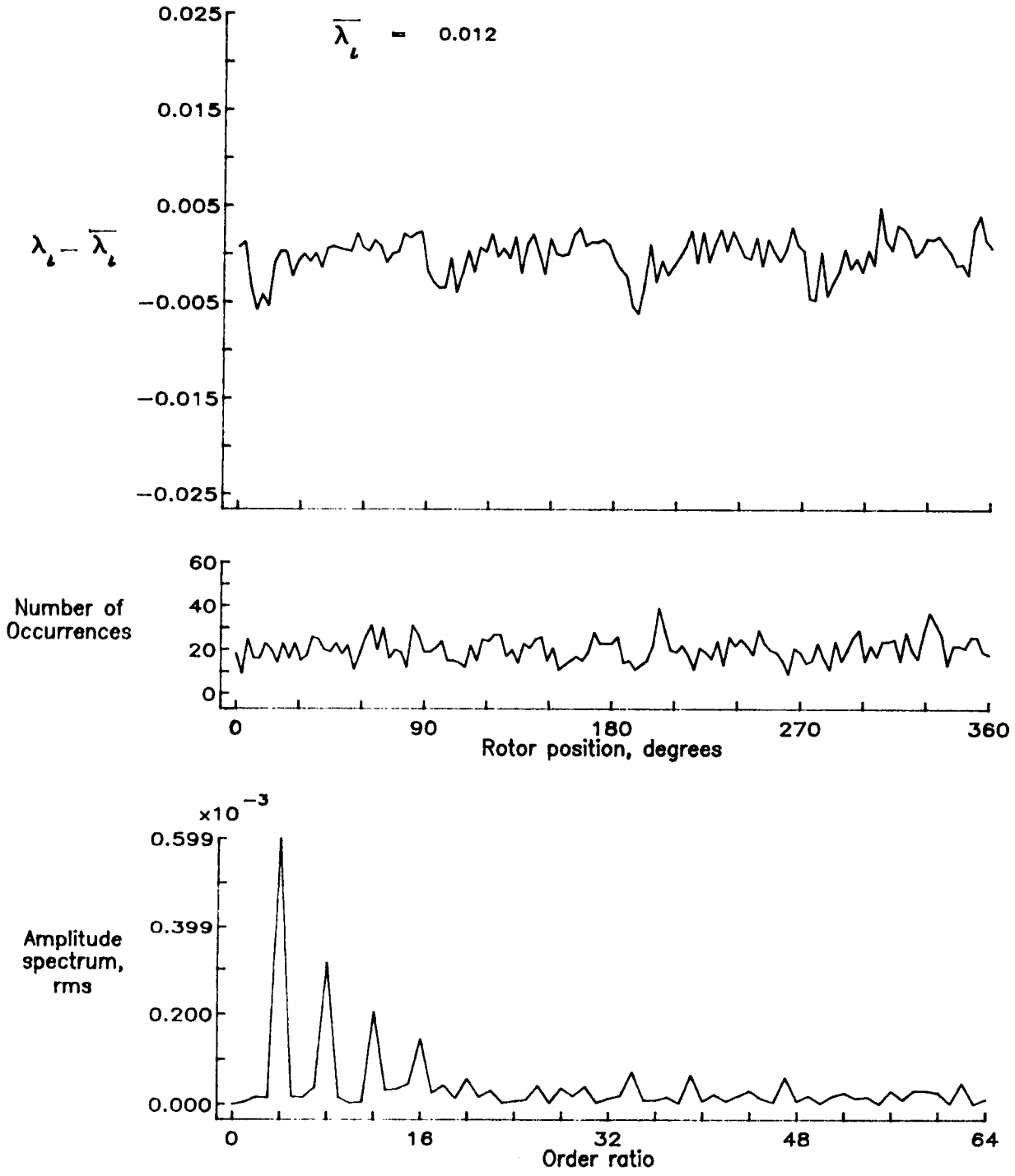

Figure 113.– Concluded.

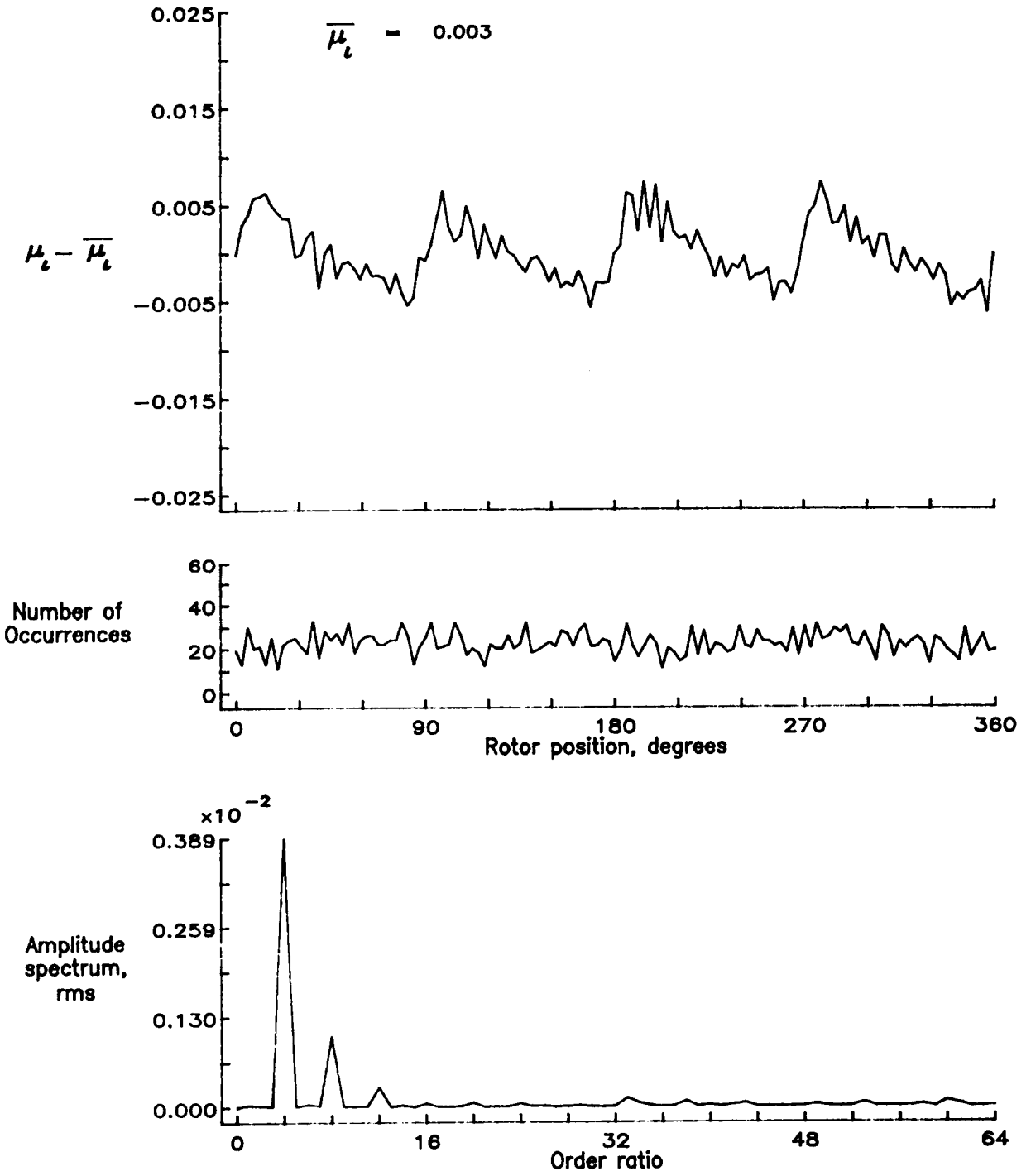

Figure 114.– Induced inflow velocity measured at 180 degrees and r/R of 0.98.

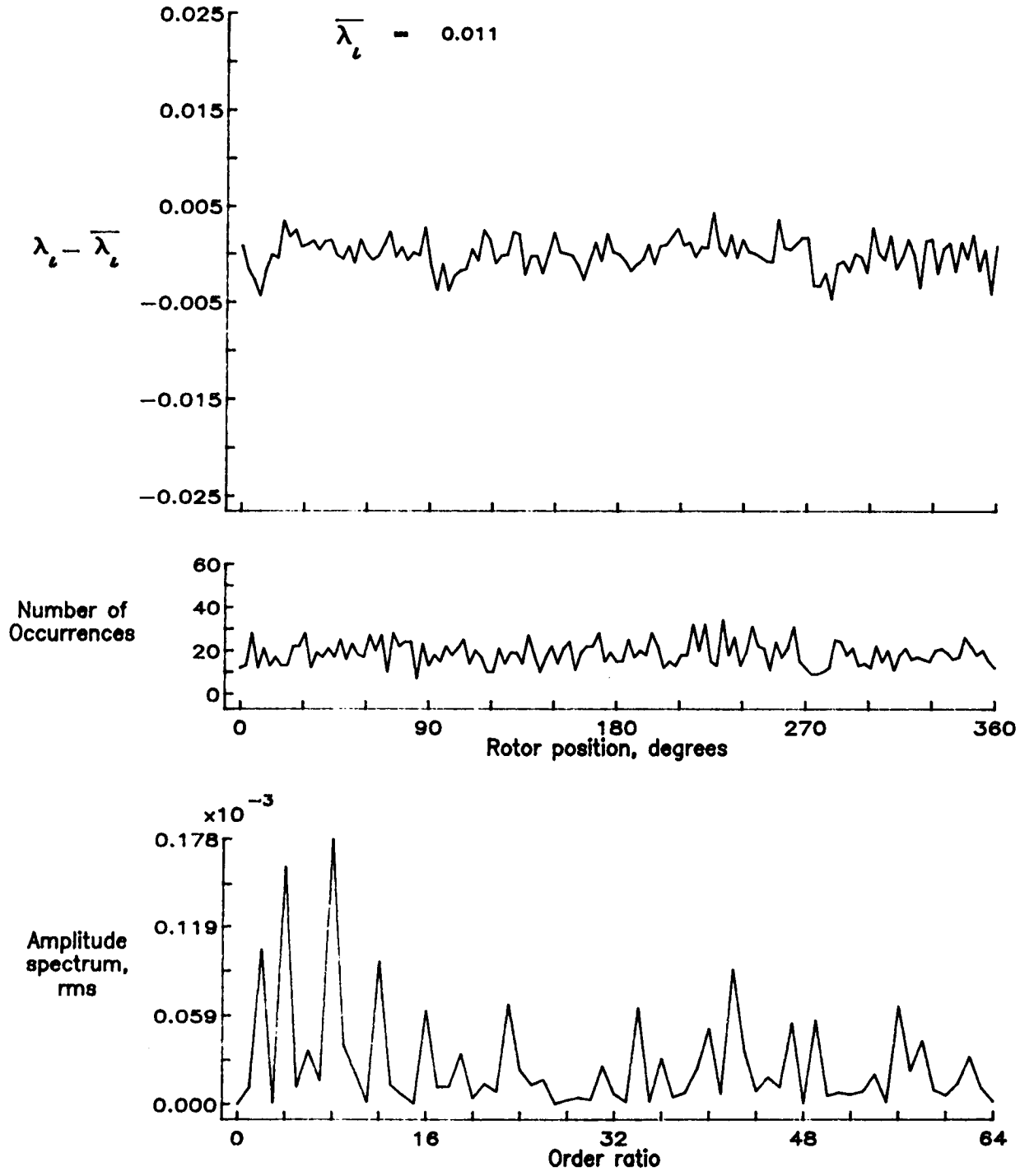

Figure 114.– Concluded.

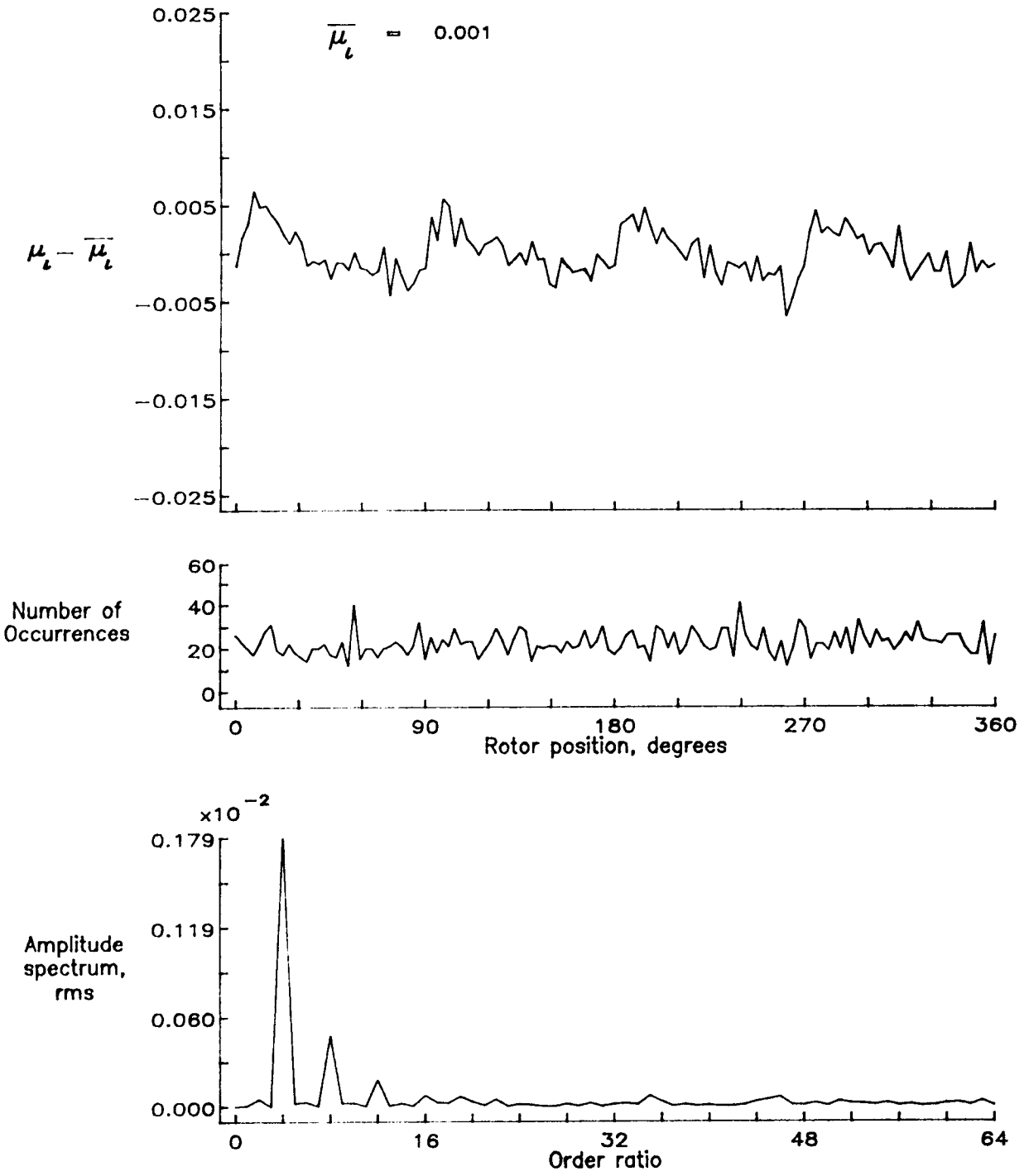

Figure 115.– Induced inflow velocity measured at 180 degrees and r/R of 1.02.

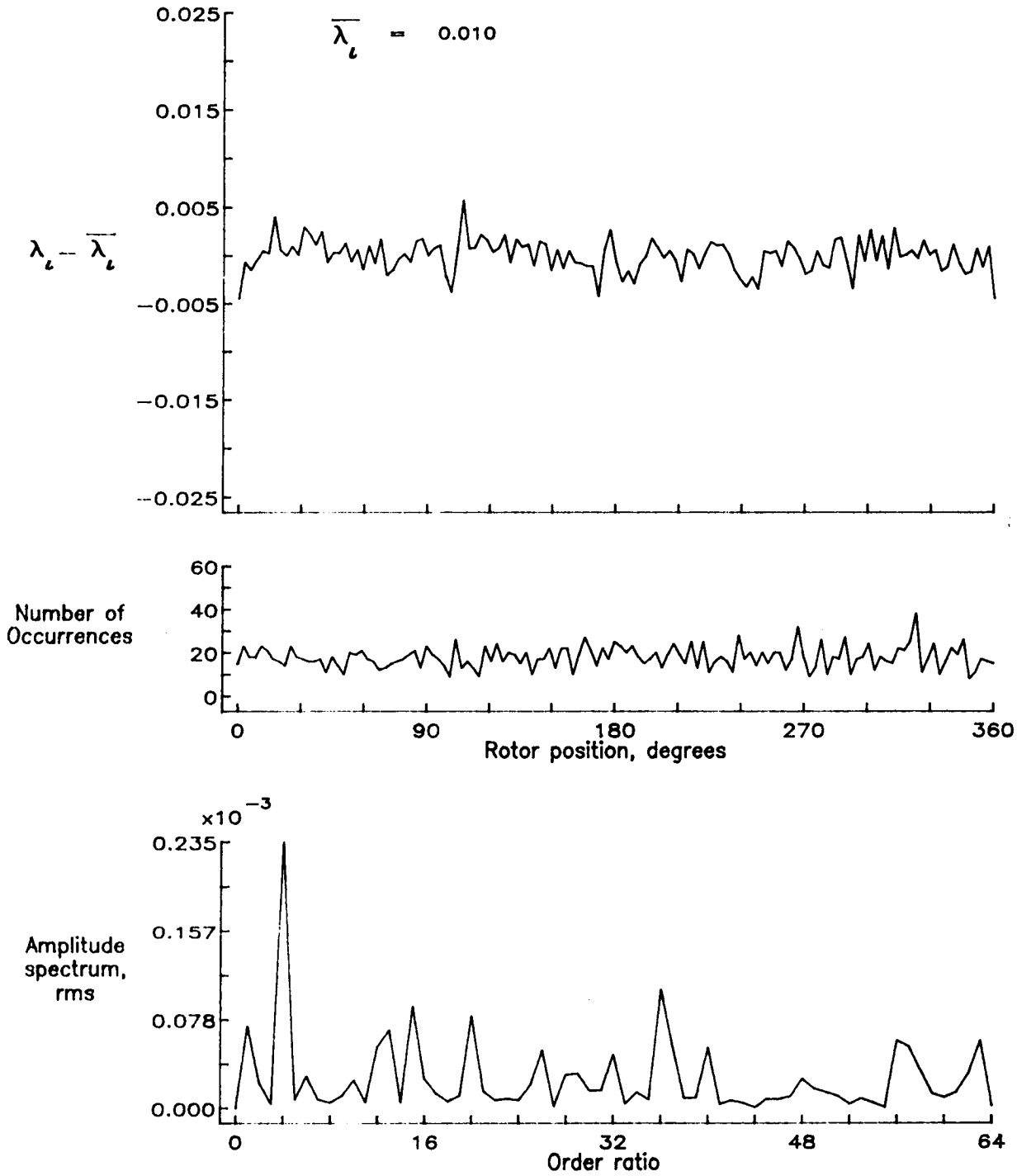

Figure 115.– Concluded.

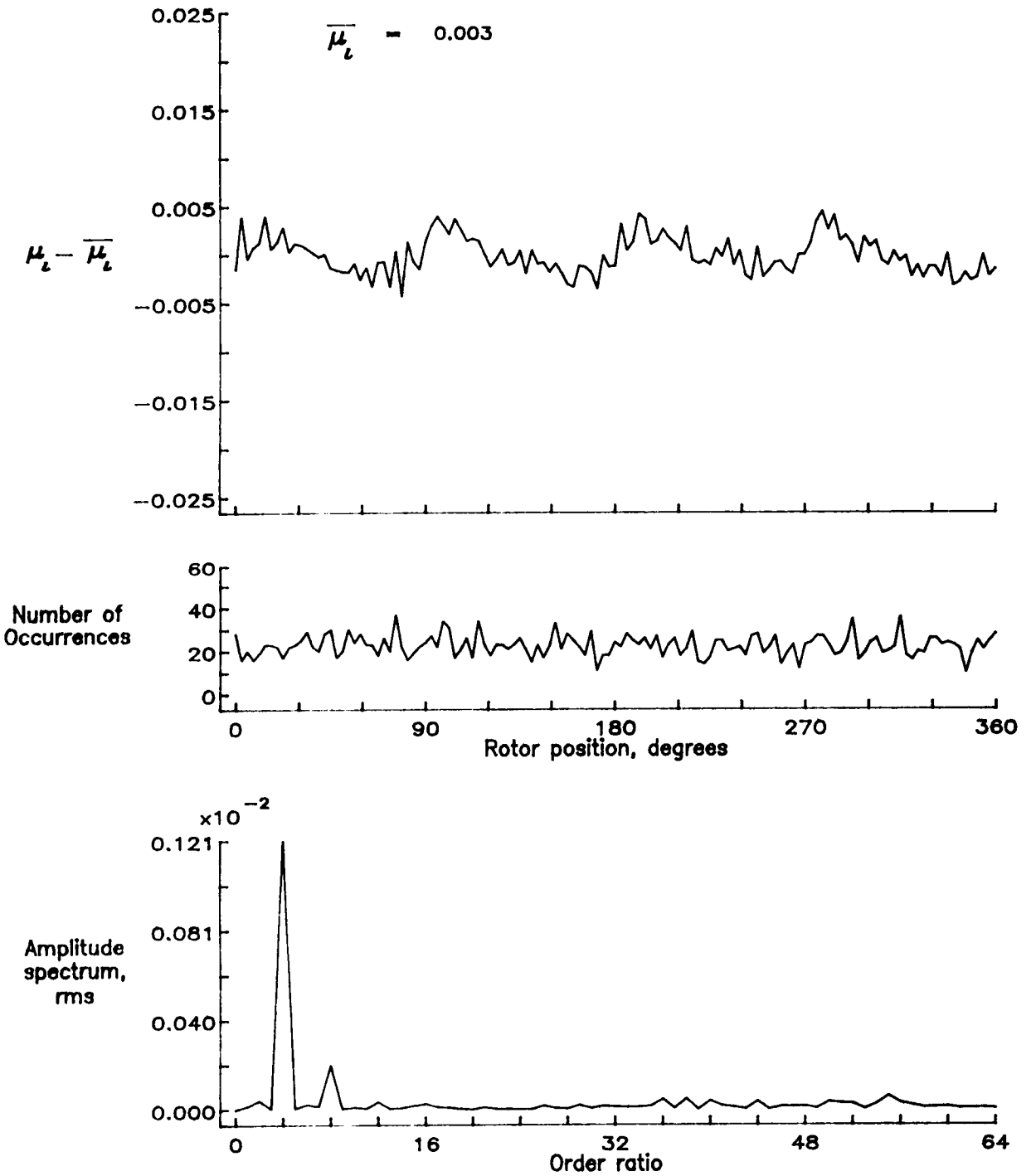

Figure 116.– Induced inflow velocity measured at 180 degrees and r/R of 1.04.

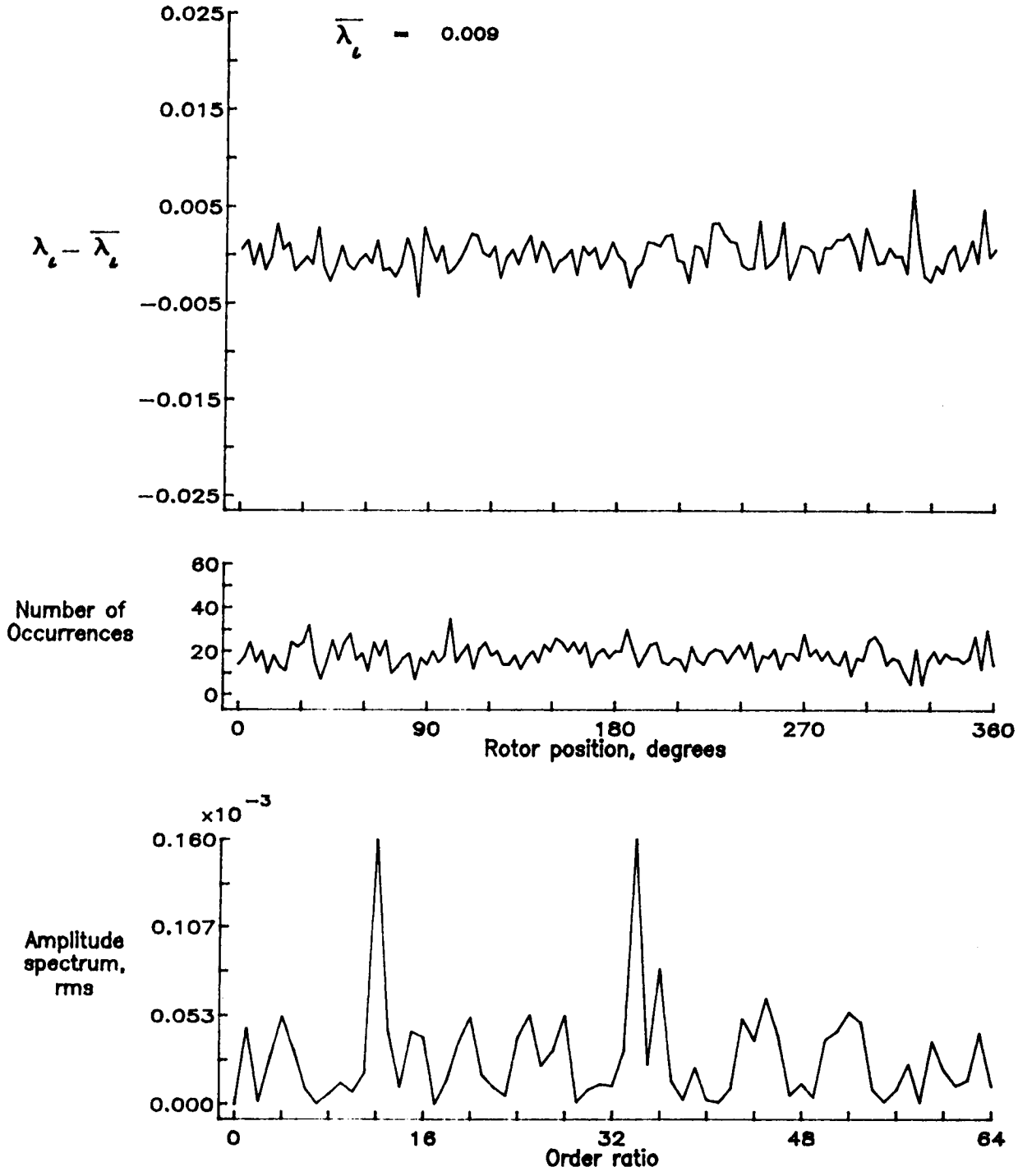

Figure 116.– Concluded.

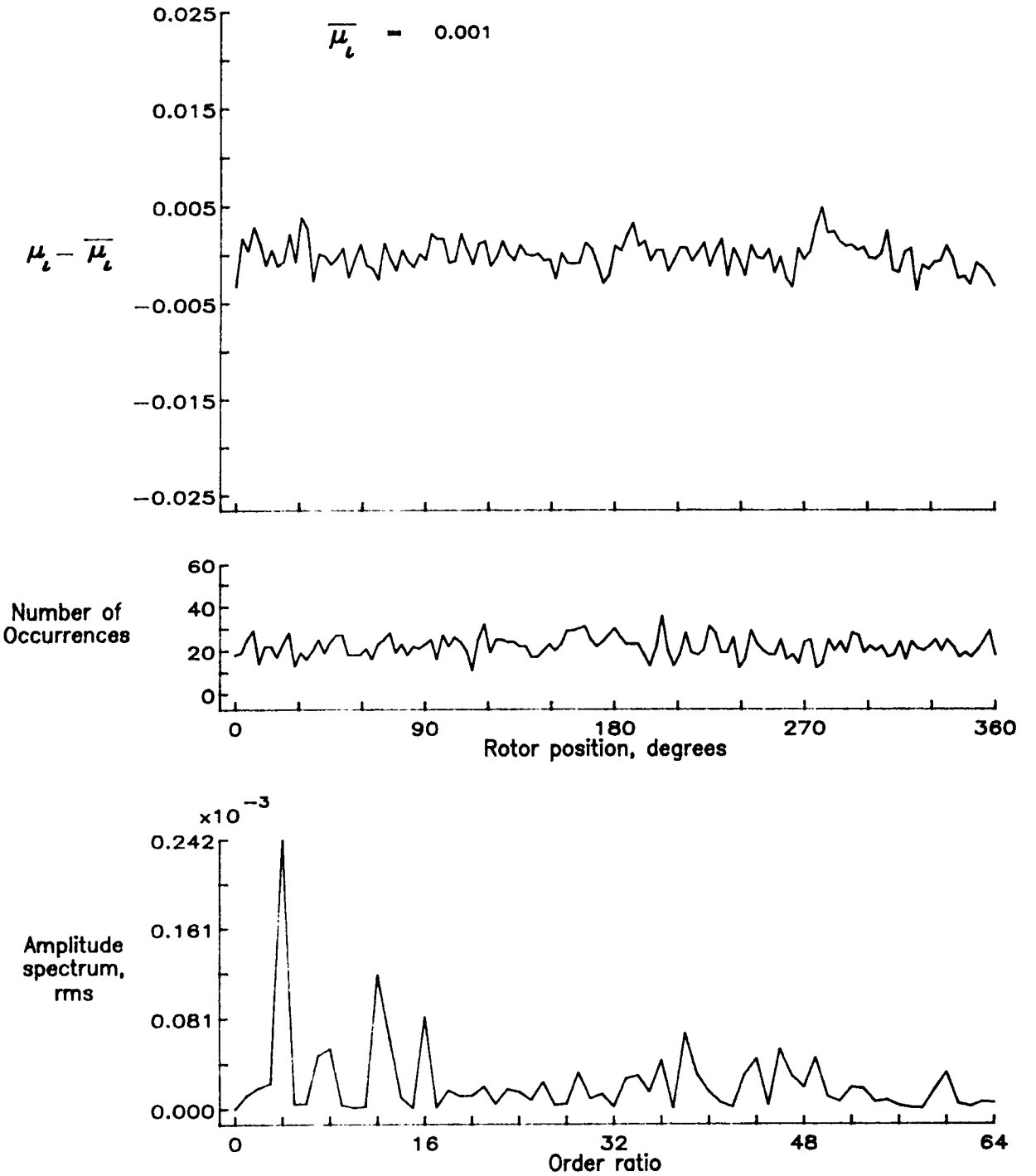

Figure 117.– Induced inflow velocity measured at 180 degrees and r/R of 1.10.

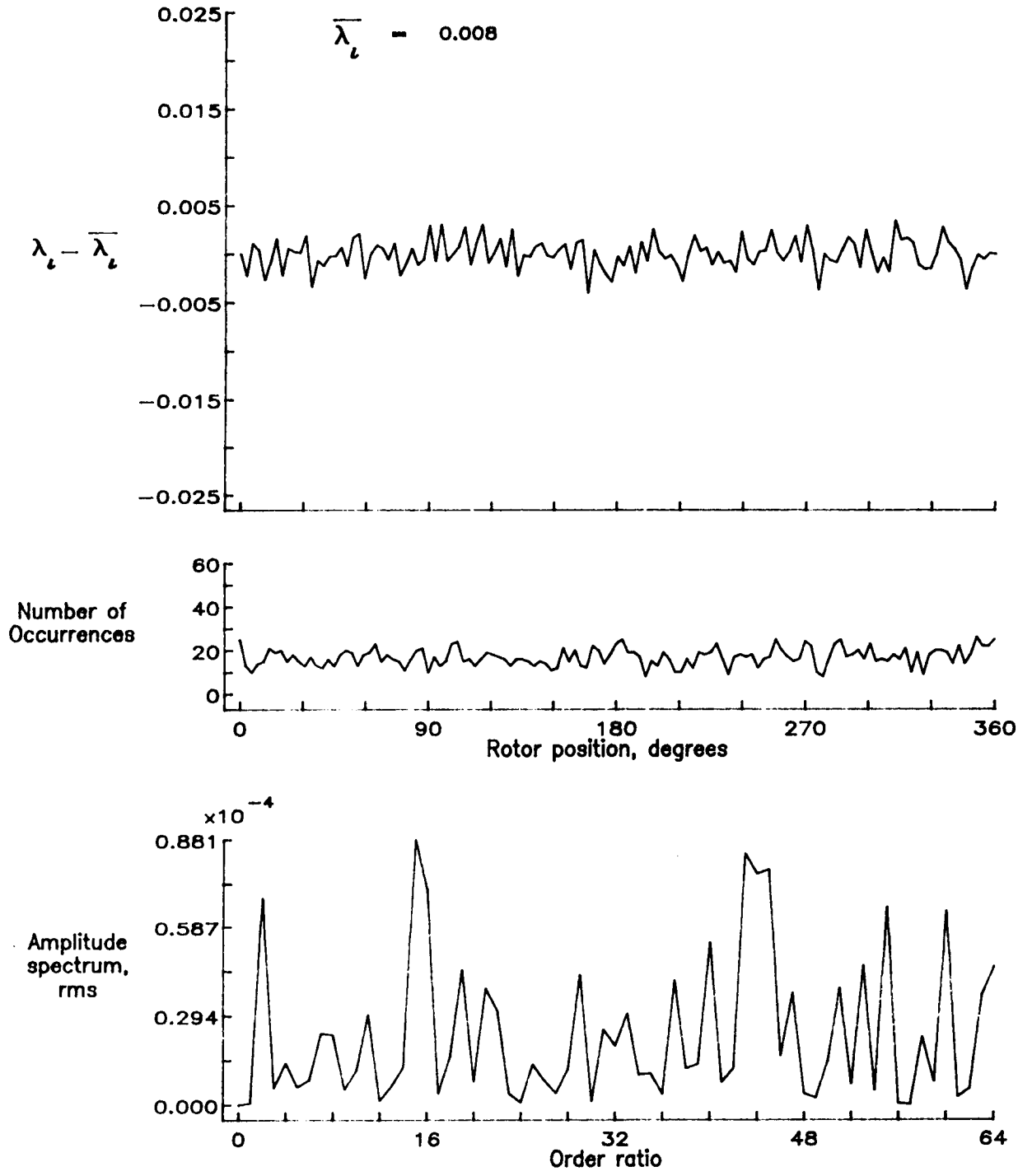

Figure 117.– Concluded.

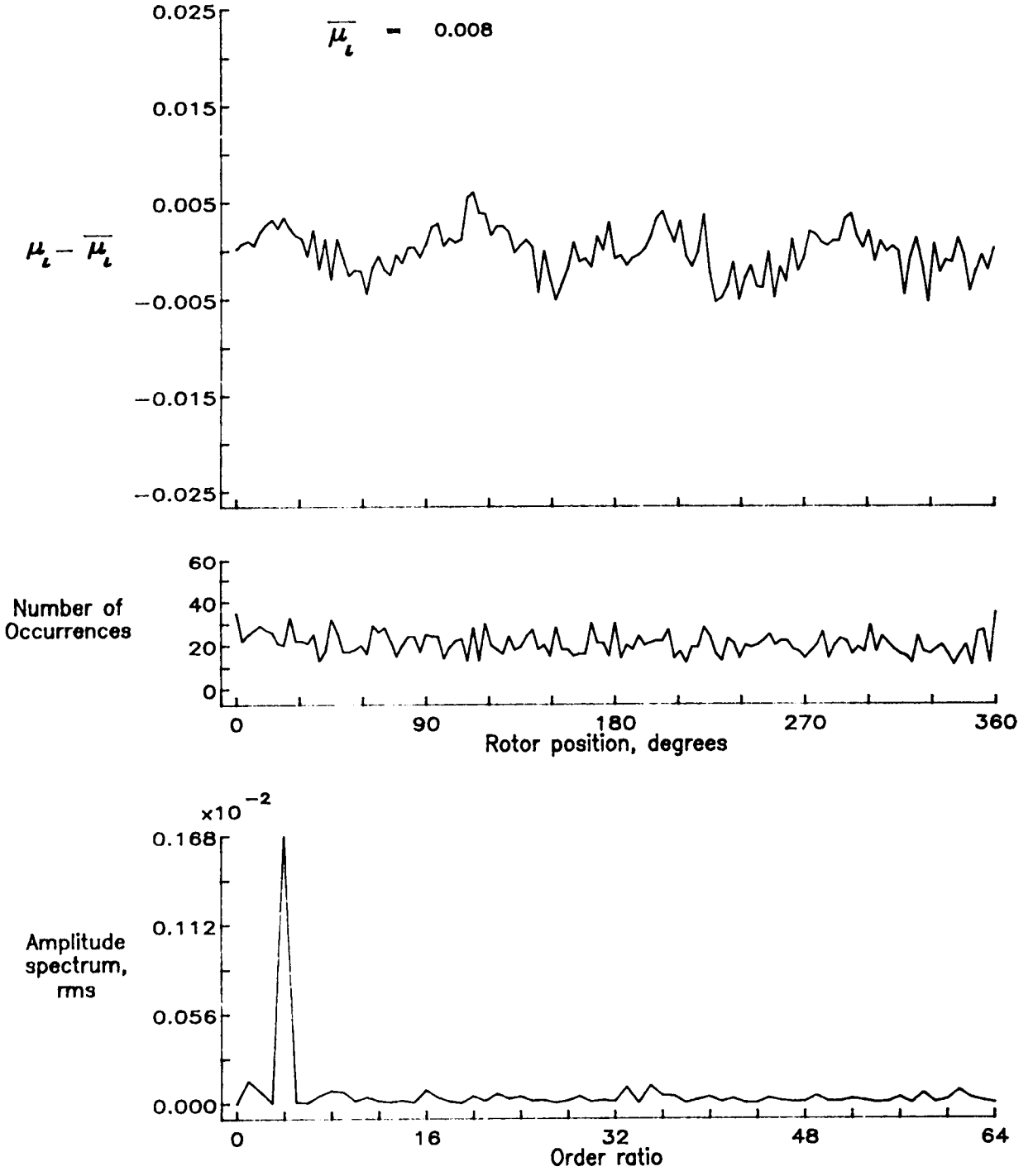

Figure 118.– Induced inflow velocity measured at 210 degrees and r/R of 0.20.

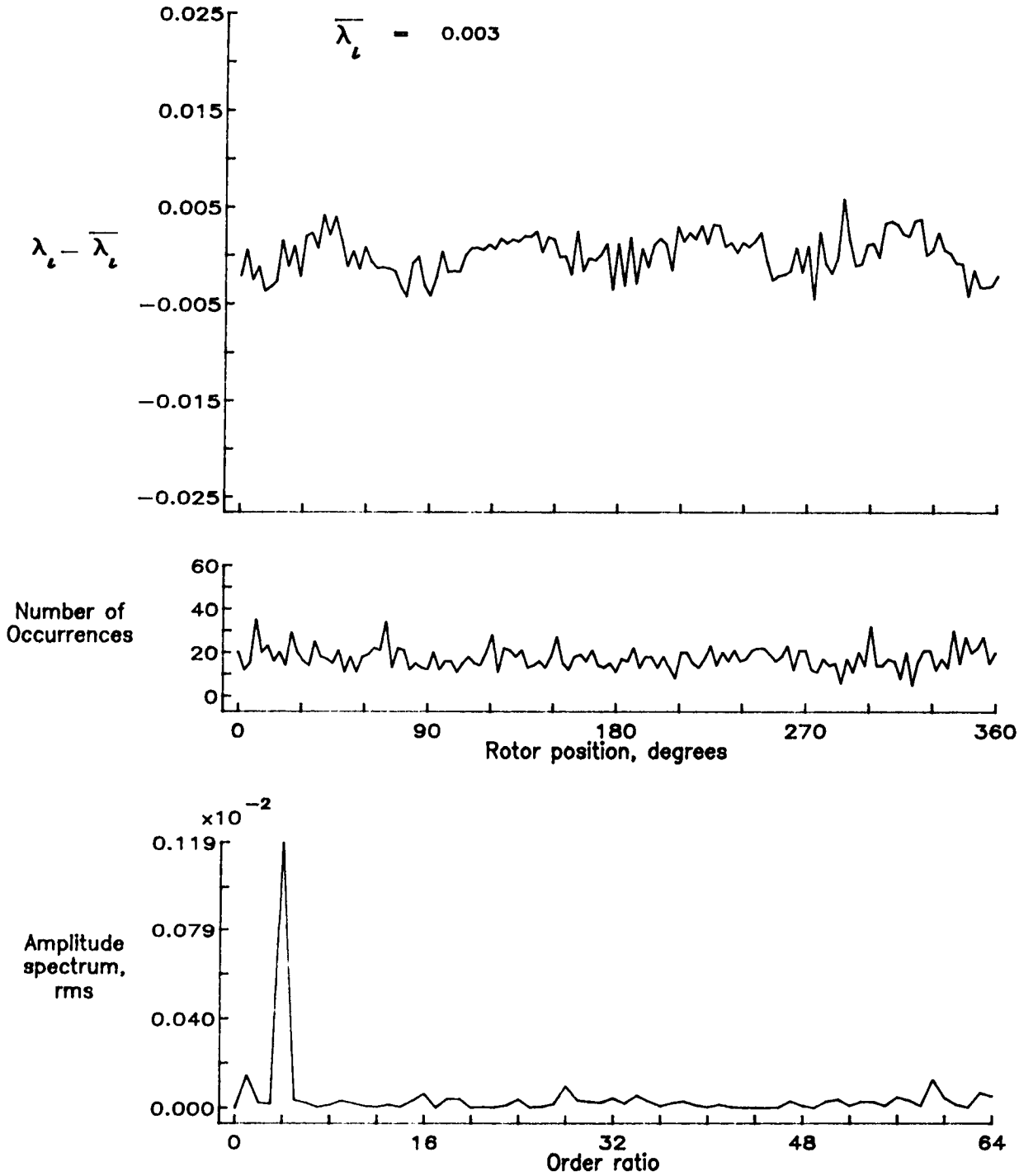

Figure 118.– Concluded.

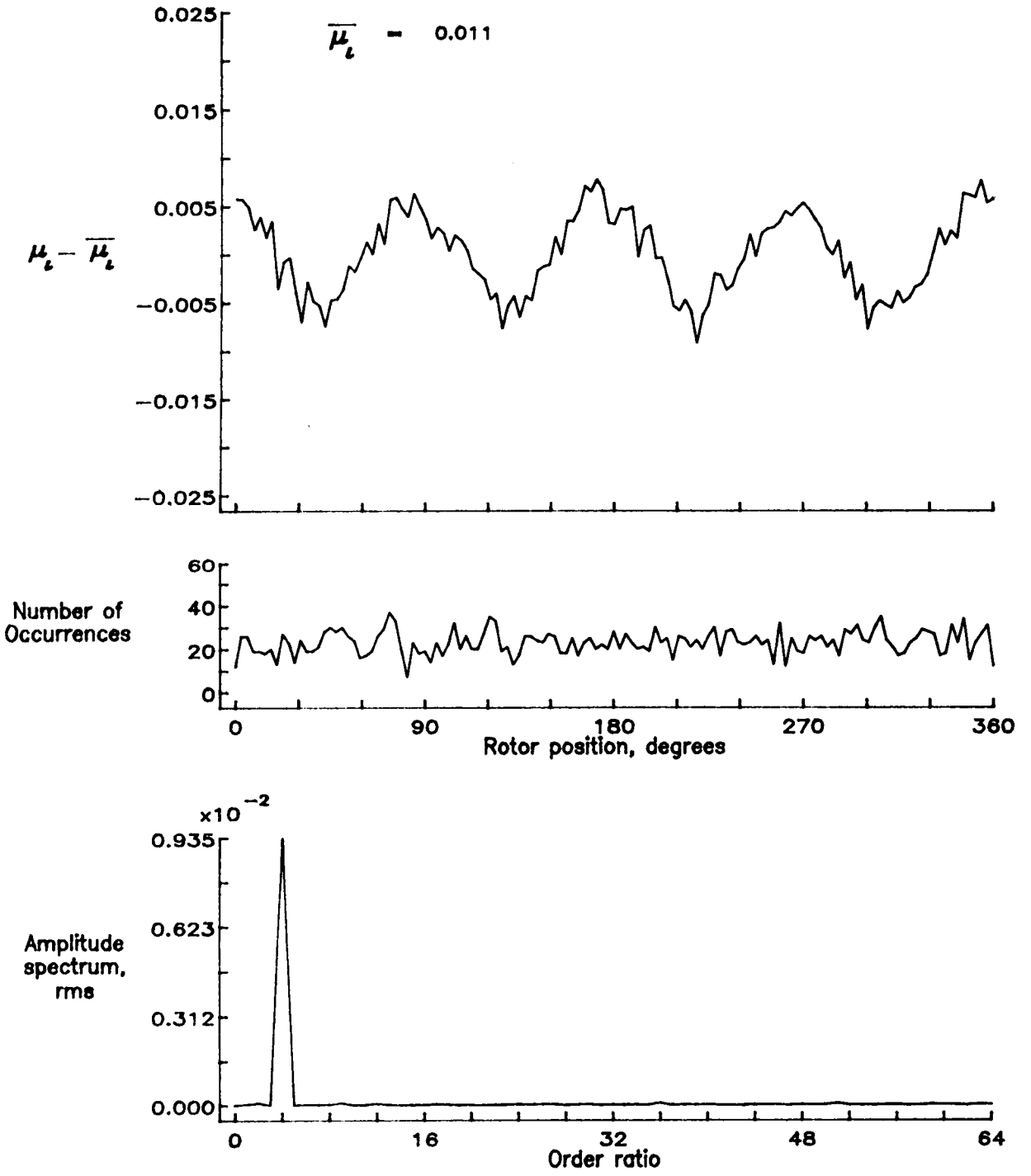

Figure 119.– Induced inflow velocity measured at 210 degrees and r/R of 0.40.

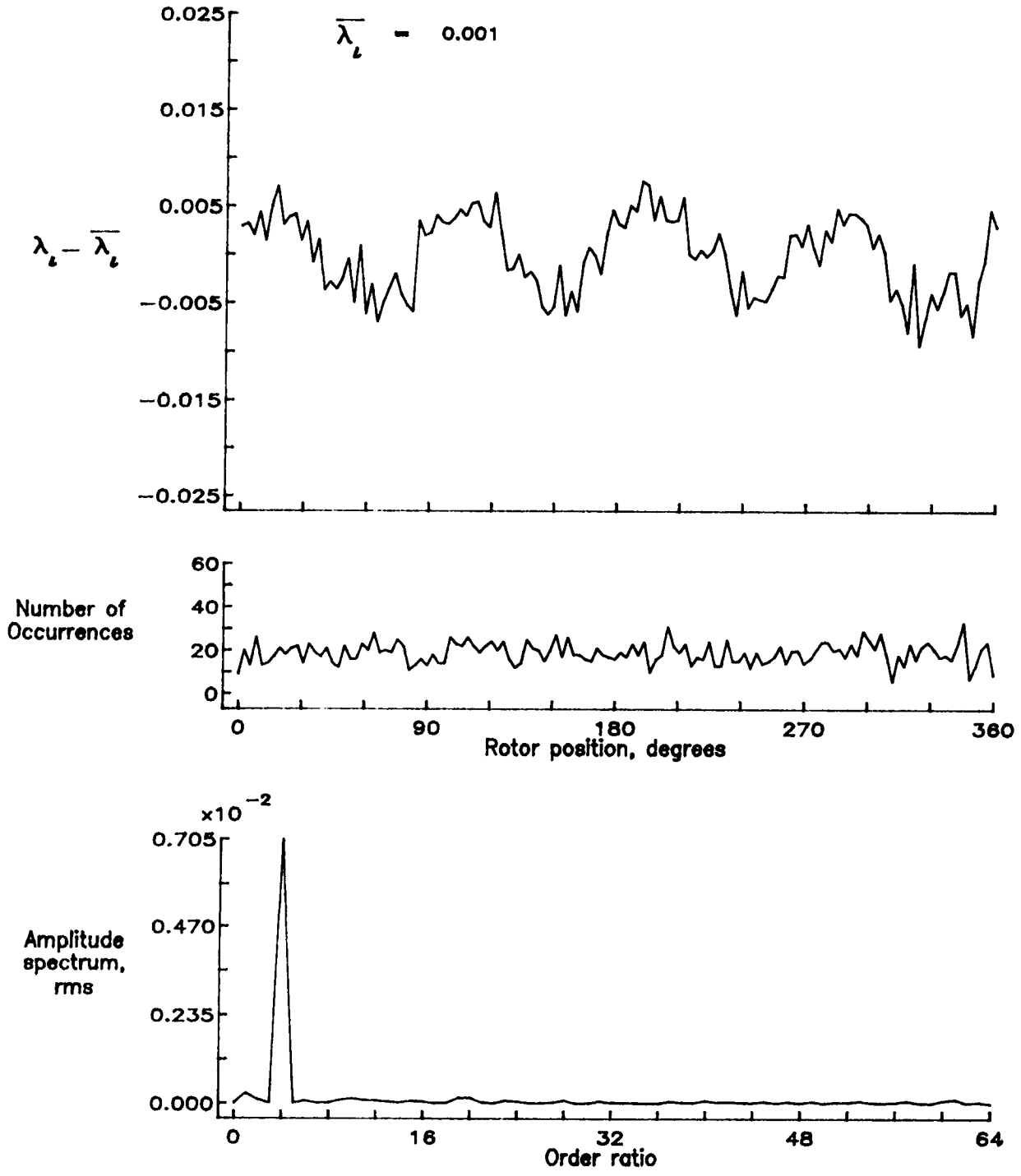

Figure 119.– Concluded.

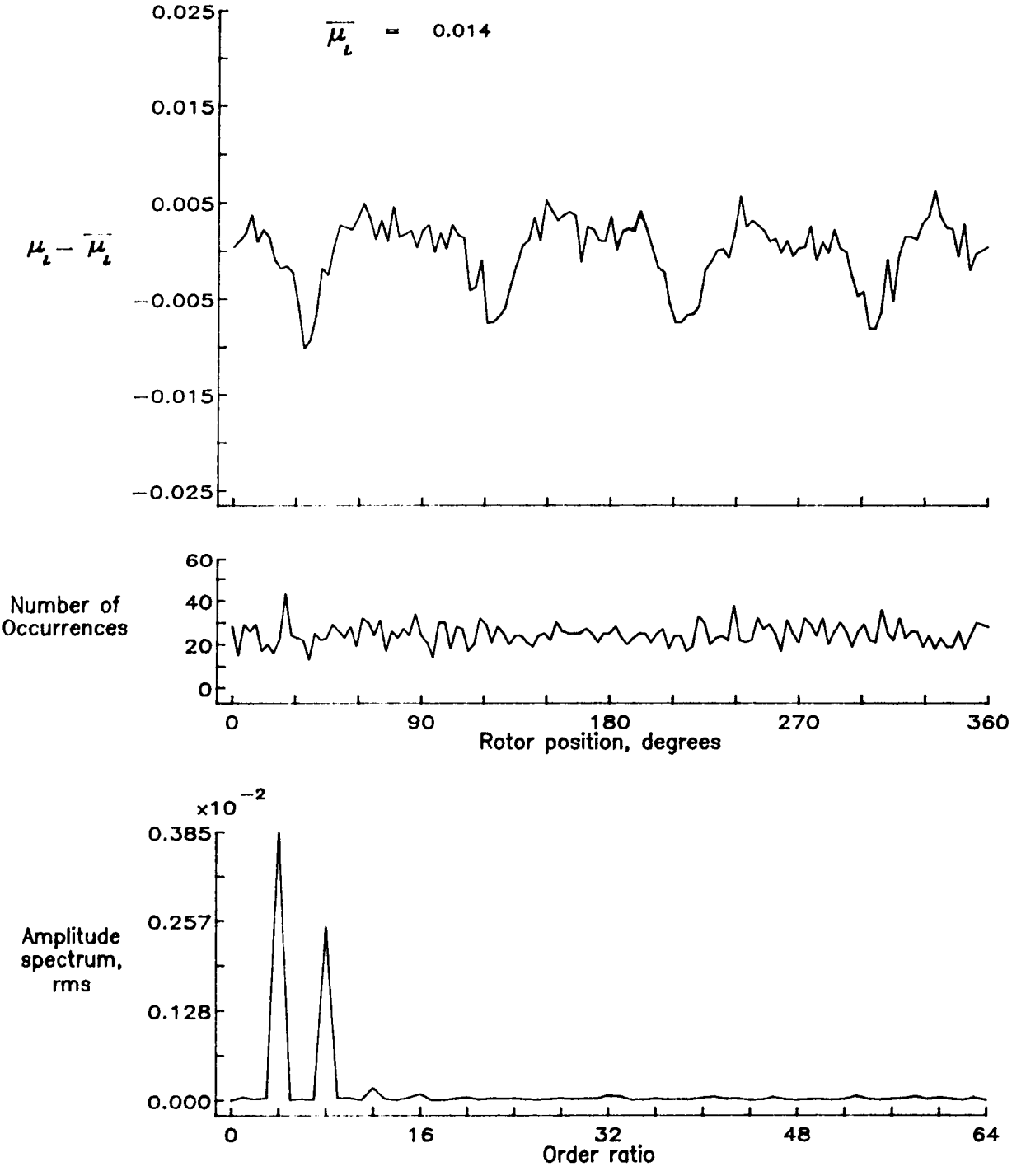

Figure 120.– Induced inflow velocity measured at 210 degrees and r/R of 0.50.

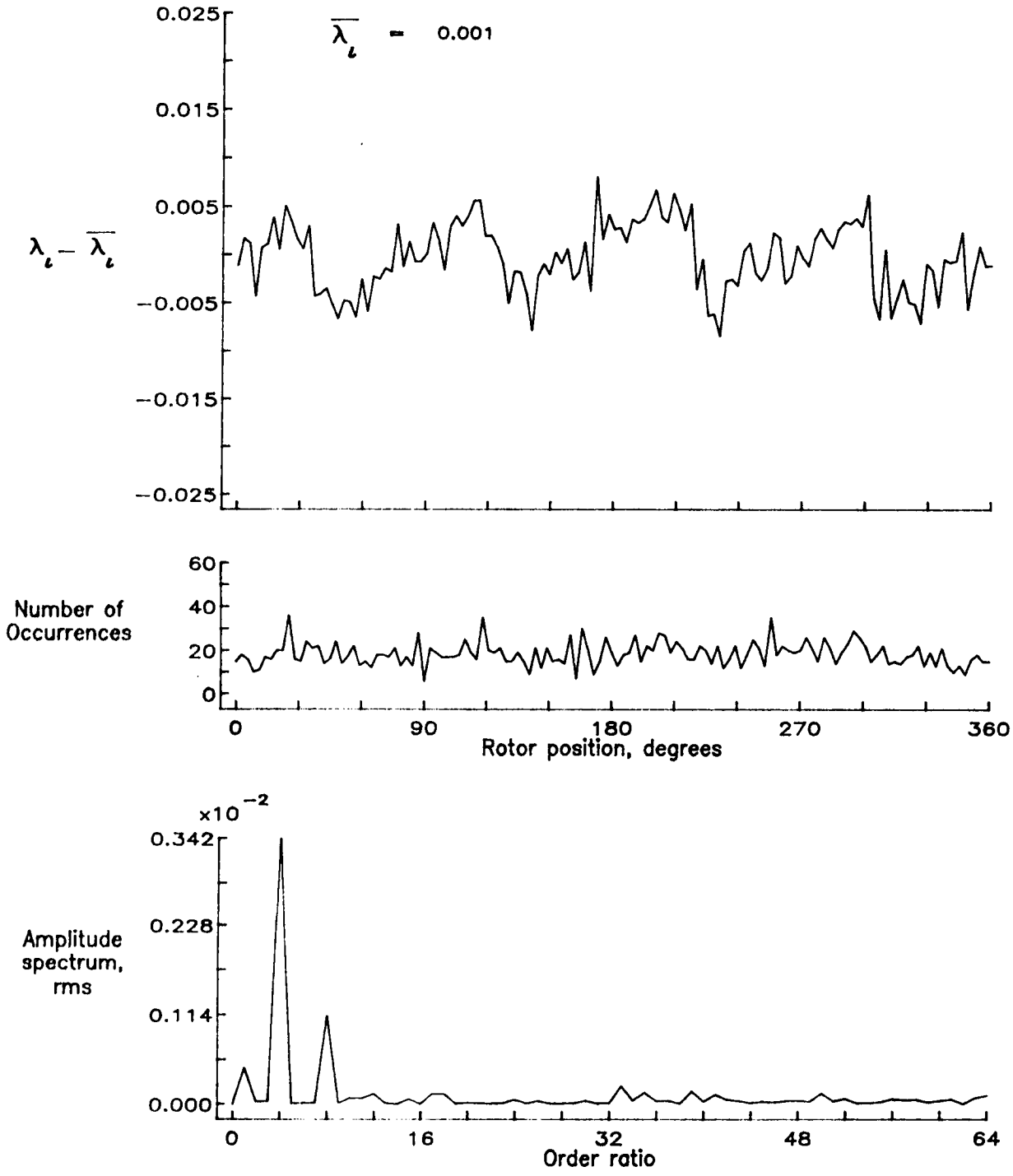

Figure 120.– Concluded.

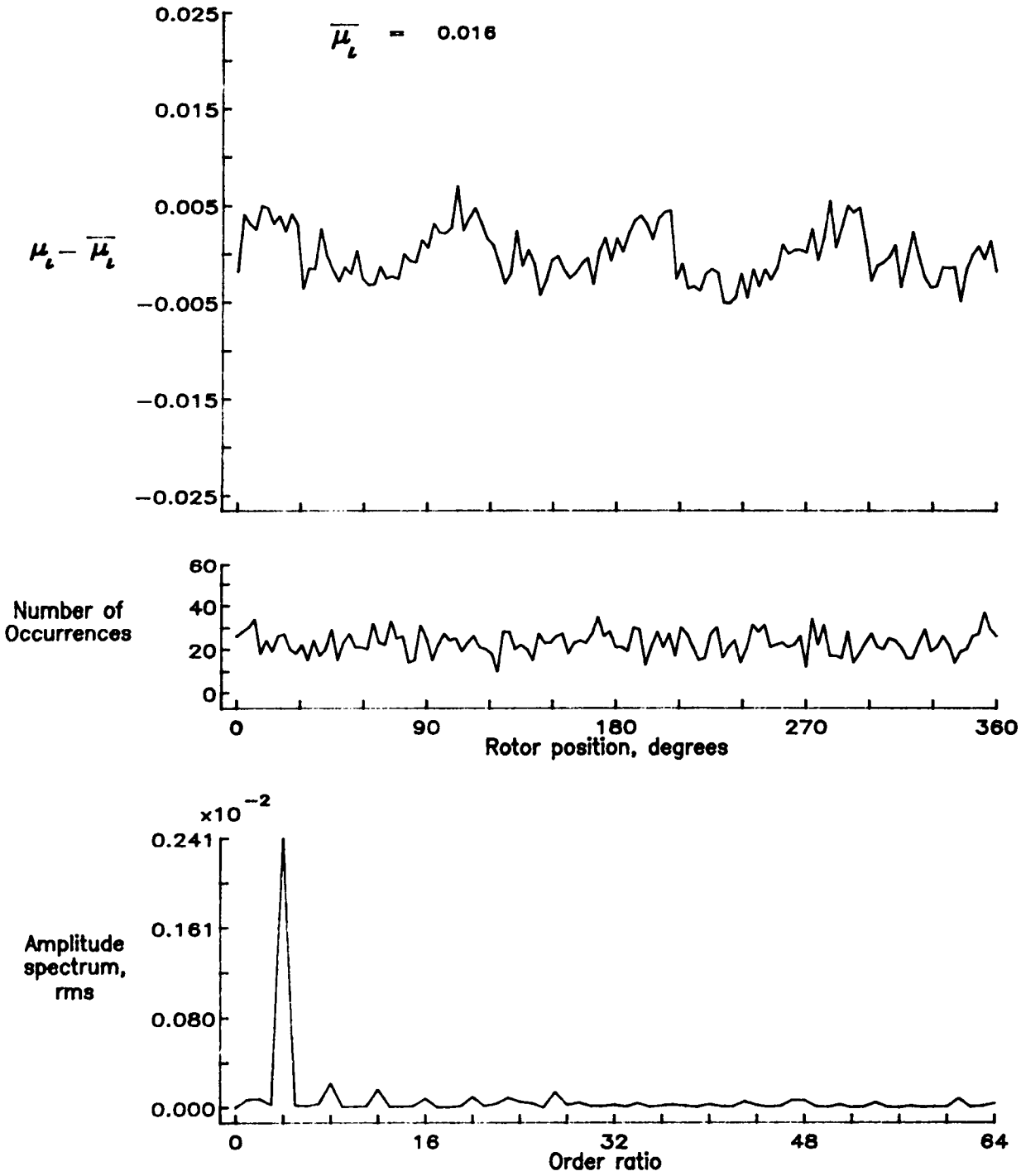

Figure 121.– Induced inflow velocity measured at 210 degrees and r/R of 0.60.

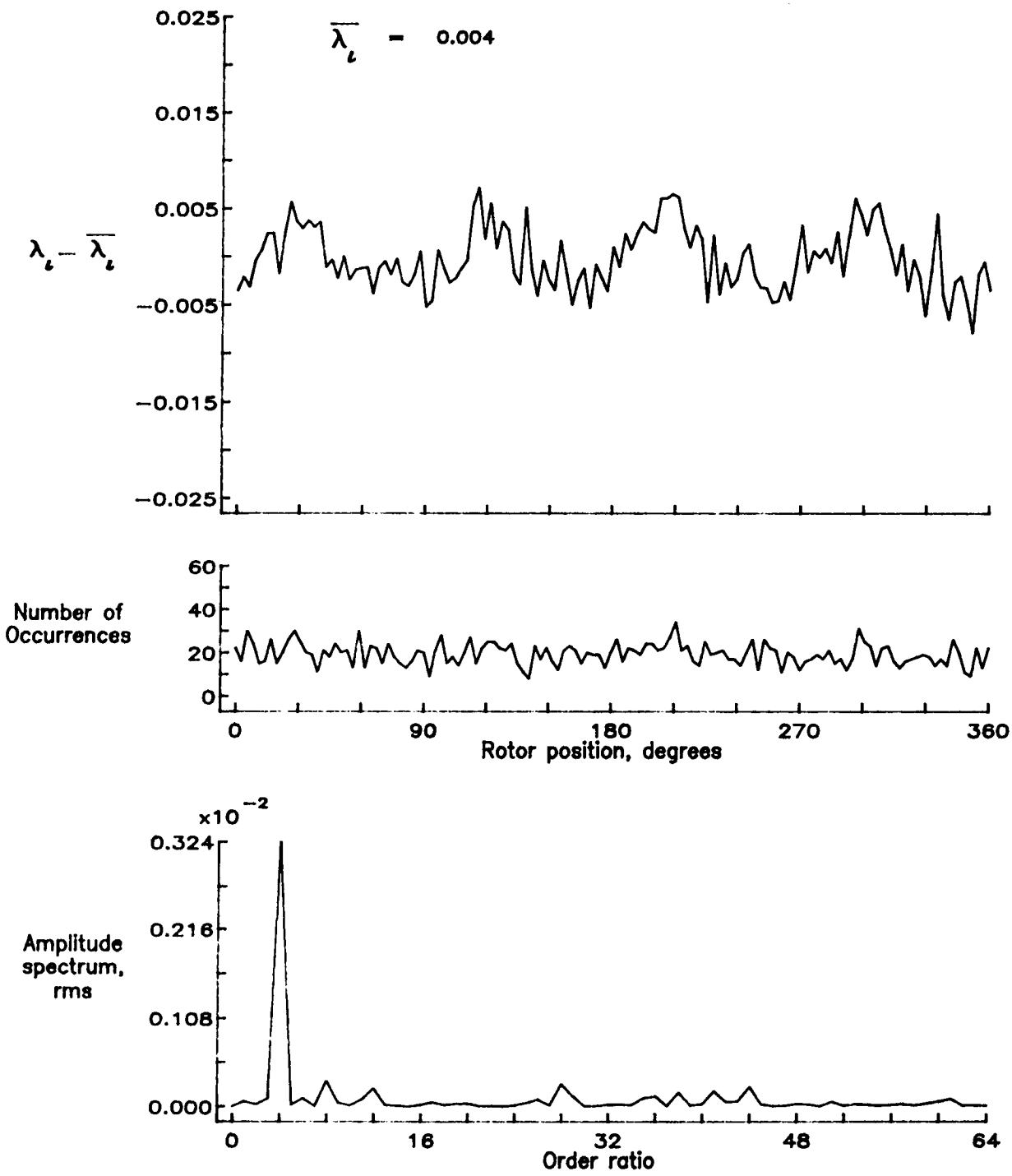

Figure 121.– Concluded.

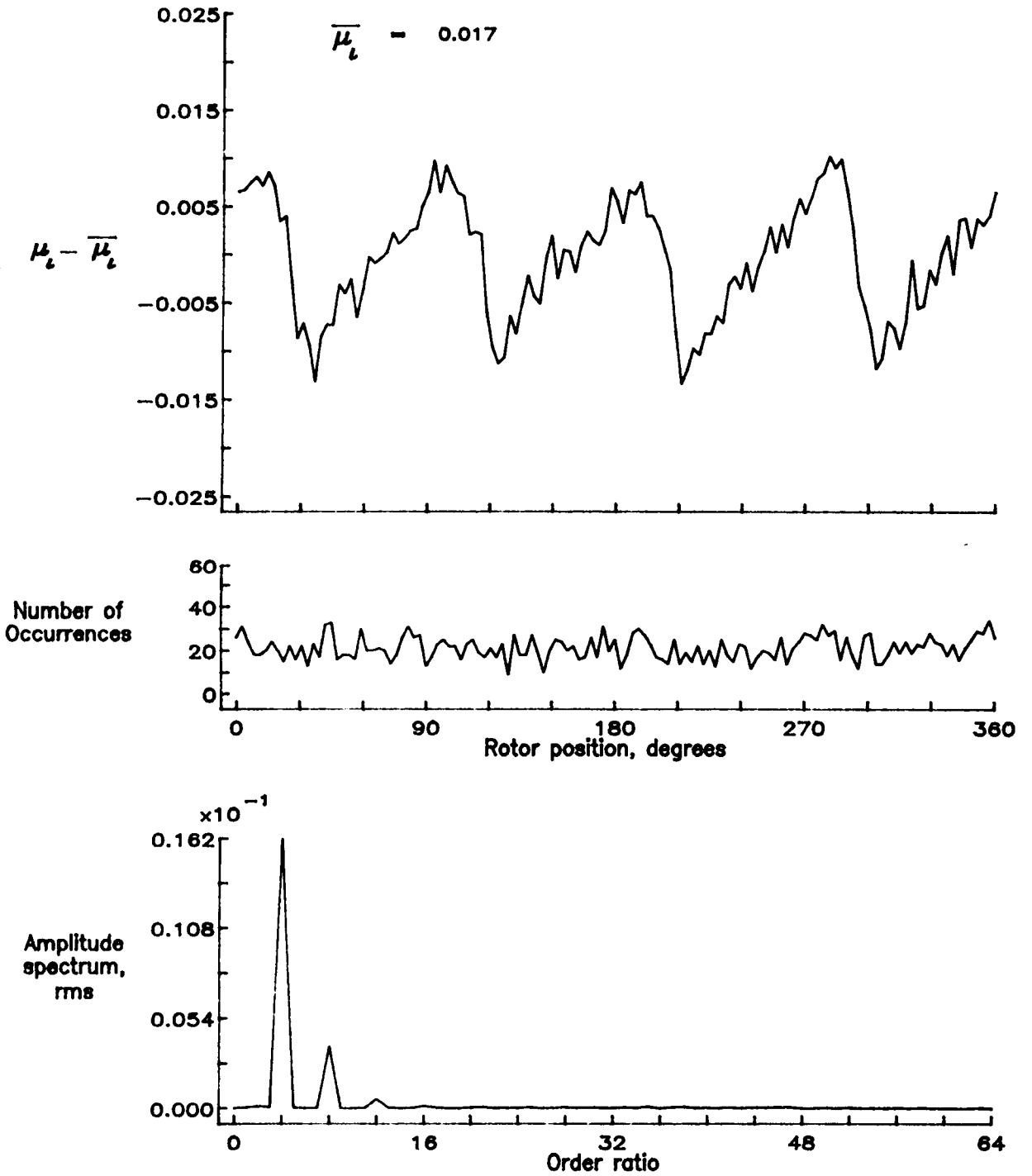

Figure 122.– Induced inflow velocity measured at 210 degrees and r/R of 0.70.

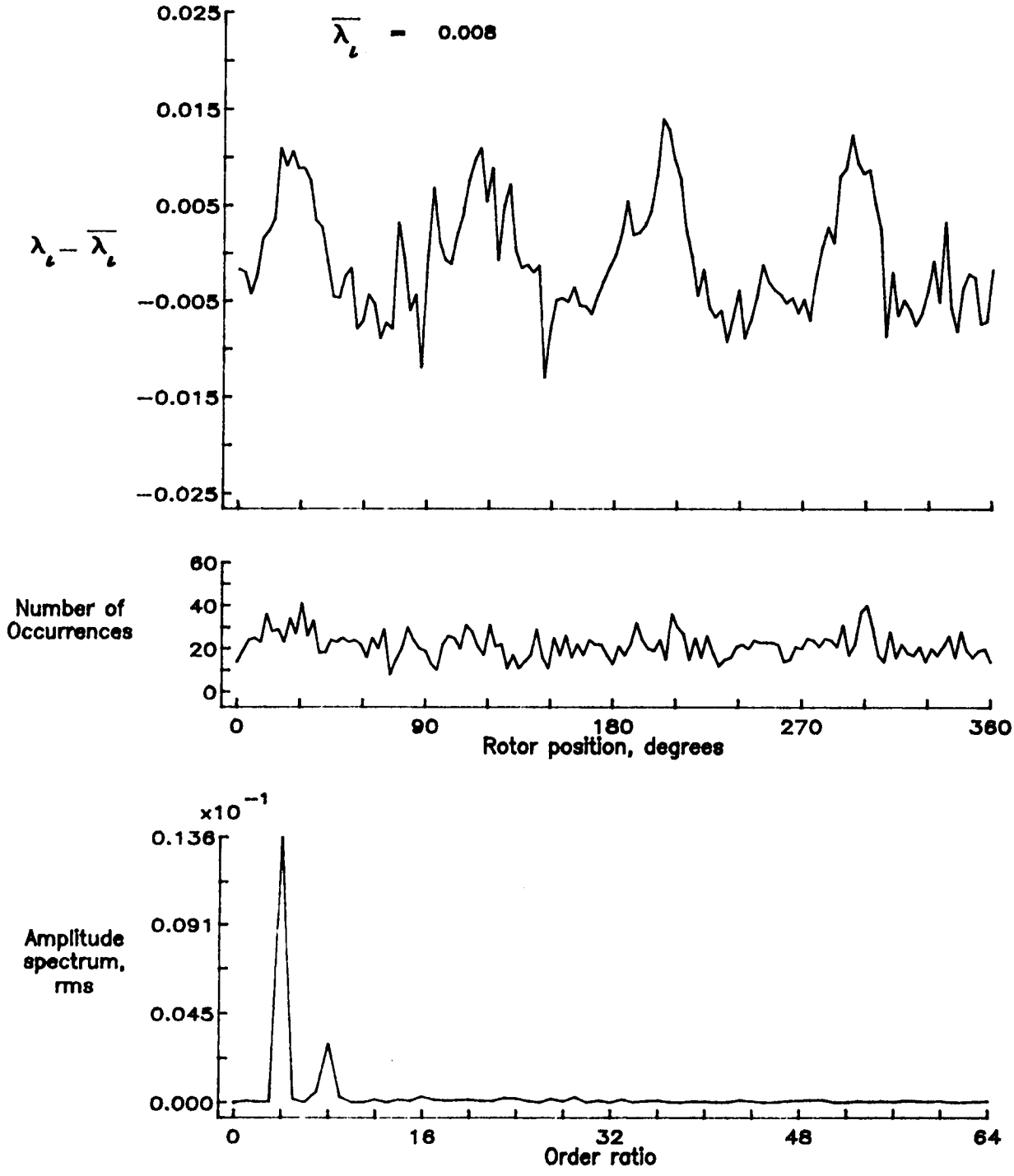

Figure 122.– Concluded.

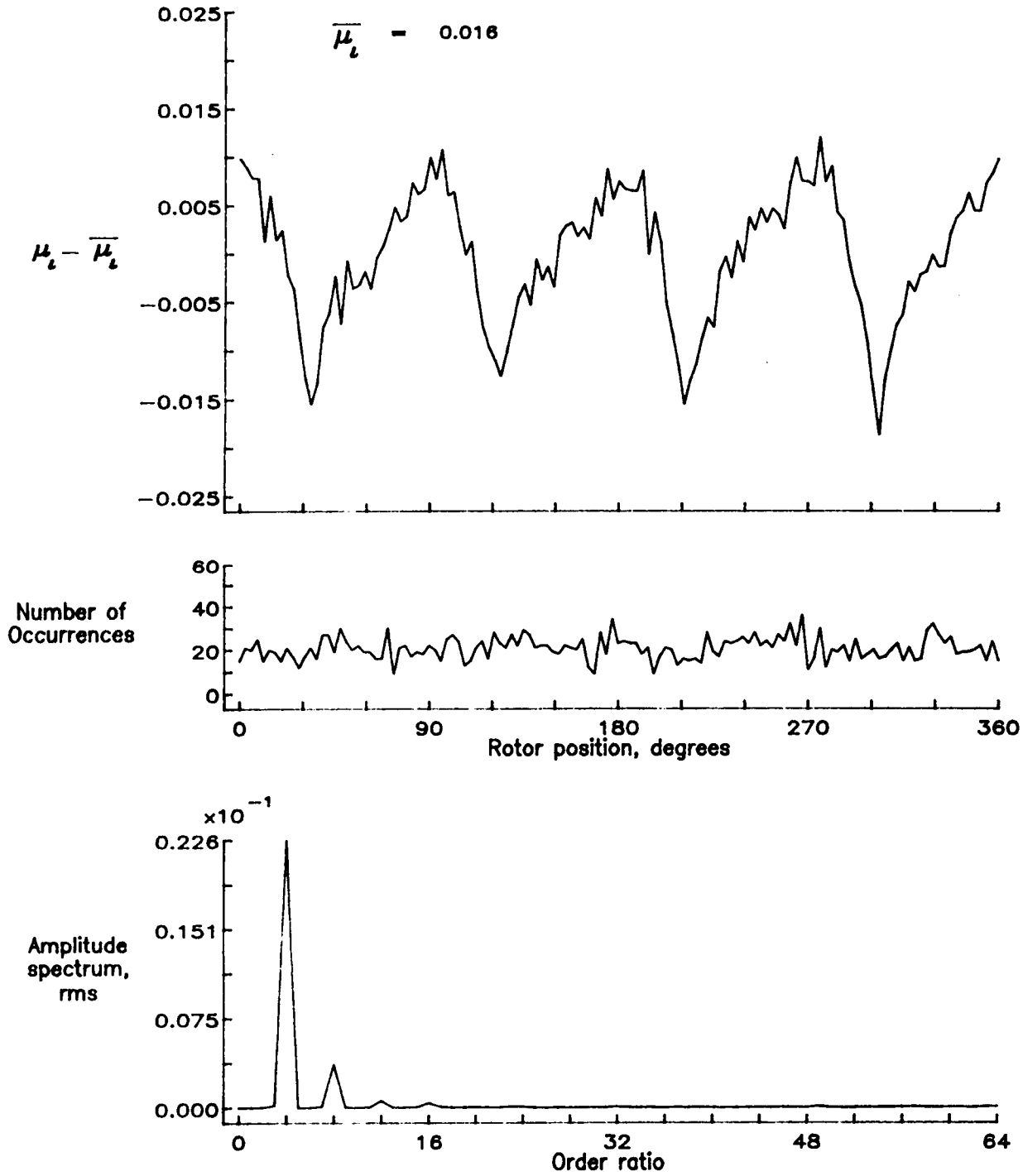

Figure 123.– Induced inflow velocity measured at 210 degrees and r/R of 0.74.

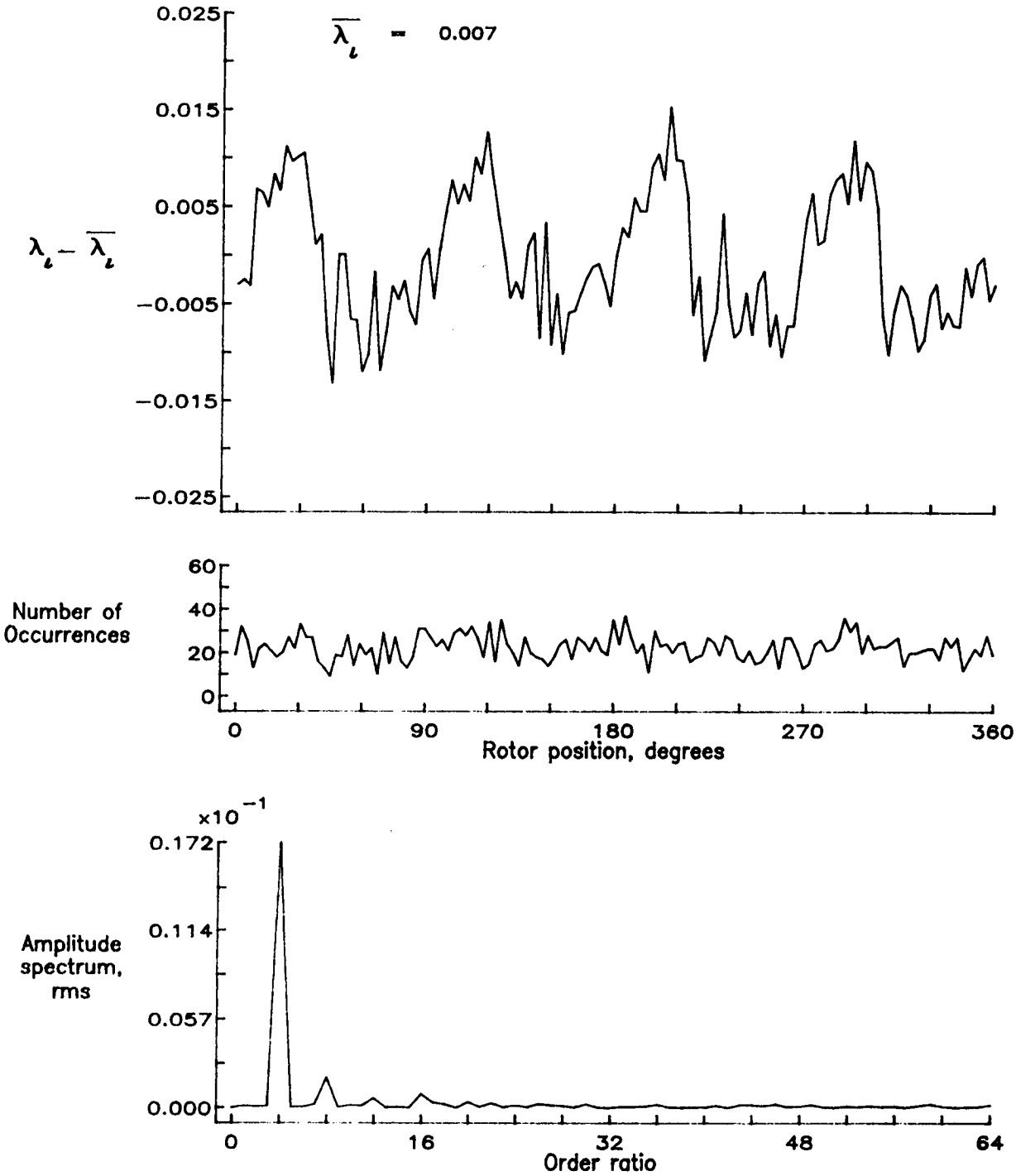

Figure 123.– Concluded.

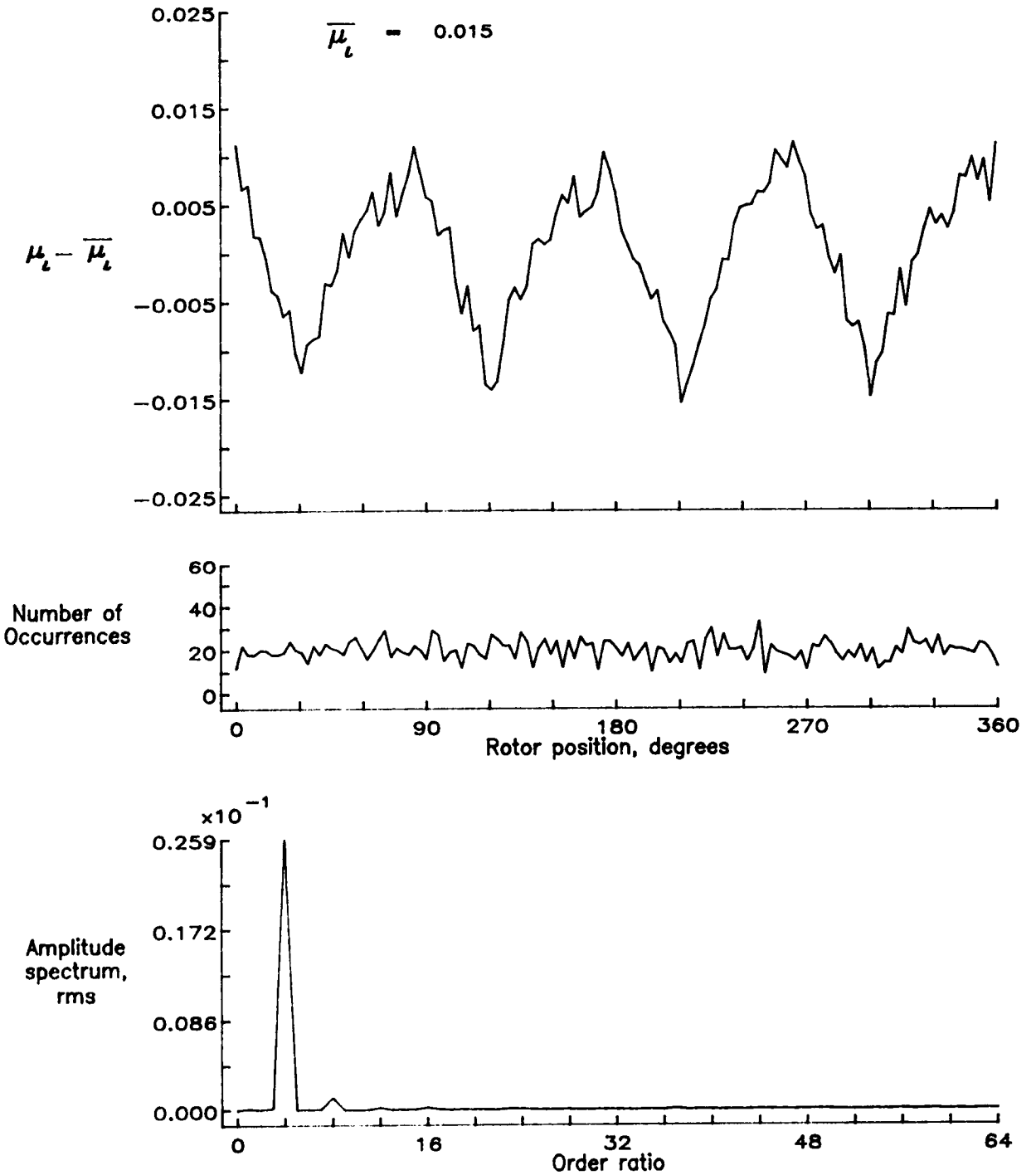

Figure 124.– Induced inflow velocity measured at 210 degrees and r/R of 0.78.

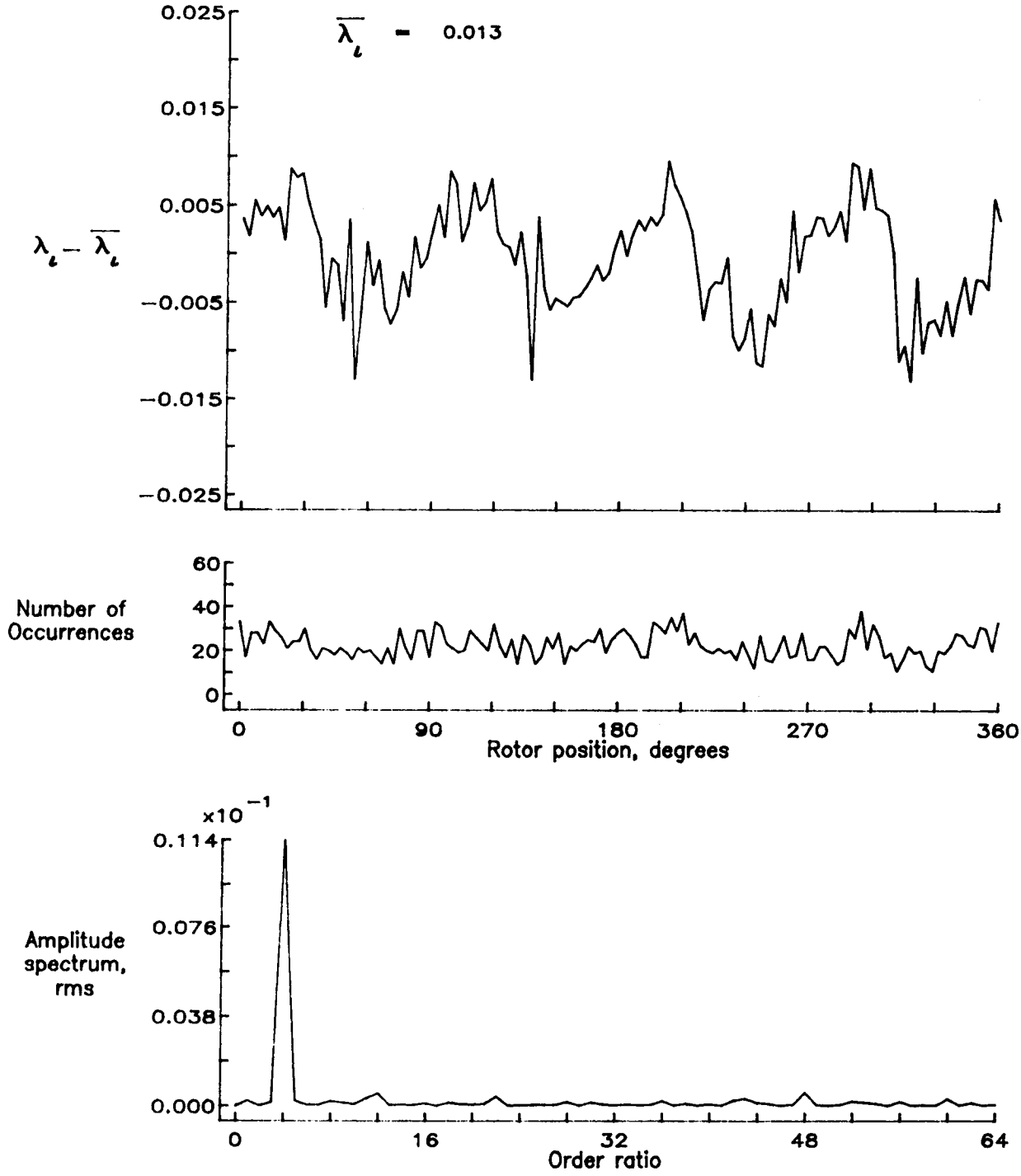

Figure 124.– Concluded.

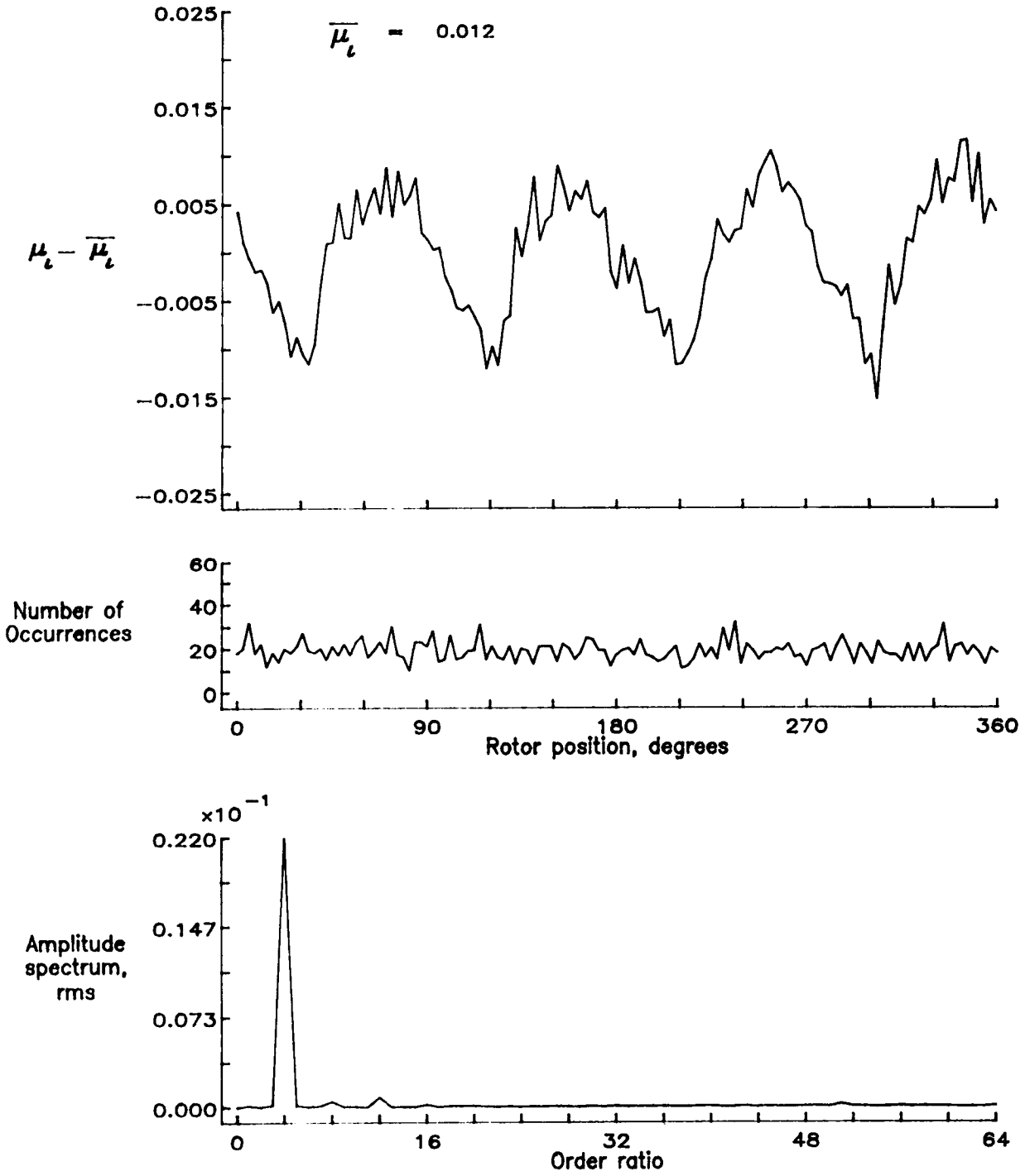

Figure 125.– Induced inflow velocity measured at 210 degrees and r/R of 0.82.

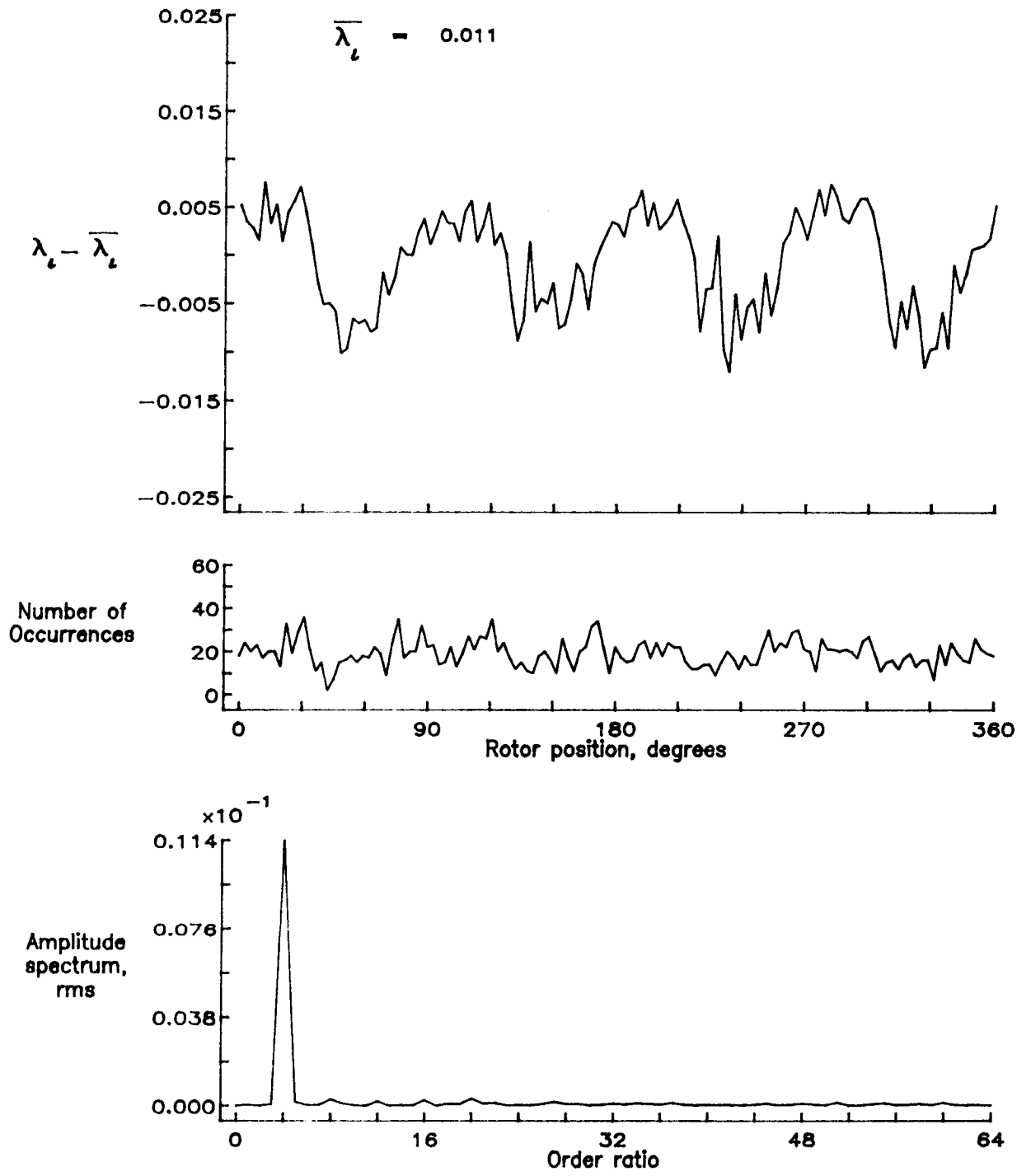

Figure 125.– Concluded.

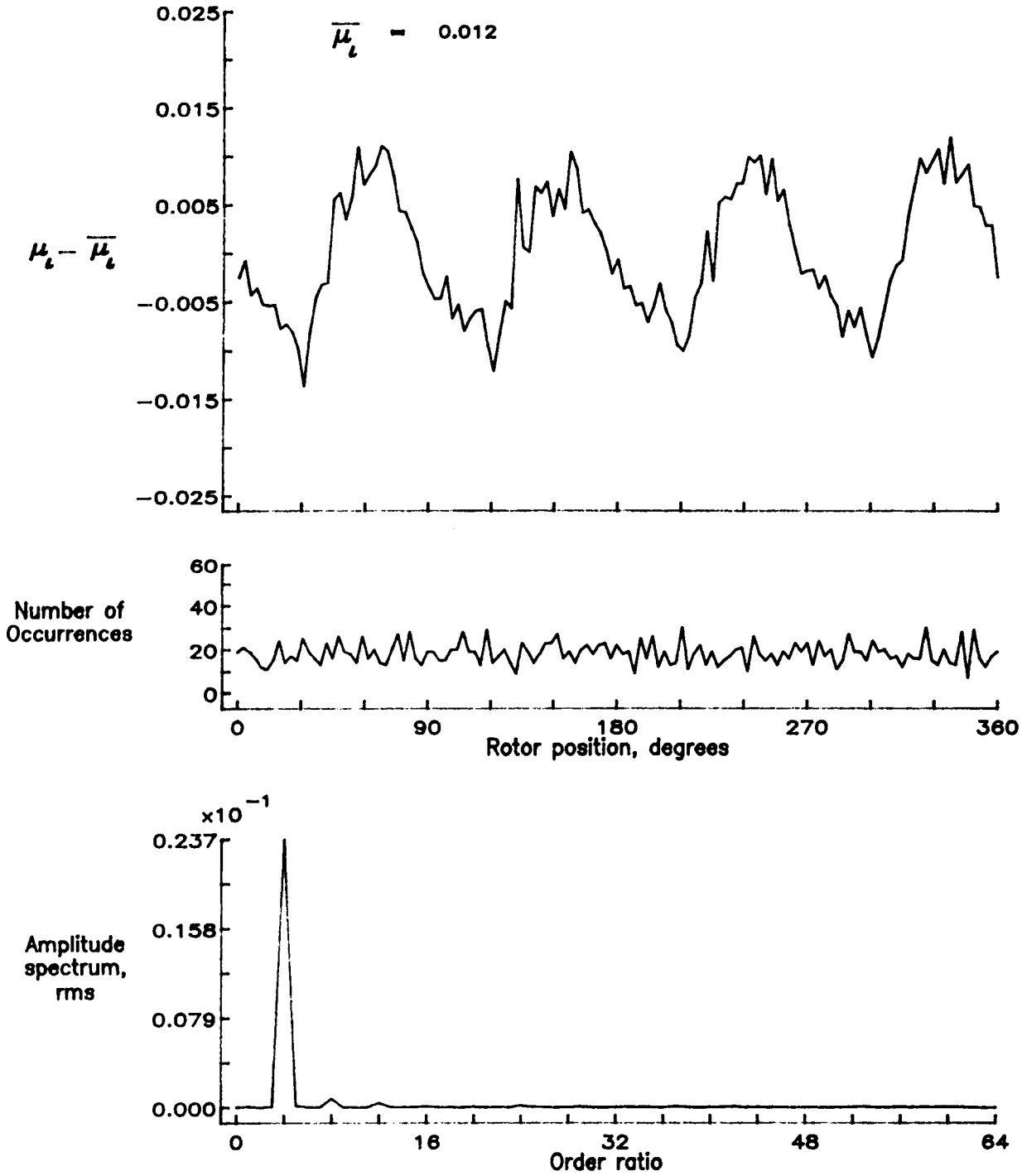

Figure 126.– Induced inflow velocity measured at 210 degrees and r/R of 0.86.

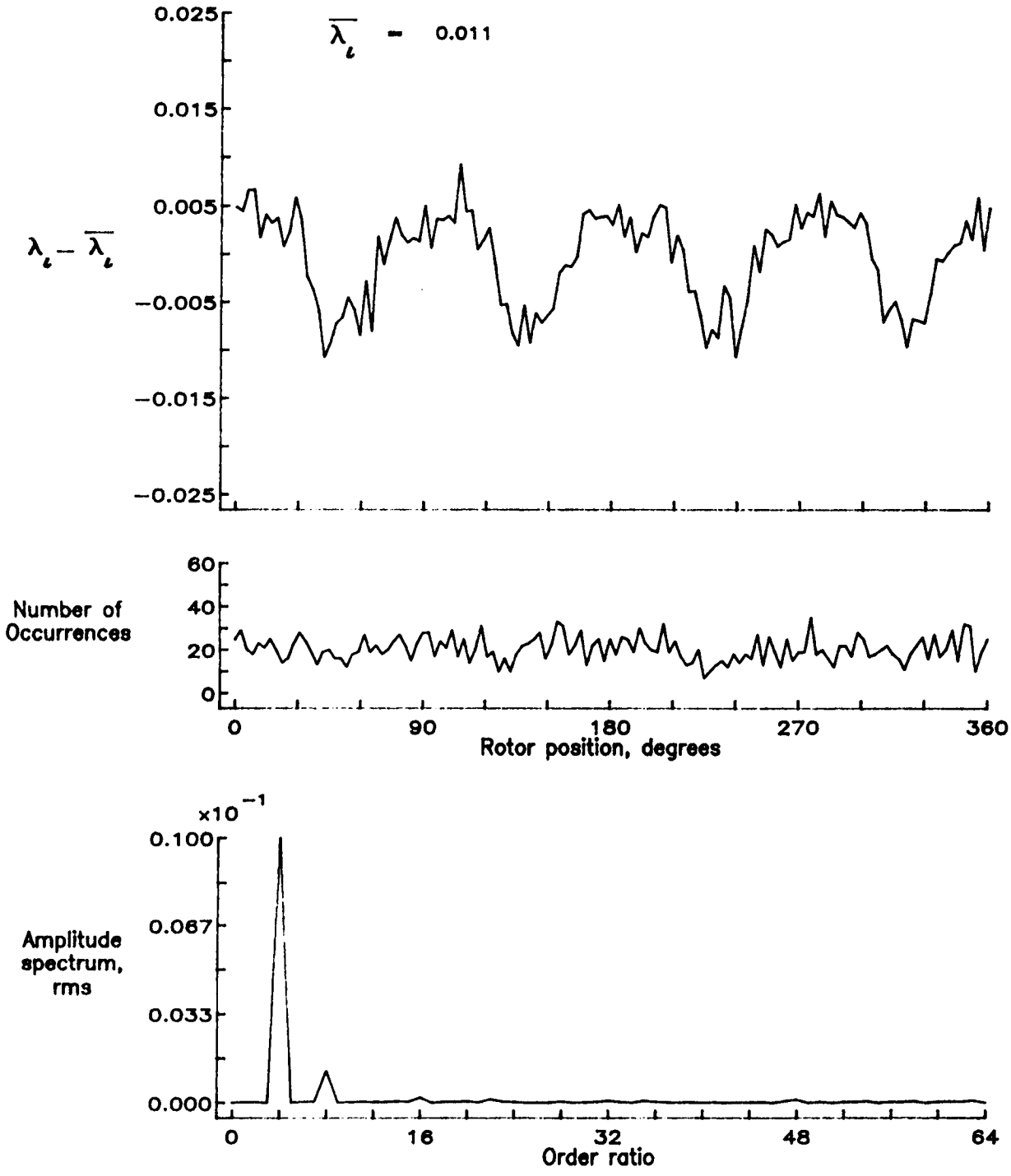

Figure 126.– Concluded.

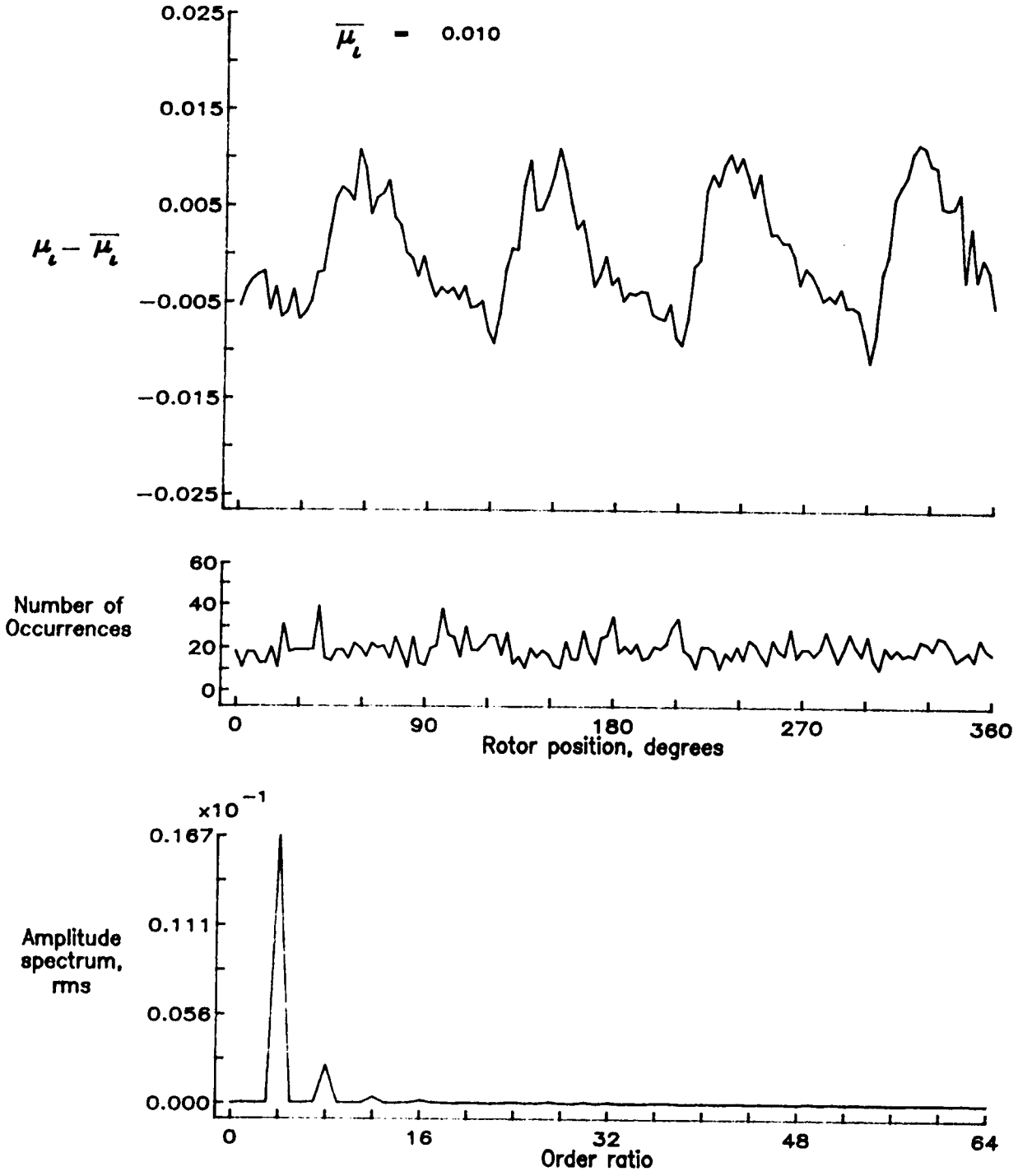

Figure 127.– Induced inflow velocity measured at 210 degrees and r/R of 0.90.

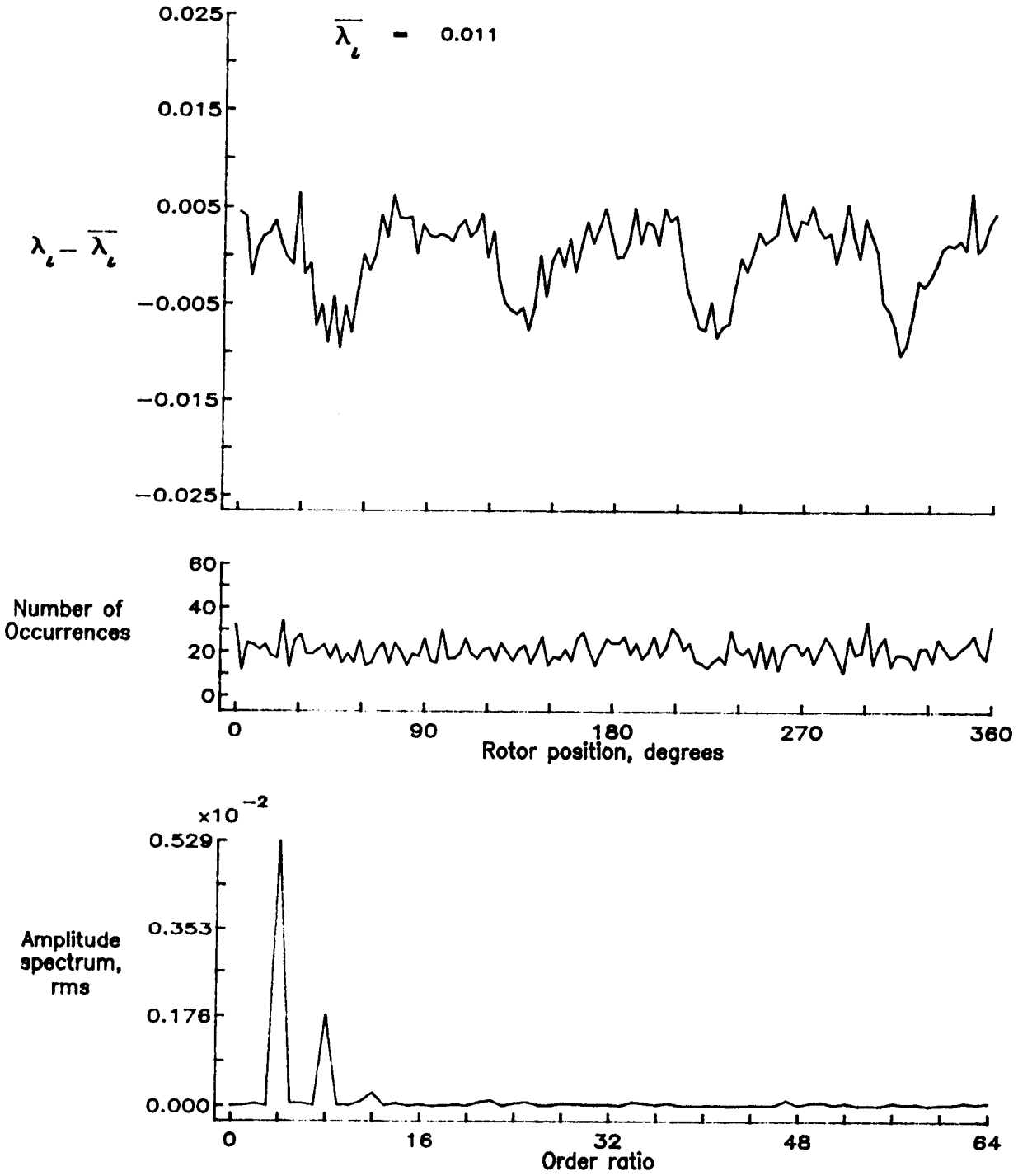

Figure 127.– Concluded.

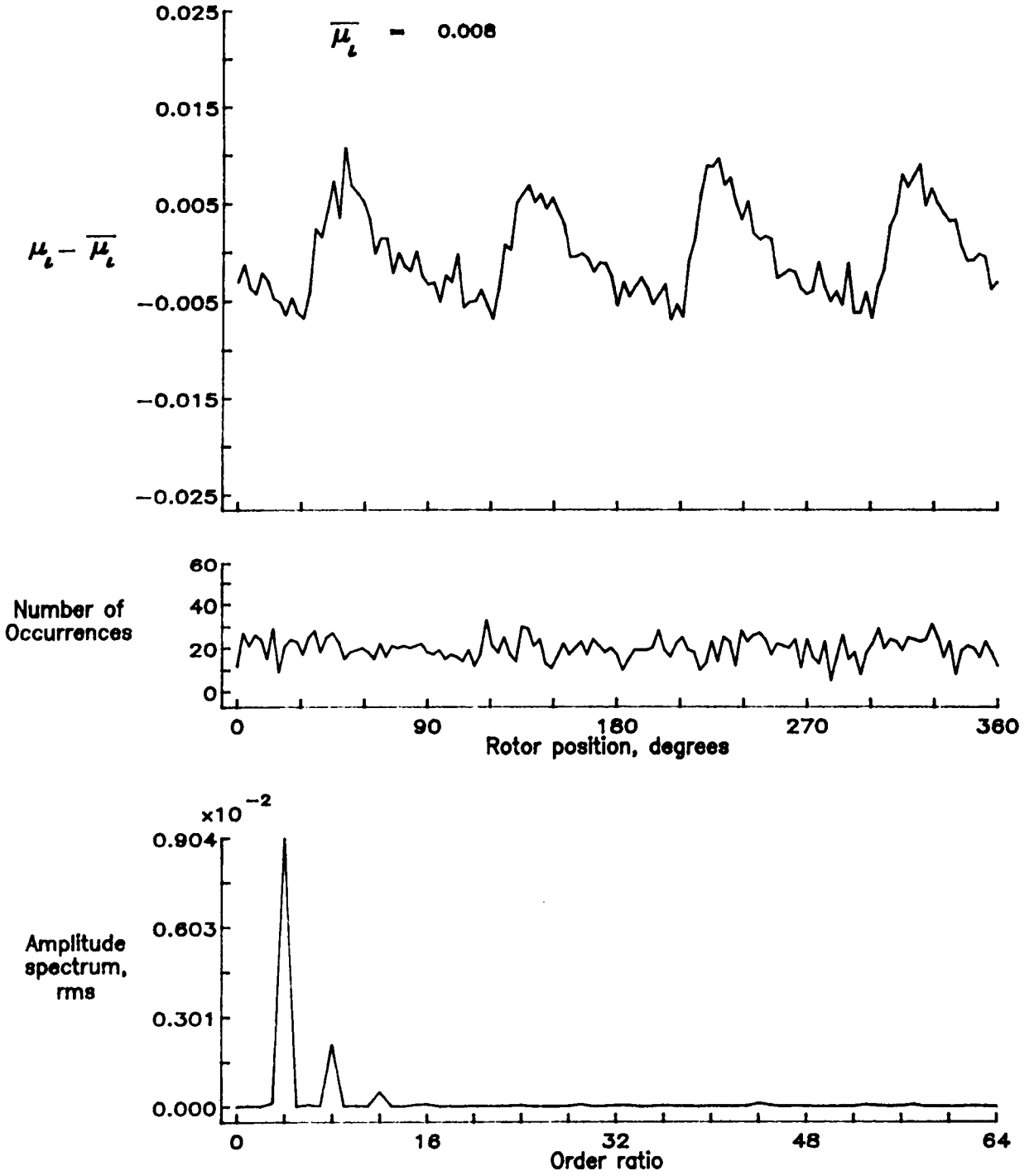

Figure 128.– Induced inflow velocity measured at 210 degrees and r/R of 0.94.

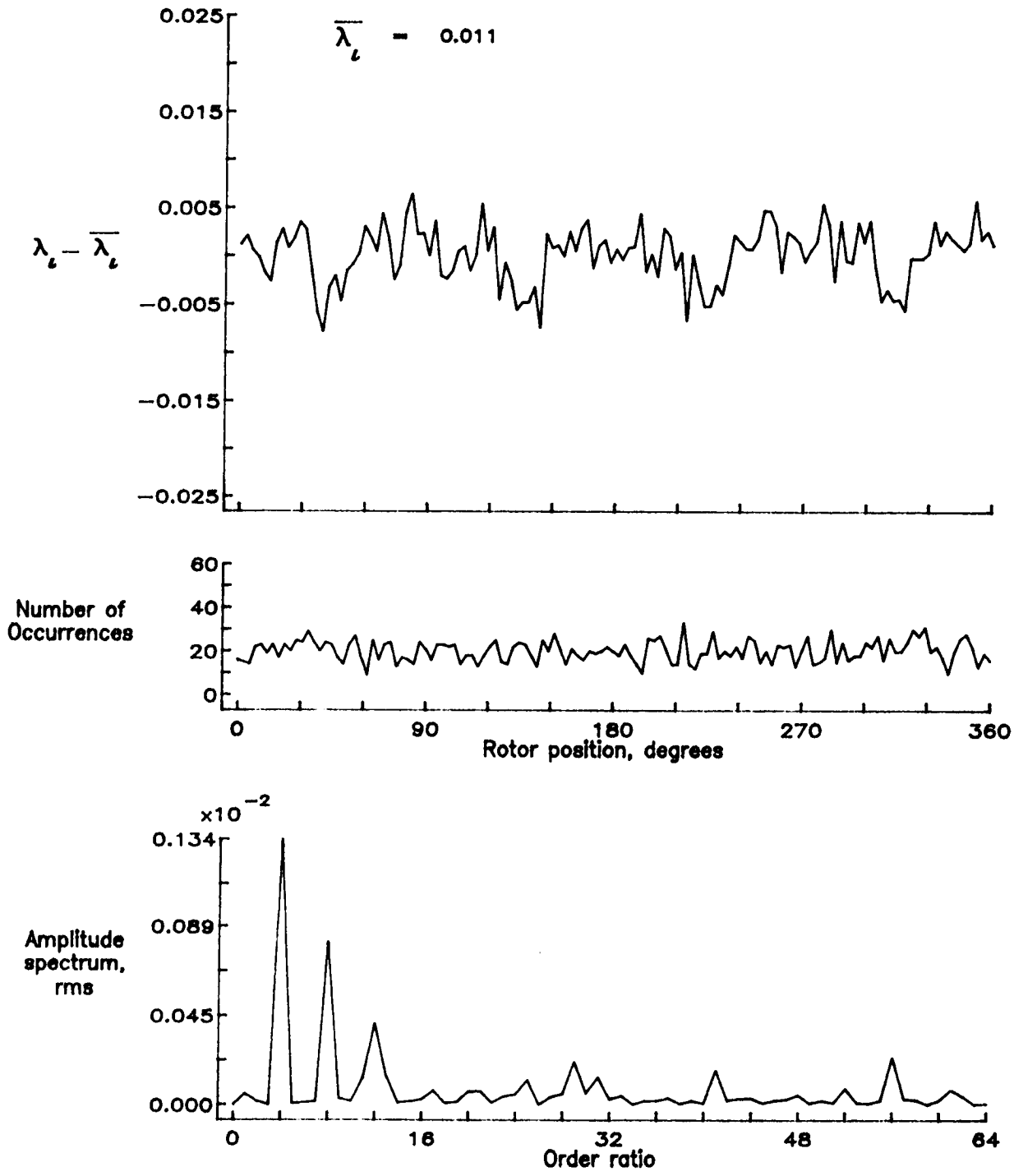

Figure 128.– Concluded.

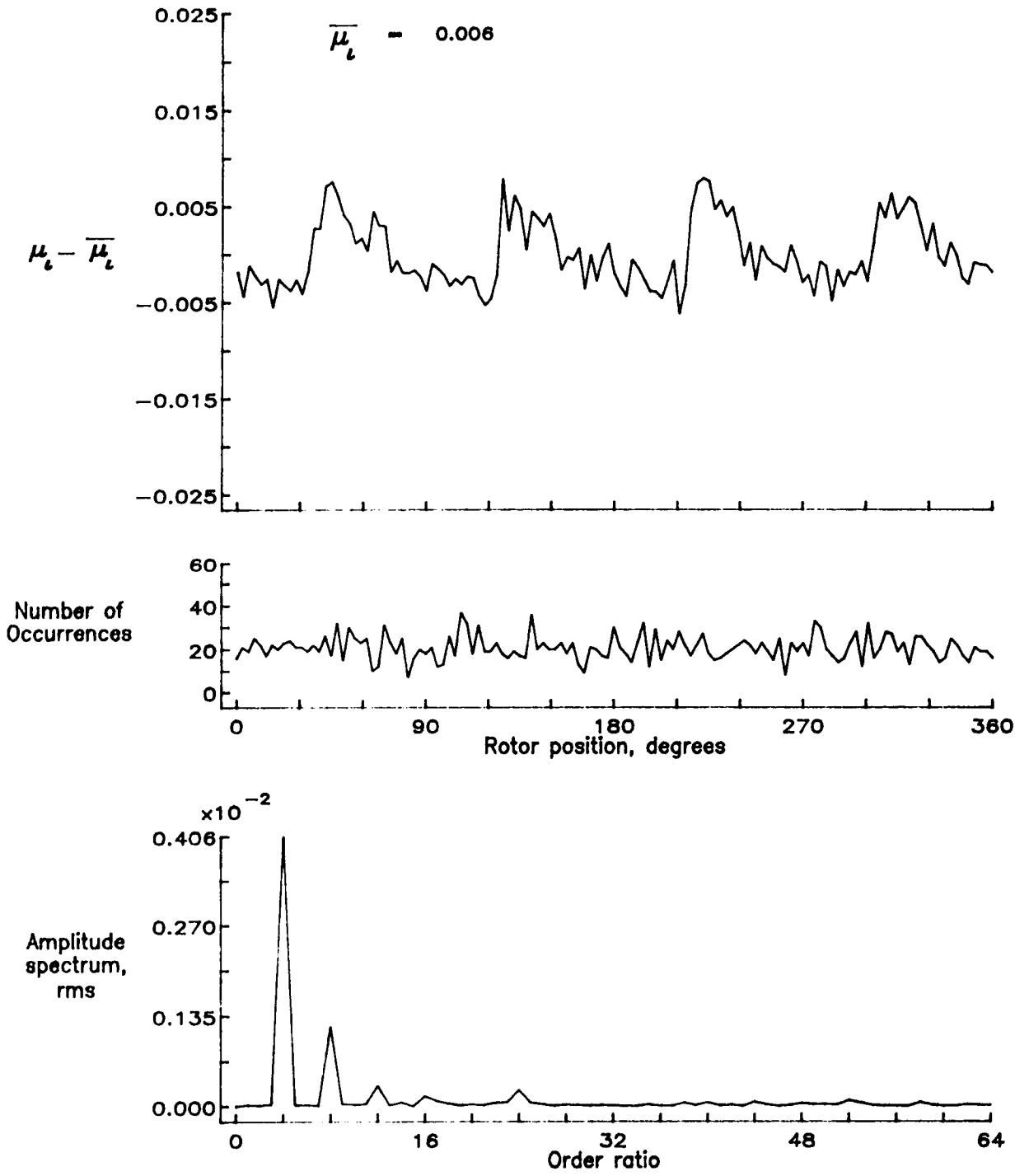

Figure 129.– Induced inflow velocity measured at 210 degrees and r/R of 0.98.

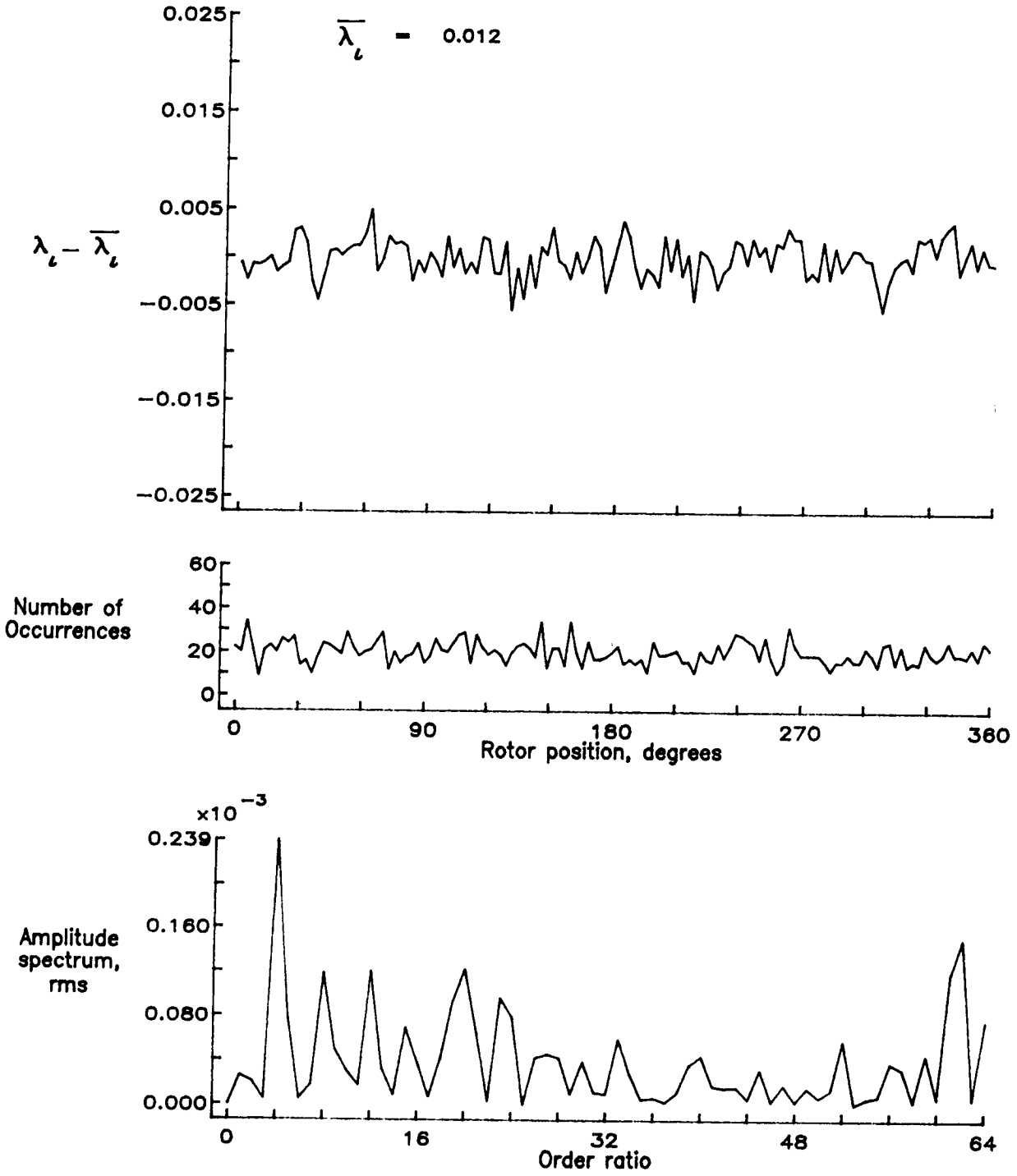

Figure 129.– Concluded.

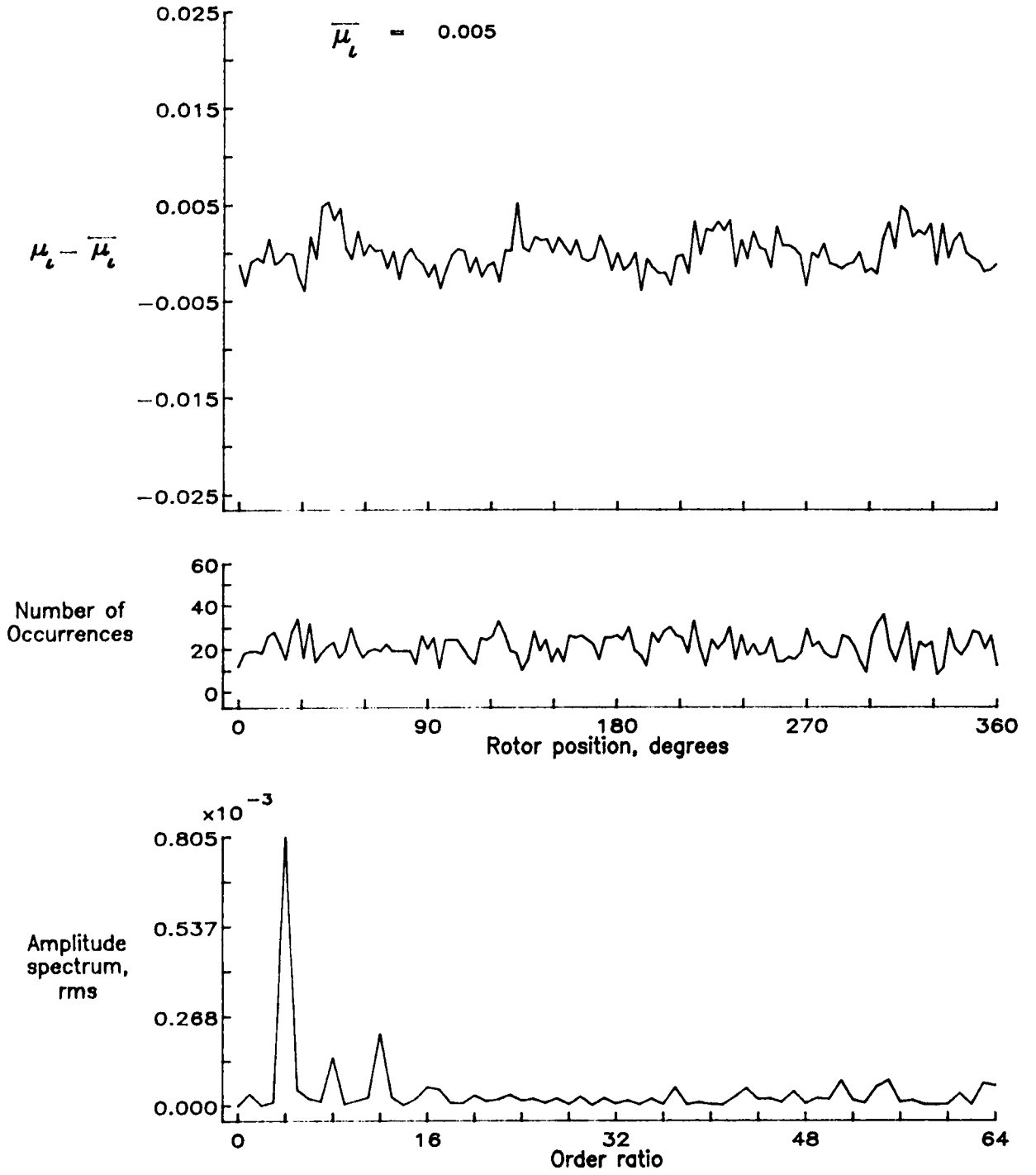

Figure 130.– Induced inflow velocity measured at 210 degrees and r/R of 1.02.

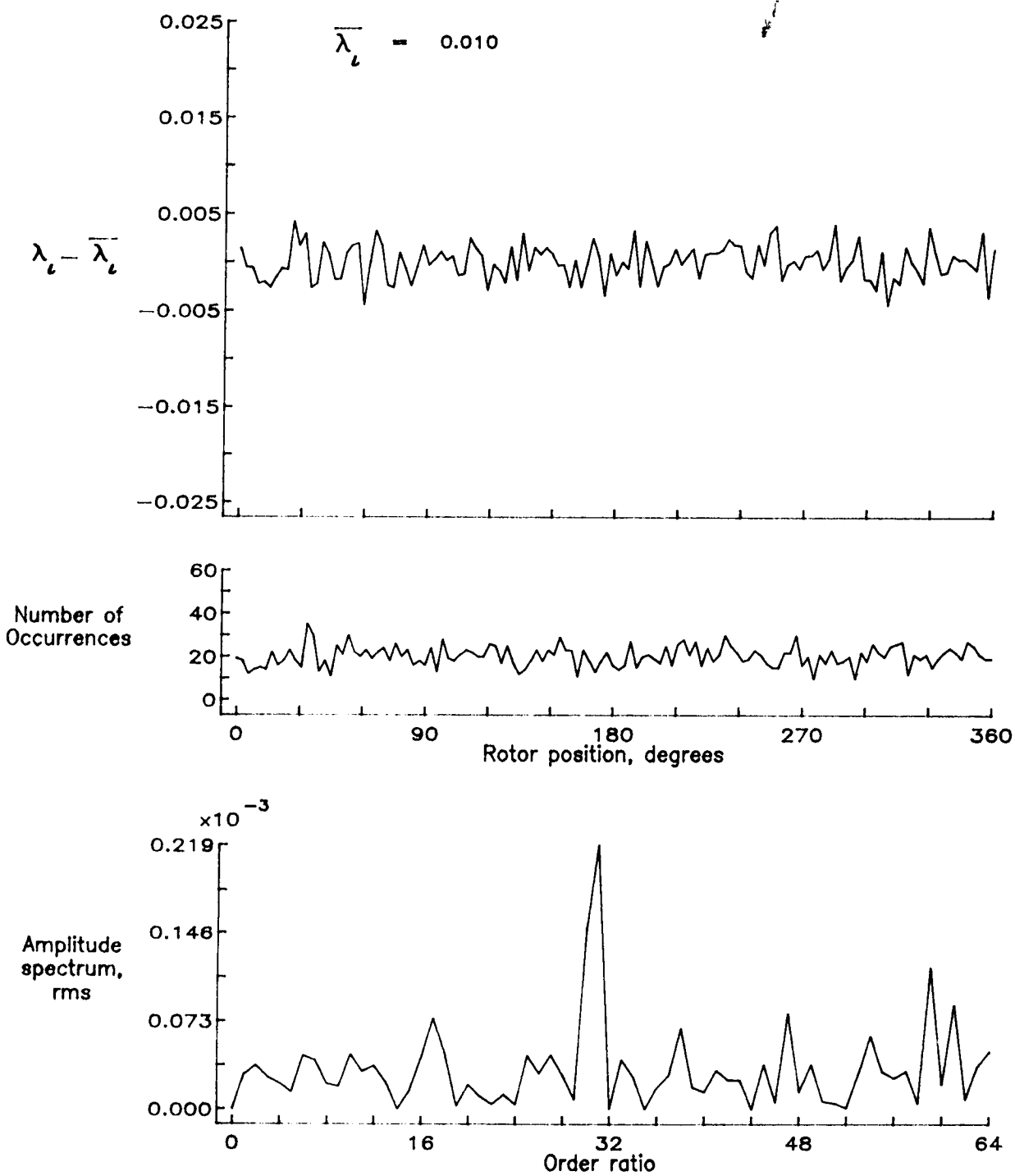

Figure 130.– Concluded.

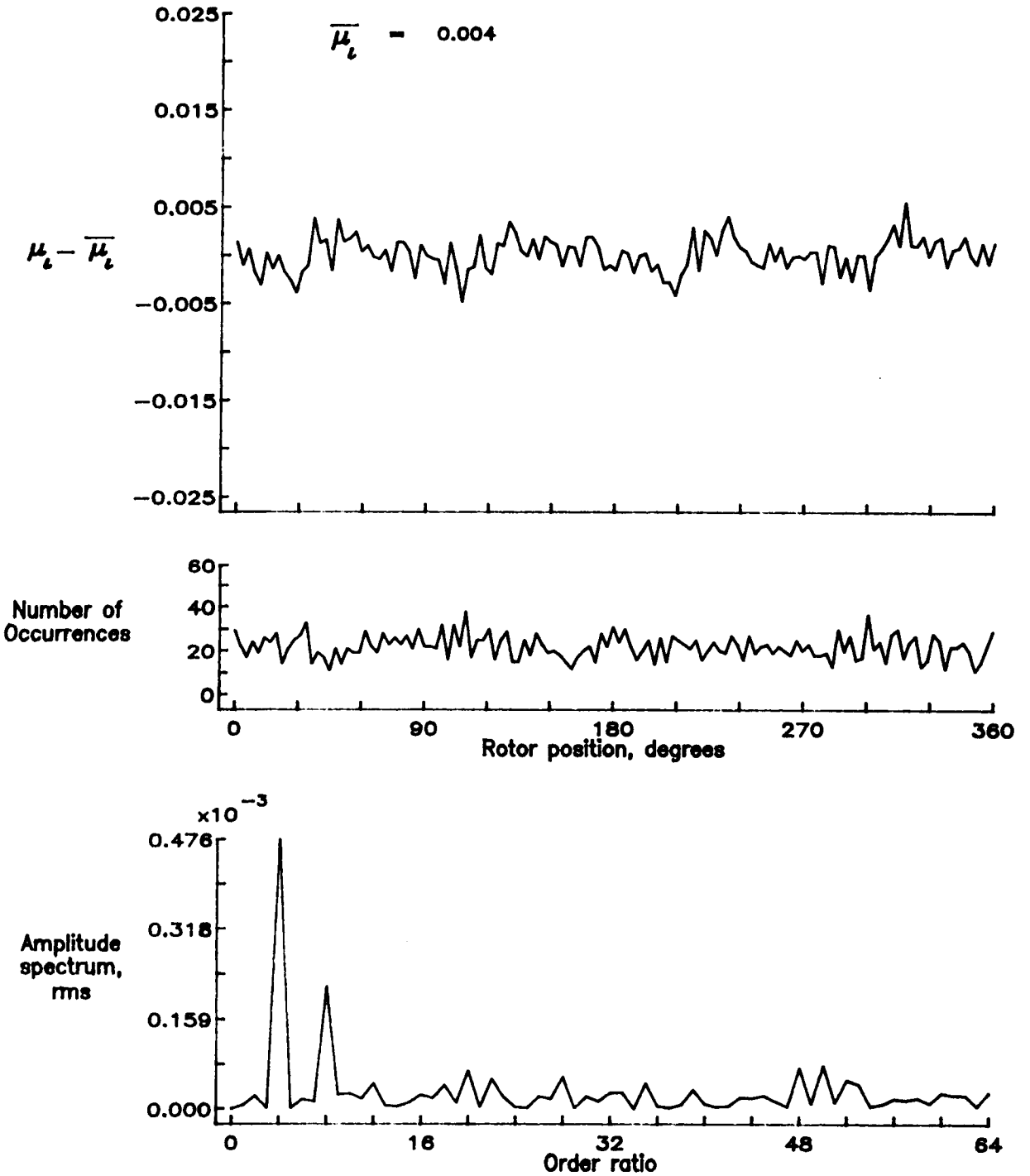

Figure 131.– Induced inflow velocity measured at 210 degrees and r/R of 1.04.

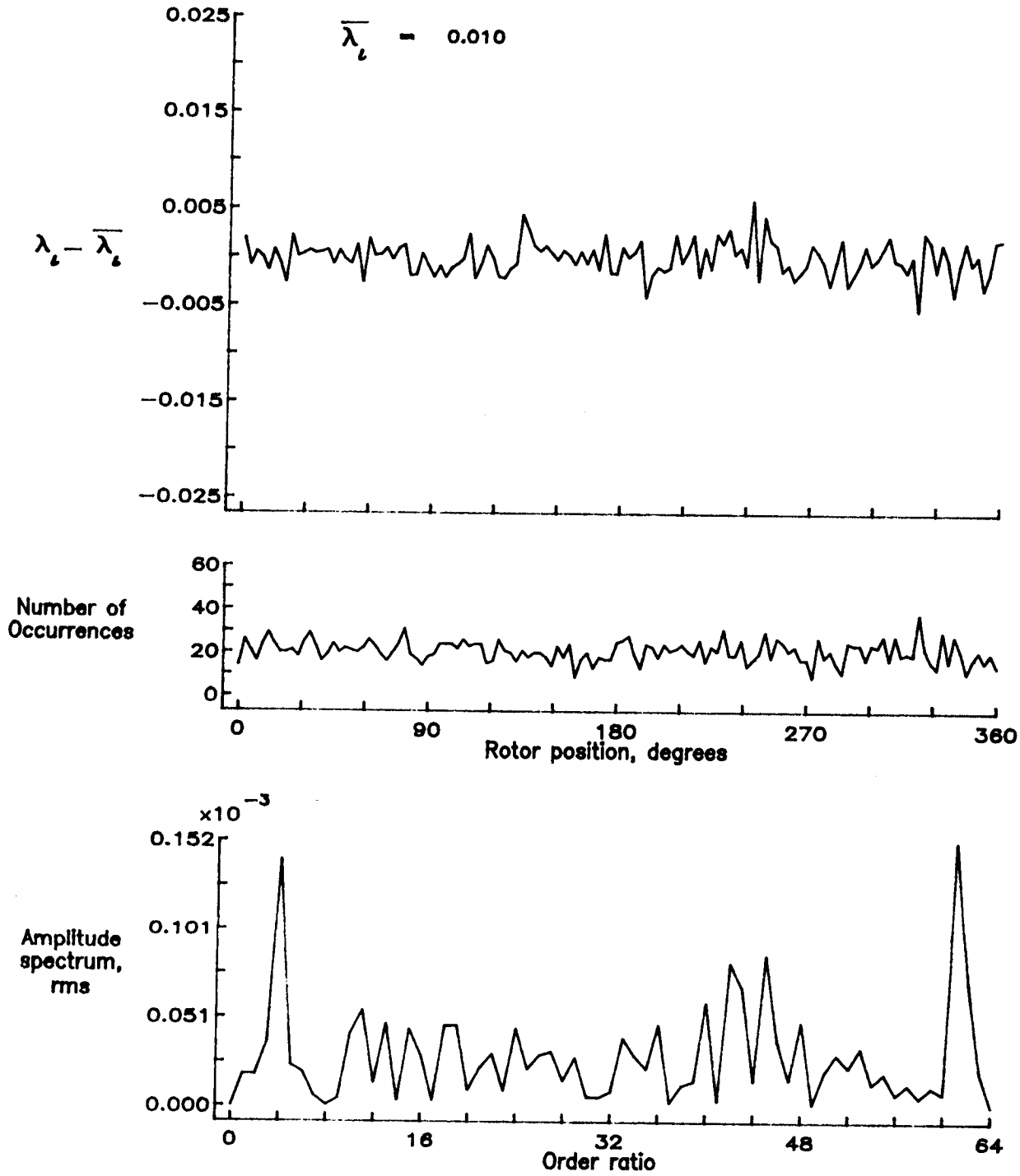

Figure 131.– Concluded.

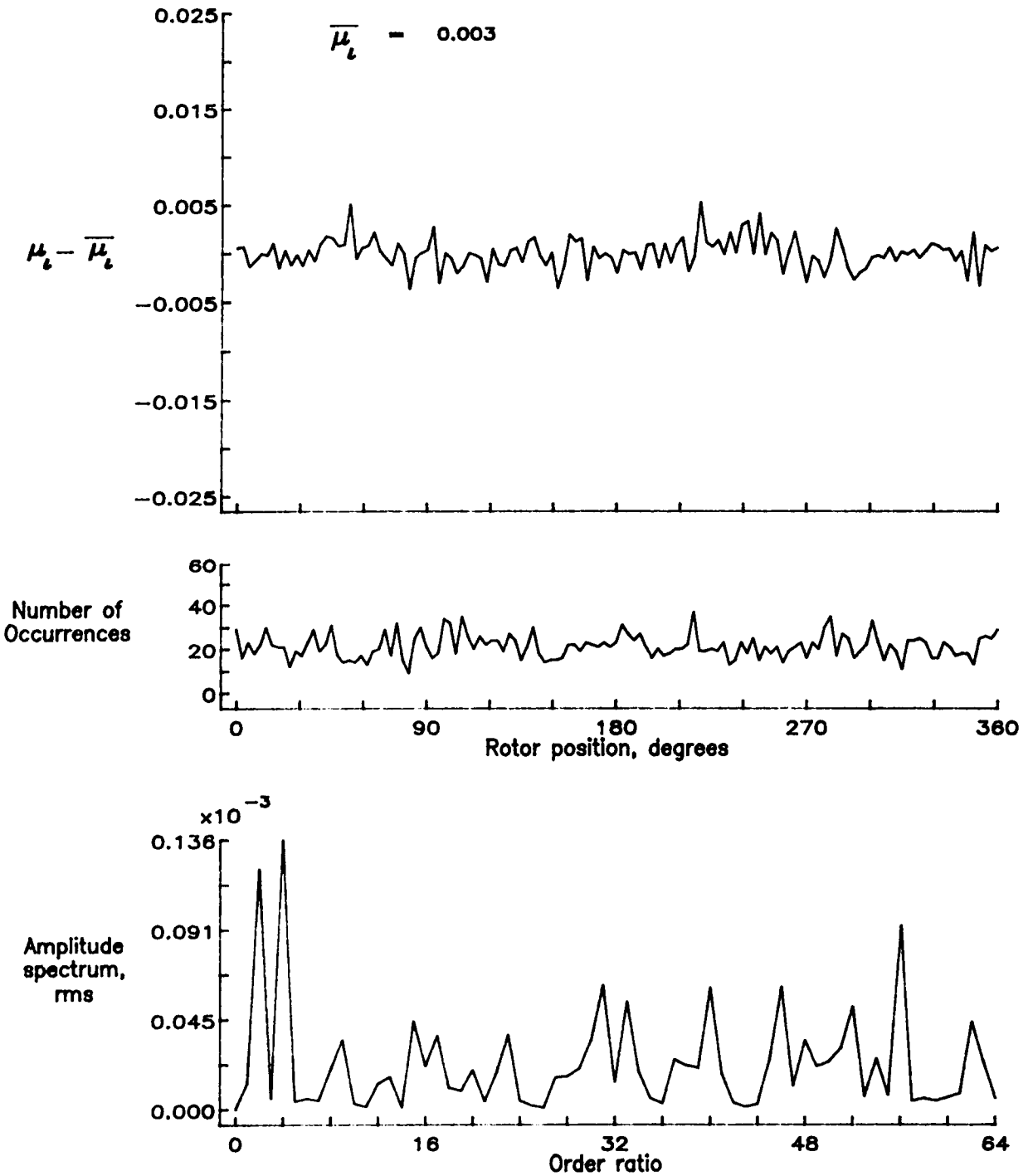

Figure 132.– Induced inflow velocity measured at 210 degrees and r/R of 1.10.

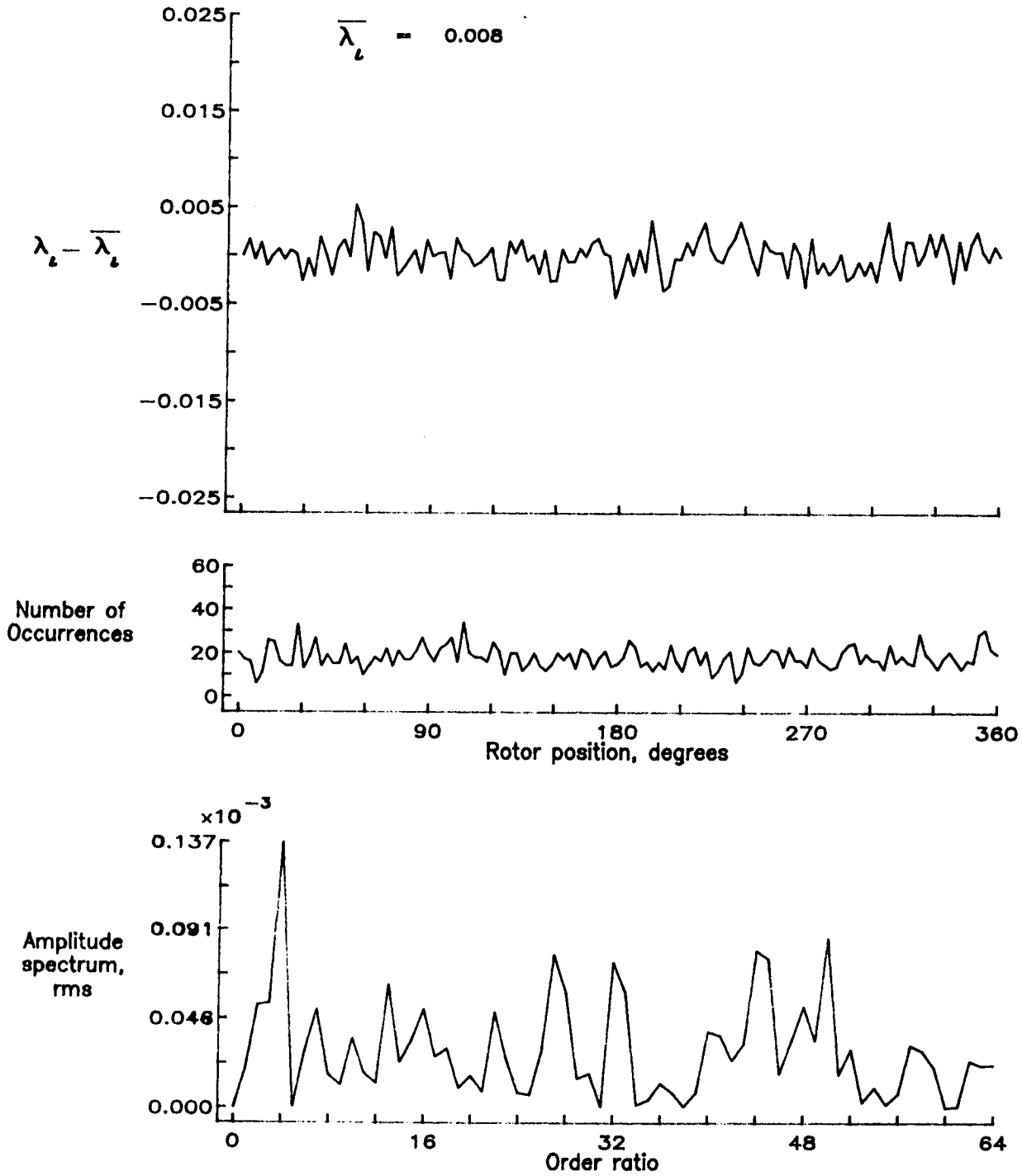

Figure 132.– Concluded.

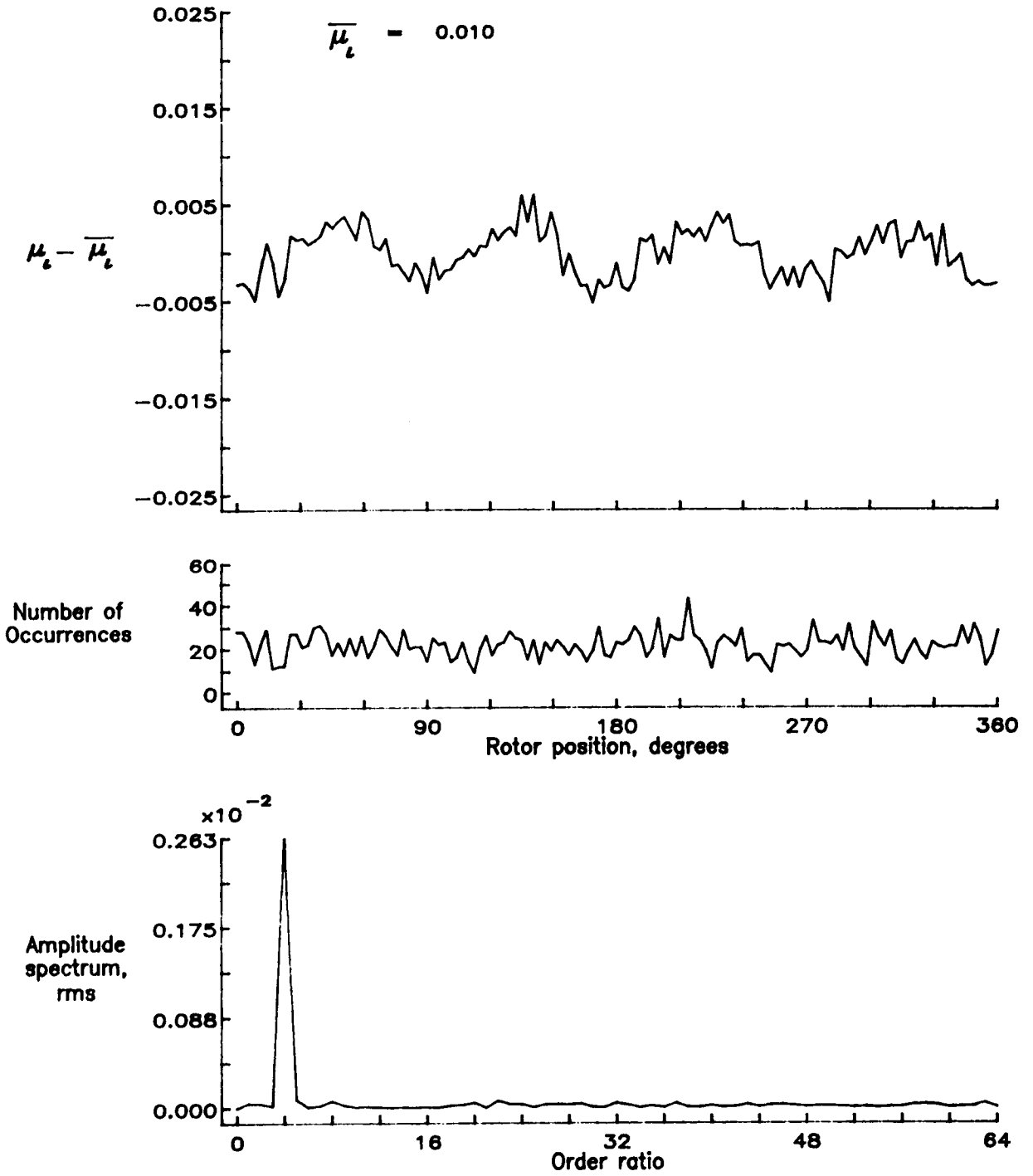

Figure 133.– Induced inflow velocity measured at 240 degrees and r/R of 0.20.

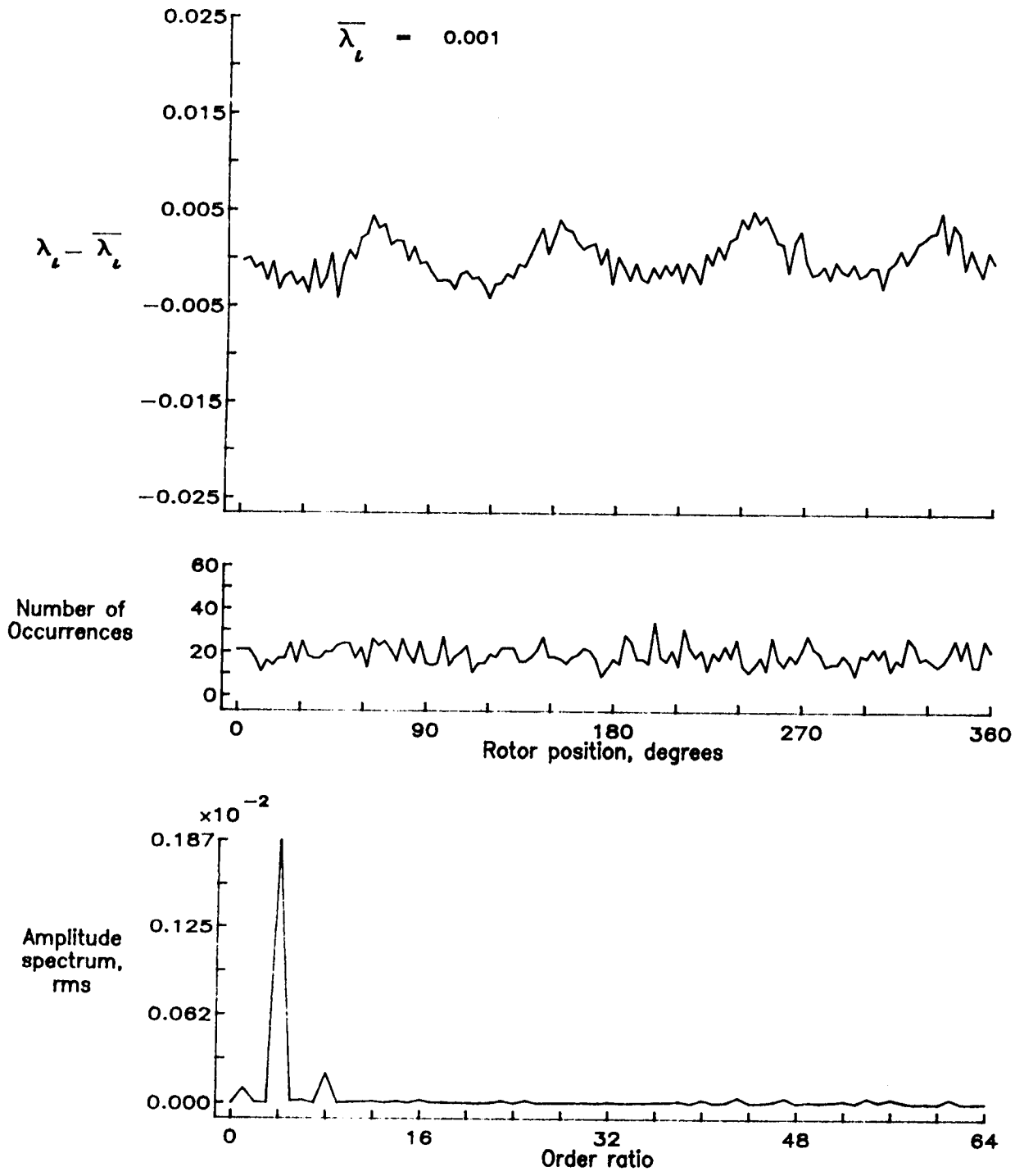

Figure 133.– Concluded.

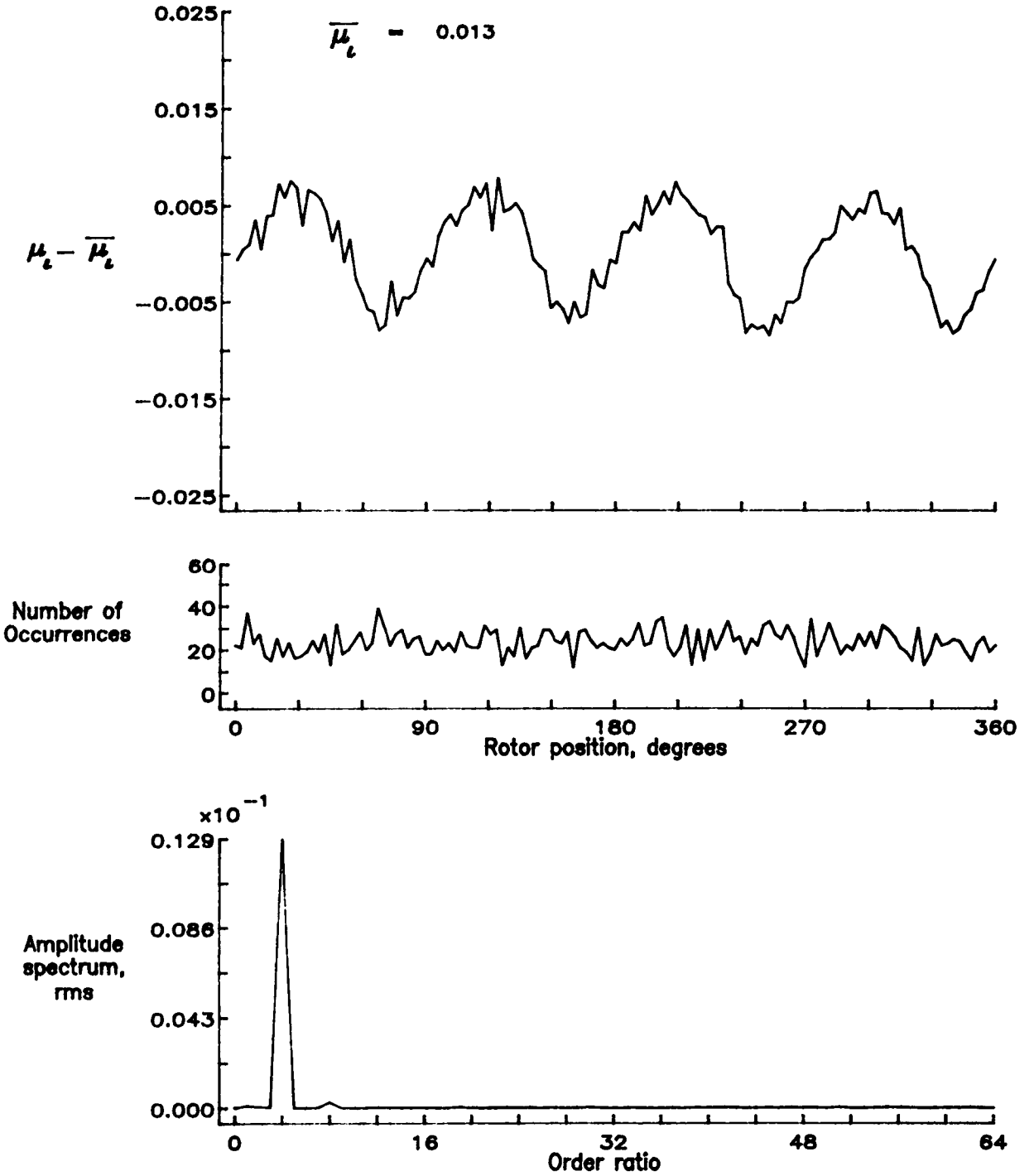

Figure 134.– Induced inflow velocity measured at 240 degrees and r/R of 0.40.

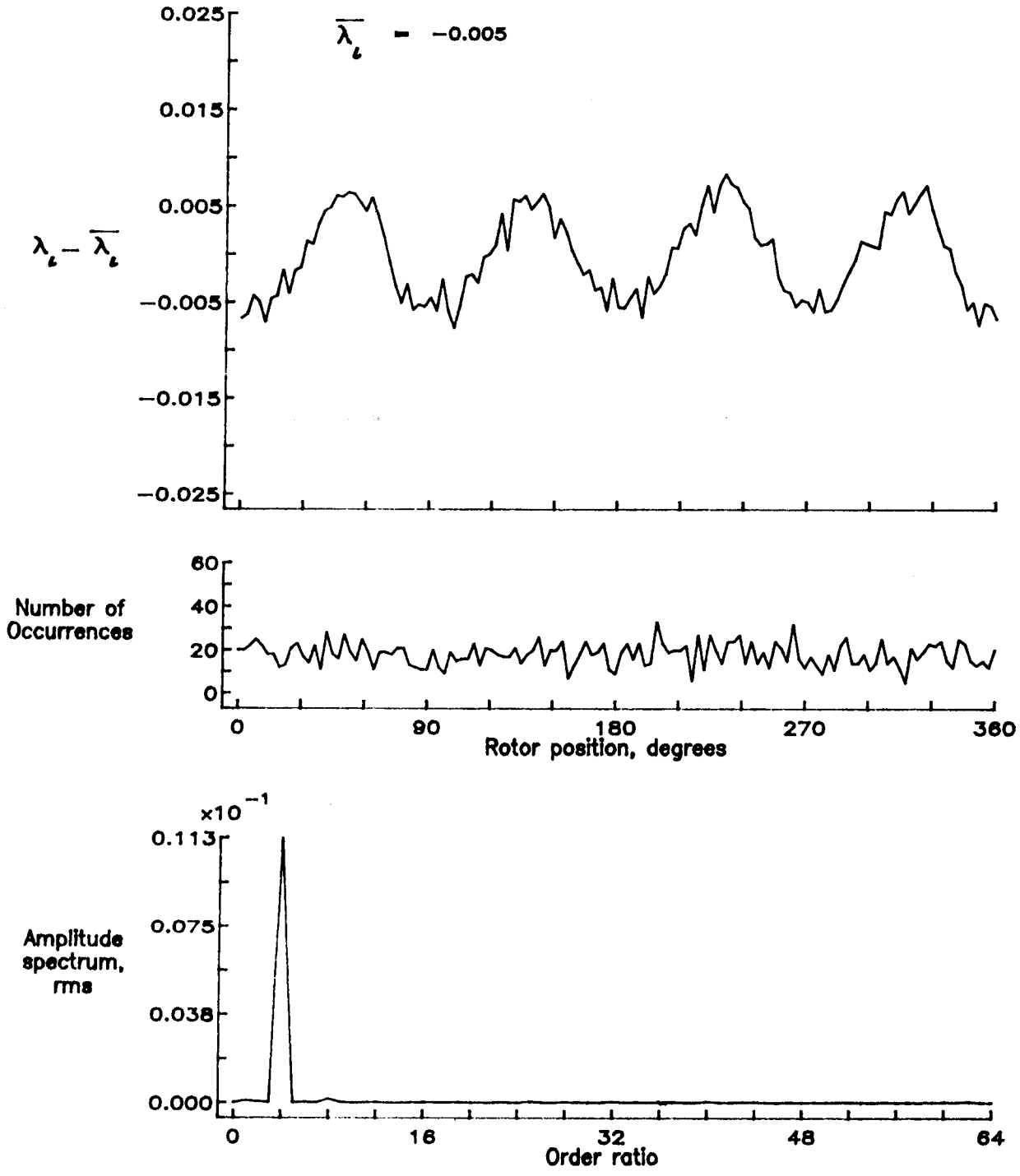

Figure 134.– Concluded.

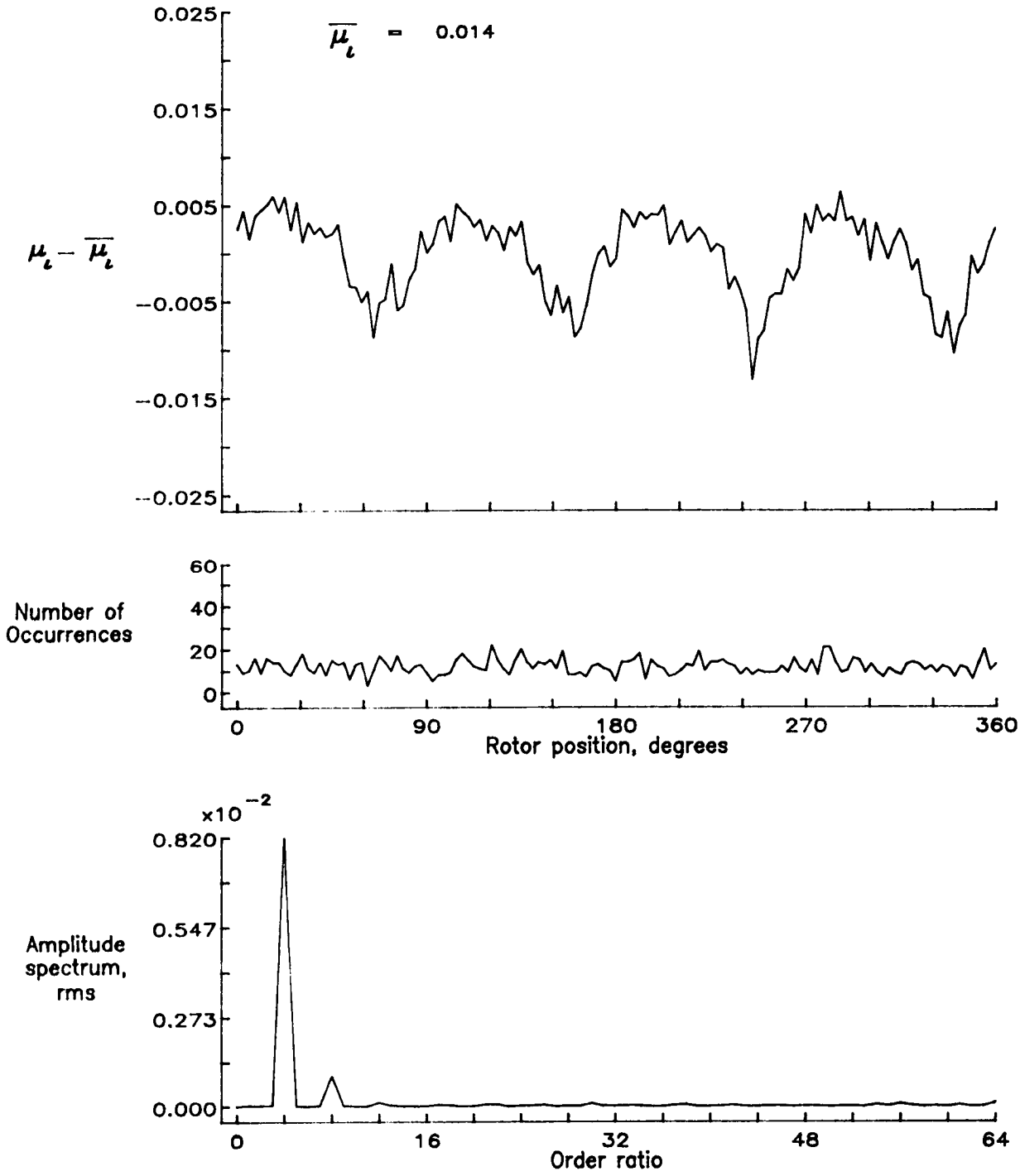

Figure 135.– Induced inflow velocity measured at 240 degrees and r/R of 0.50.

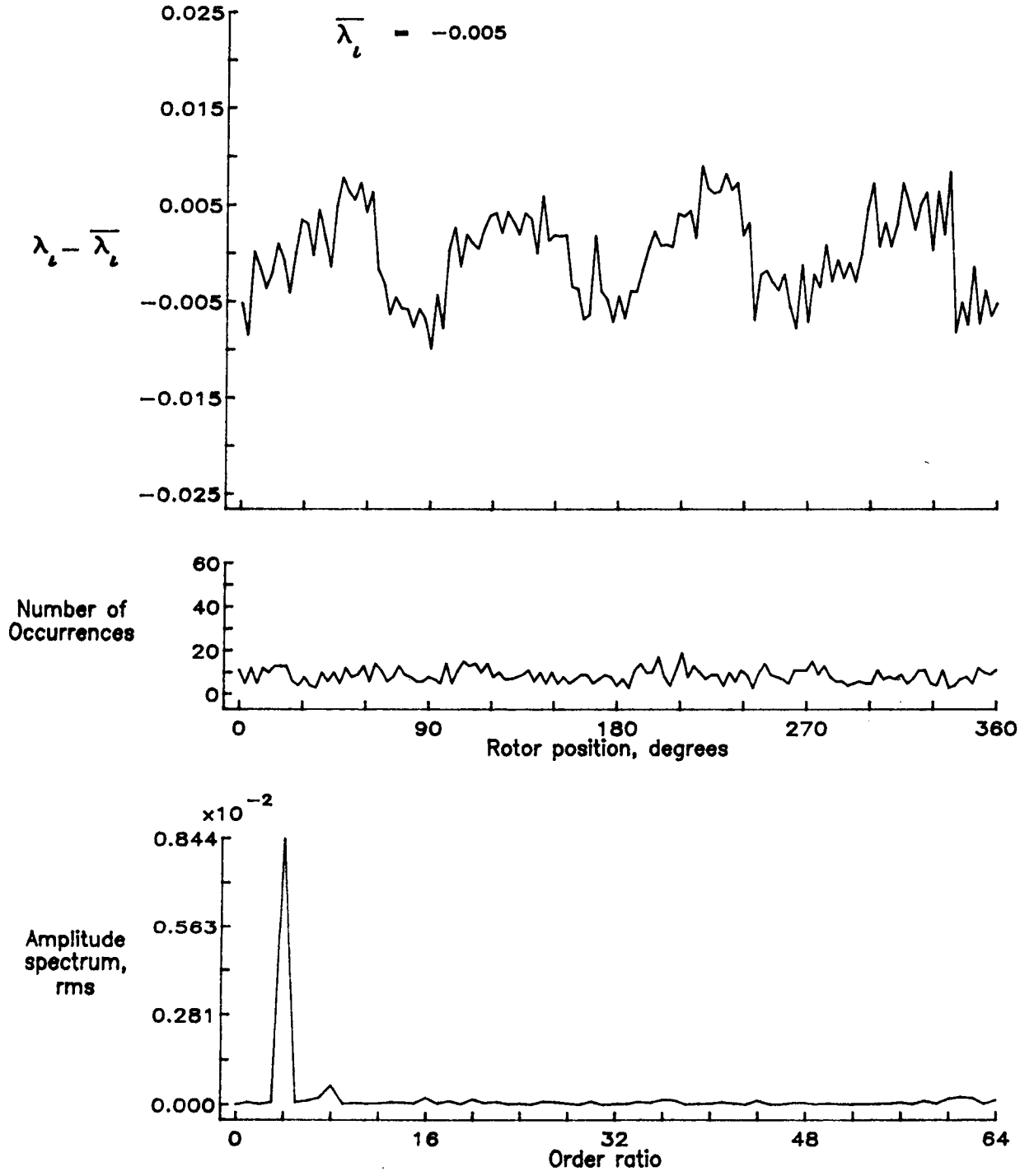

Figure 135.– Concluded.

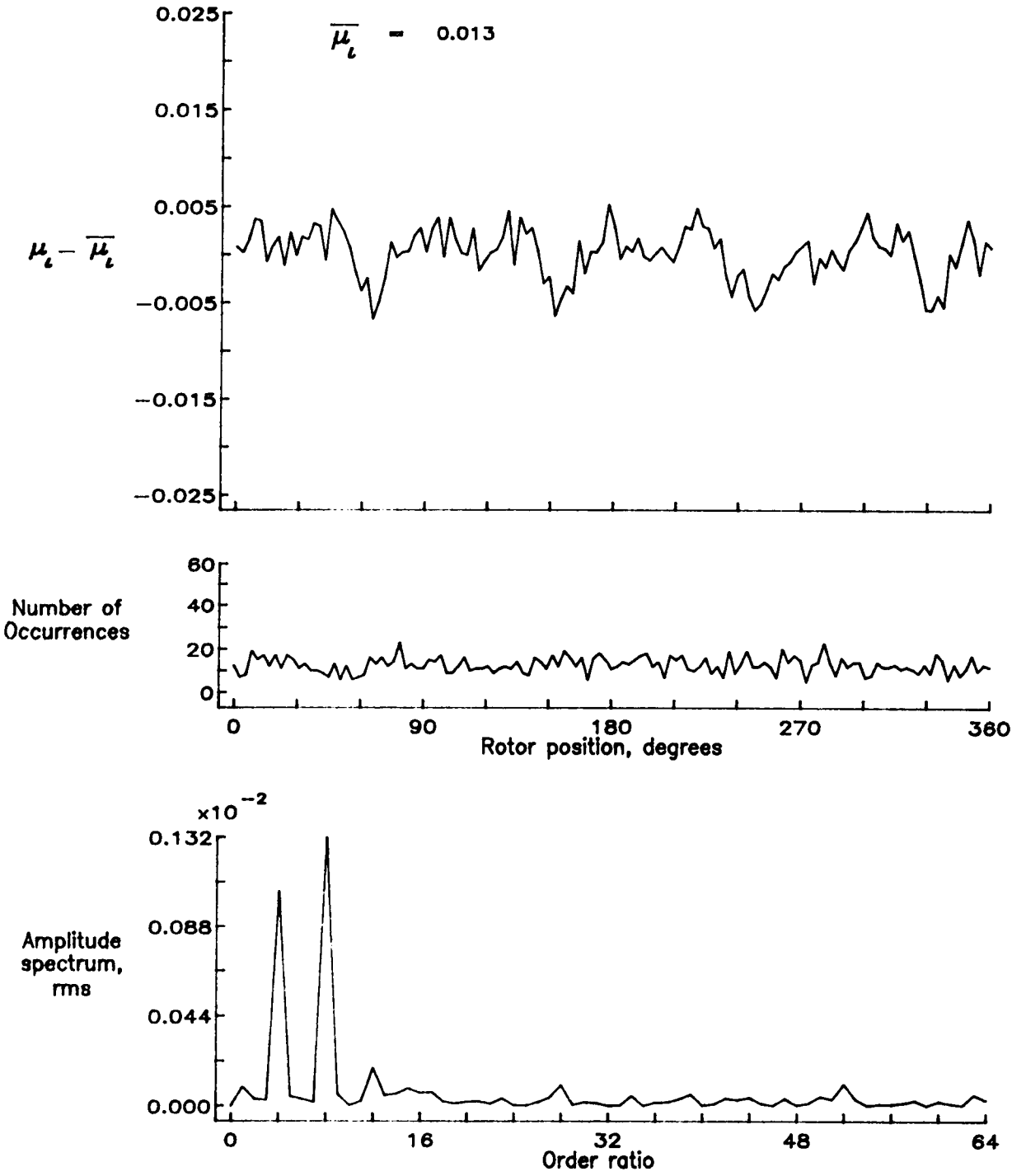

Figure 136.– Induced inflow velocity measured at 240 degrees and r/R of 0.60.

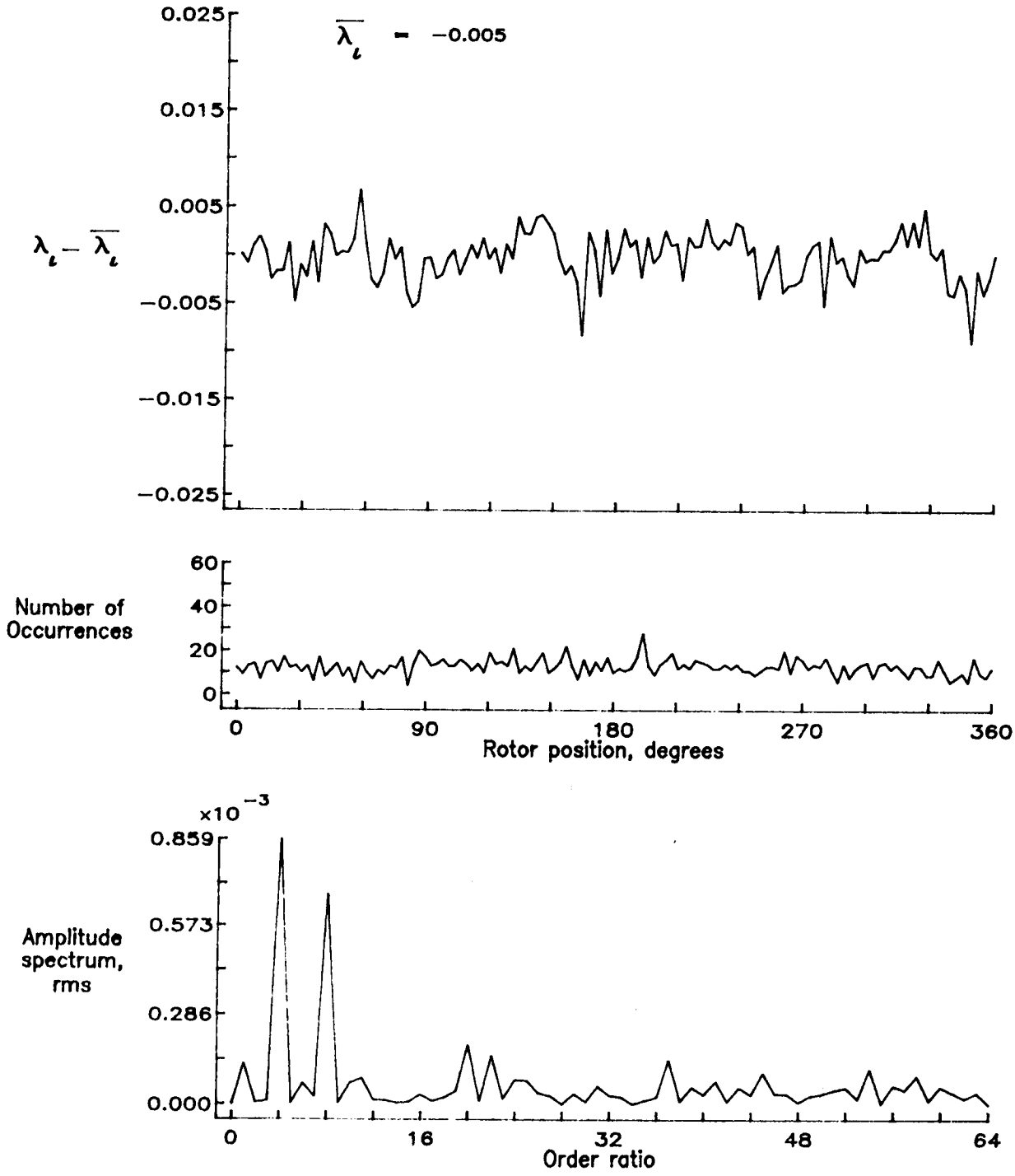

Figure 136.– Concluded.

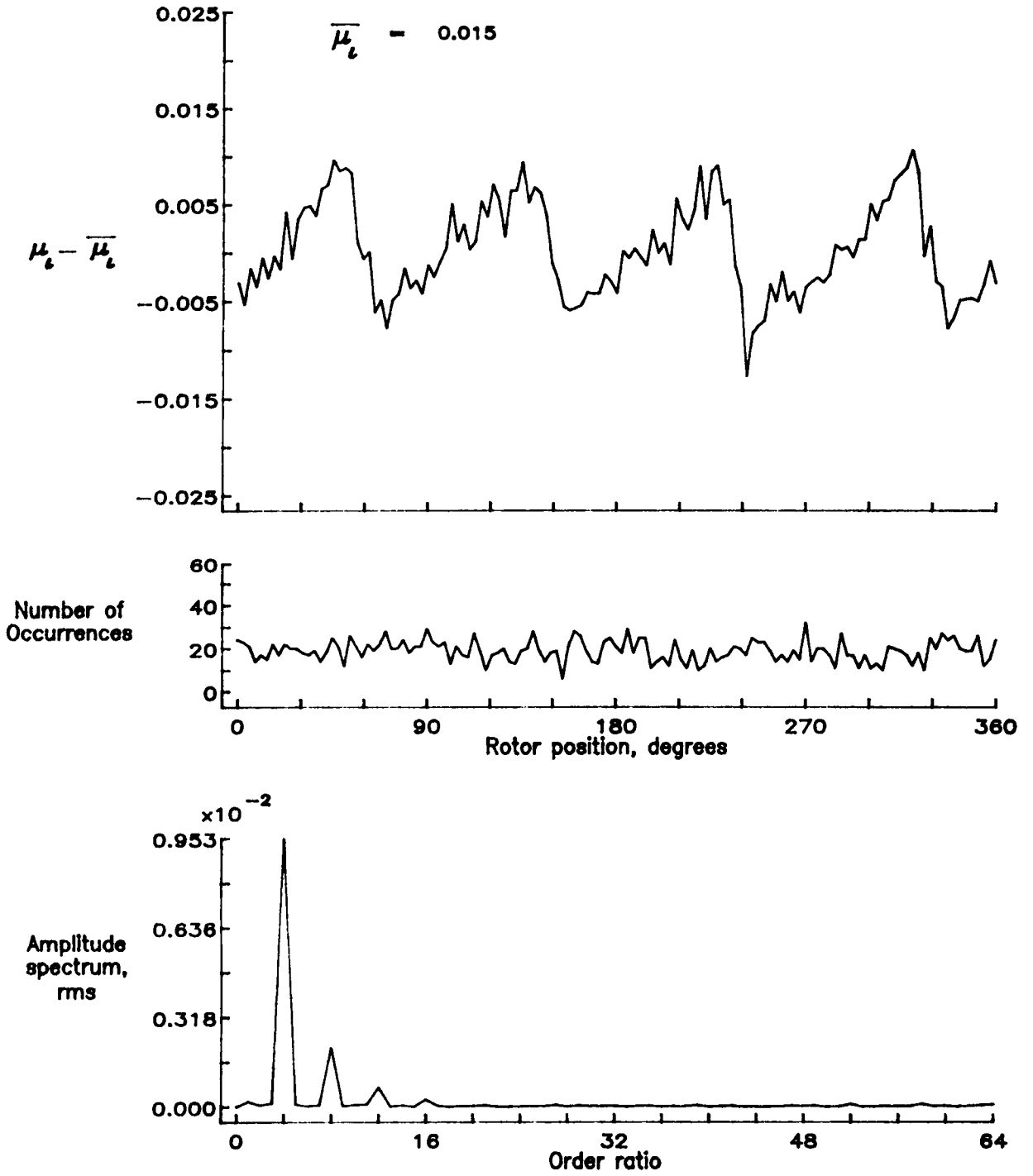

Figure 137.– Induced inflow velocity measured at 240 degrees and r/R of 0.70.

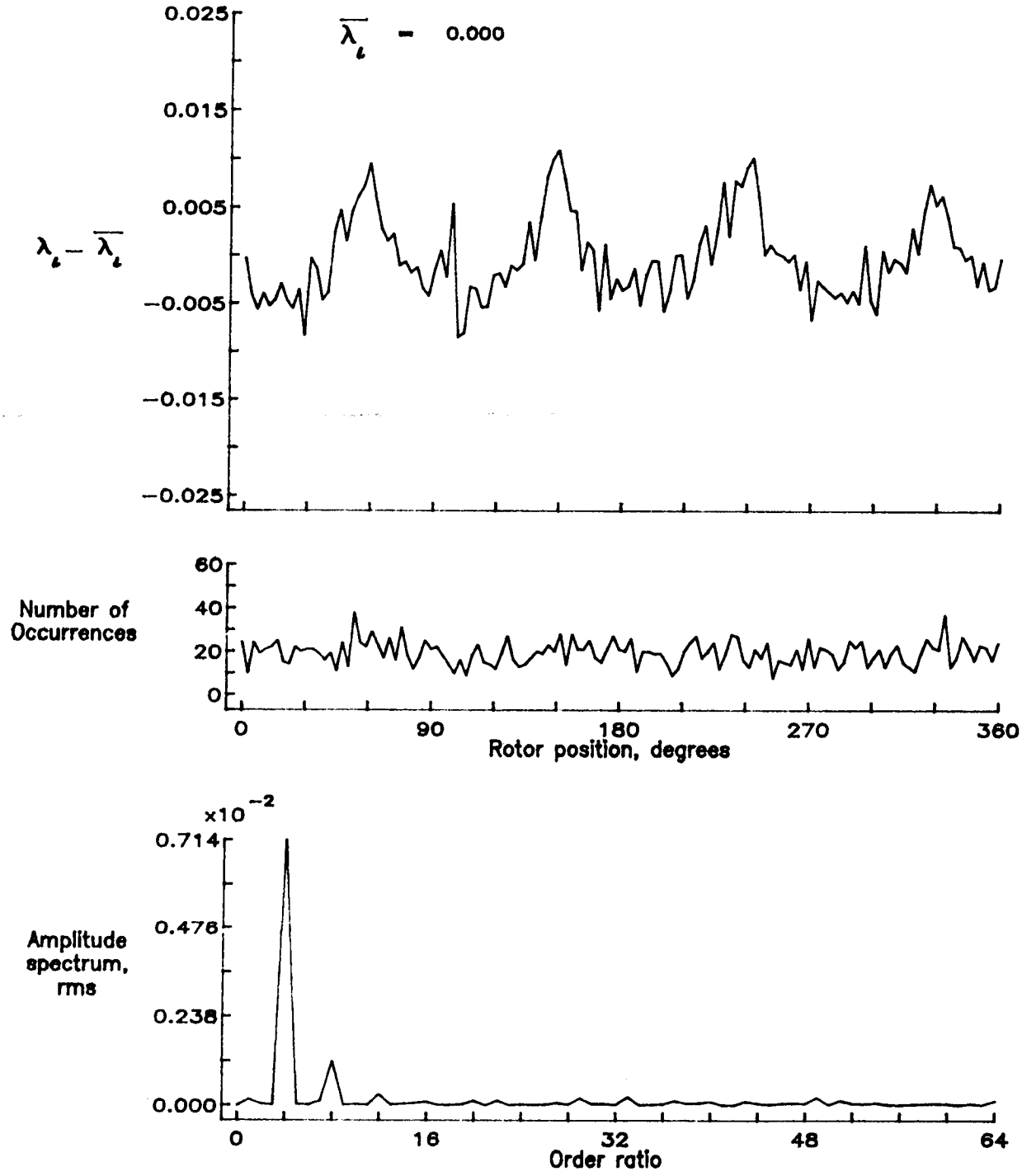

Figure 137.– Concluded.

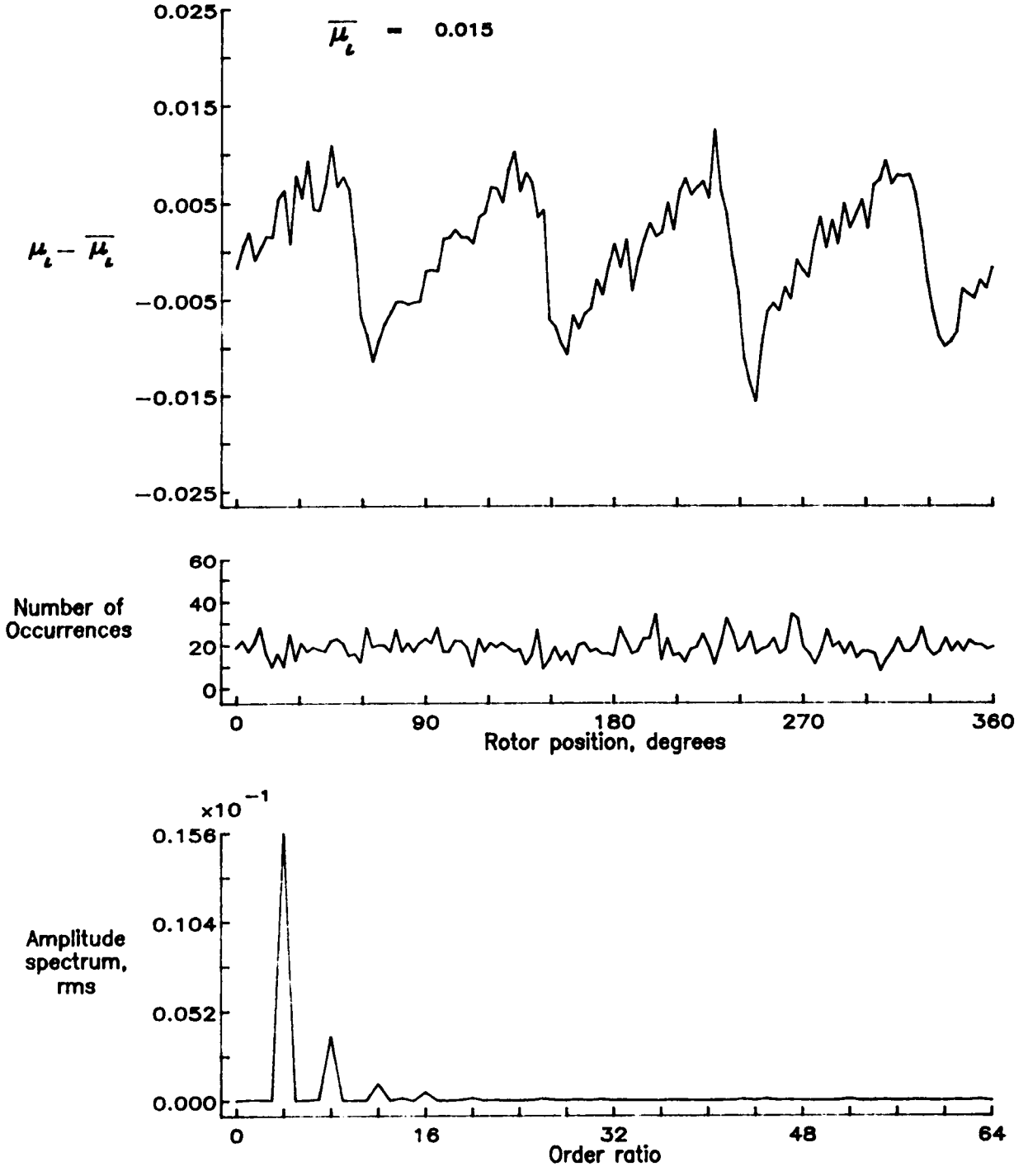

Figure 138.– Induced inflow velocity measured at 240 degrees and r/R of 0.74.

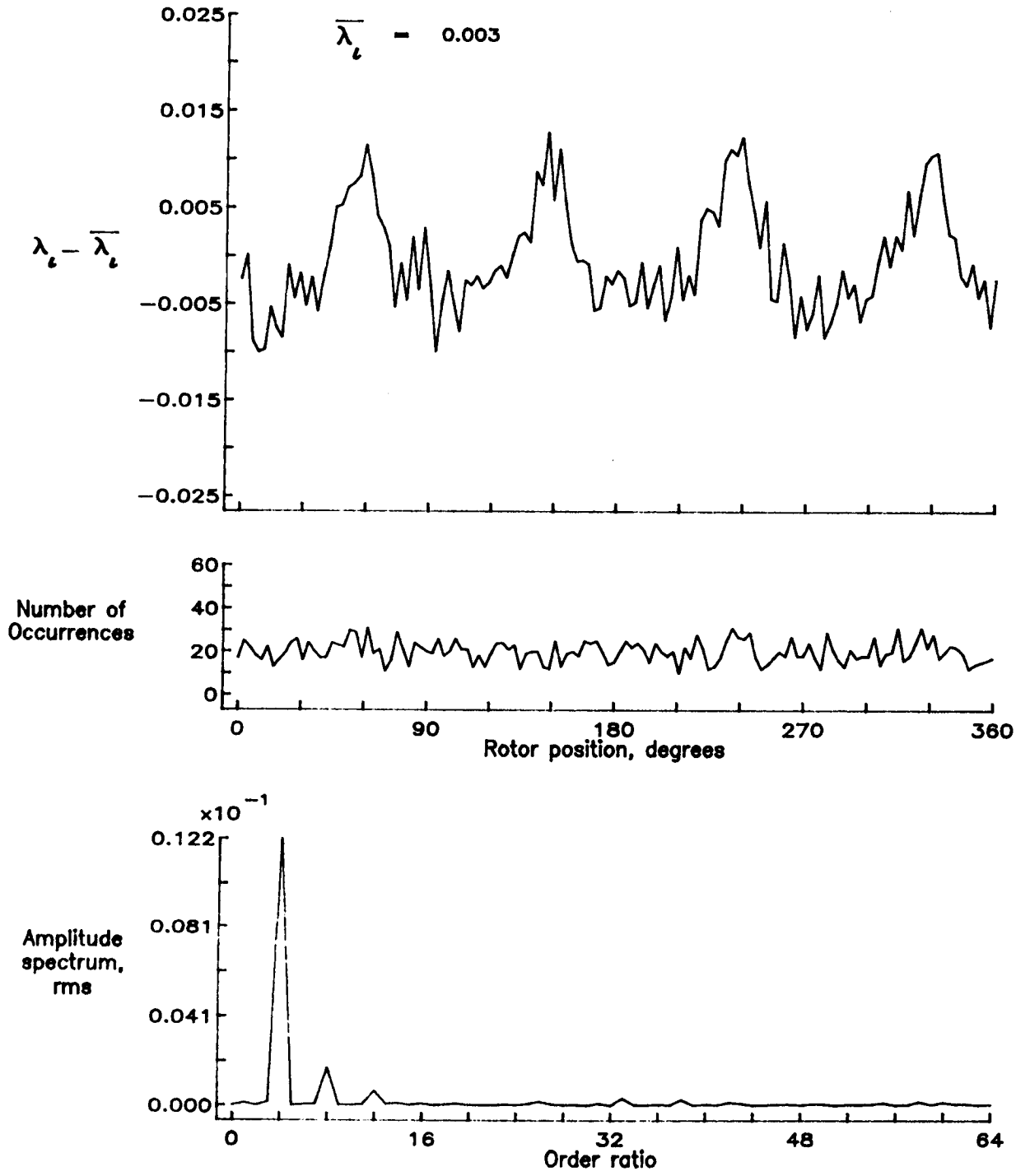

Figure 138.– Concluded.

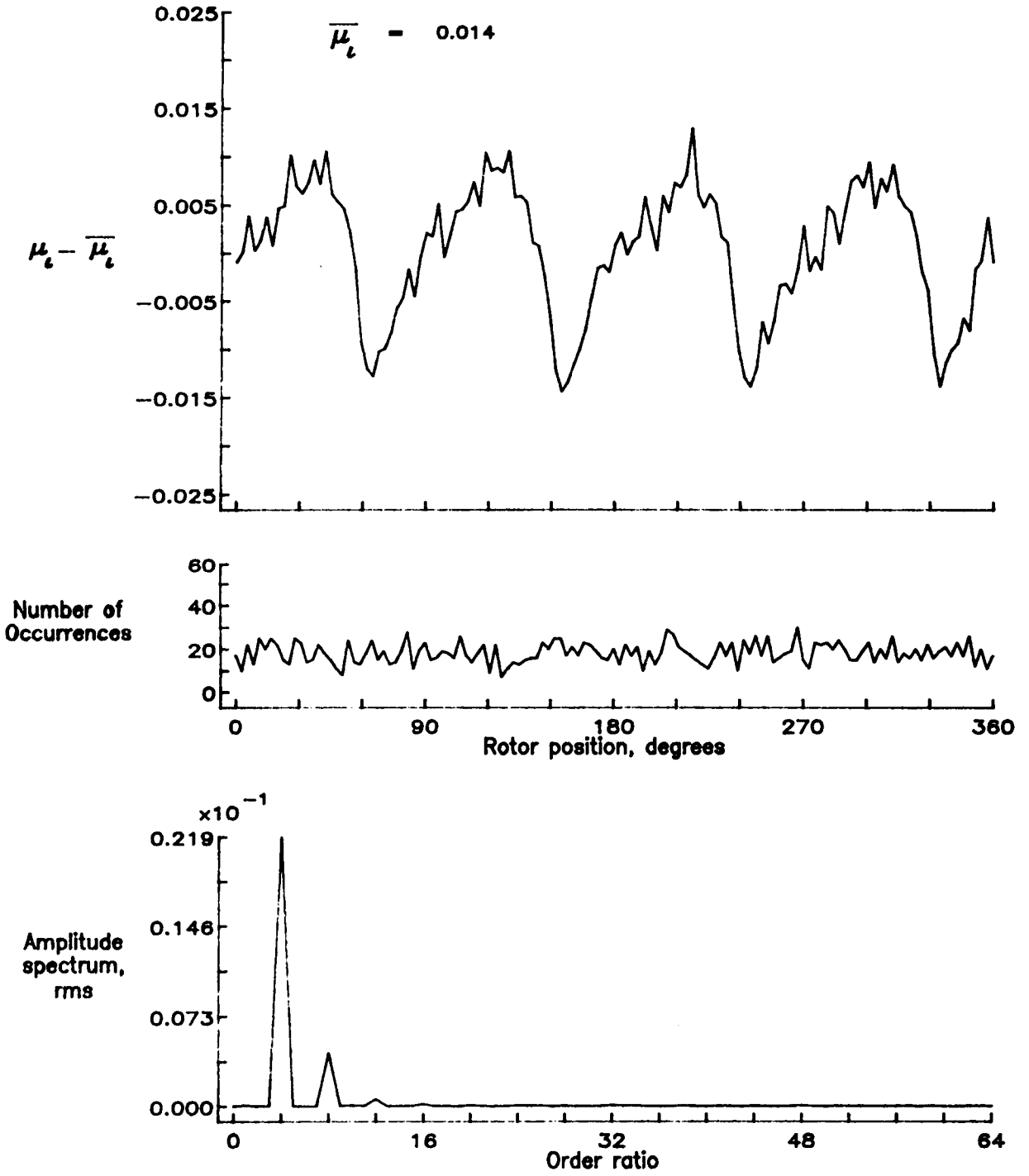

Figure 139.– Induced inflow velocity measured at 240 degrees and r/R of 0.78.

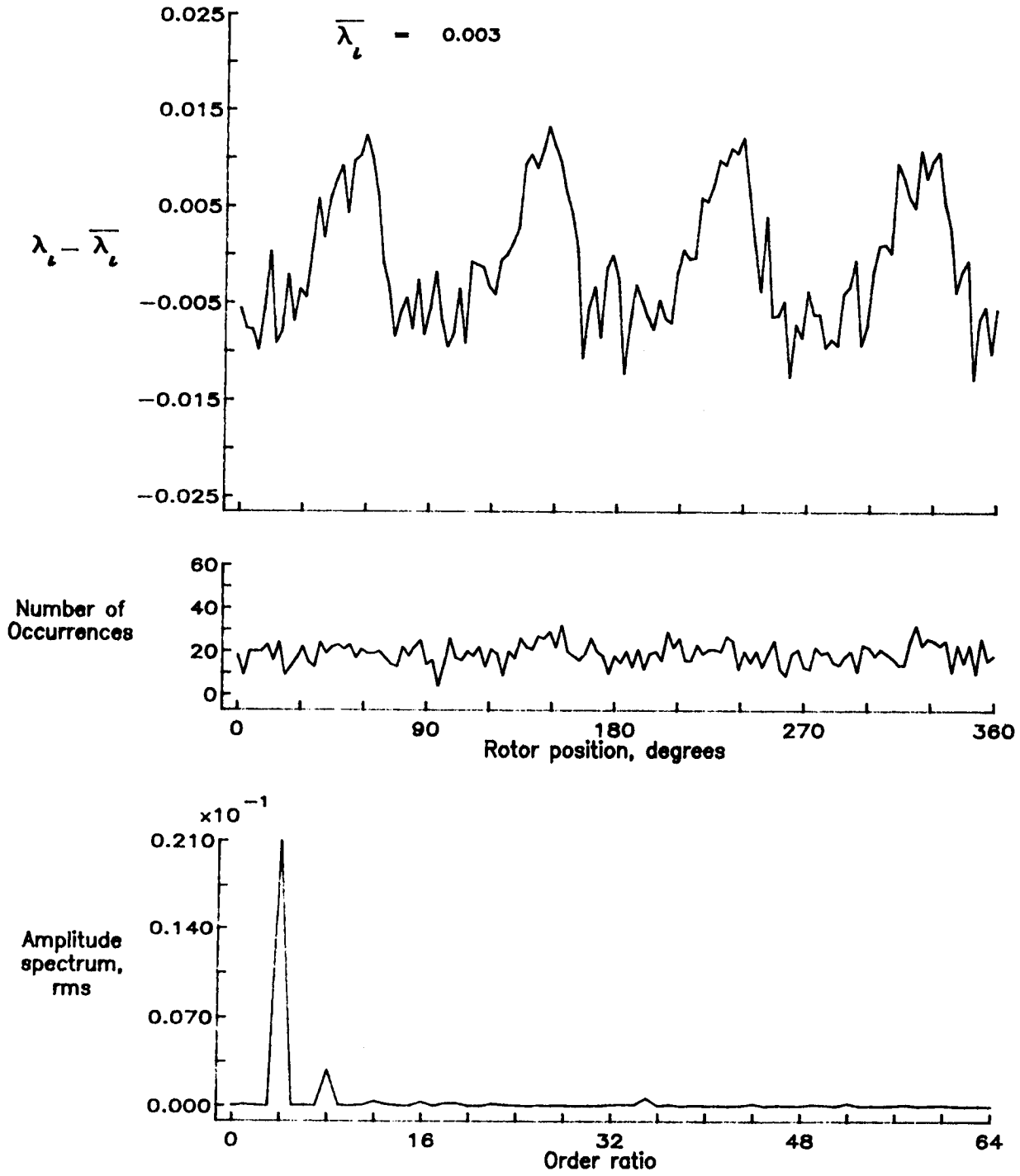

Figure 139.– Concluded.

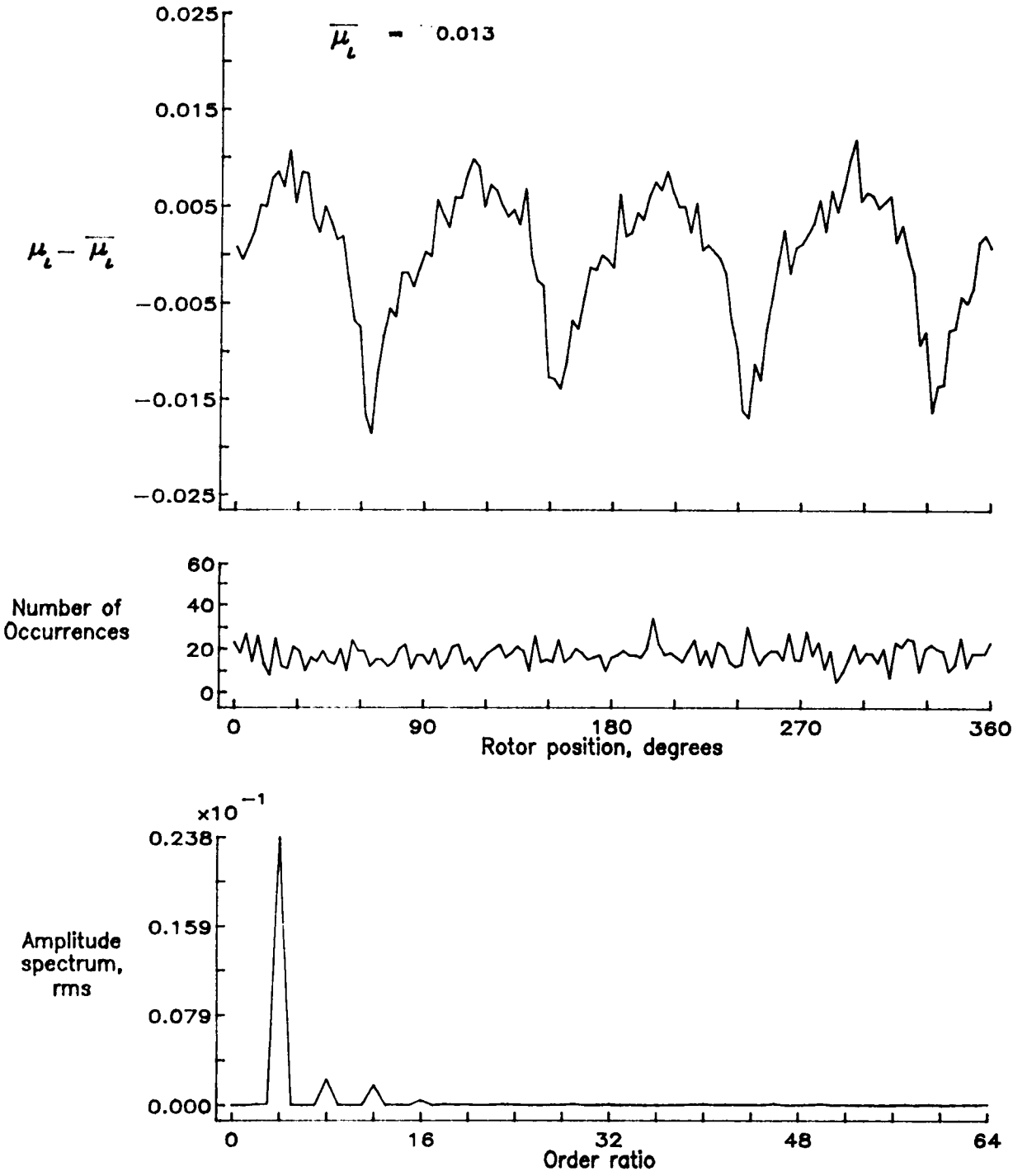

Figure 140.– Induced inflow velocity measured at 240 degrees and r/R of 0.82.

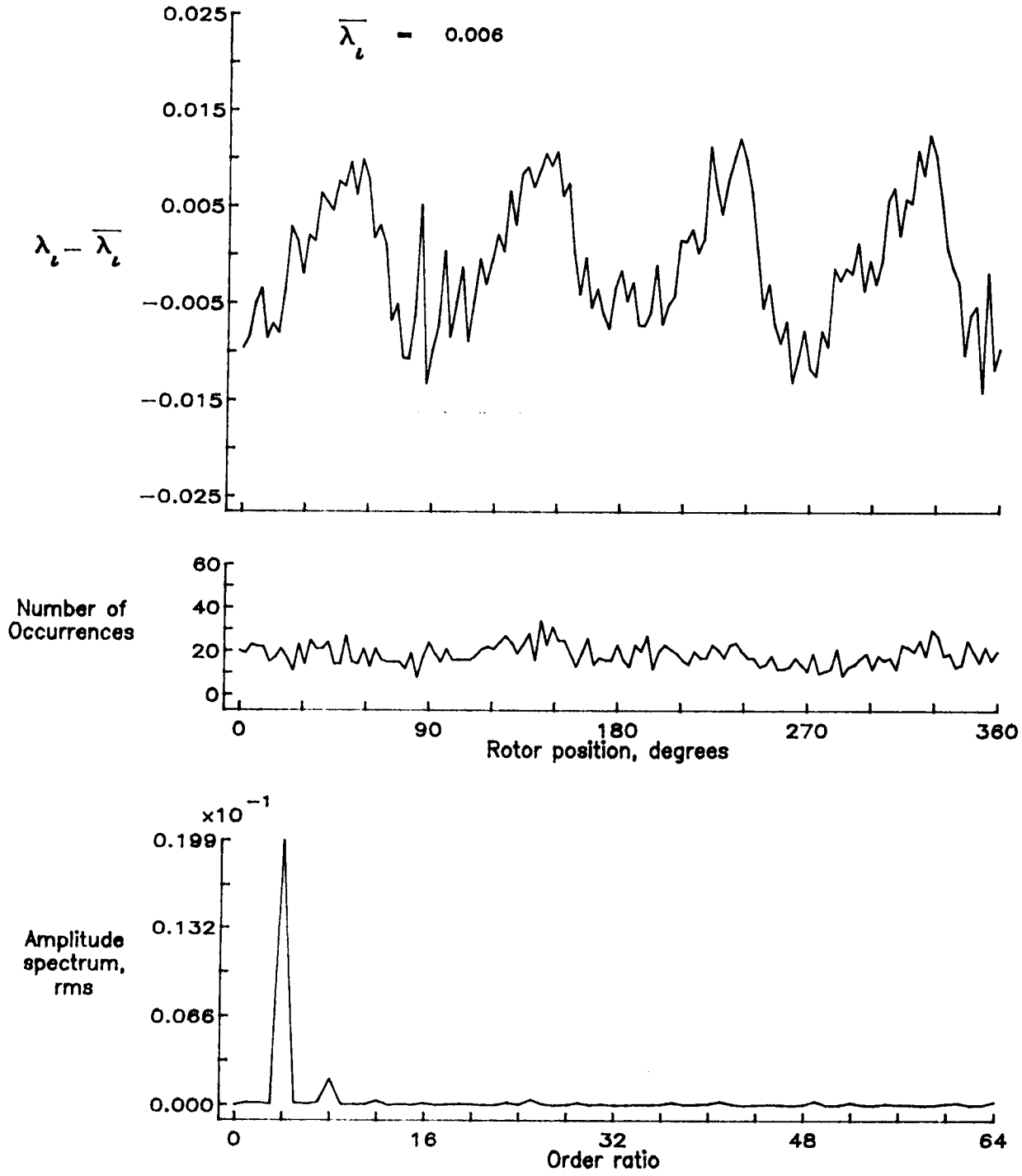

Figure 140.– Concluded.

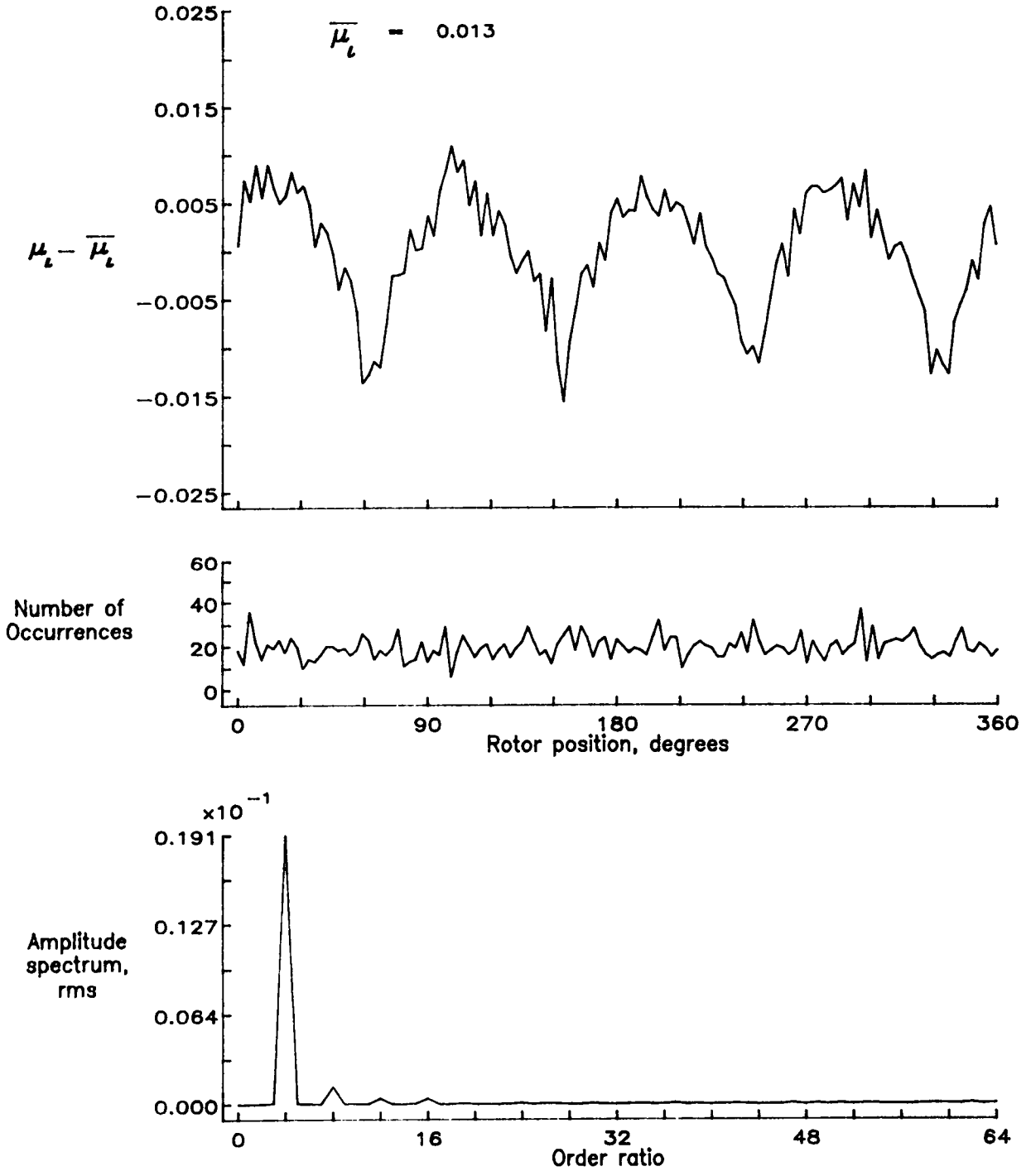

Figure 141.– Induced inflow velocity measured at 240 degrees and r/R of 0.86.

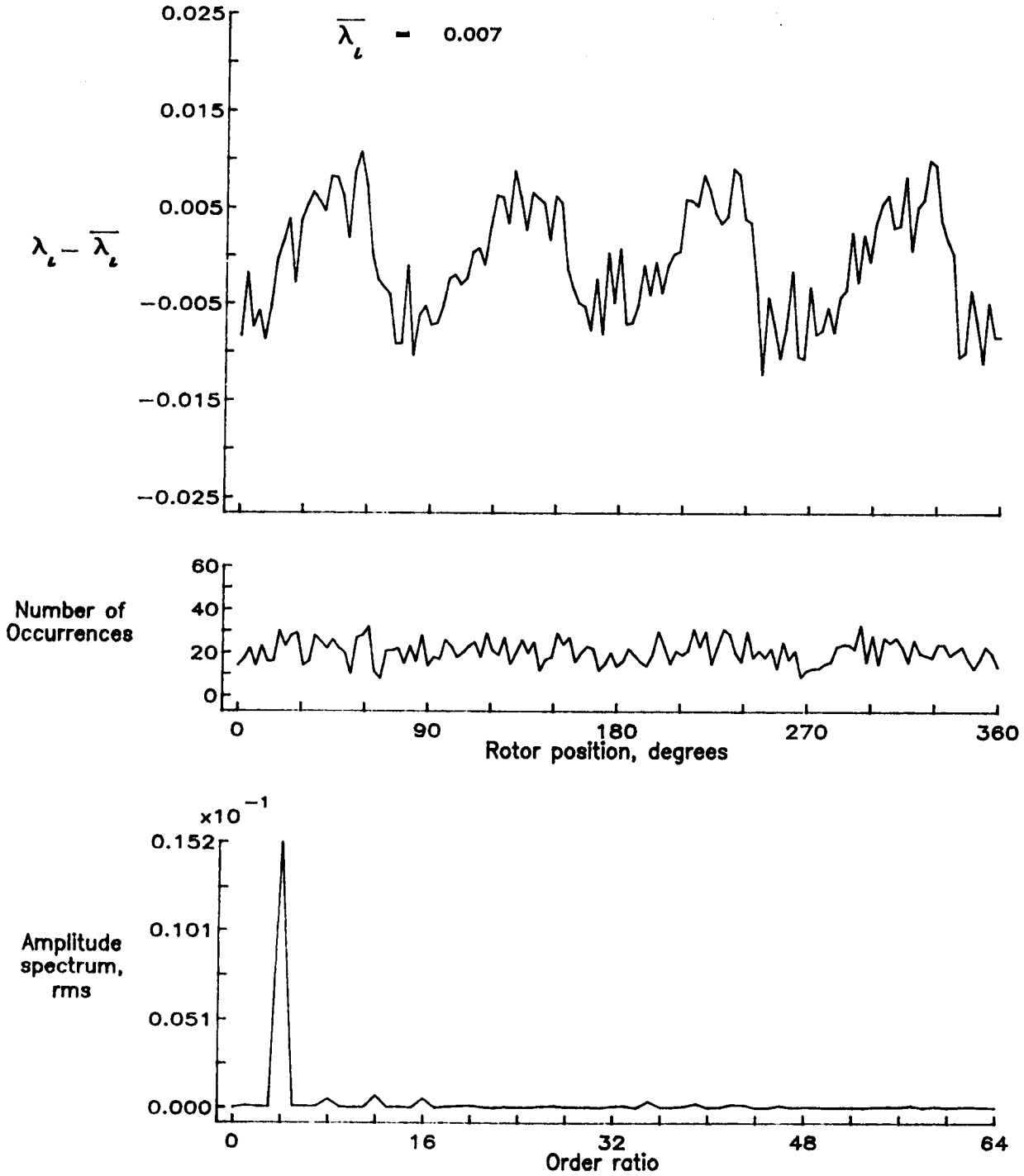

Figure 141.– Concluded.

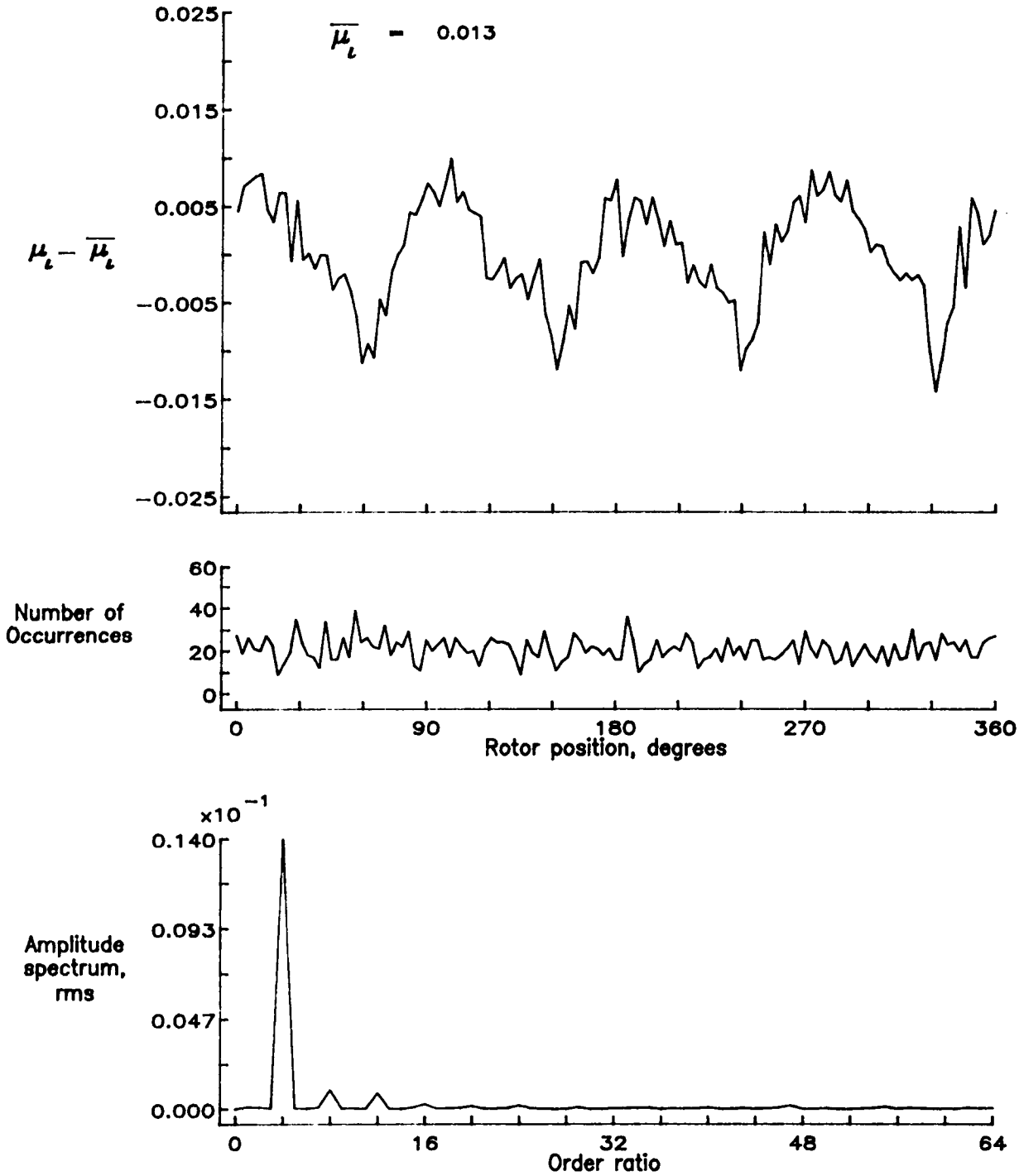

Figure 142.– Induced inflow velocity measured at 240 degrees and r/R of 0.90.

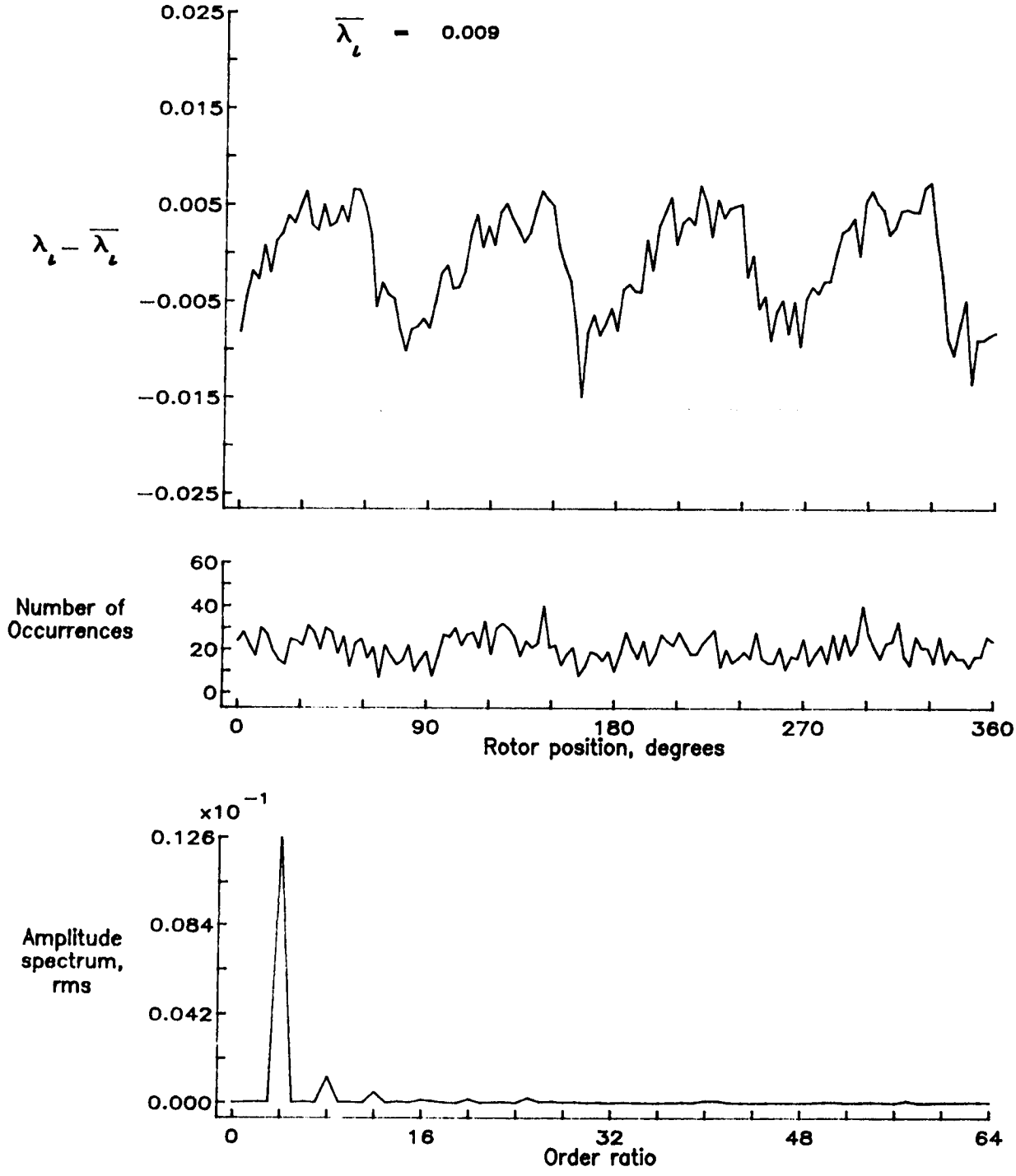

Figure 142.– Concluded.

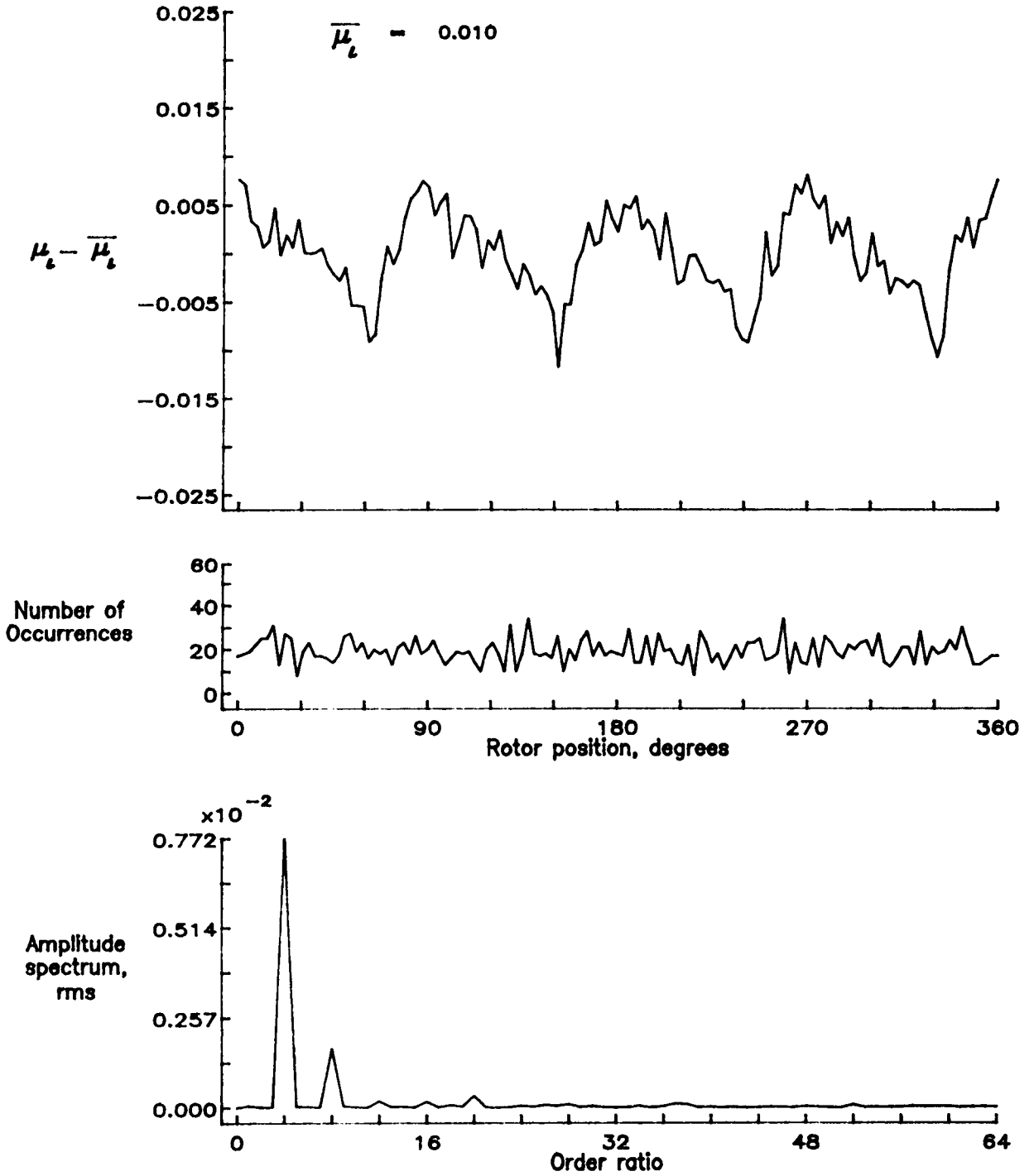

Figure 143.– Induced inflow velocity measured at 240 degrees and r/R of 0.94.

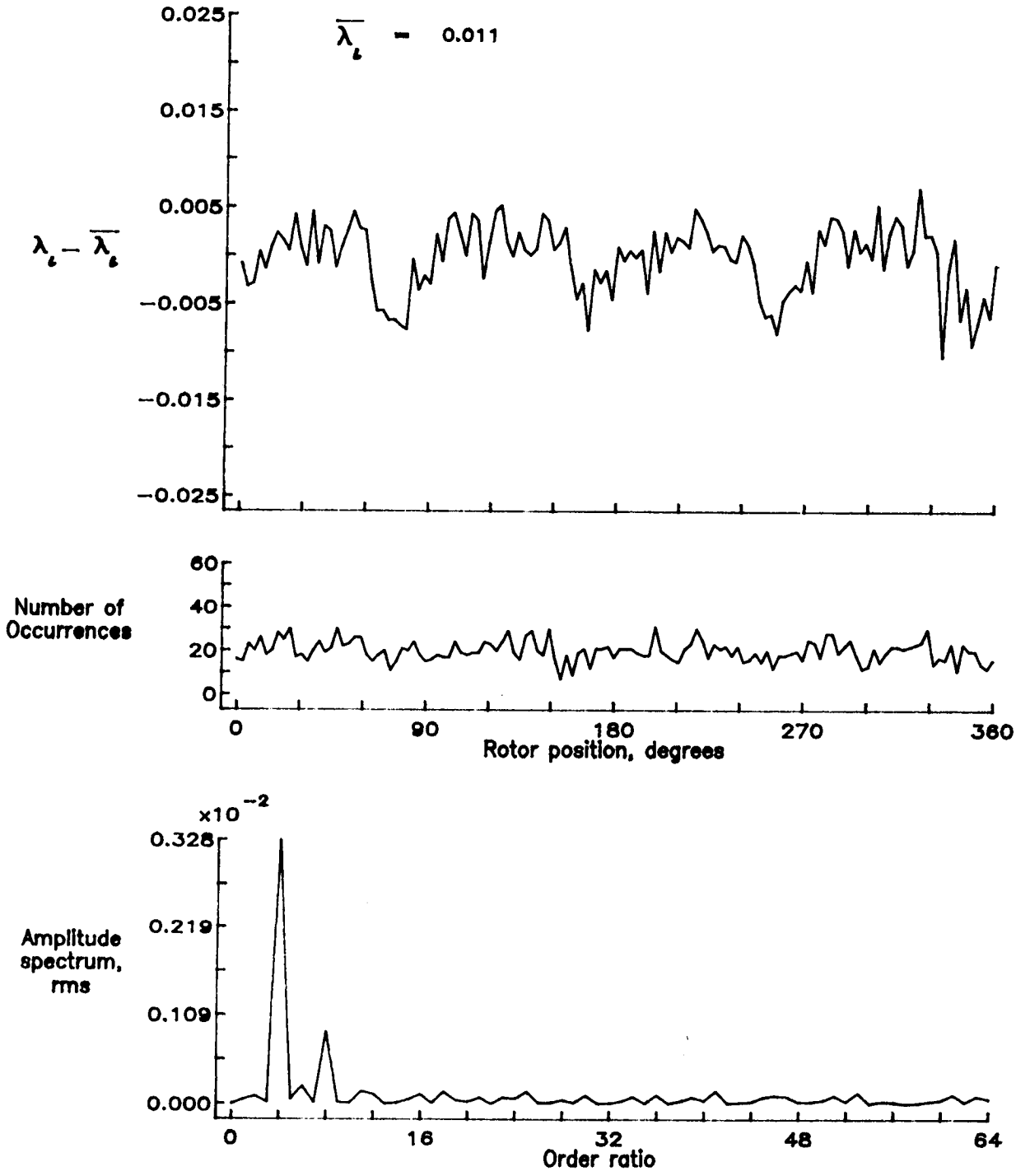

Figure 143.– Concluded.

C-4

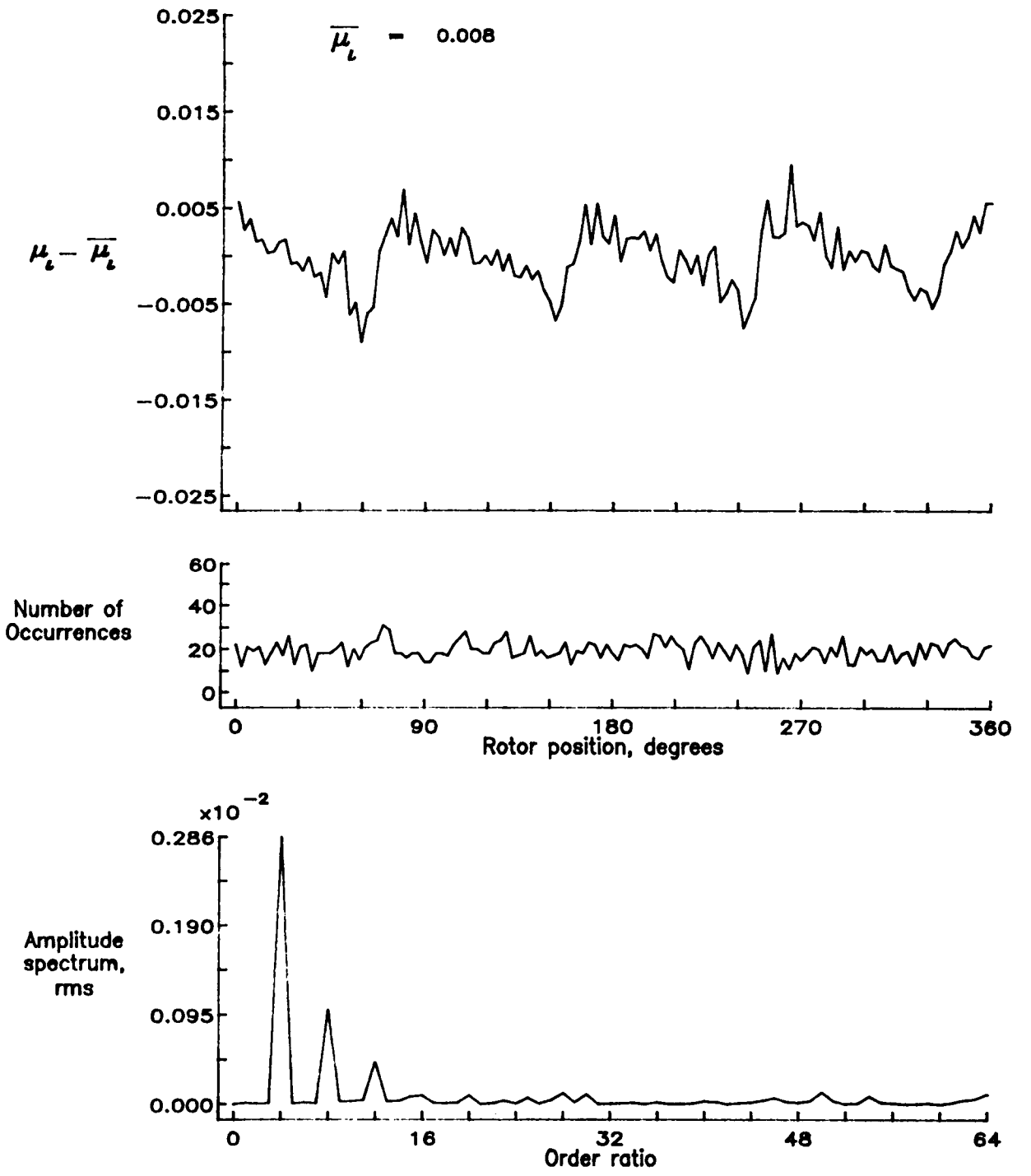

Figure 144.– Induced inflow velocity measured at 240 degrees and r/R of 0.98.

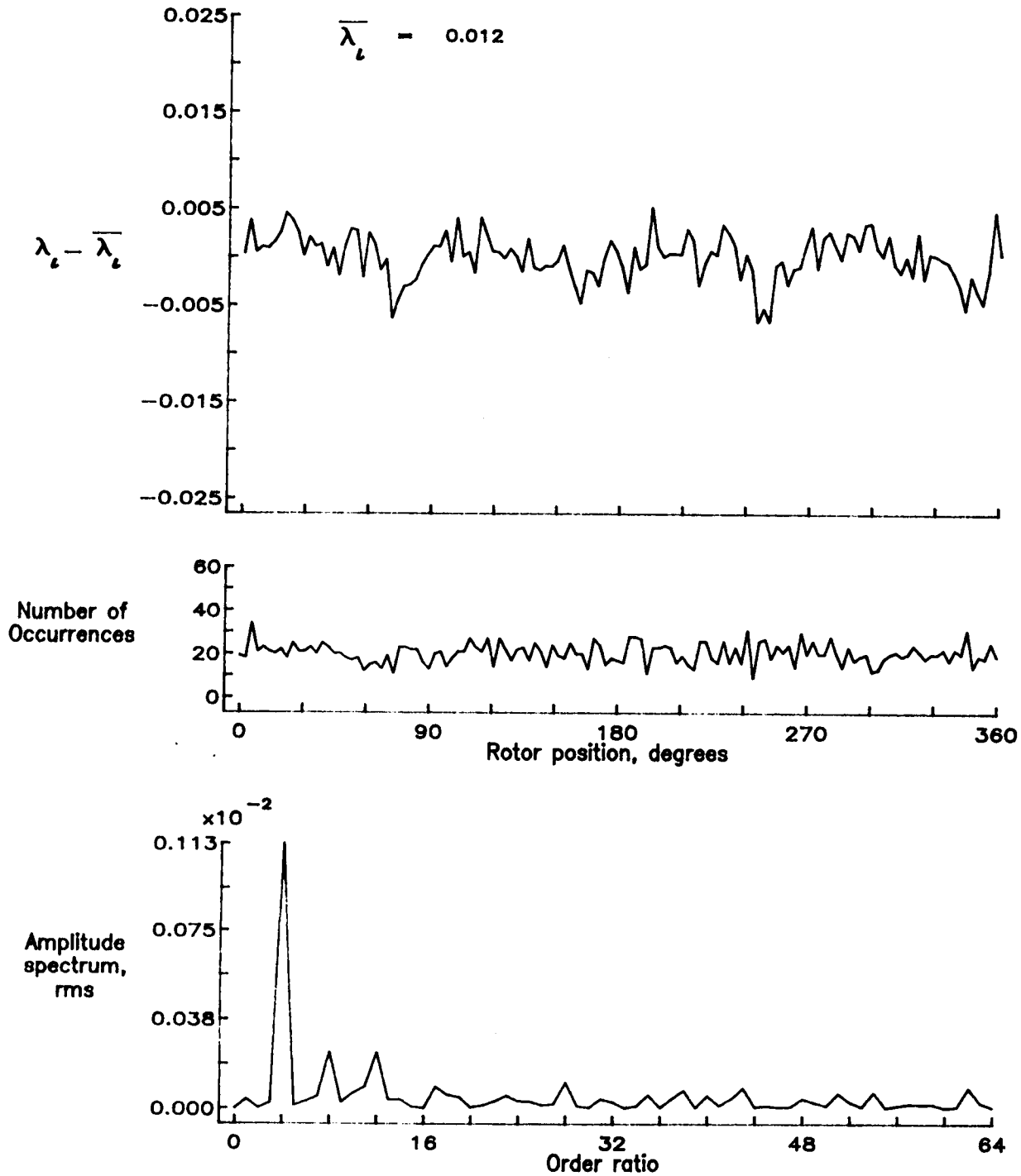

Figure 144.– Concluded.

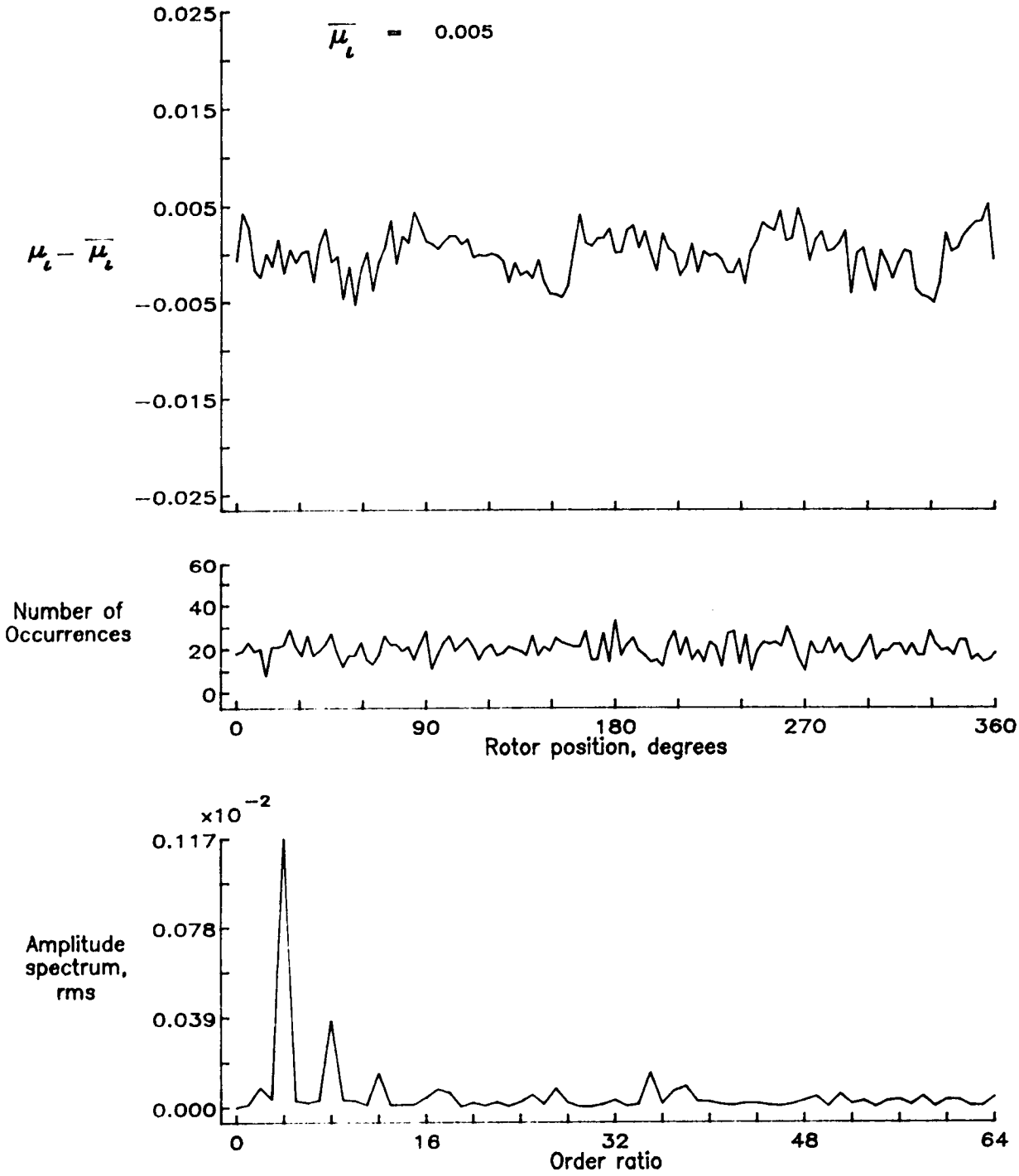

Figure 145.– Induced inflow velocity measured at 240 degrees and r/R of 1.02.

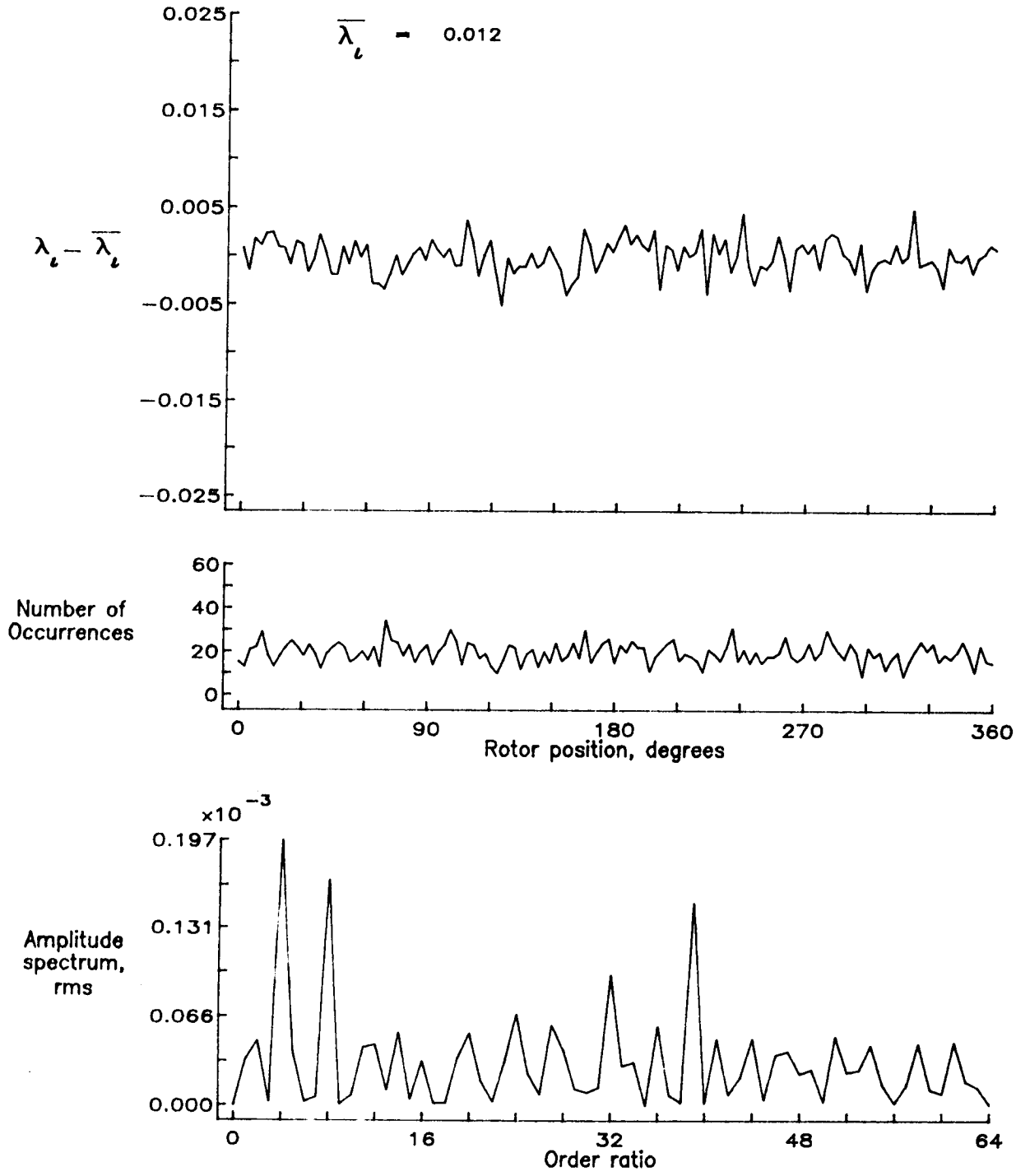

Figure 145.– Concluded.

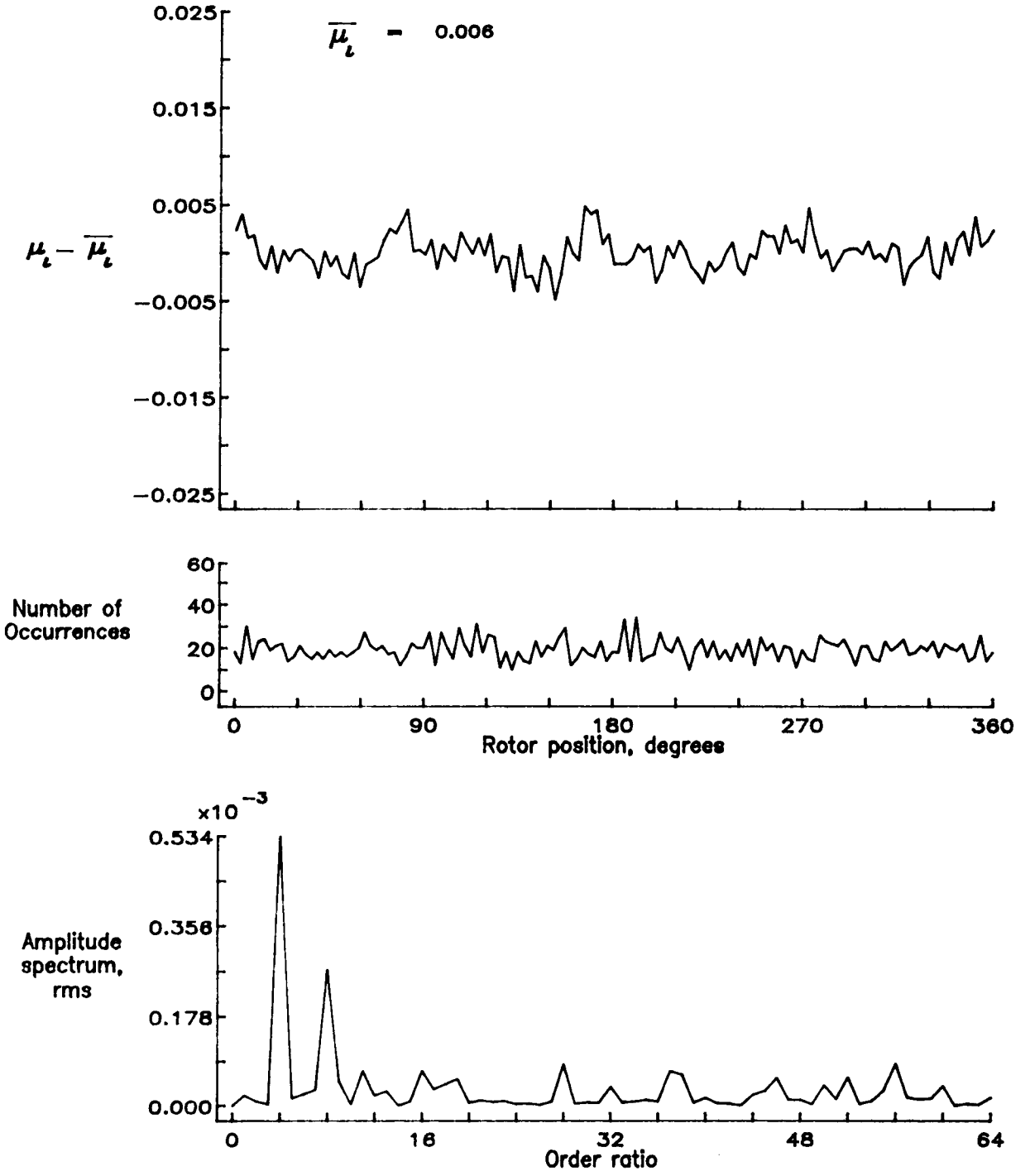

Figure 146.– Induced inflow velocity measured at 240 degrees and r/R of 1.04.

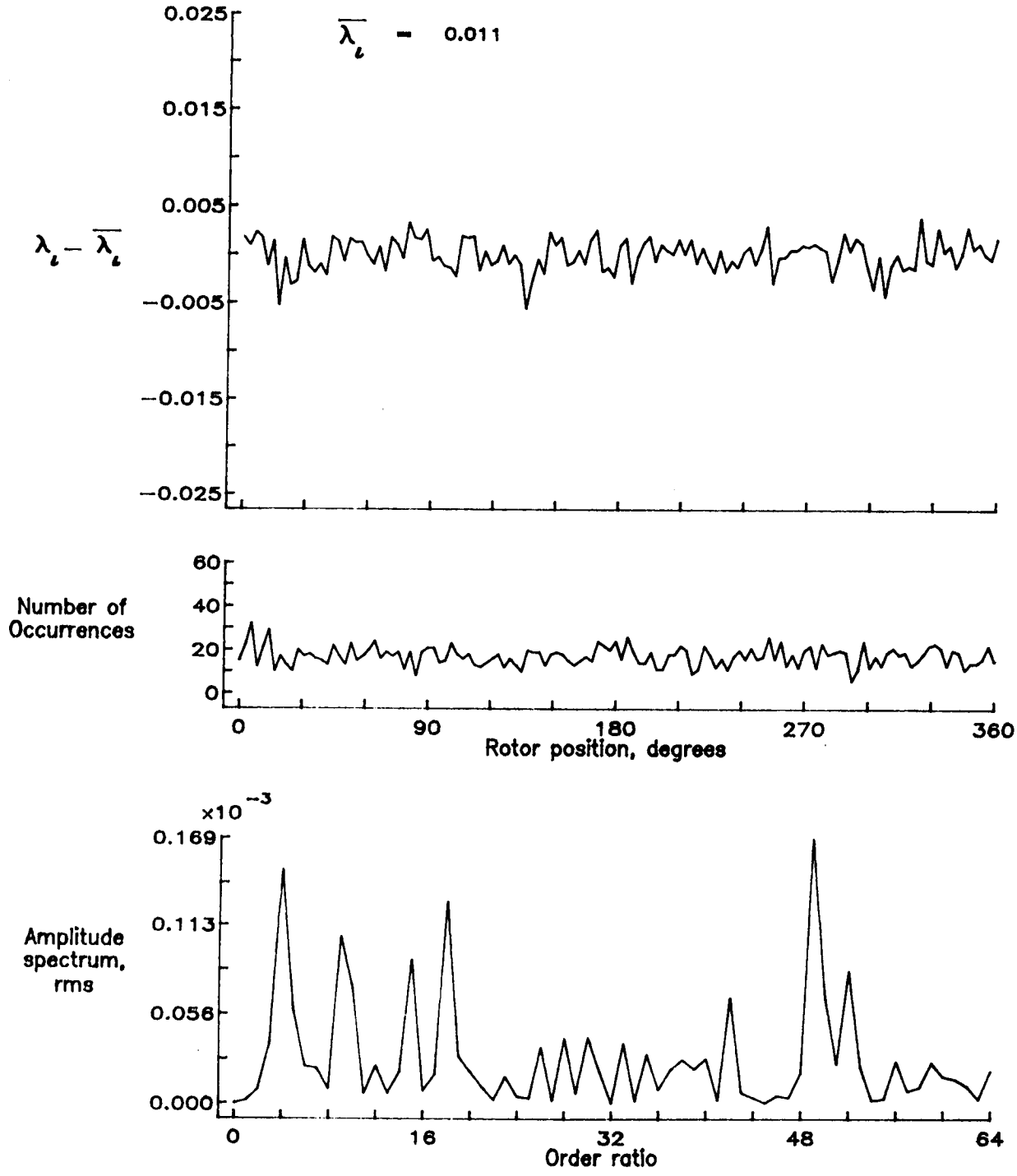

Figure 146.– Concluded.

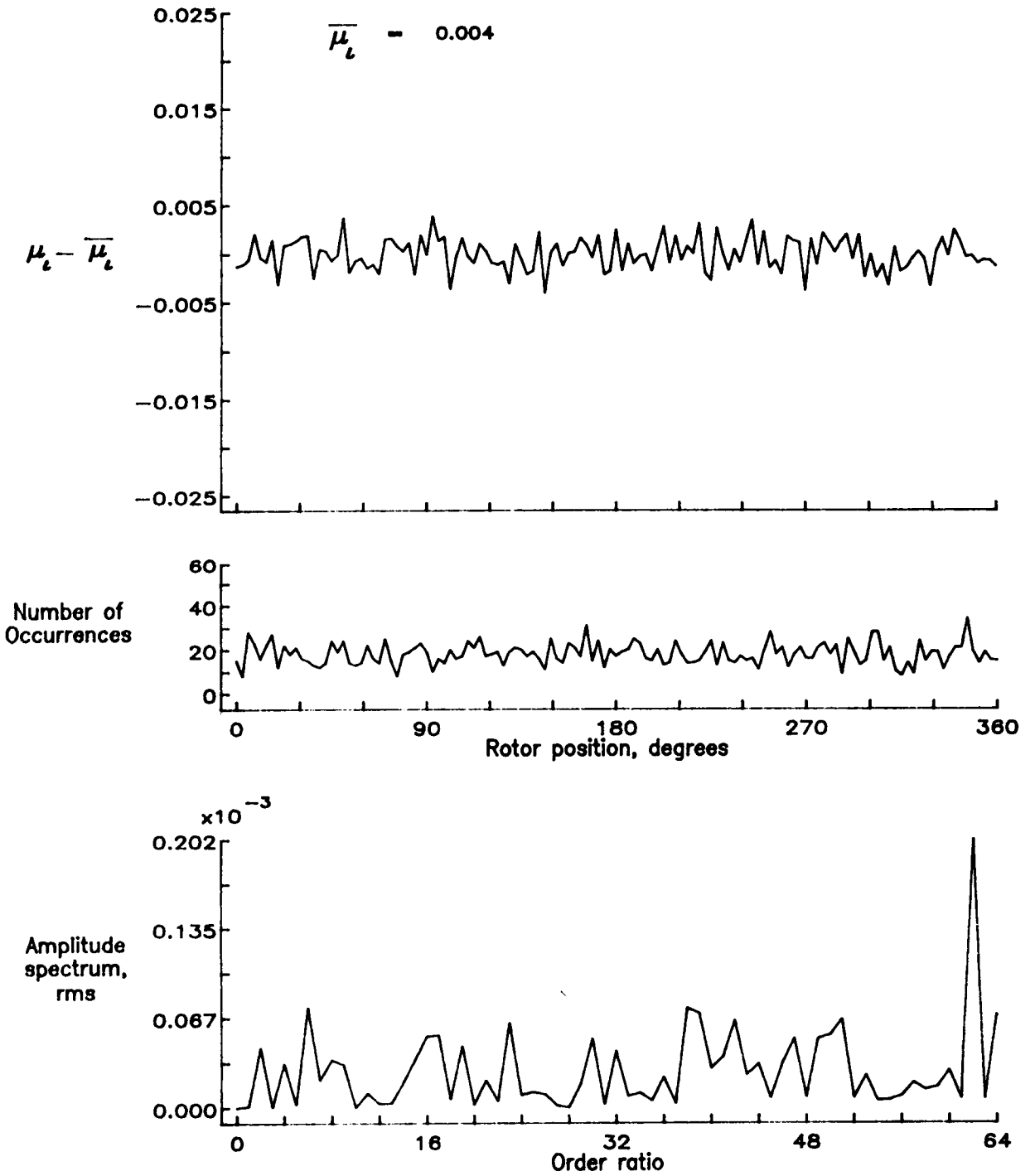

Figure 147.– Induced inflow velocity measured at 240 degrees and r/R of 1.10.

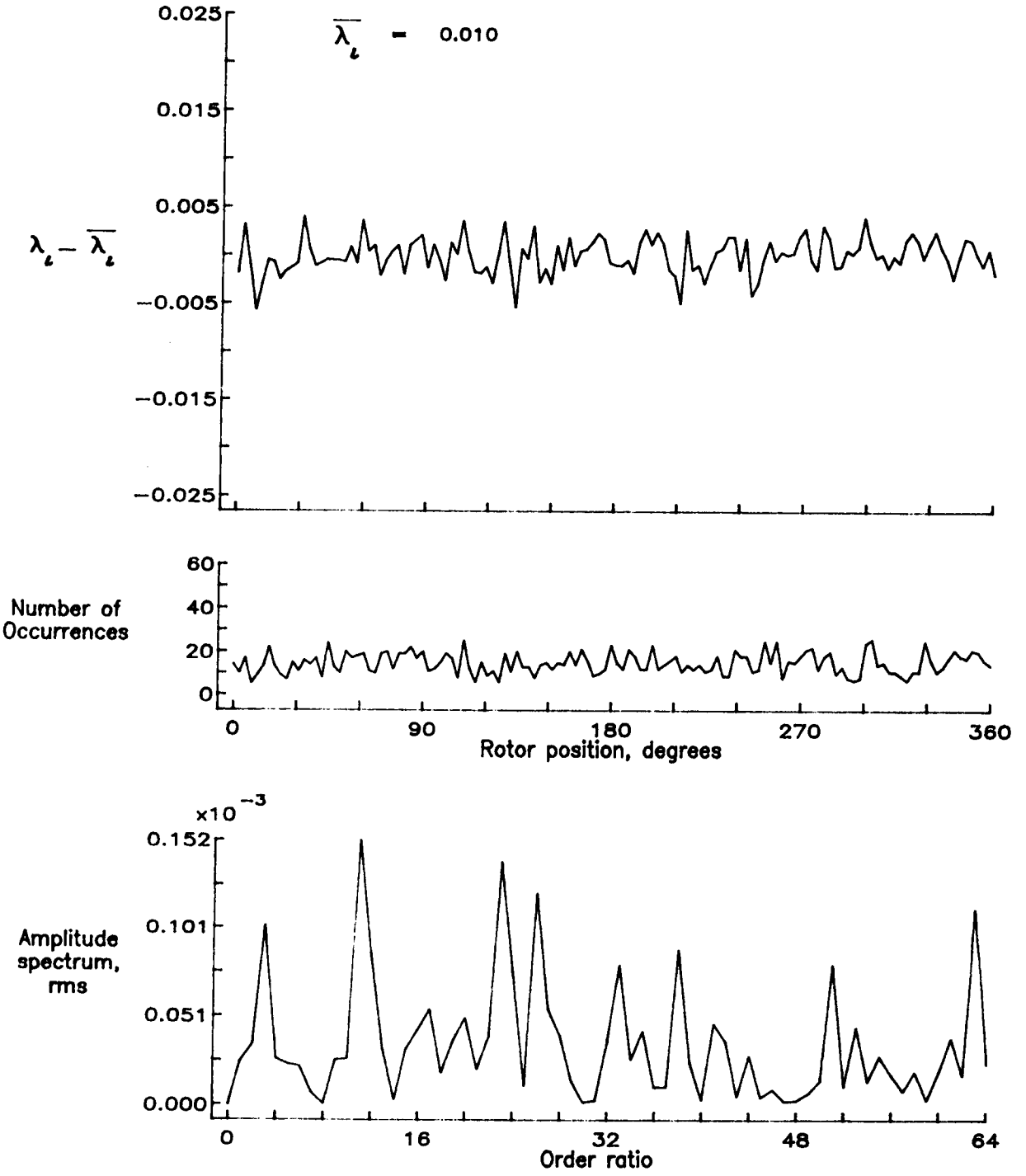

Figure 147.– Concluded.

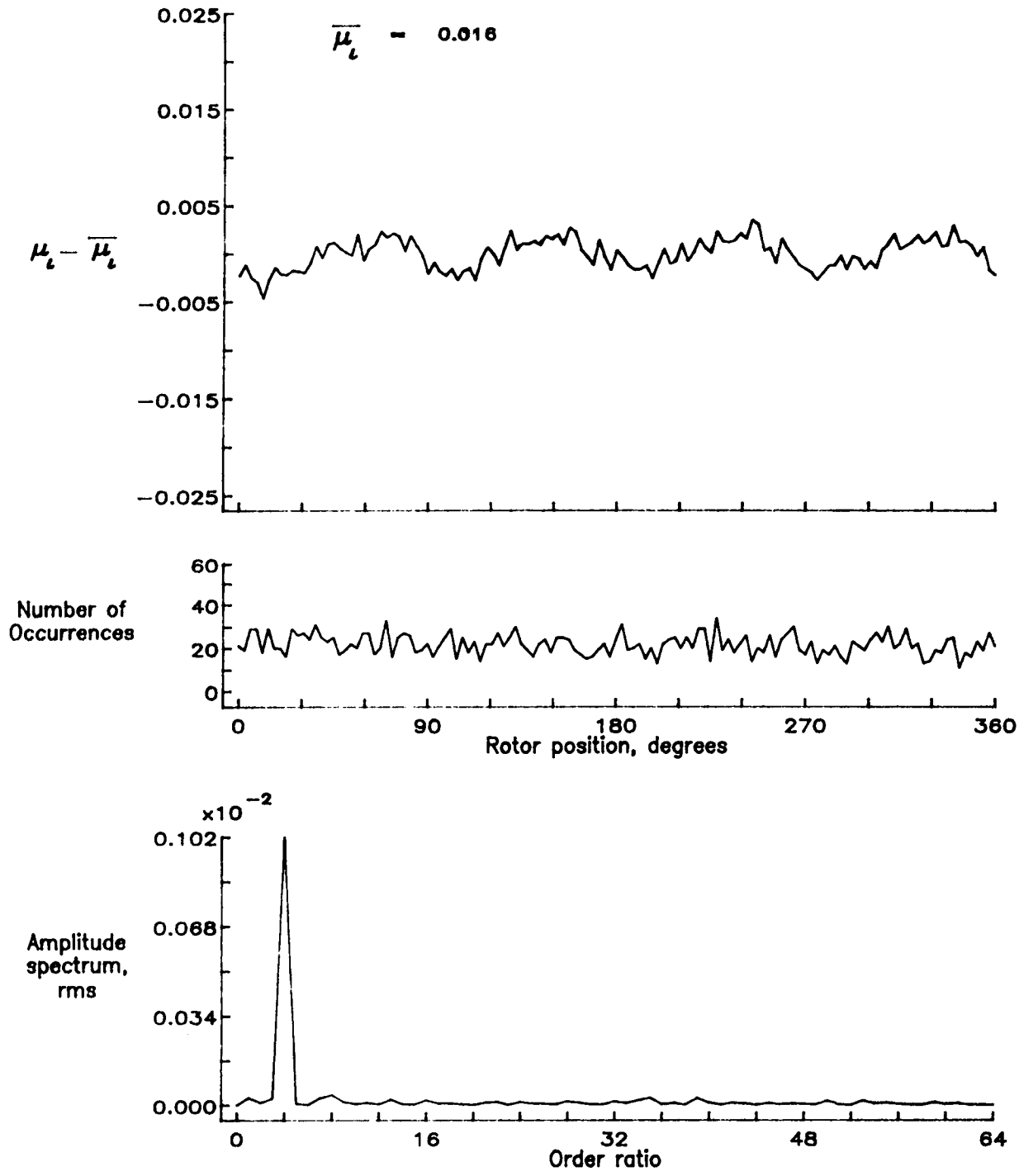

Figure 148.– Induced inflow velocity measured at 270 degrees and r/R of 0.20.

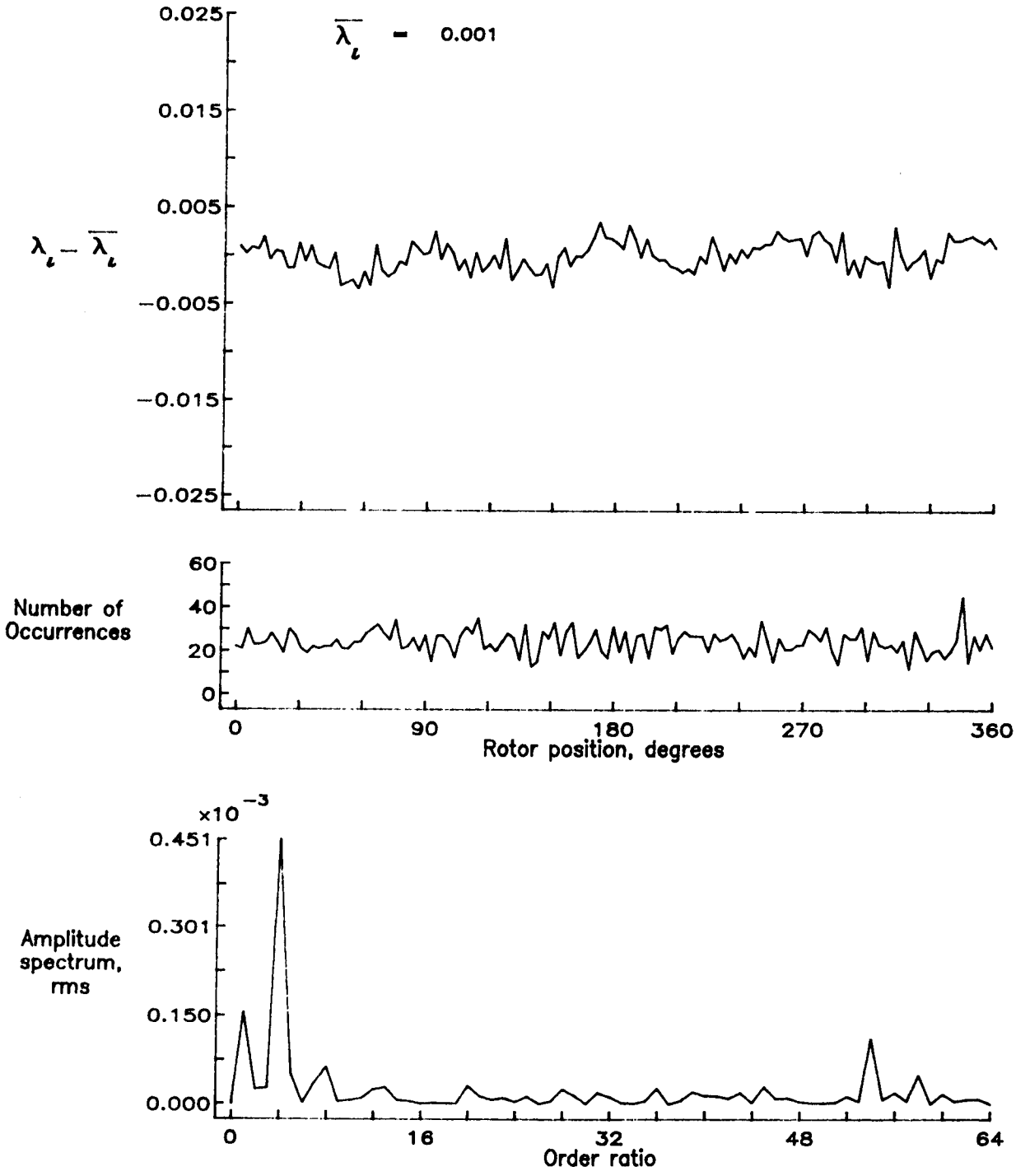

Figure 148.– Concluded.

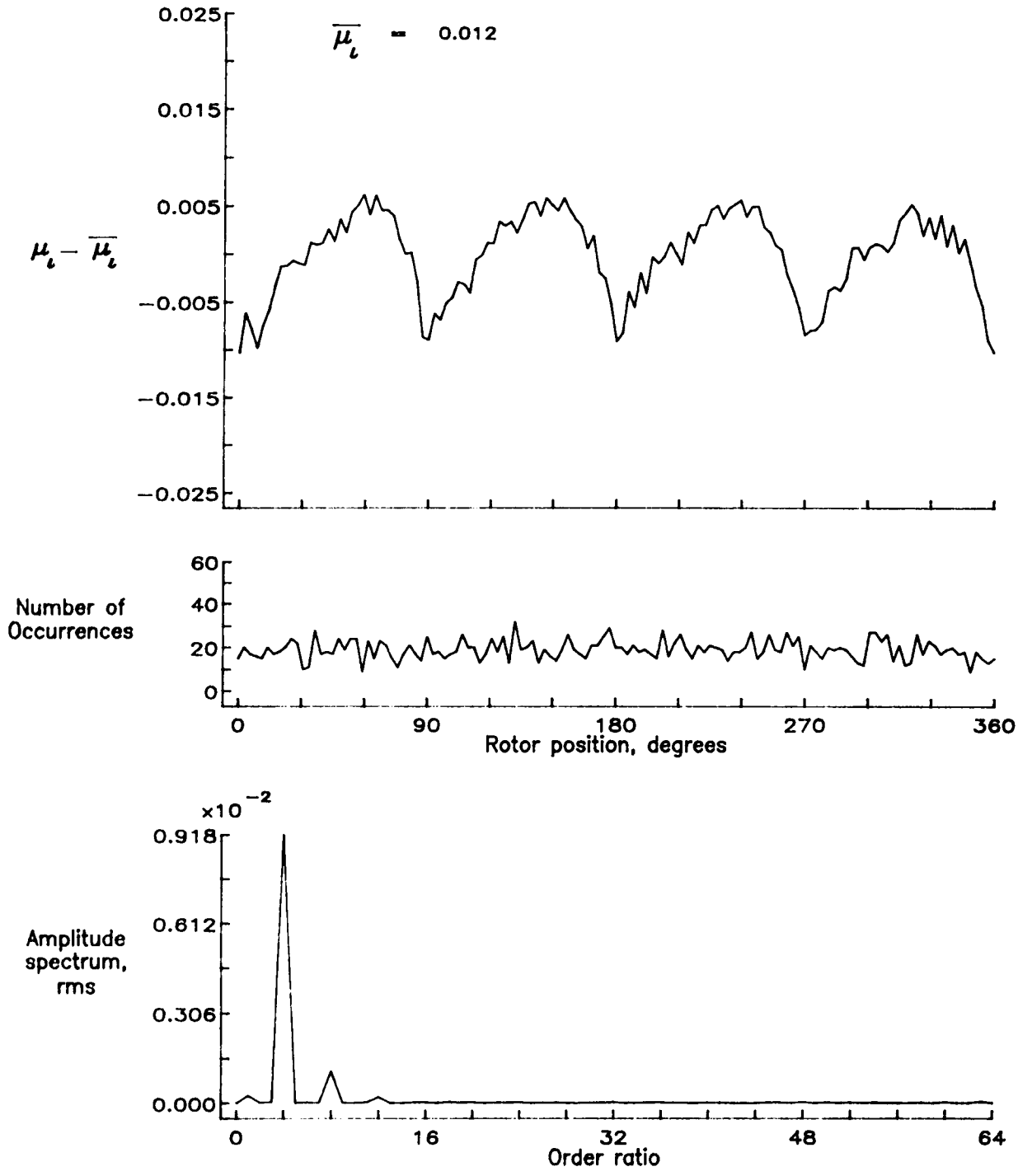

Figure 149.– Induced inflow velocity measured at 270 degrees and r/R of 0.40.

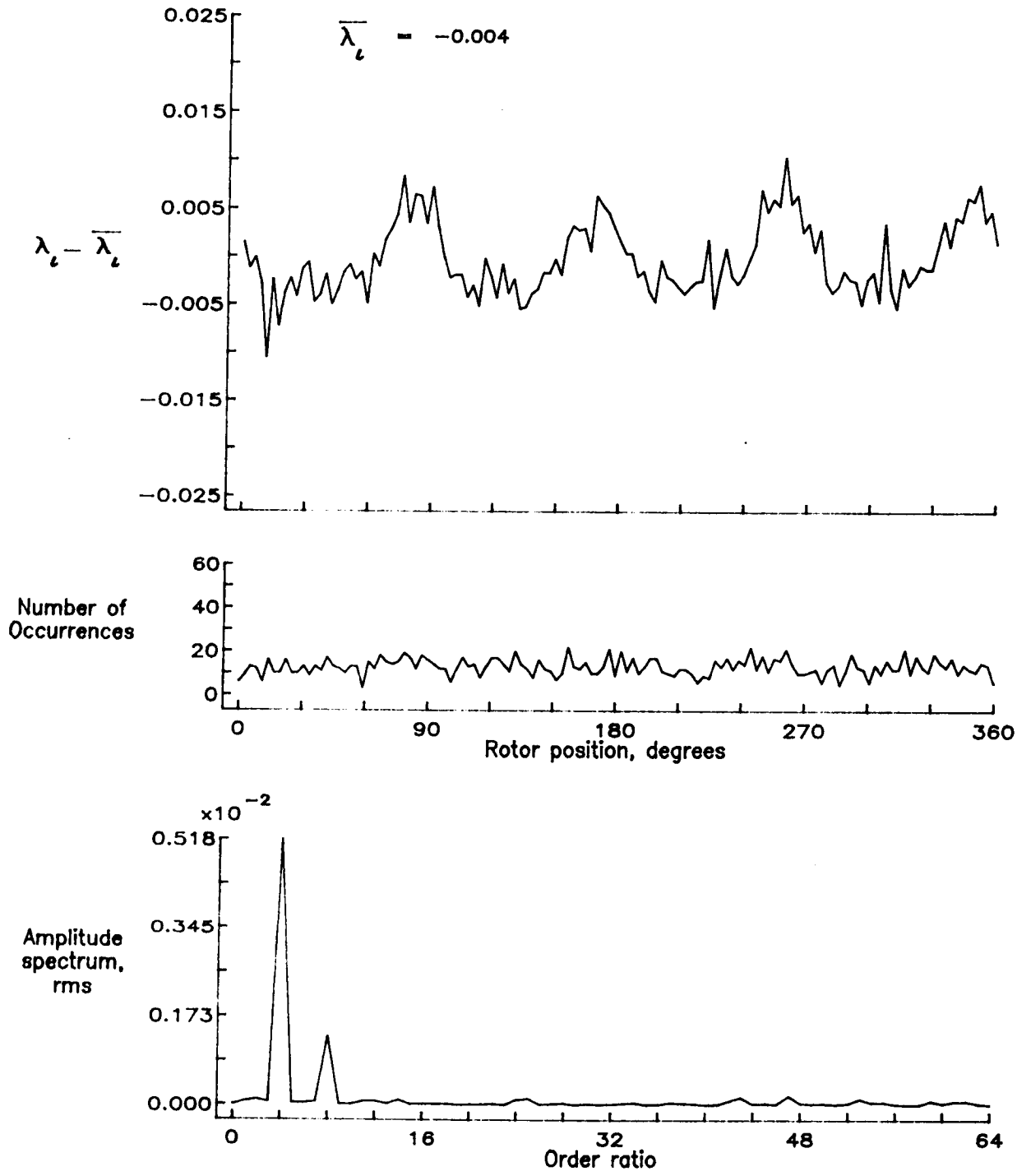

Figure 149.– Concluded.

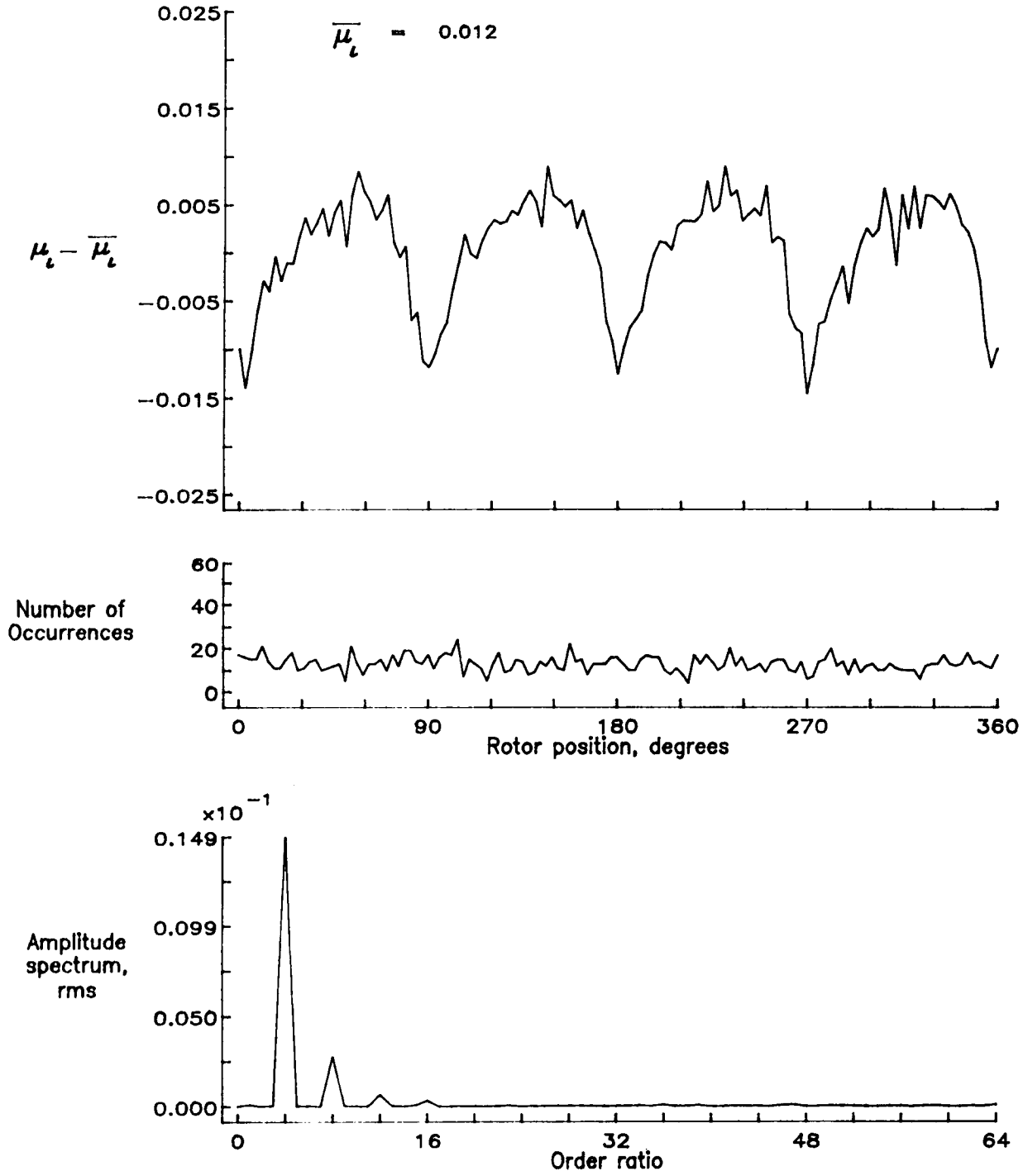

Figure 150.– Induced inflow velocity measured at 270 degrees and r/R of 0.50.

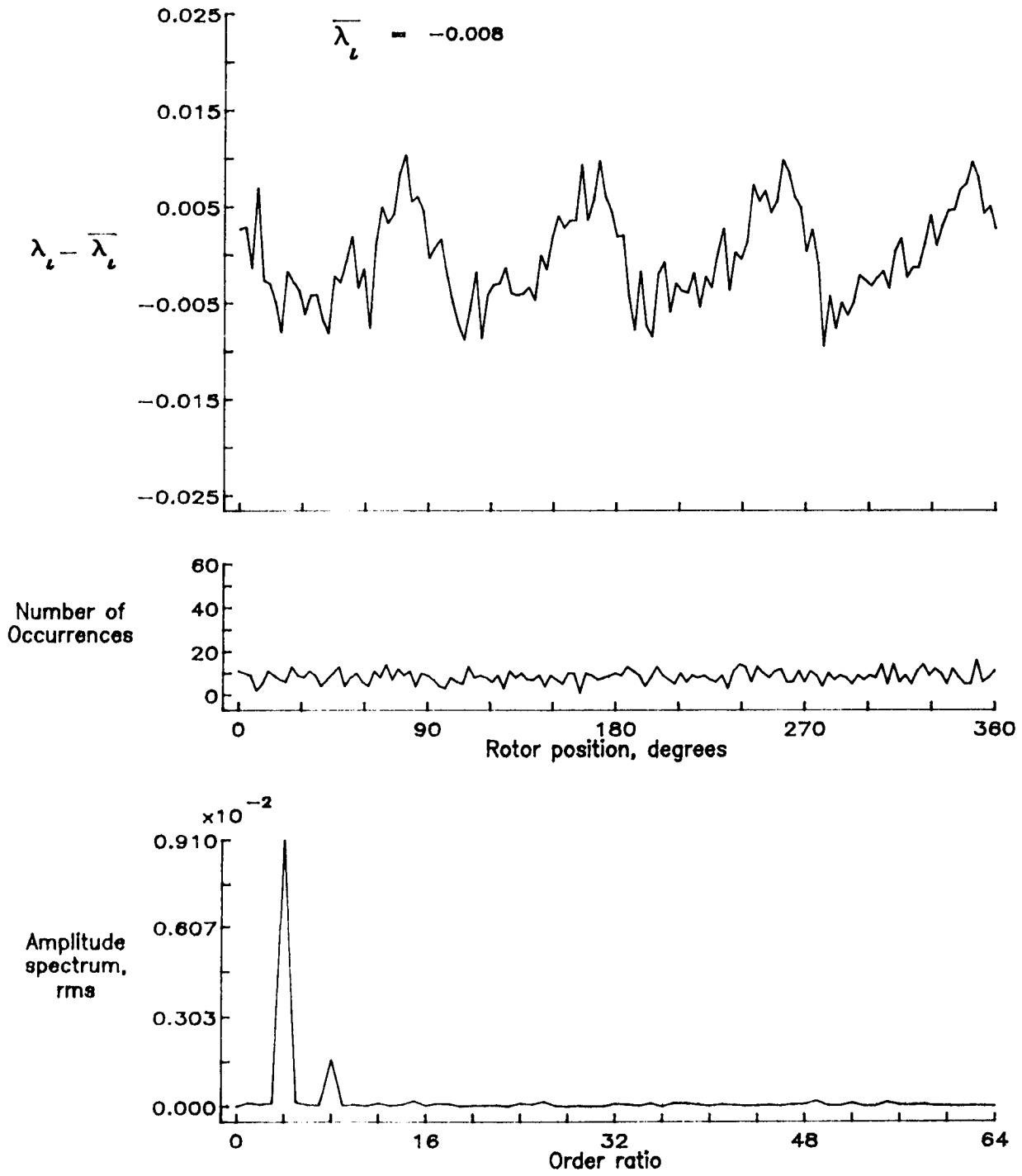

Figure 150.– Concluded.

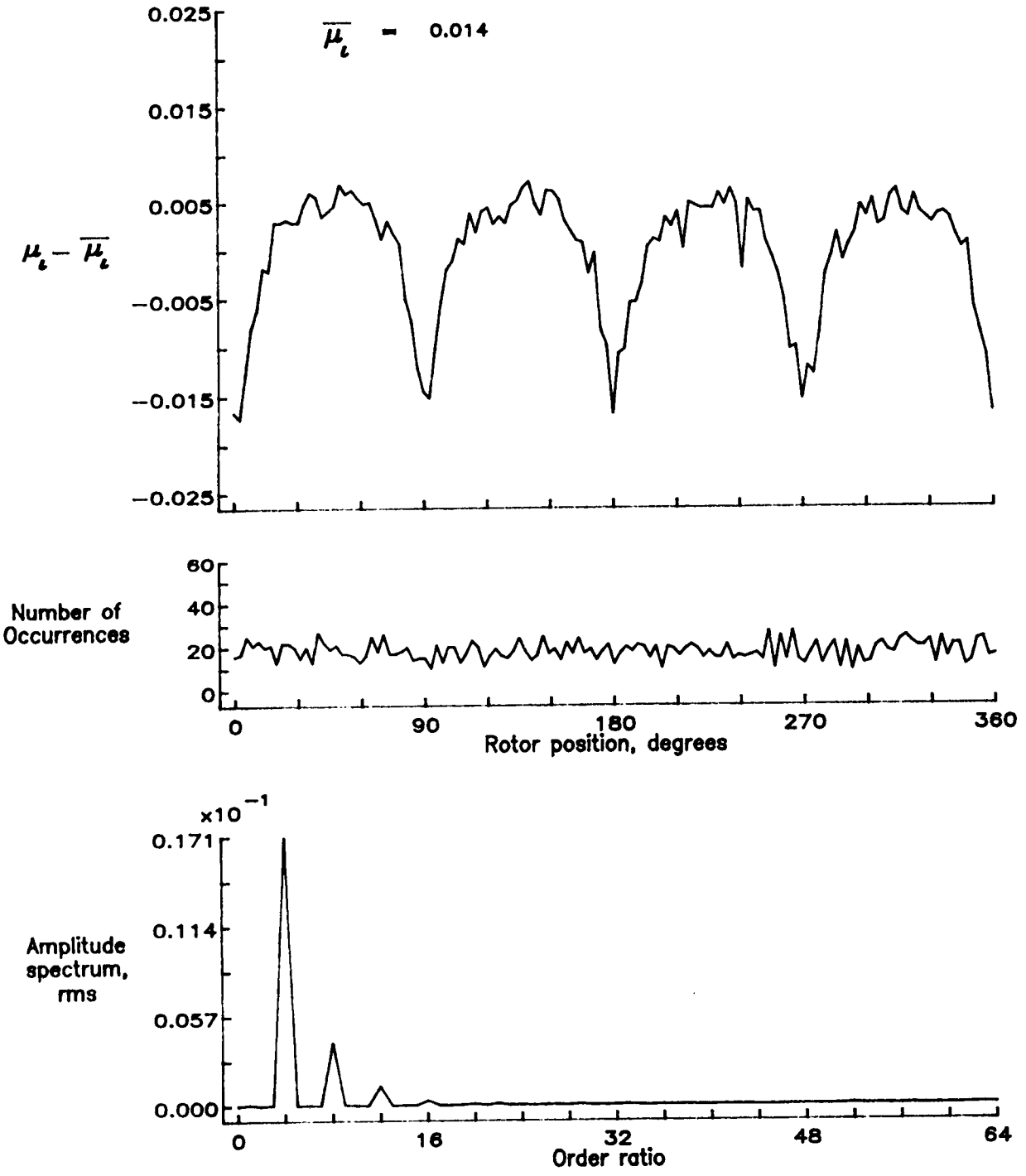

Figure 151.– Induced inflow velocity measured at 270 degrees and r/R of 0.60.

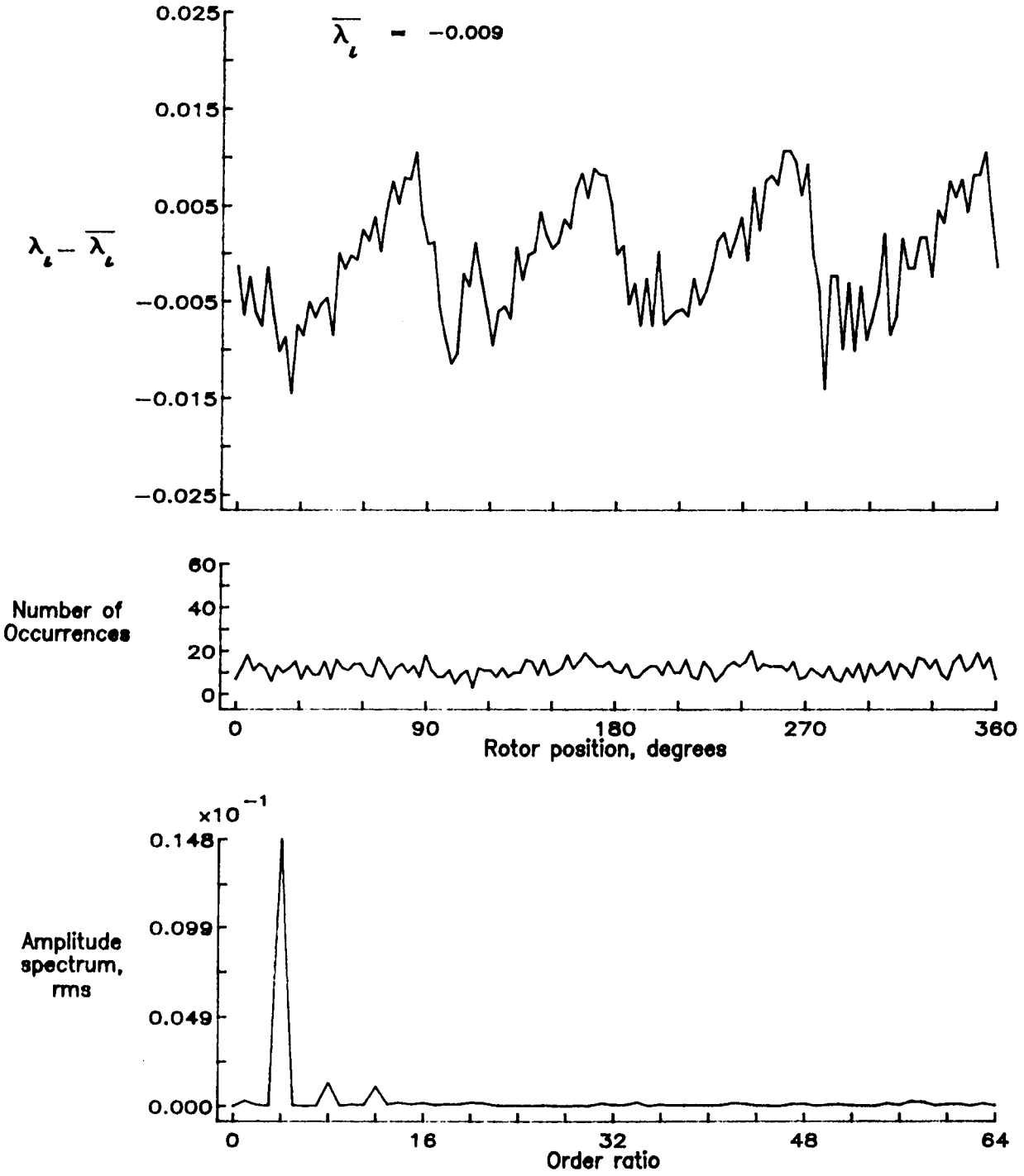

Figure 151.– Concluded.

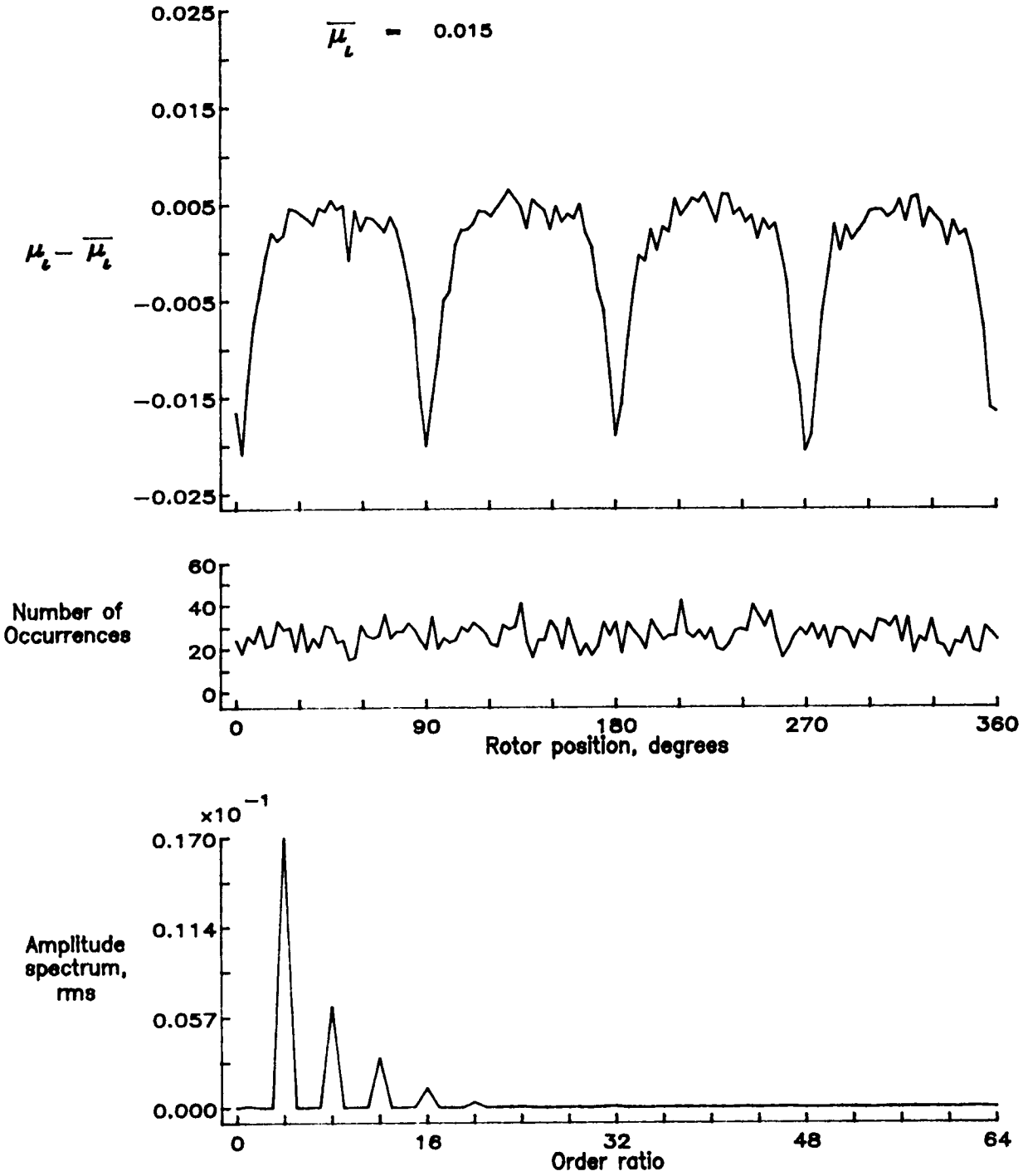

Figure 152.– Induced inflow velocity measured at 270 degrees and r/R of 0.70.

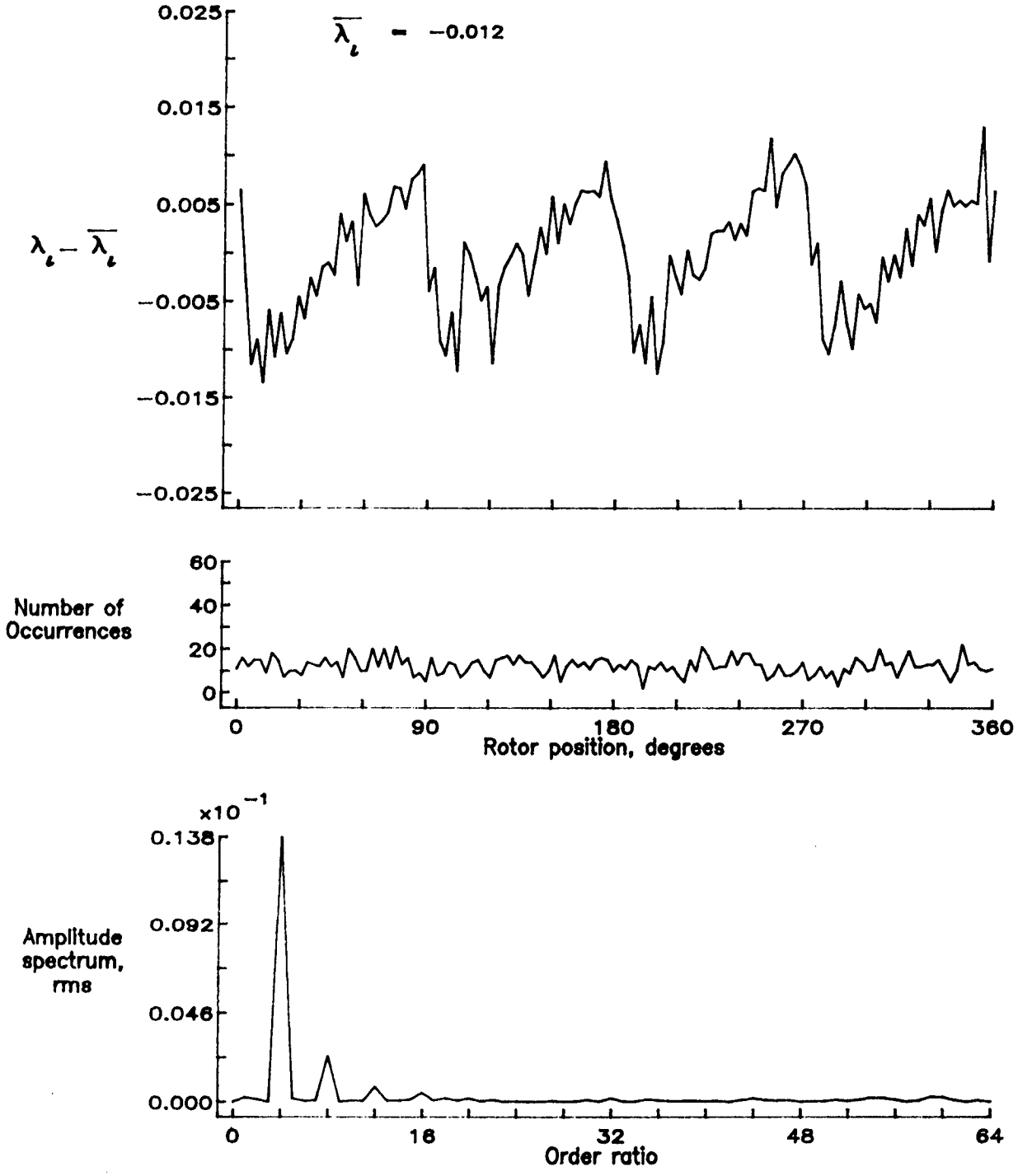

Figure 152.– Concluded.

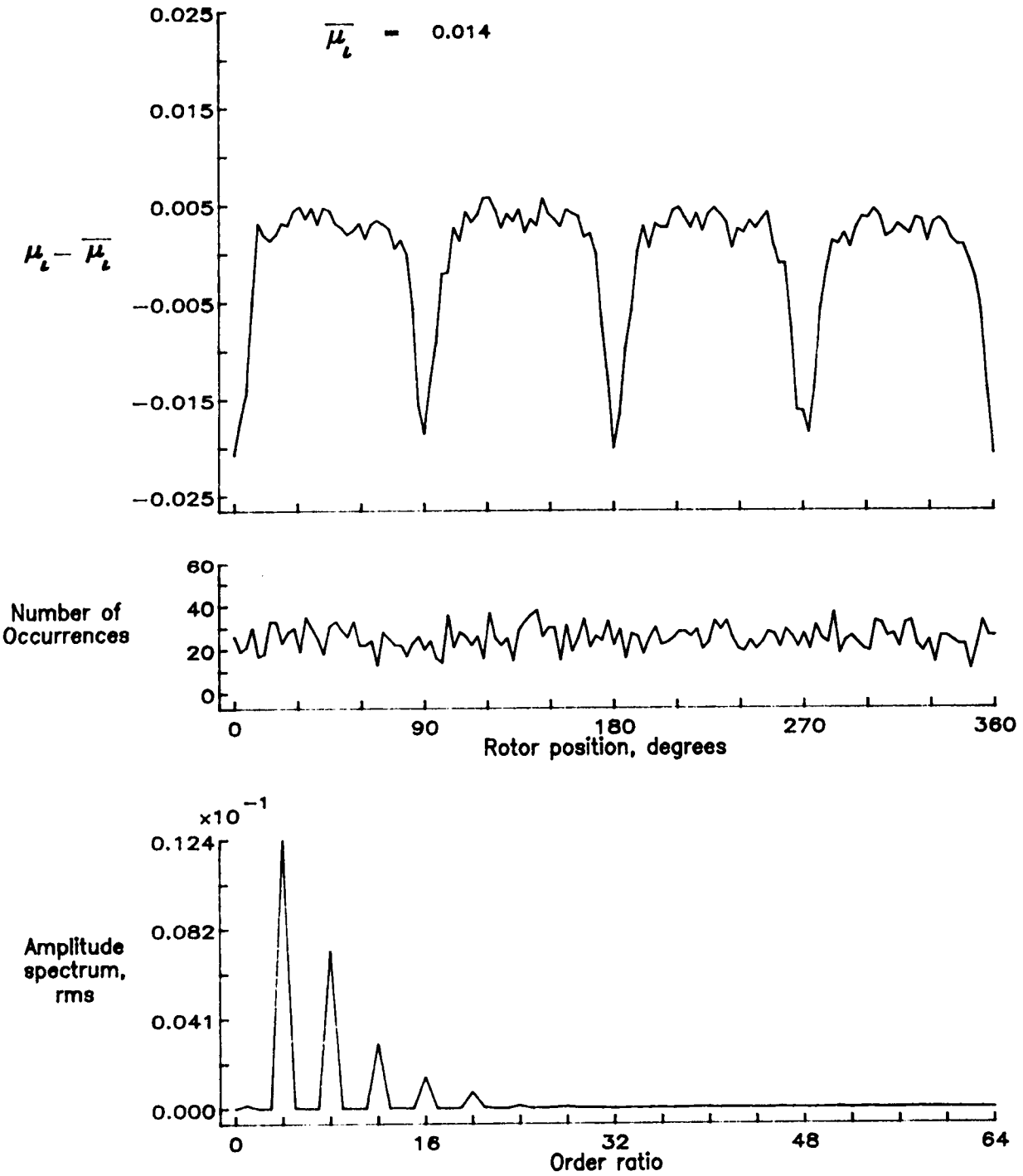

Figure 153.– Induced inflow velocity measured at 270 degrees and r/R of 0.74.

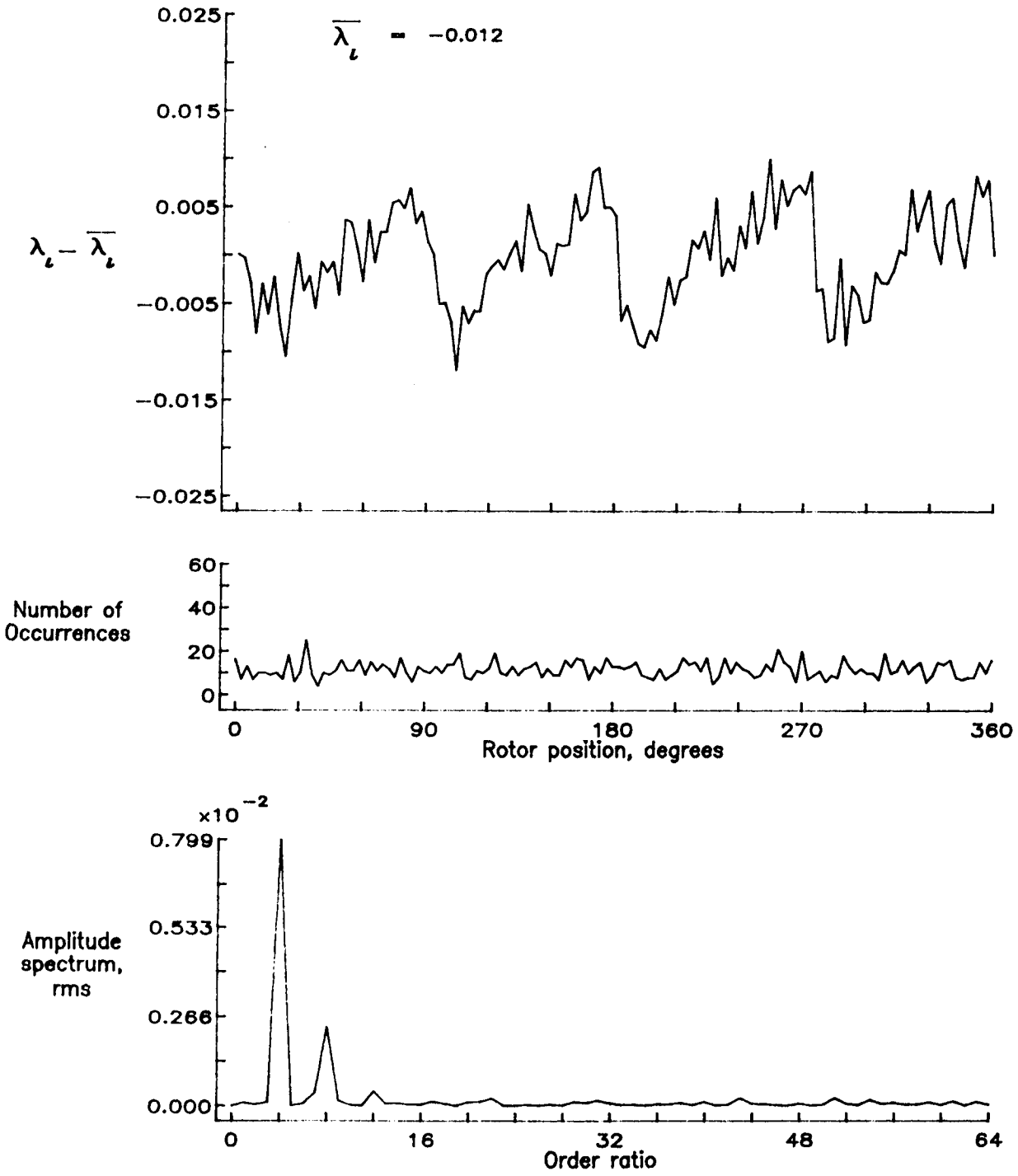

Figure 153.– Concluded.

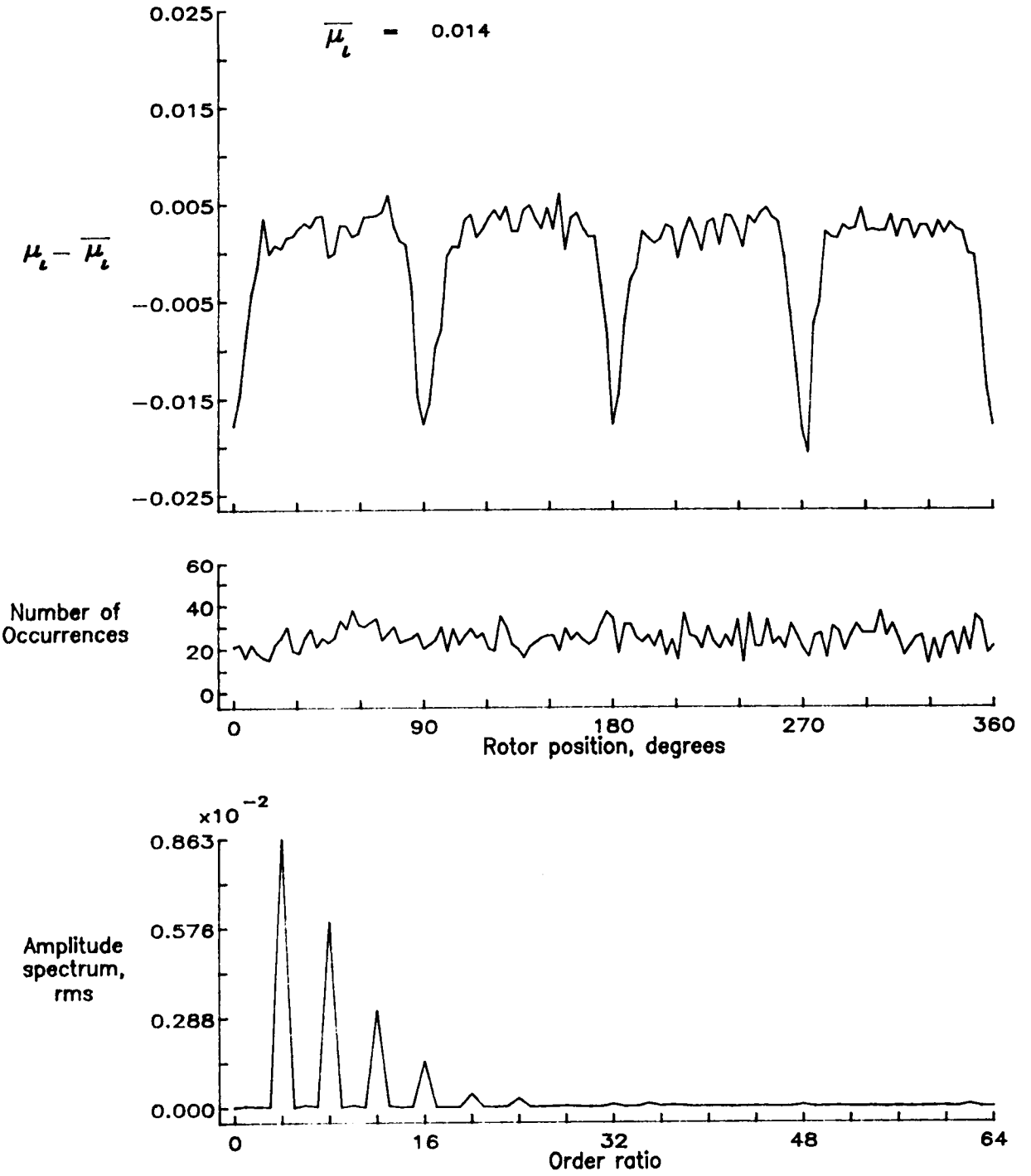

Figure 154.– Induced inflow velocity measured at 270 degrees and r/R of 0.78.

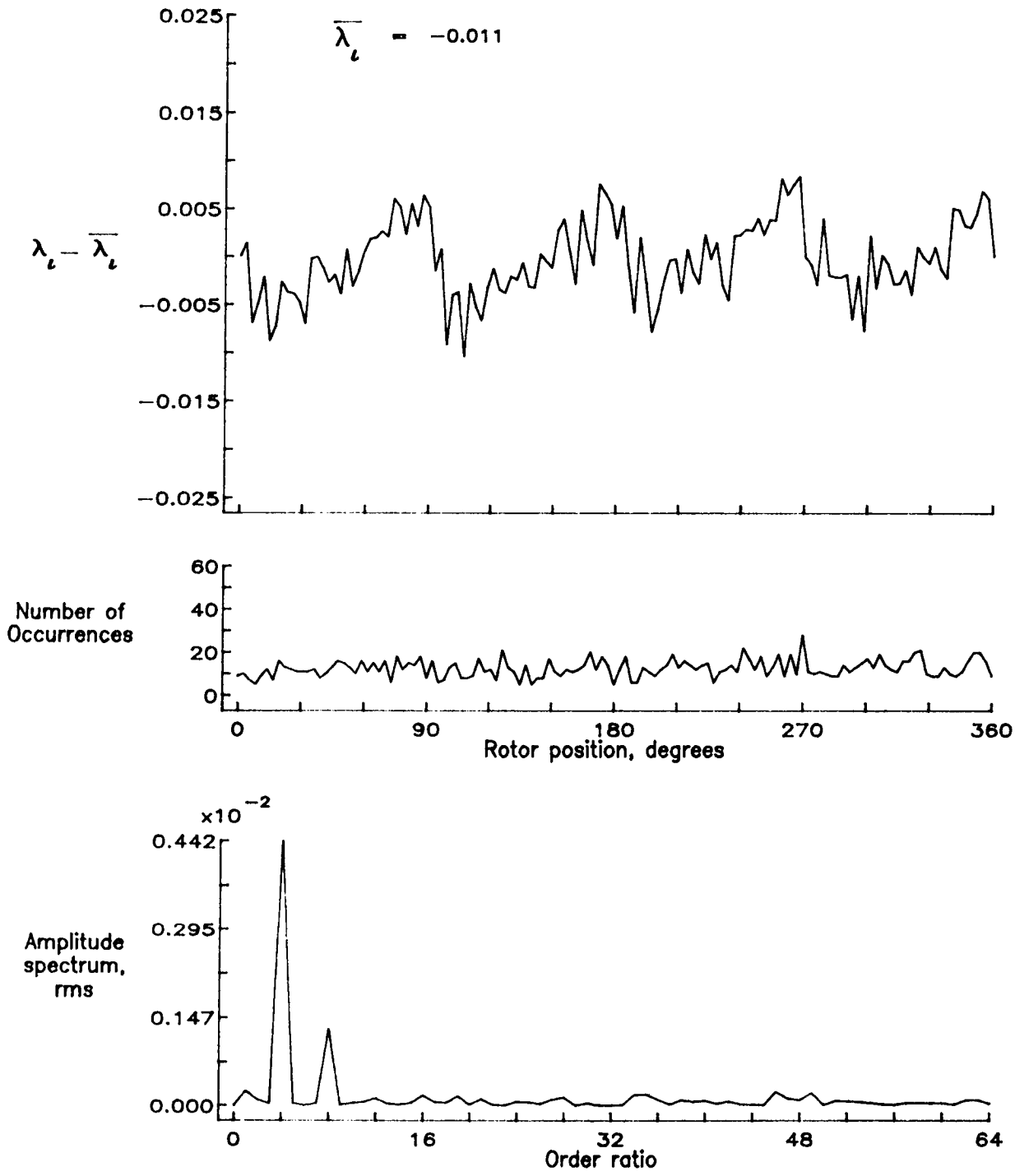

Figure 154.– Concluded.

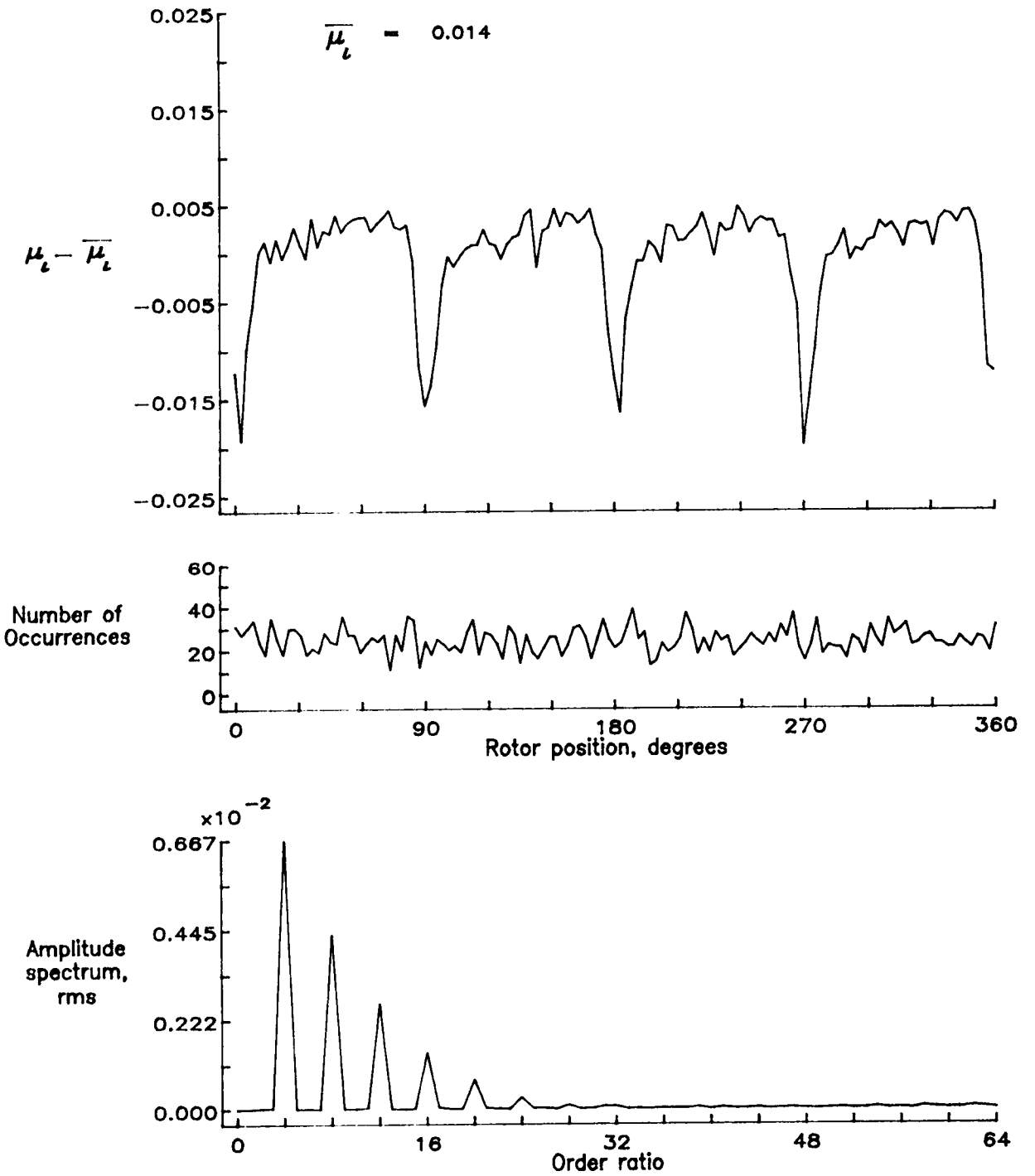

Figure 155.– Induced inflow velocity measured at 270 degrees and r/R of 0.82.

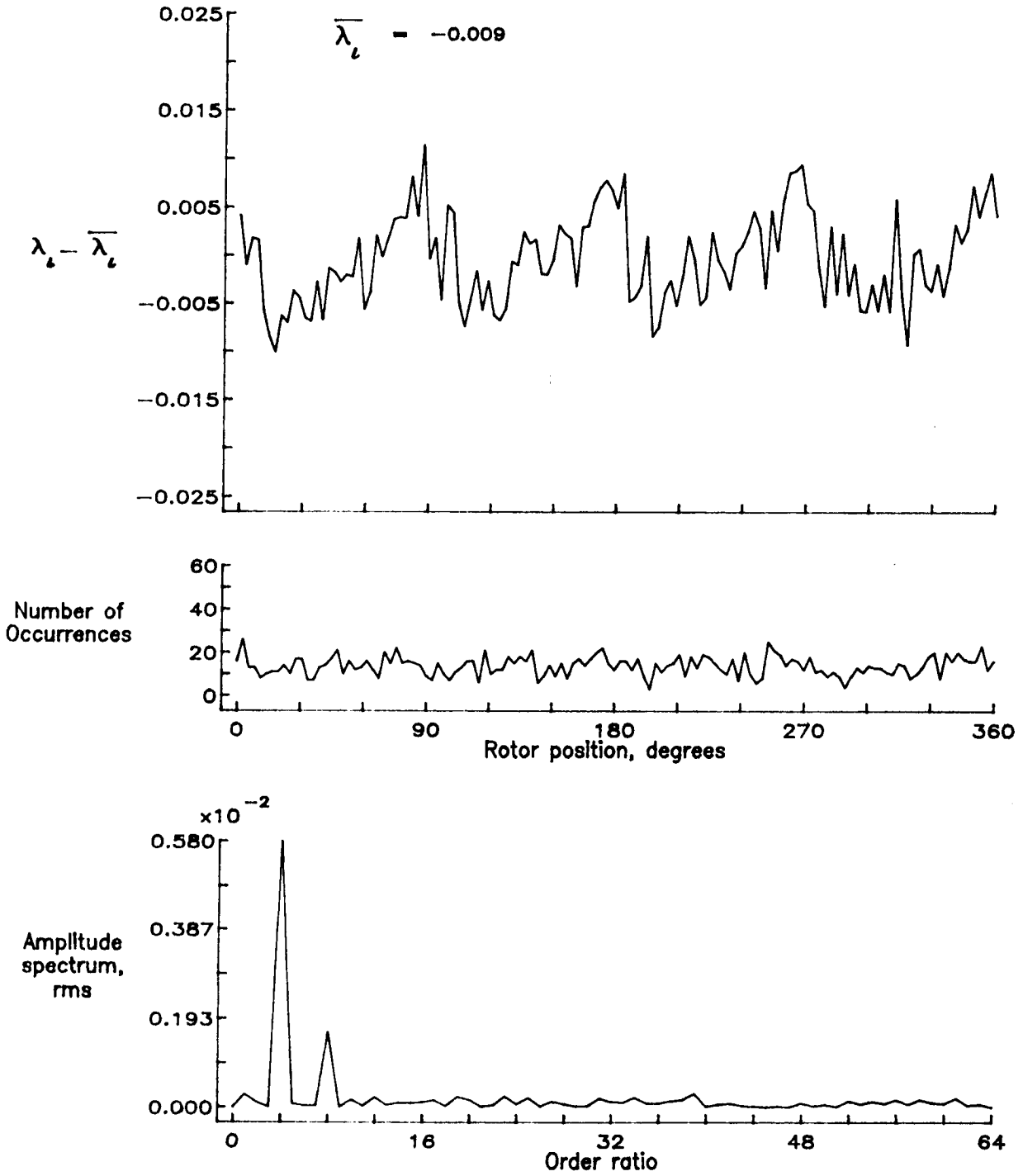

Figure 155.– Concluded.

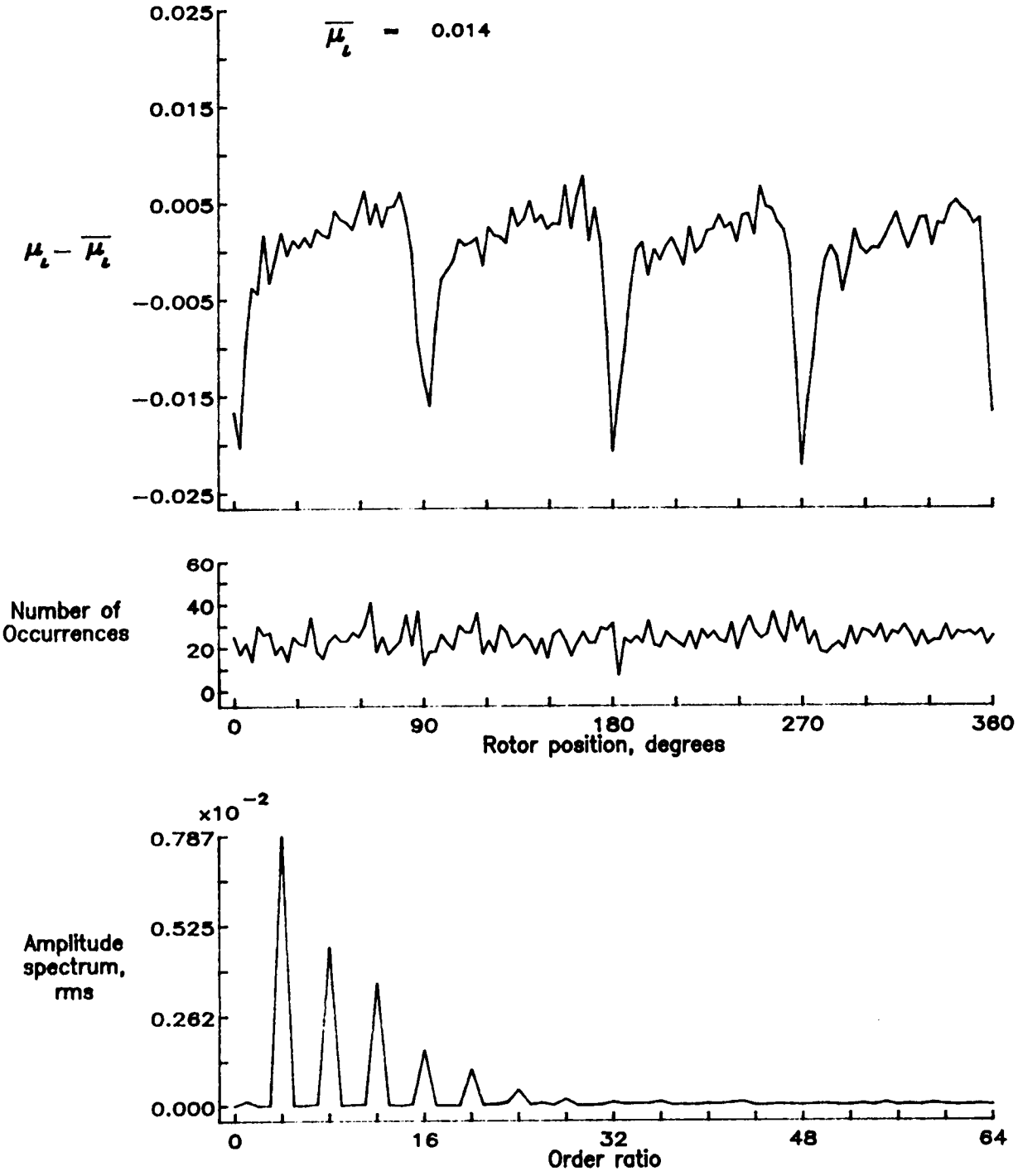

Figure 156.– Induced inflow velocity measured at 270 degrees and r/R of 0.86.

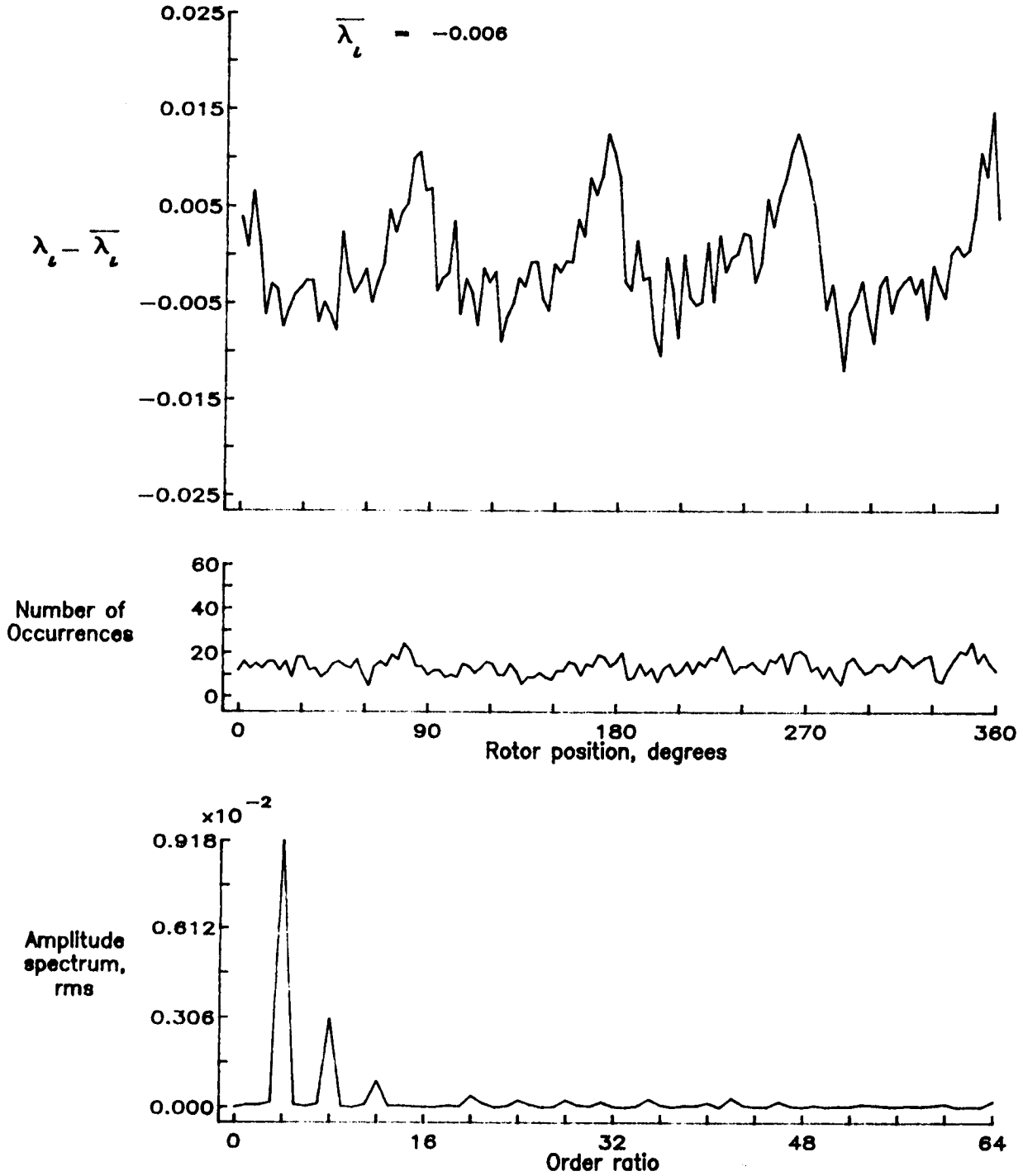

Figure 156.– Concluded.

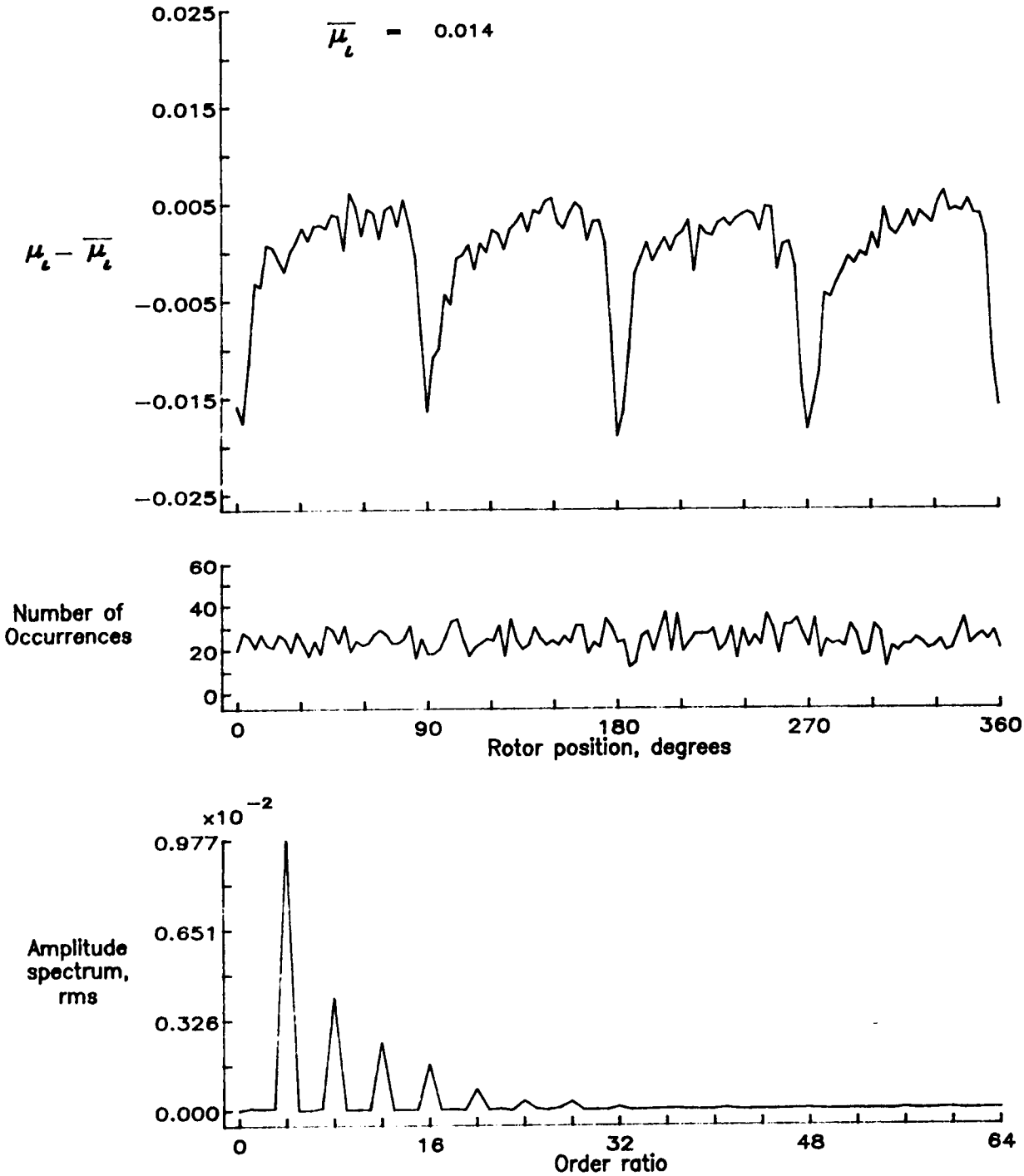

Figure 157.– Induced inflow velocity measured at 270 degrees and r/R of 0.90.

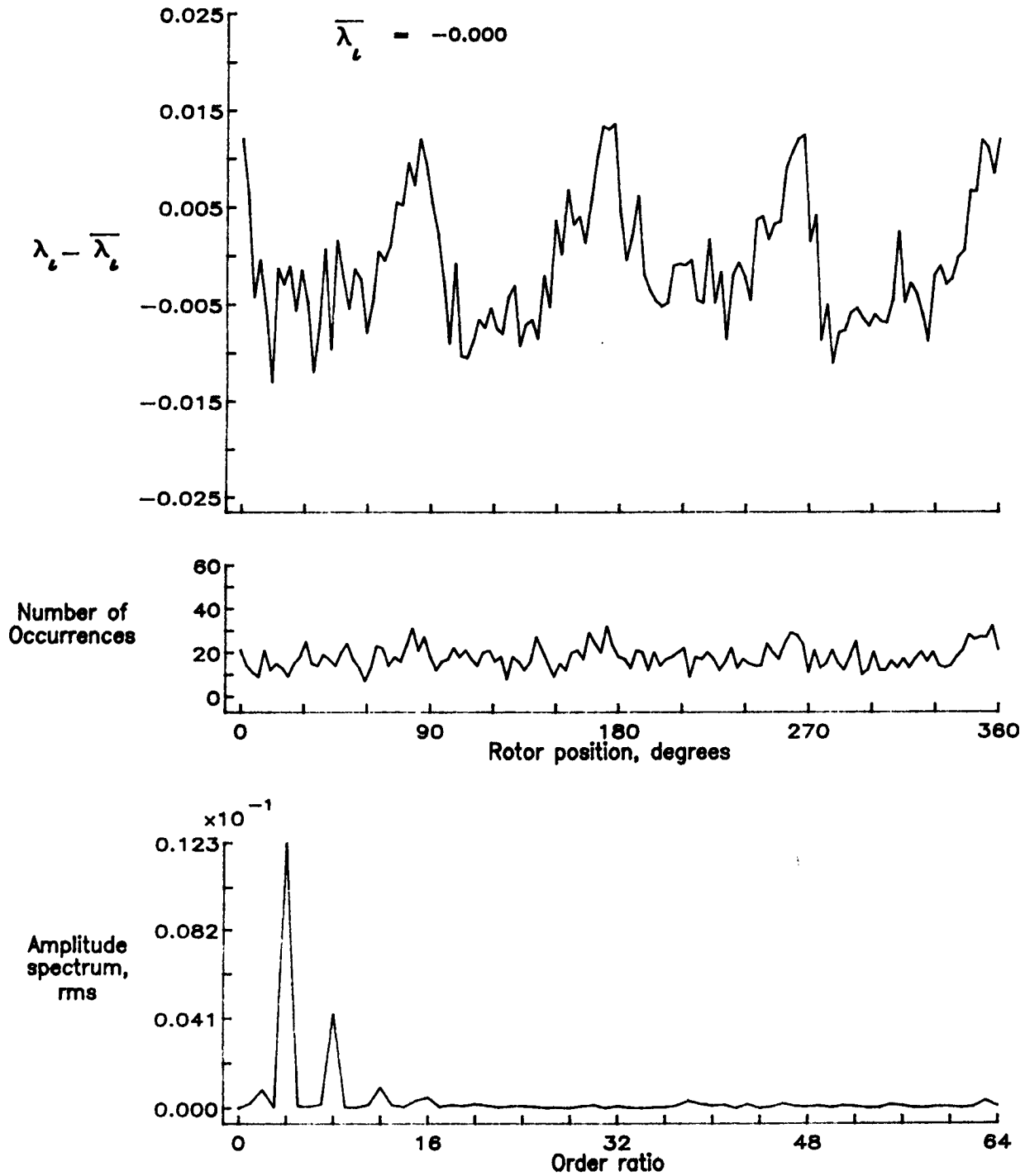

Figure 157.– Concluded.

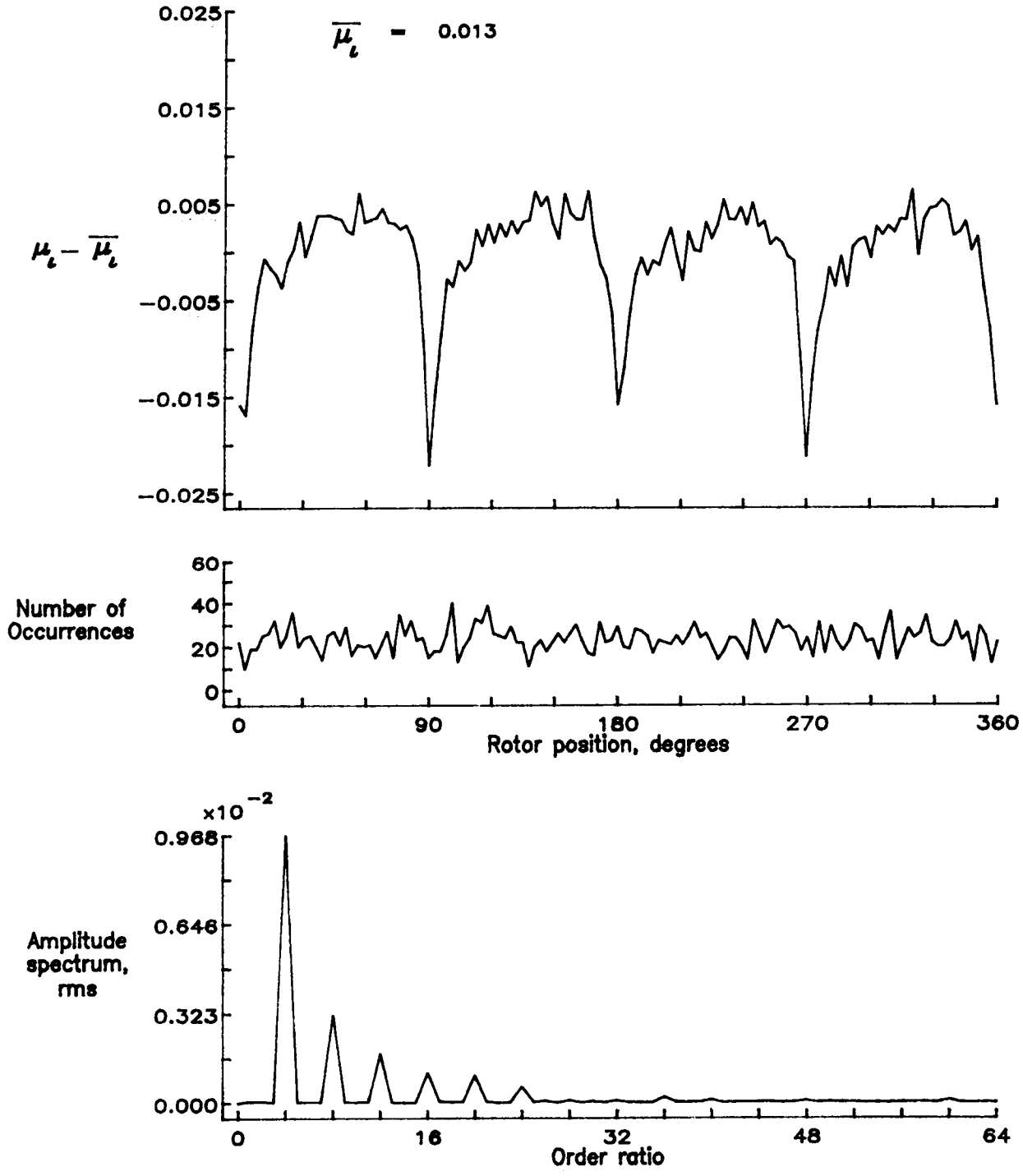

Figure 158.– Induced inflow velocity measured at 270 degrees and r/R of 0.94.

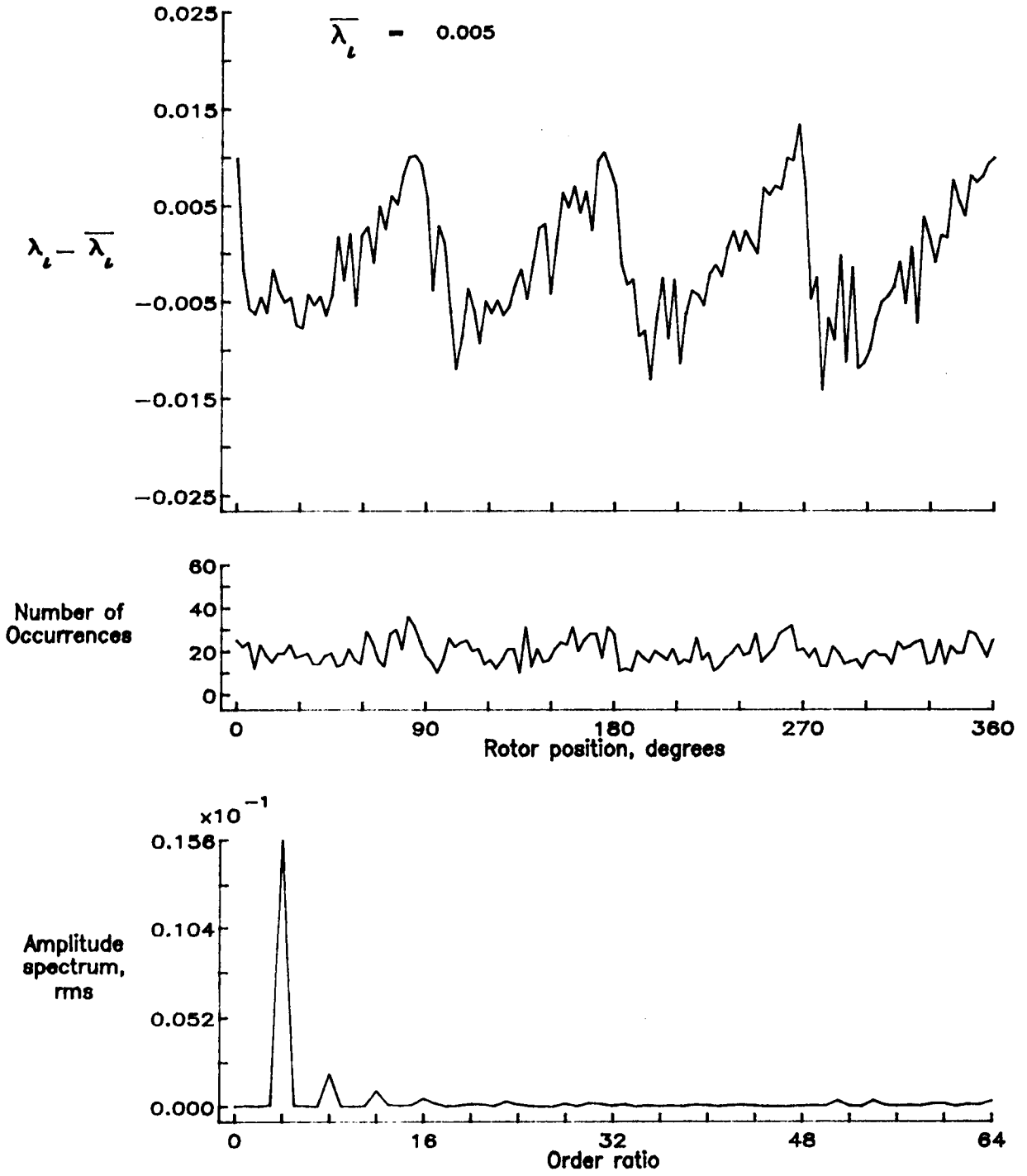

Figure 158.– Concluded.

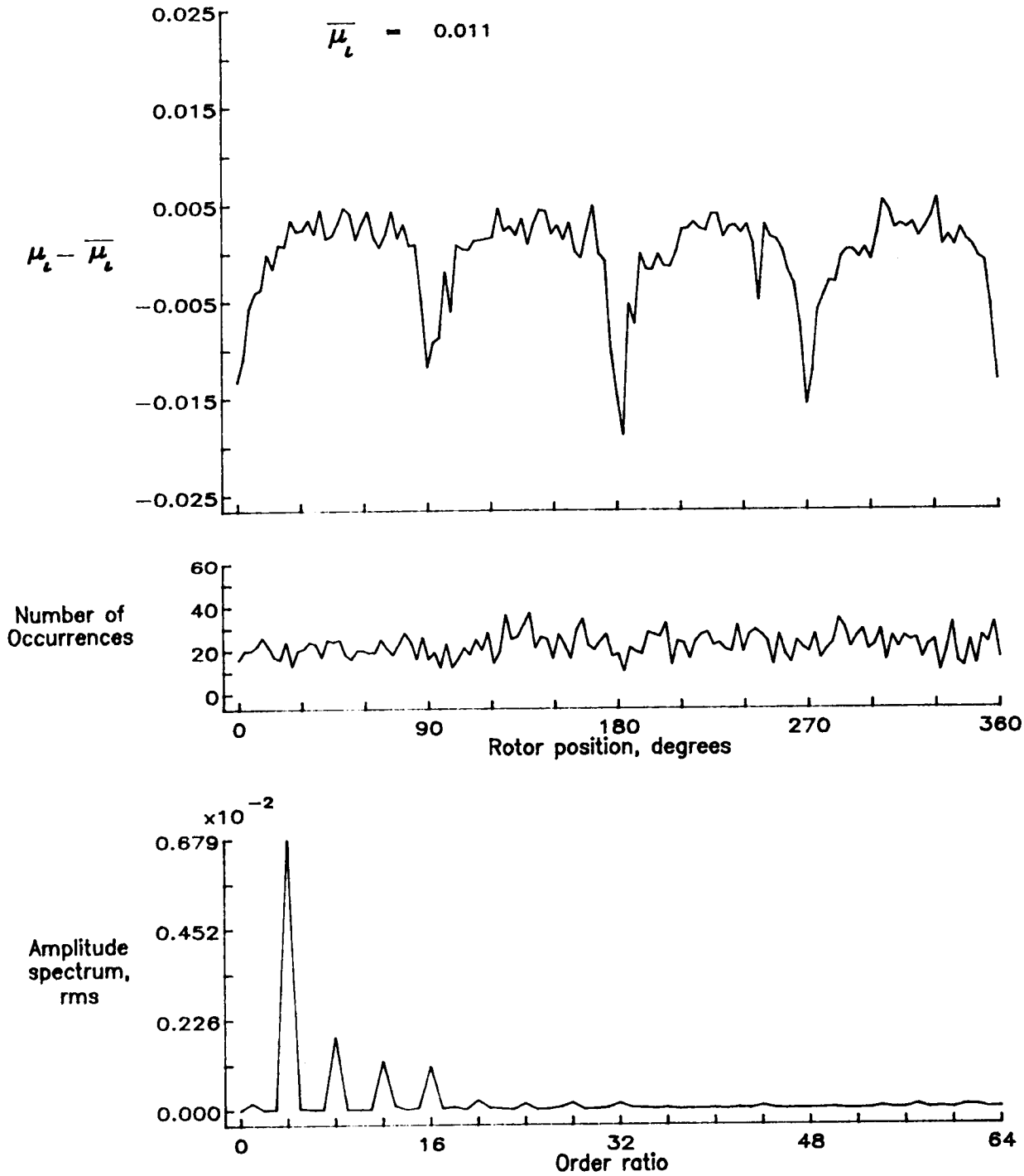

Figure 159.– Induced inflow velocity measured at 270 degrees and r/R of 0.98.

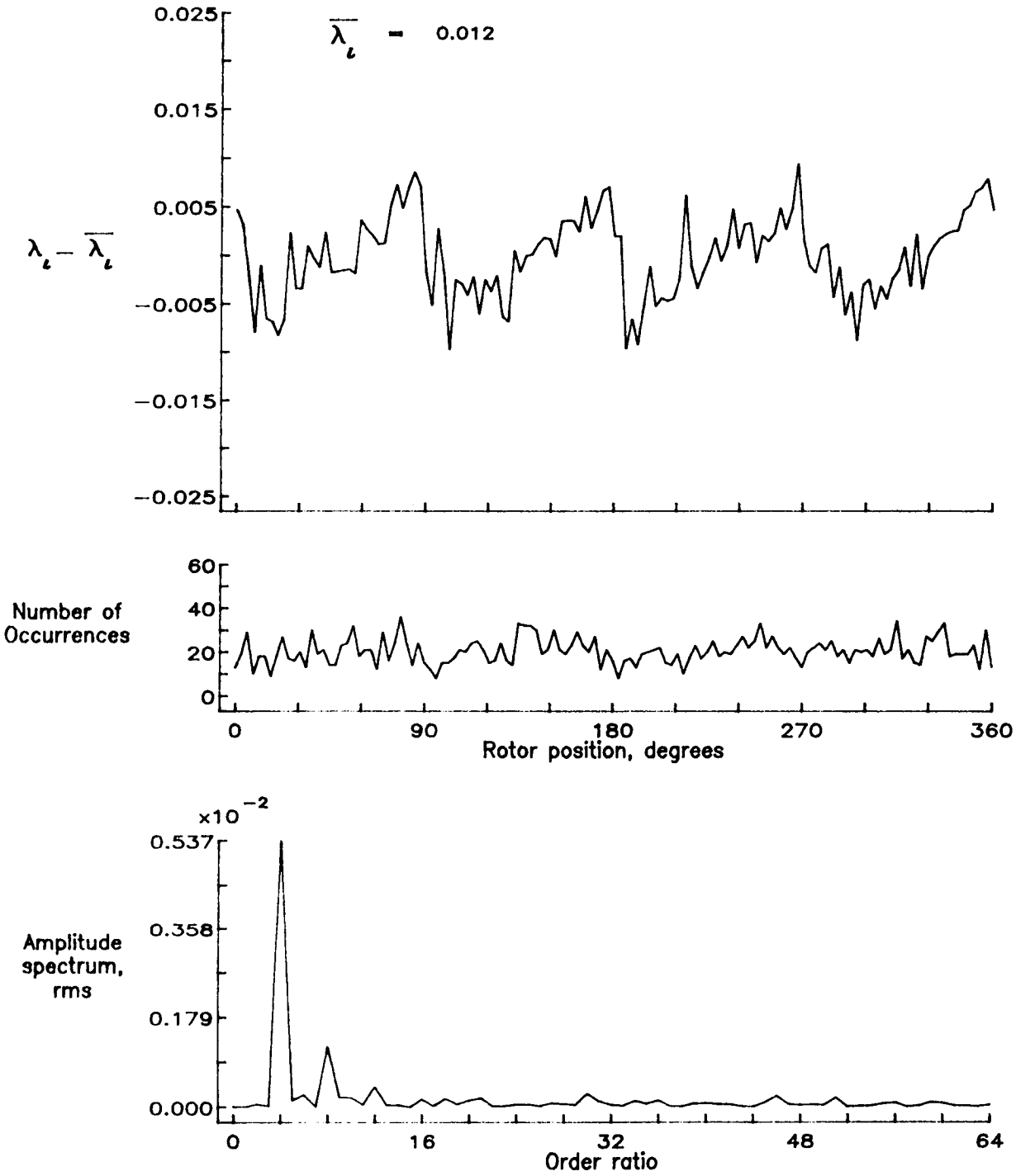

Figure 159.– Concluded.

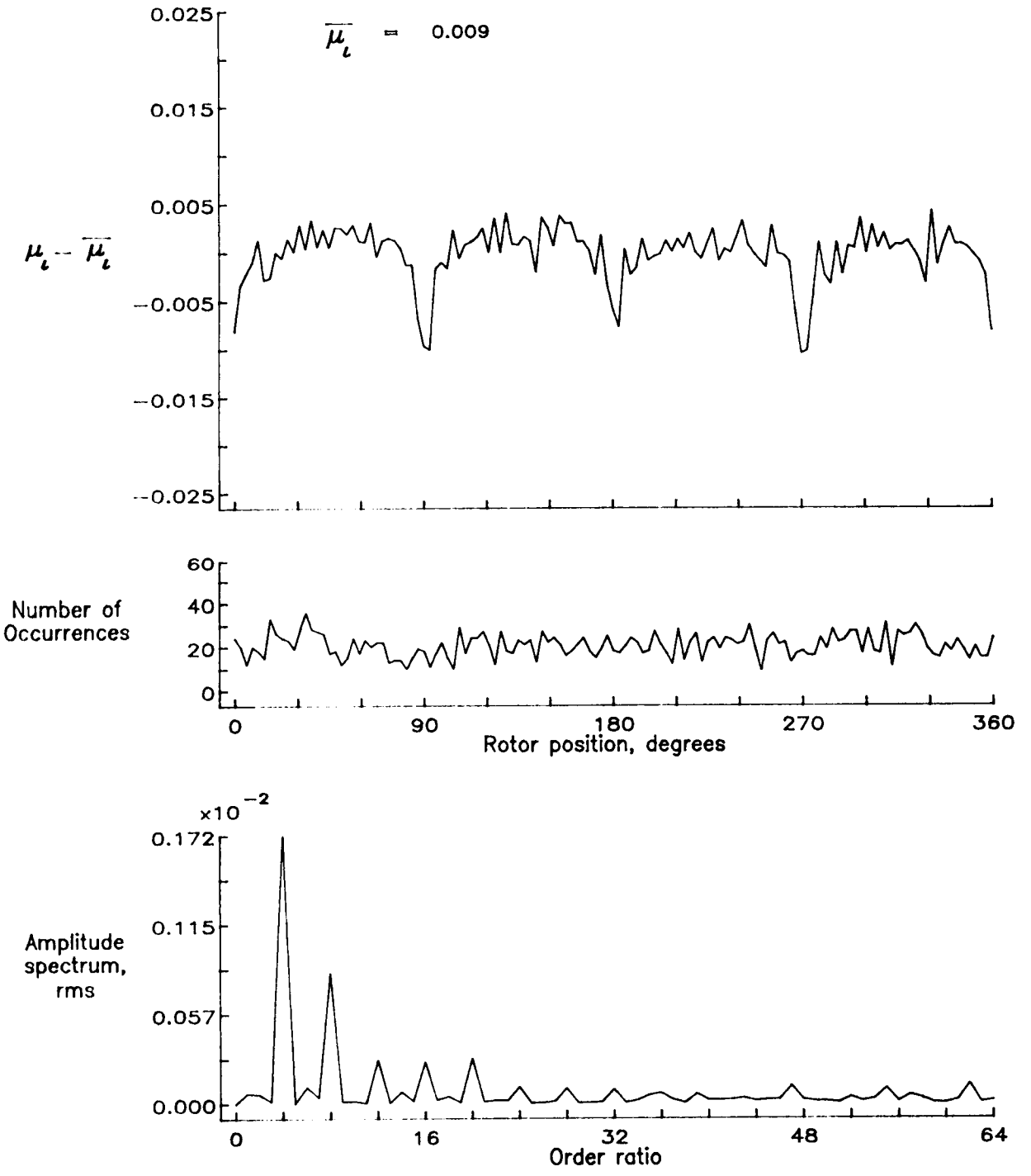

Figure 160.– Induced inflow velocity measured at 270 degrees and r/R of 1.02.

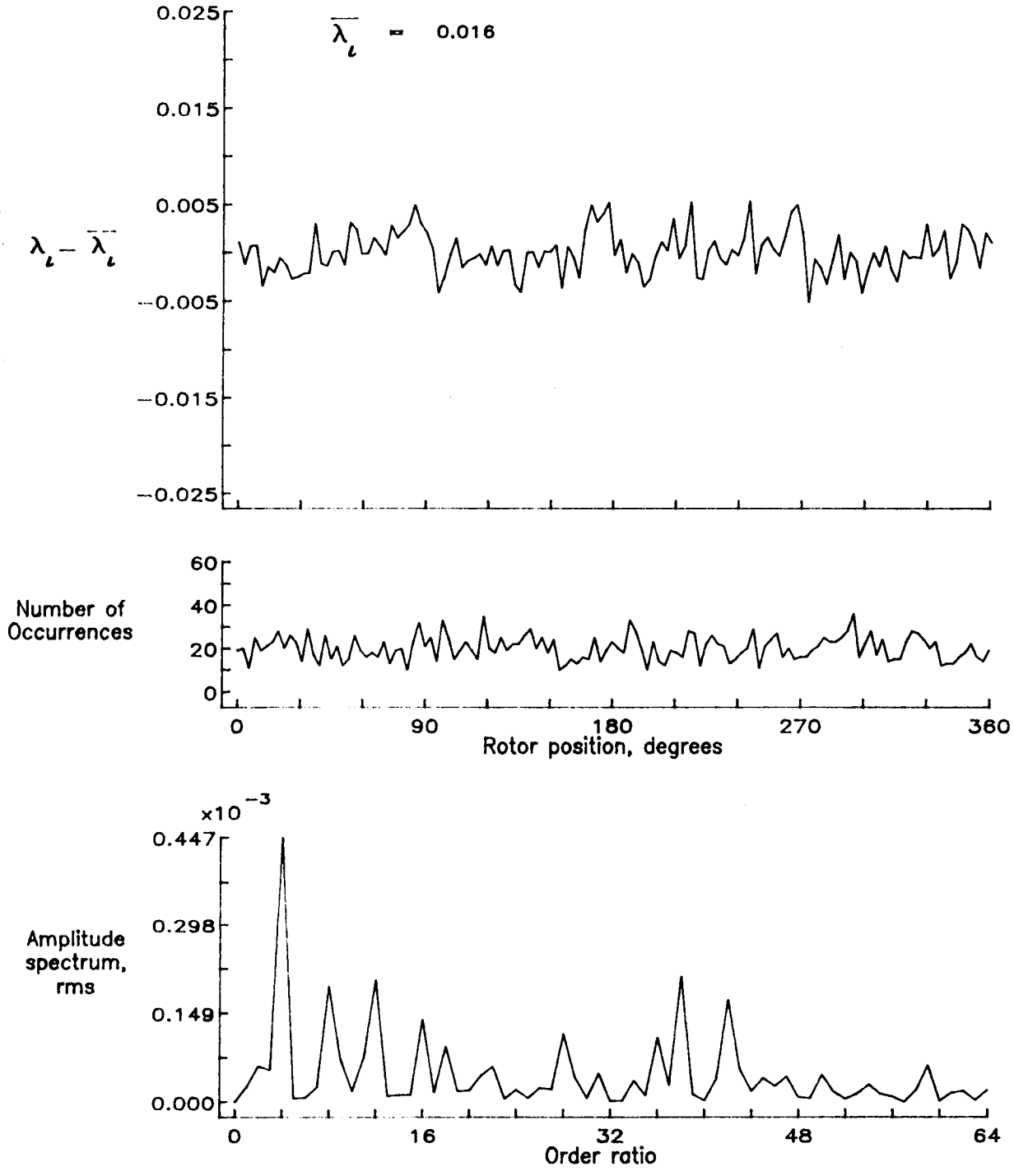

Figure 160.– Concluded.

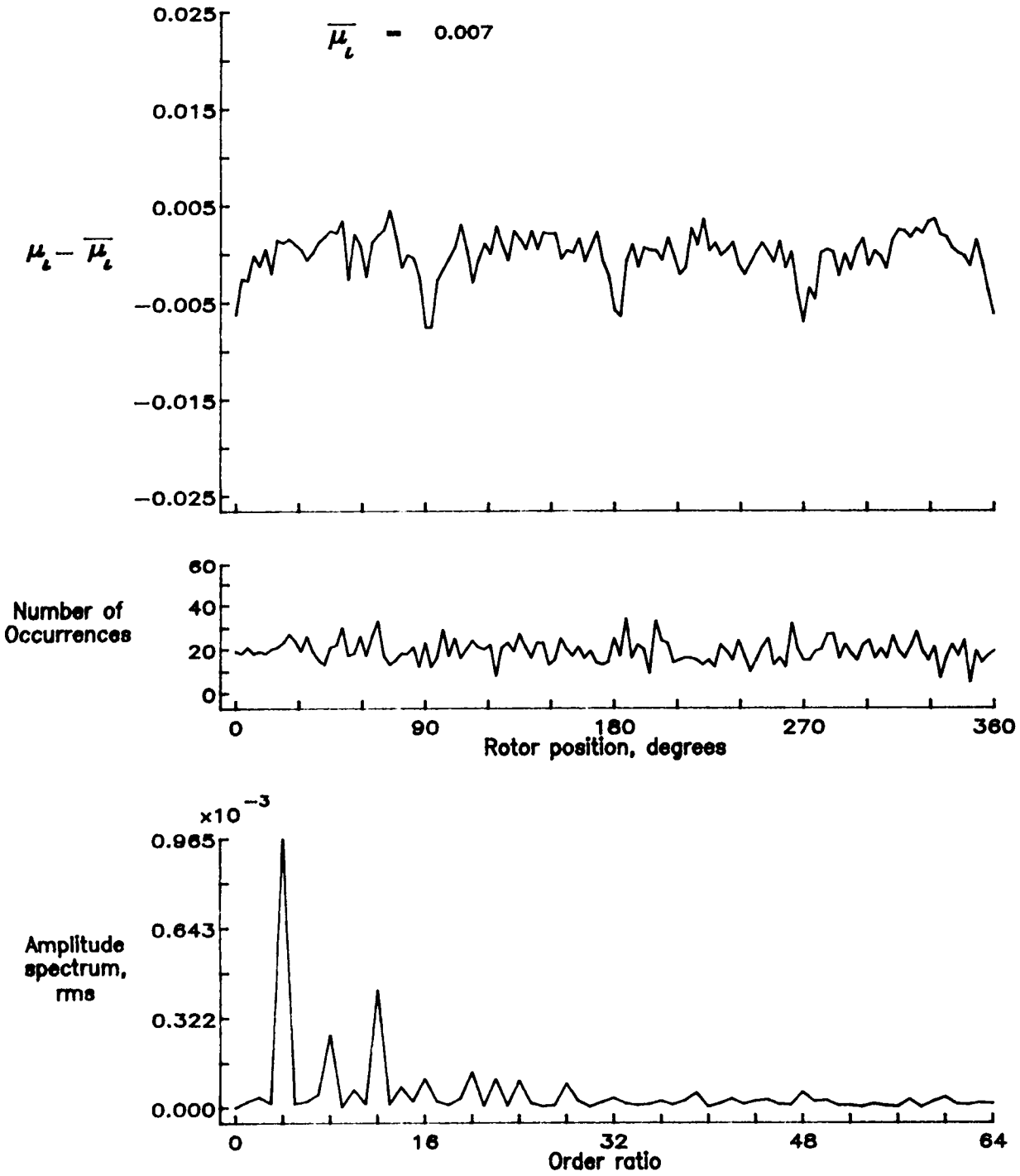

Figure 161.– Induced inflow velocity measured at 270 degrees and r/R of 1.04.

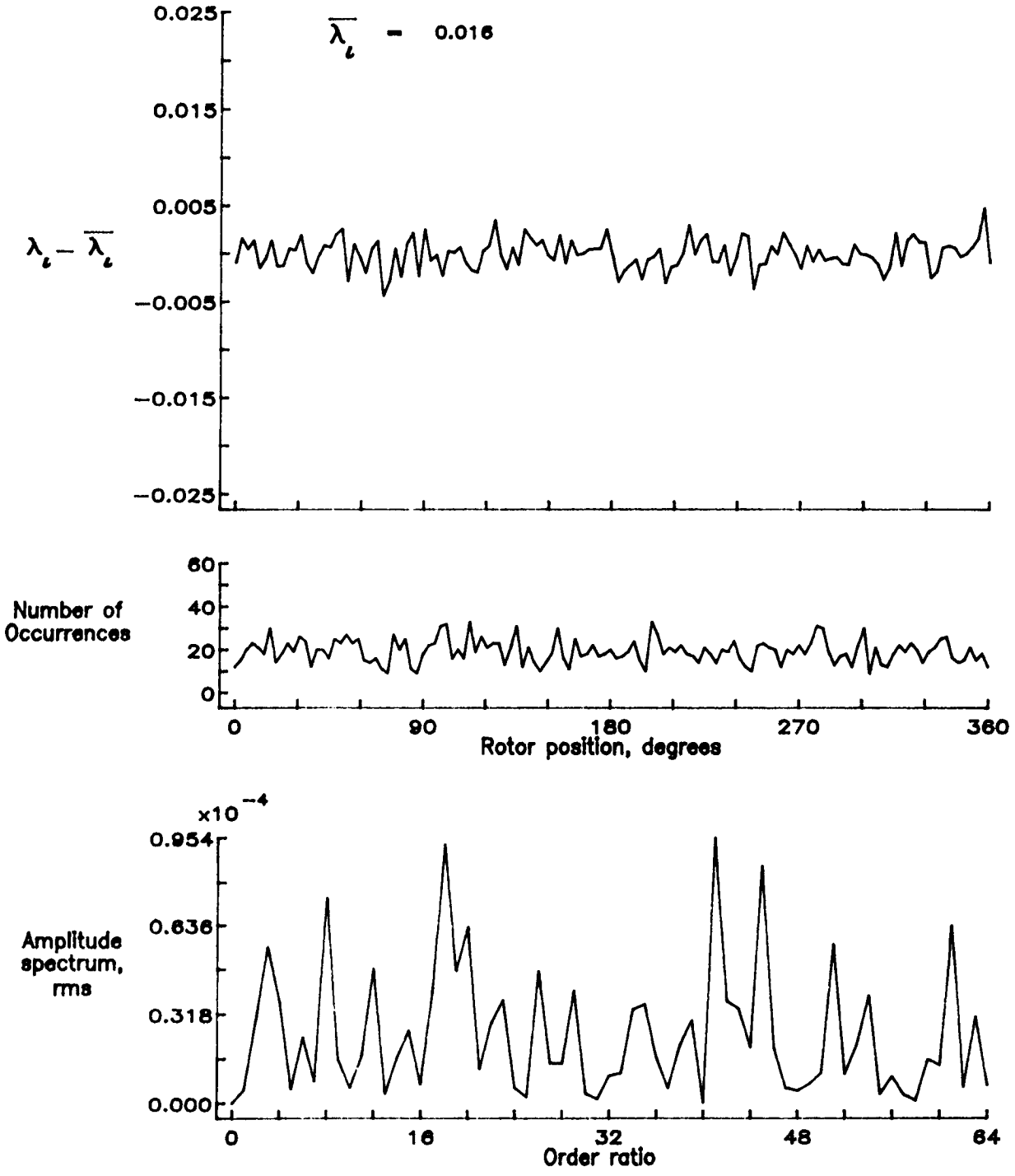

Figure 161.– Concluded.

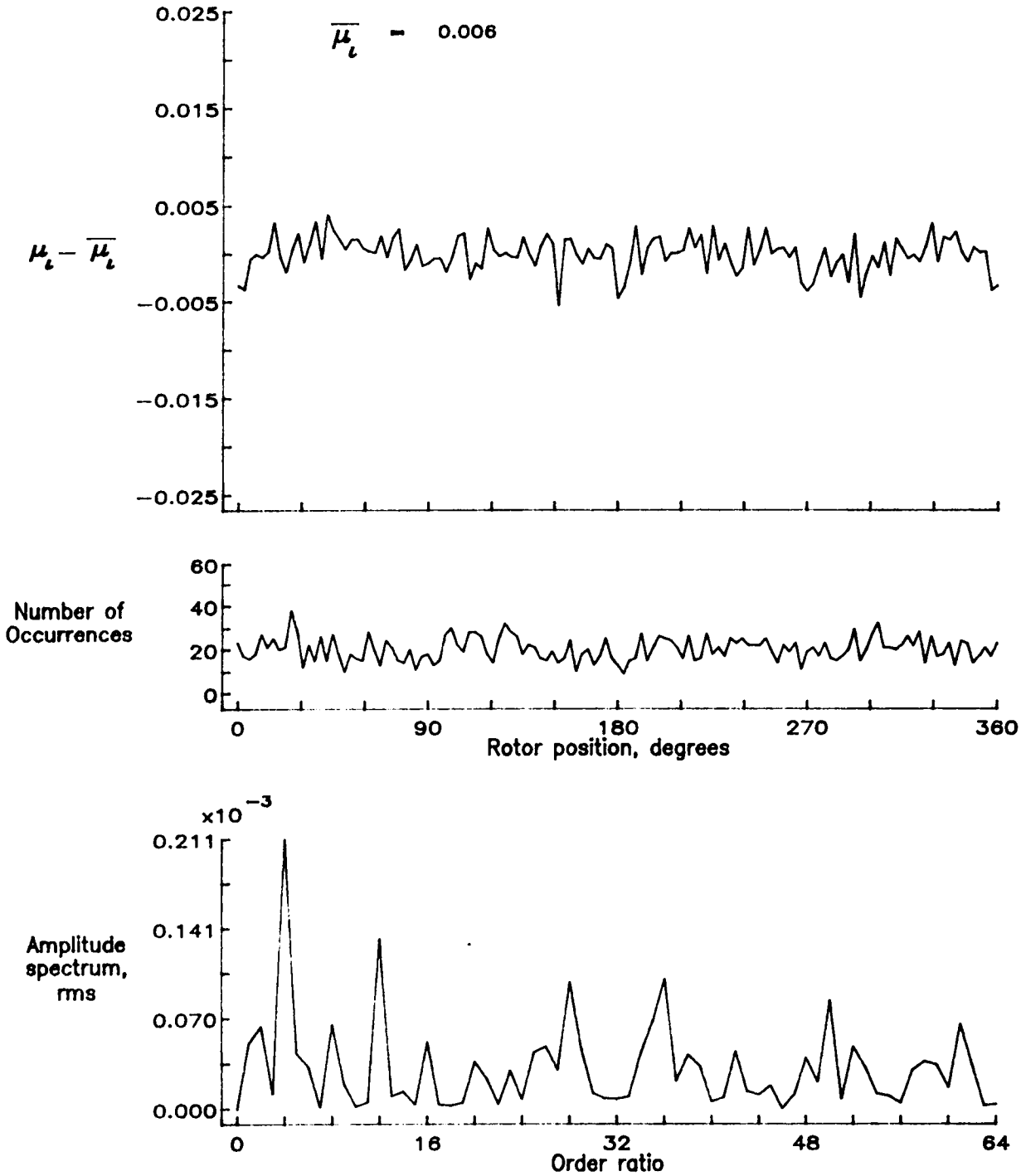

Figure 162.– Induced inflow velocity measured at 270 degrees and r/R of 1.10.

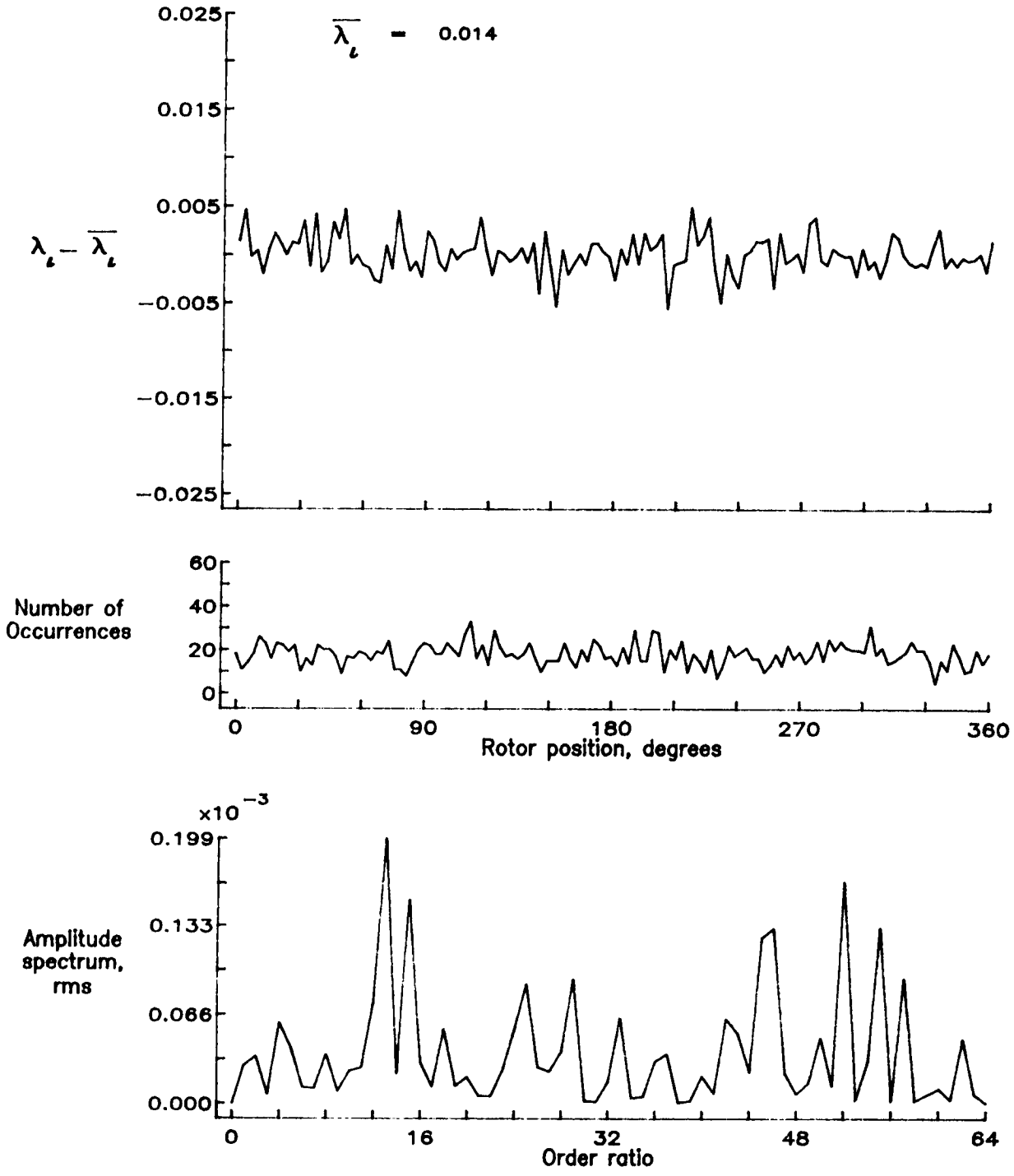

Figure 162.– Concluded.

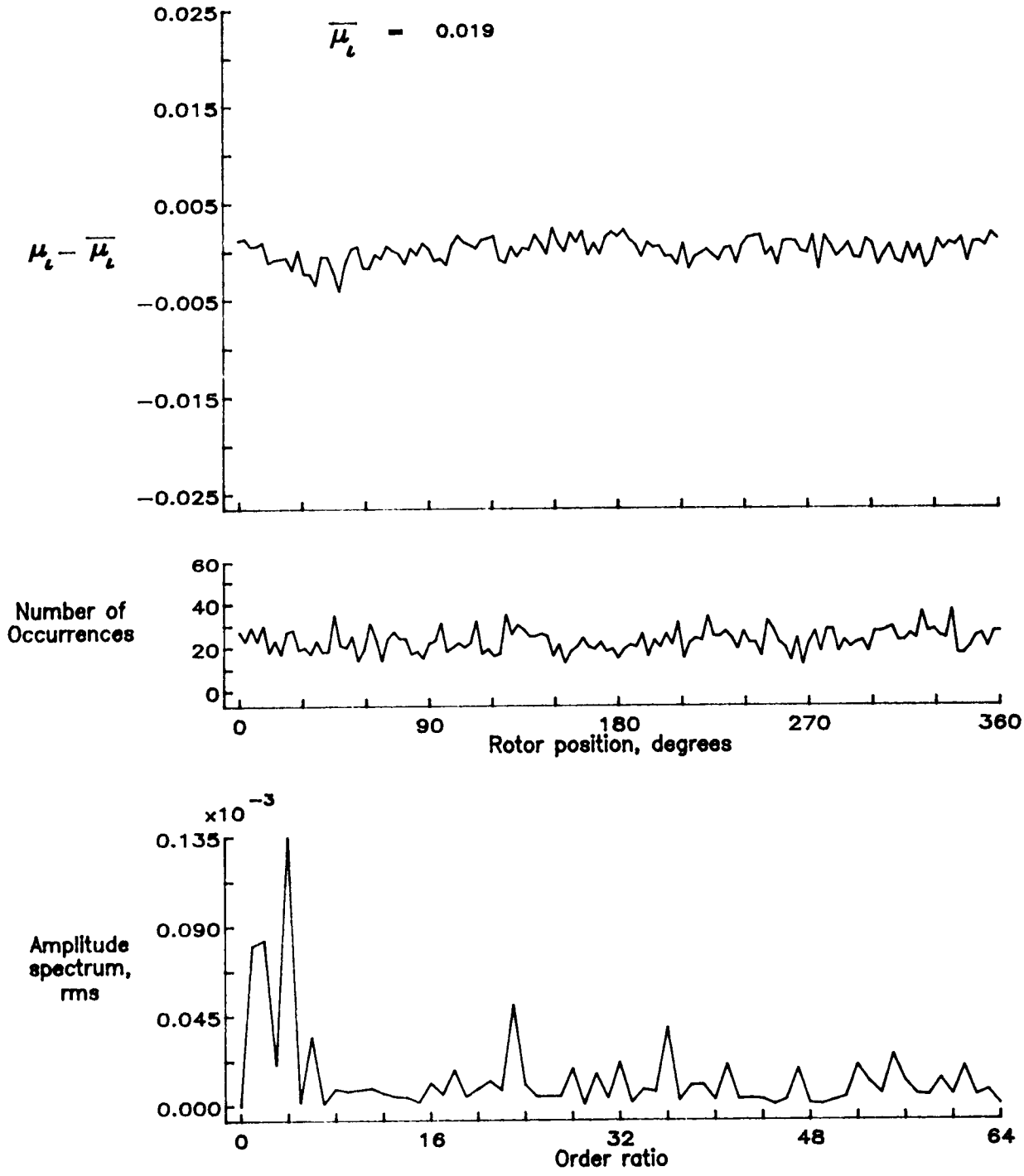

Figure 163.– Induced inflow velocity measured at 300 degrees and r/R of 0.20.

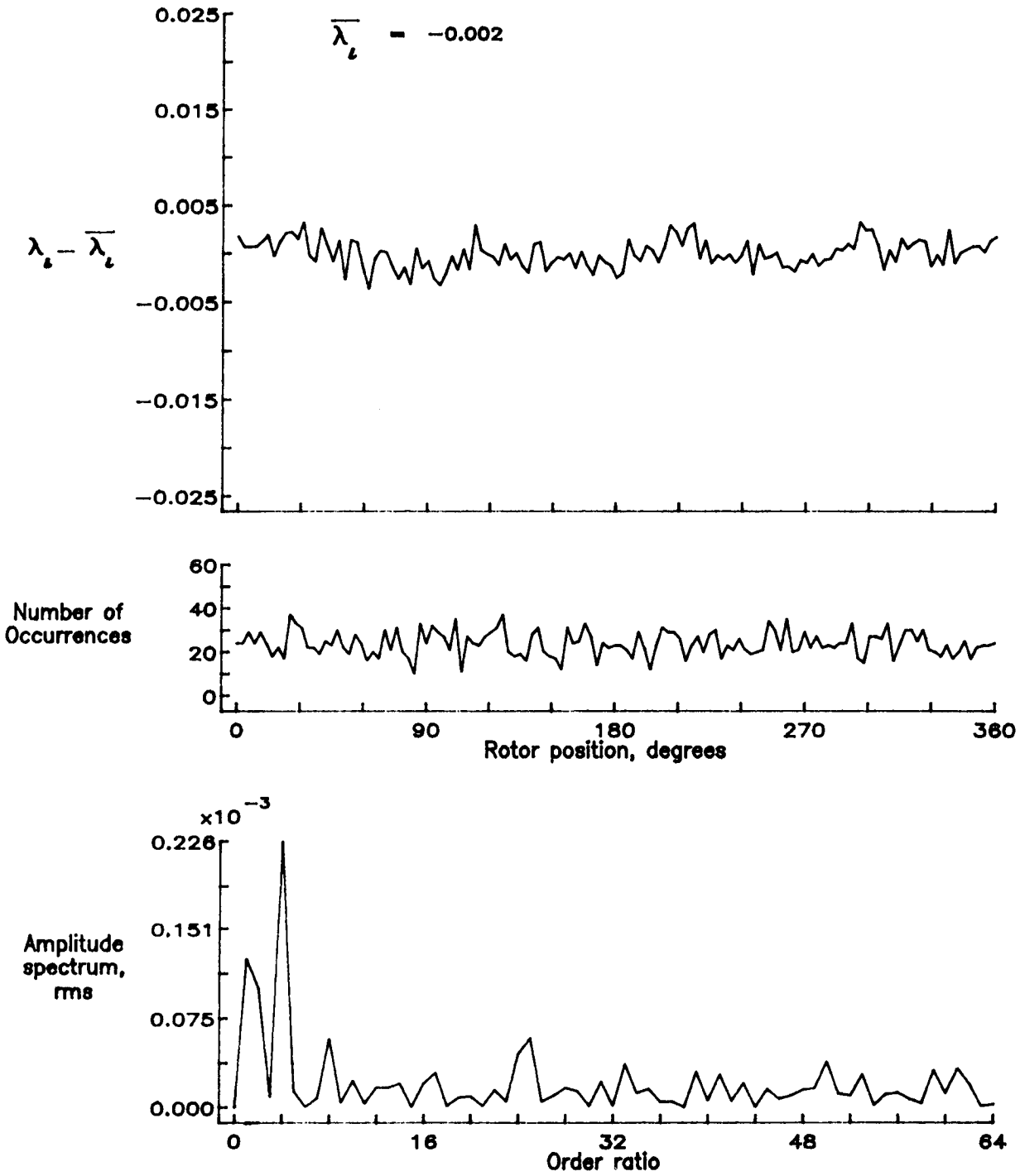

Figure 163.– Concluded.

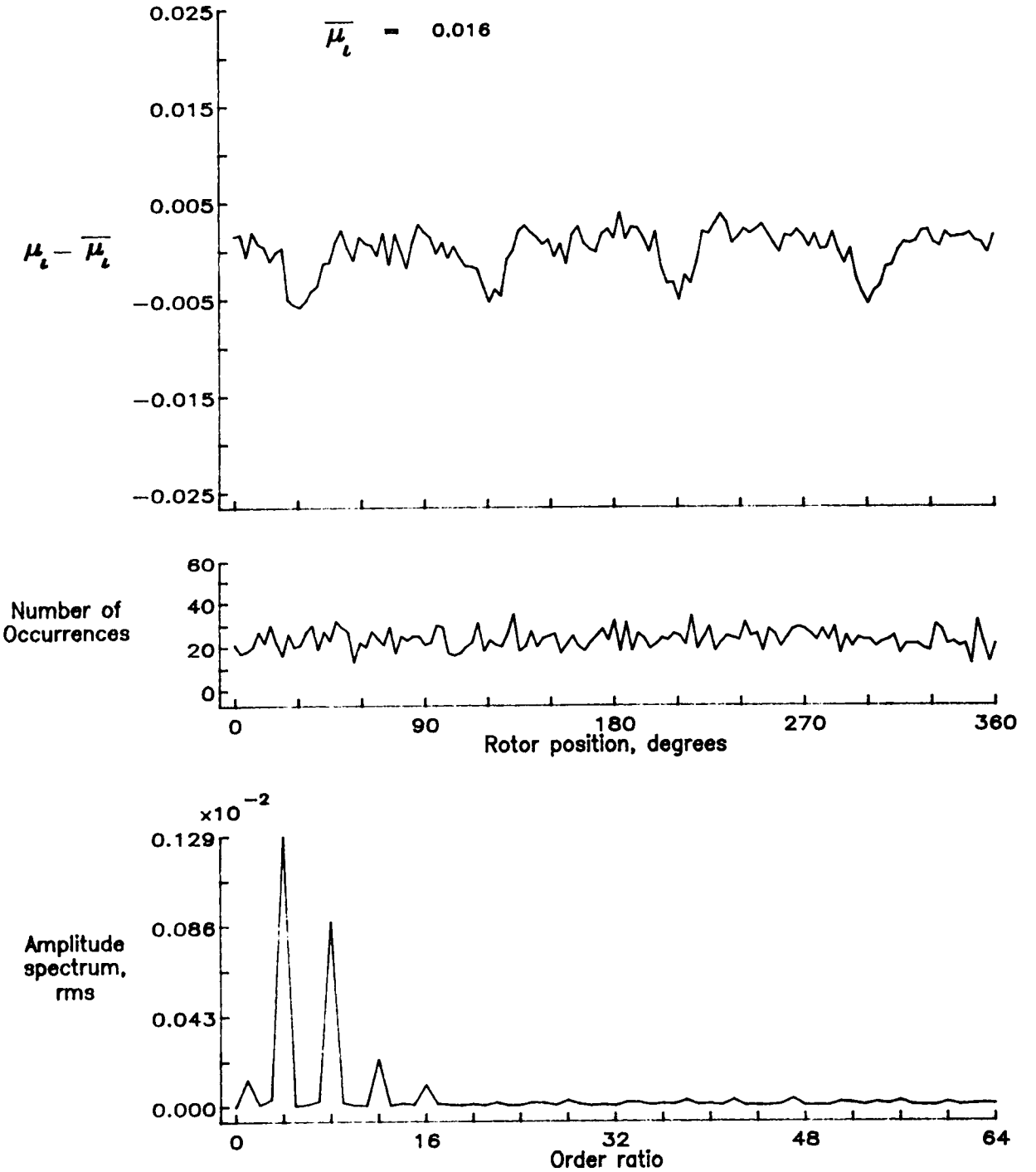

Figure 164.– Induced inflow velocity measured at 300 degrees and r/R of 0.40.

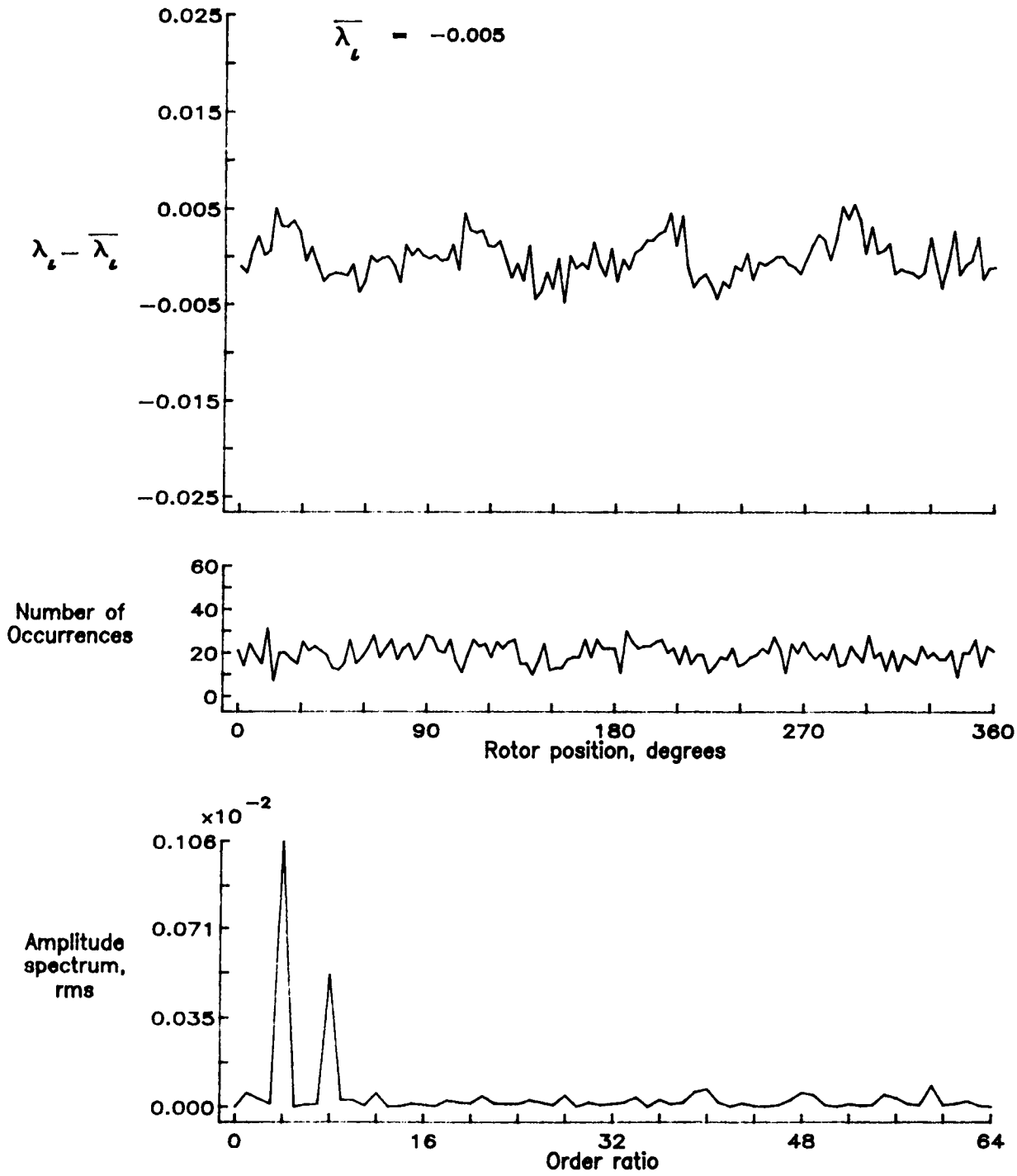

Figure 164.– Concluded.

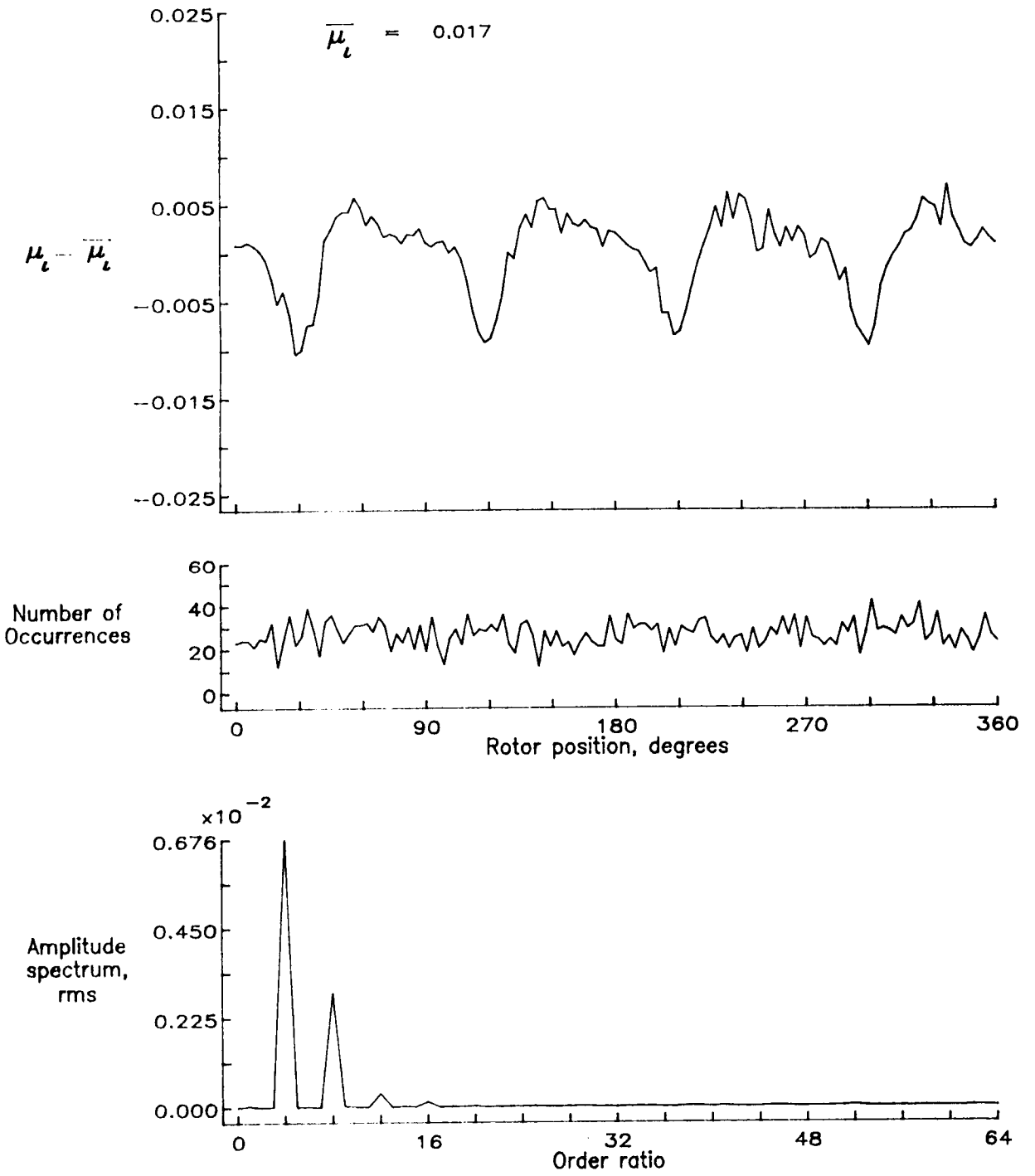

Figure 165.– Induced inflow velocity measured at 300 degrees and r/R of 0.50.

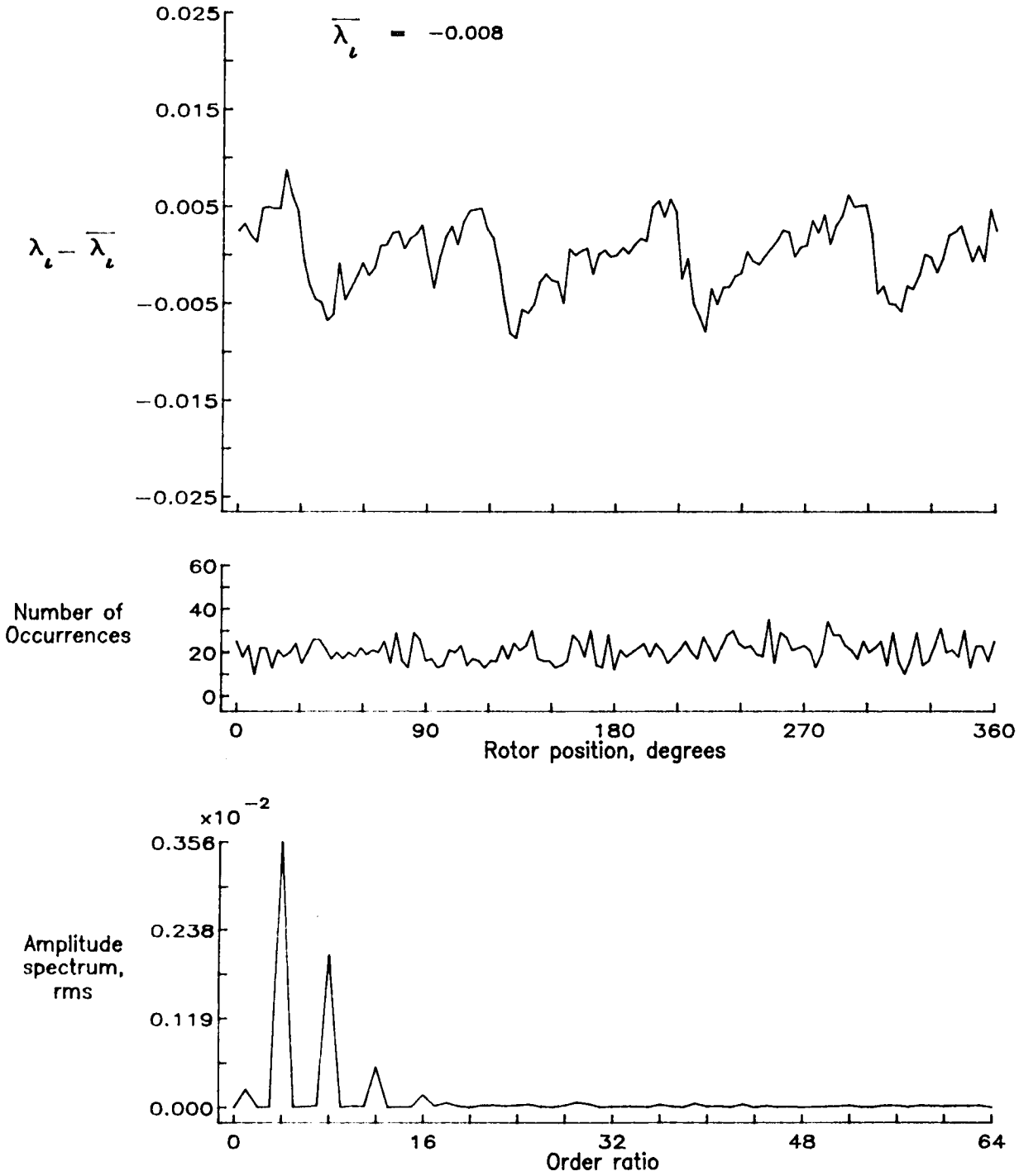

Figure 165.– Concluded.

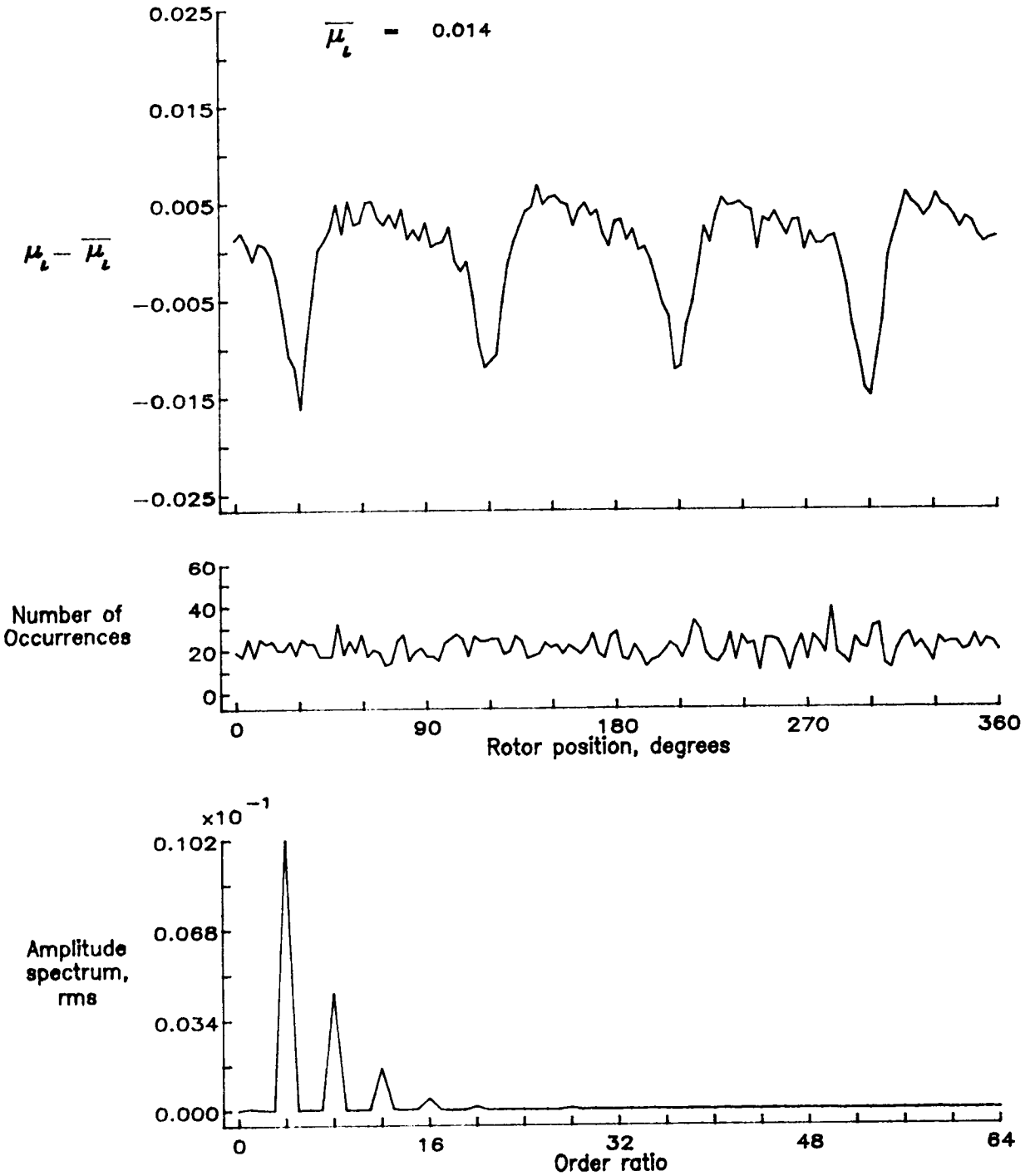

Figure 166.– Induced inflow velocity measured at 300 degrees and r/R of 0.60.

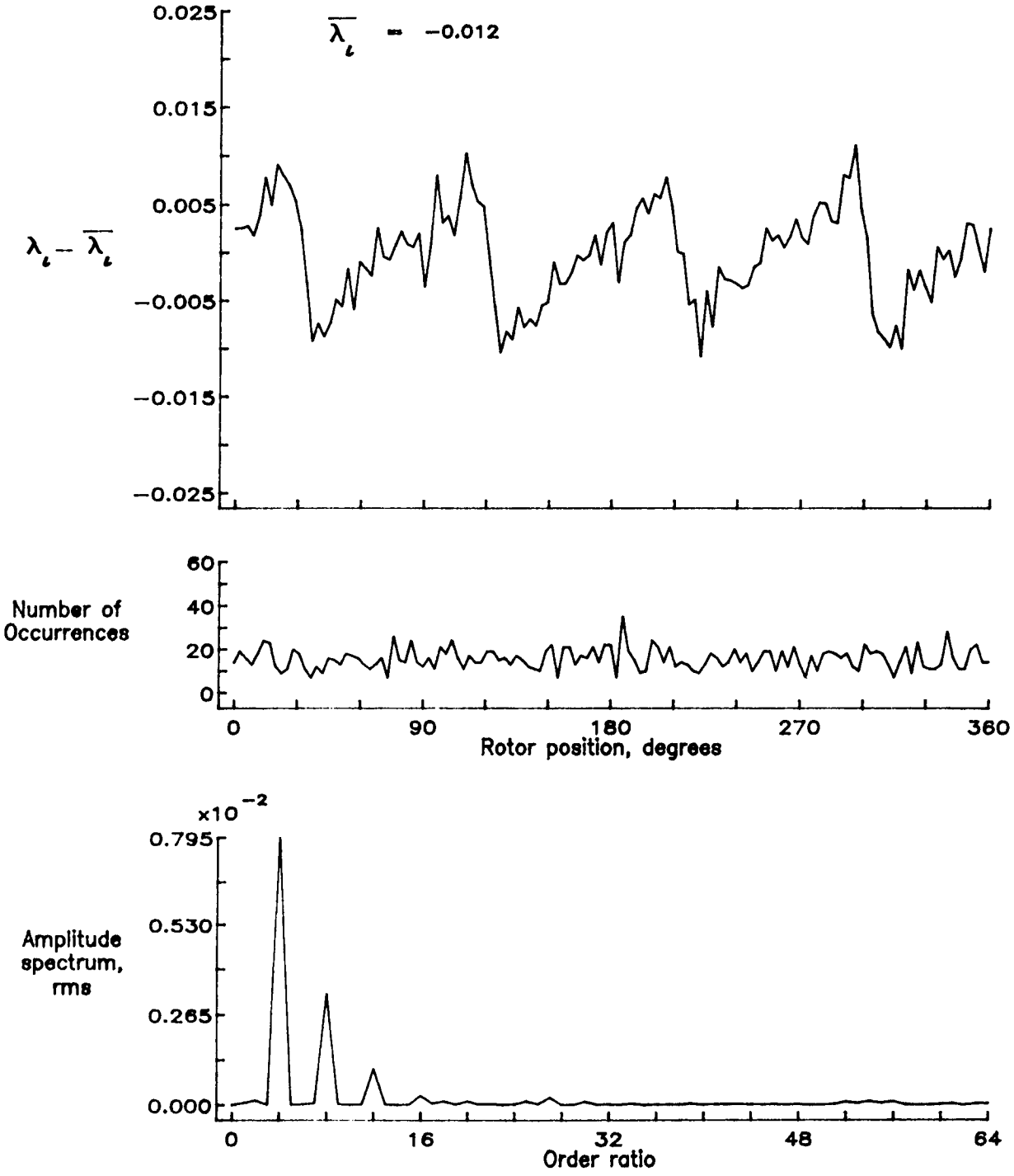

Figure 166.– Concluded.

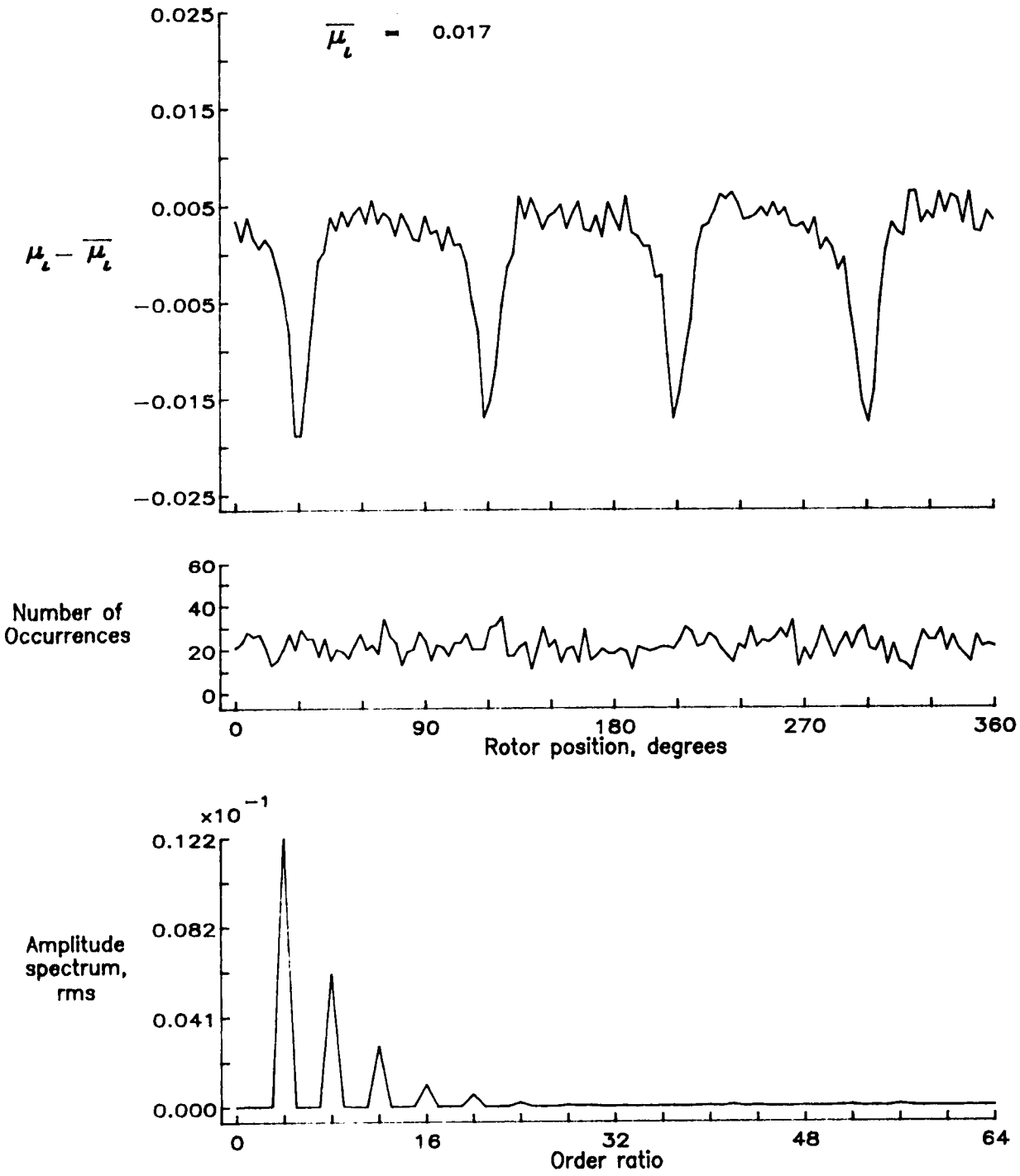

Figure 167.– Induced inflow velocity measured at 300 degrees and r/R of 0.70.

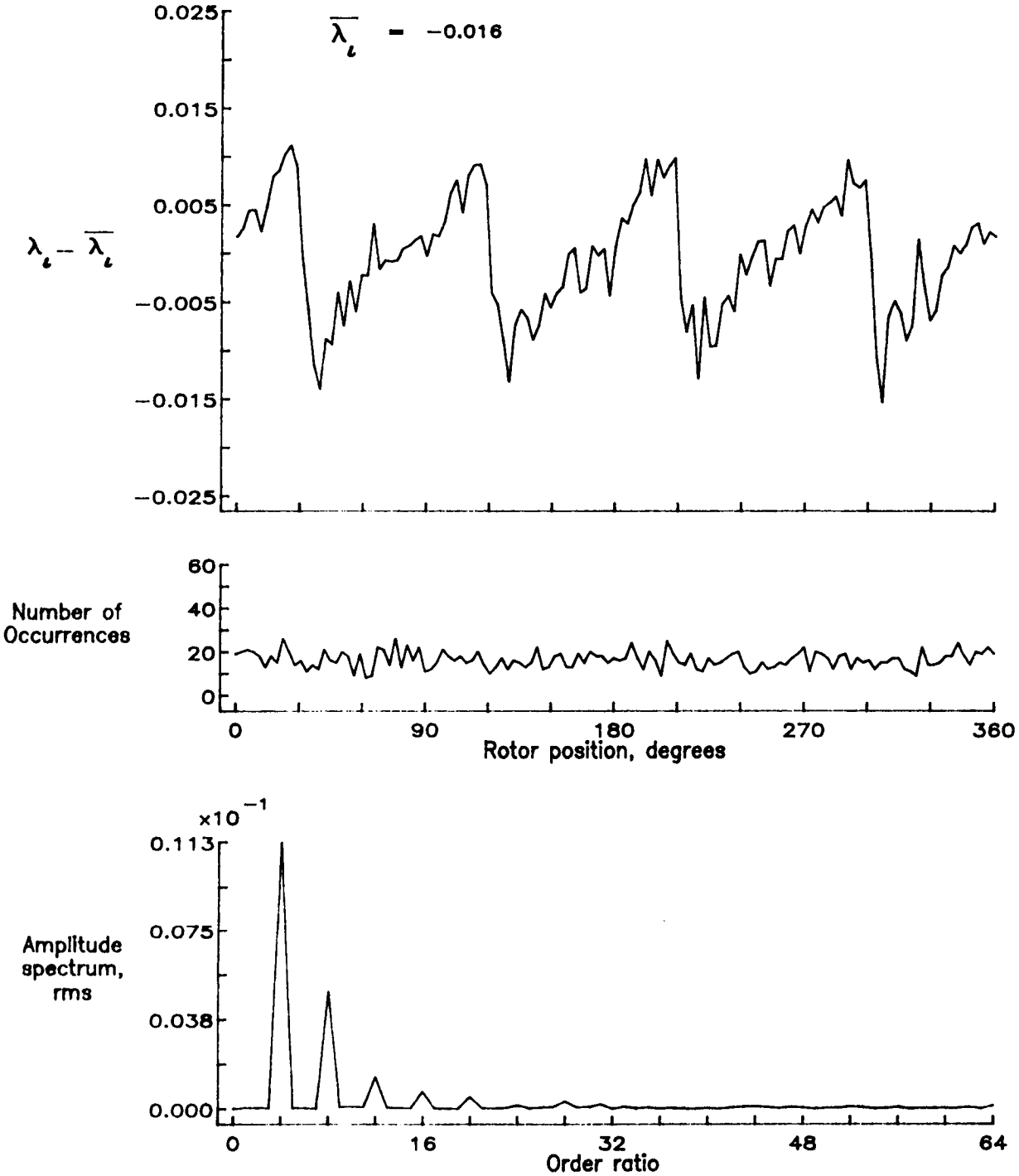

Figure 167.– Concluded.

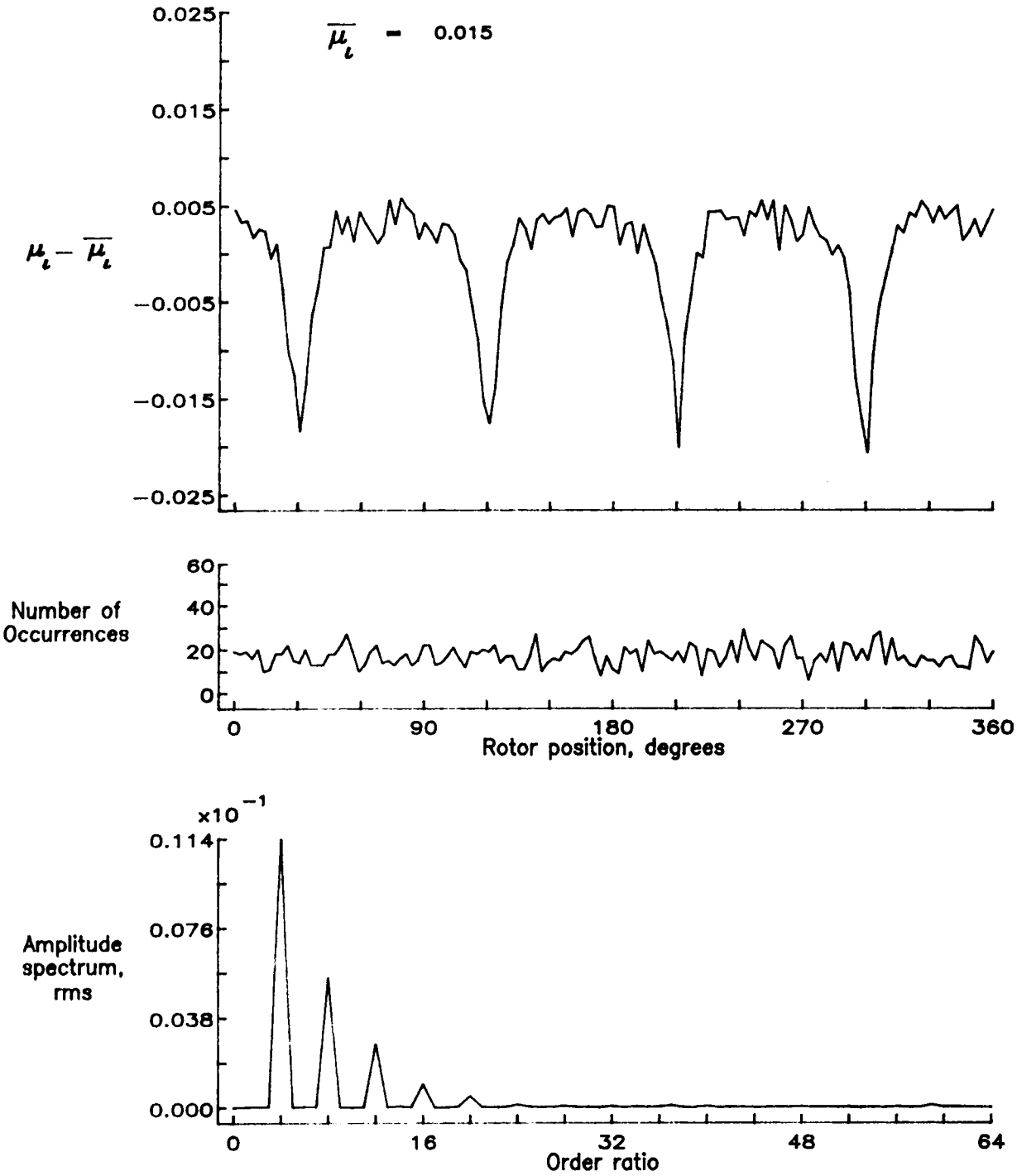

Figure 168.– Induced inflow velocity measured at 300 degrees and r/R of 0.74.

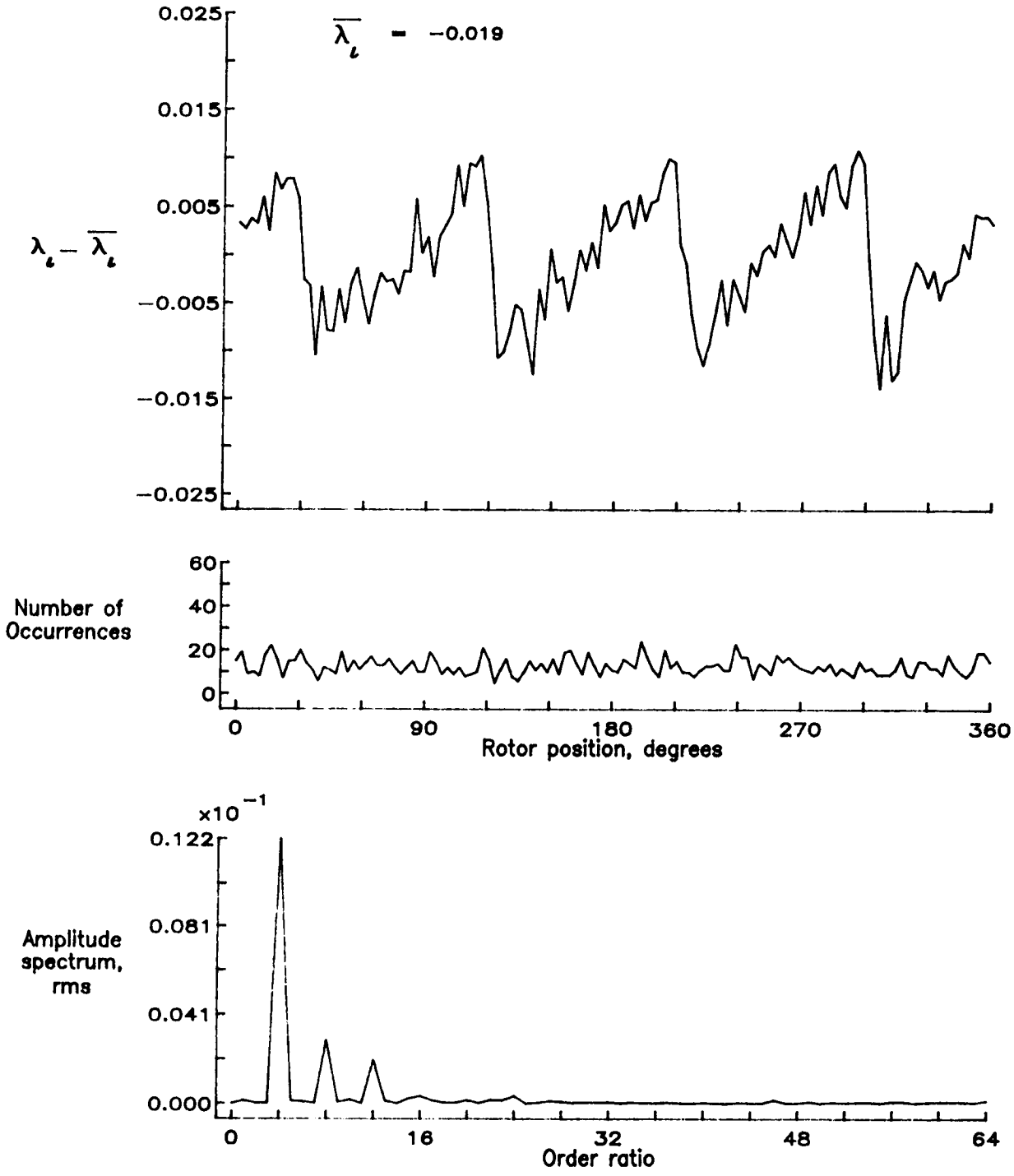

Figure 168.– Concluded.

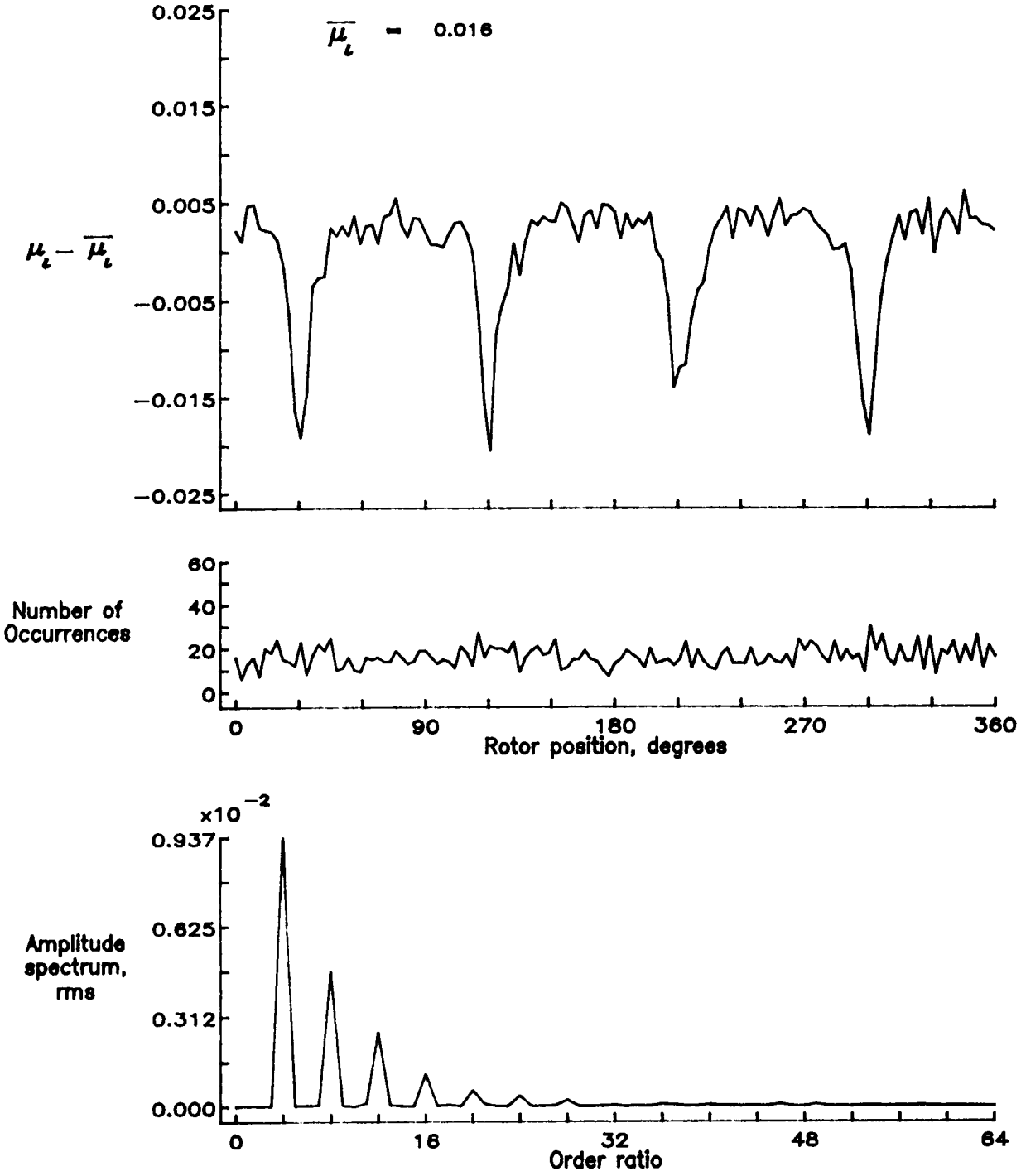

Figure 169.– Induced inflow velocity measured at 300 degrees and r/R of 0.78.

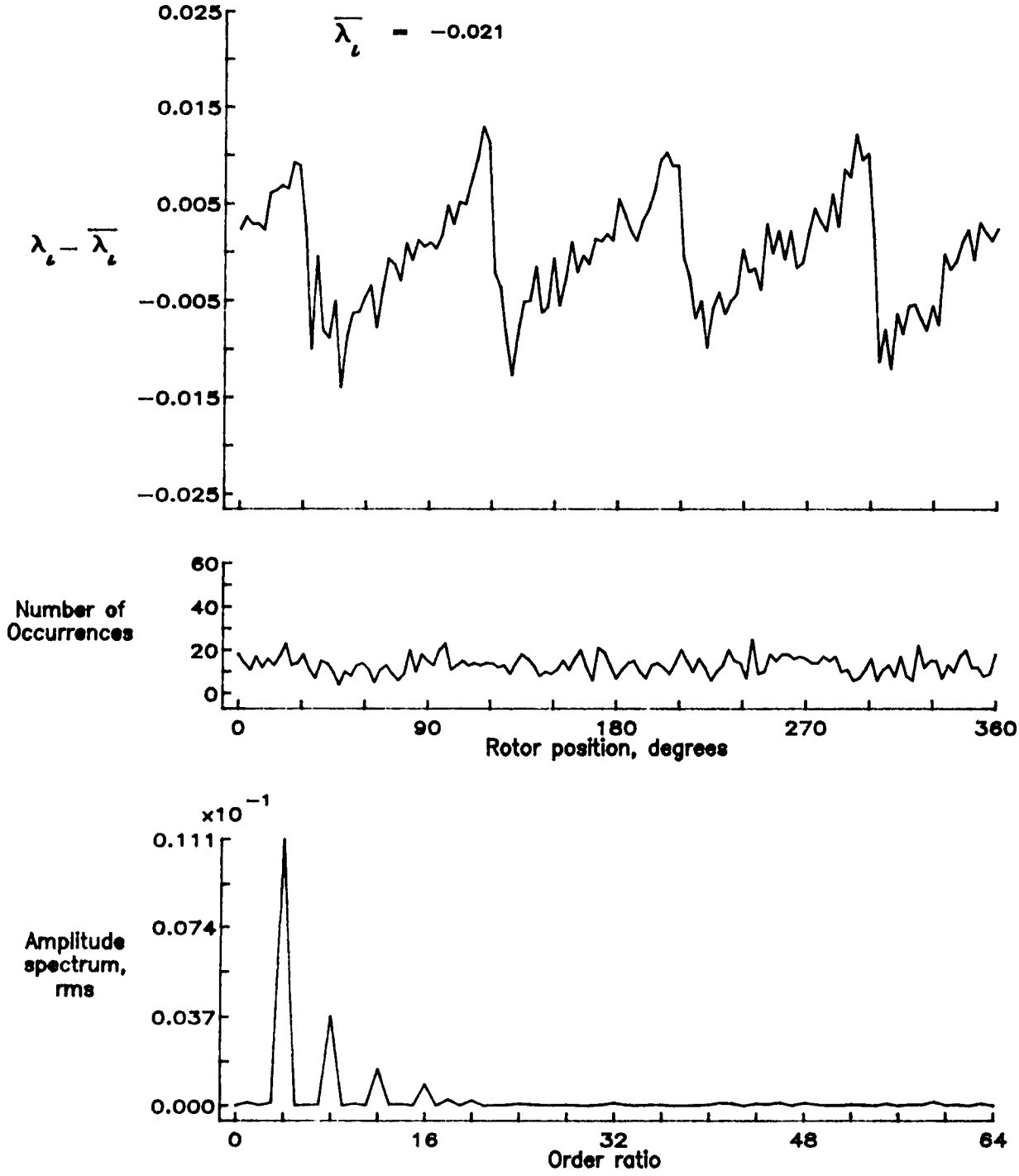

Figure 169.– Concluded.

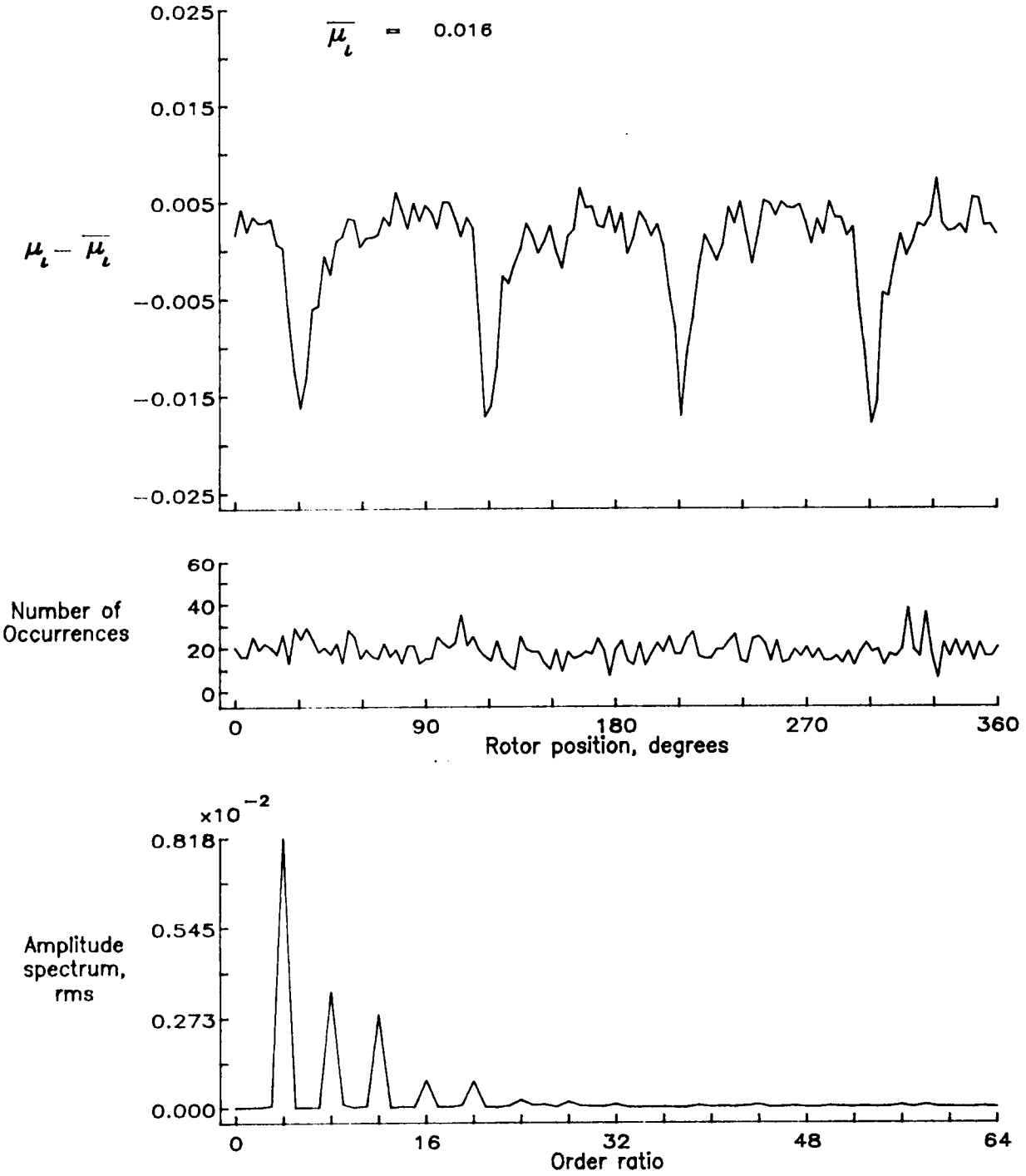

Figure 170.– Induced inflow velocity measured at 300 degrees and r/R of 0.82.

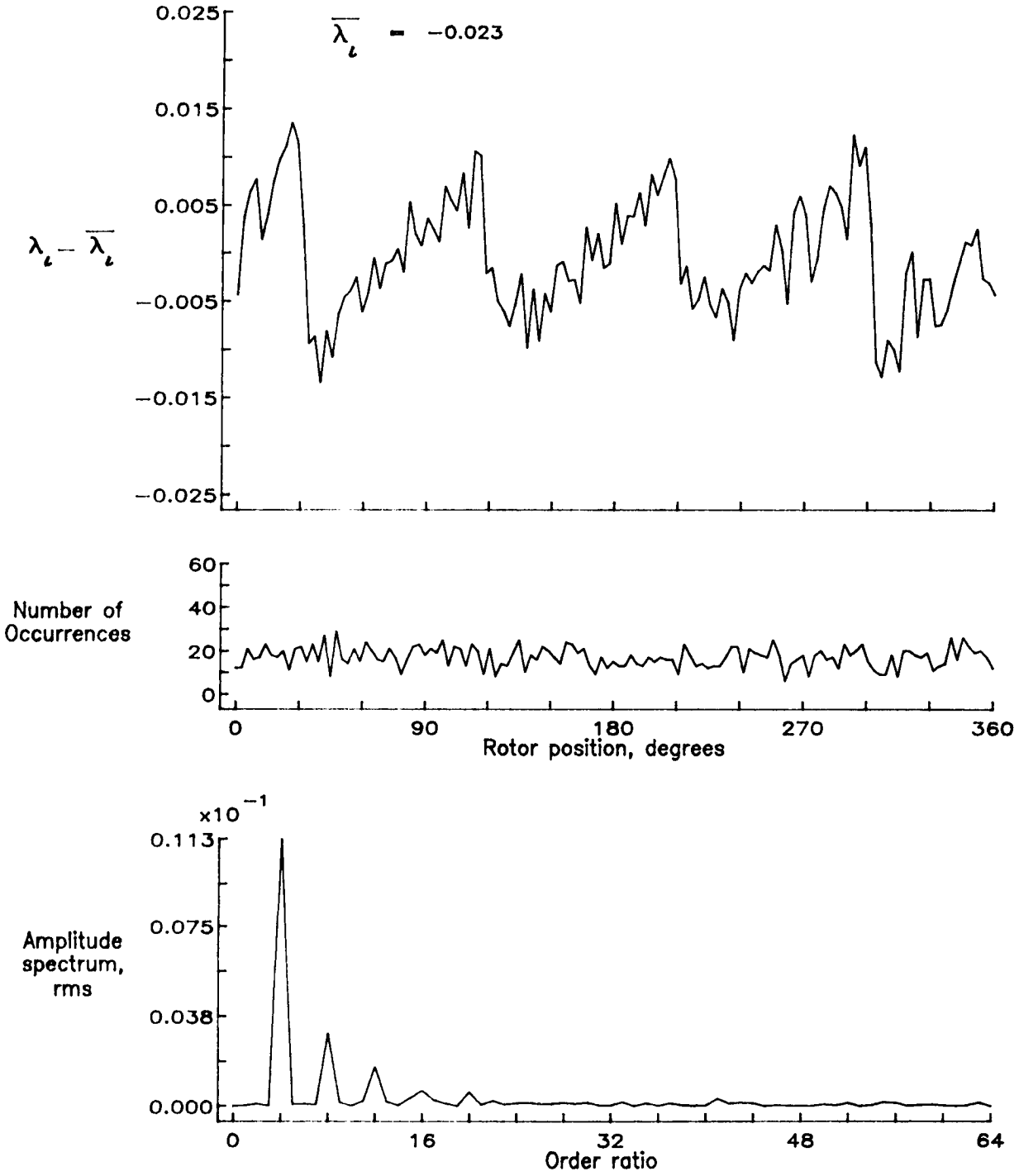

Figure 170.– Concluded.

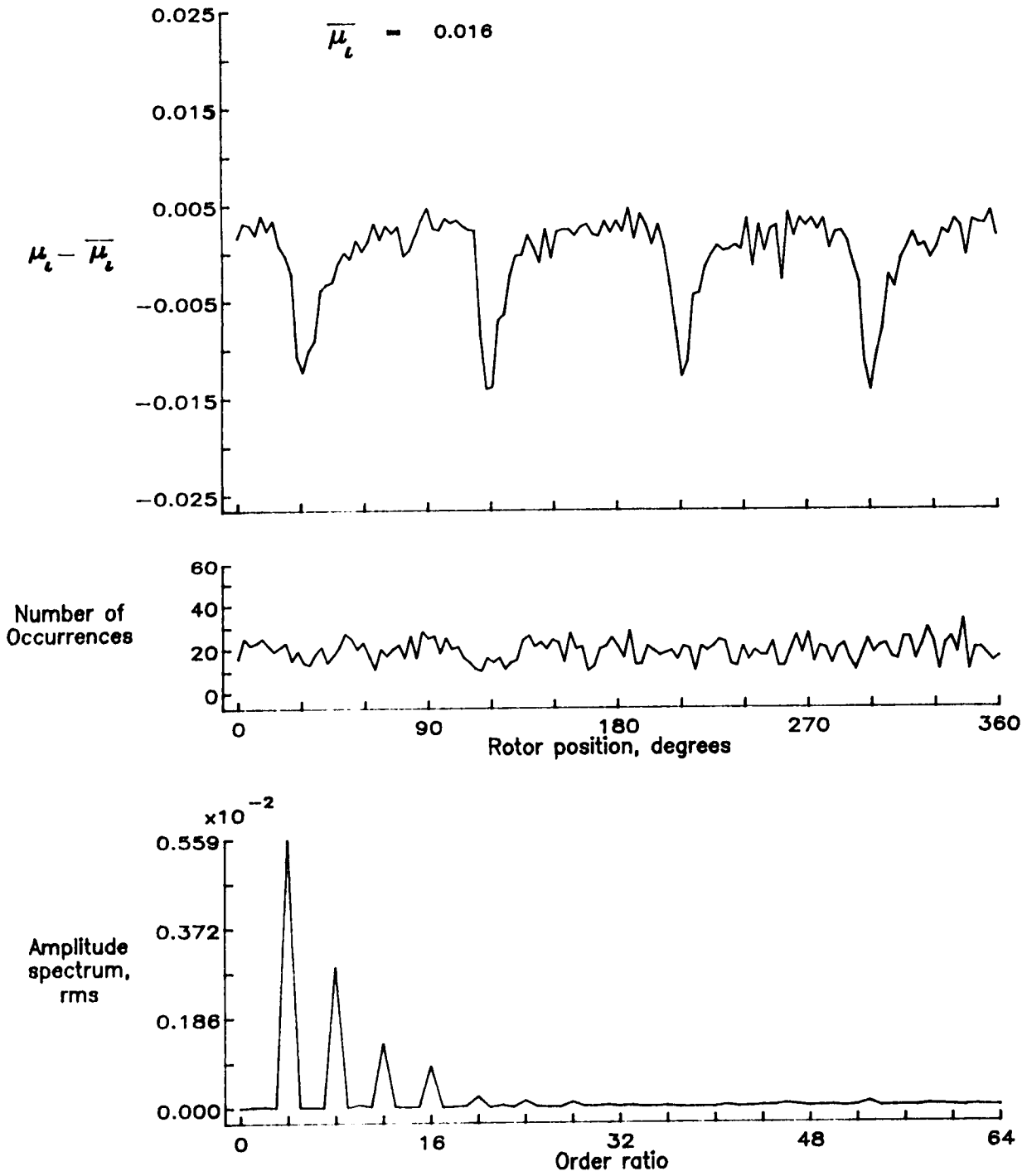

Figure 171.– Induced inflow velocity measured at 300 degrees and r/R of 0.86.

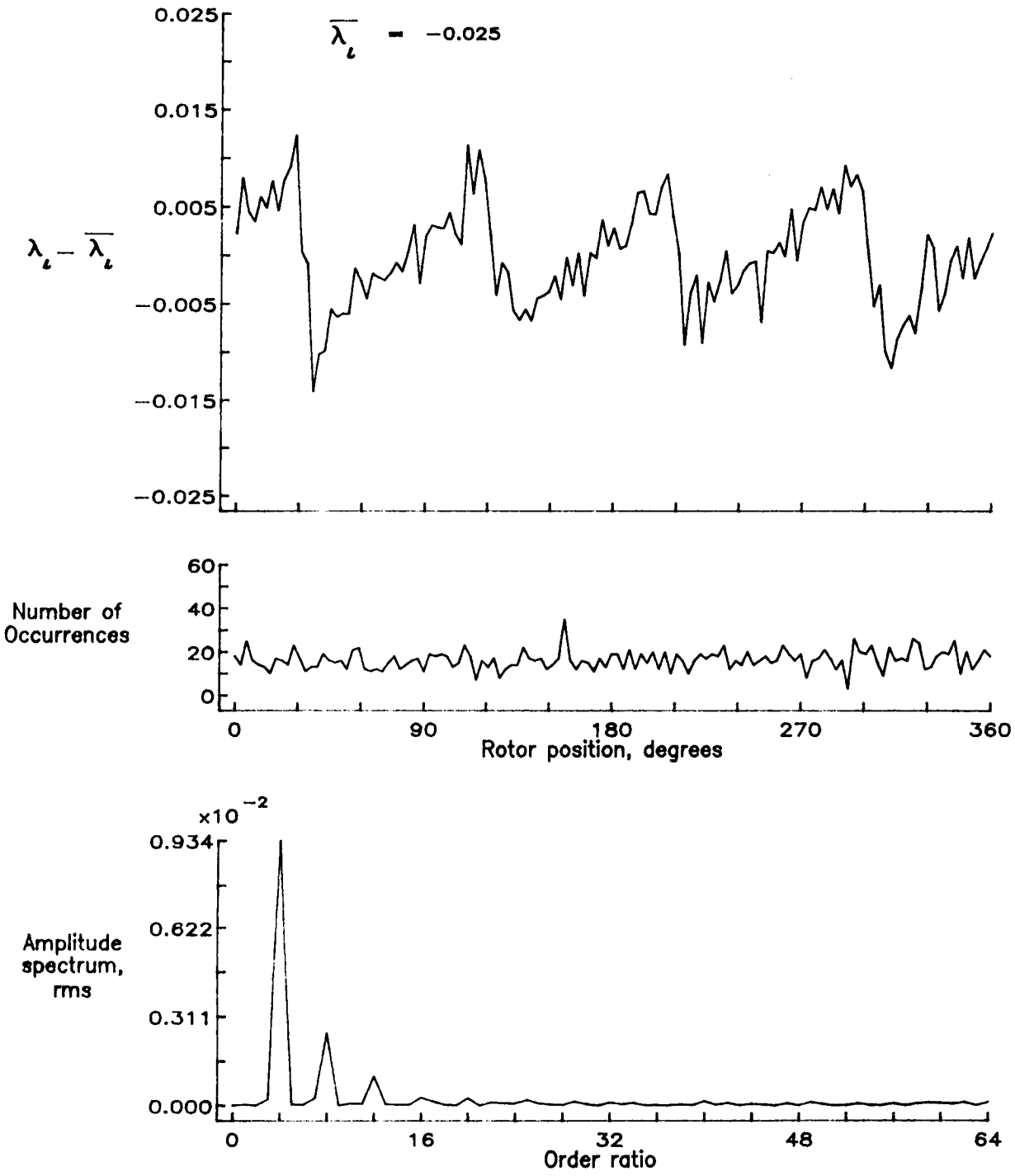

Figure 171.– Concluded.

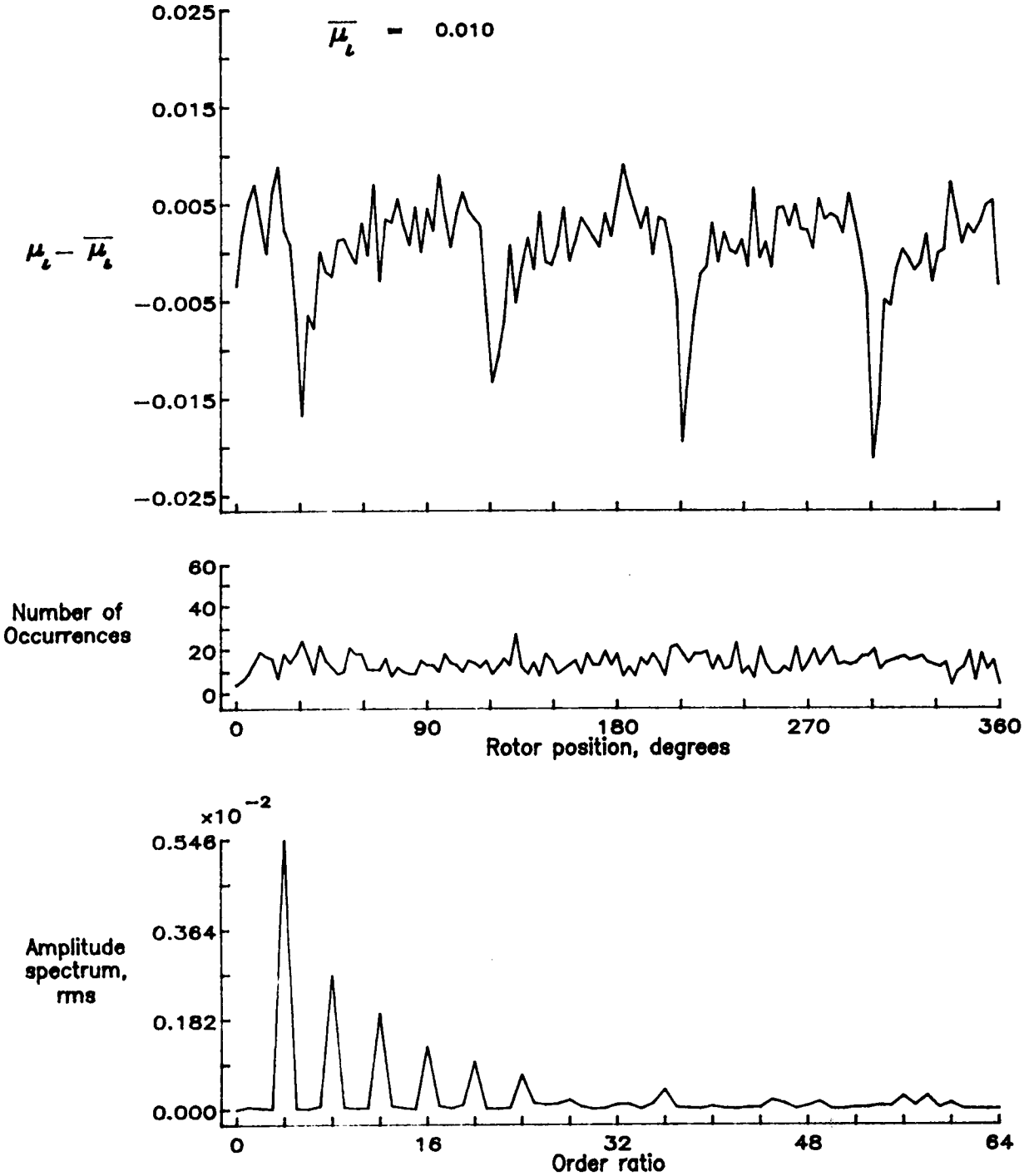

Figure 172.– Induced inflow velocity measured at 300 degrees and r/R of 0.90.

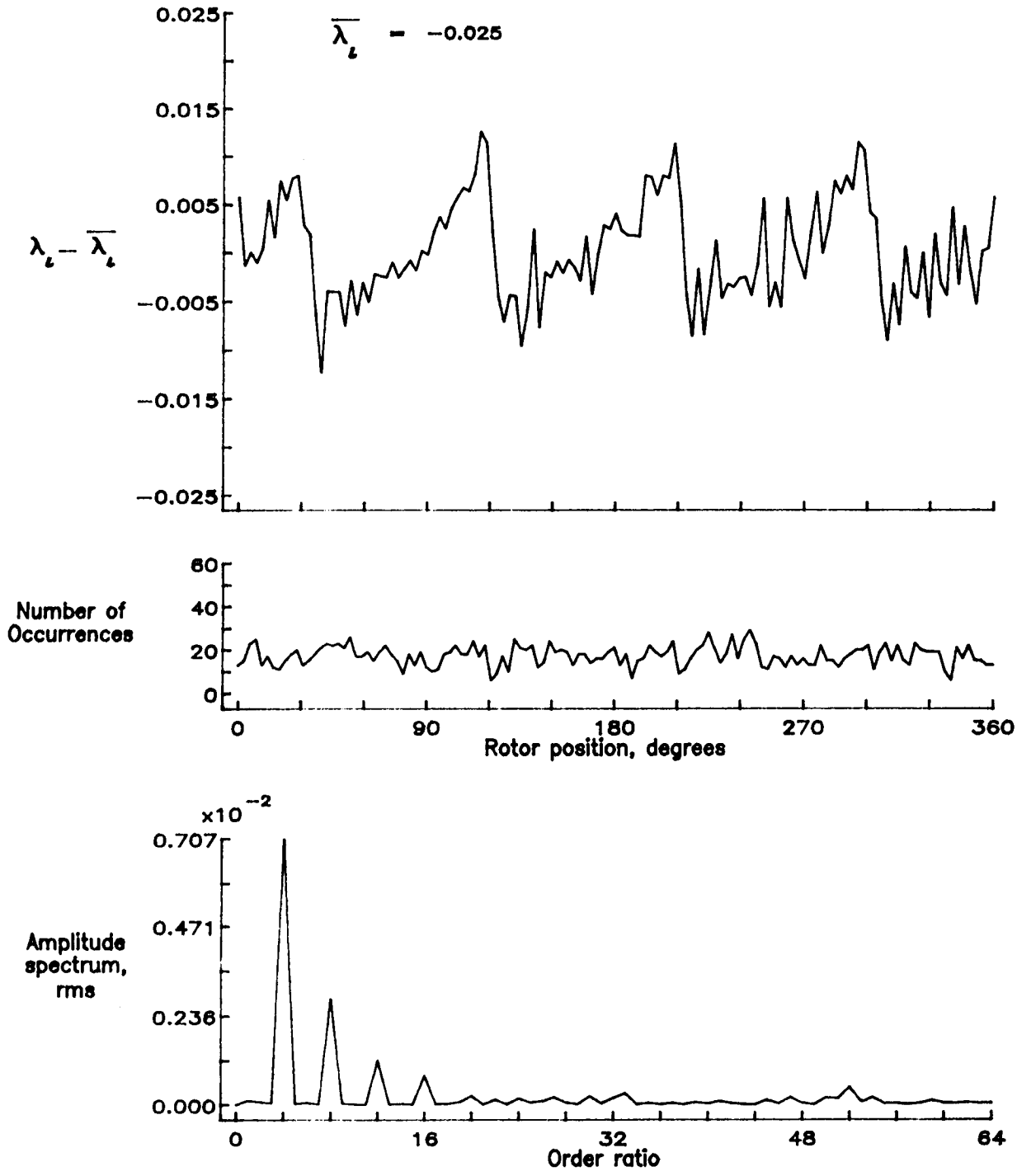

Figure 172.– Concluded.

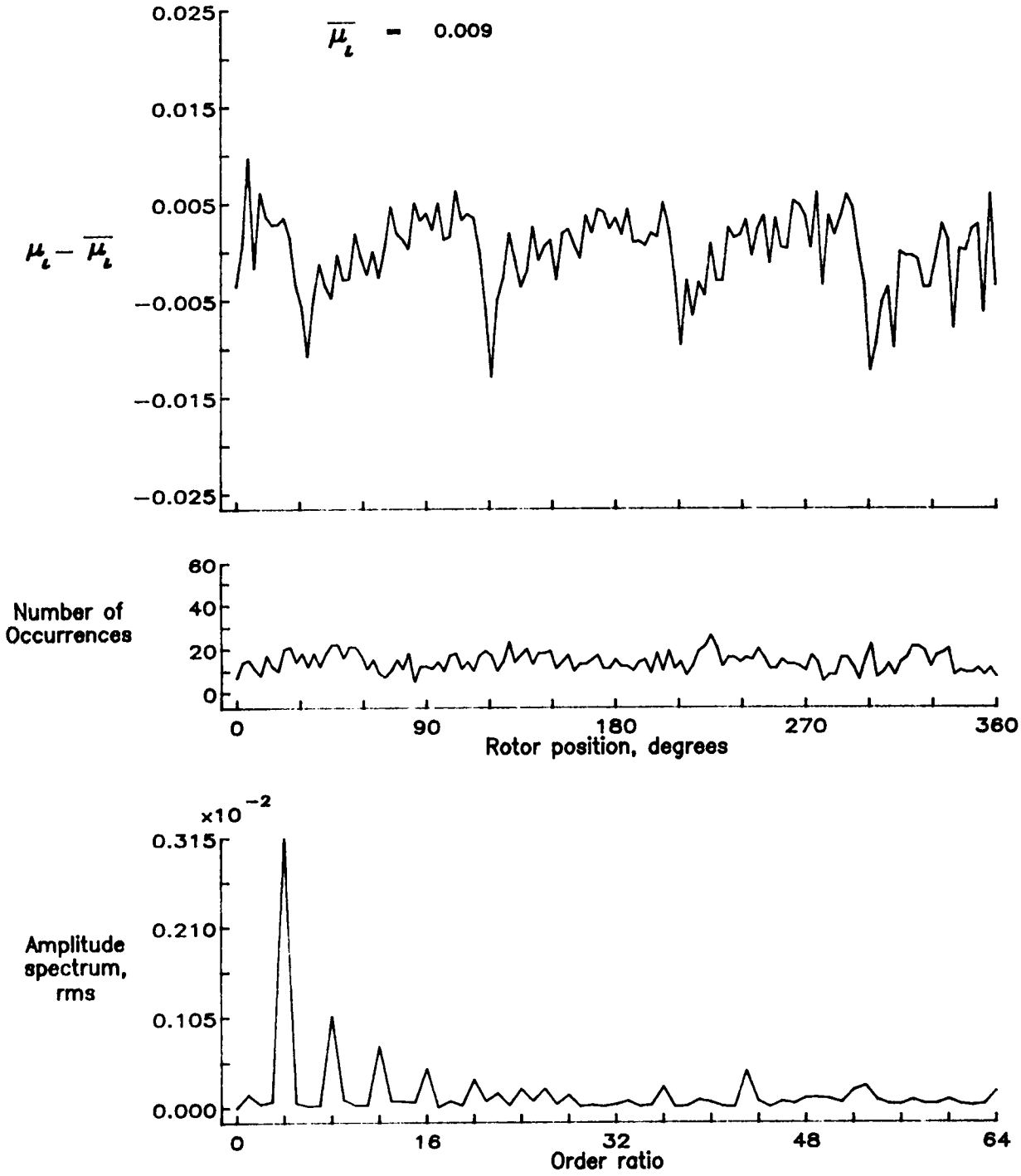

Figure 173.– Induced inflow velocity measured at 300 degrees and r/R of 0.94.

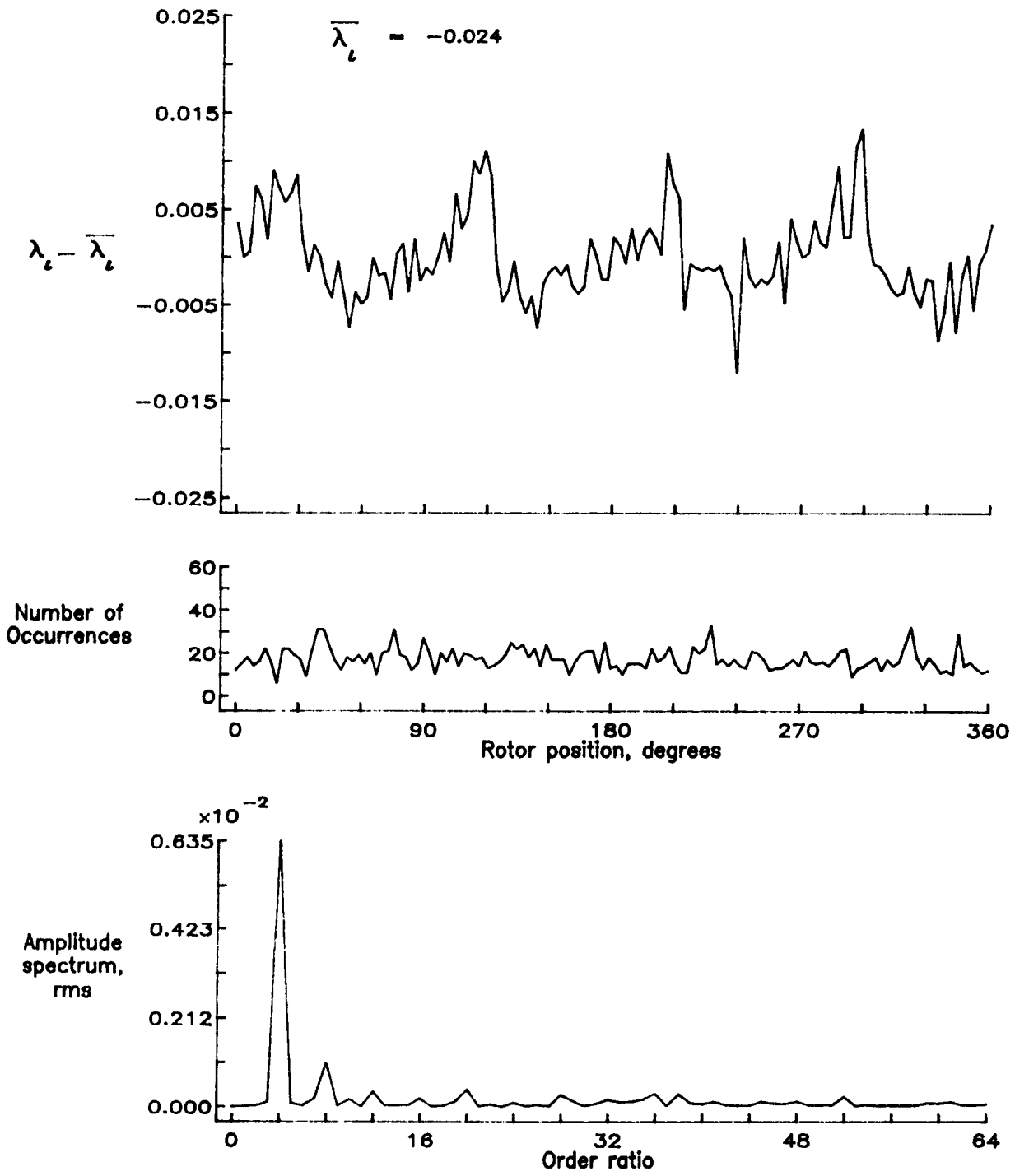

Figure 173.– Concluded.

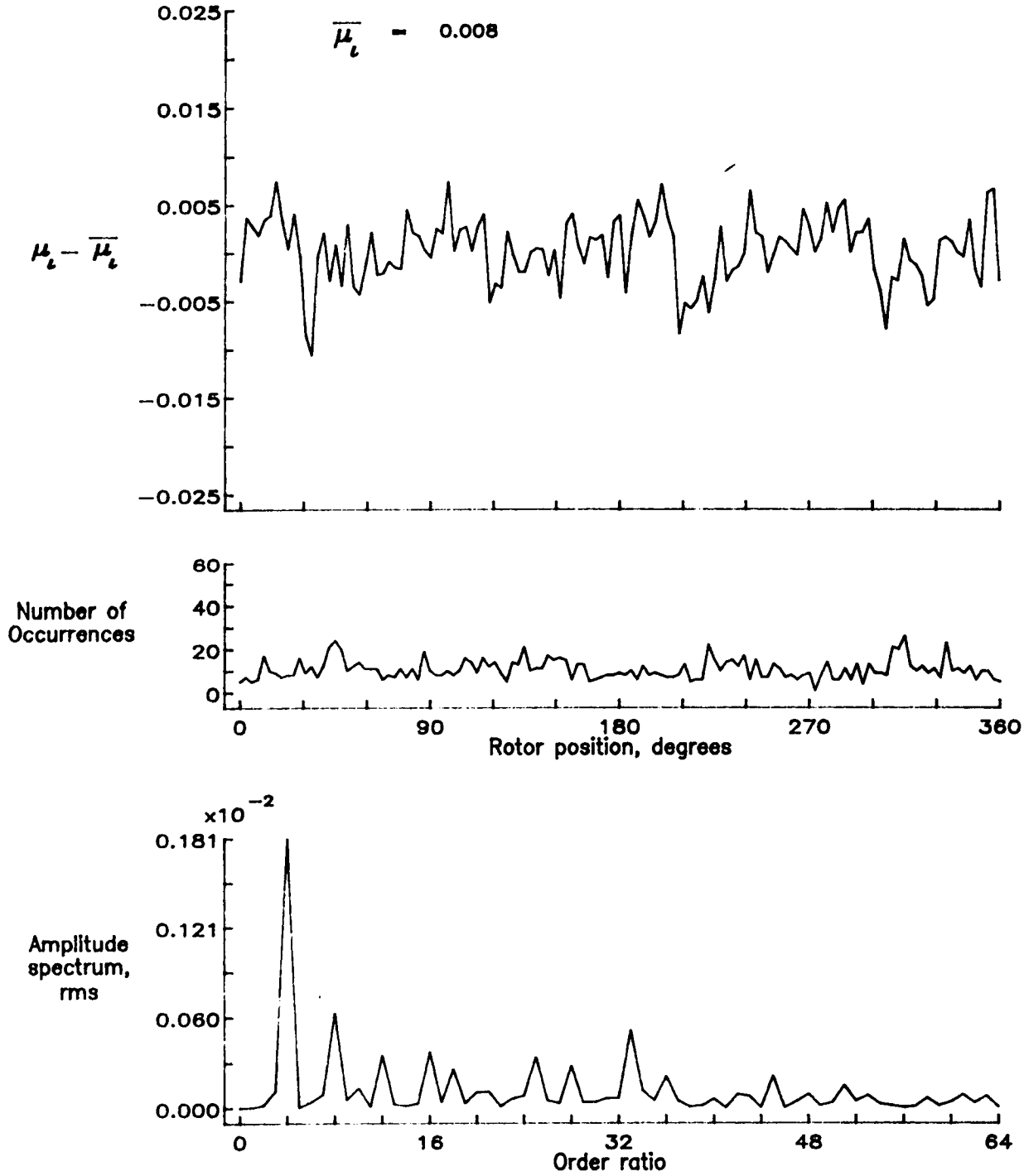

Figure 174.– Induced inflow velocity measured at 300 degrees and r/R of 0.98.

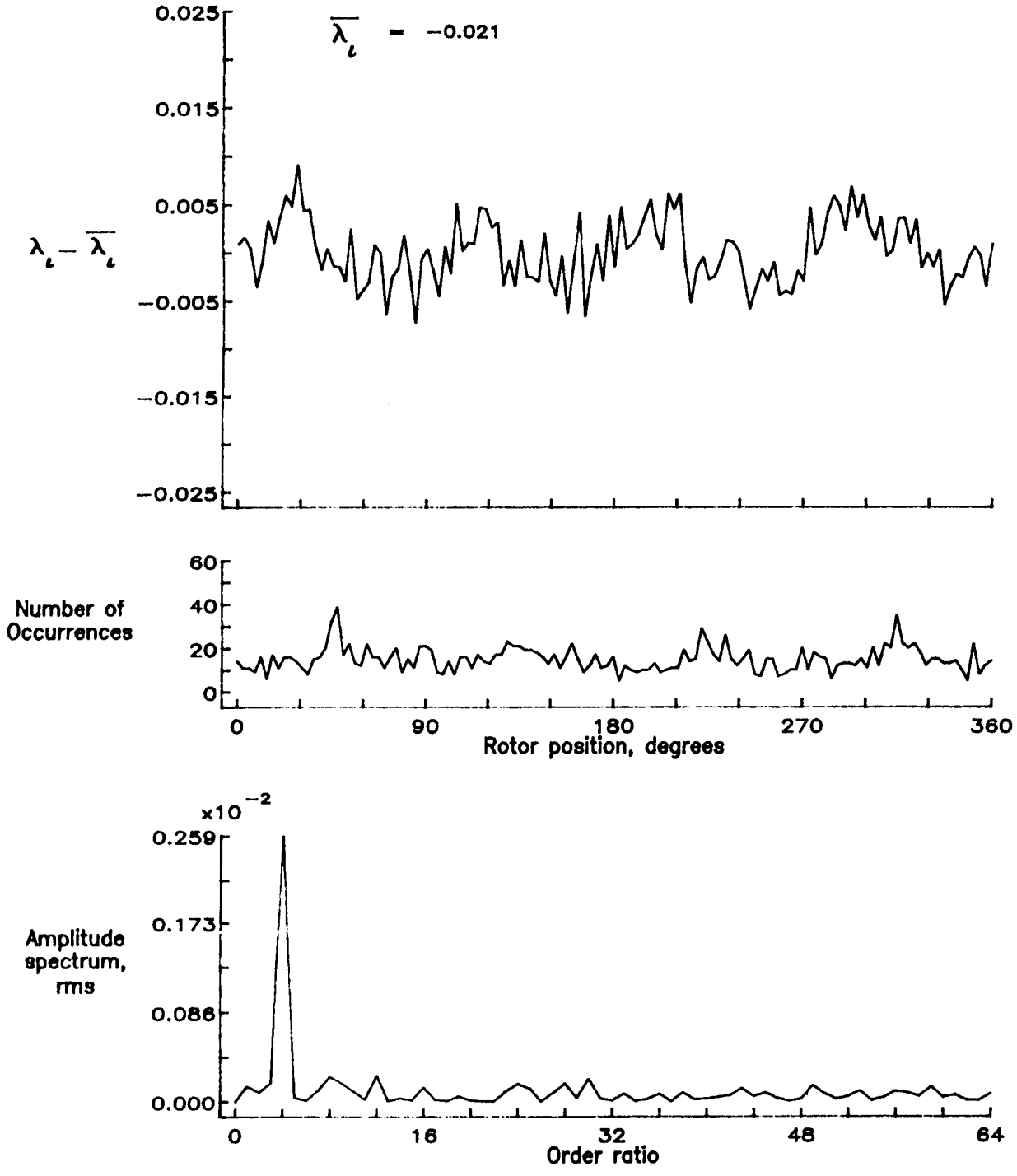

Figure 174.– Concluded.

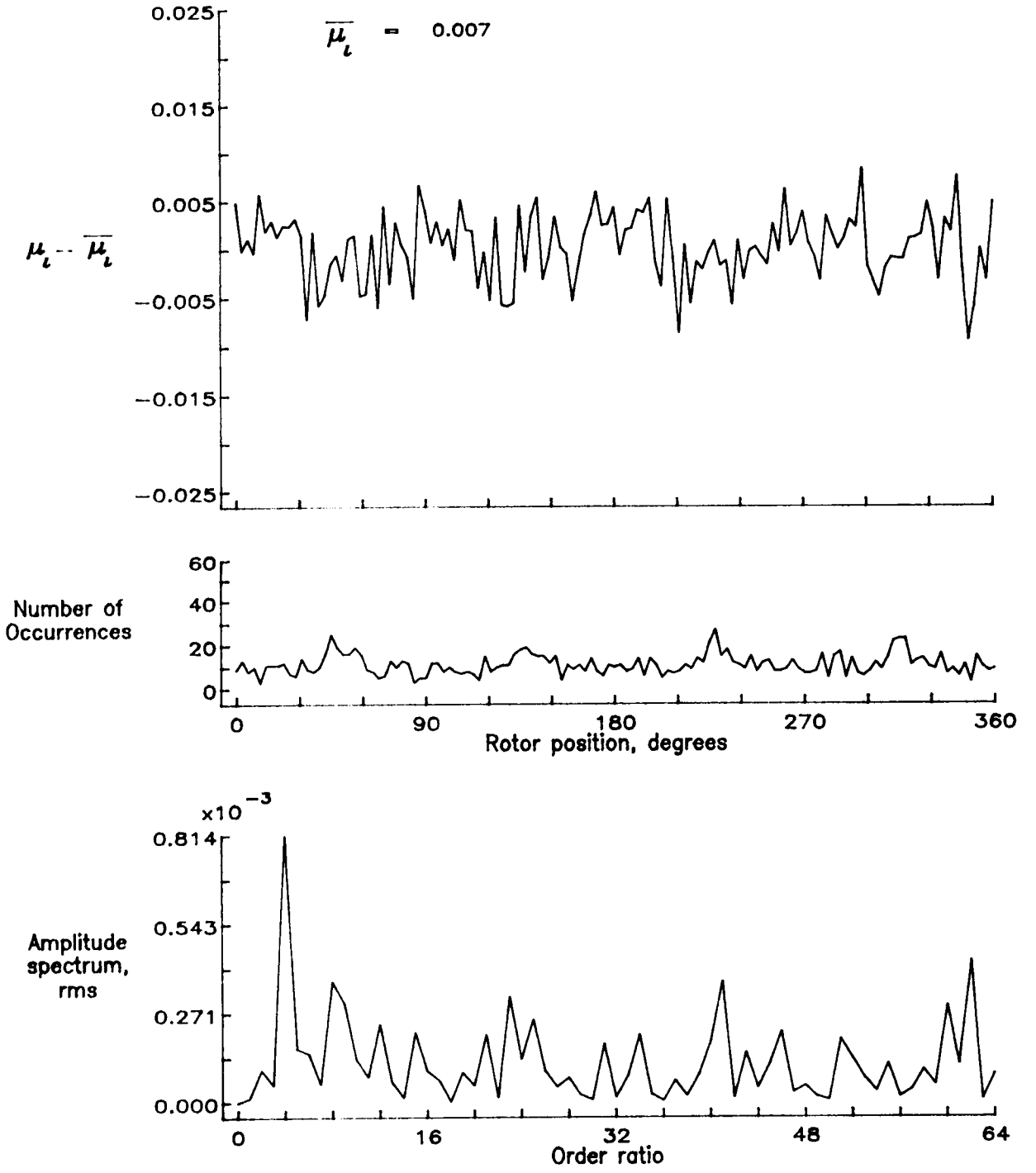

Figure 175.– Induced inflow velocity measured at 300 degrees and r/R of 1.02.

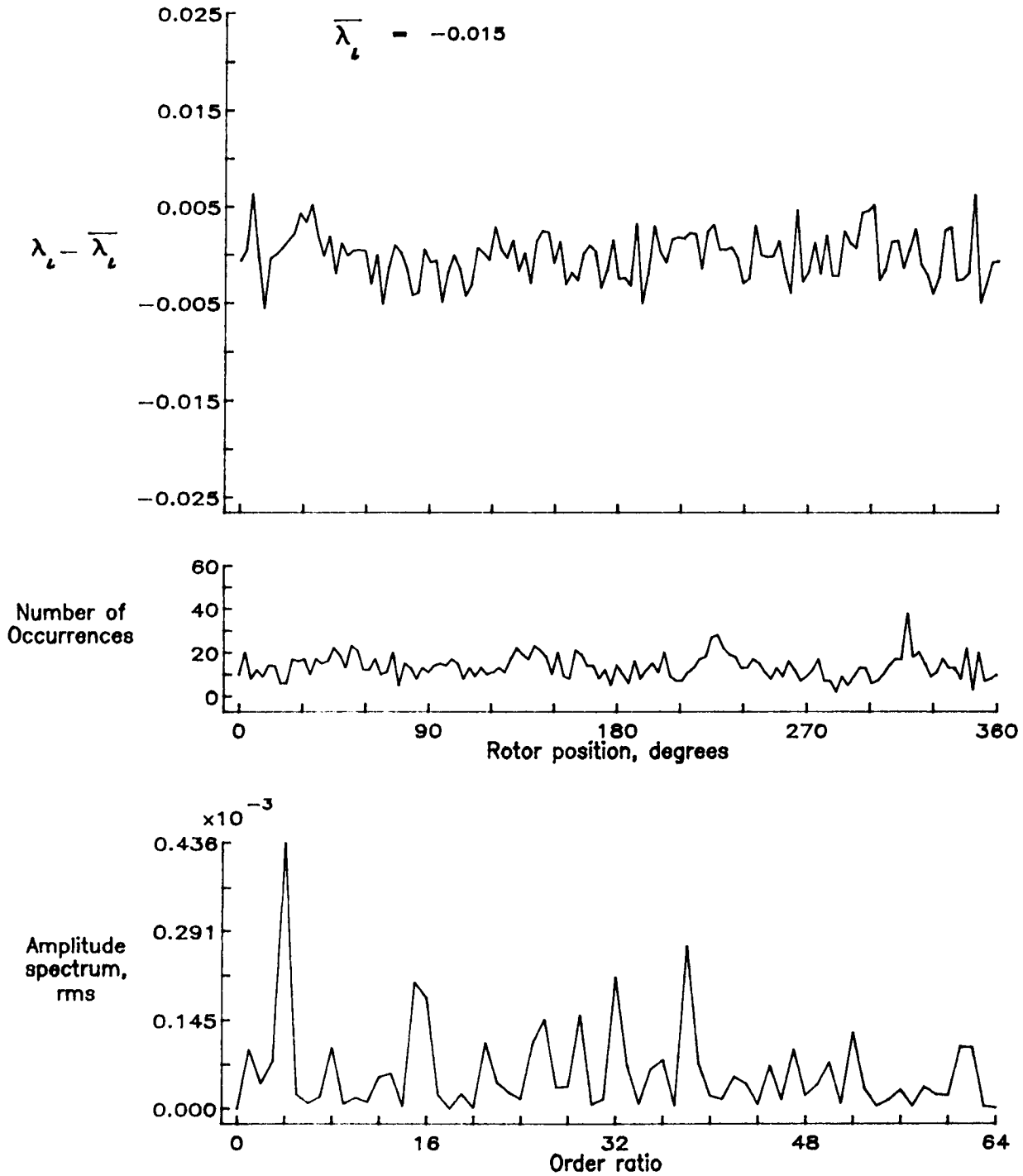

Figure 175.– Concluded.

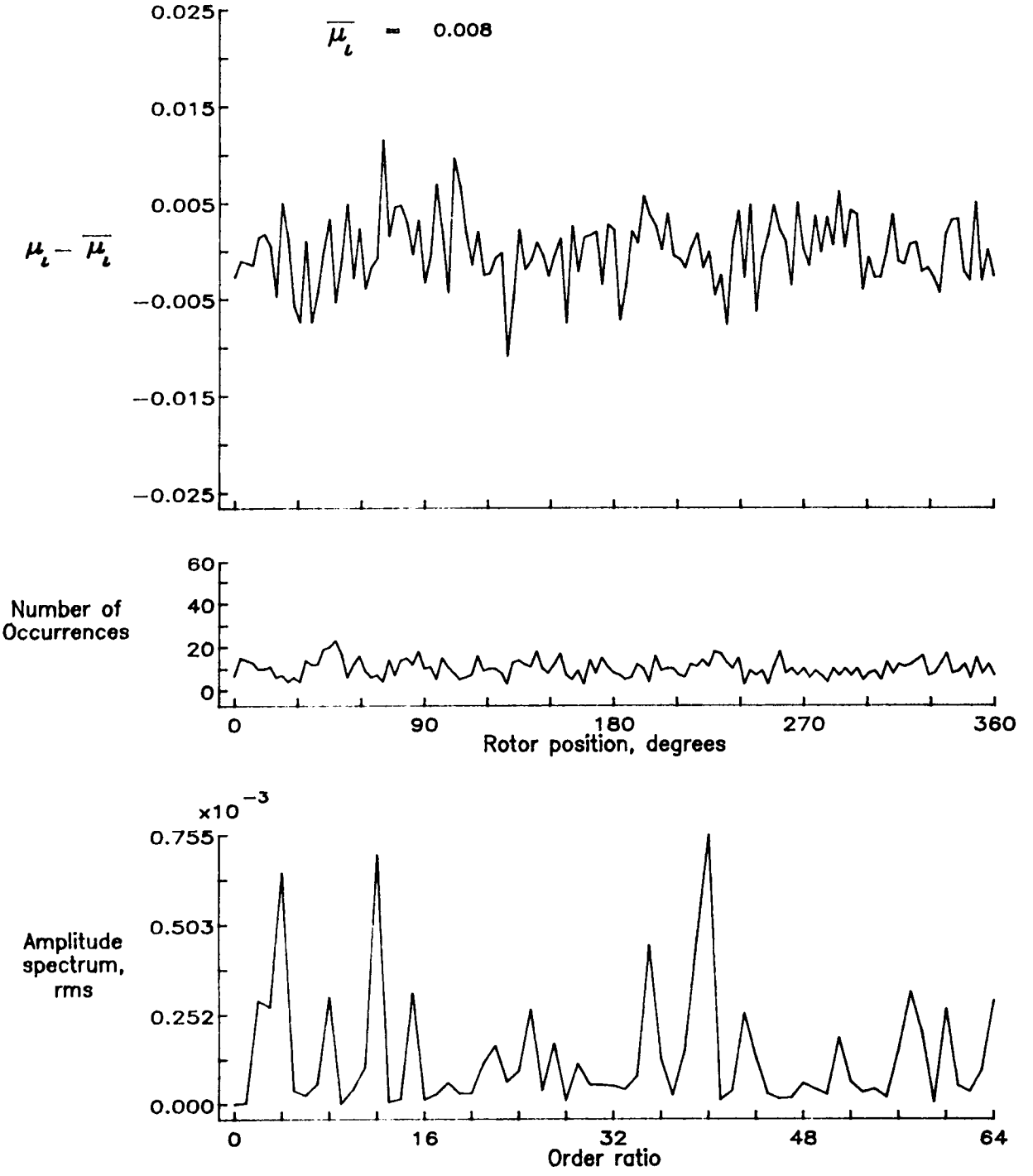

Figure 176.– Induced inflow velocity measured at 300 degrees and r/R of 1.04.

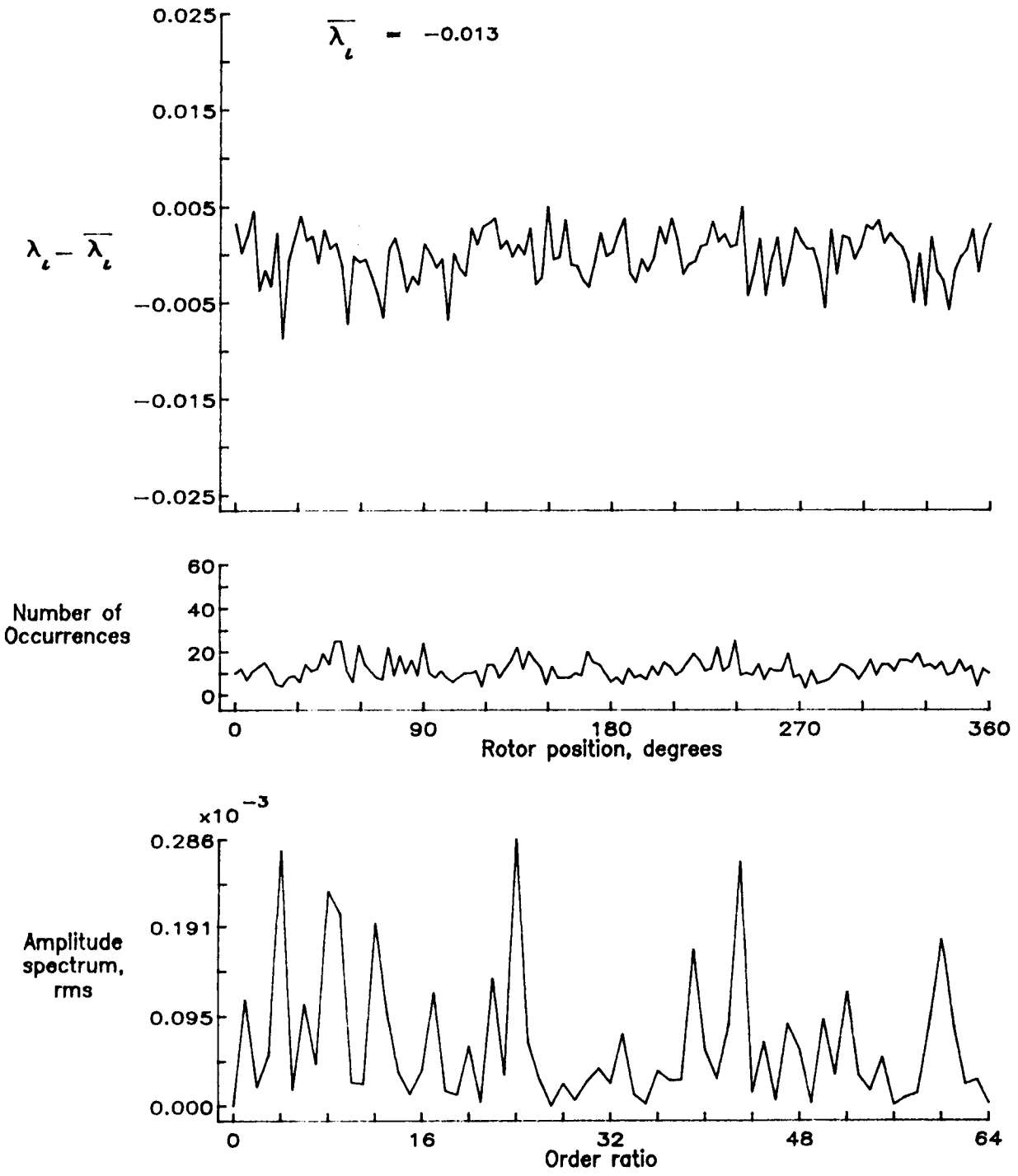

Figure 176.– Concluded.

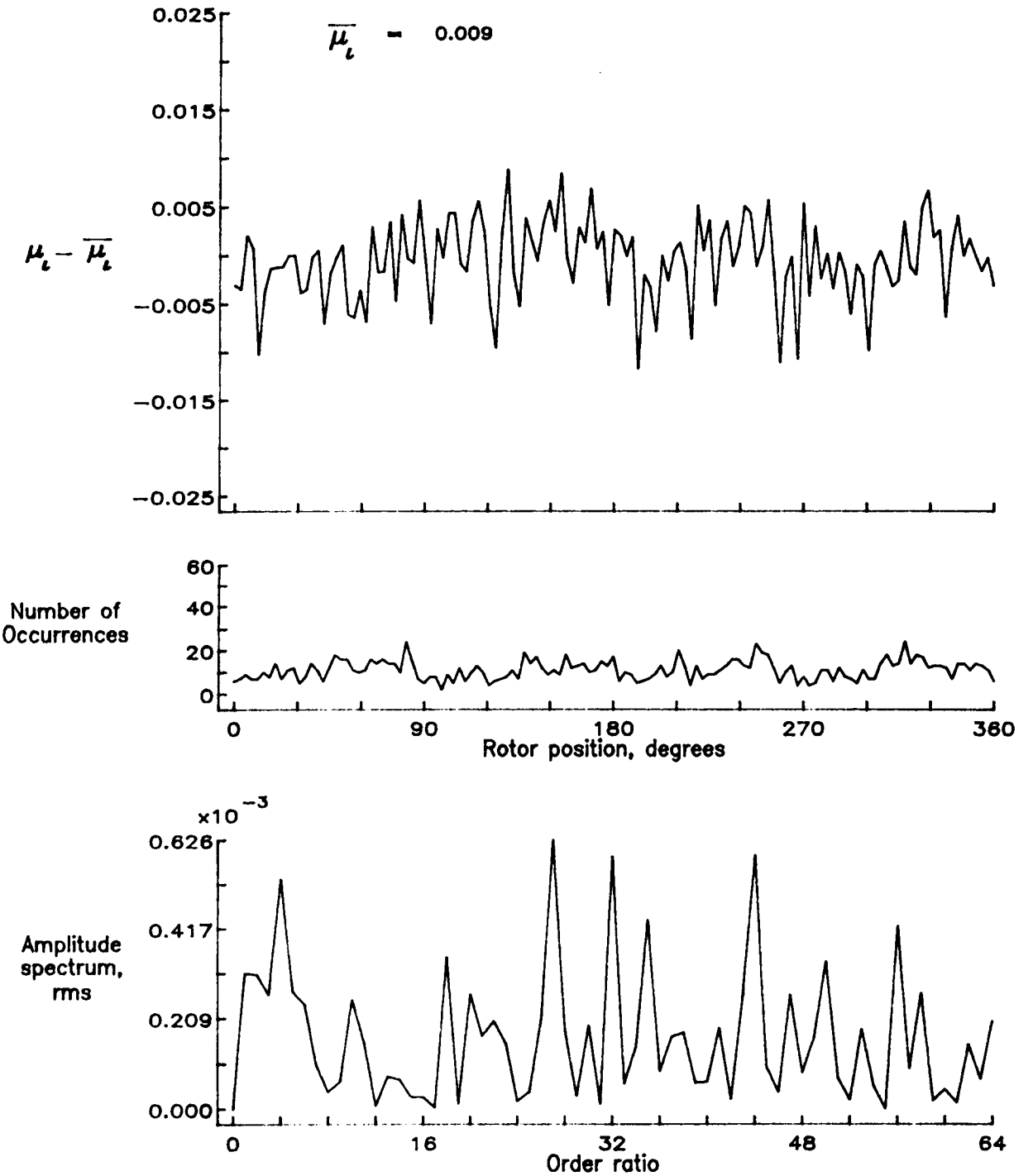

Figure 177.– Induced inflow velocity measured at 300 degrees and r/R of 1.10.

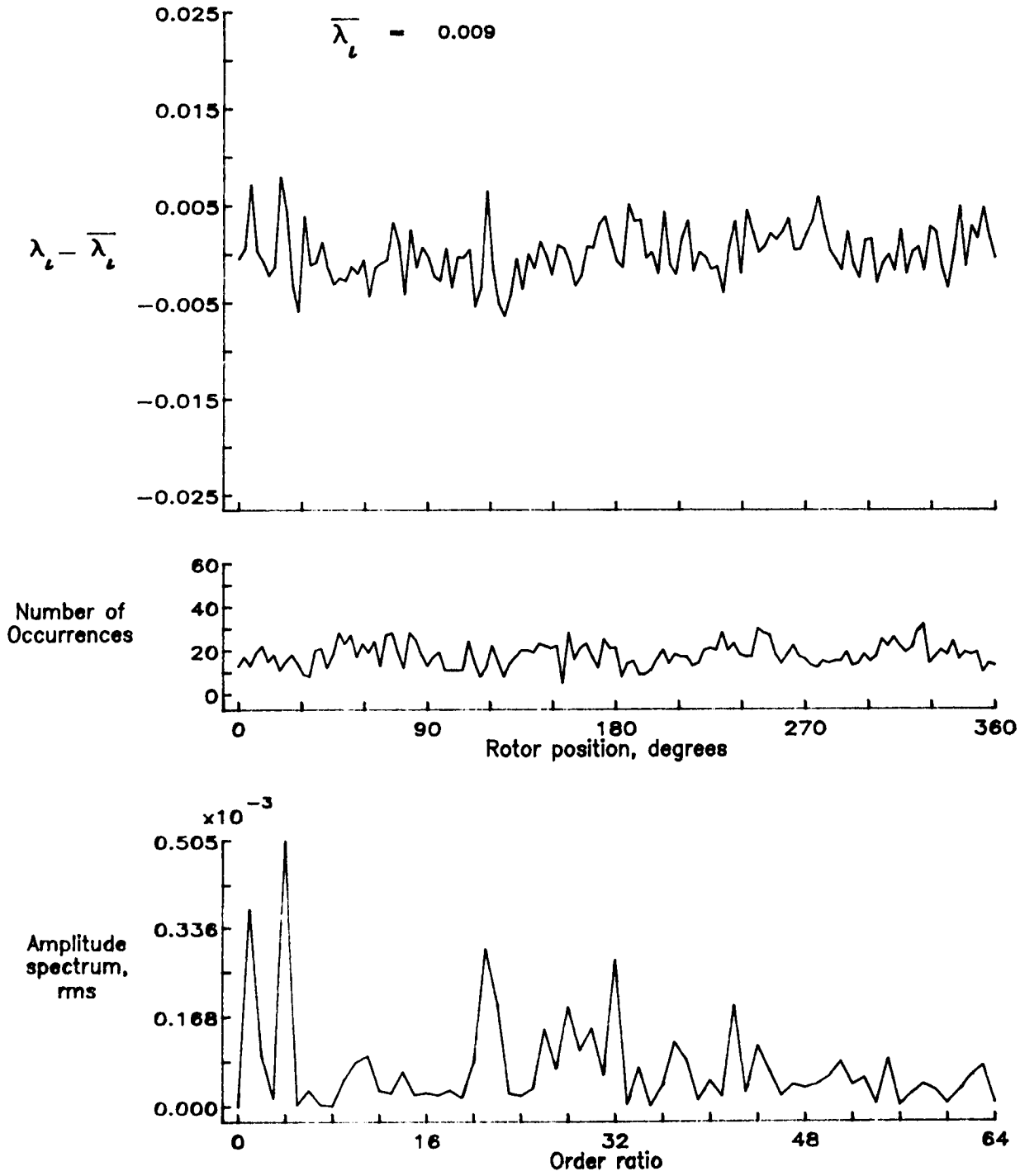

Figure 177.– Concluded.

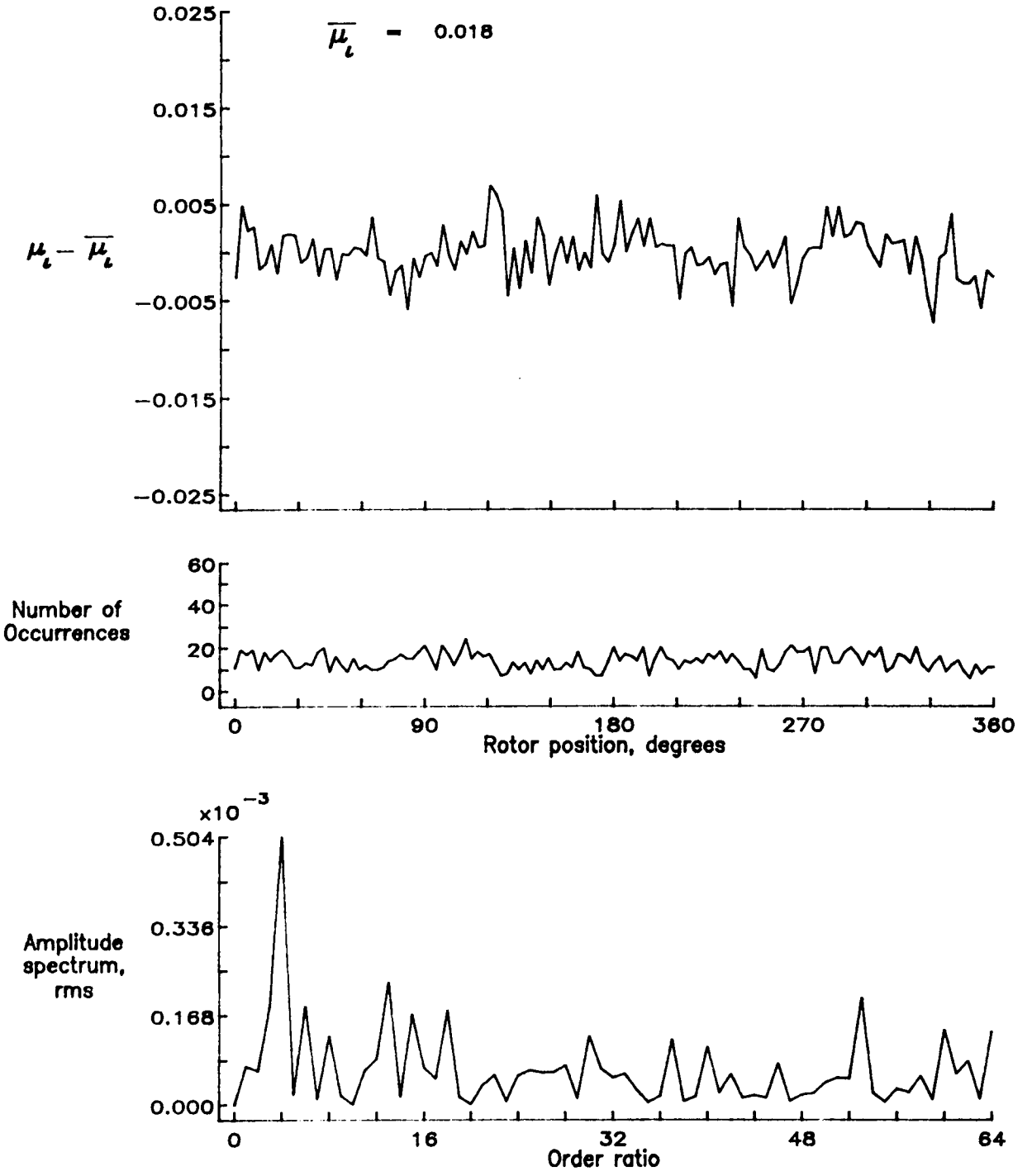

Figure 178.– Induced inflow velocity measured at 330 degrees and r/R of 0.20.

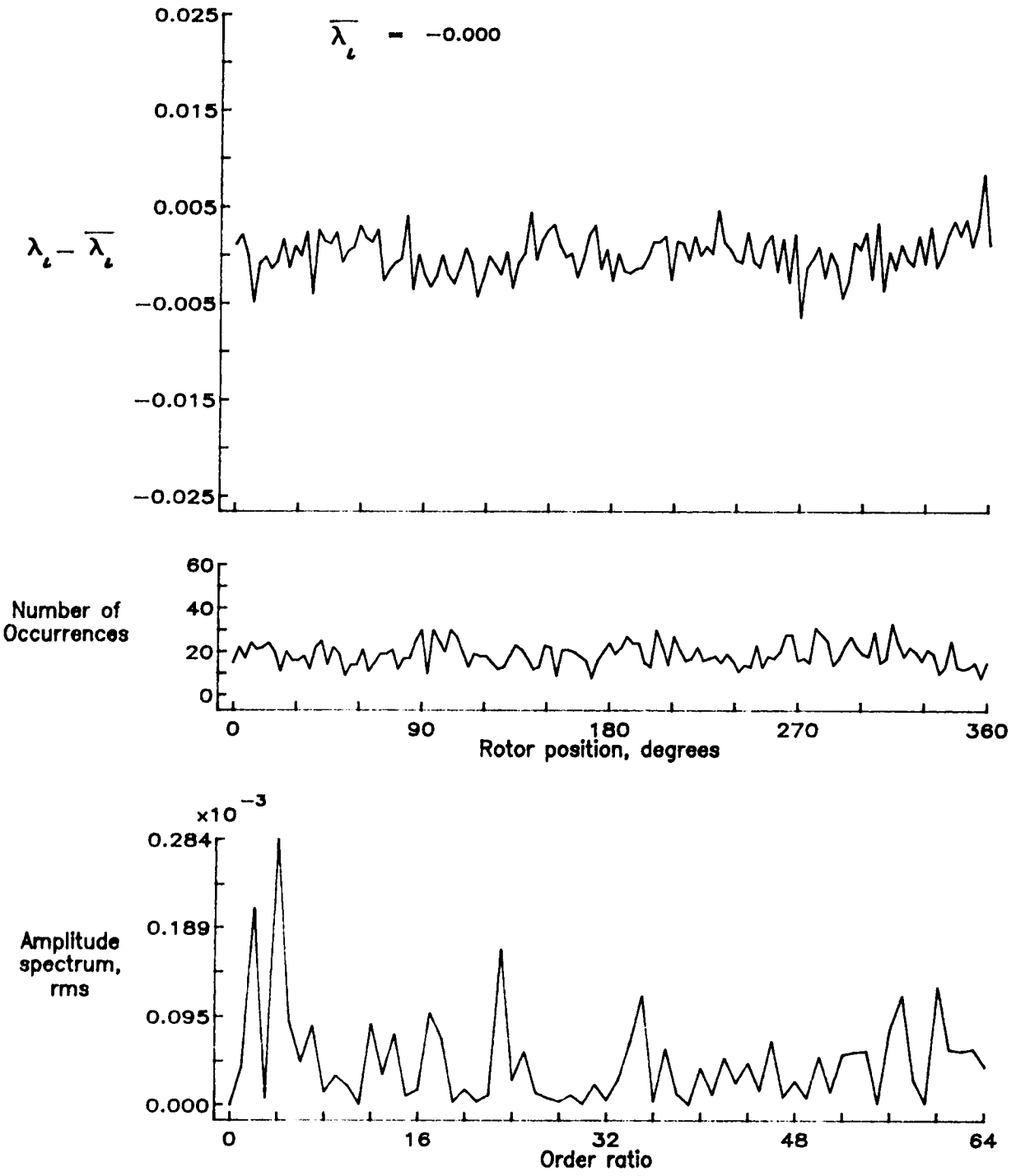

Figure 178.– Concluded.

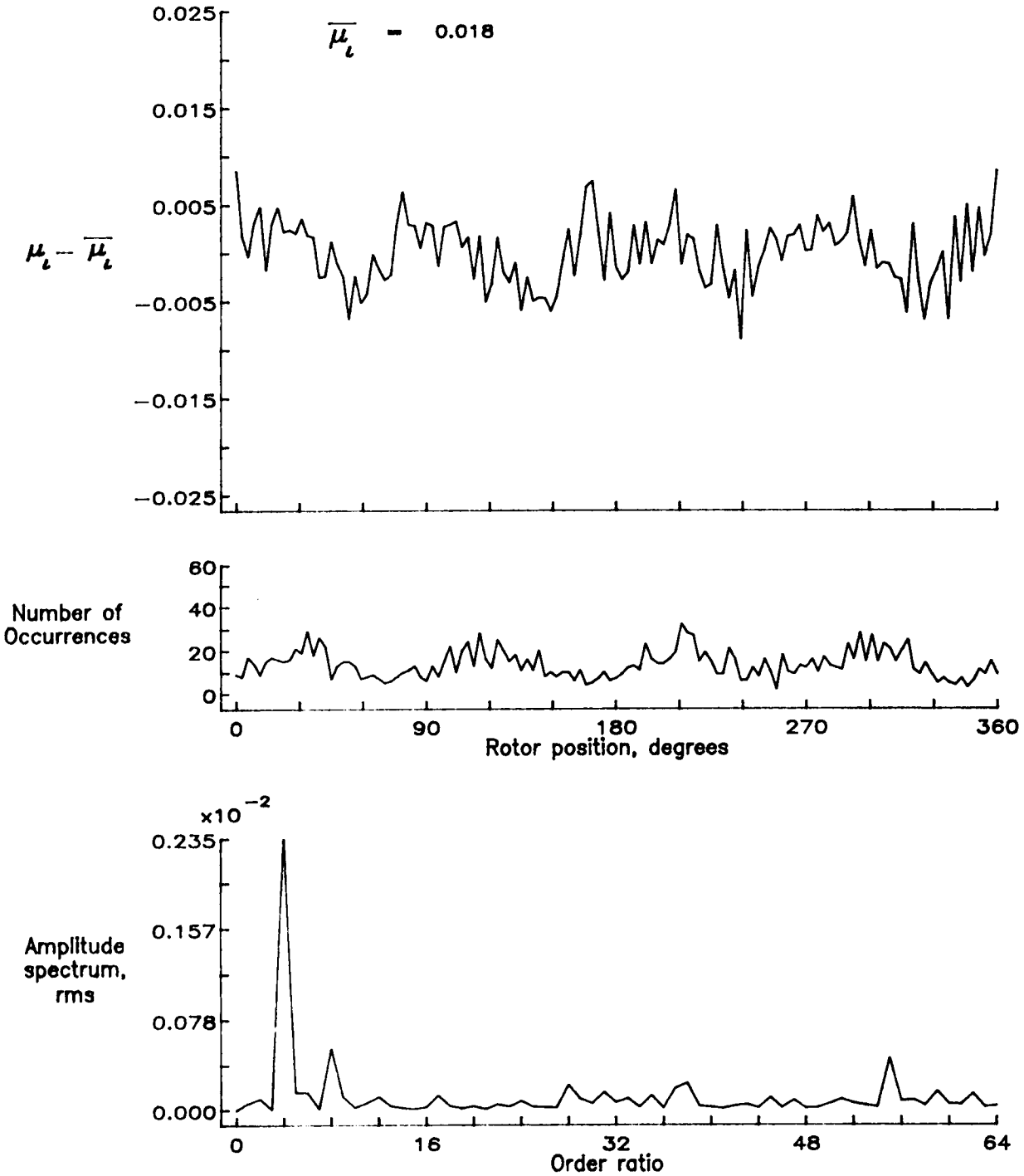

Figure 179.– Induced inflow velocity measured at 330 degrees and r/R of 0.40.

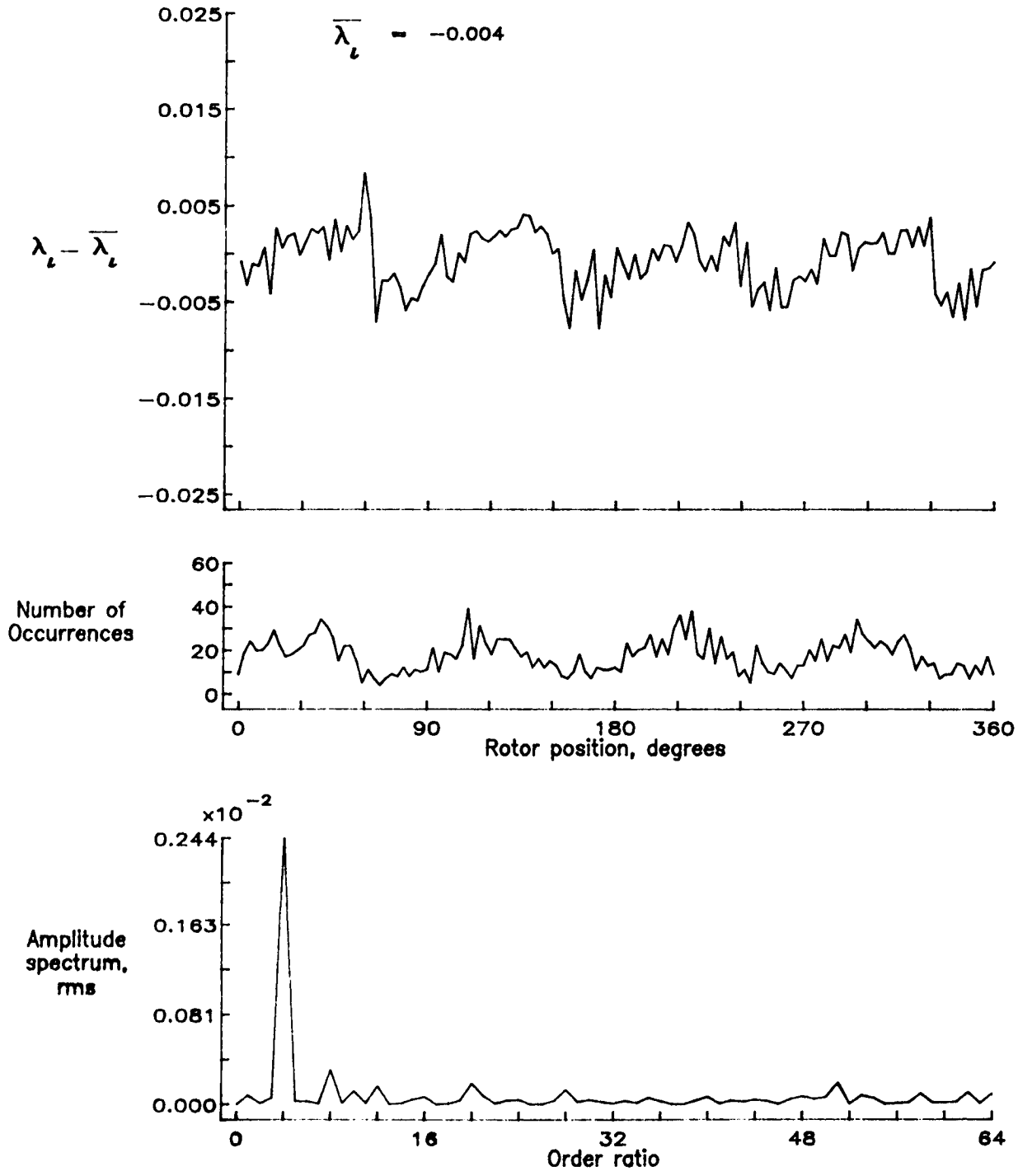

Figure 179.– Concluded.

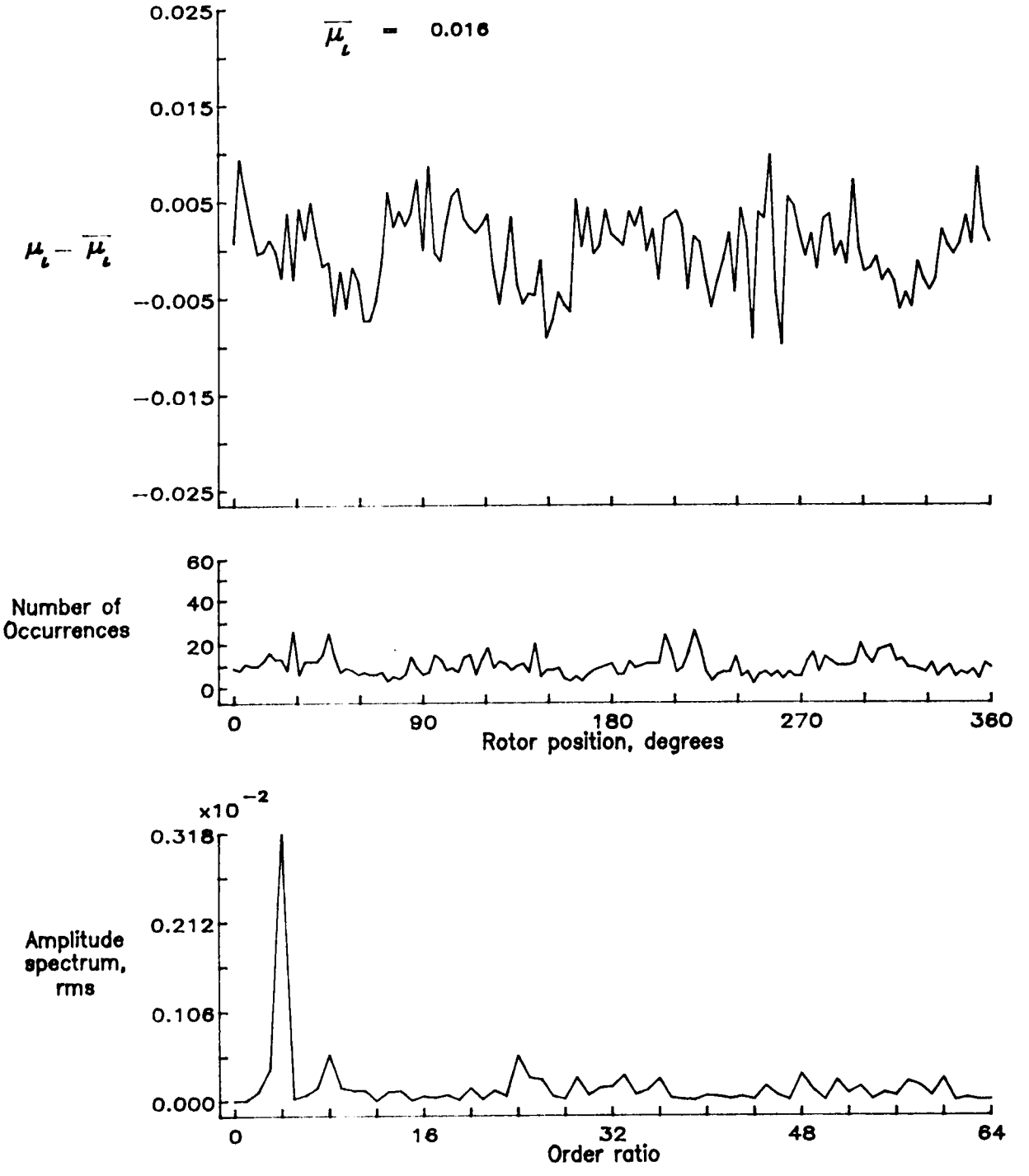

Figure 180.– Induced inflow velocity measured at 330 degrees and r/R of 0.50.

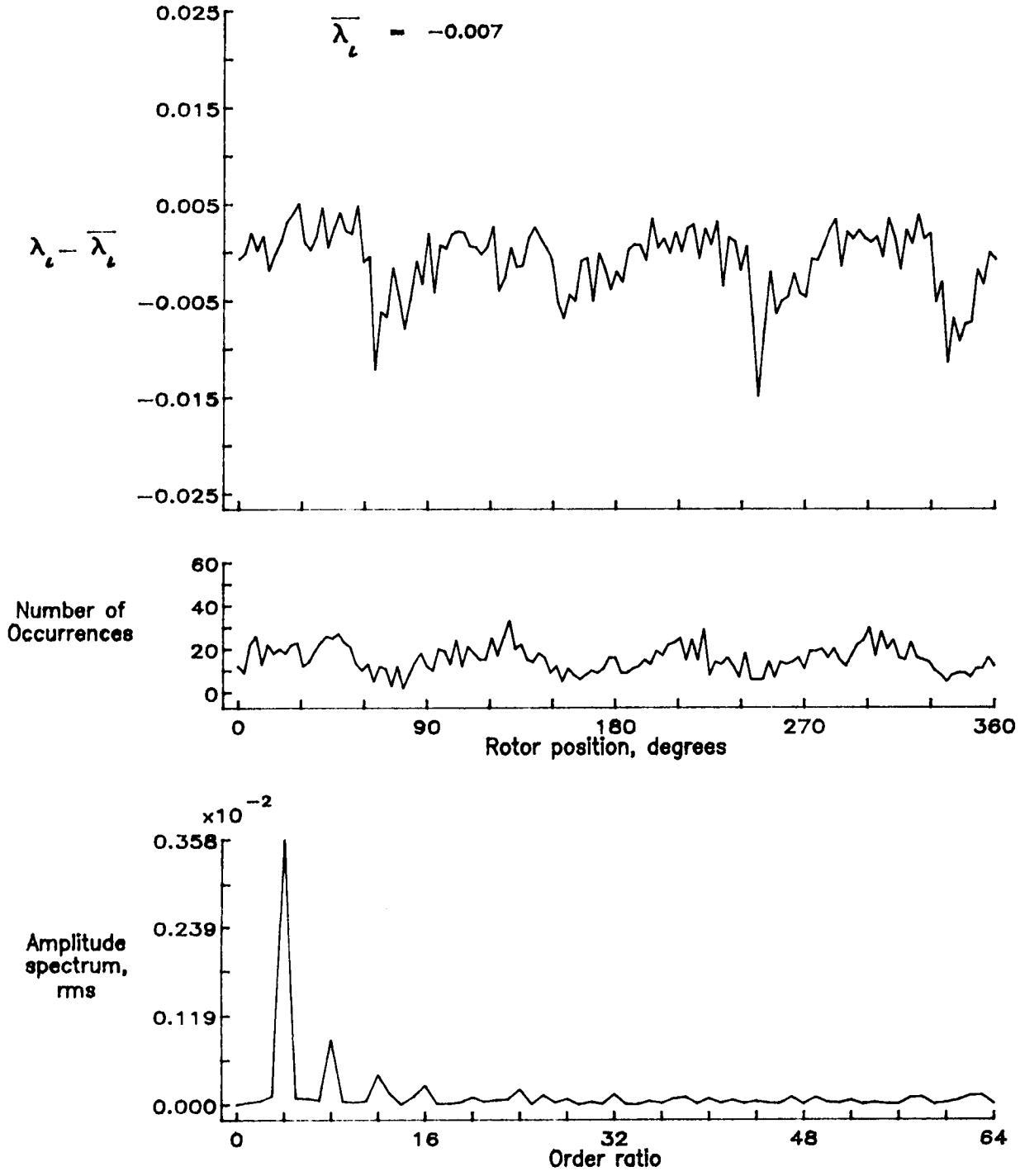

Figure 180.– Concluded.

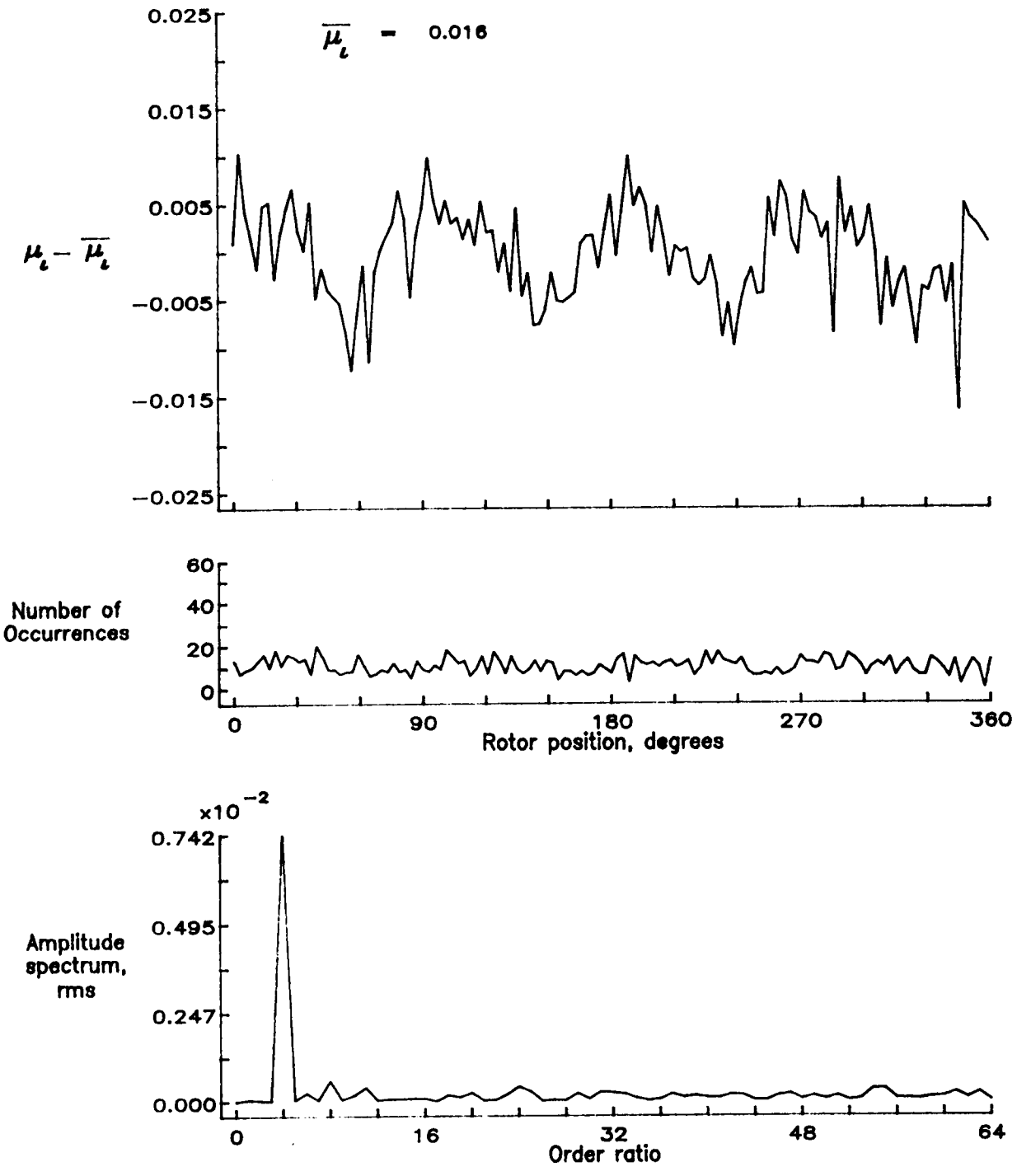

Figure 181.– Induced inflow velocity measured at 330 degrees and r/R of 0.60.

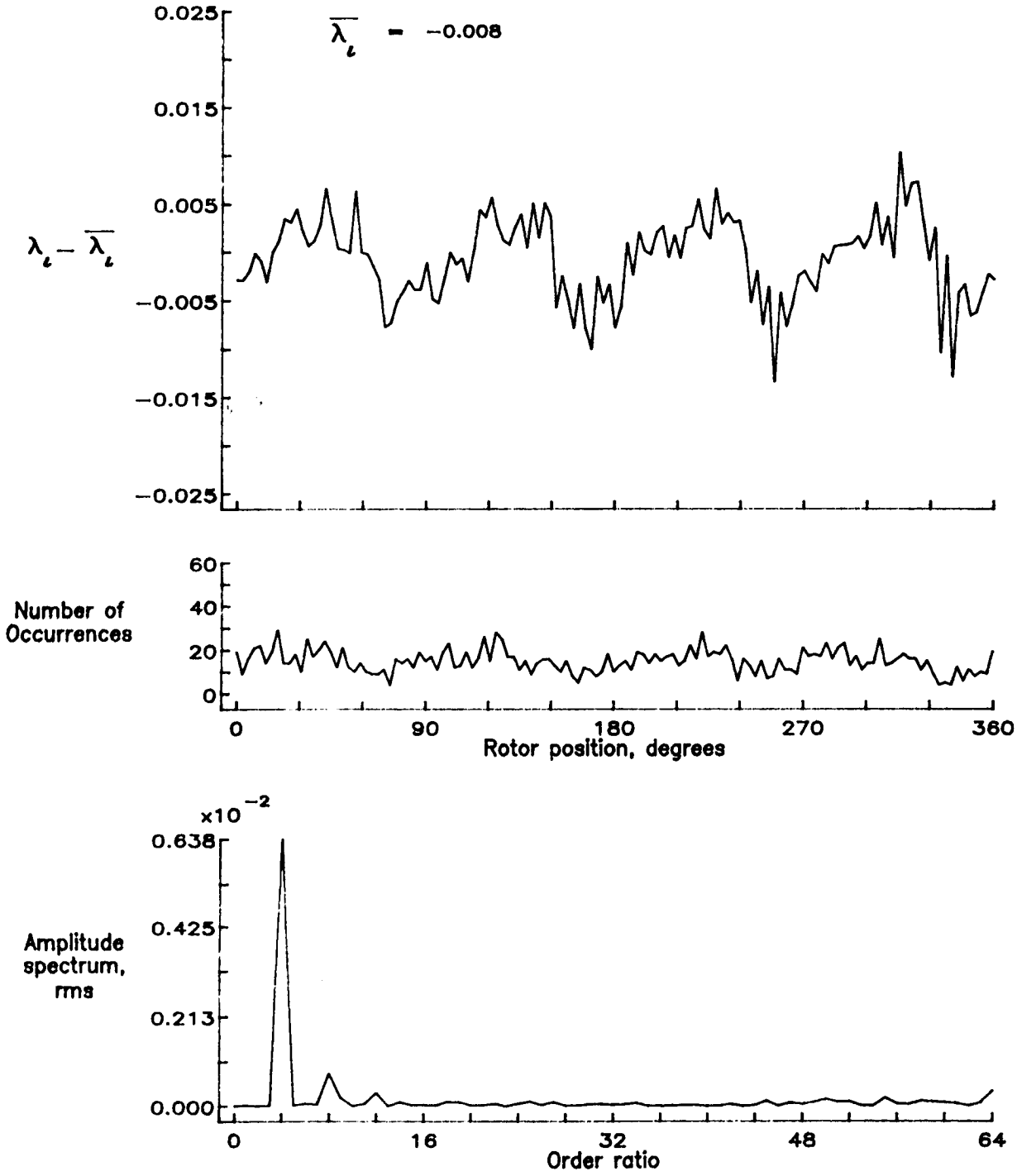

Figure 181.– Concluded.

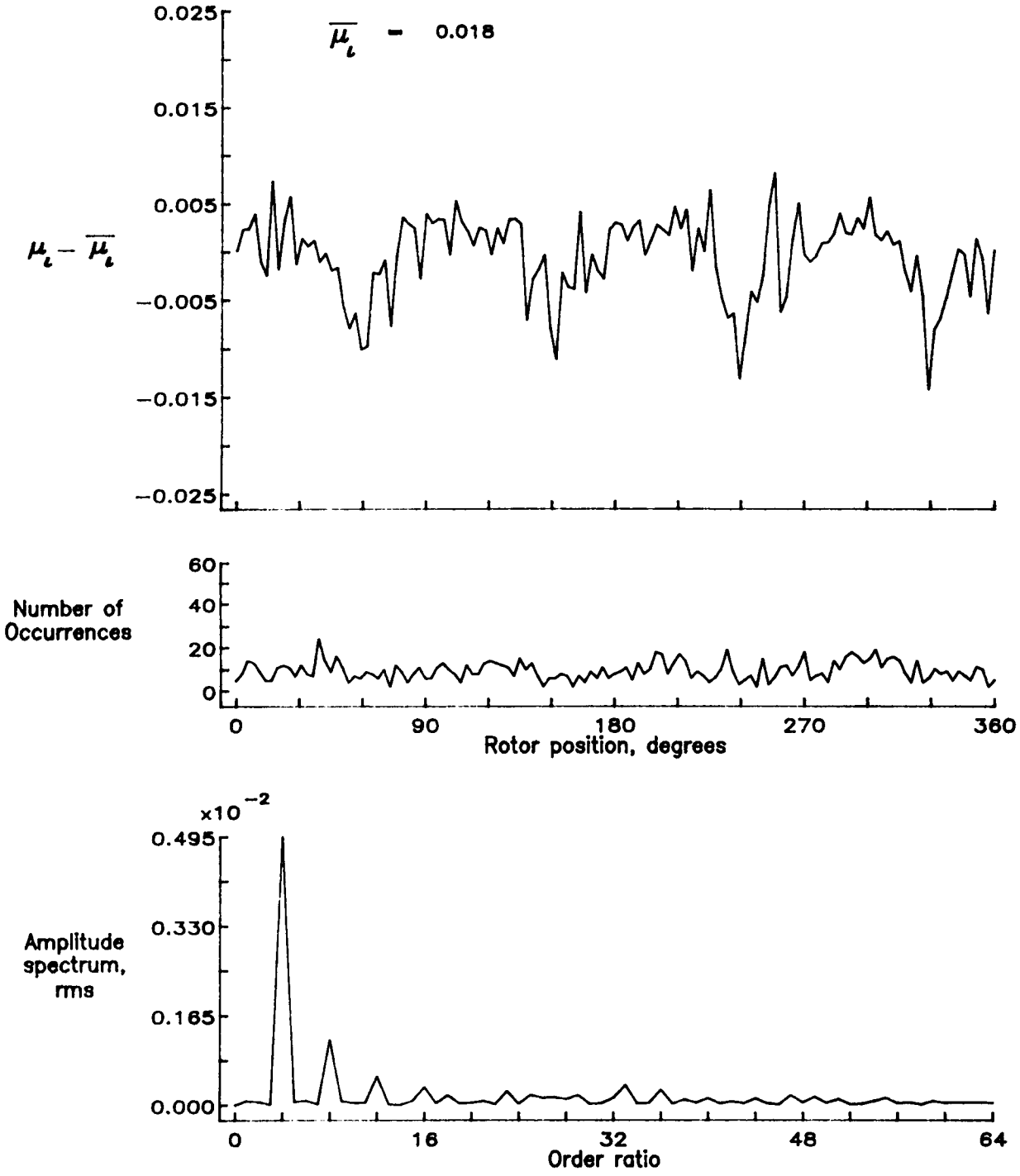

Figure 182.– Induced inflow velocity measured at 330 degrees and r/R of 0.70.

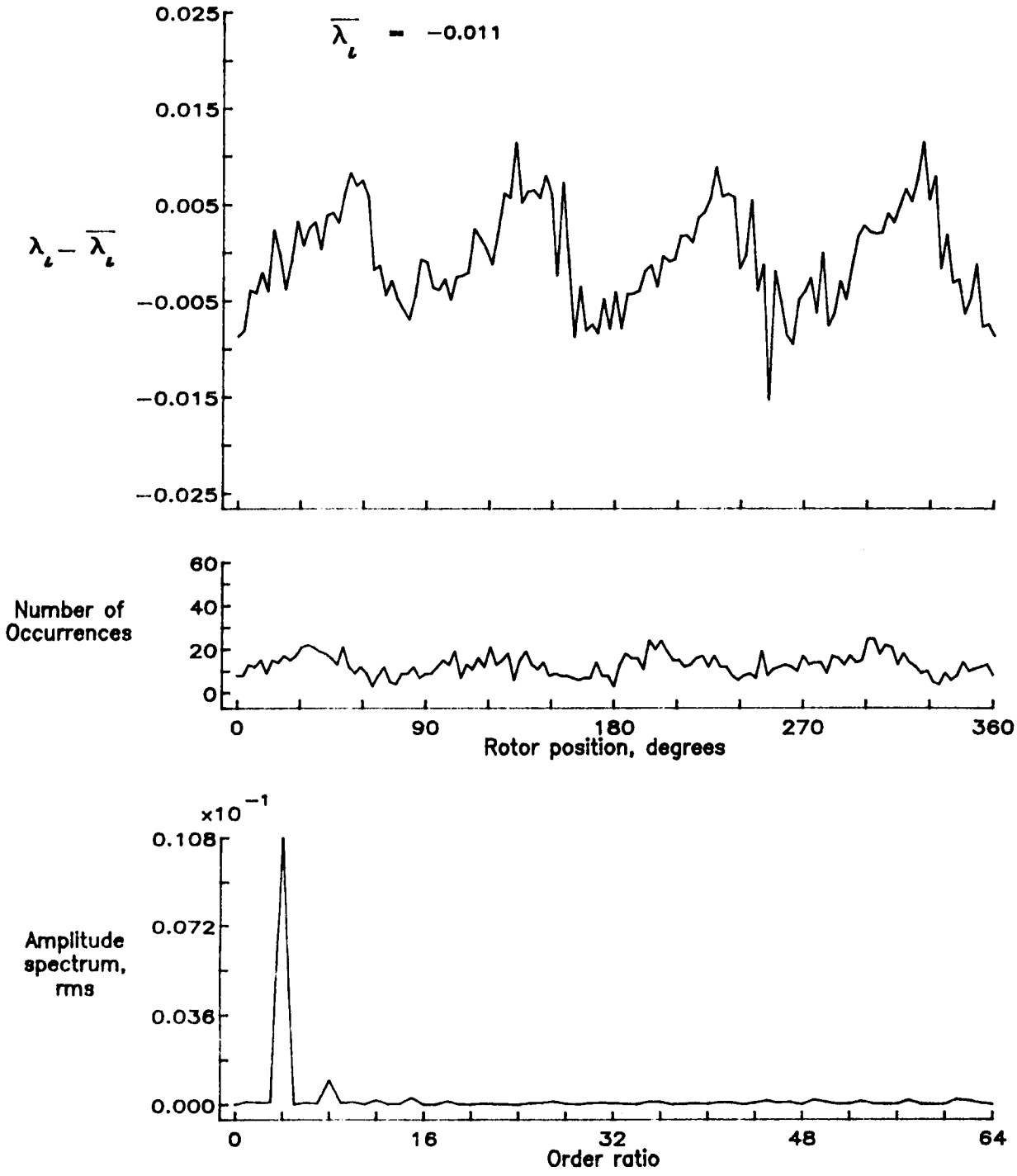

Figure 182.– Concluded.

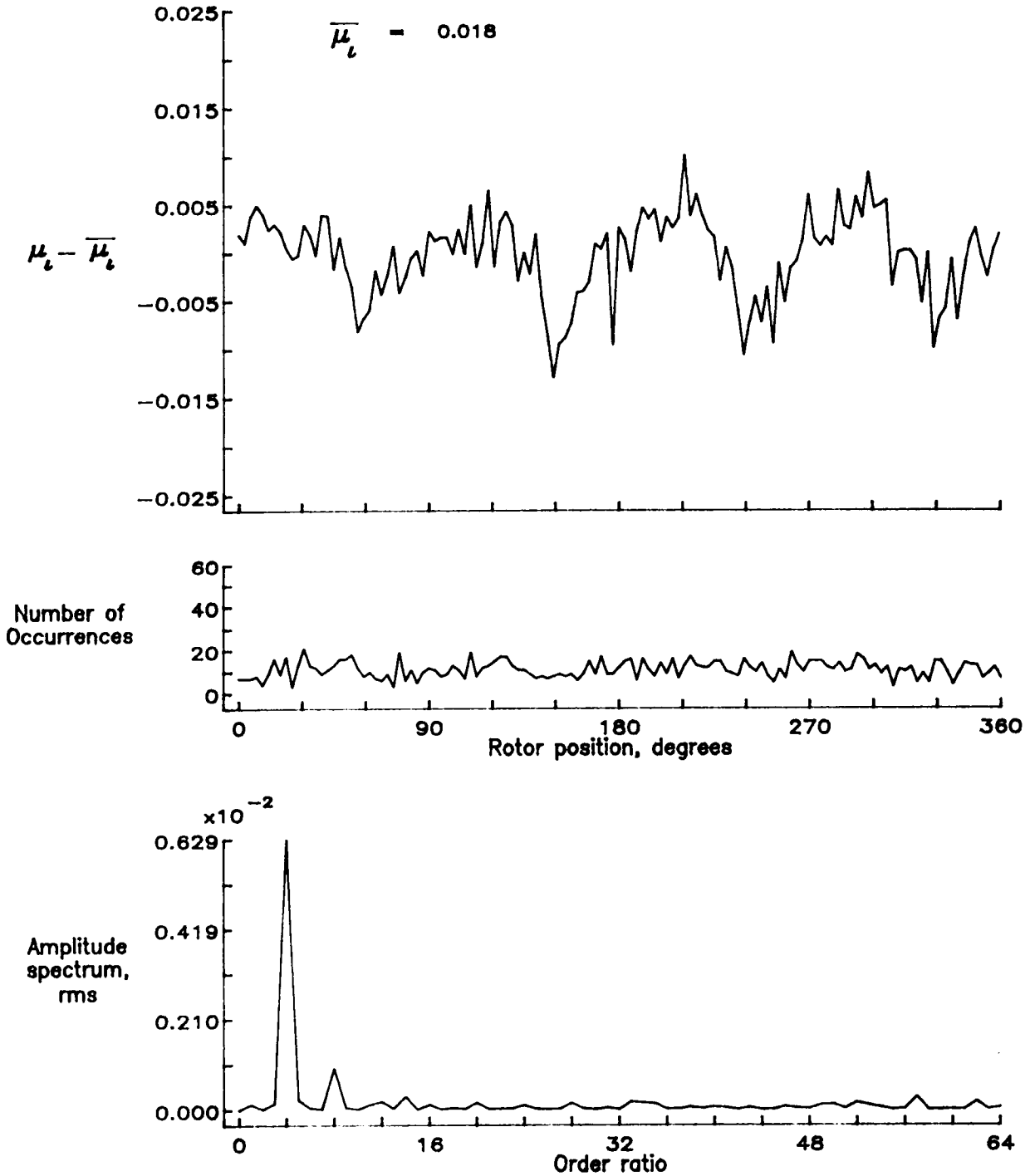

Figure 183.– Induced inflow velocity measured at 330 degrees and r/R of 0.74.

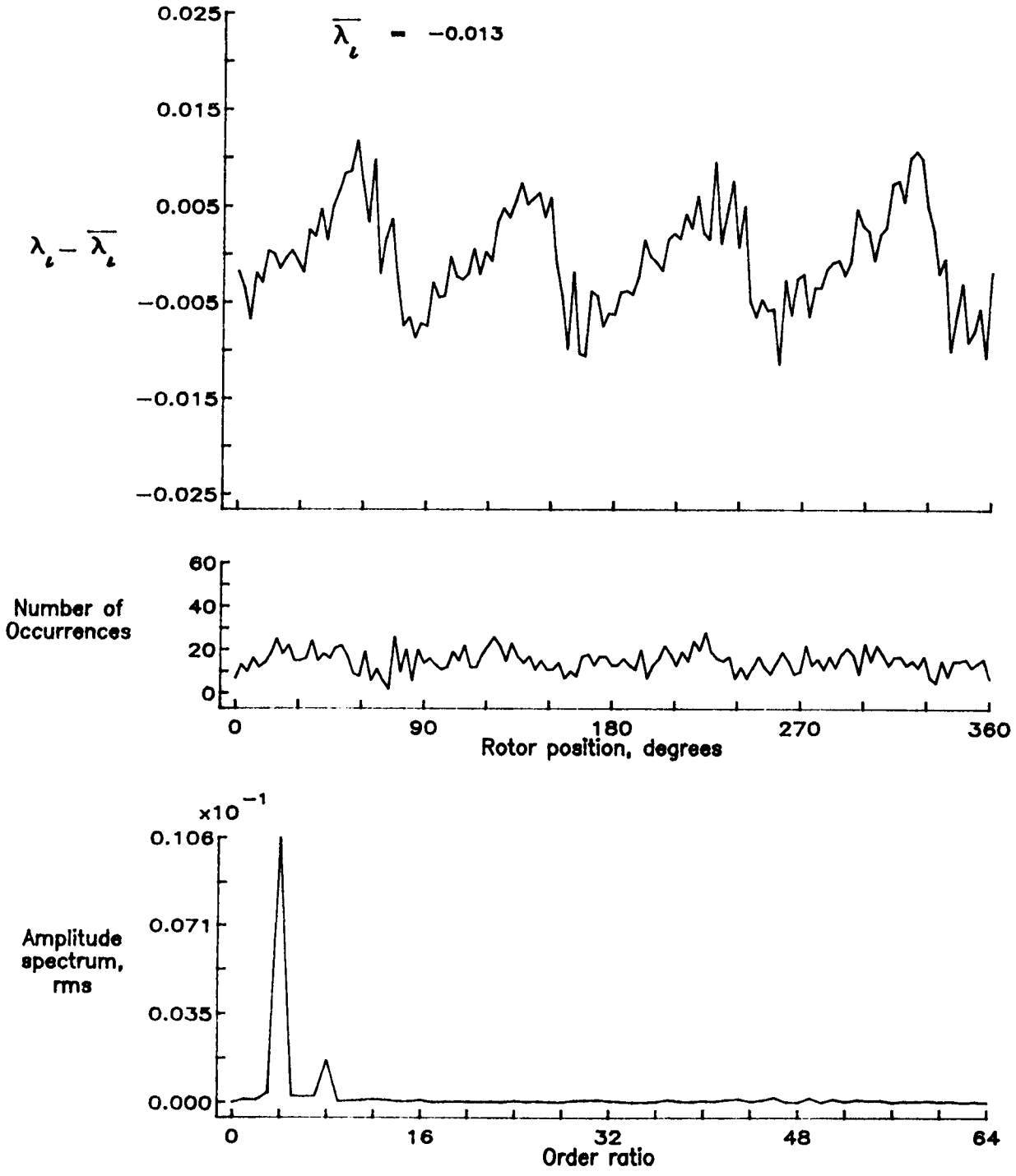

Figure 183.– Concluded.

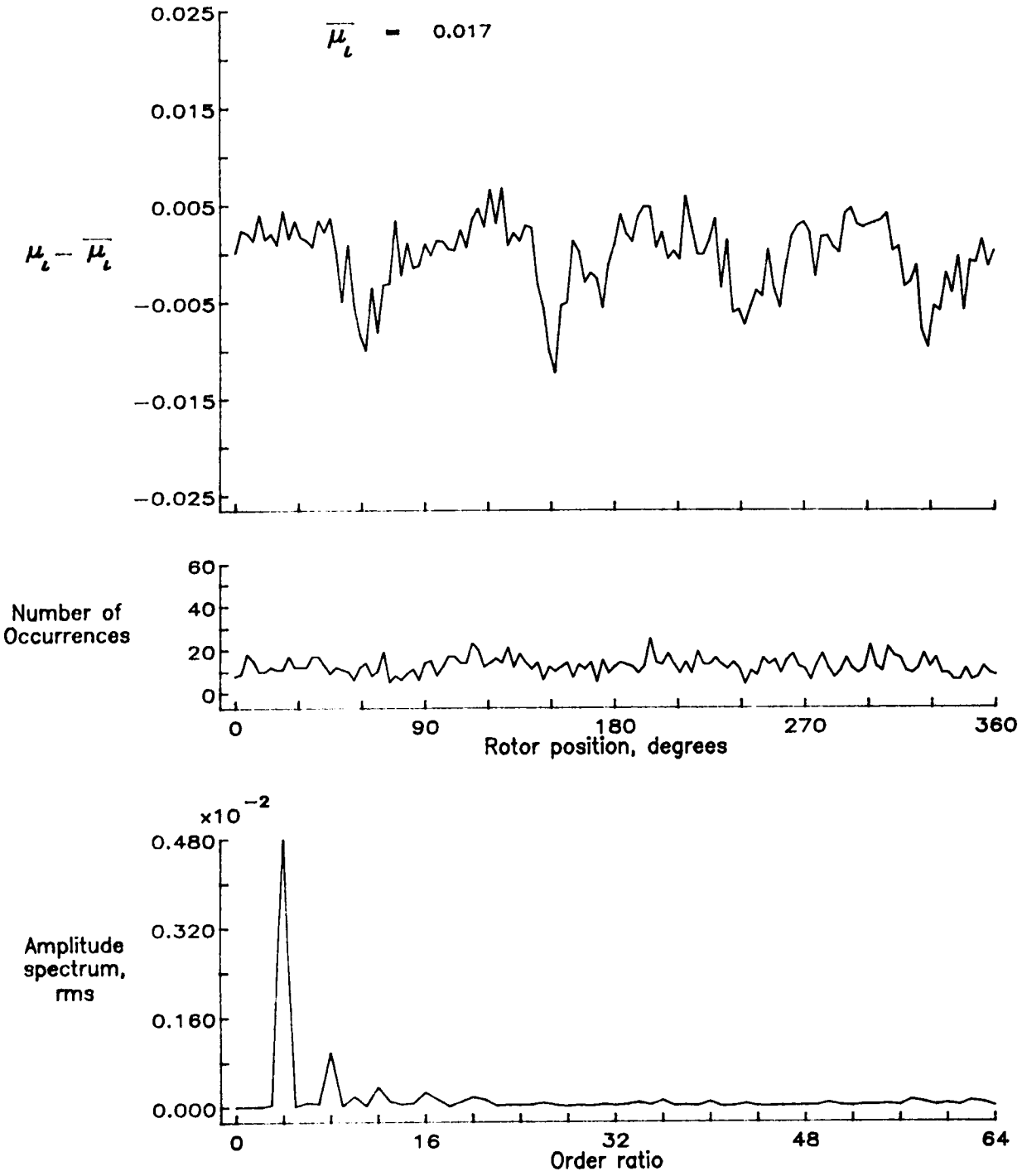

Figure 184.– Induced inflow velocity measured at 330 degrees and r/R of 0.78.

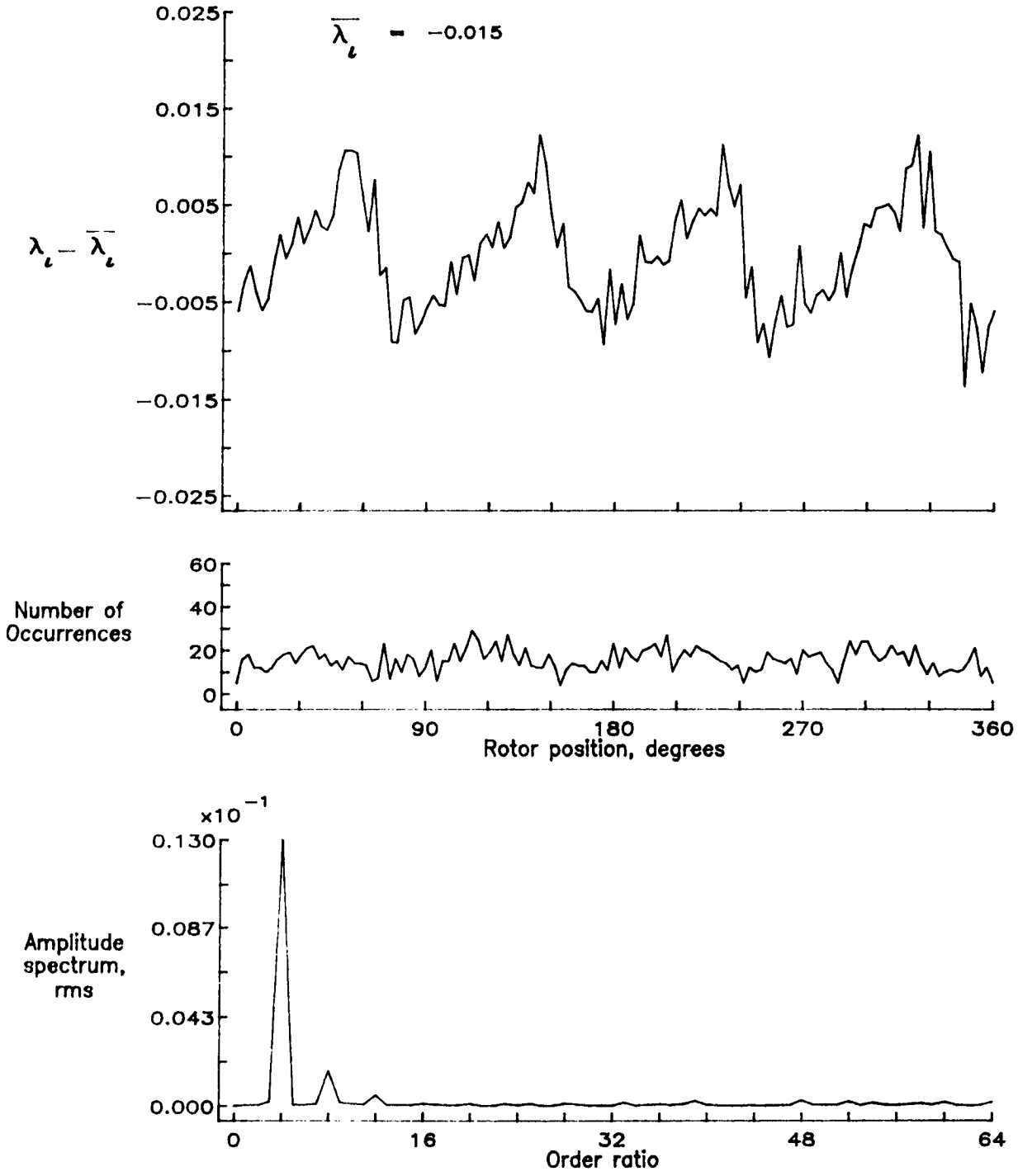

Figure 184.– Concluded.

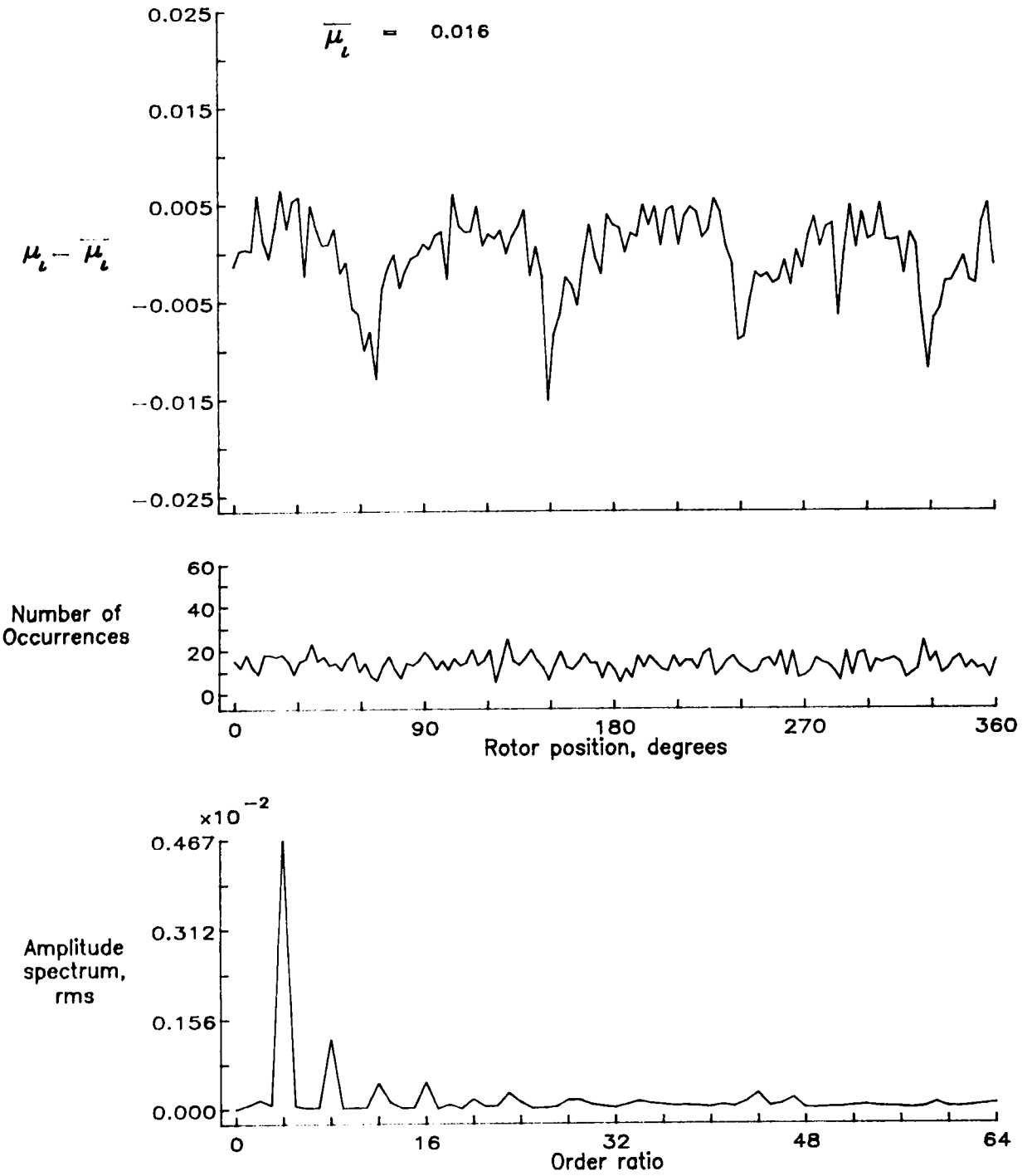

Figure 185.– Induced inflow velocity measured at 330 degrees and r/R of 0.82.

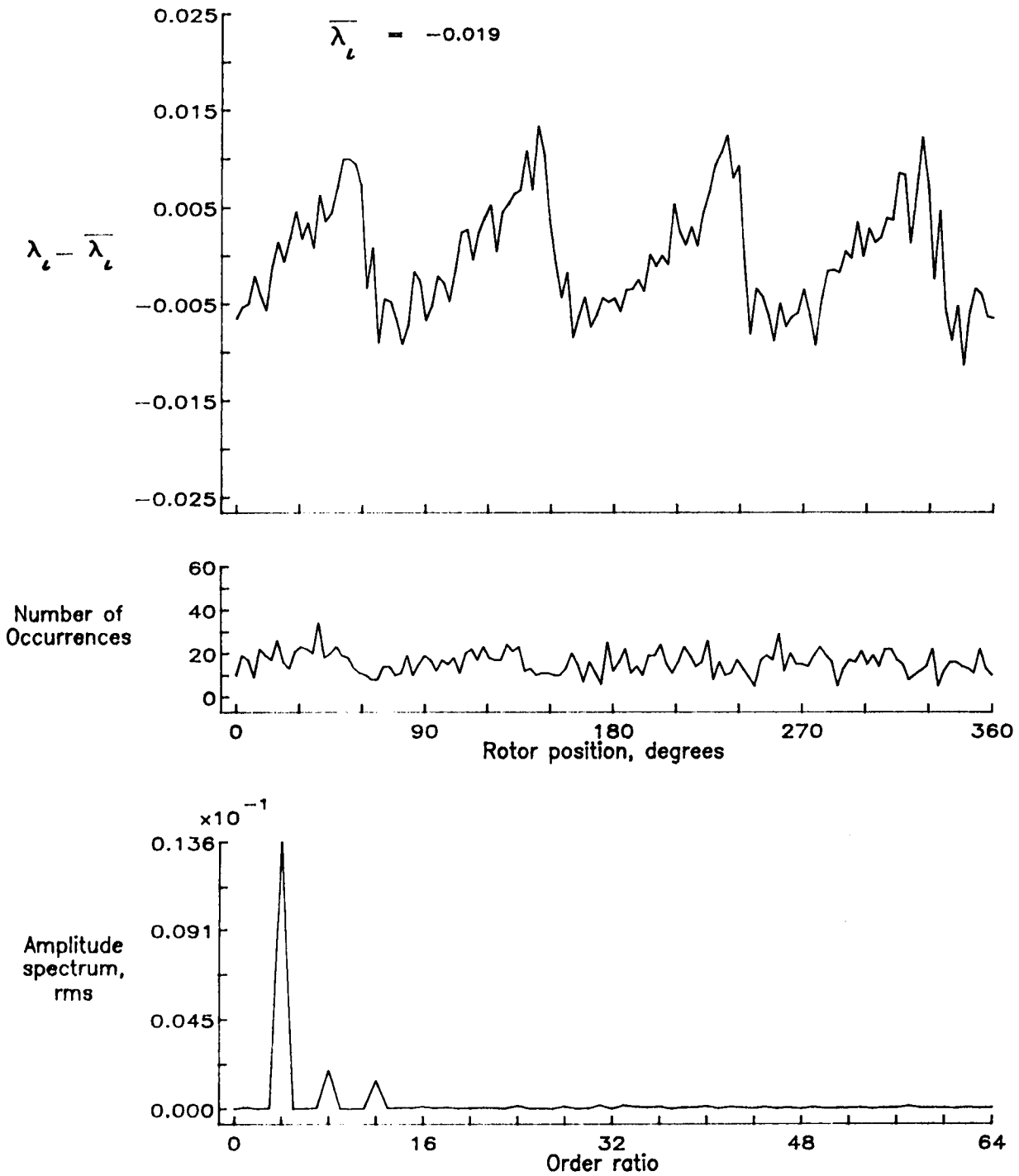

Figure 185.– Concluded.

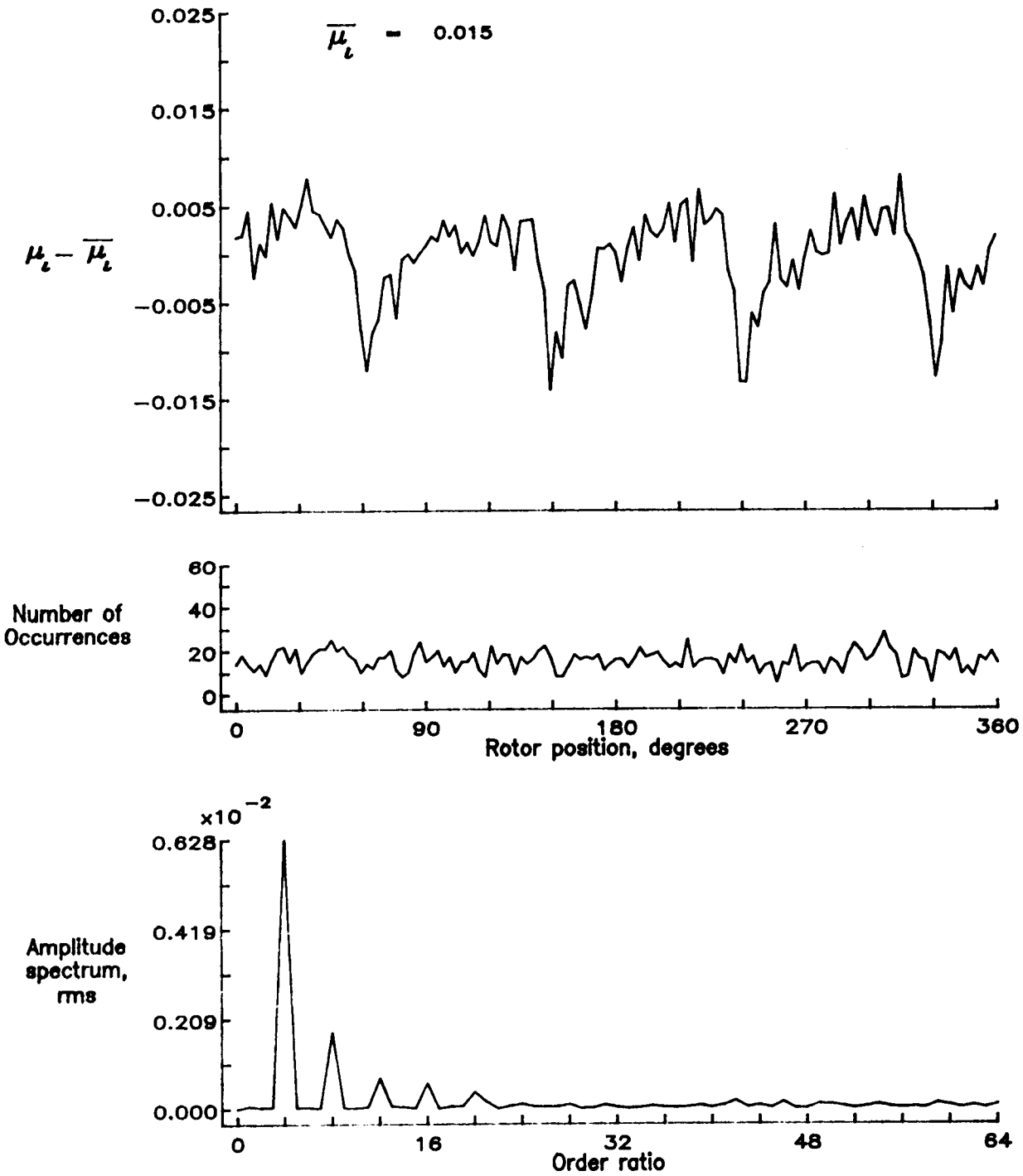

Figure 186.– Induced inflow velocity measured at 330 degrees and r/R of 0.86.

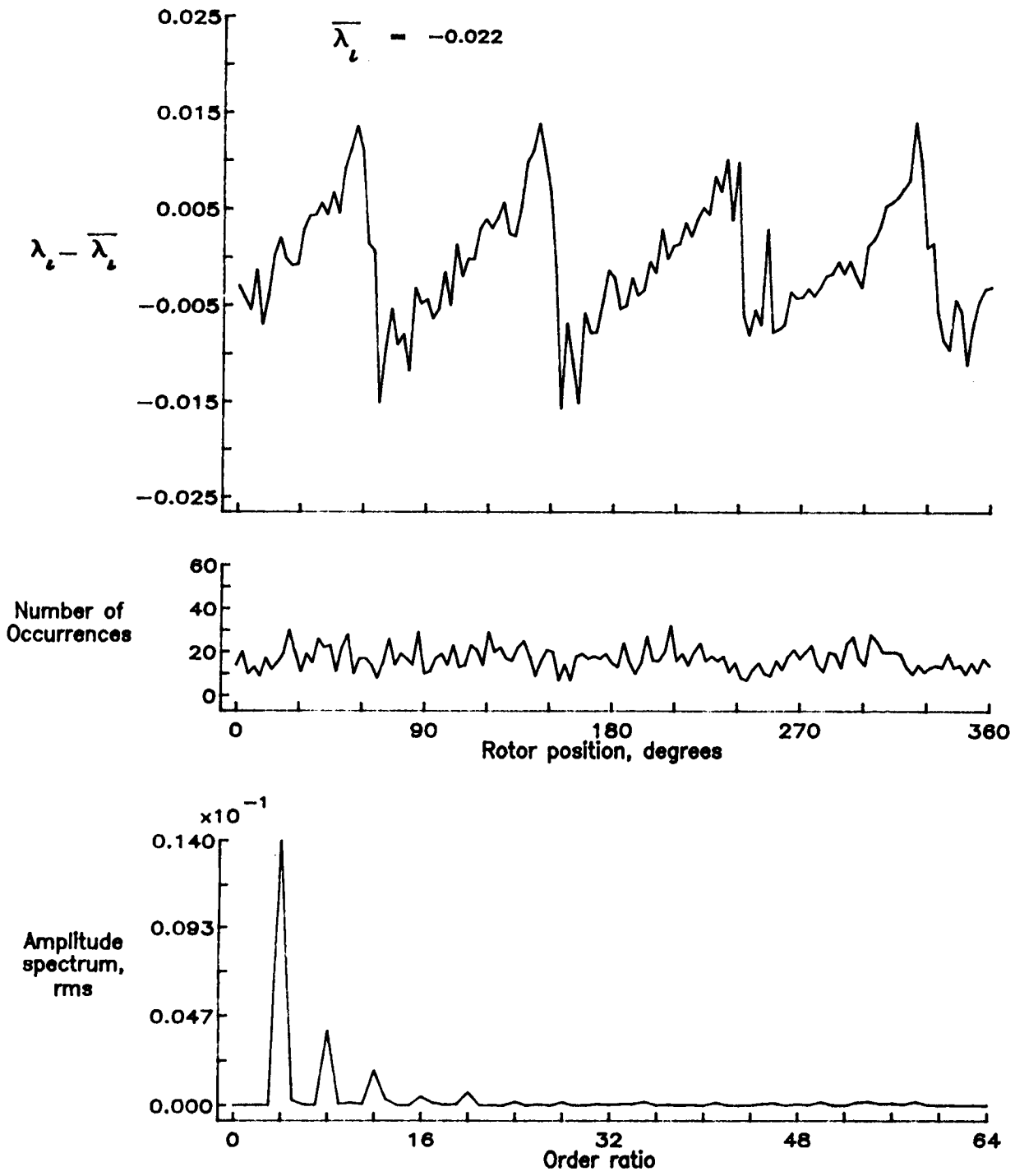

Figure 186.– Concluded.

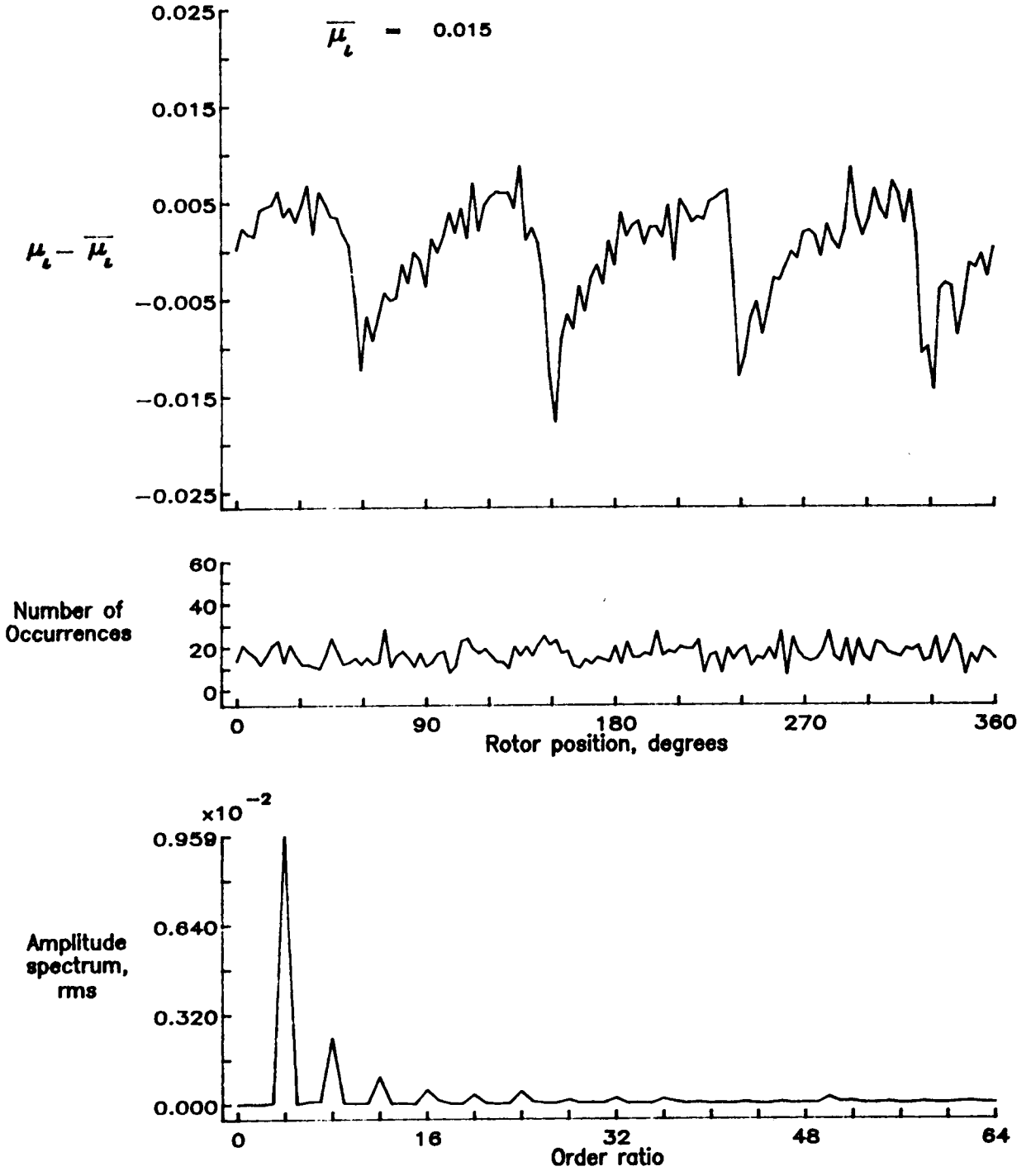

Figure 187.– Induced inflow velocity measured at 330 degrees and r/R of 0.90.

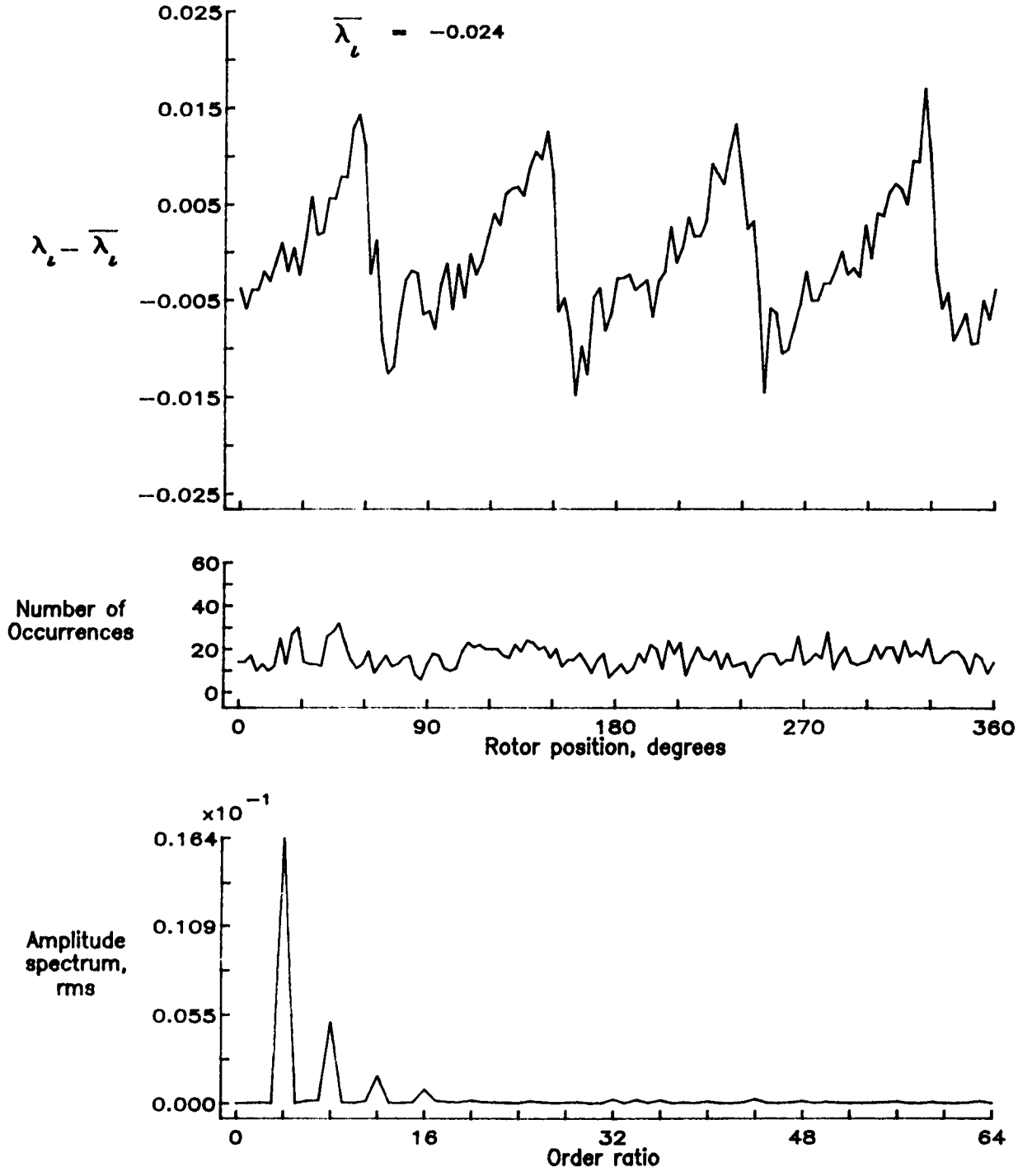

Figure 187.– Concluded.

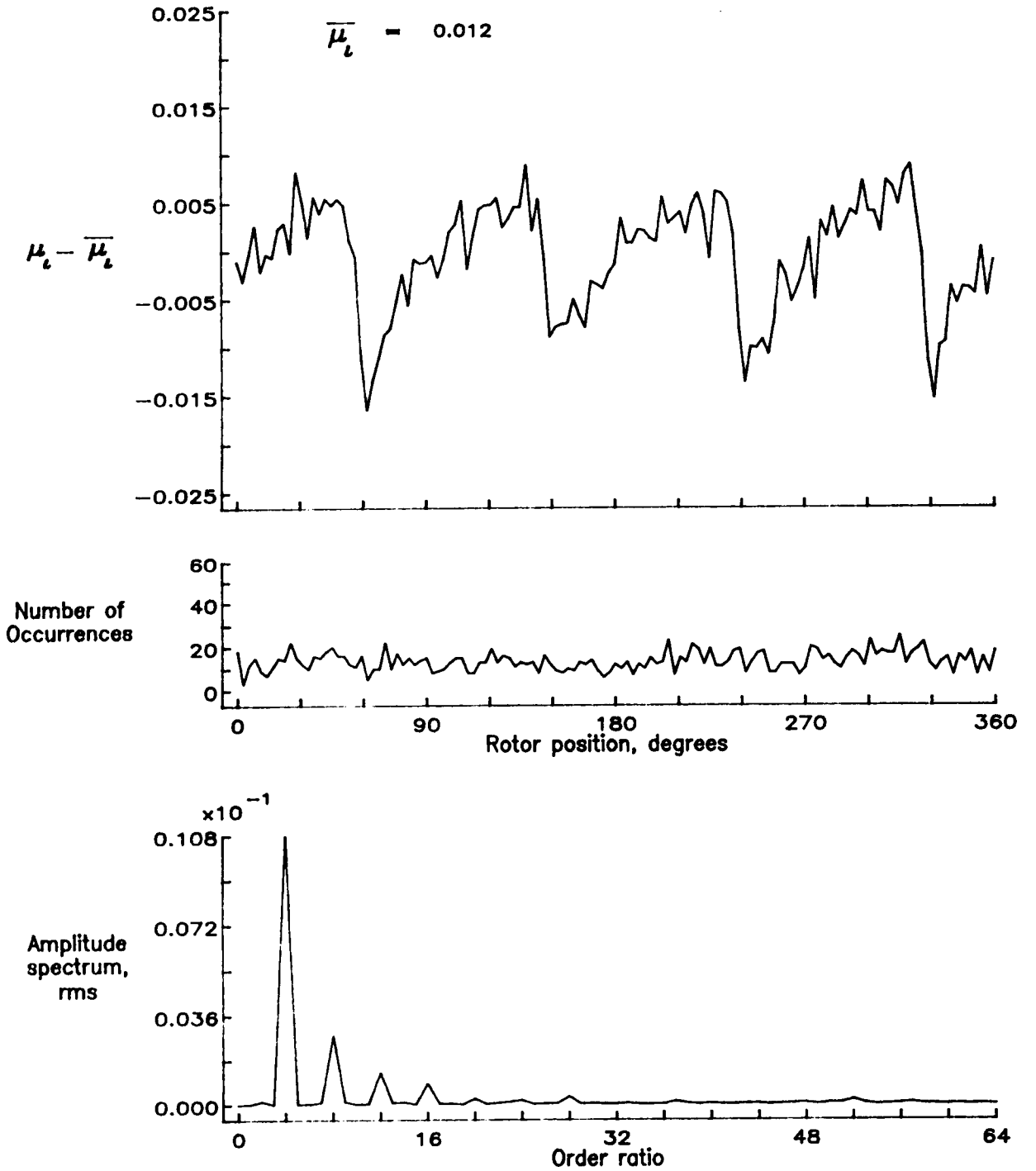

Figure 188.– Induced inflow velocity measured at 330 degrees and r/R of 0.94.

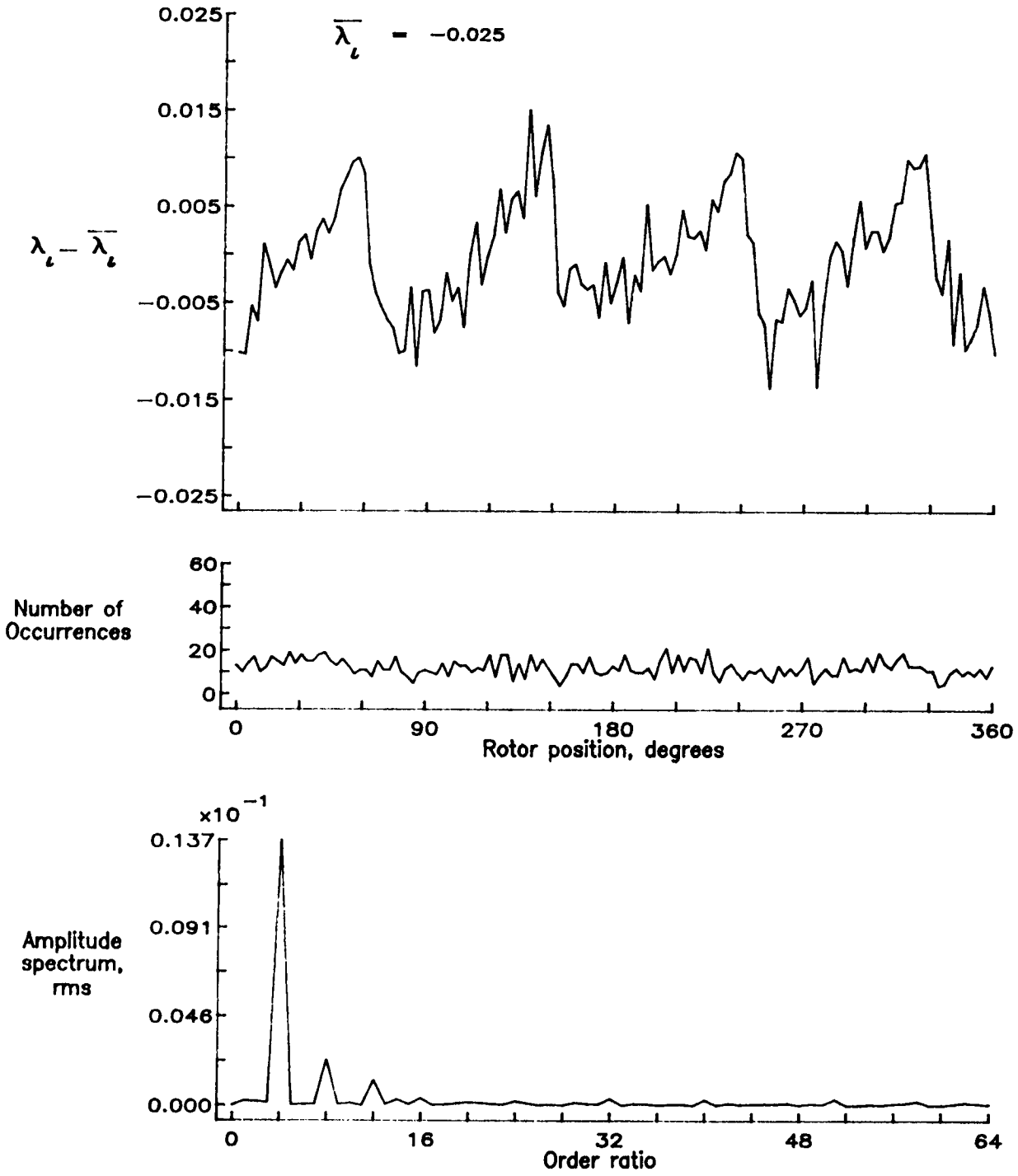

Figure 188.– Concluded.

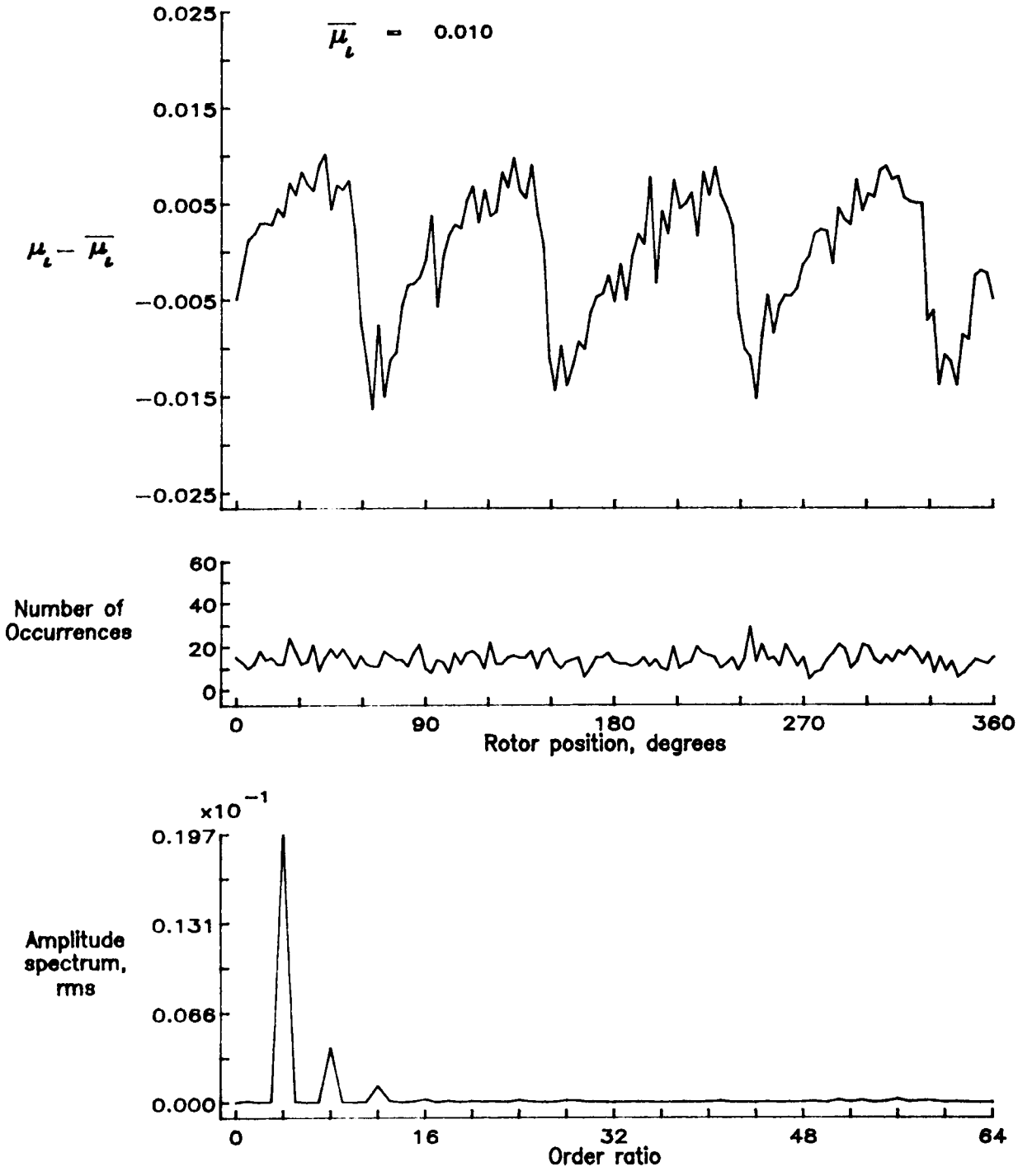

Figure 189.– Induced inflow velocity measured at 330 degrees and r/R of 0.98.

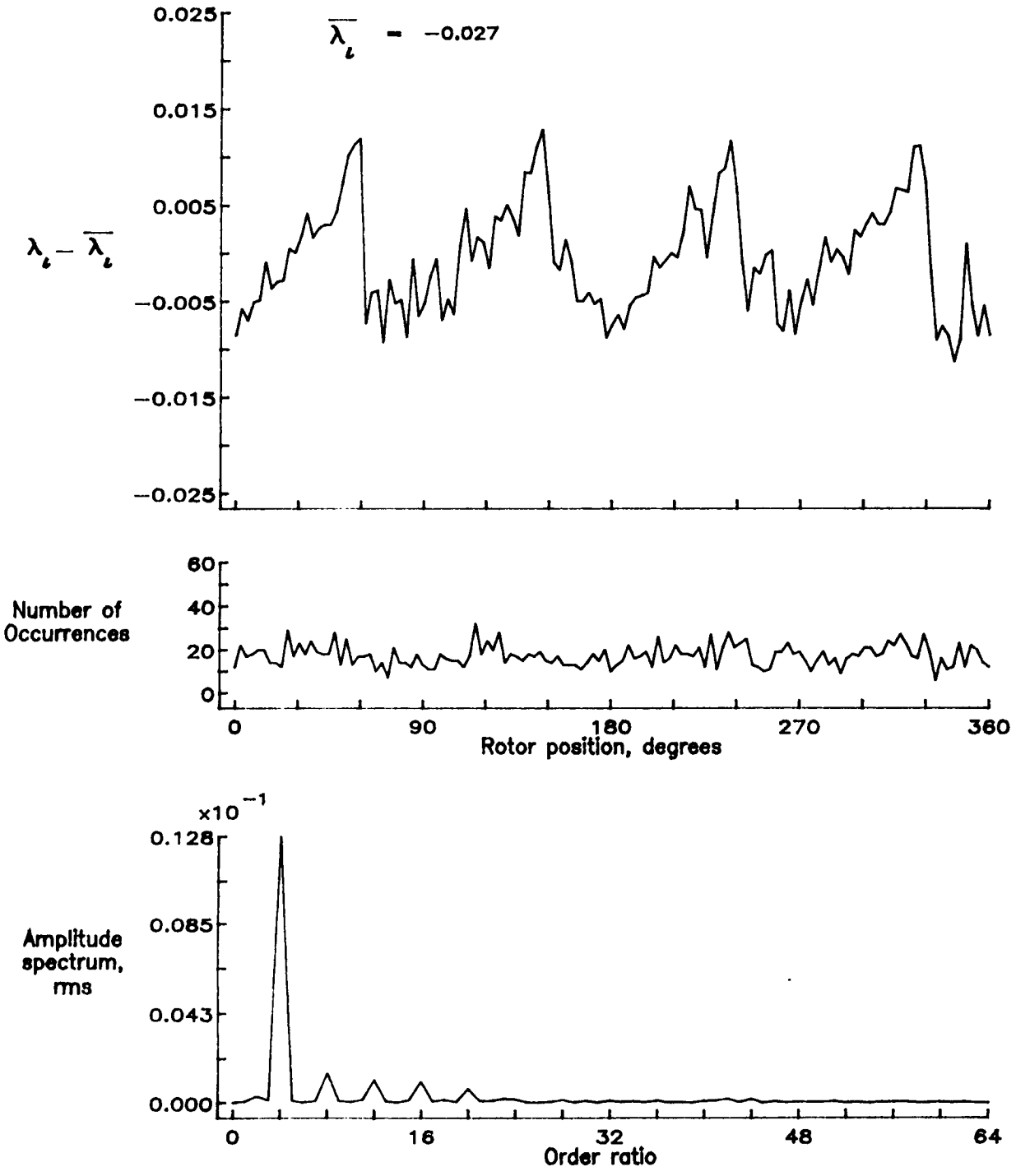

Figure 189.– Concluded.

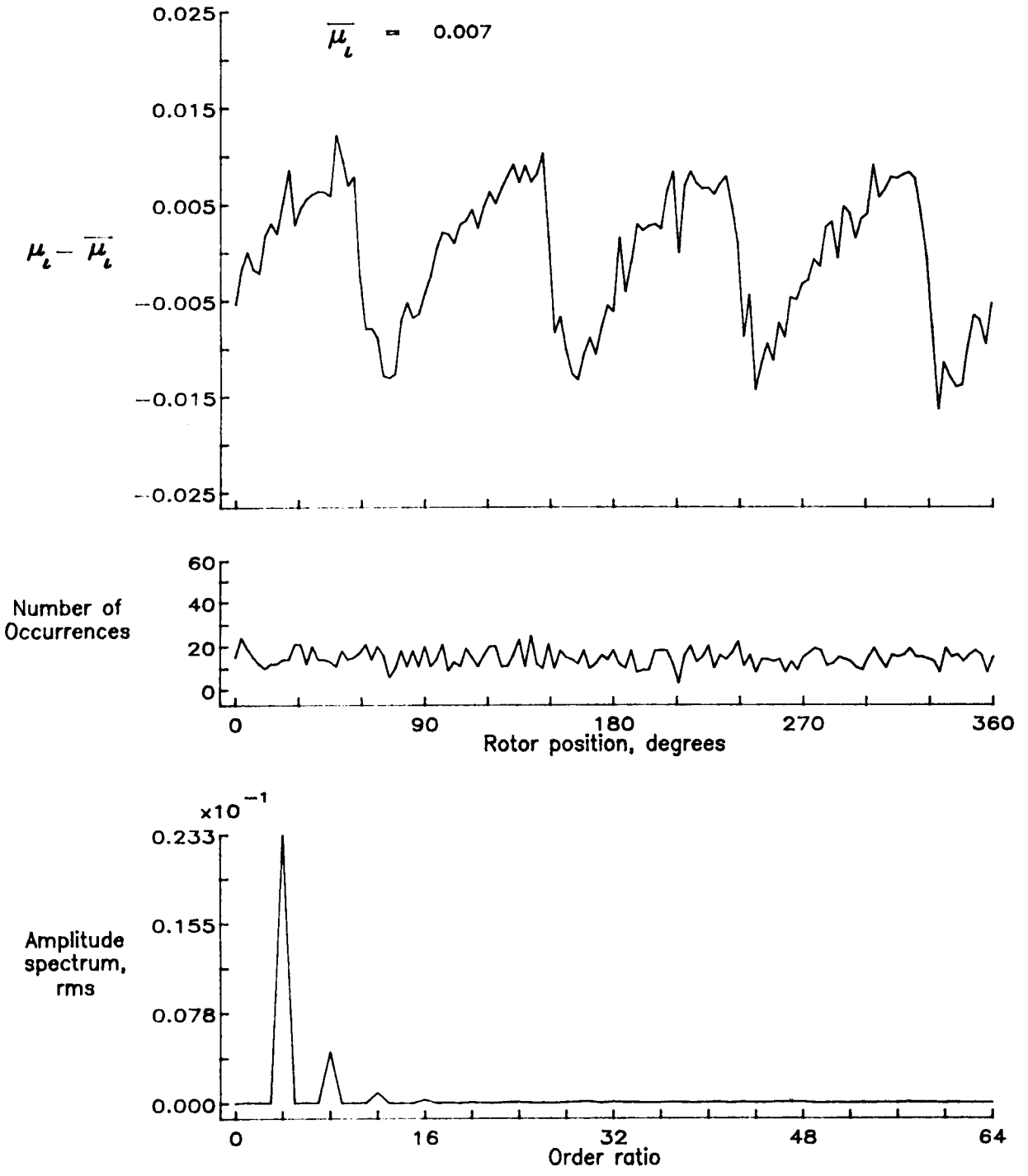

Figure 190.– Induced inflow velocity measured at 330 degrees and r/R of 1.02.

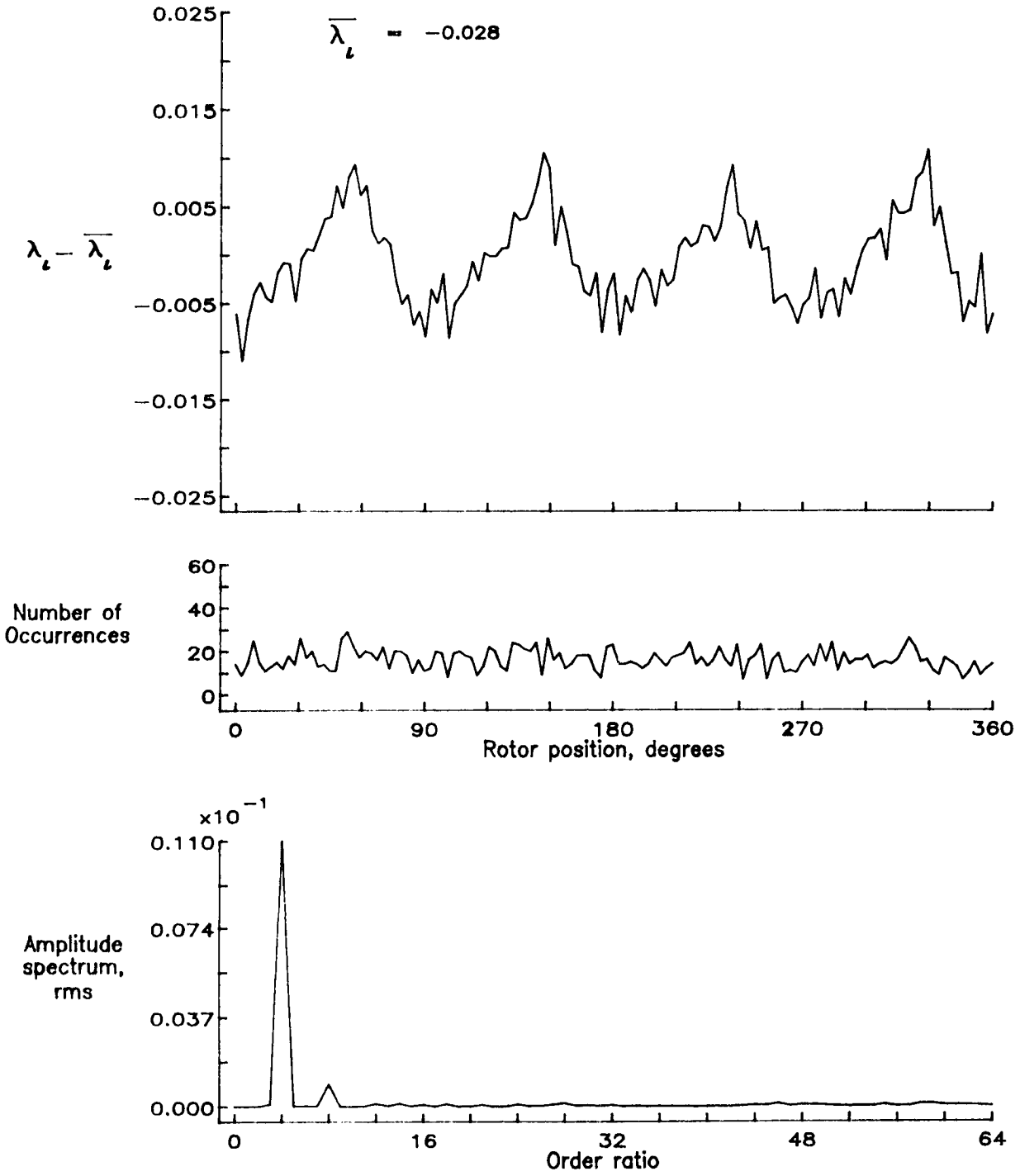

Figure 190.– Concluded.

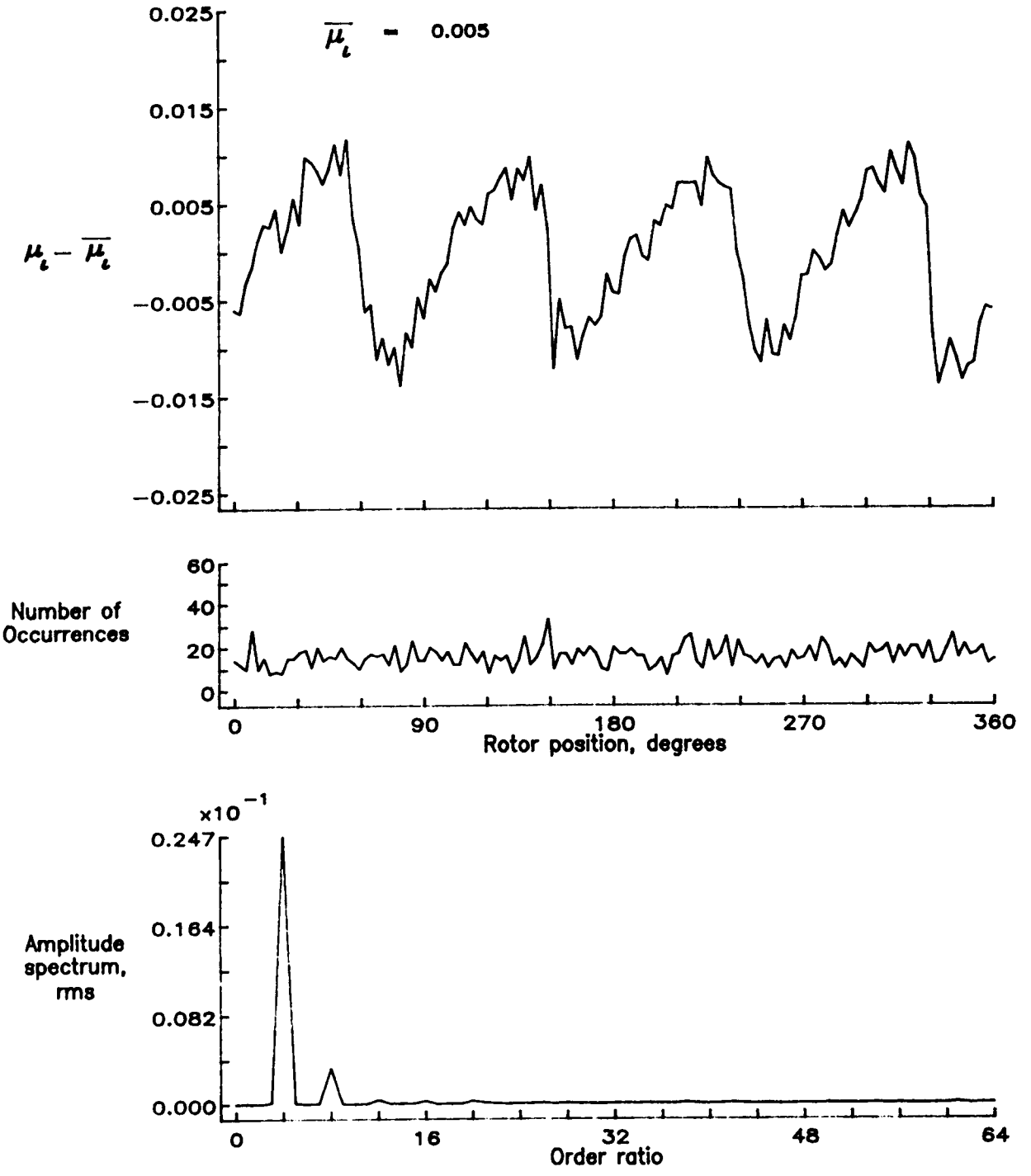

Figure 191.– Induced inflow velocity measured at 330 degrees and r/R of 1.04.

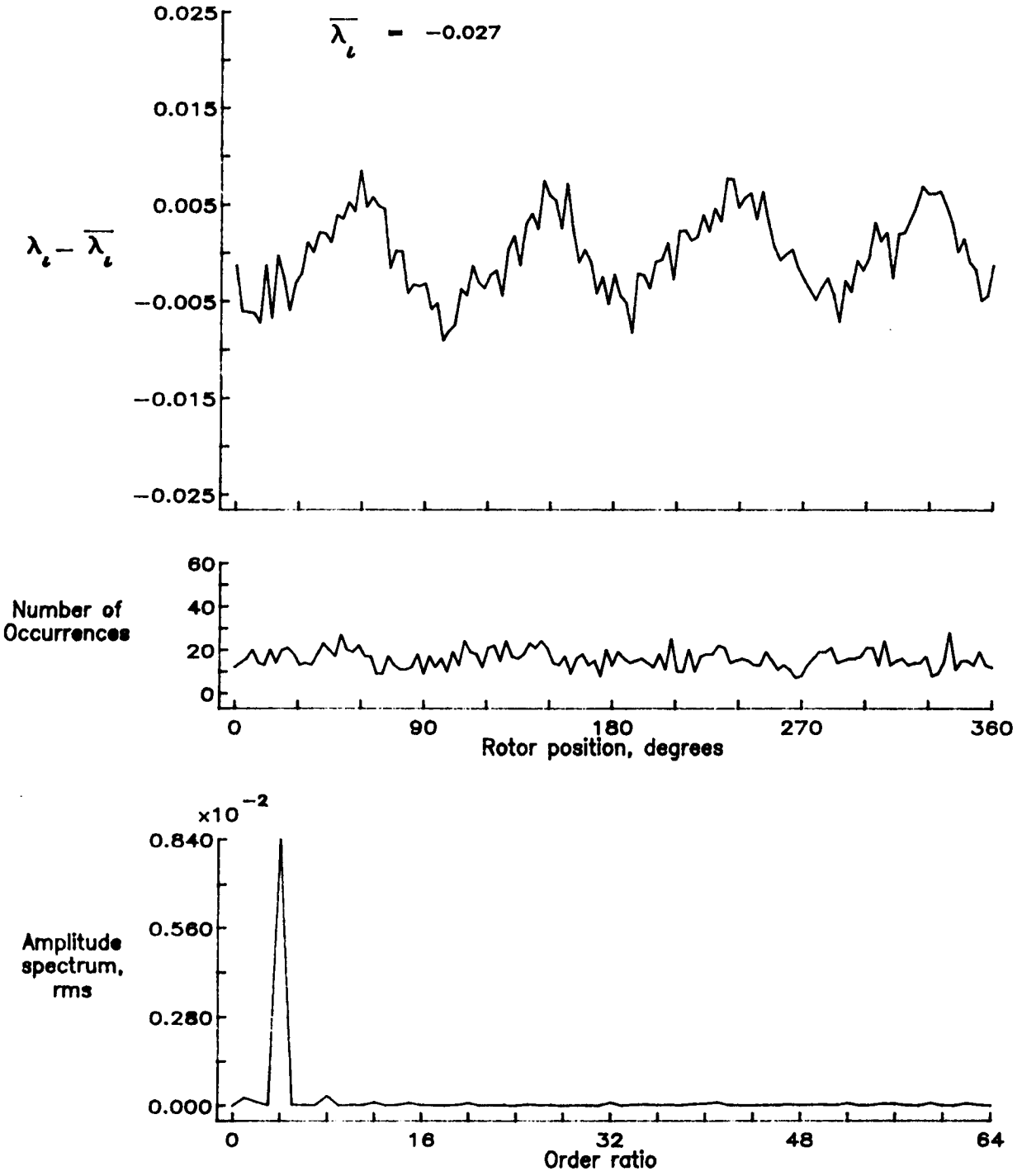

Figure 191.– Concluded.

C-5

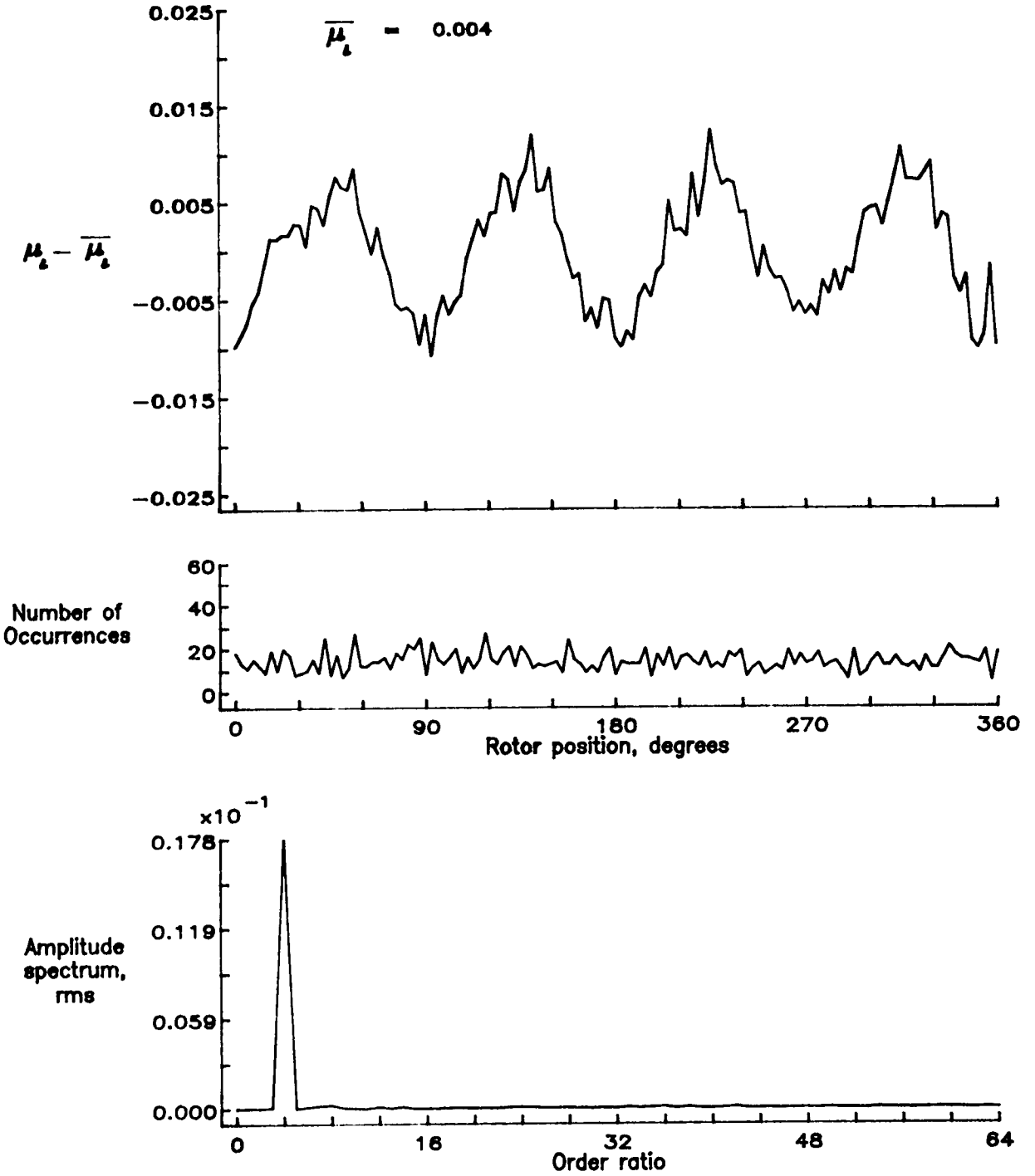

Figure 192.– Induced inflow velocity measured at 330 degrees and r/R of 1.10.

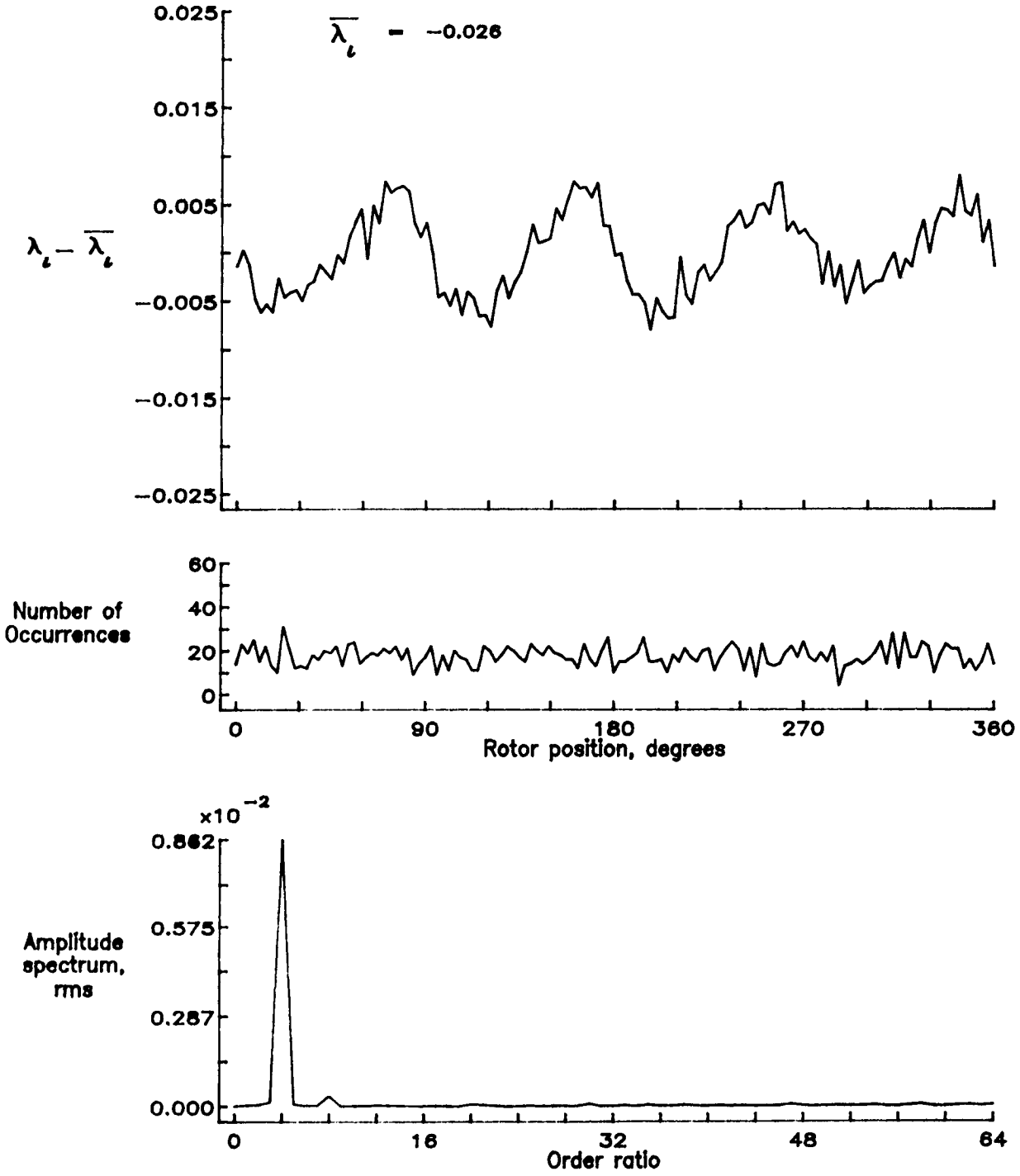

Figure 192.– Concluded.

NASA

Report Documentation Page

1. Report No.	2. Government Accession No.	3. Recipient's Catalog No.
NASA TM-100542 AVSCOM TM 88-B-005		

4. Title and Subtitle

Inflow Measurements Made With A Laser Velocimeter On A Helicopter Model In Forward Flight, Volume II Rectangular Planform Blades at an Advance Ratio of 0.23

5. Report Date	6. Performing Organization Code
April 1988	

7. Author(s)

Joe W. Elliott, Susan L. Althoff, and Richard H. Sailey

8. Performing Organization Report No.	10. Work Unit No.
	505-61-51-10

9. Performing Organization Name and Address

Aerostructures Directorate
USAARTA-AVSCOM
Langley Research Center
Hampton, VA 23665-5225

11. Contract or Grant No.	13. Type of Report and Period Covered
	Technical Memorandum

12. Sponsoring Agency Name and Address

National Aeronautics and Space Administration
Washington, DC 20546-0001 and
US Army Aviation Systems Command
St. Louis, MO 63120-1798

14. Sponsoring Agency Code

15. Supplementary Notes

Joe W. Elliott and Susan L. Althoff: Aerostructures Directorate, USAARTA-AVSCOM, Langley Research Center, Hampton, VA
Richard H. Sailey: PRC Kentron, Inc., Hampton, VA

16. Abstract

An experimental investigation was conducted in the 14- by 22-Foot Subsonic Tunnel at NASA Langley Research Center to measure the inflow into a scale model helicopter rotor in forward flight ($\mu_\infty = 0.23$). The measurements were made with a two component Laser Velocimeter (LV) one chord above the plane formed by the path of the rotor tips (tip path plane). A conditional sampling technique was employed to determine the azimuthal position of the rotor at the time that each velocity measurement was made so that the azimuthal fluctuations in velocity could be determined. Measurements were made at a total of 180 separate locations in order to clearly define the inflow character. This data is presented herein without analysis.

17. Key Words (Suggested by Author(s))	18. Distribution Statement
Rotor model Inflow Laser Velocimetry	Unclassified - Unlimited Subject Category 02

19. Security Classif. (of this report)	20. Security Classif. (of this page)	21. No. of pages	22. Price
Unclassified	Unclassified	390	A17